H. Takayasu (Ed.)

# Practical Fruits of Econophysics

## Proceedings of the Third Nikkei Econophysics Symposium

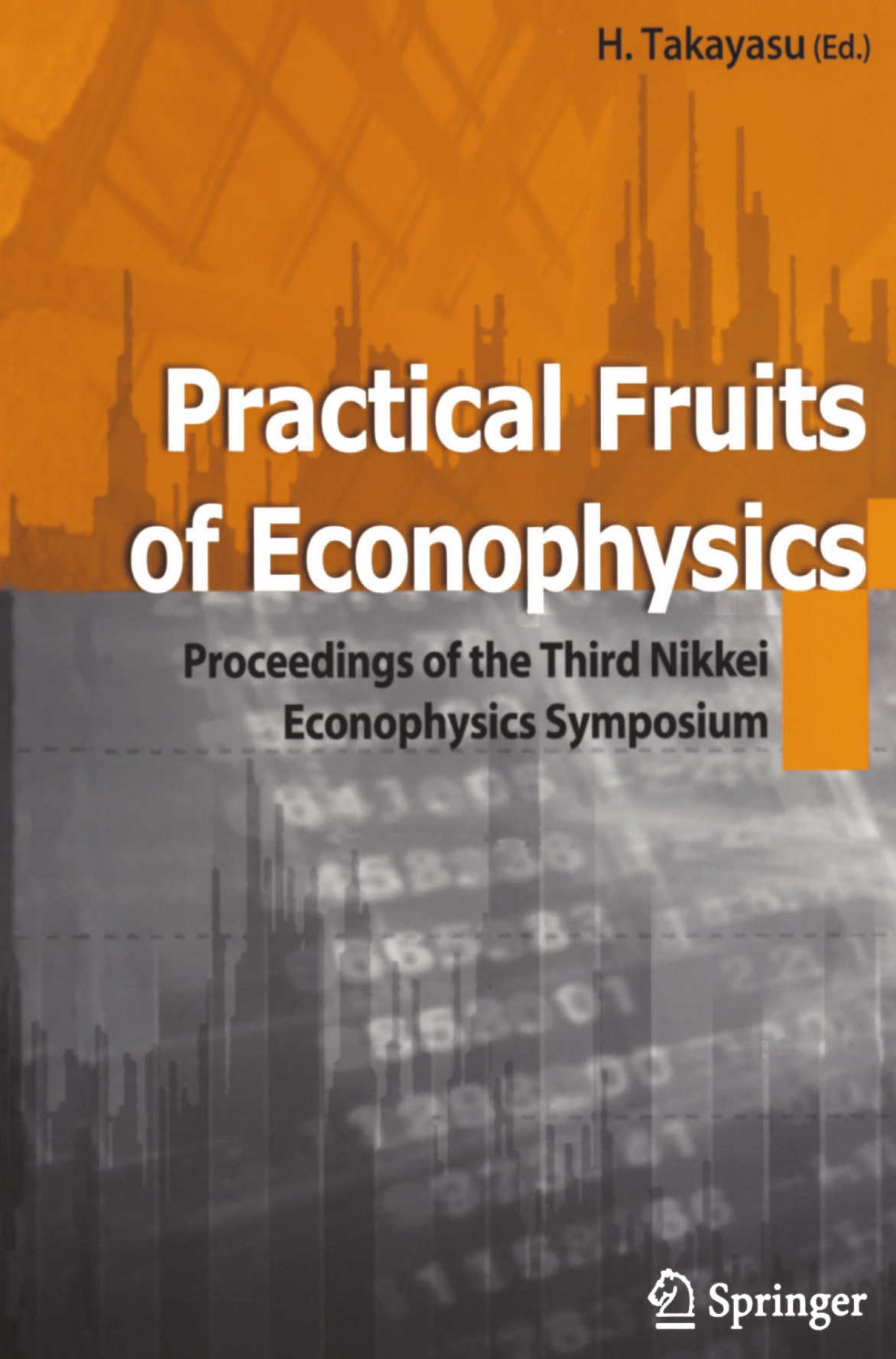

Springer

Hideki Takayasu (Ed.)

# Practical Fruits of Econophysics

Proceedings of the Third Nikkei Econophysics Symposium

Hideki Takayasu (Ed.)

# Practical Fruits of Econophysics

## Proceedings of the Third Nikkei Econophysics Symposium

With 165 Figures, Including 1 in Color

Springer

Hideki Takayasu
Senior Researcher
Sony Computer Science Laboratories, Inc.
3-14-13 Higashi-Gotanda, Shinagawa-ku
Tokyo 141-0022, Japan

Library of Congress Control Number: 2005934583

ISBN-10 4-431-28914-3 Springer-Verlag Tokyo Berlin Heidelberg New York
ISBN-13 978-4-431-28914-2 Springer-Verlag Tokyo Berlin Heidelberg New York

Printed on acid-free paper



Springer is a part of Springer Science+Business Media
springeronline.com

Printed in Japan

Typesetting: Camera-ready by the editor and authors
Printing and binding: Nihon Hicom, Japan

# Preface

Some economic phenomena are predictable and controllable, and some are impossible to foresee. Existing economic theories do not provide satisfactory answers as to what degree economic phenomena can be predicted and controlled, and in what situations. Against this background, people working on the financial front lines in real life have to rely on empirical rules based on experiments that often lack a solid foundation. "Econophysics" is a new science that analyzes economic phenomena empirically from a physical point of view, and it is being studied mainly to offer scientific, objective and significant answers to such problems.

This book is the proceedings of the third Nikkei symposium on "Practical Fruits of Econophysics," held in Tokyo, November 9–11, 2004. In the first symposium held in 2000, empirical rules were established by analyzing high-frequency financial data, and various kinds of theoretical approaches were confirmed. In the second symposium, in 2002, the predictability of imperfections and of economic fluctuations was discussed in detail, and methods for applying such studies were reported. The third symposium gave an overview of practical developments that can immediately be applied to the financial sector, or at least provide hints as to how to use the methodology.

The workshop was supported by: The Economic and Social Research Institute, Cabinet Office, Government of Japan; The Japan Center for Economic Research; The Physical Society of Japan; and The Japan Association for Evolutionary Economics. On behalf of all participants, I would like to thank those supporters, as well as the following companies without whose financial support the workshop would not have been possible: Mizuho Corporate Bank, Ltd.; Hitachi, Ltd. Business Solution Systems Division; Dresdner Kleinwort Wasserstein; Sompo Japan Insurance Inc.; and Sony Computer Science Laboratories, Inc.

As the chief organizer, I am grateful for the cooperation of the organizers, H.E. Stanley (Boston University), Hiroyuki Moriya (Sumisho Capital Management Co.), Toshiaki Watanabe (Tokyo Metropolitan University), Tsutomu Watanabe (Hitotsubashi University). I also express my thanks to the members of the conference secretariat, as represented by K. Suzuki, for their kindness and efficiency, and to the staff members of Springer-Verlag Tokyo, for editorial support. Finally, I would like to thank all the authors for their contributions to this volume.

H. Takayasu
Tokyo 2005

# Contents

## 2. Predictability of Markets

## 3. Mathematical Models

## 4. Correlation and Risk Management

## 5. Networks and Wealth Distributions

## 6. New Ideas

# 1. Market's Basic Properties

# Correlated Randomness: Rare and Not-so-Rare Events in Finance

H. E. Stanley[1], Xavier Gabaix[2], Parameswaran Gopikrishnan[1], and Vasiliki Plerou[1]

[1] Center for Polymer Studies, and Department of Physics, Boston University, Boston, MA 02215 USA
[2] Department of Economics, MIT, Cambridge, MA 02142 and National Bureau of Economic Research, Cambridge, MA 02138

**Abstract.** One challenge of economics is that the systems treated by these sciences have no perfect metronome in time and no perfect spatial architecture—crystalline or otherwise. Nonetheless, as if by magic, out of nothing but *randomness* one finds remarkably fine-tuned processes in time. To understand this "miracle," one might consider placing aside the human tendency to see the universe as a machine. Instead, one might address the challenge of uncovering how, through randomness (albeit, as we shall see, strongly correlated randomness), one can arrive at many temporal patterns in economics. Inspired by principles developed by statistical physics over the past 50 years—scale invariance and universality—we review some recent applications of correlated randomness to economics.

## 1 Introduction

The title I have given to this talk, "Correlated Randomness," I owe in part to interactions with economists, biologists, and medical researchers. Some think that *randomness* means *uncorrelated randomness.* They learn that statistical physics deals solely with random phenomena, so they imagine that our field cannot possibly yield any insights into the real world as they correctly know that no system in which they are interested corresponds to simple *uncorrelated randomness.* Hence we found using the adjective "correlated" helped persuade our collaborators that what we do may possibly be applicable to systems in which they are interested.

To help educate our collaborators, as well as ourselves, we have learned to present simple visual examples of the concept of correlated randomness. One example we found useful was comparing a simple, unbiased random walk in two dimensions (uncorrelated randomness) and a simple, *self-avoiding* random walk in two dimensions (correlated randomness). In the case of the uncorrelated walk, the spread of a $10^4$ step path is $10^2$. In the correlated random walk, the spread of a $10^4$ step path is on the order of $10^3$ steps, an order of magnitude larger (Fig. 1). A second simple example of correlated randomness that people from other fields can appreciate is critical opalescence, first discovered and interpreted—in terms of correlated randomness—by Andrews

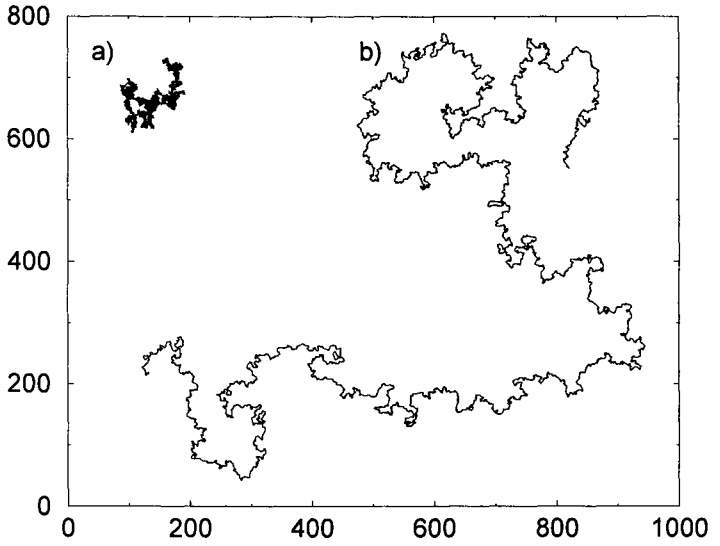


**Fig. 1.** (a) The trail of a random walk of $10^4$ steps, compared with (b) the trail of a self-avoiding random walk of the same number of steps. The "correlated randomness" of the latter results in drastically different behavior. Specifically, the characteristic diameter jumps by a factor of 10, from approximately $(10^4)^{1/2} = 100$ to approximately $(10^4)^{3/4} = 1000$, where we have used the fact that the fractal dimensions (defined as the exponent to which the length is raised to obtain the mass) are 2 and 4/3 respectively. This figure is courtesy of S. V. Buldyrev.

in 1869 [1]. The concentrations of the two components and the temperature have been adjusted so that the system is near its consolute point. The correlated fluctuations observed at that consolute point are so strong that their length scale has become comparable to the wavelength of visible light and one sees a scattering of that visible light in the form of an opalescent glow.

In this talk, I will discuss recent applications of correlated randomness to one area of science for which statistical physics is proving to be useful: economics. I organize this talk around three questions: (i) what is the question or problem that has emerged from this area of inquiry? (ii) why should we (practically and scientifically) care about this question or problem? and (iii) what have we actually done in response to this question or problem? The "we" involves a sizable set of collaborators, three of whom have consented to join me as co-authors of this opening chapter in the Nikkei Proceedings. The list of all my econophysics collaborators appears at the end of this chapter.

Our overall "take-home" message today sounds pretty general. In general systems that display correlated randomness cannot be solved exactly. Not even the simple self-avoiding random walk can be solved! Nonetheless, there are two unifying principles that have organized many of the results we will

be presenting today—scale invariance and universality. The key idea is that scale invariance is a statement not about algebraic equations of the form $x^{-3} = 1/8$ with a numerical solution ($x = 2$) but about functional equations of the form $f(\lambda x) \sim \lambda^p f(x)$ and its relevant generalizations. These functional equations have as their solutions functional forms, and the solution to this homogeneous functional equation is a power-law form.

## 2 What is the phenomenon?

One quarter of any newspaper with a financial section is filled with economic fluctuation data. Most economic graphs look approximately like the one we get when we plot the S&P 500 stock index as a function of time over 40 years We can compare this empirical data with that generated by a simple uncorrelated biased random walk, a model first used over 100 years ago by Bachelier. At first it seems that there is little difference, but looking more closely we see events in the real data that do not have counterparts in the random walk. Black Monday in October 1987 is reflected in the real data, which shows a loss of 30 percent of the total value of the market in just one day. In the random walk we do not see fluctuations anywhere near this magnitude because the probability of taking $n$ steps in the same direction of a random walk is $(1/2)^n$—it decreases exponentially with $n$.

Economists nevertheless have traditionally used this uncorrelated biased Gaussian random walk to describe real economic data, relegating events such as Black Monday to the dustbin category of "outliers" [2–6].

## 3 Why do we care?

We physicists do not like to do things this way. We do not take Newton's law seriously part of the time, and then—if we suddenly see an example of what appears to be levitation—simply call it an "outlier." We like to find laws that describe all examples of a phenomenon. All agree that understanding rare events is an unsolved problem, which is a strong motivation for us physicists to step in and try our hand—we smell a delicious scientific challenge. Also, practically speaking, catastrophic economic events such as Black Monday have extreme societal impacts; widespread suffering is the usual outcome, especially among the poor. The ability to predict economic crashes (and other large-scale risks) would have an obvious utility.

## 4 What do we do?

We return to our two graphs, the S&P 500 stock index as a function of time over 40 years and the simple uncorrelated biased random walk, and plot not the absolute value of the index but instead the *change* in the index

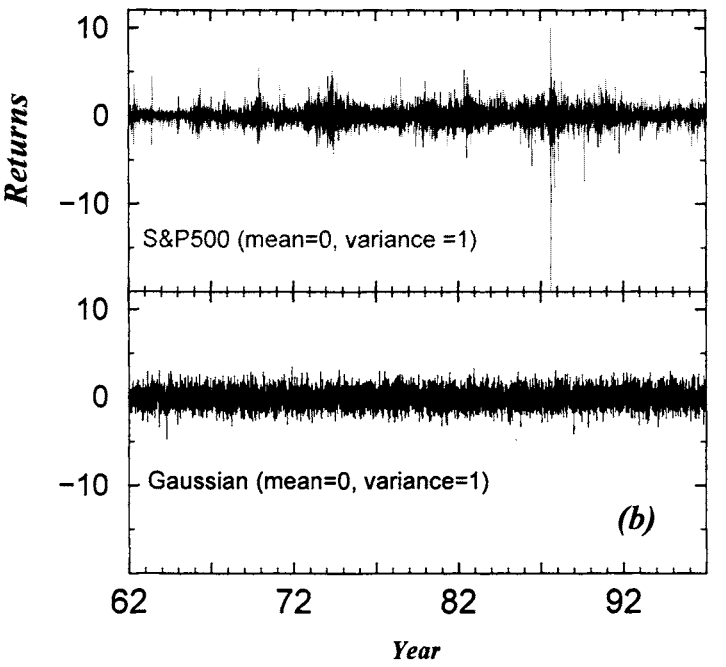


**Fig. 2.** The S&P 500 index is the sum of the market capitalizations of 500 companies. Shown is the sequence of 10-min returns for the S&P 500, normalized to unit variance, compared with sequence of i.i.d. Gaussian random variables with unit variance, which was proposed by Bachelier as a model for stock returns. The large fluctuations seen in 1987 is the market crash of October 19. Note that, in contrast to the top curve, there are no "extreme" events in the bottom curve.

(the numerical derivative, the "return"). We normalize that by the standard deviation. We look over a 13-year period rather than our original 40-year period (Fig. 2) and see, e.g., that on Black Monday the fluctuations were more than 30 standard deviations (both positive and negative) for the day, and we also see a very noisy signal. The striking thing is to look at the other curve, the uncorrelated random walk, and see the Gaussian distribution for the fluctuations—which rarely display fluctuations greater than five standard deviations. The "outliers" that the economists are content to live with are any fluctuations of the actual data that are greater than five standard deviations. In this 13-year period there are exactly 64, i.e., $2^6$. If we count only those fluctuations of the actual data that are greater than ten standard deviations, we get exactly 8, i.e., $2^3$. If we count only those that are greater than 20, we get one, i.e., $2^0$: Black Monday. Each time we double the $x$-axis we change the $y$-axis by a power of $2^3$. At the top of this presentation we made reference to a power law of the form $f(x) = x^{-3}$, which corresponds to a functional

equation, a scaling equation, with $p = -3$. The possibility that economic data obey such a scaling was pointed out in 1963 by Mandelbrot in his study of cotton price fluctuations [7].

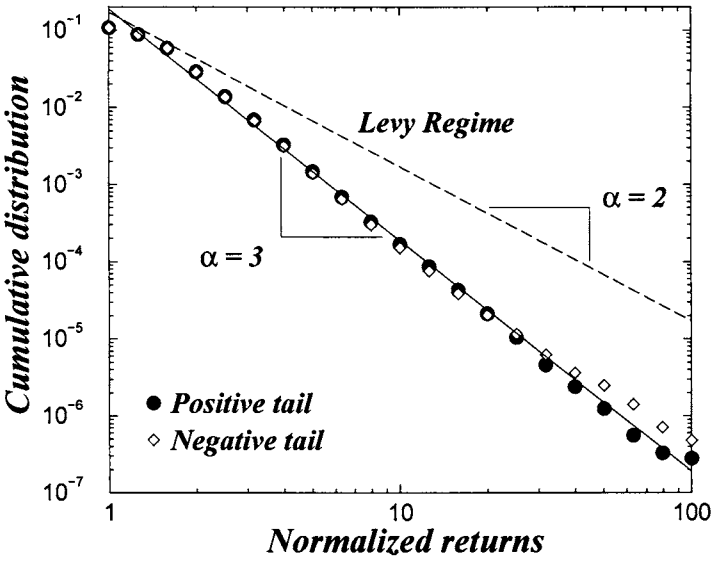


**Fig. 3.** Cumulative distributions of the positive and negative tails of the normalized returns of the 1000 largest companies in the TAQ database for the 2-year period 1994–1995. The solid line is a power-law regression fit in the region $2 \leq x \leq 80$.

If we replace our visual examination of these two graphs with a close computer analysis of not just the the S&P 500 stock index but every stock transaction over an extended time period (approximately one GB of data), we find [8–10] that the actual graph giving the number of times a fluctuation exceeds a given amount as a function of that amount is perfectly straight on log-log paper *out to 100 standard deviations* (Fig. 3). The slope of the line, $\alpha$, is indistinguishable from the value $\alpha = 3$ that we deduced from visual inspection. Note that this slope is significantly larger (by almost a factor of two) than the slope found by Mandelbrot in his research on cotton prices. Note also that our slope is outside the Lévy stable regime [11].

This is how we find laws in statistical physics, but finding them is only the first part—the empirical part—of our task. The second part—the theoretical part—is understanding them.

When we studied critical phenomena, the empirical part was a very important contributor toward our ultimate understanding of phase transitions and critical phenomena. The massing of empirical facts led to the recognition

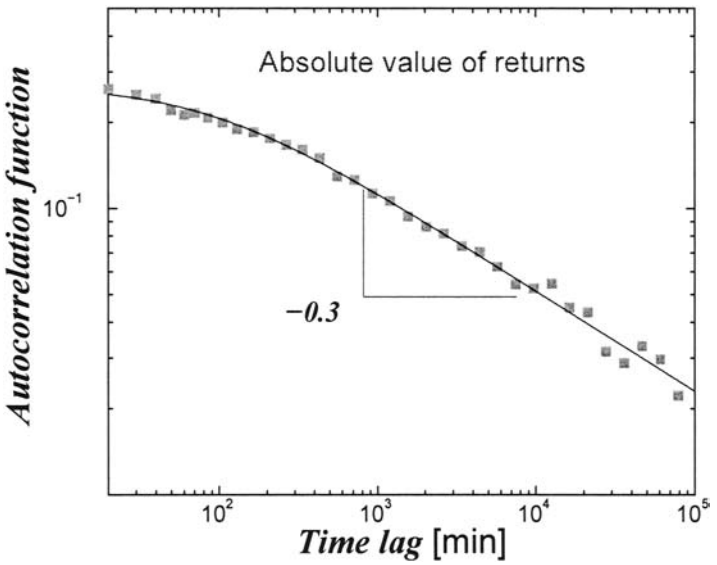


**Fig. 4.** Log-log plot of the autocorrelation function of the absolute returns. The solid line is a power-law regression fit over the entire range, which gives an estimate of the power-law exponent, $\eta \approx 0.3$. Better estimates of the exponent $\eta$ can be obtained from the power spectrum or from other more sophisticated methods.

of regularities to which certain approaches could be applied, e.g., the scaling hypothesis and the Wilson renormalization group. So also in economics we can perhaps first discover empirical regularities—e.g., the inverse cubic law—that will prove useful in ultimately understanding the economy. I wish I could say that we already have an explanation for this inverse cubic law, but I can't. We have the beginnings of an explanation, but it is only the beginning since the current theory explains the inverse cubic law of price changes, as well as the "half cubic law" of trade volume [12,13] but does not explain the strange nature of the temporal correlations. The autocorrelation function of price changes decays exponentially in time so rapidly that after 20 min it is in the level of "noise". However the autocorrelation function of changes in the *absolute value* of the price (called the "volatility") decays with a power law of exponent approximately 0.3 [14] (Fig. 4).

## 5 Quantifying fluctuations in market liquidity: analysis of the bid-ask spread

The primary function of a market is to provide a venue where buyers and sellers can transact. The more the buyers and sellers at any time, the more

efficient the market is in matching buyers and sellers, so a desirable feature of a competitive market is liquidity, i.e., the ability to transact quickly with small price impact. To this end, most exchanges have market makers (eg., "specialists" in the NYSE) who provide liquidity by selling or buying according to the prevalent market demand. The market maker sells at the "ask" (offer) price $A$ and buys at a lower "bid" price $B$; the difference $s \equiv A - B$ is the bid-ask spread.

The ability to buy at a low price and sell at a high price is the main compensation to market makers for the risk they incur while providing liquidity. Therefore, the bid-ask spread must cover costs incurred by the market maker [15–21] such as: (i) order processing costs, e.g., costs incurred in setting up, fixed exchange fees, etc., (ii) risk of holding inventory, which is related to the volatility, and (iii) adverse information costs, i.e, the risk of trading with a counter-party with superior information. Since the first component is a fixed cost, the interesting dynamics of liquidity is reflected in (ii) and (iii). Analyzing the statistical features of the bid-ask spread thus also provides a way to understand information flow in the market.

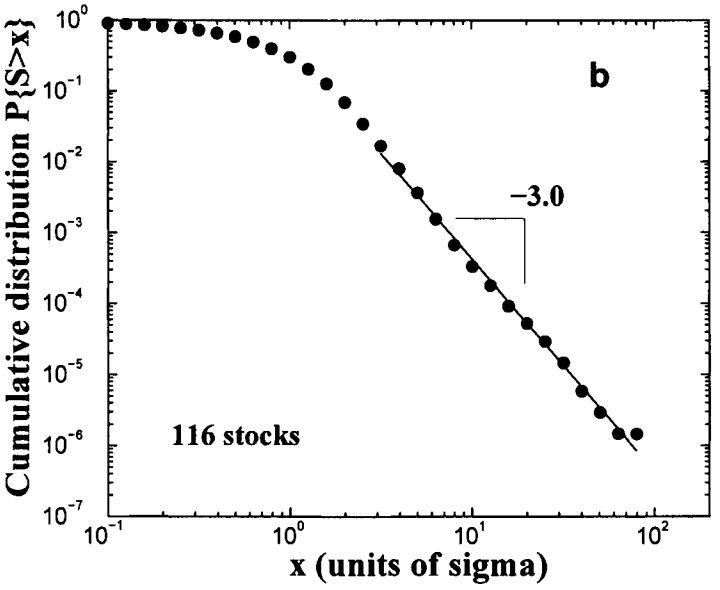


**Fig. 5.** Log-log plot of the cumulative distribution of the bid-ask spread $S_{\Delta t}$ which is normalized to have zero mean and unit variance, for all 116 stocks in our sample for the two-year period 1994–1995. A power law fit in the region $x > 3$ gives a value for the exponent $\zeta_S = 3.0 \pm 0.1$. Fits to individual distributions give similar results for the exponent values. Adapted from Ref. [22].

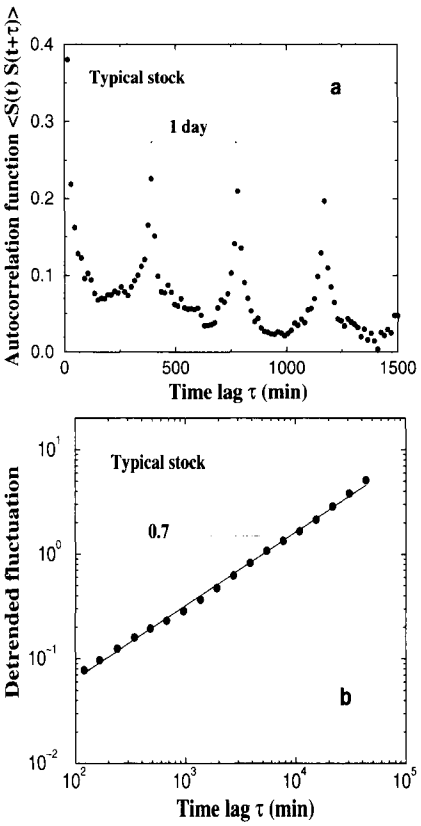


**Fig. 6.** (a) The autocorrelation function $\langle S(t)S(t+\tau)\rangle$ displays peaks at multiples of one day for Exxon Corp. (b) The detrended fluctuation function $F(\tau)$ for the same stock displays long-range power law correlations that extend over almost three orders of magnitude. (c) Histogram of slopes obtained by fitting $F(\tau) = \tau^{\nu_s}$ for all 116 stocks. We find a mean value of the exponent $\nu_s = 0.73 \pm 0.01$. The error-bar denotes the standard error of the mean of the distribution of exponents, which, under *i.i.d.* assumptions, is estimated as the ratio of the standard deviation of the distribution to the square-root of the number of points. In reality, the *i.i.d.* assumptions do not hold, so the error bar thus obtained is likely understated. Adapted from Ref. [22].

The prevalent bid-ask spread reflects the underlying liquidity for a particular stock. Quantifying the fluctuations of the bid-ask spread thus offers a way of understanding the dynamics of market liquidity. Using quote data for the 116 most-frequently traded stocks on the New York Stock Exchange over the two-year period 1994–1995, Plerou et al. [22] have recently analyzed the

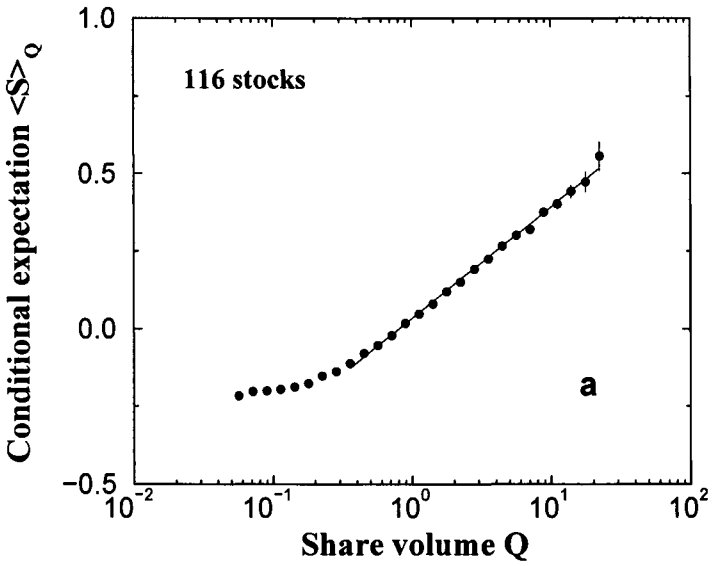


**Fig. 7.** Equal-time conditional expectation $\langle S \rangle_Q$ of the bid-ask spread for a given value of $Q$ averaged over all 116 stocks over a time interval $\Delta t = 15$ min. Here $S$ is normalized to have zero mean and unit variance, and $Q \equiv Q_{\Delta t}(t)$ is normalized by its first centered moment. The solid line shows a logarithmic fit to the data extending over almost two orders of magnitude. (b) Adapted from Ref. [22].

fluctuations of the average bid-ask spread $S$ over a time interval $\Delta t$. They find that $S$ is characterized by a distribution that decays as a power law $P\{S > x\} \sim x^{-\zeta_S}$, with an exponent $\zeta_S \approx 3$ for all 116 stocks analyzed (Fig. 5). Their analysis of the autocorrelation function of $S$ (Fig. 6)shows long-range power-law correlations, $\langle S(t)S(t+\tau)\rangle \sim \tau^{-\mu}$, similar to those previously found for the volatility. They also examine the relationship between the bid-ask spread and the volume $Q$, and find that $S \sim \log Q$ (Fig. 7). They find that a similar logarithmic relationship holds between the transaction-level bid-ask spread and the trade size. They also show that the bid-ask spread and the volatility are also related logarithmically. Finally they study the relationship between $S$ and other indicators of market liquidity such as the frequency of trades $N$ and the frequency of quote updates $U$, and find $S \sim \log N$ and $S \sim \log U$.

## 6 Unifying the power laws: a first model

There has recently been progress in developing a theory for some of the power-law regularities discussed above. For example, based on a plausible set

of assumptions, we proposed a model that provides an explanation for the empirical power laws of return, volume and number of trades [12]. In addition, our model explains certain striking empirical regularities that describe the relationship between large fluctuations in prices, trading volume, and the number of trades. In our model, large movements in stock market activity arise from the trades of the large participants. Starting from an empirical characterization of the size distribution of large market participants (mutual funds), we show that their trading behavior when performed in an optimal way, generates power-laws observed in financial data.

Define $p_t$ as the price of a given stock and the stock price "return" $r_t$ as the change of the logarithm of stock price in a given time interval $\Delta t$, $r_t \equiv \ln p_t - \ln p_{t-\Delta t}$. The probability that a return is in absolute value larger than $x$ is found empirically to be [10,23]

$$P(|r_t| > x) \sim x^{-\zeta_r} \qquad \text{with} \qquad \zeta_r \approx 3. \tag{1}$$

Empirical studies also show that the distribution of trading volume $V_t$ obeys a similar universal power law [25],

$$P(V_t > x) \sim x^{-\zeta_V} \qquad \text{with} \qquad \zeta_V \approx 1.5, \tag{2}$$

while the number of trades $N_t$ obeys [26]

$$P(N_t > x) \sim x^{-\zeta_N} \qquad \text{with} \qquad \zeta_N \approx 3.4. \tag{3}$$

The "inverse cubic law" of Eq. (1) is "universal," holding over as many as 80 standard deviations for some stock markets, with $\Delta t$ ranging from one minute to one month, across different sizes of stocks, different time periods, and also for different stock market indices [10,23]. Moreover, the most extreme events—including the 1929 and 1987 market crashes—conform to Eq. (1), demonstrating that crashes do not appear to be outliers of the distribution. We tested the universality of Eqs. (2) and (3) by analyzing the 35 million transactions of the 30 largest stocks on the Paris Bourse over a 5 yr period. Our analysis shows that the power laws (2) and (3) obtained for US stocks also hold for a distinctly different market, consistent with the possibility that Eq. (2) and (3) are as universal as (1).

We develop a model that demonstrates how trading by large market participants explains the above power laws. We begin by noting that large market participants have large price impacts [27–30]. To see why this is the case, observe that a typical stock has a turnover (fraction of shares exchanged) of approximately 50% a year, which implies a daily turnover of approximately $50\%/250 = 0.2\%$—i.e., on average 0.2% of outstanding shares change hands each day. The 30th largest mutual fund owns about 0.1% of such a stock [31]. If the manager of such a fund sells its holdings of this stock, the sale will represent half of the daily turnover, and so will impact both the price and the total volume [32–34]. Such a theory where large individual participants move

the market is consistent with the evidence that stock market movements are hard to explain with changes in fundamental values [35].

Accordingly, we perform an empirical analysis of the distribution of the largest market participants—mutual funds. We find, for each year of the period 1961–1999, that for the top 10% of distribution of the mutual funds, the market value of the managed assets $S$ obeys the power law

$$P(S > x) \sim x^{-\zeta_S}, \qquad \text{with} \qquad \zeta_S = 1.05 \pm 0.08. \tag{4}$$

Exponents of $\approx 1$ have also been found for the cumulative distributions city size [36] and firm sizes [37–39], and the origins of this "Zipf" distribution are becoming better understood [40]. Based on the assumption that managers of large funds trade on their intuitions about the future direction of the market, and that they adjust their speed of trading to avoid moving the market too much, we will see that their trading activity leads to $\zeta_r = 3$ and $\zeta_V = 1.5$,

In order to proceed, we (A) present empirical evidence for the shape of the price impact, (B) propose an explanation for this shape, and (C) show how the resulting trading behavior generates power laws (1)–(3).

### 6.1 Empirical evidence for the square root price impact of trades

The price impact $\Delta p$ of a trade of size $V$ has been established to be increasing and concave [41,42]. We hypothesize that for large volumes $V$ its functional form is

$$r = \Delta p \simeq kV^{1/2}. \tag{5}$$

for some constant $k$.

A direct statistical test of this hypothesis can be performed by analyzing $E\left[r^2 \mid V\right]$. Performing this regression using $r$ and $V$ calculated over 15 min intervals, we find

$$E\left[r^2 \mid V\right] \sim V\,. \tag{6}$$

This regression is however not definitive evidence for Eq. (5). This regression is performed in fixed $\Delta t$ so is exposed to the effect of fluctuations in the number of trades – i.e., if $N$ denotes the number of trades in $\Delta t$, $r^2 \sim N$ and $V \sim N$ so Eq. (6) could be a consequence of this effect.

Since relation (5) implies $P\left(r > x\right) \sim P\left(kV^{1/2} > x\right) = P\left(V > x^2/k^2\right) \sim x^{-2\zeta_V}$, it follows that

$$\zeta_r = 2\zeta_V. \tag{7}$$

Thus, the power law of returns, Eq. (1), follows from the power law of volumes, Eq. (2), and the square root form price impact, Eq. (5).

Recent work by Farmer and Lillo [43] reports an exponent $\approx 0.3$ for the price impact function. Apart from the quality of scaling and the limited data, one possible problem with this estimation is that large trades are usually executed in smaller traunches [44]. Ref. [43] also reports that the volume distribution is not a power-law for the LSE. Further work by Ref. [44] has

made it clear that the finding of Ref. [43] of a non-power-law distribution of volume is an artifact arising from incomplete data due to the exclusion of upstairs market trades.

We next develop a framework for explaining Eq. (2) and Eq. (5).

### 6.2 Explaining the square root price impact of trades, Eq. (5)

We consider the behavior of one stock, whose original price is, say 1. The mutual fund manager who desires to buy $V$ shares offers a price increment $\Delta p$, so that the new price will become $1 + \Delta p$. Each seller $i$ of size $s_i$ who is offered a price increase $\Delta p$ supplies the fund manager with $q_i$ shares. Elementary considerations lead us to hypothesize $q_i \sim s_i \Delta p$. The number of sellers available after the fund manager has waited a time $T$ is proportional to $T$. So, after a time $T$, the fund manager can on the average buy a quantity of shares equal to $kT\langle s\rangle \Delta p$ for some proportionality constant $k$. The search process stops (and the trades are executed simultaneously) when the desired quantity $V$ is reached—i.e., when $kT\langle s\rangle \Delta p = V$, so the time needed to find the shares is

$$T = \frac{V}{\langle s\rangle k \Delta p} \sim \frac{V}{\Delta p}. \tag{8}$$

Hence there is a trade-off between cost $\Delta p$ and the time to execution $T$; if the fund manager desires to realize the trade in a short amount of time $T$, the manager must pay a large price impact $\Delta p \sim V/T$.

Let us consider the manager's decision problem. Managers trade on the assumption that a given stock is mispriced by an amount $M$, defined as the difference between the fair value of the stock and the traded price [30,45,46]. The manager wants to exploit this mispricing quickly, as he expects that the mispricing will be progressively corrected, i.e. expects that the price will increase at a rate $\mu$. Hence, after a delay of $T$, the remaining mispricing is only $M - \mu T$. The total profit per share $B/V$ is the realized excess return $M - \mu T$ minus the price concession $\Delta p$, which gives

$$B = V\left(M - \mu T - \Delta p\right). \tag{9}$$

The fund manager's goal is thus to maximize $B$, the perceived dollar benefit from trading. The optimal price impact $\Delta p$ maximizes $B$ subject to Eq. (8), $T = aV/\Delta p$, i.e., $\Delta p$ maximizes $V(M - \mu aV/\Delta p - \Delta p)$, which we will see gives Eq. (5).

The time to execution is $T \sim V/\Delta p \sim V^{1/2}$, and the number of "chunks" in which the block is divided is $N \sim T \sim V^{1/2}$. These effects have been qualitatively documented in [27,28,42]. The last relation gives

$$\zeta_N = 2\zeta_V \tag{10}$$

which in turn predicts $\zeta_N = 3$, a value, approximately consistent with the empirical value of 3.4 [26].

Thus far, we have a theoretical framework for understanding the square root price impact of trades Eq. (5), which with Eq. (2) explains the cubic law of returns Eq. (1). We now focus on understanding Eq. (2).

### 6.3 Explaining the Power Laws.

Next we show that returns and volumes are power law distributed with tail exponents

$$\zeta_r = 3, \zeta_V = 3/2 \tag{11}$$

provided the following conditions hold (i) the power law exponent of mutual fund sizes is $\zeta_S = 1$ (Zipf's law); (ii) the price impact follows the square root law (5); (iii) funds trade in typical volumes $V \sim S^\delta$ with $\delta > 0$; (iv) funds adjust trading frequency and/or volume so as to pay transactions costs in such a way that defining

$$c(S) \equiv \frac{\text{Annual amount lost by the fund in price impact}}{\text{Value } S \text{ of the assets under management}}. \tag{12}$$

then $c(S)$ is independent of $S$ for large $S$.

The empirical validity of conditions (i) and (ii) was shown above, while condition (iii) is a weak, largely technical, assumption. Condition (iv) means that funds in the upper tail of the distribution pay roughly similar annual price impact costs $c(S)$ reaches an asymptote for large sizes. We interpret this as an evolutionary "survival constraint". Funds that would have a very large $c(S)$ would have small returns and would be eliminated from the market. The average return $r(S)$ of funds of size $S$ is independent of $S$ [47]. Since small and large funds have similarly low ability to outperform the market, $c(S)$ is also independent of $S$.

For each block trade $V(S)$ a fund of size $S$ incurs a price impact proportional to $V\Delta p$ which, from condition (ii), is $V^{3/2}$. If $F(S)$ is the fund's annual frequency of trading, then the annual loss in transactions costs is $F(S) \cdot V^{3/2}$, so

$$c(S) = F(S) \cdot [V(S)]^{3/2}/S. \tag{13}$$

Condition (iv) implies that either $V(S)$ or $F(S)$ will adjust in order to satisfy

$$F(S) \sim S \cdot [V(S)]^{-3/2}. \tag{14}$$

Condition (i) implies that the probability density function for mutual funds of size $S$ is $\rho(S) = -\partial G/\partial S \sim S^{-2}$. Since condition (iii) states that $V \sim S^\delta > x$, and since they trade with frequency given $F(S)$ in Eq. (14),

$$P(V > x) \sim \int_{S^\delta > x} F(S)\rho(S)dS \sim \int_{S > x^{1/\delta}} S^{1-3\delta/2} S^{-2} dS \sim x^{-3/2}. \tag{15}$$

which leads to a power law distribution of volumes with exponent $\zeta_V = 3/2$. Moreover, from Eq. (7), it follows that $\zeta_r = 3$. In addition, the above result does not depend on details of the trading strategy, such as the specific value of $\delta$.

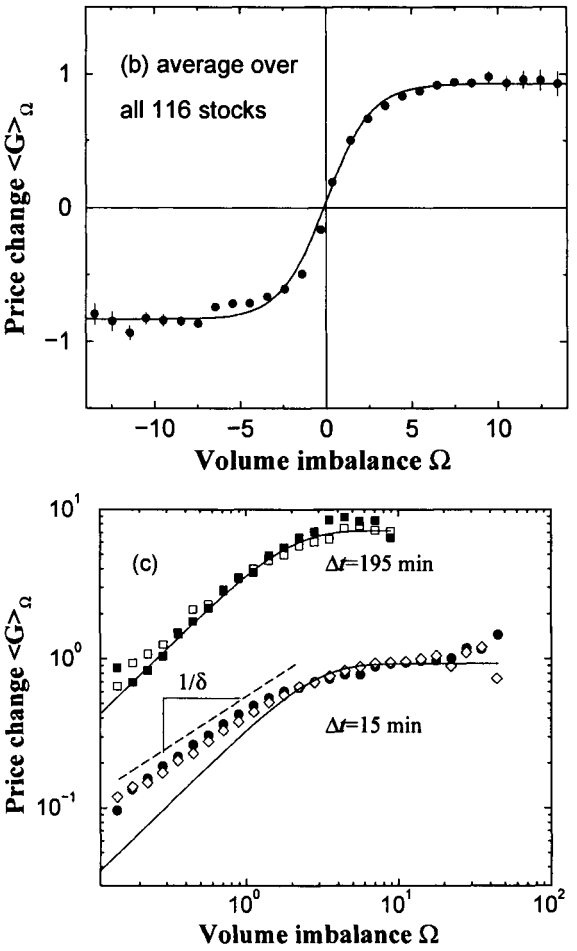


**Fig. 8.** (a) Conditional expectation $\langle G \rangle_\Omega$ averaged over all 116 stocks studied, over a time interval $\Delta t = 15$ min, where $\Omega$ is defined as the difference in number of shares traded in buyer and seller initiated trades. We normalize $G$ to have zero mean and unit variance. Since $\Omega$ has a tail exponent $\zeta = 3/2$ which implies divergent variance, we normalize $\Omega$ by the first moment $\langle |\Omega - \langle \Omega \rangle| \rangle$. We calculate $G$ and $\Omega$ for $\Delta t = 15$ min. The solid line shows a fit to the function $B_0 \tanh(B_1 \Omega)$. (b) $\langle G \rangle_\Omega$ on a log-log plot for different $\Delta t$. For small $\Omega$, $\langle G \rangle_\Omega \simeq \Omega^{1/\delta}$. For $\Delta t = 15$ min find a mean value $1/\delta = 0.66 \pm 0.02$ by fitting $\langle G \rangle_\Omega$ for all 116 stocks individually. The same procedure yields $1/\delta = 0.34 \pm 0.03$ at $\Delta t = 5$ min (interestingly close to the value of the analogous critical exponent in mean field theory). The solid curve shows a fit to the function $B_0 \tanh(B_1 \Omega)$. For small $\Omega$, $B_0 \tanh(B_1 \Omega) \sim \Omega$, and therefore disagrees with $\langle G \rangle_\Omega$, whereas for large $\Omega$ the fit shows good agreement. For $\Delta t = 195$ min ($\frac{1}{2}$ day) (squares), the hyperbolic tangent function shows good agreement.

## 7 Concluding Remarks

One reason the economy is of interest to statistical physicists is that, like an Ising model, the economy is a system made up of many subunits. The subunits in an Ising model are called spins, and the subunits in the economy are buyers and sellers. During any unit of time these subunits of the economy may be either positive or negative as regards perceived market opportunities. People interact with each other, and this fact often produces what economists call "the herd effect." The orientation of whether we buy or sell is influenced not only by our neighbors but also by news. If we hear bad news, we may be tempted to sell. So the state of any subunit is a function of the states of all the other subunits and of a field parameter.

On a qualitative level, economists often describe a price change as a hyperbolic-tangent-like function of the demand. The catch is that "demand" is not quantified. So one of the first things we had to do was quantify demand [41].

We did this by analyzing huge databases comprising every stock bought or sold—which gives not only the selling price and buying price, but also the asking price and the offer price. If we go to the open market to buy presents we will often be given an asking price we are not willing to pay, and we may counter with a much smaller offer. Ultimately when the sale is struck, the price may be above the midpoint between the asking price and the offer—and we assign a variable $a_i = +1$ to the sale—if below the midpoint, $a_i = -1$. If we sum all these indices $a_i$ over a time interval $\Delta t$

$$H \equiv \sum_{i-1}^{N} a_i = \begin{cases} + & \text{[Big Demand]} \\ - & \text{[Small Demand]} \end{cases}$$

$$N = N_{\Delta t} = \quad \text{Number of sales in } \Delta t,$$

then we can calculate the analog of a magnetic field, which provides a way of quantifying demand. If most of the $a_i$ are positive, the field will be positive, and vice versa. A hint that this definition of magnetic field makes sense is the fact that a plot of price change as a function of the "magnetic field" variable defined above remarkably resembles a plot of the magnetization of a magnet as a function of the magnetic field [41] (Fig. 8). The full implications of the remarkable observation that a plot of price change as a function of the "magnetic field" resembles a plot of the magnetization in a magnet are a challenging problem.

**Acknowledgments** We thank the NSF economics program (SES-0215823 and SRS-0140554) for financial support and we thank our many collaborators, among whom are S. V. Buldyrev, D. Canning, P. Cizeau, S. Havlin, Y. Lee, Y. Liu, P. Maass, R. N. Mantegna, K. Matia, M. Meyer, B. Rosenow, M. A. Salinger, and M. H. R. Stanley, and most especially L. A. N. Amaral. We also thank H. Takayasu for organizing the November 2004 Nikkei Conference.

## References


1. T. Andrews, *Phil. Trans.* **159**, 575 (1869).
2. H. Takayasu, ed., *Empirical Science of Financial Fluctuations The Advent of Econophysics* (Springer Verlag, Berlin, 2002).
3. A. Bunde, H. J. Schellnhuber, and J. Kropp, eds., *The Science of Disasters Climate Disruptions, Heart Attacks, and Market Crashes* (Springer-Verlag, Berlin, 2002).
4. R. N. Mantegna and H. E. Stanley, *An Introduction to Econophysics: Correlations and Complexity in Finance* (Cambridge University Press, Cambridge, 2000).
5. J. P. Bouchaud and M. Potters, *Theory of Financial Risk* (Cambridge University Press, Cambridge, 2000).
6. H. E. Stanley, Physica A **318**, 279–292 (2003).
7. B. B. Mandelbrot, *J. Business* **36**, 394 (1963).
8. P. Gopikrishnan, M. Meyer, L. A. N. Amaral, and H. E. Stanley, *Eur. Phys. J. B* **3**, 139 (1998).
9. V. Plerou, P. Gopikrishnan, L. A. N. Amaral, M. Meyer, and H. E. Stanley, *Phys. Rev. E* **60**, 6519 (1999).
10. P. Gopikrishnan, V. Plerou, L. A. N. Amaral, M. Meyer, and H. E. Stanley, *Phys. Rev. E* **60**, 5305 (1999).
11. K. Matia, L. A. N. Amaral, S. Goodwin, and H. E. Stanley, Phys. Rev. E Rapid Communications **66**, 045103 (2002).
12. X. Gabaix, P. Gopikrishnan, V. Plerou, and H. E. Stanley, Nature **423**, 267 (2003).
13. X. Gabaix, P. Gopikrishnan, V. Plerou, and H. E. Stanley, "The Fat-Tailed Distributions of Financial Variables," Quarterly Journal of Economics (submitted).
14. Y. Liu, P. Gopikrishnan, P. Cizeau, M. Meyer, C.-K. Peng, and H. E. Stanley, "The Statistical Properties of the Volatility of Price Fluctuations," *Phys. Rev. E* **60**, 1390–1400 (1999).
15. T. Copeland and D. Galai, J. Finance **38**, 5 (1983).
16. D. Easley and M. O'Hara, J. Fin. Econom. **19**, 69 (1987).
17. R. Roll, J. Finance **39**, 1127 (1984).
18. J. Y. Campbell, A. Lo, and A. C. MacKinlay, *The Econometrics of Financial Markets* (Princeton University Press, Princeton, 1999).
19. Y. Amihud and H. Mendelson, J. Fin. Econom. **8**, 31 (1980).
20. L. Glosten and P. Milgrom, J. Fin. Econom. **14**,71 (1985).
21. J. Hasbrouck, J. Fin. Econom. **22**, 229 (1988).
22. V. Plerou, P. Gopikrishnan, and H. E. Stanley, Phys. Rev. E Rapid Communications **71**, 046131 (2005).
23. T. Lux, "The Stable Paretian Hypothesis and the Frequency of Large Returns: An Examination of Major German Stocks," *Appl. Finan. Econ.* **6**, 463–475 (1996).
24. D. M. Guillaume et al., "From the Bird's Eye to the Microscope: A Survey of New Stylized Facts of the Intra-Daily Foreign Exchange Markets," *Fin. and Stochastics* **1**, 95–129 (1997).
25. P. Gopikrishnan, V. Plerou, X. Gabaix, and H. E. Stanley, "Statistical Properties of Share Volume Traded in Financial Markets," *Phys. Rev. E* **62**, R4493–R4496 (2000).

26. V. Plerou, P. Gopikrishnan, L. A. N. Amaral, X. Gabaix, and H. E. Stanley, "Diffusion and Economic Fluctuations," *Phys. Rev. E* **62**, R3023–R3026 (2000).
27. D. Keim and A. Madhavan, "Transactions Costs and Investment Style: An Inter-Exchange Analysis of Institutional Equity Trades," *J. Fin. Econ.* **46**, 265–292 (1997).
28. L. Chan and J. Lakonishok, "The Behavior of Stock Prices around Institutional Trades," *J. Fin.* **50**, 1147–1174 (1995).
29. J. Wurgler and K. Zhuravskaya, "Does Arbitrage Flatten Demand Curves for Stocks?" *J. Business* **75**, 583–608 (2002).
30. L. Bagwell, "Dutch Auction Repurchases: An Analysis of Shareholder Heterogeneity," *J. Fin.* **47**, 71–105 (1992).
31. Source `http//gsbwww.uchicago.edu/research/crsp/` (Center for Research in Security Prices).
32. A. S. Kyle, "Continuous Auctions and Insider Trading," *Econometrica* **53**, 1315–1335 (1985).
33. S. Grossman and M. Miller, "Liquidity and Market Structure," *J. Fin.* **43**, 617–633 (1988).
34. M. O'Hara, *Market Microstructure Theory* (Blackwell, Oxford, 1997).
35. D. Cutler, J. M. Poterba, and L. H. Summers, "What Moves Stock Prices?" *J. Portfolio Management* **15**, 4–12 (1989).
36. G. Zipf, *Human Behavior and the Principle of Least Effort* (Addiston-Wesley, Cambridge, 1949).
37. M. H. R. Stanley, S. V. Buldyrev, S. Havlin, R. Mantegna, M.A. Salinger, and H. E. Stanley, "Zipf plots and the size distribution of Firms," Economics Lett. **49**, 453–457 (1995).
38. K. Okuyama, M. Takayasu, and H. Takayasu, "Zipf's Law in Income Distribution of Companies," *Physica A* **269**, 125–131 (1999).
39. R. Axtell, "Zipf Distribution of U.S. Firm Sizes," *Science* **293**, 1818–1820 (2001).
40. X. Gabaix, "Zipf's Law for Cities: An Explanation," *Quart. J. Econ.* **114**, 739–767 (1999).
41. V. Plerou, P. Gopikrishnan, X. Gabaix, and H. E. Stanley, Phys. Rev. E **66**, 027104 (2002).
42. J. Hasbrouck, "Measuring the Information Content of Stock Trades," *J. Finance* **46**, 179–207 (1991).
43. J. D. Farmer and F. Lillo, "On the Origin of Power Law Tails in Price Fluctuations" Quant. Fin. **4**, C7 (2004).
44. V. Plerou, P. Gopikrishnan, X. Gabaix, and H. E. Stanley, "On the Origin of Power Law Fluctuations in Stock Prices" Quant. Fin. **4**, C11 (2004).
45. K. Daniel, D. Hirshleifer, and A. Subrahmanyam, "Investor Psychology and Security Market Under- and Over-reactions," *J. Fin.* **53**, 1839–1885 (1998).
46. A. Shleifer, *Inefficient Markets An Introduction to Behavioral Finance* (Oxford University Press, Oxford, 2000).
47. X. Gabaix, R. Ramalho, and J. Reuter, "Investor Behavior and the Evolution of Mutual Funds," Mimeo (2005).

# Non-trivial scaling of fluctuations in the trading activity of NYSE

János Kertész[1,2] and Zoltán Eisler[1]

[1] Department of Theoretical Physics, Budapest University of Technology and Economics, Budafoki út 8, H-1111 Budapest, Hungary

[2] Laboratory of Computational Engineering, Helsinki University of Technology, P.O.Box 9203, FIN-02015 HUT, Finland

**Summary.** Complex systems comprise a large number of interacting elements, whose dynamics is not always a priori known. In these cases – in order to uncover their key features – we have to turn to empirical methods, one of which was recently introduced by Menezes and Barabási. It is based on the observation that for the activity $f_i(t)$ of the constituents there is a power law relationship between the standard deviation and the mean value: $\sigma_i \propto \langle f_i \rangle^{\alpha}$. For stock market trading activity (traded value), good scaling over 5 orders of magnitude with the exponent $\alpha = 0.72$ was observed. The origin of this non-trivial scaling can be traced back to a proportionality between the rate of trades $\langle N \rangle$ and their mean sizes $\langle V \rangle$. One finds $\langle V \rangle \propto \langle N \rangle^{0.69}$ for the $\sim 1000$ largest companies of New York Stock Exchange. Model independent calculations show that these two types of scaling can be mapped onto each other, with an agreement between the error bars. Finally, there is a continuous increase in $\alpha$ if we look at fluctuations on an increasing time scale up to 20 days.

**Key words:** econophysics; stock market; fluctuation phenomena

## 1 Introduction

Although there is no generally recognized definition of complex systems, one of their widely accepted properties is that they comprise a large number of interacting constituents (or nodes) whose collective behavior forms spatial and/or temporal structures. Some of them are labeled "physical" because they are treated in the regular framework of physics. Nevertheless, the above scheme itself applies to a much wider range of systems, including the world economy consisting of companies that trade and compete. Human agents can interact with each other, e.g., by social networks or on the trading floor. We have little or no a priori knowledge about the laws governing these systems. Thus, very often our approach must be empirical. Recently, an increasing number of such systems have become possible to monitor through multichannel measurements. These offer the possibility to record and characterize the simultaneous time dependent behavior of many of the constituents. On the ground of these new datasets, an emerging technique (de Menezes and Barabási 2004a) seems to be able to grasp important features of the internal dynamics in a model independent framework.

## 2 Scaling of fluctuations in complex systems

The method is based on a scaling relation that is observed for a growing range of systems: The standard deviation $\sigma_i$ and time average $\langle f_i \rangle$ of the signal $f_i(t)$ capturing the time dependent activity of elements $i = 1, \ldots, N$ follows the power law

$$\sigma_i \propto \langle f_i \rangle^{\alpha}, \tag{1}$$

where we define

$$\sigma_i = \sqrt{\left\langle (f_i - \langle f_i \rangle)^2 \right\rangle}, \tag{2}$$

and $\langle \cdot \rangle$ denotes time averaging.

This relationship is not unmotivated from a physicist's point of view. The constant $\alpha$ – while not a universal exponent in the traditional sense – is indeed the fingerprint of the microscopic dynamics of the system. Applications range from Internet traffic through river networks to econophysics. The latest advances (Menezes and Barabási 2004b, Eisler and Kertész 2005) have shown several possible scenarios leading to various scaling exponents:

1. The value $\alpha = 1$ always prevails in the presence of a *dominant external driving force*. An example is web page visitation statistics. Here the main contribution to fluctuations comes from the fluctuating number of users surfing the web: a factor that is not intrinsic in the structure of the network. The situation is very similar for networks of roads or rivers.
2. There are systems, where the different mean activity of constituents comes exclusively from a different mean number of events. Individual events have the same mean contribution (impact) to a node's activity, only for more active nodes more of these events occur. When the *central limit theorem* is applicable to the events, $\alpha = 1/2$. This behavior was observed for the logical elements of a computer chip and the data traffic of Internet routers.
3. Two mechanisms have been documented so far that can give rise to an intermediate value $1/2 < \alpha < 1$:
   a) Because of the competition of external driving and internal fluctuations, it is possible that $\sigma$'s measured for finite systems display a crossover between $\alpha = 1/2$ and $\alpha = 1$ at a certain node strength $\langle f \rangle$. Then there exists an effective, intermediate value of $\alpha$, but actual scaling breaks down.
   b) The other possibility is related to a very distinct character of internal dynamics: when elements with higher activity do not only experience more events, but those are also of larger impact. We call this property *impact inhomogeneity*. Stock market trading belongs to this third group with $\alpha \approx 0.72$ for short time scales (see also Eisler et al. 2005).

In a recent model (Eisler and Kertész 2005), the effect of impact inhomogeneity has been studied. Tokens are deposited on a Barabási-Albert network (Albert and Barabási 2002) and they are allowed to jump from node to node in every time step. Activity is generated when they arrive to a site. Every token that steps to a node $i$

generates an impact $V_i$ whose mean depends on the node degree $k_i$: $\langle V_i \rangle \propto k_i^{\beta}$. This gives rise to a scaling relation:

$$\langle V_i \rangle \propto \langle N_i \rangle^{\beta} . \tag{3}$$

The result of Eisler and Kertész (2005) can then then be generalized as

$$\alpha = \frac{1}{2}\left(1 + \frac{\beta}{\beta + 1}\right). \tag{4}$$

Simulation results shown in Fig. 1(a) are in perfect agreement with formula (4). This is an example that the value of $\alpha$ is basically determined by this impact inhomogeneity. If $\beta = 0$, i.e., the mean impact generated on all nodes is equal regardless of their degree, one recovers $\alpha = 1/2$. When $\beta > 0$, the events on more frequently visited nodes are also larger on average. Correspondingly, $\alpha > 1/2$.

## 3 Application to stock market data

Let us now turn to the case of the stock market. Data for the period 2000–2002 was taken from the TAQ Database (New York Stock Exchange 2003). We define the activity $f_i(t)$ of stock $i$ as the capital flow in time windows of size $\Delta t$. In window $t$, $f_i(t)$ is the sum of $N_i(t)$ trading events. If we denote the value exchanged in the $n$'th trade of time window $t$ by $V_i(t;n)$, then the total traded value of stock $i$ is

$$f_i(t) = \sum_{n=1}^{N_i(t)} V_i(t;n). \tag{5}$$

Then, $\langle V \rangle$ is the *mean value per trade*, while $\langle N \rangle$ is the *mean rate of trades*.

As we wish to calculate the mean and the standard deviation of this activity, it is essential that these quantities at least exist. Traded volumes and consequently traded values $f_i(t)$ are often considered to have a power law tail ($Prob(f > x) \propto x^{-\lambda}$) with an exponent $\lambda_i \sim 1.5 - 1.7$ (Gopikrishnan et al. 2000). This would imply, that the standard deviation is already divergent. Recent measurements, however, indicate that both of these quantities exist and that there is no unique $\lambda_i$ for a stock (Eisler and Kertész unpublished).

Then, it is possible to test the scaling relation (1) and one finds good scaling over more than 5 orders of magnitude in $\langle f \rangle$ with $\alpha \approx 0.72$. This is a value which can be – at least partly – explained in terms of impact inhomogeneity. We found [1] that for the stocks of the $\sim$ 1000 largest companies of NYSE, $\beta = 0.69 \pm 0.09$ (see Fig. 1(b)). Substituting this into (4) we expect $\alpha = 0.71 \pm 0.01$, which is very close to the actual result seen from Fig. 2(a). Note that although large error bars prevent us from testing (4) for smaller stocks, we still find that the scaling law (1) holds. The exponent is unchanged, but this can only be explained by a detailed analysis of fluctuations.

[1] The result is qualitatively similar to those of Zumbach (2004) for the FTSE 100. He shows that both $\langle N \rangle$ and $\langle V \rangle$ scale as power laws with company capitalization for large companies. Capitalization dependence can be eliminated to recover (3).

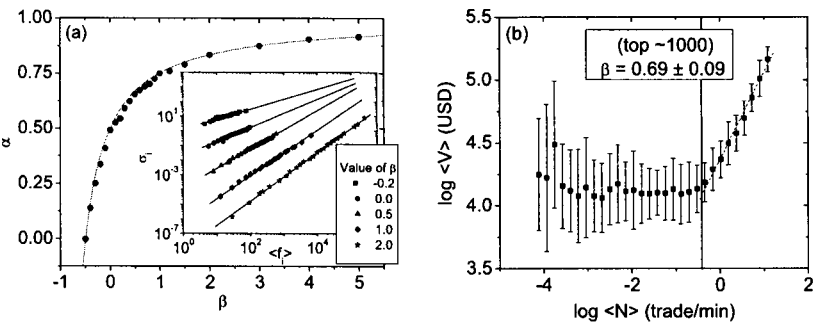


**Fig. 1. (a)** The value of $\alpha$ as a function of $\beta$ for the random walk model introduced by Eisler and Kertész (2005). Circles give simulation results, while the solid line corresponds to (4). The inset shows actual scaling plots for various values of $\beta$. **(b)** Plot of mean value per trade $\langle V \rangle$ versus mean rate of trades $\langle N \rangle$ for NYSE. For smaller stocks there is no clear tendency. For the top $\sim$ 1000 companies, however, there is scaling with an exponent $\beta = 0.69 \pm 0.09$.

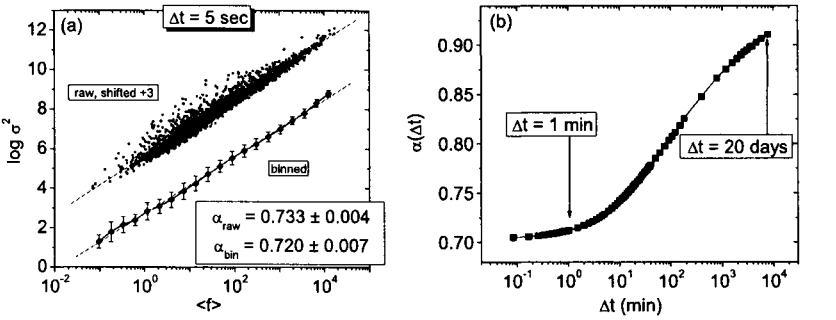


**Fig. 2. (a)** The scaling $\sigma \propto \langle f \rangle^{\alpha}$ for fluctuations of traded value at NYSE, $\Delta t = 5$ sec. Dots show raw results for each stock (shifted vertically for better visibility), the fitted slope is $\alpha_{raw} = 0.733 \pm 0.004$. Diamonds show average $\sigma$'s for multiple stocks in a range of $\log \langle f \rangle$. This method corrects for bias that comes from the large number of stocks with low $\langle f \rangle$, one finds $\alpha_{binned} = 0.720 \pm 0.007$. **(b)** The dependence of $\alpha$ on the time window $\Delta t$ for the NYSE data. One finds that up to $\Delta t = 1$ min, $\alpha \approx 0.72$, as expected from independent approximations. Then by increasing $\Delta t$, the value of $\alpha$ increases. This is due to the presence of strong autocorrelations in the activities $f(t)$ stemming from the clustering of trades.

The mechanism leading to non-trivial $\alpha$ via the scaling (3) can be considered dominant only if the events are not strongly correlated. This condition is satisfied for short time windows $\Delta t$, when $\langle N \rangle \ll 1$. Interestingly, the value of $\alpha$ does not change noticably up to $\Delta t \sim 1$ min. There is, however, another effect that is relevant to the value of $\alpha$ for longer time windows. For the NYSE data, $\alpha(\Delta t)$ increases continuously with $\Delta t$ (see Fig. 2(b)). Previously (Eisler et al. 2005) this was attributed to the growing influence of external news: a kind of "driving". With longer

time given for information to spread, the system was assumed to converge to the externally driven limit $\alpha = 1$. That mechanism would, however, lead to a *crossover* to $\alpha = 1$ with increasing $\Delta t$ (Menezes and Barabási 2004b). What is observed, is in fact *not* a crossover. There is no breakdown of scaling as a function of $\langle f \rangle$ for intermediate $\Delta t$'s as one would expect between the regime of the two limiting exponents (Menezes and Barabási 2004b). On the other hand, it is well known (see, e.g., Gopikrishnan et al. 2000), that the number of trades $N_i(t)$ is correlated. Individual trades tend to cluster together and this causes enhanced fluctuations in $N_i(t)$. This mechanism sets in at time windows for which the probability for two trades to coincide is no longer negligible. The scaling law (1) itself is preserved, but the exponent $\alpha$ is strongly affected.

## 4 Conclusions

In the above we have outlined a recent type of scaling analysis for the fluctuations of activity in complex systems. We have shown that systems can be classified according to the scaling exponents $\alpha$. Then we have discussed how impact inhomogeneity and long range correlations give rise to non-trivial scaling exponents. Further research should clarify the interplay between fluctuations in the number of trades and in traded volumes/values in order to deepen the understanding of the market mechanism.

Acknowledgments: JK is member of the Center for Applied Mathematics and Computational Physics, BUTE. This research was supported by OTKA T049238. Thanks are due to A.-L. Barabási and M.A. de Menezes.

## References

Albert R, Barabási A-L (2002) Statistical mechanics of complex networks, Rev Mod Phys 74:47–97

Eisler Z, Kertész J (2005) Random walks on complex networks with inhomogeneous impact. arXiv:cond-mat/0501391, submitted to Phys Rev E

Eisler Z, Kertész J, Yook S-H, Barabási A-L (2005) Multiscaling and non-universality in fluctuations of driven complex systems. Europhys Lett 69:664–670

Gopikrishnan P, Plerou V, Gabaix X, Stanley HE (2000) Statistical properties of share volume traded in financial markets. Phys Rev E 62:R4493-4496

de Menezes MA, Barabási A-L (2004a) Fluctuations in Network Dynamics. Phys Rev Lett 92:28701

de Menezes MA, Barabási A-L (2004b) Separating internal and external dynamics of complex systems. Phys Rev Lett 93:68701

New York Stock Exchange (2003) The Trades and Quotes Database for 2000-2002. New York

Zumbach G (2004) How the trading activity scales with the company sizes in the FTSE 100. arXiv:cond-mat/0407769, to appear in Quant Fin

# Dynamics and predictability of fluctuations in dollar-yen exchange rates

A.A. Tsonis[1], K. Nakada[1], and H. Takayasu[2]

[1]Department of Mathematical Sciences, University of Wisconsin-Milwaukee Milwaukee, WI 53201-0413, USA

[2] Sony Computer Science Laboratories Inc. 3-14-13 Higashigotanda, Shinagawa-ku, Tokyo, 141-0022, Japan

**Summary.** Analysis of tick data of yen-dollar exchange using random walk methods has showed that there exists a characteristic time scale approximately at 10 minutes. Accordingly, for time scales shorter than 10 minutes the market exhibits anti-persistence, meaning that it self-organizes so that to restore a given tendency. For time scales longer than 10 minutes the market approaches a behavior appropriate to pure Brownian motion. This property is explored here to elucidate the predictability of this type of data. We find that improvement in predictability is possible provided that the data are not "contaminated" with noise.

**Key words.** Econophysics, Fractals, Anti-Pesristence, Brownian Motions

## Introduction

In an earlier paper (Tsonis et al., 2001) we analyzed two tic data sets of dollar-yen exchange rates using random walk methods. The data were collected by Bloomberg from representative dealers. The dealers report their prices to Bloomberg whenever they trade and then Bloomberg announces immediately the prices to the rest of the world. As a result the sampling of these data is not constant but it varies from 0 to 20 minutes with the mean interval being about 7 seconds. Data set 1 covers the period from 26 October to 30 November 1998 (267,398 values) and data set 2 covers the period from 4 January to 12 March 1999 (578,509 values). In the analysis the data were assumed as having been sampled at a constant time step. The effect of the non-uniformity in the sampling time is discussed in Tsonis et al. (2001).

For each data set the root mean square fluctuation $F(t)$ about the average displacement, $F^2(t) = \overline{[\Delta y(t)]^2} - \overline{[\Delta(y(t)]}^2$ was estimated. Hare the bars indicate

an average over all positions $t_0$ in the walk and $\Delta y(t) = y(t_0 + t) - y(t_0)$. The derivative of this function is shown in figure 1 for data set 1 (top) and data set 2 (bottom). The derivative is used to delineate scaling regimes in the data where *F(t)* varies as $F(t) \propto t^H$ (Triantafyllou et al., 1994). Both plots indicate that in the range $2<\log_{10}t<4$ (which would approximately correspond to time scales between 10 minutes and 20 hours), $F(t) \propto t^H$ with $H$=0.5. An interesting feature in this figure is that for time scales less than 10 minutes the exponent $H$ is clearly less than 0.5 indicating negative correlations (anti-persistence). This is an important result because it implies a tendency to restore trends in the data. The only difference is that for data set 2 there is more fluctuation in the derivative, which could be due to several factors (see below for more details).

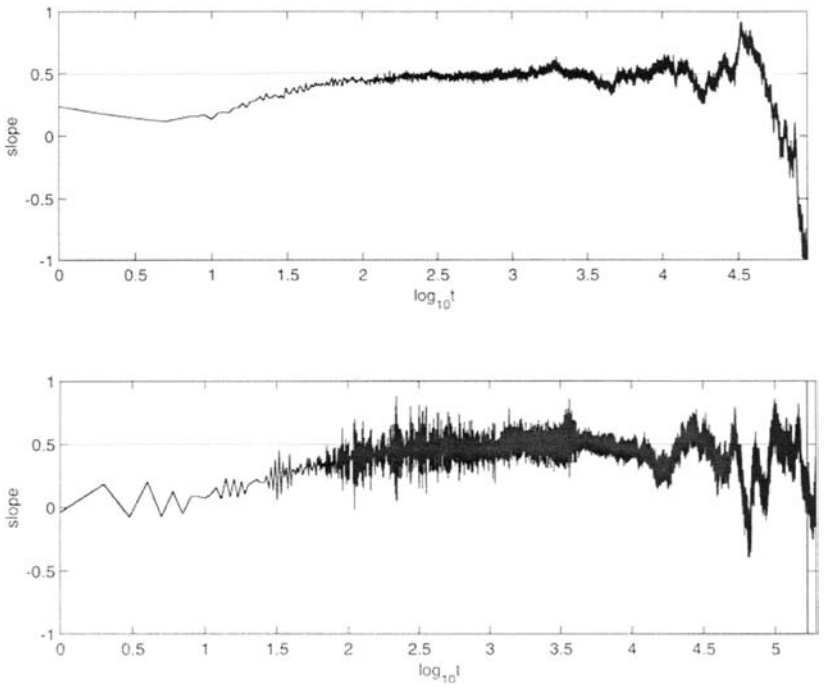


**Fig. 1.** Log-log plot of the derivative of function *F(t)* versus *t* for data set 1(top) and for data set 2 (bottom).

The statistical significance of the scaling properties derived in figure 1 has been investigated in Tsonis et al. (2001). There, it is shown that the characteristic time scale of 10 minutes is statistically significant and not the result of the uneven sampling interval. Note that, using other variants of the method (such as detrended

fluctuation analysis [DFA]) yields very similar results. Similar analyses using other type of economic time series have reported other values for $H$. For example, Podbnik et al. (2000) have analyzed stock market prices and found a characteristic time scale of 30 minutes separating persistence from pure Brownian motion. Also, Vandewalle and Ausloos (1998) have applied DFA for various financial time series and have reported various values for $H$. Dynamically speaking, different types of financial time series may not exhibit similar characteristics. The demand and trading characteristics are different and as such different exponents should be expected.

The above results are important because they suggest that for some time (though short) the market (in this case the dollar-yen exchange rate) acts to restore a given past tendency. In this case, the behavior of the data for time scales less than 10 minutes may be modeled as a fractional Brownian motion with $H<0.5$, whereas for longer time scales it should be modeled as a pure Brownian motion ($H=0.5$). Also, it suggests that monitoring local trends may improve short-term predictions, since any given tendency will have to be reversed.

This is investigated next. In order to address the issue of predictability we first considered data set 1 and divided it into non-overlapping windows of 20 values and estimated the trend in the first 10 values (trend 1) and the trend in the second 10 values (trend 2) in each window, and plotted trend1 versus trend2 (figure 2, top left panel). The period covered by 10 values (on the average about 70 seconds) corresponds to a time scale in the anti-persistence region. On the top right panel, the same is shown, but now the windows are 500 values wide and the trends are calculated over 250 values (which corresponds to a time scale of about 30 minutes in the pure Brownian motion region). On the top right panel the points are distributed in a rather circular pattern, indicating that a given trend over a period of 30 minutes is likely to be followed, with equal probability, by a trend in the next 30 minutes that can be either of the same sign or the opposite sign. The pattern on the top left panel, however, is markedly different. Even though a positive (negative) trend over a period of 70 seconds is not always followed by a negative (positive) trend in the following 70 seconds, clearly a large positive (negative) trend1 is associated with a much smaller positive (negative) or a negative (positive) trend2. This is consistent with the theoretical expectations.

Thus, monitoring local trends may improve short-term predictions. One, however, must be careful of possible noise or other effects that may act as added noise. As we can see in figure 1, while the scaling behavior is very similar in both plots, there exists more variation superimposed on the bottom plot. This may indicate added noise or some other problem in the data. How does this affect predictability? To answer this question we considered data set 2 and repeated the analysis.

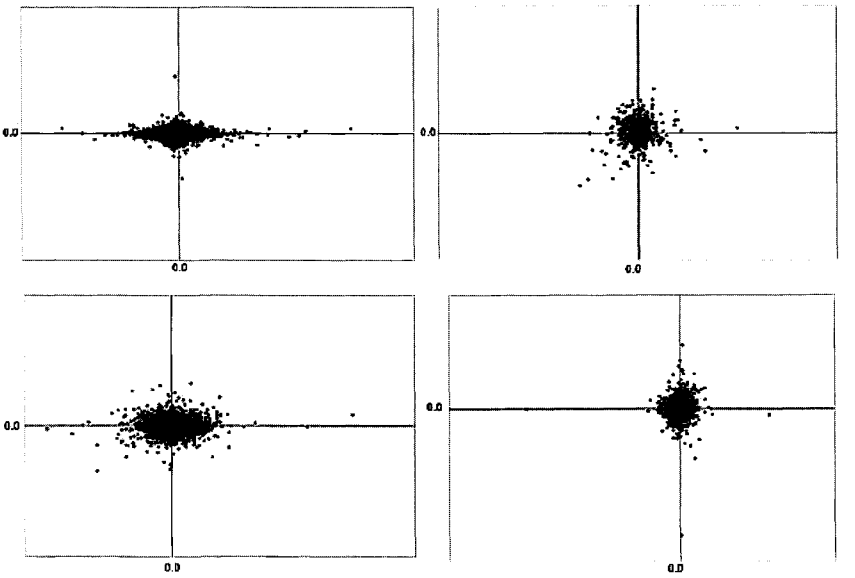

**Fig. 2** Top left: Data set 1 is used and divided into non-overlapping windows of 20 values. For each window we estimate the trend in the first 10 values (trend 1) and the trend in the second 10 values (trend 2). This figure shows trend1 versus trend2. The period covered by 10 values (on the average about 70 seconds) corresponds to a time scale in the anti-persistence region. Top right: Same as top but the non-overlapping windows are 500 values wide and the trends are calculated over 250 values (which corresponds to a time scale of about 30 minutes in the pure Brownian motion region). Bottom left: same as top left but for data set 2. Bottom right: Same as top right but for data set 2.

The results are shown on the bottom panels of figure 2. Now we observe that, while the noise has not affected the results in the pure Brownian motion region (as one might expected), it has affected the results in the anti-persistence region. Even though we still see that the pattern is not circular, we observe that now the pattern is somewhere between the pattern in the top right and the pattern in the top left. Thus, while some of the predictability shown in the top left panel still exists it has been affected by the noise. We conclude that, while improvements in predictability might be possible in the anti-persistence regime, one must be careful with data that may include some kind of influences "acting" like noise. It is interesting to note here that in the period covered by data set 2, the euro was introduced to the market. Apparently, such an introduction might have created uncertainty, thus introducing an effect acting as noise compared to the data before its introduction.

## Conclusions

A characteristic time scale in a certain type of finance data has been documented. This characteristic time scale corresponds to about 10 minutes and separates anti-persistence from pure randomness. This is an important finding as it suggests that for some time (though short) the market (in this case the dollar-yen exchange rate) acts to restore a given past tendency. In this case, the behavior of the data for time scales less than 10 minutes may be modeled as a fractional Brownian motion with $H<0.5$, whereas for longer time scales it should be modeled as a pure Brownian motion ($H=0.5$). Also, it suggests that monitoring local trends may improve short-term predictions, since any given tendency will have to be reversed. Indeed, we show here that improvements in prediction are feasible provided that the data do not include effects which may introduce uncertainty and act as noise.

## References


Podbnik B, Ivanov PC, Lee Y, Chessa A, Stanley HE (2000) Systems with correlations in the variance:generating power-law tails in the probability density. Europhysics Lett 50:711-717.

Triantafyllou GN, Picard R, Tsonis AA (1994) Exploiting geometric signatures to accurately derive properties of attractors. Appl Math Lett 7:19-24.

Tsonis AA, Heller F, Takayasu H, Maruno K, Shimizu T (2001): A characteristic time scale in dollar-yen exchange rates. PhysicaA 291:574-582.

Vandewalle N, Ausloos M (1998) Extended detrended fluctuation analysis for financial data. Int J Compu Anticipat Syst 1:343-349.

Viswanathan GM, Afanasyev V, Buldyrev SV, Murphy EV, Prince PA, Stanley HE (1996) Lévy flight search patterns of wandering albatrosses. Nature 381:413-415.

# Temporal characteristics of moving average of foreign exchange markets

Misako Takayasu[1], Takayuki Mizuno[1], Takaaki Ohnishi[2], Hideki Takayasu[3]

[1] Department of Computational Intelligence and Systems Science, Interdisciplinary Graduate School of Science and Engineering, Tokyo Institute of Technology, 4259 Nagatsuta-cho, Midori-ku, Yokohama 226-8502, Japan
[2] Graduate School of Law and Politics, The University of Tokyo, 7-3-1 Hongo, Bunkyo-Ku, Tokyo, 113-0033, Japan
[3] Sony Computer Science Laboratories, 3-14-13 Higashi-Gotanda, Shinagawa-ku, Tokyo 141-0022, Japan

**Summary.**
We firstly introduce an optimal moving average for Yen-Dollar tick data that makes the residual term to be an independent noise. This noise separation is realized for weight functions decaying nearly exponentially with characteristic time about 30 seconds. We further introduce another moving average applied to the optimal moving average in order to elucidate underlying force acting on the optimal moving average. It is found that for certain time scale we can actually estimate potential force that satisfies a simple scaling relation with respect to the time scale of moving average.

**Key words.** Foreign exchange market, optimal moving average, potential force, scaling relation.

## 1. Introduction

In the first Nikkei symposium we showed that the statistics of trade intervals is well characterized by a Poisson process with its mean given by a moving average of trade intervals for about two minutes [1]. Such type of stochastic process is named as the self modulation process and its basic properties have been analyzed theoretically [2]. Although the moving average covers only a short time scale the self modulation can cause a large time scale effect such as the 1/f power spectrum or long tails in the autocorrelation function of trade intervals [3].

As known from this example clarification of the meaning of moving average is one of the most important tasks in econophysics. In this paper we pay attention to Yen-Dollar exchange rates and report quite non-trivial behaviors derived from a combination of moving average analysis of different time scales.

## 2. The optimal and super moving averages

We introduce so-called the optimal moving average that can separate uncorrelated noises from the market data. Denoting the tick data of Yen-Dollar rate by $P(t)$ the moving average procedure is given by the following equations:

$$P(t+1) = \overline{P(t)} + f(t), \tag{1}$$

$$\overline{P(t)} = \sum_{k=1}^{K} w(k) \cdot P(t-k), \tag{2}$$

where $\{w(k)\}$ give the optimal weight factors that make the residue $f(t)$ almost an independent random noise [4, 5]. The estimated weight factors generally decay exponentially such as $w(k) \propto \exp(-0.3k)$.

In order to elucidate potential forces acting on $\overline{P(t)}$ we introduce another moving average called the super moving average of scale $M$:

$$\overline{P_M(t)} \equiv \frac{1}{M} \sum_{k=1}^{M} \overline{P(t-k)} \quad . \tag{3}$$

We observe the time difference of optimal moving averages, $\overline{P(t+1)} - \overline{P(t)}$, versus the price difference of optimal moving average and super moving average at time $t$, $\overline{P(t)} - \overline{P_M(t)}$ for various values of $M$ ranging from 4 to 2000 ticks. In Fig.1we can confirm the following linear relation approximately.

$$\overline{P(t+1)} - \overline{P(t)} \propto \overline{P(t)} - \overline{P_M(t)} \tag{4}$$

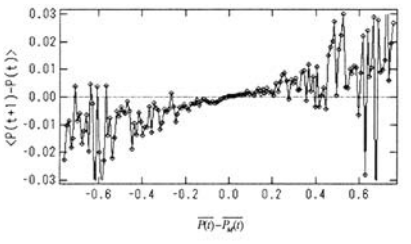


Fig.1 Price difference vs Temporal change

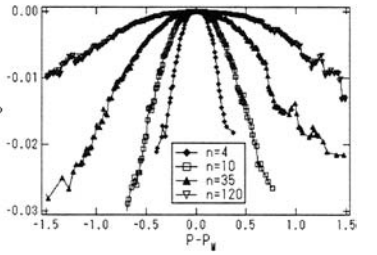


Fig.2 Potential forces observed in the Yen-Dollar market

The potential function can be calculated by integrating along the horizontal axis of Fig.1 as shown in Fig.2. In this case the estimated potential functions are always parabolic for various values of $M$. It should be noted that this type of non-trivial potential function can not be found if the market price change follows a simple random walk.

## 3. Scaling relation of the potential force

The $M$-dependence of the parabolic potential functions is analyzed by plotting the coefficient of the quadratic term $(\overline{P(t)}-\overline{P_M(t)})^2$ as a function of $M$ in Fig.3. It is found that the coefficient generally decays proportional to $1/(M-1)$, therefore, all the potential functions observed for different values of $M$ collapse into one parabolic function as shown in Fig.4.

Applying these results we have the following dynamics as for the optimal moving average:

$$\overline{P(t+1)}-\overline{P(t)}=-\frac{d}{d\overline{P}}U(\overline{P(t)}-\overline{P_M(t)}) \qquad (5)$$

where

$$U(\overline{P(t)}-\overline{P_M(t)})=\frac{1}{2}\cdot\frac{b(t)}{M-1}\cdot(\overline{P(t)}-\overline{P_M(t)})^2 \quad . \qquad (6)$$

The value of $b(t)$ changes slowly and it takes both positive and negative values.

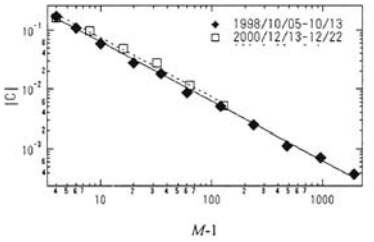


Fig.3. Potential coefficient vs the size of super moving average

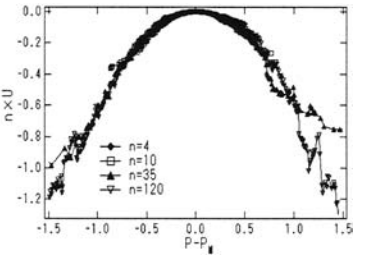


Fig.4. Scaled potential functions

## 4. Discussion

The underlying potential force in the market we observed in this paper is expected to be closely related to the "God's invisible hand" proposed by Adam Smith about 200 years ago. In the case of positive $b(t)$ the attractive force is considered to be realized by "demand and supply". On the other hand a negative value of $b(t)$ implies that the market is quite unstable. Real time characterization of market stability in terms of $b(t)$ will be of practical use in the near future.


## Acknowledgement

The authors would like to show appreciation to H. Moriya of Oxford Financial Education for providing us the data of high-frequency exchange rate. T.M. is supported by the Ministry of Education, Science, Sports and Culture, Grant-in-Aid for JSPS Fellows.


## References


[1] M. Takayasu, H. Takayasu, and M. P. Okazaki, Transaction Interval Analysis of High Resolution Foreign Exchange Data, in Empirical Science of Financial Fluctuations – The Advent of Econophysics, (Springer Verlag, Tokyo, 2002), 18-25.

[2] M. Takayasu and H. Takayasu, Self-modulation processes and resulting generic 1/f fluctuations, Physica A 324, 101-107, 2003.

[3] M. Takayasu, Self-modulation processes in financial markets, in The Application of Econophysics – Proceedings of the Second Nikkei Econophysics Symposium, (Springer Verlag, Tokyo. 2003), 155-160.

[4] T. Ohnishi, T. Mizuno, K. Aihara, M. Takayasu and H. Takayasu, Statistical properties of the moving average price in dollar–yen exchange rates, Physica A 344, 207-210, 2004.

[5] T. Mizuno, M. Takayasu and H. Takayasu, Modeling a foreign exchange rate using moving average of Yen-Dollar market data, in this volume.

# Characteristic market behaviors caused by intervention in a foreign exchange market

Takayuki Mizuno[1], Yukiko Umeno Saito[2], Tsutomu Watanabe[2,3], and Hideki Takayasu[4]

[1] Department of Computational Intelligence and Systems Science, Interdisciplinary Graduate School of Science and Engineering, Tokyo Institute of Technology, 4259 Nagatsuta-cho, Midori-ku, Yokohama 226-8502, Japan
[2] Fujitsu Research Institute Inc., 1-16-1 Kaigan, Minato-ku, Tokyo 105-0022, Japan
[3] Institute of Economic Research, Hitotsubashi University, 2-1 Naka, Kunitachi City, Tokyo 186-8603, Japan
[4] Sony Computer Science Laboratories, 3-14-13 Higashi-Gotanda, Shinagawa-ku, Tokyo 141-0022, Japan

**Summary.** In foreign exchange markets monotonic rate changes can be observed in time scale of order of an hour on the days that governmental interventions took place. We estimate the starting time of an intervention using this characteristic behavior of the exchange rates. We find that big amount of interventions can shift the averaged rate about 1 yen per 1 dollar in an hour, and the rate change distribution becomes asymmetric for a few hours.

**Key words.** Intervention, Foreign exchange market, Econophysics.

## 1. Introduction

The central banks intervene in foreign exchange markets in order to stabilize the currency exchange rates. The amount of one transaction is typically several million dollars in the yen-dollar market, while the amount of intervention by the bank of Japan sometimes exceeds 10 billion dollars in one day. Due to such extraordinary big amount the intervention is generally expected to show remarkable influence on the market. For the basic study of foreign exchange markets it is important to clarify the influence of interventions quantitatively and statistically.

Among various studies on foreign exchange markets the effects of interventions have been investigated by using the daily data [1][2]. In order to clarify the response of markets to an intervention in more detail, we investigate average rate shifts after the intervention in the time scale of several minutes.

As the intervention starting times of the Bank of Japan are not announced, we first estimate the starting time using characteristics of rate changes on intervention days. By analyzing the yen-dollar market's tick data for 10 years comparing the information of intervention about amounts and dates, we find statistical laws of rate changes for typical intervention influences.

## 2. Asymmetrical rate changes on intervention days

In Fig.1 we show yen-dollar fluctuations on 2/11/1994 as a typical example of an intervention day. It is announced that the United States' governmental bank intervened in the foreign exchange market from 11:00AM on this day. Right after the start of the intervention the exchange rate went up nearly monotonically for about 30 minutes. We can find similar rate changes also on other intervention days. The monotonic rate changes cause an asymmetric probability density distribution of rate changes on the intervention day.

We investigate the skewness of rate changes on intervention days. Denoting yen-dollar rate at a time $t$ by $P(t)$ and its change with time interval $T$ by $dP(t,T) = P(t+T) - P(t)$ the skewness is defined by the following formula:

$$\text{Skewness} = \frac{\left\langle \left( dP(t,T) - \left\langle dP(t,T) \right\rangle \right)^3 \right\rangle}{\sigma^3}, \qquad (1)$$

where $\sigma$ is the standard deviation of the rate change. We plot the skewness as a function of time scale $T$ in Fig.2. White diamonds ($\diamond$) denote the averaged skewness on non-intervention days. The rate change distributions on the non-intervention days are nearly symmetric as known from the value of the skewness being around zero [3]. Black diamonds ($\blacklozenge$) show the averaged skewness on days of "yen-selling intervention". Within the time scales between 10 and 60 minutes, non-zero skewness is clearly observed on the intervention days. Namely, the rate change distribution on intervention days is asymmetric in this time scale.

## 3. Intervention starting time estimation

The number of Japanese interventions is much larger than that of any other country. For example, in the yen-dollar exchange market from 1991 to 2004, the total number of Japanese interventions was 342, while that of the United States'

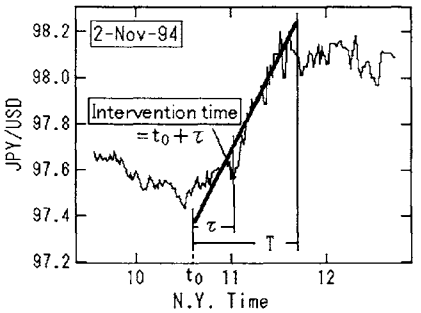


**Fig.1** An example of intervention in the yen-dollar exchange market. The figure shows the rate in 2/11/1994. America intervened at 11:00AM.

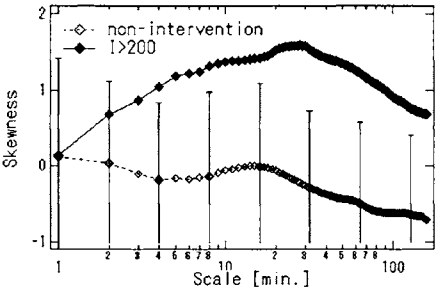


**Fig.2** Skewness of the rate change on a time scale between 1 minute and 3 hours. ◇ is the averaged skewness by non-intervention days and ◆ is the averaged skewness of days of "yen-selling intervention" more than 200 billion yen. Error bars are estimated by the standard deviation of the skewness for non-intervention days.

interventions was only 10. In order to analyze statistical properties we focus on Japanese interventions. The dates of Japanese interventions are now announced and each amount is also announced, however, the starting times are never announced. Therefore, we have to develop a method of estimating the starting time of Japanese intervention from given rate change data.

On an intervention day a large rate change can often be found in the time scale between 10 to 60 minutes as mentioned. We assume that such a large rate change occurs due to the intervention and define a characteristic time $t_0$ that gives the starting time of the largest rate change smoothed over time scale of 60 minutes on each intervention day as indicated in Fig.1. In Table.1 we show a relationship between the intervention time and the characteristic time $t_0$ through the period in which the starting times of the United States' interventions were announced. We find that the actual intervention starting time is given $t_0 + 20$ minutes. We apply this estimation method for the estimation of starting times of Japanese interventions.

**Table.1** The United States' interventions from 1994 to 2000. The table shows intervention dates, intervention times, characteristic times $t_0$, and the intervened market. The characteristic time $t_0$ is defined during a time when the largest rate change for 60 minutes occurred as shown in Fig.1.

| Date | time | $t_0$ | $t_0$+20minutes | Market |
|---|---|---|---|---|
| 29-Apr-94 | 11:30 | 11:20 | 11:40 | Yen-Dollar |
| 4-May-94 | 8:30 | 8:20 | 8:40 | Yen-Dollar |
| 24-Jun-94 | 9:30 | 9:20 | 9:40 | Yen-Dollar |
| 2-Nov-94 | 11:00 | 10:40 | 11:00 | Yen-Dollar |
| 3-Nov-94 | 11:00 | 10:40 | 11:00 | Yen-Dollar |
| 3-Mar-95 | 9:10 | 8:30 | 8:50 | Yen-Dollar |
| 3-Apr-95 | 11:20 | 13:50 | 14:10 | Yen-Dollar |
| 5-Apr-95 | 10:20 | 10:00 | 10:20 | Yen-Dollar |
| 17-Jun-98 | 7:55 | 7:35 | 7:55 | Yen-Dollar |
| 22-Sep-00 | 7:11 | 7:10 | 7:30 | Dollar-Euro |

## 4. Influence of intervention

We introduce a conditional average: $\langle P(t_0+dt)-P(t_0)\,|\,I_{c1}<I<I_{c2}\rangle$, that is the average of rate changes $P(t_0(n)+dt)-P(t_0(n))$ for yen-selling intervention of which amount is in the range of $I_{c1}<I<I_{c2}$. Here, $t_0(n)$ denotes the characteristic time of the $n$-th intervention. We show the results $\langle P(t_0+dt)-P(t_0)\,|\,I_{c1}<I<I_{c2}\rangle$ for three ranges of the intervention amounts in Fig.3. The time $dt=20$ minutes is expected to give the starting of interventions. For big size interventions of $I>200$ billion yen the average rate shifts monotonically for about an hour and it becomes nearly flat after that. From Fig.3 we find that the average rate shift depends on the amount of intervention. Although the shift is within the error bars for $I<200$ billion yen, the over all rate shift due to the intervention is approximated by a linear function,

$$\langle P(t_0+dt)-P(t_0)\,|\,I\rangle = I\times 10^{-3}, \qquad (2)$$

where, $dt=190$ minutes and a unit of the intervention price $I$ is one billion yen.

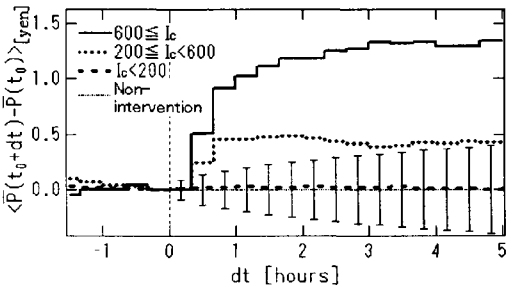


**Fig.3** Average rate change after intervention times. The top (solid) line indicates cases in which the interventions are larger than 600 billion yen, the middle line represents cases of interventions from 200 billion yen up to 600 billion yen, and the bottom line indicates cases in which interventions are less than 200 billion yen. Error bars are standard deviations of a rate change on non-intervention days.

## 5. Discussion

We introduced an estimation method of intervention times and clarified influences of the intervention on a foreign exchange market. The exchange rate drifts for about an hour after the start of an intervention time. After an hour the rates fluctuate randomly with no drift. The shift of the averaged rate is approximated by a linear function of the intervention price. For example, typically an intervention of size 1 trillion yen can shift 1 yen in the yen-dollar exchange rates.

## Acknowledgement

The present authors would like to show appreciation to Hiroyuki Moriya in Oxford Financial Education for providing us with the CQG data of high-frequency exchange rate, Prof. Tohru Nakano for stimulating discussions. T. Mizuno is supported by Research Assistant Fellowship of Chuo University, and the Ministry of Education, Science, Sports and Culture, Grant-in-Aid for JSPS Fellows.

## References

[1] T. Ito, Is Foreing exchange intervention effective? The Japanese experiences in the 1990s, NBER Working Paper No. 8914, 2002.

[2] A. P. Chaboud and O. F. Humpage, An analysis of Japanese foreign exchange interventions, 1991-2002, Federal Reserve bank of Cleveland, Working Paper 03-09, 2003.

[3] T. Mizuno, S. Kurihara, M. Takayasu, H. Takayasu, Analysis of high-resolution foreign exchange data of USD-JPY for 13 years, Physica A 324, 296-302, 2003.

# Apples and Oranges: the difference between the Reaction of the Emerging and Mature Markets to Crashes.

Adel Sharkasi, Martin Crane and Heather J. Ruskin

School of Computing, Dublin City University, Dublin 9, IRELAND.

## Summary.

We study here the behavior of the eigenvalues of the covariance matrices of returns for emerging and mature markets at times of crises. Our results appear to indicate that mature markets respond to crashes differently to emerging ones and that emerging markets take longer to recover than mature markets. In addition, the results appear to indicate that the *second largest* eigenvalue gives additional information on market movement and that a study of the behavior of the other eigenvalues may provide insight on crash dynamics.

**keyword**. Covariance Matrix, Eigenvalues and Stock Crashes.

## Introduction.

Recently, several studies have applied the concepts and methods of physics to the areas of economics and finance, particularly to the study the covariance (or correlation) between price changes (returns) of different stocks [e.g. Meric and Meric (1997), Kwapien et al. (2002), Keogh et al. (2003) and Kwapien et al. (2004)]. Thus far, the magnitude of the *maximum eigenvalue* of the correlation (or covariance) matrices for different sectors in one stock market index only, has predominantly been studied with no attention paid to the other eigenvalues. The differences in the current work are twofold; firstly, to highlight the information obtained from the subdominant eigenvalue as well as the dominant eigenvalue and study their behaviour. Secondly, to compare this for stock market indices for two different classes, namely emerging and mature markets.

Our objectives in this article are thus; **(a)** To study the distribution of the eigenvalues of the Covariance matrices for equal-interval sliding windows, including the week before the Crisis, together with those of Covariance matrices for windows, including both the week of the Crisis and a week after. This, in order

to see the qualitative difference between emerging and mature markets to crashes in term of the eigenvalues (the $\lambda$'s). **(b)** To study the distribution of the ratio of the *largest* to the *second largest* eigenvalue of the Covariance matrices for sliding windows of equal sizes. This, we believe, a measure of the degree of agreement (or coherence) in agent views of the market.

The remainder of this paper is organized as follows: The method of estimating the Covariance matrices is described briefly below (Section 2), with data and results presented in Section 3. Our brief discussion and conclusions form the final section.

## Covariance matrix estimation.

The Variance-Covariance matrix can be computed easily, using the following formula, (full details see Litterman and Winkelmann (1998)):

$$\sigma_{ij}^{T}(M) = (\sum_{s=0}^{T} \omega_{T-s} r_{i,T-s} r_{j,T-s}) / (\sum_{s=0}^{T} \omega_{T-s}) \quad (1)$$

Where $r_{(i,T)}$ is the return on the $i^{th}$ market at date T and $\omega_T$ is the weight applied at date T over horizon M. In our study, we use weekly returns of stock market indices (i=13 indices and T=20 for emerging and i=14 indices and T=20 for major markets for our data) and each week, previous to the current, receives 90% of the weight of the following week (where $\omega_T$=1) as suggested in e.g. Litterman and Winkelmann.

## Data and Results.

The data used in the following analysis consists of the weekly prices of a set of thirteen **emerging** market indices and a set of fourteen **mature** market indices during the period from the second week of January 1997 to the third week of March 2003. As each market uses its local currency for presenting the index values, we use the weekly *returns* instead of the weekly prices, where the following formula applies: **Weekly Return = Ln($P_t/P_{t-1}$),** where $P_t$ and $P_{t-1}$ are the closing prices of the index at week t and t-1 respectively. The Variance-Covariance matrices for overlapping windows of size 20 weeks have been calculated using Equation (1).

### Empirical results.

Figures 1 and 2, for the emerging and mature markets respectively, show the distribution of the eigenvalues of the Covariance matrices for overlapping windows of size 20, before and after the Asian Crisis in July 1997, the Global

Crisis in October 1998, the Dot-Com Crash in March 2000 and the September the 11th Crash in 2001.

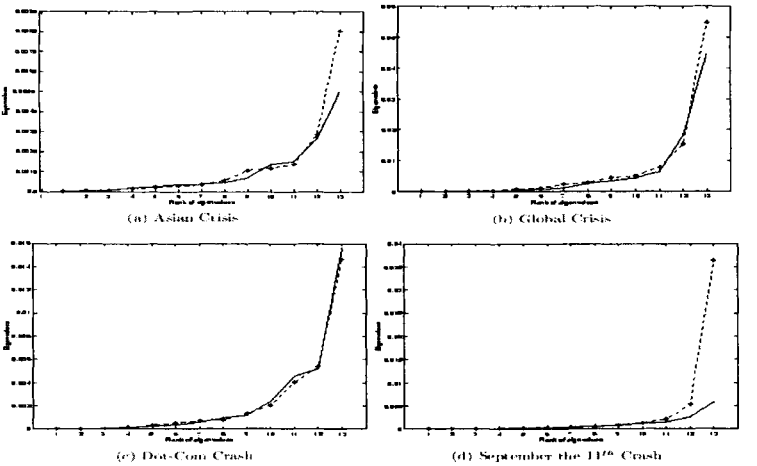

**Fig. 1.** The distribution of the eigenvalues of the covariance matrices before **(Solid line)** and after **(Dashed line)** the crash for Emerging markets[1].

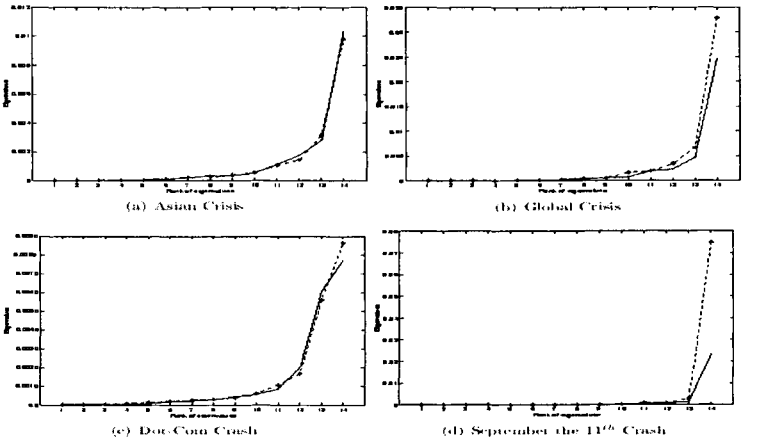

**Fig. 2.** The distribution of the eigenvalues of the covariance matrices before **(Solid line)** and after **(Dashed line)** the crash for Mature markets[1].

[1] In figures 1 and 2, the **Eigenvalues** are given on the **y-axis** while their **Ranks** are given on the **x-axis**.

Figures 1(a) and 2(a) show that the value of the maximum eigenvalue ($\lambda_1$) increased, for emerging markets, after the Asian Crisis, which began in July 1997 in Thailand, but did not change markedly for developed markets. This implies that the crisis mainly affected emerging markets but not the mature ones. However, Figures 1(c) and 2(c) show that the Dot-Com Crash influenced major markets but not emerging ones and took longer than a week to show a strong effect.

From Figures 1(b) and 2(b), we can see that the Global Crisis in 1998 affected emerging and mature markets comparably in the same week.

Figures 1(d) and 2(d) show that the value of $\lambda_1$ after the September 11$^{th}$ crash, which could not have been predicted by most people, hugely increased for **both** emerging and mature markets. This implies that stock markets around the world were hit very hard and that the markets moved in *coordination* to make a recovery after falling so sharply or being oversold.

The ratio of the *Largest* ($\lambda_1$) to the *Second Largest* ($\lambda_2$) eigenvalues of the Covariance matrices for emerging and mature markets are shown in Figures 3(a) and 3(b) respectively. These show a *qualitative difference* in the way emerging and mature markets deal with crises, (especially unexpected ones). For major markets, there are three highly significant points in the distribution of this ratio representing the third week of October 1999 (the 12$^{th}$ anniversary of the October 19 stock market crash)}, the second week of September 2001 *(9/11 crash)* and the third week of March 2004 *(Madrid Bomb)* respectively. However, for emerging markets, there is only one highly significant point representing the second week of September 2001 *(9/11 crash)*.

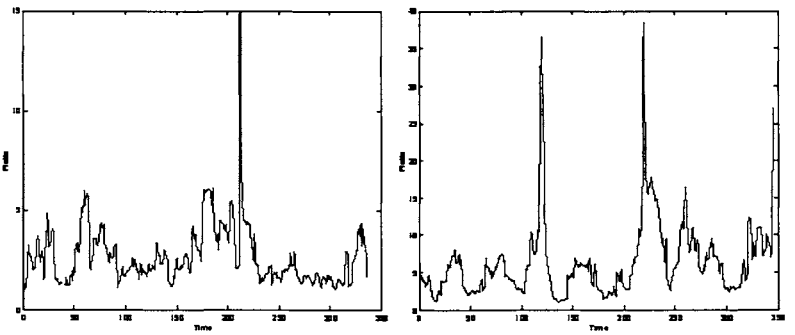

(a) Emerging Markets (b) Major Markets

**Fig. 3.** The distribution of ratio of *Dominant* ($\lambda_1$) to *Subdominant* ($\lambda_2$) eigenvalues of covariance matrices for equal overlapping time windows

The results also show that the mature markets move together immediately after the crash to bounce back faster than emerging markets. In other words, the recovery time from crisis for developed markets is shorter than that for developing ones.

## Conclusion.

Our aims were to study the distribution of the eigenvalues of covariance matrices for emerging and mature markets at crisis points (namely, the Asian Crisis, Global Crisis, Dot-Com Crash and September the $11^{th}$ Crash). In particular, we wished to distill the information from the ratio of the Largest to the Second Largest eigenvalues of these covariance matrices. Our findings can be summarized as follows: **(i)** The Asian Crisis in 1997 disproportionately affected the emerging markets compared to the major ones while the Dot-Com Crash influenced major markets but affected emerging ones far less. **(ii)** The Global Crisis in 1998 affected developing markets as much as developed ones in the same week. **(iii)** The September $11^{th}$ Crash hit both emerging and mature markets very hard because it was totally unpredictable. **(iv)** The distribution of the ratio of $\lambda_1$ to $\lambda_2$ appears to show that emerging and mature markets deal with crashes differently especially unexpected ones. This means that mature markets move together immediately after the crash to bounce back faster than emerging markets. In other words, the recovery time from crisis for emerging markets is longer than that for mature ones.

## REFERENCES.


Keogh G, Sharifi S, Ruskin H, Crane M, (2003) Epochs in Market Sector Index Data - Empirical or Optimistic?. Proceedings of the 2nd Nikkei Econophysics Symposium - Application of Econophysics, Takayasu, H. (Eds), Lecture Notes in Computer Science, Springer, November, 2003, pp 83-89, ISBN 4-431-14028-X

Kwapien J, Drozdz S, Speth J (2002) Alternation of Different Scaling Regimes in the Stock Market Fluctuation, (Available from
www.fz-juelich.de/ikp/ publications/AR2002/CHAP4/409.pdf}, [Accessed 11 May 2004].

Kwapien J, Drozdz S, Speth J (2004) Time Scale involved in Emergent Market Coherence. Physica A, Vol 337, pp 231-242.

Litterman R, Winkelmann K (1998) Estimating Covariance Matrices: in Goldman-Sachs Risk Management Series, Krieger R, (Eds), Goldman, Sachs & Co.

Meric I, Meric G. (1997) Co-movements of European Equity Markets before and after the 1987 crash, Multinational Finance Journal, Vol 1(2), pp 137-152.

# Scaling and Memory in Return Loss Intervals: Application to Risk Estimation

Kazuko Yamasaki[1,2], Lev Muchnik[3], Shlomo Havlin[3], Armin Bunde[4], and H. Eugene Stanley[1]

[1] Center for Polymer Studies and Department of Physics
Boston University, Boston MA, 02215 USA
[2] Tokyo University of Information Sciences, Chiba, Japan
yamasaki@rsch.tuis.ac.jp
[3] Minerva Center and Department of Physics, Bar-Ilan University, Ramat-Gan, Israel
[4] Institut für Theoretische Physik III, Justus-Liebig-Universität, Giessen, Germany

**Summary.** We study the statistics of the return intervals $\tau_q$ between two consecutive return losses below a threshold $-q$, in various stocks, currencies and commodities. We find the probability distribution function (pdf) of $\tau_q$ scales with the mean return interval $\bar{\tau}_q$ in a quite universal way, which may enable us to extrapolate rare events from the behavior of more frequent events with better statistics. The functional form of the pdf shows deviation from a simple exponential behavior, suggesting memory effects in losses. The memory shows up strongly in the conditional mean loss return intervals which depend significantly on the previous interval. This dependence can be used to improve the estimate of the risk level.

**Key words:** return loss intervals, scaling, universality, value-at-risk

## 1 INTRODUCTION

A common indicator of risk in the financial world [1, 2] is the value-at-risk (VAR) indicator, which is defined by the risk at a level of loss $\Lambda$

$$\int_{-\infty}^{-\Lambda} p_\Delta(r)dr = p^* \tag{1}$$

where $p^*$ is the probability of loss and $p_\Delta(r)$ is the probability density of return $r(t) = \log[p(t)/p(t-\Delta)]$, which depends on the time interval $\Delta$. Here we propose a simple method which enables us to improve the estimate of

VAR using historical information. We study the statistics of the return intervals $\tau \equiv \tau_q$ between two consecutive losses below a threshold $-q$, in various stocks, currencies and commodities (for illustration, see Fig. 1). We find scaling and memory effects—similar to those found in stock and currency market volatilities [3] and in climate fluctuations [4]—that can be used to improve

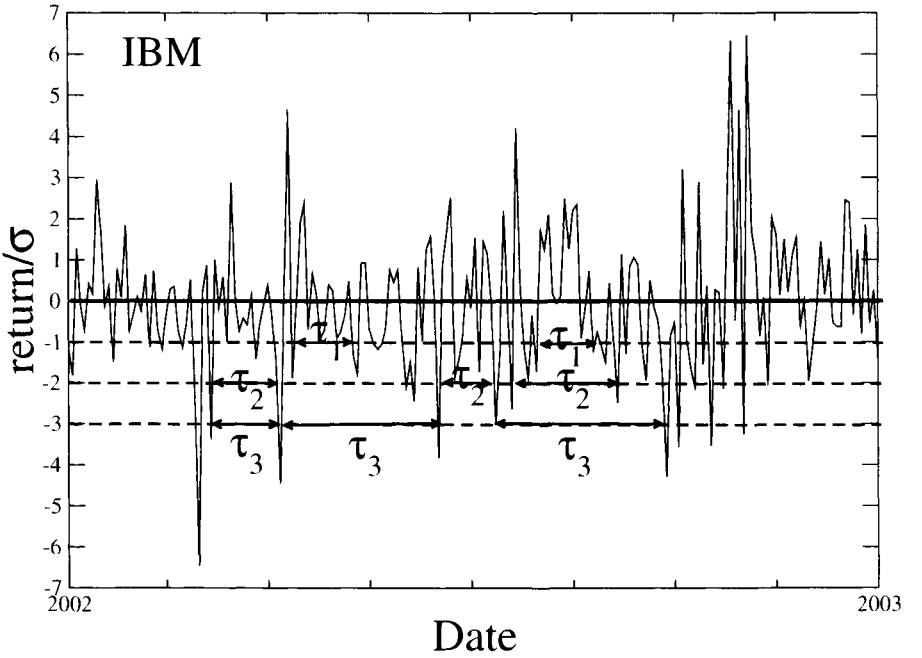


**Fig. 1.** Schematic illustration of the loss intervals $\tau_q(l)$, for three threshold values $q = -1$, $-2$ and $-3$ for the return losses of IBM stock prices. The return is normalized by its standard deviation $\sigma$.

## 2 SCALING

We study the pdf of the return loss intervals, $P_q(\tau)$, of three daily stocks in NYSE, three daily currencies and three daily commodities. Our results in Fig. 2 suggest that $P_q(\tau)$ is not a function of two independent variables $\tau$ and $q$, but depends only on the scaled parameter $\tau/\bar{\tau}_q$,

$$P_q(\tau) = \frac{1}{\bar{\tau}_q} f\left(\frac{\tau}{\bar{\tau}_q}\right), \tag{2}$$

where the $q$-dependence is contained in the mean return loss interval

$$\bar{\tau}_q \equiv \frac{1}{N_q} \sum_{i=1}^{N_q} \tau_q(i), \tag{3}$$

and $N_q$ is the total number of return loss intervals for a given $q$. Similar scaling has been also found in earthquakes[5, 6, 7] and in the volatility of stocks and currencies [3] as well as in various phenomena, such as climate fluctuations, that exhibit long term memory [4].

Figure 2 shows both scaled and unscaled $P_q(\tau)$ of IBM's stock returns (11700 days). Curves of the data for different $q$ values collapse to a single curve, consistent with the scaling relation, Eq. (2).

Figure 3 shows the scaled pdf $P_q(\tau)\bar{\tau}_q$ of stocks, currencies and commodities as functions of the scaled return loss intervals $\tau/\bar{\tau}_q$. Note that the scaling function $f(x)$ in Eq. (2) does not depend explicitly on $q$, a result that is supported by this figure. This result may be useful if $P_q(\tau)$ is known for one value of $q$, one can estimate it for other $q$—in particular for very large $q$ (rare events), which are difficult to study due to lack of statistics.

## 3 UNIVERSALITY

Our results in Fig. 3 also indicate that the scaled pdf $P_q(\tau)\bar{\tau}_q$ is very similar for different stocks, currencies, and commodities, suggesting universality of $f(x)$ for the economic fluctuations. The universality is more easily seen when we include stocks, currencies, and commodities in the same plot. It is more flat for smaller values of $\tau/\bar{\tau}_q$ and faster for large values of $\tau/\bar{\tau}_q$. Figure 4 shows the scaled pdf $P_q(\tau)\bar{\tau}_q$ of three stocks, three currencies, and three commodities with $q = 1.0$ and 2.0. We can see nine curves of scaled data for each $q$ that collapse to an approximated single curve. Note the similarity of these results to the analogous results for the volatility [3].

The scaled function $f(x)$ includes more information than just the return intervals distribution, since shuffled data with the same return distribution has an $f(x)$ function that differs from that of the unshuffled return data. As seen in Fig. 3, curves of the data from different stocks, currencies and commodities respectively collapse to a single function form, while after shuffling the original return records the function is modified. The function is more flat for small values of $\tau/\bar{\tau}_q$ and falls more rapidly for large values of $\tau/\bar{\tau}_q$ compared to the unshuffled graph.

## 4 ESTIMATION OF VAR

It is easy to see that $\bar{\tau}_q$ and VAR are related by

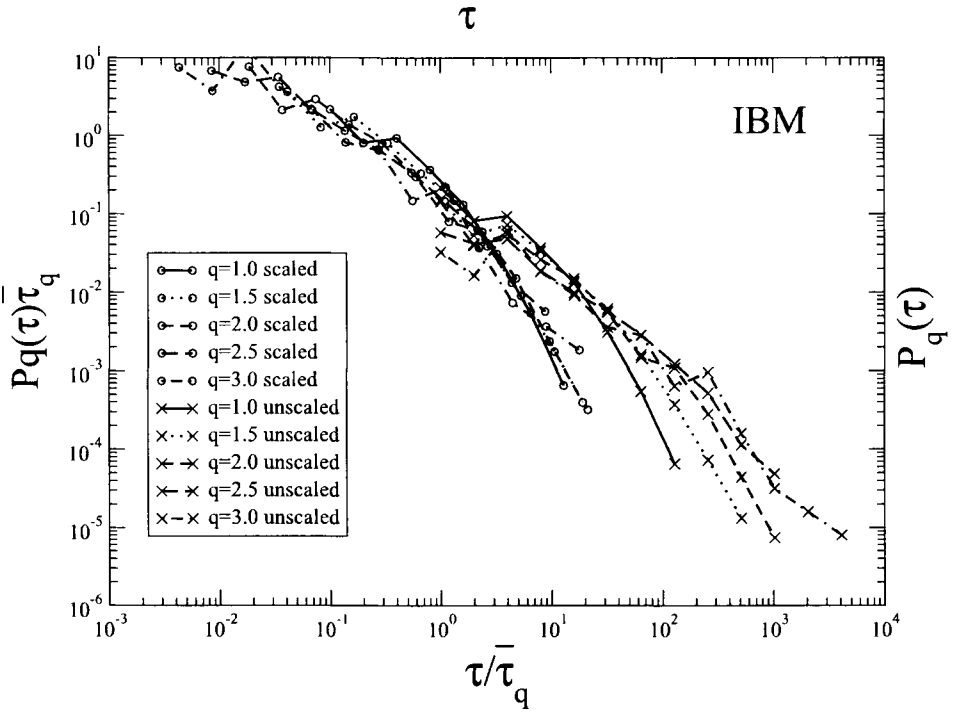


**Fig. 2.** Scaled and unscaled $P_q(\tau)$ of IBM's stock returns are shown. While systematic derivation occur for $P_q(\tau)$, the curves collapse to a single curve when plotted in the scaled form $P_q(\tau)\bar{\tau}_q$ vs. $\tau/\bar{\tau}_q$.

$$\frac{1}{\bar{\tau}_q} = \int_{-\infty}^{-q} p_\Delta(r)dr = \frac{\text{number of days with } r < -q}{\text{total number of days}} \tag{4}$$

where $\bar{\tau}_q$ is defined in (3),

$$\sum_{i=1}^{N_q} \tau_q(i) \approx \text{total number of days}, \tag{5}$$

and

$$N_q + 1 = \text{number of days with } r < -q. \tag{6}$$

Thus $\bar{\tau}_q^{-1}$ represents the probability of loss for a risk level of loss $-q$.

As discussed above, $P_q(\tau)$ includes more information than $p_\Delta(r)$ and therefore more than the VAR. In the following we suggest the use of this information

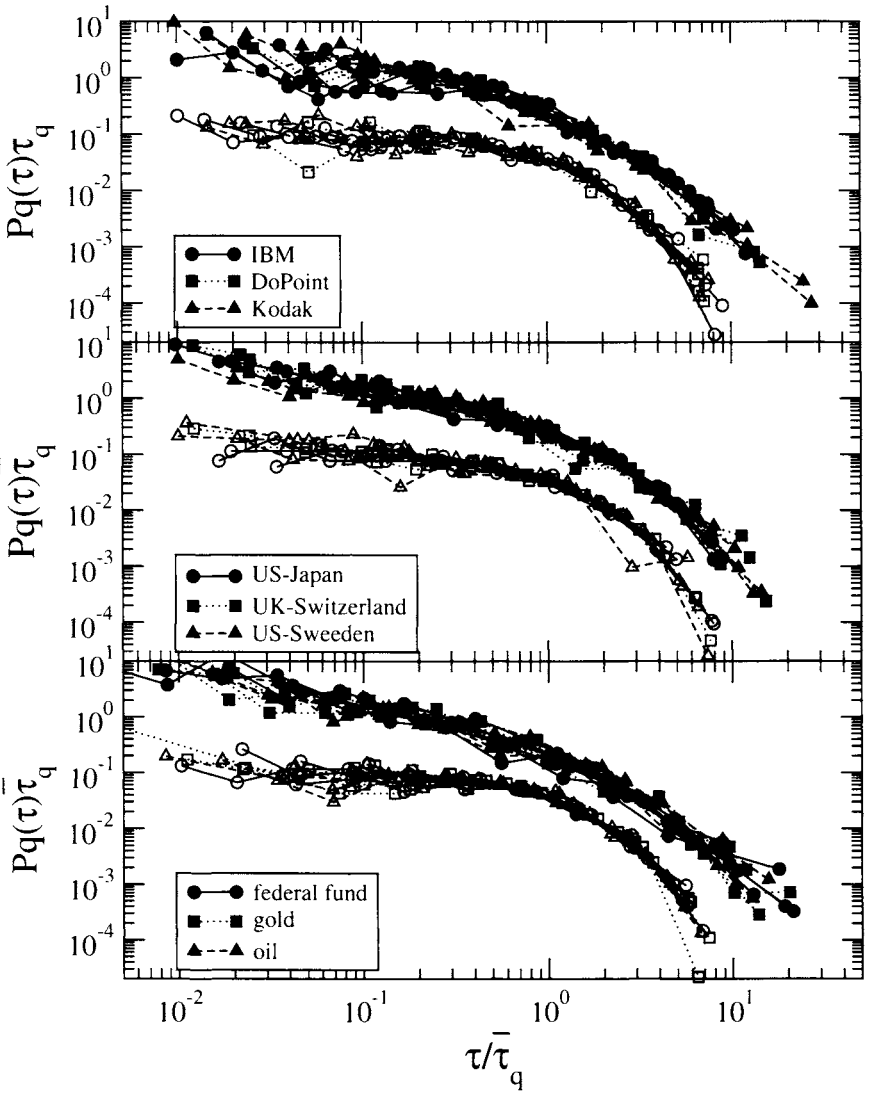


**Fig. 3.** The scaled pdf $P_q(\tau)\bar{\tau}_q$ of three stocks as functions of the scaled return loss intervals $\tau/\bar{\tau}_q$ with $q = -1.0$, $-1.5$, $-2.0$, $-2.5$, and $-3.0$ are shown. Curves of the data from different $q$ collapse to a single curve. Note that curves of the data from different stocks also collapse to a single curve. The lower plots represent the scaled $P_q(\tau)\bar{\tau}$ vs. $\tau/\bar{\tau}$ after shuffling the return records, thereby removing the correlations. The lower plots were divided by a factor of 10, i.e., $P_q(\tau)\bar{\tau}/10$.

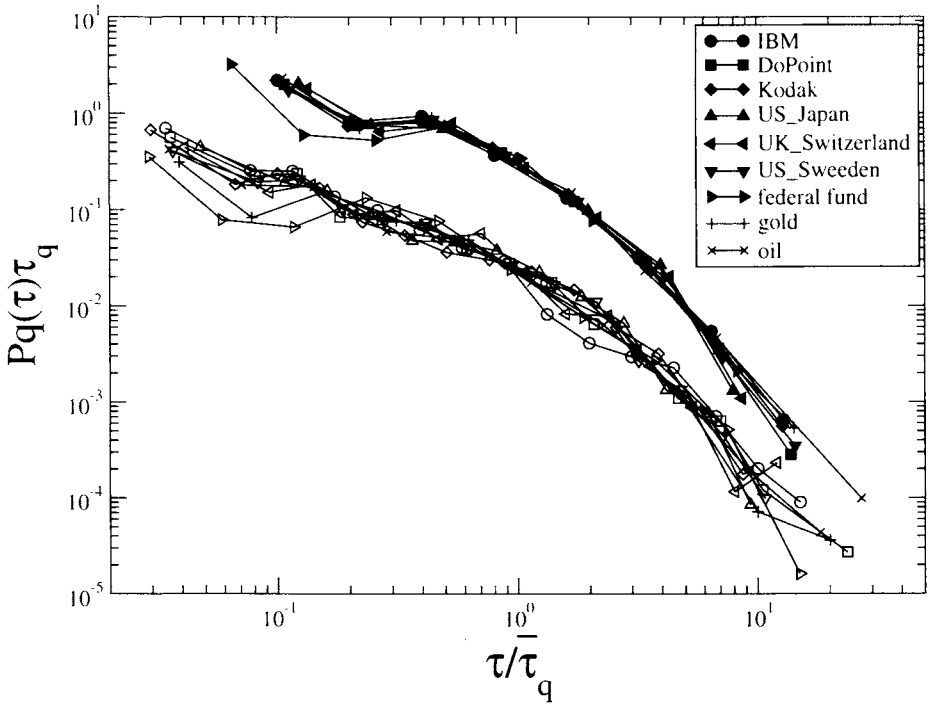


**Fig. 4.** Scaled pdf, $P_q(\tau)\bar{\tau}_q$, of 3 stocks, 3 currencies and 3 commodities with $q = -1.0$ (upper plots) and $q = -1.7$ (lower plots). The lower plots were divided by a factor of 10, i.e., $P_q(\tau)\bar{\tau}/10$. We can see nine curves clearly collapse to a curve in each q value.

to improve the estimation of the risk level of loss $-q$. First we estimate the conditional mean return loss interval $\bar{\tau}_q(\tau_0)$ which depend on the previous return interval $\tau_0$. We also expect that

$$\frac{1}{\bar{\tau}_q(\tau_0)} = \int_{-\infty}^{-q} p_\Delta(r|\tau_0)dr. \tag{7}$$

Here $p_\Delta(r|\tau_0)$ is the probability that a return $r$ will follow a return interval $\tau_0$. Figure 5 shows the conditional mean of interval $\bar{\tau}_q(\tau_0)$ of IBM. It can be approximated by

$$\log\left(\frac{\bar{\tau}_q(\tau_0)}{\bar{\tau}_q}\right) = 0.25\log\left(\frac{\tau_0}{\bar{\tau}_q}\right). \tag{8}$$

From the inset of Fig. 5, $\bar{\tau}_q^{-1}$ can be estimated by

$$\frac{1}{\bar{\tau}_q} = 0.21 q^{-3.3} \quad q \geq 1.5 \tag{9}$$

Equations (8) and (9) enable us to estimate $\bar{\tau}_q(\tau_0)$ for large values of $q$. Figure 6 shows $\bar{\tau}_q(\tau_0)$, which is the inverse of a certain probability of loss $p^*$. Thus, if we want to know the risk level corresponding to 1% probability of loss within the time interval of $\Delta$ = one day, we only look at intersections between the horizontal line of $\bar{\tau}_q(\tau_0) = 100$ and lines with fixed $q$ in Fig. 6. The condition $\tau_0$ which is the previous intervals of losses below $-q$, is changing every day. So the risk level is changing every day and can be estimated in this way. Thus our method provides a simple practical tool for estimation of risk.

## 5 CONCLUSION

We study the statistics of the return loss intervals $\tau_q$ between two consecutive losses below a threshold $-q$, in various stocks, currencies and commodities. We find that the pdf of the return loss intervals, $P_q(\tau)$, is not a function of the two independent variables $\tau$ and $q$, but depends only on the scaled parameter $\tau/\bar{\tau}_q$. This scaling allows us to extrapolate rare events from the behavior of frequent events, with therefore good statistics.

A universal feature of the scaled pdf, $P_q(\tau)\bar{\tau}_q$, is that shapes are almost the same for different stocks, currencies, and commodities. We show a relation between $\bar{\tau}_q$ and VAR and use it to estimate the conditional mean return loss interval, $\bar{\tau}_q(\tau_0)$, which enables us to improve the risk estimate of loss $-q$.

## References


1. Bouchaud, J.-P. & Potters, M. (2003) Theory of Financial Risks, Cambridge University Press, Cambridge.
2. Mantegna, R., & Stanley, H.E. (1999) An Introduction to Econophysics, Cambridge University Press, Cambridge.
3. Yamasaki, K., Muchnik, L., Havlin, S., Bunde, A. & Stanley, H.E. (2005) Scaling and Memory in Volatility Return Intervals in Financial Market, PNAS 102:9424 9428.
4. Bunde, A., Eichner, J. F., Kantelhardt, W. & Havlin, S. (2005) Long-Term Memory: A Natural Mechanism for the Clustering of Extreme Events and Anomalous Residual Times in Climate Records, Phys. Rev. Lett. vol.99 048201.

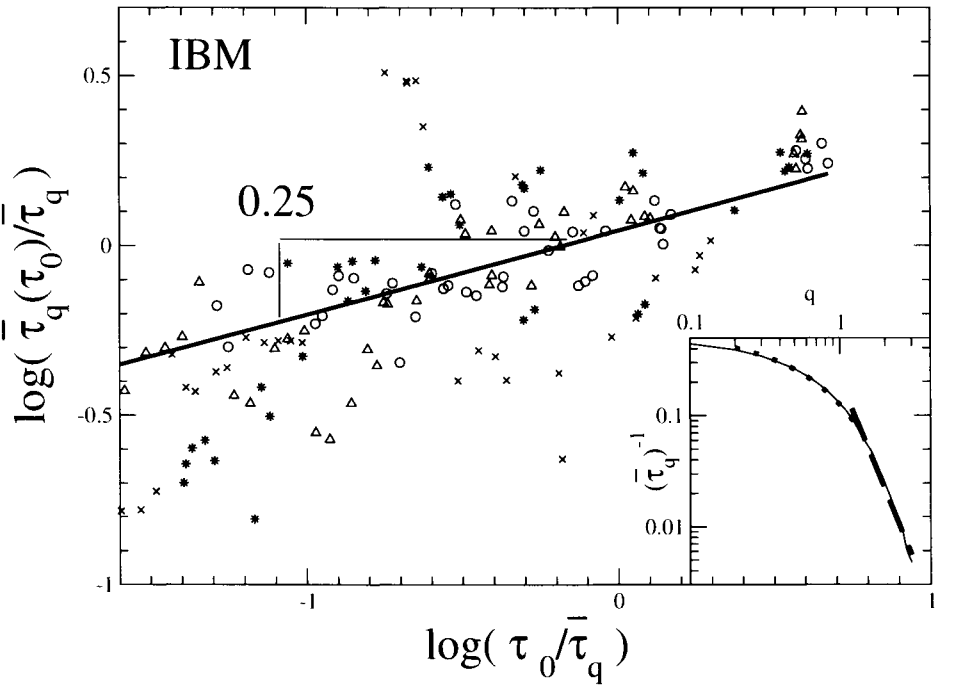


**Fig. 5.** The conditional mean of interval $\bar{\tau}_q(\tau_0)$ is shown for IBM. The condition $\tau_0$ is the previous return interval. ○ shows $q = 1.0 \sim 1.4$ , △ $q = 1.5 \sim 1.9$, $*$ $q = 2.0 \sim 2.4$, × $q = 2.5 \sim 2.9$. The mean seems to depend on $\tau_0/\bar{\tau}_q$ by a certain power, Eq. (8). The inset shows the estimation of $\bar{\tau}_q^{-1}$, Eq. (9).


5. Lillo, F. & Mantegna, R. N. (2003) Power-law relaxation in a complex system: Omori law after a financial market crash, Phys. Rev. E 68:016119.
6. Corral, A. (2004) Long-Term Clustering, Scaling, and Universality in the Temporal Occurrence of Earthquakes, Phys. Rev. Lett. 92:108501.
7. Livina, V., Tuzov, S., Havlin, S. & Bunde,A. (2005) Recurrence intervals between earthquakes strongly depend on history, Physica A 348:591 595.
8. Black, F. & Scholes, M. (1973) Tne pricing of options and corporate liabilities, J. Political Economy 81:637 654.
9. Lux, T. & Ausloos, M. (2002) Market Fluctuations 1: Scaling, Multiscaling, and Their possible Origins, The Science of Disasters: Climate Disruptions, Heart Attacks, and Market Crashes, edited by A. Bunde, J. Kropp, and H. J. Schellnhuber , Springer-Verlag,Berlin, pp373 409.

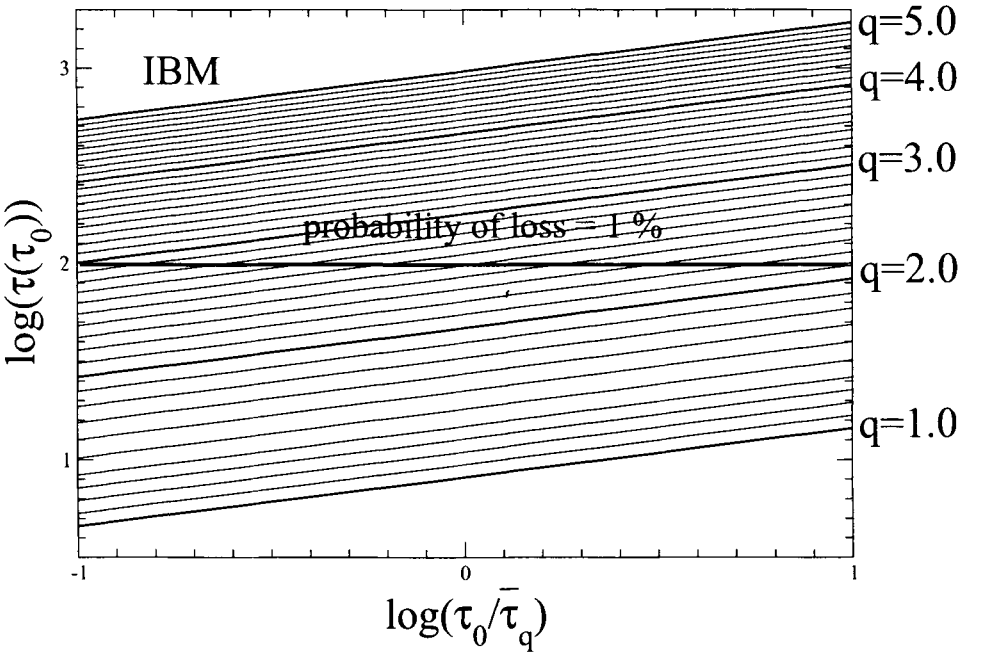


**Fig. 6.** The estimation of conditional mean $\bar{\tau}(\tau_0)$ using Eqs. (8) and (9). Equation (3) suggests that $\bar{\tau}_q(\tau_0)$ is the inverse of a certain probability of loss $p^*$. To estimate the risk level corresponding to 1% probability of loss within the time interval of $\Delta$, one must look at the intersections between the horizontal line of $\bar{\tau}_q(\tau_0) = 100$ and lines with fixed $q$. The condition $\tau_0$, which represent the previous intervals of losses below $-q$, changes with time. Thus the risk level changes and can be estimated from such a figure.

# Recurrence analysis near the NASDAQ crash of April 2000

Annalisa Fabretti[1] and Marcel Ausloos[2]

[1] Department of Mathematics for Economy, Insurances and Finance Applications, University of Roma 1, La Sapienza I-00100 Rome, Italy
annalisa.fabretti@uniroma1.it
[2] SUPRATECS, B5, University of Liège, B-4000 Liège, Euroland
marcel.ausloos@ulg.ac.be

**Summary.** Recurrence Plot (RP) and Recurrence Quantification Analysis (RQA) are signal numerical analysis methodologies able to work with non linear dynamical systems and non stationarity. Moreover they well evidence changes in the states of a dynamical system. It is shown that RP and RQA detect the critical regime in financial indices (in analogy with phase transitions) before a bubble bursts, whence allowing to estimate the bubble initial time. The analysis is made on NASDAQ daily closing price between Jan. 1998 and Nov. 2003. The NASDAQ bubble initial time has been estimated to be on Oct. 19, 1999.

**Key words:** Endogenous crash, Financial bubble, Recurrence Plot, Recurrence Quantification Analysis, Nonlinear Time Series Analysis, NASDAQ

## 1 Introduction

Recent papers have shown some analogy between crashes and phase transitions [1, 2, 3]; like in earthquakes, log periodic oscillations have been found before some crashes [4, 5]. It was proposed that an economic index $y(t)$ increases as a complex power law, whose first order Fourier representation is

$$y(t) = A + B\ln(t_c - t)\{1 + C\cos[\omega \ln(t_c - t) + \phi]\} \quad (1)$$

where $A$, $B$, $C$ , $\omega$, $\phi$ are constants and $t_c$ is the critical time (rupture time).

An endogenous crash is preceded by an unstable phase where any information is amplified; this critical period takes the name of 'speculative bubble'.

Recurrence Plots are graphical tools elaborated by Eckmann, Kamphorst and Ruelle in 1987 and are based on Phase Space Reconstruction [6]. In 1992, Zbilut and Webber [7] proposed a statistical quantification of RPs and gave it the name of 'Recurrence Quantification Analysis' (RQA). RP and RQA are

good in working with non stationarity and noisy data, in detecting changes in data behavior, in particular in detecting breaks, like a phase transition [8], and in informing about other dynamic properties of a time series [6]. Most of the applications of RP and RQA are at this time in the field of physiology and biology, but some authors have already applied these techniques to financial data [9, 10]. We have used RP and RQA techniques for detecting critical regimes preceding an endogenous crash seen as a phase transition and whence estimating the initial bubble time.

After simulating an arbitrary log periodic signal for preliminary RP analysis, a similar one is made on the NASDAQ, taken over a time span of 6 years including the known crash of April 2000 [5]. The series is also divided into subseries in order to investigate local changes in the evolution of the signal. Then the RPs of all time series are observed, compared and discussed. This work is extracted from [12].

## 2 Recurrence Analysis

The changing state of a dynamic system can be indeed represented by sequences of 'state vectors' in the phase space. Each unknown point of the phase space at time $i$ is reconstructed by the delayed vector $y(i) = X_i, X_{i+d}, ..., X_{i+(m-1)d}$ in an $m$-dimensional space.

*Recurrence Plot*

The Recurrence Plot (RP) is a matrix of points $(i, j)$ where each point is said to be recurrent and marked with a dot if the distance between the delayed vectors $y(i)$ and $y(j)$ is less than a given threshold $\epsilon$. As each coordinate $i$ represents a point in time, RP provides information about the temporal correlation of phase space points [6].

Therefore RPs can be used to test a system deterministic behavior through the percentage of recurrent points belonging to parallel lines. In fact for a periodic or a deterministic signal patterns like parallel lines appear. In so doing, RPs are useful tools for the preprocessing of experimental time series and provide a comprehensive image of the dynamic course at a glance [8].

*Recurrence Quantification Analysis*

RQA quantifies the presence of patterns, like parallel lines of RPs, with 5 RQA variables: the percentage of recurrent points (%REC); the percentage of recurrent points forming line segments parallel to the main diagonal (%DET); the longest line segment measured parallel to the main diagonal (MAXLINE); the slope of line-of-best-fit through %REC as a function of the displacement from the main diagonal (excluding the last 10% range) (TREND); the Shannon entropy of the distribution of the length of line segments parallel to the main diagonal (ENT).

## 3 Analysis and Conclusions

In order to study the crash from the point of view of a phase transition with log periodic precursors, a log periodic signal, generated by equation (1), has been simulated; its RP is shown in Fig. 1(lhs). The 'arrow' shape is due to the trend, the not smooth border ('color') lines are due to the log periodicity. It has been also considered as a phase transition signature. In Fig. 2(lhs) an arbitrary signal is plotted before and after a peak, taking into account the anti-bubble phenomenon after a crash [11]. The RP aspect of Fig. 2(rhs) reveals a feature far from the normal signal evolution; note the well marked black bands corresponding to the crash time.

The whole NASDAQ time series data has been divided into subseries of 200 days, overlapping each other by almost 5 months, in order to further analyze whether and how the data changes.

Fig. 3(rhs) is the RP of NASDAQ between Jan. 05, 1998 and Nov. 21, 2003. Of interest is the dark grey vertical band surrounded by a lighter grey area, delimited by horizontal coordinates $x = 452$ and $x = 690$ corresponding to Oct. 19, 1999 and Sept. 27, 2000. In the period during which the bubble grows, RQA variables take the highest absolute values [12].

It is worth to note the same RP shape for the phase transition signature in Fig. 2(rhs). Considering that each coordinate in RP is linked with the time series, the border line of a grey or black band reveals the time when the data behavior starts to change. Noting that the dates here above fall in the same time interval as the bubble and the subsequent crash, it can be supposed that the initial bubble time occurs at $x = 452$ (Oct. 19,1999). We can thus deduce that on such a day the evolution of the system changes, i.e. the evolution passes from a normal regime to a critical regime. This is an a posteriori estimation of the initial bubble time, but through the analysis of the subseries one can argue that one is able to recognize the beginning of the bubble with some delay before the bubble grows. In fact, while the RPs of the first (I), the second (II) and of the third (III) subseries do not present any remarkable pattern [12] (they are quite homogeneous except for some local maximum reached by the index) the fourth subseries presents an interesting pattern: the RP in Figure 1(rhs) shows the characteristic shape typical of a strong trend in a speculative bubble as studied and pointed out in Fig. 1(lhs). The trend starts to be significant in the middle of Oct. 1999. This indicates that the RP has changed indeed when the bubble has started. Even the RQA variables, in Table 1, evidence in this period their highest values. It has to be underlined that this IV period does not include the crash time, but stops in Dec. 1999 before the bubble bursts. Even in the fifth (V) subseries RP, the bubble beginning is not so evident as in the fourth subseries.

In conclusion it has been shown that, with some delay as respect to the beginning but enough time before the crash (3 months in this particular case), a crash warning could be given, RP and RQA techniques do detect a difference in state and recognize the critical regime.

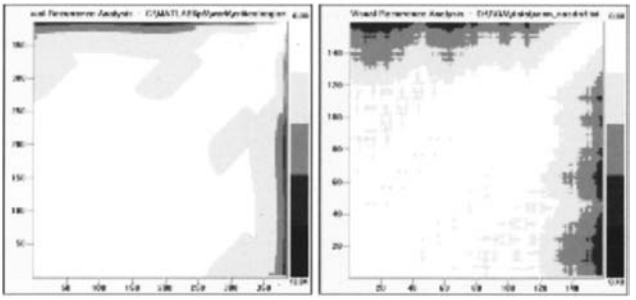

**Fig. 1.** (lhs) RP of a log periodic signal as generated by equation (1). The arrow shape on the lhs plot is the sign of a strong trend; the curve lines are due to the log periodicity. (rhs) RP of the NASDAQ subseries (IV) from Jan., 1999 to Dec., 1999. It is worth to note the similarity between these two RPs

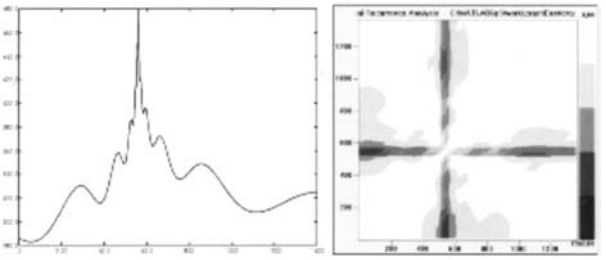

**Fig. 2.** (rhs) the RP of a simulated phase transition of a signal (lhs) following the law (1) before and after the critical event.

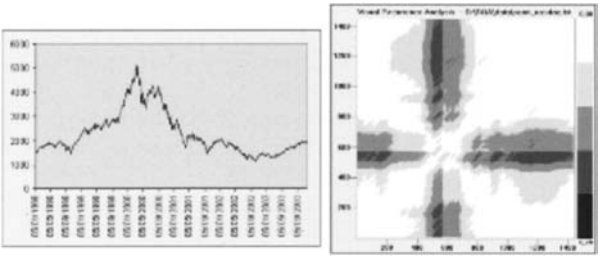

**Fig. 3.** (lhs)daily closing price of NASDAQ from Jan. 05, 1998 to Nov. 21, 2003; (rhs) RP of NASDAQ from Jan. 05, 1998 to Nov. 21, 2003. The dark grey band delimited by horizontal coordinates $x = 504$ and $x = 566$, encircled by a grey area delimited by horizontal coordinates $x = 452$ and $x = 690$, is the 'image' of the crash of April 2000. It is a 'strong event' but afterwards the normal regime is restored

**Table 1.** RQA variables for the 5 NASDAQ subseries, each of 200 days long.

| Subseries | I | II | III | IV | V |
|---|---|---|---|---|---|
| periods | Jan.1998 | June 1998 | Oct.1998 | Feb.1999 | July 1999 |
| | Oct.1998 | Feb.1999 | July1999 | Dec.1999 | May2000 |
| %REC | 6.075 | 9.141 | 5.513 | 17.146 | 9.246 |
| %DET | 35.980 | 36.119 | 29.079 | 45.018 | 54.511 |
| MAXLINE | 125 | 158 | 83 | 179 | 166 |
| ENT | 2.522 | 3.547 | 2.585 | 4.054 | 3.301 |
| TREND(units/1000points) | -105.125 | -155.824 | -97.808 | -273.775 | -138.501 |

## References


1. Sornette D, Johansen A, Bouchaud JP (1996) Stock Market Crashes, Precursors and Replicas. J Phys I France 6 :167–175
2. Feigenbaum JA, Freund PGO (1996) Discrete scale invariance in Stock Market before crashes. Int J Mod Phys B 10:3737–3745
3. Vandewalle N, Boveroux Ph, Minguet A, Ausloos M (1998) The crash of October 1987 seen as a phase transition. Physica A 255:201–210
4. Vandewalle N, Ausloos M, Boveroux Ph, Minguet A (1998) How the financial crash of October 1997 could have been predicted. Eur Phys J B 4:139–141
5. Johansen A, Sornette D (2000) The Nasdaq crash of April 2000: yet another example of log-periodicity in a speculative bubble ending in a crash. Eur Phys J B 17:319–328
6. Eckmann JP, Kamphorst SO, Ruelle D (1987) Recurrence Plot of dynamical system. Europhys Lett 4:973–977
7. Zbilut JP, Webber CL (1992) Embedding and delays as derived from quantification of Recurrence Plot. Phys Lett A 171:199–203
8. Lambertz M, Vandenhouten R, Grebe R, Langhorst P (2000) Phase transition in the common brainstem and related systems investigated by nonstationary time series analysis. Journal of the Autonomic Nervous System 78:141–157
9. Antoniou A, Vorlow CE (2000) Recurrence Plot and financial time series analysis. Neural Network World 10:131–145
10. Holyst JA, Zebrowska M (2000) Recurrence Plots and Hurst exponent for financial market and foreign exchange data. Int J Theoretical and Applied Finance 3:419
11. Johansen A, Sornette D (1999) Financial 'Anti-Bubbles': Log Periodicity in Gold and Nikkei collapses. Int J Mod Phys C 10:563–575
12. Fabretti A, Ausloos M (2005) Recurrence Plot and Recurrence Quantification Analysis techniques for detecting a critical regime. Examples from financial market indices. Int J Mod Phys C (to be printed)

# Modeling a foreign exchange rate using moving average of Yen-Dollar market data

Takayuki Mizuno[1], Misako Takayasu[1], Hideki Takayasu[2]

[1] Department of Computational Intelligence and Systems Science, Interdisciplinary Graduate School of Science and Engineering, Tokyo Institute of Technology, 4259 Nagatsuta-cho, Midori-ku, Yokohama 226-8502, Japan
[2] Sony Computer Science Laboratories, 3-14-13 Higashi-Gotanda, Shinagawa-ku, Tokyo 141-0022, Japan

**Summary.** We introduce an autoregressive-type model with self-modulation effects for a foreign exchange rate by separating the foreign exchange rate into a moving average rate and an uncorrelated noise. From this model we indicate that traders are mainly using strategies with weighted feedbacks of the past rates in the exchange market. These feedbacks are responsible for a power law distribution and characteristic autocorrelations of rate changes.

**Key words.** Foreign exchange market, Self-modulation effect, Autoregressive (AR) process, Econophysics.

## 1. Introduction

The probability densities of rate changes of foreign exchange markets generally have fat tails compared with the normal distribution and the volatility always shows a long autocorrelation [1]. In order to clarify the mechanism of these nontrivial behaviors, we introduce an auto-regressive type model with self-modulation effects for the exchange rate by using the new technique of separating moving average rates and residual uncorrelated noises [2,3]. We are going to show that these nontrivial behaviors are caused by traders' strategies with weighted feedbacks of the past rates. In this paper we use a set of tick-by-tick data provided by CQG for the yen-dollar exchange rates from 1989 to 2002.

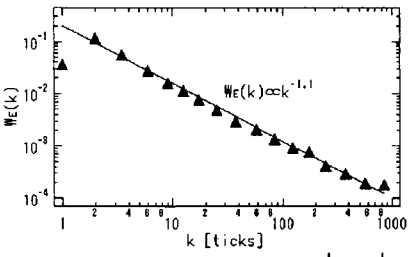


Fig.1 Weight factors $w_\varepsilon(k)$ of the absolute value $|\varepsilon(t)|$ of the yen-dollar rate. The line indicates a power function $w_\varepsilon(k) \propto k^{-1.1}$.

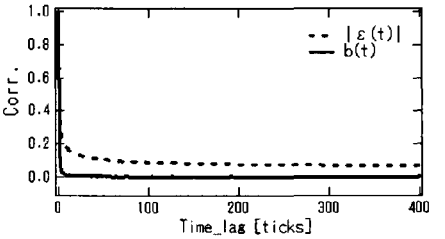


Fig.2 Autocorrelations of the absolute value $|\varepsilon(t)|$ and the factor $b(t)$.

## 2. The best moving average

Traders are generally predicting future exchange rates using various types of moving averages. We first introduce so-called the best moving average rate that separates uncorrelated noises from the market data.

A foreign exchange rate $P(t+1)$ is generally separable into a moving average rate $\overline{P}(t)$ and its residue $\varepsilon(t)$,

$$P(t+1) = \overline{P}(t) + \varepsilon(t), \tag{1}$$

$$\overline{P}(t) = \sum_{k=1}^{K} w_P(k) \cdot P(t-k+1), \tag{2}$$

where $w_p(k)$ gives the weight factors where the time is measured by ticks. By tuning the weight factors we tried to find the best set of weights that makes the autocorrelation of the term $\varepsilon(t)$ almost zero. It is found that such condition is satisfied generally by weights which decay nearly exponentially with a characteristic time about a few minutes.

Although the correlation of $\varepsilon(t)$ is nearly zero, its absolute value shows a long autocorrelation [2]. In order to characterize this stochastic dynamics we also

separate the absolute value $|\varepsilon(t+1)|$ into a moving average $\langle|\varepsilon(t)|\rangle$ and an uncorrelated noise term, $b(t)$. We apply an autoregressive process to $\log|\varepsilon(t+1)|$ as follows,

$$\log|\varepsilon(t+1)| = \log\langle|\varepsilon(t)|\rangle + \log b(t), \tag{3}$$

$$\log\langle|\varepsilon(t)|\rangle = \sum_{k=1}^{K'} w_\varepsilon(k)\cdot\log|\varepsilon(t-k+1)|, \tag{4}$$

where $w_\varepsilon(k)$ is the weight factor which is estimated from the foreign exchange data. The weight factors $w_\varepsilon(k)$ of the yen-dollar rate decay according to power law $w_\varepsilon(k)\propto k^{-1.1}$ with a characteristic time about a few minutes as shown in Fig.1. The autocorrelation of the term $b(t)$ becomes nearly zero as shown in Fig.2. Namely, the fluctuation of the logarithm of absolute value of $\varepsilon(t)$ can be approximated by an autoregressive type stochastic process.

From these results, we find that the characteristic time of the best moving average is generally about a minute, namely, most traders are expected to be watching only very latest market data of order of a few minutes.

## 3. Self modulation process for foreign exchange rate

As a mathematical model of foreign exchange market that is directly compatible with the tick-by-tick data, we now introduce an auto-regressive type model with self-modulation effects as follows,

$$\begin{cases} P(t+1) = \overline{P}(t) + \varepsilon(t) & (5) \\ \varepsilon(t+1) = \alpha(t)\cdot b(t)\cdot\langle|\varepsilon(t)|\rangle + f(t) & (6) \end{cases},$$

where the moving averages $\overline{P}(t)$ and $\langle|\varepsilon(t)|\rangle$ are given by Eqs.(2) and (4), $\alpha(t)$ is chosen randomly from 1 or -1 with probability 0.5. We introduce an additive term $f(t)$ independent of $\langle|\varepsilon(t)|\rangle$ in order to take into account effects such as sudden big news or interventions by the central banks or other uncertain events.

We simulate the rate changes numerically by using Eqs.(5) and (6). In the simulation the noise $b(t)$ is chosen randomly from the observed probability density for "$b$" in Eq.(3). As for the weight function in the moving average in Eq.(5), we apply an exponential function, $w_p(k)=0.43e^{-0.35k}$. The external noise factor $f(t)$ is given by a Gaussian noise with the average value 0 and its standard deviation 0.001.

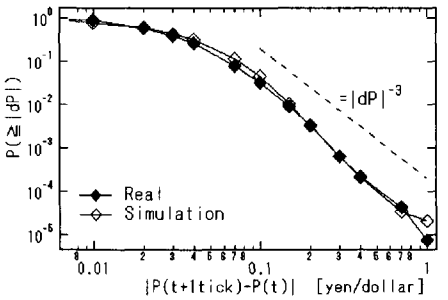

Fig.3 Cumulative distributions of rate changes.

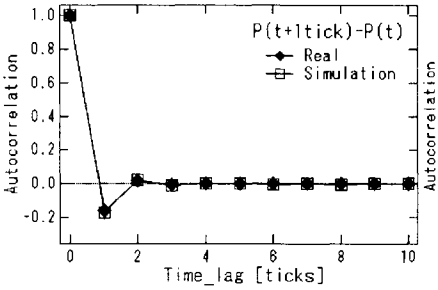

Fig.4 Autocorrelations of rate change.

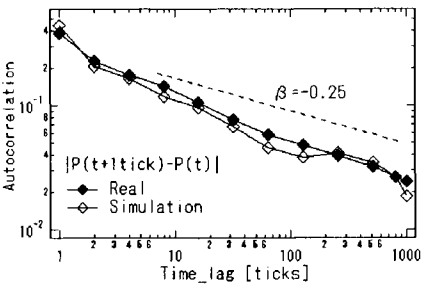

Fig.5 Autocorrelations of volatility.

We compare the simulated rates to the real yen-dollar rates. In Fig.3 the cumulative distribution of rate changes $|P(t+1\text{tick})-P(t)|$ by our simulation is plotted together with the real data. The two graphs fit quite nicely both showing power law behaviors as indicated in the figure.

This power law property can be understood theoretically from the view point of self-modulation process that is a stochastic process of which basic parameters such as the mean value are modulated by the moving average of its own traces [4,5,6]. According to the results of self-modulation processes it is a natural consequence that the resulting market rates show power law properties when the multiplicative factor $b(t)$ in Eq.(6) fluctuates randomly.

The autocorrelation of rate changes and that of the volatility are plotted in Fig.4 and Fig.5, respectively. In both cases the simulation results fit with the real data quite nicely. It should be noted that the functional form of the autocorrelation functions depend on the weight factors $w_p(k)$ and $w_\varepsilon(k)$, and the interesting point is that the weight factors work quite well, namely, the principle of making the residue terms independent is effective.

## 4. Discussion

We introduced a new type of foreign exchange rate equation that describes very short time characteristics of markets consistent with the real data. It is well-known that traders are generally using moving average methods for predicting the future rates. Our model represents this general property of traders by introducing the best weight factors of the moving averages $w_P(k)$, $w_\varepsilon(k)$ and the noise factors $b(t)$ that expresses responses of dealers to the past market rate changes. From our model it is confirmed that this feedback of information is responsible for the power law distribution of rate changes and characteristic autocorrelations of rate changes and volatility.


## Acknowledgement

The authors would like to show appreciation to Hiroyuki Moriya of Oxford Financial Education for providing us the data of high-frequency exchange rate, Prof. Tohru Nakano of Chuo Univ. for stimulating discussions. T. Mizuno is supported by Research Assistant Fellowship of Chuo University, and the Ministry of Education, Science, Sports and Culture, Grant-in-Aid for JSPS Fellows.


## References


[1] T. Mizuno, S. Kurihara, M. Takayasu, H. Takayasu, Analysis of high-resolution foreign exchange data of USD-JPY for 13 years, Physica A 324, 296-302, 2003.

[2] T. Ohnishi, T. Mizuno, K. Aihara, M. Takayasu and H. Takayasu, Statistical properties of the moving average price in dollar–yen exchange rates, Physica A 344, 207-210, 2004.

[3] T. Mizuno, T. Nakano, M. Takayasu and H. Takayasu, Traders' strategy with price feedbacks in financial market, Physica A 344, 330-334, 2004.

[4] M. Takayasu, H. Takayasu, and M. P. Okazaki, Transaction Interval Analysis of High Resolution Foreign Exchange Data, in Empirical Science of Financial Fluctuations – The Advent of Econophysics, (Springer Verlag, Tokyo, 2002), 18-25.

[5] M. Takayasu, Self-modulation processes in financial markets, in The Application of Econophysics – Proceedings of the Second Nikkei Econophysics Symposium, (Springer Verlag, Tokyo. 2003), 155-160.

[6] M. Takayasu and H. Takayasu, Self-modulation processes and resulting generic 1/f fluctuations, Physica A 324, 101-107, 2003.

# Systematic tuning of optimal weighted-moving-average of yen-dollar market data

Takaaki Ohnishi[1], Takayuki Mizuno[2], Kazuyuki Aihara[3], Misako Takayasu[4] and Hideki Takayasu[5]

[1] Graduate School of Law and Politics, The University of Tokyo, 7-3-1 Hongo, Bunkyo-Ku, Tokyo, 113-0033, Japan
[2] Department of Physics, Faculty of Science and Engineering, Chuo University, 1-13-27 Kasuga, Bunkyo-ku, Tokyo 112-8551, Japan
[3] Institute of Industrial Science, The University of Tokyo, 4-6-1 Komaba, Meguro, Tokyo 153-8505, Japan and ERATO Aihara Complexity Modelling Project, JST, 45-18 Oyama, Shibuya-ku, Tokyo 151-0065, Japan
[4] Department of Computational Intelligence and Systems Science, Interdisciplinary Graduate School of Science and Engineering, Tokyo Institute of Technology, 4259 Nagatsuta-cho, Midori-ku, Yokohama, 226-8503, Japan
[5] Sony Computer Science Laboratories Inc., 3-14-13 Higashi-gotanda, Shinagawa-ku, Tokyo 141-0022, Japan

**Abstract.** We introduce a weighted-moving-average analysis for the tick-by-tick data of yen-dollar exchange market: price, transaction interval and volatility. The weights are determined automatically for given data by applying the Yule-Walker formula for autoregressive model. Although the data are non-stationary the resulting moving average gives a quite nice property that the deviation around the moving-average becomes a white noise.

## 1 Moving-average analysis

From the viewpoint of physics one of the interesting features of market is that prices look quite stochastic in general, however, in some cases especially at the time of large fluctuations such as crashes or bubbles, they show rather dynamical behaviors. To clarify such behaviors we try to extract the component of white noises from the data by introducing a moving-average analysis [1].

For the time series $x(t)$ with mean zero, the moving-average model is given by the following well-known linear autoregressive form:

$$x(t) = \sum_{i=1}^{n} w_i \, x(t-i) + \epsilon(t) \, . \tag{1}$$

Here, $w_i$ are the weights, $n$ is the total number of weights and $\epsilon(t)$ denotes a random noise. We determine the values of $w_i$ by minimizing the averaged square prediction error:

$$E = \left\langle \left( x(t) - \sum_{i=1}^{n} w_i \, x(t-i) \right)^2 \right\rangle , \tag{2}$$

where $\langle \cdot \rangle$ denotes average over period studied. Hence, $w_i$ can be obtained by the Yule-Walker equations:

$$R_i = \sum_{j=1}^{n} R_{j-i} \, w_j , \tag{3}$$

where $i = 1, 2, \ldots, n$ and the autocovariance $R_\tau$ is defined as $R_\tau = R_{-\tau} = \langle x(t) \, x(t+\tau) \rangle$. The weights are determined automatically for given data by applying this formula. The resulting moving average gives a quite nice property that the deviation around the moving-average becomes a white noise.

It should be noted that the Yule-Walker method is rigorous only for stationary time series, however, the market time series are generally not stationary. Therefore, the validity of this method must be checked carefully in this case. For this purpose we separate the tick data into two time zones and compare the results. In the following section, we analyze the time series of Price, transaction interval and volatility by this method.

## 2 Price

We analyze tick-by-tick data of yen-dollar exchange rate, $P(t)$, of data size 291,215 ticks [2]. We define the zero-mean price by

$$x(t) = P(t) - \langle P(t) \rangle . \tag{4}$$

Fig. 1 shows the obtained cumulative amount of weights defined by $\sum_{j=i}^{n} w_j$ for two time zones. The weights decay exponentially in all cases. It is quite interesting that the weights vanish around 2 minutes which coincide to the known results of transaction intervals [3, 4]. Hence, we believe that our method can capture a feature of dealers' action. The weight distribution indicates the property of price fluctuation. Actually, the weights for daily data become 0 immediately, namely, the daily data is quite close to an ideal random walk.

In Fig. 2 we show the autocorrelation functions of the residue of fluctuations, $\epsilon(t)$. The correlation is almost 0 as expected for a white noise, that is, the prices go up and down randomly around the moving-averaged value. As illustrated in Fig 3 optimal weighted-moving-average vary with time so that it may take the value near the actual price.

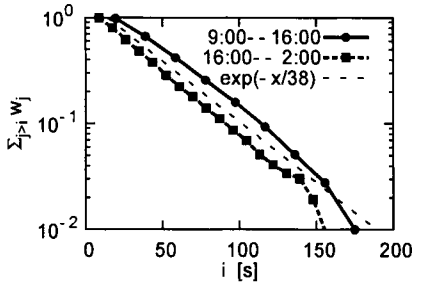


**Fig. 1.** Semi-log plot of the cumulative distribution of weight for the price.

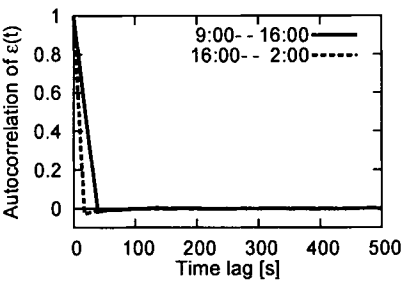


**Fig. 2.** Autocorrelation function of $\epsilon(t)$ for the price.

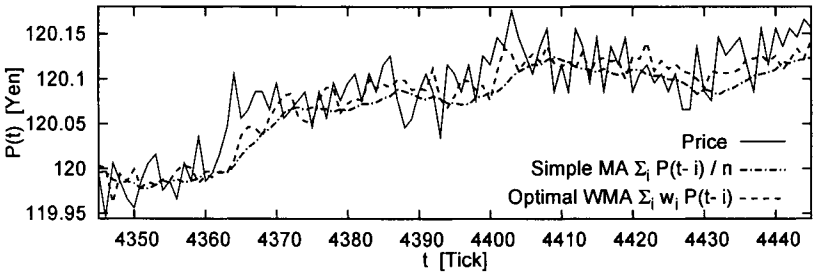


**Fig. 3.** Time series of price, simple moving-average and optimal weighted-moving-average.

## 3 Transaction interval

We consider the transaction interval $T$ which can be given by $T_i = t_{i+1} - t_i$, where $t_i$ is the time transaction occurs. It is recently reported that the transaction interval can be modeled by self-modulation process:

$$T(t) = \epsilon(t) \frac{1}{n} \sum_{i=1}^{n} T(t-i) , \tag{5}$$

where $n$ is the maximum integer that makes $\sum_{i=1}^{n} T(t-i) > \tau$ and $\epsilon(t)$ denotes a random noise. The parameter $\tau$ have to be determined by the trial and error. In the case of $\tau = 150$ seconds, $\epsilon(t)$ appears to be almost no correlation as shown in Fig. 4 [3, 4].

We apply the moving-average analysis to the transaction interval by defining the zero-mean transaction interval as

$$x(t) = \ln T(t) - \langle \ln T(t) \rangle . \tag{6}$$

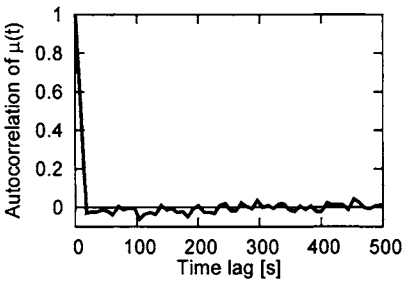


**Fig. 4.** Autocorrelation function of $\epsilon(t)$ for the self-modulation process ($\tau = 150$).

Then, $T(t)$ is described as the geometric mean type of the self-modulation process:

$$T(t) \;=\; \text{const} \cdot \prod_{i=1}^{n} T(t-i)^{w_i} \cdot \exp\bigl(\epsilon(t)\bigr) \;. \tag{7}$$

As shown in Fig. 5 and Fig. 6 the obtained weights decay exponentially and $\epsilon(t)$ has no correlation. Differing from original model, this model has the superiority that the weights are determined automatically and the correlation can be completely eliminated.

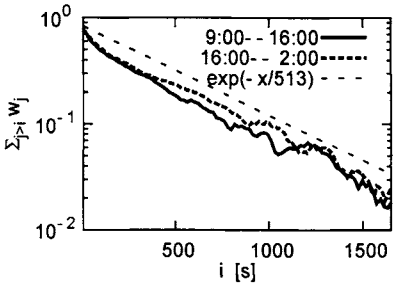


**Fig. 5.** Semi-log plot of the cumulative distribution of weight for the transaction interval.

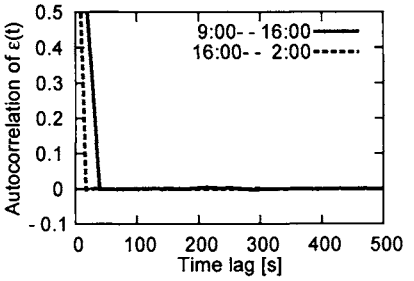


**Fig. 6.** Autocorrelation function of $\epsilon(t)$ for the transaction interval.

## 4 Volatility

Fig. 7 and Fig. 8 give the results for volatility calculated as

$$x(t) \;=\; \ln V(t) \;-\; \langle \ln V(t) \rangle \;, \tag{8}$$

where the volatility $V(t)$ is given by $V(t) = |P(t+1) - P(t)|$. The weights show power law decay and $\epsilon(t)$ has no correlation. The reason for power weight distribution is not apparent but may be related to the long-range volatility correlations.

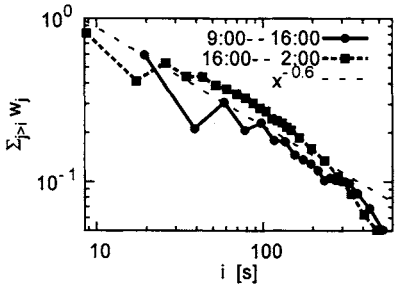


**Fig. 7.** Log-log plot of the cumulative distribution of weight for the volatility.

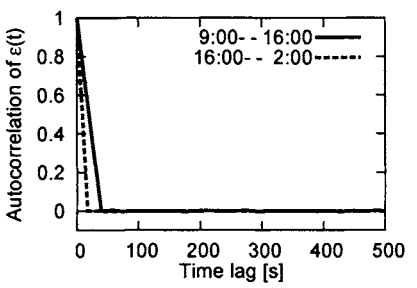


**Fig. 8.** Autocorrelation function of $\epsilon(t)$ for the volatility.

## 5 Conclusion

In this paper we showed that by using Yule-Walker method we can separate the yen-dollar market data into the dynamical component described by the weighted-moving-average and noise component. As a future work we are investigating the dynamical component which would serve to clarify the market dynamics at time scale more than a few minutes.

## References


1. M.G. Lee, A. Oba, H. Takayasu, Parameter Estimation of a Generalized Langevin Equation of Market Price, in: H. Takayasu (Ed.), Empirical Science of Financial Fluctuations, Springer, 2002, 260–270.
2. T. Ohnishi, T. Mizuno, K. Aihara, M. Takayasu, H. Takayasu, Statistical properties of the moving average price in dollar-yen exchange rates, Physica A 344 (2004) 207–210.
3. M. Takayasu, H. Takayasu, M.P. Okazaki, Transaction Interval Analysis of High Resolution Foreign Exchange Data, in: H. Takayasu (Ed.), Empirical Science of Financial Fluctuations, Springer, 2002, 18–25.
4. M. Takayasu, H. Takayasu, Self-modulation processes and resulting generic 1/f fluctuations, Physica A 324 (2003) 101–107.

# Power law and its transition in the slow convergence to a Gaussian in the S&P500 index

Ken Kiyono, Zbigniew R. Struzik, and Yoshiharu Yamamoto

Educational Physiology Laboratory, Graduate School of Education, The University of Tokyo, 7–3–1 Hongo, Bunkyo-ku, Tokyo 113–0033, Japan
k_kiyono@p.u-tokyo.ac.jp z.r.struzik@p.u-tokyo.ac.jp,yamamoto@p.u-tokyo.ac.jp

We study non-Gaussian behaviour of logarithmic returns of the U.S. S&P500 index from a stochastic point of view. The non-Gaussian behaviour indicates an unexpectedly high probability of a large price change, which is of the utmost importance in risk analysis and a central issue in understanding the statistics of price changes [1, 2, 3, 4, 5]. We assess the temporal dependence (evaluated in sliding time intervals) of the non-Gaussian behaviour, and demonstrate as an empirical fact that a precursor of the October 1987 crash can be observed in the index fluctuations at a relatively short time scale $\sim$ 10 minutes.

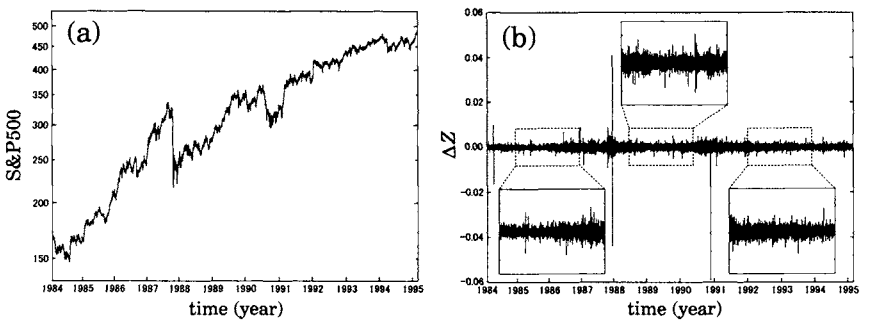


**Fig. 1.** (a) Semilog plot of the S&P500 index time series over the period 1984 - 1995. (b) The 2-min log returns of the S&P500 index: $\Delta Z \equiv (\ln Z(t+s) - \ln Z(t))$, where $s = 2$ min.

Figure 1(a) shows the S&P 500 index $Z(t)$ from 1984 to 1996 in semi-log scale, and figure 1(b) shows time series of the 2-min log return, *i.e.* $\Delta_s Z(t) = \ln Z(t+s) - \ln Z(t)$, where $s = 2$ min. Here we investigate the probability

density function (PDF) of the *detrended* log returns at different time scales, where the non-stationarity of the data has been eliminated by local detrending [6]. To eliminate the trends present in the time series $\{B(t)\}$, where $B(t) \equiv \ln Z(t)$, in each subinterval $[1+s(k-1), s(k+1)]$ of length $2s$, where $k$ is the index of the subinterval, we fit $B(t)$ using a linear function, which represents the exponential trend of the original index in the corresponding time window. After this detrending procedure, we define detrended log returns at a scale $s$ as $\Delta_s B(i) = B^*(i+s) - B^*(i)$, where $1+s(k-1) \leq i \leq sk$ and $B^*(i)$ is a deviation from the fitting function.

After this procedure, we obtain the standardized PDF (the variance has been set to one) of the detrended log-returns, as shown in Fig. 2(a). In addition, we also study a truncated Lévy flight as a representative example of non-Gaussian fluctuations, as shown in Fig. 2(b). We can see a non-Gaussian PDF with heavy tails at small scales $s$ ($\sim$ min), and its convergence to a Gaussian, as the scale $s$ increases.

It has been demonstrated that a non-Gaussian PDF with fat tails can be generated by assuming random multiplicative processes [7, 8, 9, 10]. For instance, let us assume phenomenologically that the increment is represented by the following multiplicative form:

$$\Delta_s B(i) = \xi_s(i) \mathrm{e}^{\omega_s(i)}, \tag{1}$$

where $\xi_s$ and $\omega_s$ are both Gaussian random variables and independent of each other. The PDF of $\Delta_s B(i)$ has fat tails depending on the variance of $\omega_s(i)$, and is expressed by

$$P_s(\Delta_s B) = \int F_s\left(\frac{\Delta_s B}{\sigma}\right) \frac{1}{\sigma} G_s(\ln\sigma) \mathrm{d}(\ln\sigma), \tag{2}$$

where $F_s$ and $G_s$ are both Gaussian,

$$G_s(\omega_s) = \frac{1}{\sqrt{2\pi}\lambda} \exp\left(-\frac{\omega_s^2}{2\lambda^2}\right). \tag{3}$$

In this case, $P_s$ converges to a Gaussian when $\lambda \to 0$. The equation (2) is the same as that for a log-normal cascade model, which was originally introduced to study fully developed turbulence.

For a quantitative comparison, we fit the data to the above function [Eq. (2)] and estimate $\lambda^2$ in Eq. (3) [7]. As shown in Fig. 2(a) and (b) in solid lines, the PDF's of detrended log returns and the truncated Lévy flight are approximated by Eq. (2). Strictly speaking, the function of the PDF for the truncated Lévy distribution is not exactly the same form of the approximated PDF based on Eq. (2). However, through the convergence process to the Gaussian, the difference between the truncated Lévy distribution and the approximated PDF becomes much smaller according to a power law decay. This means that in practical applications, it is impossible to distinguish between the truncated Lévy distribution and the approximated PDF. So we use

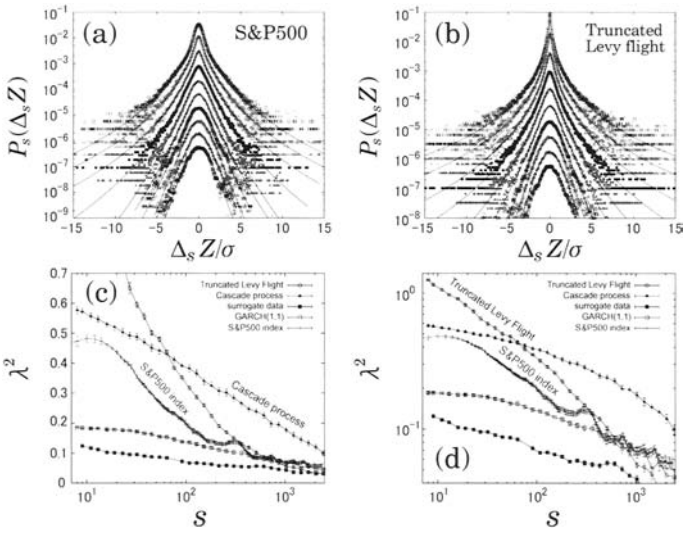


**Fig. 2.** Continuous deformation of increment PDF's, across scales; (**a**) the S&P500 index, (**b**) a truncated Lévy flight. Standardized PDF's at scales (from top to bottom) $s = 8, 16, 32, 64, 128, 256, 512, 1024, 2048, 4096$. In the solid line, we have superimposed Castaing's equation with the normal self-similarity kernel. The scale dependence of the fitting parameter of Castaing's equation for the S&P500 index, its surrogate and the models is plotted as $\lambda^2$ vs. $\log s$ (**c**), and $\log \lambda^2$ vs. $\log s$ (**d**).

a single parameter $\lambda^2$ in Eq. (3) in order to characterise the non-Gaussian PDF of detrended log returns. The scale dependence of $\lambda^2$ for the detrended log returns shows the existence of a power law scaling, rather than a logarithmic decay like cascade models (compare Fig. 2(d) with Fig. 2(c)).

An important point is that the large value of $\lambda^2$ indicates a high probability of a large price change. The probability of a large price change shows a sharp increase. For instance, if the value of $\lambda^2$ has doubled from 0.2 to 0.4, the probability of a large change greater than $10\sigma$, where $\sigma$ is a standard deviation, is about twelve times ($P_{\lambda^2=0.4}(|X| > 10\sigma) \approx 10^{-4}$), and if the value of $\lambda^2$ has doubled from 0.4 to 0.8, the probability of large change greater than $20\sigma$ is about 18 times ($P_{\lambda^2=0.8}(|X| > 20\sigma) \approx 5 \times 10^{-5}$). To date, the volatility of stock price changes has been used as a measure of how much the market is liable to fluctuate, which is of interest to traders because it quantifies the risk and is the key input for the option pricing model of Black and Scholes [11]. Therefore, the statistical properties of the volatility have been intensely studied by economists and recently by physicists. As we will see, it is necessary for a risk analysis to quantify not only the volatility, but also the non-Gaussian nature of the price fluctuations at a relatively short time scale ($\sim$ 10 min).

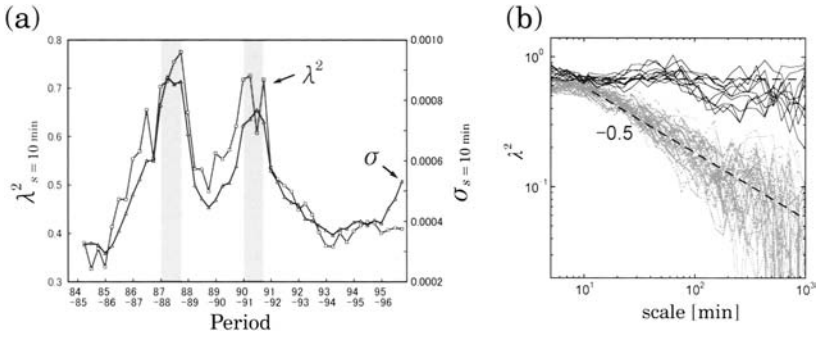


**Fig. 3.** (a) Log-log plot of the scalewise dependence of $\lambda^2$ for five consecutive time intervals before the Black Monday crash. A gradual, systematic increase of $\lambda^2$ at $s = 10$ is evident on approaching the crash date, together with an abrupt transition of $\lambda^2$ scaling just before the Black Monday crash. (b) The temporal dependence of the $\lambda^2$ over a large time span of index evolution shows two instances, in '87 and '90, of apparent tuning towards a critical state.

Here we assess the temporal dependence (evaluated in sliding time intervals) of the $\lambda^2$, together with the volatility defined as the local standard deviation of $\Delta B_s$ at scale $s$ over $N$ data points, *i.e.*

$$\sigma_s = \sqrt{\frac{1}{N}\sum_{i=1}^{N} \Delta B_s^2(i\Delta t)}, \tag{4}$$

where $\Delta t$ is the sampling time interval.

The local temporal variation of $\sigma_{10\mathrm{min}}$ and $\lambda^2_{10\mathrm{min}}$ over a one-year period before the Black Monday crash in '87 shows a gradual, systematic increase on approaching the crash date [Fig. 3(a)]. Because the large $\lambda_s^2$ and $\sigma_S$ mean a high probability of occurrence of extremely large fluctuations, our observation suggests that, through the internal dynamics, the system gradually approached a "critical" state with large fluctuations, which might result in a crash. In addition, we observe an abrupt transition of $\lambda^2$ scaling in the periods including the Black Monday crash, as shown in Fig. 3(b). The scaling law after the transition also suggests that the market was in a state with a high probability of occurrence of large fluctuations at various time scales.

After the Black Monday crash in '87, another increase of $\lambda_s^2$ and $\sigma_S$ is observed before '90, although the crash transition like the Black Monday crash is not observed. It is well known that Iraq's attack on Kuwait, which began in August 1990, and the Persian Gulf War (1991) led to declining and sluggish stock prices (see Fig. 1(a)). Our findings might suggest that the market was approaching a 'critical' state with a high probability of the occurrence of extremely large fluctuations before the attack by Iraq, but the external factor

of the war brought about a radical change in the internal dynamics of the stock market, which prevented a crash transition like the Black Monday crash.

To summarize, we have characterised the non-Gaussian nature of the detrended log-returns of the U.S. S&P500 index from 1984 to 1995 by introducing a simple multiplicative model, and have found the empirical fact that the temporal dependence of fat tails in the PDF shows a gradual, systematic increase of the probability of the appearance of large increments on approaching Black Monday in October 1987. Our finding suggests the importance of the non-Gaussian nature for risk analysis.

## References


[1] R. N. Mantegna and H. E. Stanley. Scaling behavior in the dynamics of an economic index. *Nature*, 376:46–49, 1995.

[2] S. Ghashghaie, W. Breymann, J. Peinke, P. Talkner, and Y. Dodge. Turbulent cascades in foreign exchange markets. *Nature*, 381:767–770, 1996.

[3] J. F. Muzy, J. Delour, and E. Bacry. Modelling fluctuations of financial time series: from cascade process to stochastic volatility model. *Eur. Phys. J. B*, 17:537–548, 2000.

[4] N. Kozuki and Nobuko Fuchikami. Dynamical model of financial markets: fluctuating 'temperature' causes intermittent behavior of price changes. *Physica A*, 329:222–230, 2003.

[5] M. Ausloos and K. Ivanova. Dynamical model and non-extensive statistical mechanics of a market index on large time windows. *Phys. Rev. E*, 68:046122, 2003.

[6] C. K. Peng, J. Mietus, J. M. Hausdorff, S. Havlin, H. E. Stanley, and A. L. Goldberger. Long–range anticorrelations and non–Gaussian behavior of the heartbeat. *Phys. Rev. Lett.*, 70:1343–1346, 1993.

[7] B. Castaing, Y. Gagne, and E. J. Hopfinger. Velocity probability density-functions of high Reynolds-number turbulence. *Physica D*, 46:177–200, 1990.

[8] Hideki Takayasu, A. H. Sato, and M. Takayasu. Stable infinite variance fluctuations in randomly amplified langevin systems. *Phys. Rev. Lett.*, 79:966–969, 1997.

[9] U. Frisch and D. Sornette. Extreme deviations and applications. *J. Phys. I France*, 7:1155–1171, 1997.

[10] E. Bacry, J. Delour, and J. F. Muzy. Multifractal random walk. *Phys. Rev. E*, 64:026103, 2001.

[11] F. Black and M. Scholes. The pricing of options and corporate liabilities. *J. Political Economy*, 81:637–654, 1973.

# Empirical study of the market impact in the Tokyo Stock Exchange

Jun-ichi Maskawa

Department of Management Information, Fukuyama Heisei University, Fukuyama, Hiroshima 720-0001, Japan maskawa@heisei-u.ac.jp

**Summary.** We analyze the trades and quotes database of the TSE (Tokyo Stock Exchange) to derive the average price response to transaction volumes.Through the analysis, we point out that the assumption of the independence of the amplitude of returns on the size of transactions cannot fully explain the profile of the average price response .

## 1 Introduction

The understanding of the market impact (or price impact), that is the price reaction to a transaction volume, is of a practical importance in order to avoid the risk of paying a large transaction cost, when individual investors or brokerage firms place a large size of order. From many prior works about this subject, it seems to be established that the functional form of the average price impact is monotonically increase and concave. Especially, in the recent work of Gabaix et al[1], a square root law has been proposed as a specified functional form of the price impact in the context of a theory of power law distribution of returns, based on the analysis of the 35 million transaction records of the 30 largest stocks on the Paris Bourse over the 5 years period 1994-1999. In their paper, the functional form appeared as the relation between the optimal price change and the volume intended by fund managers for maximizing the benefit of trading, when they place large size of orders.

On the other hand, in the very recent work by Farmer et al[2], an entirely different interpretation has been proposed about the origin of large price changes. They has argued that large returns are not caused by large orders, while the large gaps between the occupied price levels in the orderbook lead to large price changes in each transaction, and actually showed that the gap distribution closely matches the return distribution, based on the analysis of the orderbook as well as the transaction records of 16 large stocks on the LSE (London Stock Exchange) in the 4 years period 1999-2002. They have also showed by the experiment of the virtual market orders of a constant size

that non-intelligent manner of market order placement produces the actual fat tail of return distribution, in contrast to the claim of Gabaix et al. As another work in this direction, Weber and Rosenow analyzed the Island ECN (Electronic communications network), which is automated ATS ( Alternative Trading System) of NASDAQ, and derived the conclusion that large price changes are mainly caused by the lack of liquidity[3].

In this paper, we analyze the trades and quotes database of the TSE (Tokyo Stock Exchange) to derive the average price response to transaction volumes, and consider the origin of the profile. We also study the price changes caused by the block of trades as well as each trade. In the study of the block of trades, we deal with the price change and the volume over a successive sell or buy market orders. The aggregated price change roughly corresponds to the price change for a fixed time interval analyzed by Gabaix et al[1] or the virtual price change by virtual market order by Farmer et al[2]. Through the analysis, we point out that the assumption of the independence of the amplitude of returns on the size of transactions cannot fully explain the profile of the average price response. In section 2, we empirically derive the average price response to transaction volume of each trade. In section 3, the analysis of the aggregated price change caused by successive trades is given. Section 4 is devoted to conclusion.

## 2 Market impact by each trade

The TSE has two trading sessions per day. The morning session starts at 9:00 A.M. and ends at 11:00 A.M. Trading resumes as the afternoon session at 12:30 A. M. and ends at 3:00 A. M. The opening and closing prices for each session are determined by a single price auction called *Itayose*. The continuous auction called *Zaraba* follows Itayose. We can place two kind of orders throughout sessions. One is market order, which does not indicate the specific price, and are executed at the best available price. Second is limit order, which indicate the price as well as the size that a trader want to sell or buy. Limit orders are stored in orderbook, if the immediate transaction is impossible. The market mechanism is fully computerized and there are no designated market makers for the TSE. The situation is the same as in the Paris Bourse, the downstairs market of the LSE and the Island ECN of NASDAQ analyzed in the papers [1], [2] and [3] respectively.

We analyze all transactions and quotes for the 21 stocks listed on the first section of the TSE over one year period from Nov. 1999 through Oct. 2000. Those are the most frequently traded stocks during the period concerned and consist of 10 electric companies, 4 communication companies, 3 security firms, 3 information service companies and 1 game company. This study deal with the logarithmic returns of the best quote (ask or bit price) occurred by the trades during Zaraba. All trades are divided into four classes according to the price p(t) at which the trade is executed at the time t, that is, the trade are

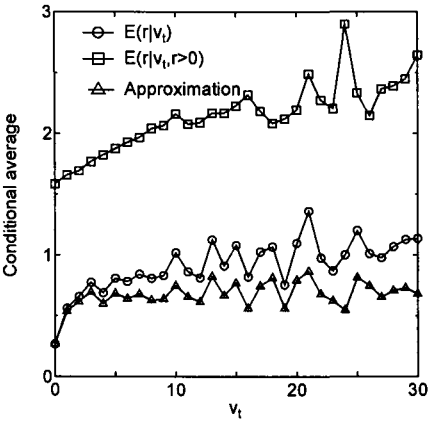


**Fig. 1.** Conditional average of the return of the best quote. The result shown here is for the ask price, and the result for the bit price is very similar. We normalized the return by the average of the absolute value of the price return of each stock, and normalized the volume by the average transaction volume of each stock. Circle represents the average of returns under a given transaction volume $v_t$, and box the average of returns conditioned by $r > 0$ besides a given transaction volume. Triangle gives an approximation which is explained in the text.

executed at the ask price a(t) (the best available sell price), the bit price b(t) (the best available buy price), inside spread ($b(t) < p(t) < a(t)$) or inside book ($p(t) < b(t)$ or $a(t) < p(t)$). In our data, 99.9% of trades are executed at the best bit or offer price. In this paper, we will concentrate on those trades.

First of all, we show the conditional average of the return of the best quote by a given transaction volume $v_t$ in Fig. 1.

The conditional probability density function for the return r by a given transaction volume $v_t$ is decomposed into two parts as the following equation,

$$p(r|v_t) = P(r = 0|v_t)\delta(r) + P(r > 0|v_t)p(r|v_t, r > 0)\theta(r), \tag{1}$$

where $\delta(r)$ and $\theta(r)$ are the Dirac delta function and the step function, that is, $\theta(r) = 0, r \leq 0$ and $\theta(r) = 1, r > 0$. Using this equation, the conditional average is factorized as,

$$E(r|v_t) = P(r > 0|v_t)E(r|v_t, r > 0), \tag{2}$$

where $E(r|v_t, r > 0)$ is the conditional average by the conditional probability density function $p(r|v_t, r > 0)$. The first factor $P(r > 0|v_t)$ represents the probability that the best price shifts by the trade with the transaction volume $v_t$, and is coincident with the probability that the integrated amount $v_a(v_b)$ of limit orders stored at the ask(bit) price is cleared by the market order $v_t$. On

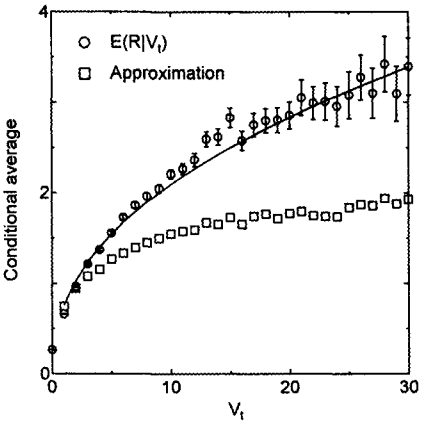


**Fig. 2.** Conditional average of the aggregated return of the best quote. The result shown here is for the ask price, and the result for the bit price is very similar. Circle represents the average of aggregated returns under a given aggregated transaction volume $V_t$, and the error bar gives the 95% confidence interval. Box represents an approximation which is explained in the text. Solid line gives the power law fit by the regression $ln(E(R|V_t)) = aV_t + b$. The parameter estimation gives $a = 0.46(0.01), b = -0.32(0.03)$ and $R^2 = 0.98$

the other hand, $P(r|v_t, r > 0)$ represents the probability that the gap between the best and the second best price is r. The dependence of this quantity on the transaction volume $v_t$ means that the trader change the size of order according to the gap in the limit orderbook. In our data, this dependence is not negligible. The approximation $E(r|v_t, r > 0) = const.$ cannot fully explain the profile of $E(r|v_t)$ as shown in Fig. 1.

## 3 Market impact by the block of trades

In this section, we study the price changes caused by the block of trades. We deal with the price change and the volume over a successive sell or buy market orders, for example, the ask price change over the 3 successive buy market orders. The aggregated price change is considered to roughly correspond to the price change for a fixed time interval analyzed by Gabaix et al[1]. or the virtual price change by virtual market order by Farmer et al[2]. The result for our data and its power law fit are shown In Fig. 2.

The conditional average of aggregated return is given by the equation,

$$E(R|V_t) = \sum_R RP(R|V_t) = \sum_R R \sum_n \frac{P(R, V_t|n)P(n)}{P(V_t)}, \tag{3}$$

where n is the number of successive trades. If we put the ansatz

$$P(R, V_t|n) = P(R|n)P(V_t|n) \tag{4}$$

which indicates that the aggregated return is irrelevant to the aggregated transaction volume, we have an approximation,

$$E(R|V_t) = \sum_n E(R|n)P(n|V_t). \tag{5}$$

As we can see in Fig. 2, the ansatz fails especially in the region of large transaction volume.

## 4 conclusion

The claim that a large transaction volume does not cause a large return fails in the TSE in the period from Nov. 1999 through Oct. 2000. This period coincide with the period of IT bubble and its crash in Japan. I am not sure how the nature of the period enhances the relevance between price changes and transaction volumes. However, it is true that the correlation between the market order size and the limit orderbook should be taken into account in general, when we model the trade in stock markets.

## References


1. Gabaix X, Gopikrishnan P, Plerou V, Stanley HE (2003) A theory of power law distributions in financial market fluctuations, Nature 423:267–270
2. Farmer J. D,Gillemot L, Lillo F, Mike S, Sen A (2004) What really causes large price change? http://xxx.lanl.gov/cond-mat/0312703
3. Weber P, Rosenow B (2004) Large stock price changes: volume or liquidity? http://xxx.lanl.gov/cond-mat/0401132

# Econophysics to unravel the hidden dynamics of commodity markets

Sary Levy-Carciente[1], Klaus Jaffé[2], Fabiola Londoño[1], Tirso Palm[1], Manuel Pérez[1], Miguel Piñango[1] and Pedro Reyes[1]

[1]Economic and Social Science Research Institute "Rodolfo Quintero", Av. Rectorado, Res. A-1, P-3, Los Chaguaramos, Caracas, Venezuela
[2] Center of Strategic Studies, Simon Bolivar University, A.P. 89000, Caracas, Venezuela

**Summary**. Commodity prices act as leading indicators and have important implications for output and business fluctuations, but their dynamics are not well understood. We used some econophysic tools to evaluate five agricultural commodities traded at the NYBOT (cocoa, coffee, cotton, frozen orange juice and sugar), both in price and volume. Results show important differences between price and volume fluctuations and among the commodities. All commodities have high volatile but non-random dynamic, the less so the larger their market.

**Keywords**. Econophysics, Non linear dynamics, Derivative, Agricultural commodity, Futures

## Introduction

Some economists look at commodity prices as leading indicators to anticipate economic processes in the sectors affected by the commodity. This can be viewed as a sort of reversal from the usual direction of causation, as commodity markets are known to have important implications for output and fluctuations in business. Their assessment is particularly important for less-developed-countries that depend on agriculture exports and that spend a lot of resources regulating this sector. Some studies assume commodity markets follow a random walk (Brennan and Schwartz 1985; Paddock et al. 1988) and others consider a mean-reverting price behavior hypothesis (Laughton and Jacoby 1993; Dixit and Pindyck 1994). Both perspectives have elements of truth, while the unpredictability, volatility and instability of commodity market are still a major concern in economics.

There are basically two ways to cope with this problem: increasing the stability of the cash market through artificial controls of volume and price supports – which means the investment of significant amount of resources on the regulation of the agricultural sector and their regulation boards - or through the derivative markets.

Derivative markets serve a risk-shifting function, and can be used to lock-in prices instead of relying on uncertain price developments. Being a vehicle for risk transfer among hedgers and speculators, futures markets also play a role in price discovery, as well as in price information. The risk transfer function allows to match risk exposure of the cash market price with its opposite in the same market or at the future market as a profit opportunity.

Following the expectations theory hypothesis, the current future price is a consensus forecast of the value of the spot price in the future. So, future prices give necessary indications to producers and consumers about the likely future ready price and demand and supply conditions of the commodity traded.

Commodity derivatives have a crucial role to play in the price risk management process in any economy, especially in agriculture dominated countries and even more in less developed agricultural commodity exports dependent countries. Agricultural prices depend on specific circumstances and many commodity exchanges fail to provide an efficient hedge against the risk emerging from volatile prices of many products in which they carry out futures trading. Some recent studies with new insights have shown that complex structures of financial time series may reveal its fundamentals (Mantegna and Stanley 1999; Gabaix et al. 2003).

The fundamental hypothesis explored here is that there are underlying non linear mechanisms of the market, which provide it with some structure. These structures in market behavior might be revealed with the use of tools from econophysics, by studying the series of commodity derivatives either in price and/or volume transacted.

## Data and methods

We worked with the volume and close price of the first nearby contract of the agricultural commodities futures traded daily in the New York Board of Trade, NYBOT[1] (cocoa, coffee, cotton, frozen concentrated orange juice and sugar).

We used the nearby future contracts as these are the contracts closest to expiration and represent the benchmark for the spot (or cash) market, and the first nearby contract is the closest one to expire and theoretically with the smallest basis (difference between the price of a future contract and the underlying commodity's spot price). It's important to remark that there is a substantial variation across futures markets in the pattern of open interest with respect to contract maturity: in currency and financial indexes most of open interest is highly concentrated in the first two nearby contracts (80%), in metals and agricultural, open interest tends to be less concentrated and in energy markets is evenly distributed among nearby and distant futures (Hong 2001).

[1] www.nybot.com/library/cocoa.xls., www.nybot.com/library/coffee.xls, www.nybot.com /library/cotton.xls, www.nybot.com/library/fcoj.xls, www.nybot.com/library/sugar11.xls.

The data series used were from June 01, 1999 to May 28, 2004 in a daily basis, exhibiting series of 1243 records. Time series were analyzed using program facilities of *Excel®*, *Minitab®*, and the analysis software *Chaos Data Analyzer* (Sprott and Rowlands 2003).

## Main results

### Statistical Analysis

Data series of the different commodities have their particularities and similarities. The commodity series do not follow a typical Gaussian distribution, but show a asymmetric distribution or a multimodal one with specific frequency concentrations and leptokurtic distributions. As data series were neither random nor stationary, there was evidence of an underlying model. Volume series showed an apparent cyclical behavior.

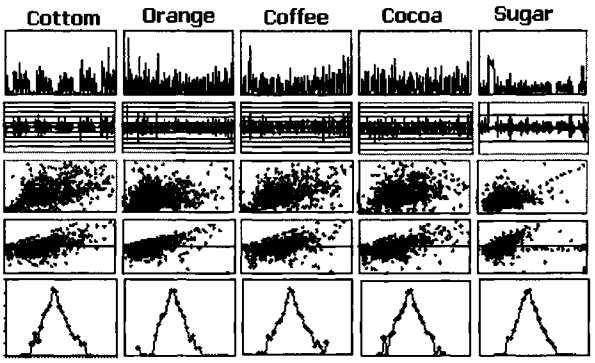


**Fig. 1**. Dynamics of VOLUME traded. First row: Time path (x: time; y: R/S: 0-10 times the average value). Second row: Difference, time vs. change at t+1(-10,10 sd). Third row: Return map v(t) vs v(t+1) (4-4). Forth row: Phase space (-5:5). Fifth row: Histogram, log of observations vs sd (-8:9).

### Bivariate outcome and Portraits

Price and volume showed weak linear correlations, nevertheless, it is important to clarify that they seemed to have some kind of relationship as the data was not distributed randomly in the phase space, suggesting some non linear association or presence of attractors and clusters. The presence of attractors was most relevant for cacao. On the other hand, cotton showed an apparent cyclical behavior with change of levels in the time path. The difference plot and the phase-space plots

showed that Orange juice had much less variance that the rest, and that the patterns of the two commodities causing addiction (cocoa and coffee) were more similar among them than the rest. Variance in volume series was about two times that of price series. Each commodity showed a unique characteristic temporal pattern in the variance of volumes traded. This particularity was not evident in price fluctuations.

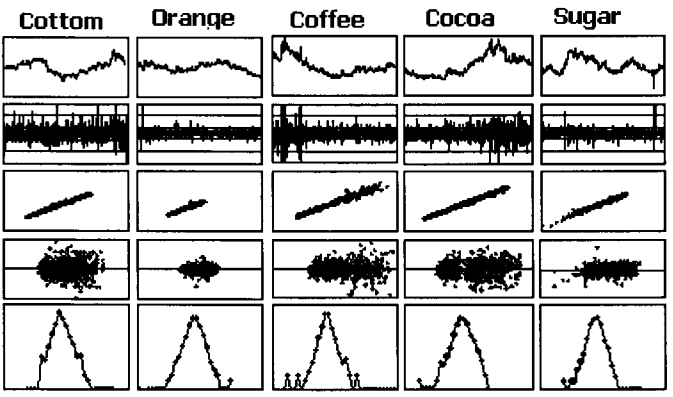


**Fig. 2**. Dynamics of PRICE. First row: Time path (x: time; y: R/S: 0-10 times the average value), Second row: Difference, time vs. change at t+1(-5,5 sd). Third row: Return map p(t) vs p(t+1) (0.2-2). Forth row: Phase space (-5:5). Fifth row: Histogram, log of observations vs sd (-8:8).

## Hurst exponent

The Hurst exponents of both volume and price series showed they were not independent, and carry memory. The fat tails of the distributions shown in the histograms confirm this. Their value –minor than 0.5- showed antipersistence, indicating that past trends tends to reverse in the future.

| | Hurst exponent | | Lyapunov exponent | |
|---|---|---|---|---|
| Commodities | Volume | Price | Volume | Price |
| Cocoa | 0.168 | 0.265 | 0.541 *(0.086)* | 0.214 *(0.046)* |
| Orange juice | 0.079 | 0.079 | 0.653 *(0.056)* | 0.215 *(0.052)* |
| Coffee | 0.182 | 0.183 | 0.504 *(0.090)* | 0.197 *(0.047)* |
| Sugar | 0.275 | 0.291 | 0.548 *(0.090)* | 0.246 *(0.043)* |
| Cotton | 0.178 | 0.178 | 0.551 *(0.073)* | 0.311 *(0.045)* |

## Conclusions

Our results show that the dynamics of prices and volume traded in the future commodity markets differ, and that each commodity market shows particular dynamics in the trade of futures. The dynamics of these markets seem to depend on both, the structure of the market itself and economic factors affecting demand. These results call for caution when insights from one market are extrapolated to another. That is, the use of leading indicators to understand a sector of the economy might be misleading.

Price and volume of the futures of the commodities traded at the NYBOT, show a deterministic non-lineal path with the presence of strange attractors. The underlying mechanisms producing those particular behaviors may be revealed by a deeper understanding of the trade system of each market and the economic variables affecting the demand of each commodity.

The clear antipersistence (Hurst exponent <0.5) of the time series studied contrast with the persistence found in stock markets (Peters 1996). This antipersistence seems to be a common character of commodities (Levy-Carciente et al. 2004). A more detailed analysis of specific commodity markets should reveal more about the economics underlying these dynamics.

## References


Brennan M, Schwartz E (1985) Evaluating natural resource investments. J Bus 58:135-157.

Dixit, A, Pindyck R (1994) Investment Under Uncertainty. Princeton, New Jersey: Princeton University Press.

Gabaix X, Gopikrishnan P, Plerou V, Stanley H (2003) A theory of power-law distributions in financial market fluctuations. Nature 423:267-270

Hong H (2001) Stochastic Convenience Yield, Optimal Hedging and the Term Structure of Open Interest and Futures Prices [www.princeton.edu/~hhong/hong-futures.pdf]

Laughton D, Jacoby H (1993) "Reversion, Timing Options, and Long-Term Decision Making", Financ Manage 22:225-240.

Levy-Carciente S, Sabelli H, K Jaffe (2004) Complex Patterns in the Oil Market *Interciencia* Vol.29(6):320-323 [http://www.interciencia.org/v29_06/jaffe.pdf]

Mantegna RN, HE Stanley (2000) An Introduction to Econophysics: Correlations and Complexity in Finance., Cambridge University Press, NY.

Paddock J, Siegel D, Smith J (1988) Option valuation of claims on physical assets: The case of offshore petroleum leases. Q J Econ 103:479-503.

Peters EE (1996) Chaos and order in the Capital Markets. Wiley 274 pp.

Sprott JC, Rowlands G (2003) Chaos Data Analyzer, *CDA* sprott.physics.wisc.edu/cda/htm

# A characteristic time scale of tick quotes on foreign currency markets

Aki-Hiro Sato

Department of Applied Mathematics and Physics, Graduate School of Informatics, Kyoto University, Kyoto 606-8501, Japan

**Summary.** This study investigates that a characteristic time scale on an exchange rate market (USD/JPY) is examined for the period of 1998 to 2000. Calculating power spectrum densities for the number of tick quotes per minute and averaging them over the year yield that the mean power spectrum density has a peak at high frequencies. Consequently it means that there exist the characteristic scales which dealers act in the market. A simple agent model to explain this phenomenon is proposed. This phenomena may be a result of stochastic resonance with exogenous periodic information and physiological fluctuations of the agents. This may be attributed to the traders' behavior on the market. The potential application is both quantitative characterization and classification of foreign currency markets.

**Key words. power spectrum density, agent-based model, stochastic resonance**

## 1 Introduction

Empirical analysis of high-frequency financial data have been attracting significant interest among physicists as well as economists during a decade (Mantegna and Stanley 2000, and Dacorogna 2001). Many features of financial markets have been clarified by many successive studies.

Actually it is well-known that the markets have a characteristic time scale in long period (daily, weekly, and monthly). However recent studies (Takayasu 2003, Ohnishi 2004 and Mizuno 2004) on time-series analyses in financial markets show that the market has a characteristic time scale in short period and propose the reason why traders are mainly using strategies with weighted feedbacks of past prices. Furthermore using the self-modulation process Takayasu *et al.* have found that the characteristic time scale is about 2 minutes in the JPY/USD market (Takayasu 2003) (abbreviated as MT).

On the other hand Baninec and Krawiech and Hołst proposed a possibility that stochastic resonance occurs in markets (Babinec 2002 and Krawiech 2003)

through an Ising-like agent model. They suggest that a periodicity in the market results from exogenous periodical information (abbreviated as BKH).

In order to clarify the mechanism of this characteristic time I think that we should examine it on a different standpoint from MT and BKH. Both studies focus on prices or price returns. However, in this article, we focus on the number of tick quotes in foreign currency rates (USD/JPY) and investigate the statistical properties of them by utilizing the power spectrum technique. As the results of examining the number of tick quotes in USD/JPY market it is found that the power spectrum density (PSD) has some peaks at about 2 minutes (the peak frequency depends on the currency markets).

In order to explain this phenomena a simple agent model based on double-threshold noisy device (Sato 2004) is proposed. From a result of numerical simulations of the model it is found that the high periodicity of the number of tick quotes may happen. This result leads to a hypothesis that this periodicity is caused by common exogenous periodical information.

The purposes of this study are as follows: (1) to examine the number of high-frequency quotes lead us to deeply understand microscopic market activities. (2) this may provide useful information for market players to consider their trading strategy.

## 2 Data Analysis

The number of ask quotes per minute in USD/JPY is counted for a period of 1998 to 2000. Utilizing the data we calculated three PSDs for 2,048 points in weekday and average them over the year. The averaged power spectrums on the semi-log scale are shown in Fig. 1. They all have a peak at 0.4 (1/min), namely 2.5 minutes. We consider that these peaks exhibit characteristic time scales of dealers' activities, i.e., the dealers act having the periodicity of 2.5 minutes.

## 3 Dealer model

We introduce a simple agent model based on double-threshold noisy devices in order to understand the characteristic time scales found in the averaged power spectrum density. This model contains $N$ dealers and the $i$th dealer has double-threshold ($\theta_i^{(1)} > \theta_i^{(2)}$) to decide buy(1), sell(-1) and wait(0), and noise source $\xi_i(t)$ to model an uncertainty in their mind. We assume that the $i$th dealer must choose a decision (output) into the three ones $y_i(t) = \{1, 0, -1\}$ based on information (input) $x_i(t)$ with an uncertainty $\xi(t)$ in his/her mind:

$$y_i(t) = \begin{cases} 1 & (x_i(t) + \xi_i(t) > \theta_i^{(1)}) \\ 0 & (\theta_i^{(2)} \leq x_i(t) + \xi_i(t) \leq \theta_i^{(1)}) \\ -1 & (x_i(t) + \xi_i(t) < \theta_i^{(2)}) \end{cases} . \quad (1)$$

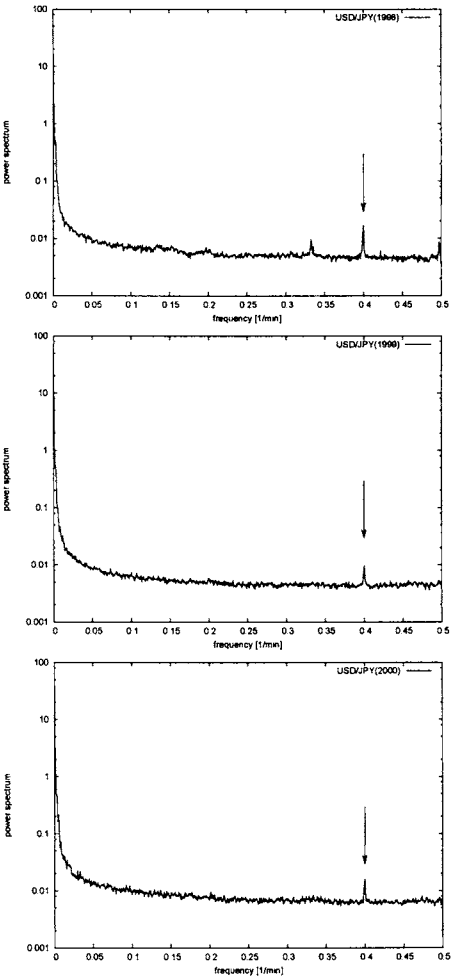


**Fig. 1.** Semi-log plots of the averaged power spectrum density of the number of tick quotes (USD/JPY) over the year for a period of 1998 (top), 1999 (middle), and 2000 (bottom). They all have a peak at 0.4 (1/min), i.e., 2.5 minutes.

Here we assume that $\xi_i(t)$ is identically independent Gaussian distribution,

$$G(\xi) = \frac{1}{\sqrt{2\pi}\sigma_i} \exp\Big( - \frac{\xi^2}{2\sigma_i^2} \Big), \tag{2}$$

where $\sigma_i$ are standard deviations of the $i$th dealer.

It is assumed that the input of each dealer is exogenous periodic information $s(t) = A\sin(2\pi f t)$, where $A$ represents an amplitude, and $f$ a frequency.

For $s(t) > 0$ the dealers feel it good news and tend to decide a buy, while for $s(t) < 0$ they do it bad news and to decide a sell.

Furthermore the number of tick quotes per unit time $X(t)$ is defined as

$$X(t) = \frac{1}{N} \sum_{i=1}^{N} |y_i(t)|. \tag{3}$$

For simplicity assume $\theta_i^{(1)} = \theta$ and $\theta_i^{(2)} = -\theta$. Obviously the activity $X(t)$ is always zero if $\sigma = 0$ and $A < \theta$, so that, there is no uncertainty of the dealers in their mind and the exogenous information is weaker than the threshold for the dealers to decide their action. However if there is uncertainty $\sigma > 0$ then the activity $X(t)$ can exhibit periodicity despite of $A < \theta$ due to stochastic resonance (see Gammaitoni Hänggi Jung and Marchesoni (1998)).

As shown in Fig. 2 it is found that the PSD has some peaks from numerical simulations of the dealer model for $\sigma > 0$ and $A < \theta$. This peak is caused by stochastic resonance.

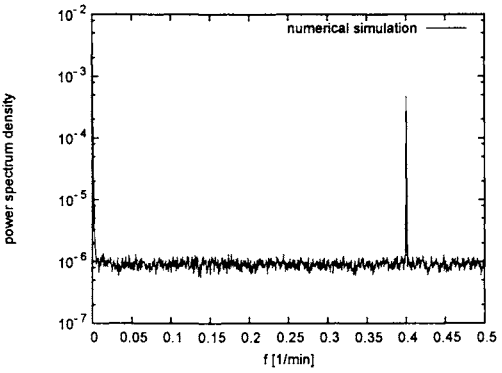


**Fig. 2.** Semi-log plots of the averaged power spectrum of $X(t)$ at $\sigma = 0.3$, $\theta = 1.0$, $A = 0.4$, and $f = 0.2$. It has a peak at 0.4.

## 4 Discussion and Conclusion

We empirically investigate the number of the tick quotes per unit time in foreign currency market (USD/JPY). It is found that the power spectrum densities of them for a period 1998 to 2000 all have a peak at 0.4 [1/min]. From the results it is conclude that a periodical action of dealers exists.

In order to explain this phenomena a simple dealer model based on the double-threshold noisy devices is proposed. Under a hypothesis that the mechanism of this periodicity is stochastic resonance the market activity in the

model shows periodicity due to uncertainty of dealers' decision even though the exogenous periodical information is weaker than the threshold for dealers to decide their action. In fact this model is a feedforward one, however, real markets contains complicated (positive and negative) feedbacks. The future work is to consider the feedbacks to improve the dealer model.

Moreover the source of this periodicity is open problem. One possibility is an endogenous feedback mechanism of dealers as shown in MT. The other is an exogenous periodical information as shown in this paper. More detailed data analyses let us clarify the mechanism of this phenomena. To consider this problem is expected to contribute to a deep understanding of fluctuations and structure in the market.

## References


1. Mantegna R.N. and Stanley H.E. (2000) Introduction to econophysics, Cambridge University Press.
2. Dacorogna M.M., Genćay R, Müller U., Olsen R.B. and Pictet O.V. (2000) An Introduction to High-Frequency Finance, Academic Press (San Diego).
3. Mizuno T., Kurihara S., Takayasu M. and Takayasu H. (2003) Analysis of high-resolution foreign exchange data of USD-JPY for 13 years. Physica A **324**:296–302.
4. Takayasu M. (2003) in ; The Application of Econophyisc–Proceedings of the Second Nikkei Econophysics Symposium, H. Takayasu (Ed.), Springer(Tokyo): 155-160; Takayaus M. and Takayasu H. (2003) Self-modulation processes and resulting generic 1/f fluctuations. Physica A **324**: 101–107.
5. Ohnishi T., Mizuno T., Aihara K., Takayasu M. and Takayasu H. (2004) Statistical properties of the moving average price in dollar-yen exchange rates, Physica A **344**:207–210.
6. Mizuno T., Nakano T., Takayasu M. and Takayasu H. (2004) Traders' strategy with price feedbacks in financial market. Physica A **344**:330–334.
7. Babinec, P (2002) Stochastic resonance in an interacting-agent model of stock market. Chaos, Solutions and Fractals **13**: 1767–1770.
8. Krawiecki A. and Hołyst J.A. (2003) Stochastic resonance as a model for financial market crashes and bubbles. Physica A **317**: 597–608.
9. Sato A.-H., Ueda M. and Munakata T., Signal estimation and threshold optimization using an array of bithreshold elements. (2004) Physical Review E, **70**:021106.
10. Gammaitoni L., Hänggi P., Jung P., and Marchesoni F. (1998) Stochastic resonance. Rev. Mod. Phys. **70**:223–287.

# 2. Predictability of Markets

# Order book dynamics and price impact

Philipp Weber and Bernd Rosenow

Institut für Theoretische Physik, Universität zu Köln, D-50937 Köln, Germany

**Summary.** The price impact function describes how prices change if stocks are bought or sold. Using order book data, we explain the shape of the average price impact function by a feedback mechanism due to a strong anticorrelation between price changes and limit order flow. We find that the average price impact function has only weak explanatory power for large price changes. Hence, we study the time dependence of liquidity and find it to be a necessary prerequisite for the explanation of extreme price fluctuation.

## 1 Introduction

Market participants, especially those who manage a large amount of capital, need to know how the market price changes in reaction to their transactions because this price change contributes to trading costs. Generally, the influence of excess supply or demand on price changes is described by the price impact function [1, 2, 3, 4, 5, 6, 7, 8, 9, 10, 11]. Excess supply and demand can be described by the volume imbalance, the difference between the volume (number of shares) of buyer and seller initiated trades.

The average price impact function is a concave function of volume imbalance, hence one large trade seems to have a smaller price impact than two smaller ones. We argue that this property of the average price impact function can be explained by the influence of resiliency, i.e. price recovery from a random uninformative shock. The price impact function can be used to elucidate the mechanism behind the occurence of large price fluctuations, which cause the fat tails of the distribution of stock price changes [12, 13, 14]. In [15] the average price impact function was approximated by a square root law, and large price fluctuations are suggested to be due to large volume imbalances. This theory was criticized by the authors of [16] who argue that large gaps in the order book are responsible for large price changes.

Our contribution to this discussion is an analysis of fluctuations of price impact. Since we find that the average price impact function can not well

explain large price changes, we analyze fluctuations of the actual price impact, i. e. fluctuations of liquidity [17, 18, 19, 20, 21, 22, 23], and show that they must be taken into account in order to explain large price changes.

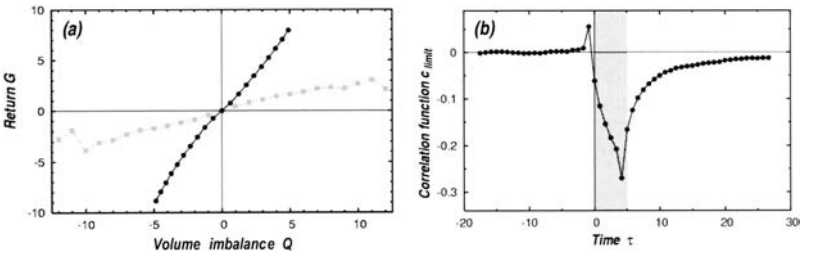


**Fig. 1.** (a) The virtual price impact function $I_{<\text{book}>}(Q)$ (black circles) calculated from the average limit order book is a convex function of order volume and much steeper than the average price impact of market orders (grey squares). Both functions are calculated for the ten most frequently traded stocks from the Island ECN in the year 2002. (b) Correlation function between return and signed limit order flow (buy minus sell orders). Limit orders preceding returns have weak positive correlations with them, while equal time correlations are strongly negative. The region of overlapping time intervals is shaded.

## 2 Price impact and resiliency

An impatient trader who wants to buy or sell a certain number of shares at the best price available initiates a trade by placing a market order. In an electronic market place, market orders execute limit orders which indicate that a trader is willing to trade at a given or better price. A market buy order is matched with the limit sell orders offering the stock for the lowest price, the ask price $S_{\text{ask}}$. Similarly, a market sell order is matched with the limit buy orders offering the highest price, the bid price $S_{\text{bid}}$. In this analysis, we study midquote returns $G_{\Delta t}(t) = \ln S_{\text{M}}(t+\Delta t) - \ln S_{\text{M}}(t)$ where $S_{\text{M}} = \frac{1}{2}(S_{\text{bid}} + S_{\text{ask}})$ is the midquote price and with $\Delta t = 5\text{min}$. Returns can be connected with the volume imbalance $Q$ in a five minute interval via the average price impact function

$$I_{\text{market}}(Q) = \langle G_{\Delta t}(t) \rangle_Q \quad . \tag{1}$$

We calculate $I_{\text{market}}(Q)$ using order book data from the Island ECN for the ten most frequently traded companies in the year 2002 [24] and find that it is a concave function which levels off at above average volume imbalances (Fig. 1a). This shape is quite surprising because it would be an incentive to execute large trades in one step instead of splitting them into several smaller ones as it is done in practice to reduce trading costs.

In order to understand the shape of $I_{\text{market}}(Q)$, we compare it to the virtual price impact calculated from limit orders stored in the order book.

Limit orders are described by their density $\rho_{\text{book}}(\gamma_i, t)$ as a function of time and their position $\gamma_i$ in the order book on a grid with spacing $\Delta\gamma$. For each limit price $S_{\text{limit}}$, we define the coordinate $\gamma_i$ as

$$\gamma_i = \begin{cases} [(\ln(S_{\text{limit}}) - \ln(S_{\text{bid}}))/\Delta\gamma]\,\Delta\gamma & \text{limit buy order} \\ [(\ln(S_{\text{limit}}) - \ln(S_{\text{ask}}))/\Delta\gamma]\,\Delta\gamma & \text{limit sell order} \end{cases} . \tag{2}$$

Here, the function $[x]$ denotes the smallest integer larger than $x$. Execution of a market order with volume

$$Q_{\text{book}}(G, t, k) = \sum_{\gamma_i \leq G} \rho_{\text{book}}(\gamma_i, t, k)\Delta\gamma \tag{3}$$

causes a return $G$ at time $t$ for stock $k$. The inverse of this relation is the virtual price impact $I_{\text{book}}(Q, t, k)$. We now calculate the average order book density $\rho_{\langle\text{book}\rangle}(\gamma_i)$ from $\rho_{\text{book}}(\gamma_i, t, k)$ by averaging over both time and stocks. Replacing $\rho_{\text{book}}(\gamma_i, t, k)$ by $\rho_{\langle\text{book}\rangle}(\gamma_i)$ in Eq. 3, we can obtain the virtual price impact function $I_{<\text{book}>}(Q)$ again by inversion.

We find that $I_{<\text{book}>}(Q)$ is four times steeper than the average price impact $I_{\text{market}}(Q)$ (Fig. 1a). Besides the possible influence of discretionary trading, meaning that large trades are only done when price impact is low, this surprising discrepancy can be explained by resiliency described by time dependent correlations

$$c_{\text{limit}}(\tau) = \frac{\langle Q_{\text{limit}}(t+\tau)G(t)\rangle - \langle Q_{\text{limit}}(t)\rangle\langle G(t)\rangle}{\sigma_{Q_{\text{limit}}}\sigma_G} \tag{4}$$

between limit order flow and returns. The limit order flow

$$Q_{\text{limit}}(t) = \sum_{-\infty}^{\infty} \text{sign}(-\gamma_i)\,(Q_{\delta t}^{\text{add}}(\gamma_i) - Q_{\delta t}^{\text{canc}}(\gamma_i))\,\Delta\gamma \tag{5}$$

is the net volume of limit buy orders minus the net volume of limit sell orders placed in the time interval $\delta t$. Here, $Q_{\delta t}^{\text{add}}(\gamma_i)$ is the volume of limit orders added to the book at a depth $\gamma_i$, and $Q_{\delta t}^{\text{canc}}(\gamma_i)$ is the volume of orders canceled from the book.

We find that limit orders are anticorrelated with returns (see Fig. 1b) in contrast to positive correlations between returns and market orders [25]. Thus, rising prices produce an additional flow of limit sell orders reducing the virtual price impact and contributing to resiliency. These additional limit orders may be due to value traders selling when the price deviates from their perceived fair price. They could also be caused by order management systems. They automatically split large orders into smaller ones that are placed consecutively as soon as the previous one is executed and thus produce an additional limit order flow when prices change. In a more sophisticated analysis, one finds that dynamical effects provide a quantitative link between virtual and average price impact [25].

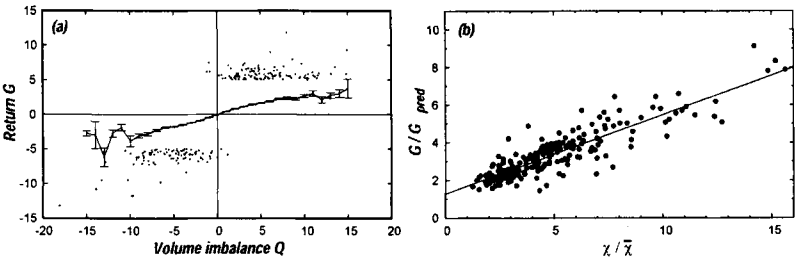


**Fig. 2.** (a) Price changes larger than five standard deviations cluster in the region of small volume imbalance, all of them are clearly outside the error bars of the average price impact function $I_{\text{markct}}(Q)$. (b) Ratio of actual price change to predicted price change plotted against the normalized slope $\chi/\overline{\chi}$ of the actual price impact function $I_{\text{actual}}(Q,t)$. The data points cluster in the vicinity of a linear fit.

## 3 Large stock returns and thin order book

We now ask the question whether the average price impact function can shed light on the origin of large price changes. The shape of $I_{\text{market}}(Q)$ suggests that large returns should occur at large volume imbalances. In Figure 2a all events with returns larger than five standard deviations are compared with the average price impact function $I_{\text{market}}(Q)$. Surprisingly, we find that large events cluster at quite small volume imbalances.

Having in mind the importance of dynamical effects, we now analyze liquidity fluctuations to explain the deviations of the large events from $I_{\text{market}}(Q)$. Therefor, we include dynamical effects in our description of order book density. By definition, $\rho_{\text{book}}(\gamma_i,t)$ is an order book snapshot taken at the beginning of a five minute interval, but during five minutes many additional limit orders are placed in the order book and can also be matched with incoming market orders. Hence, we define another density function $\rho_{\text{flow}}(\gamma_i,t,\Delta t)$ describing the additional limit orders placed or cancelled within the five minute interval. Thus, for each time interval we can reconstruct the actual price impact function $I_{\text{actual}}(Q,t)$ by inversion of the equation for the dynamically corrected order book density

$$Q_{\text{actual}}(G,t) = \sum_{\gamma_i \le G} \Delta\gamma(\rho_{\text{book}}(\gamma_i,t) + \rho_{\text{flow}}(\gamma_i,t,\Delta t)) \quad . \tag{6}$$

We now use the slope $\chi(t)$ of the actual price impact function $I_{\text{actual}}(Q,t)$ as a liquidity measure. In Figure 2b, the ratio of actual return $G$ to the return $G_{\text{pred}}$ predicted by the average price impact function $I_{\text{market}}(Q)$ is plotted against $\chi(t)$ normalized by the slope $\overline{\chi}$ of the average price impact function. The large correlation coefficient $R^2 = 0.79$ suggests that extreme returns can be explained quantitatively by taking into account both order flow and liquidity [26]. Our analysis suggests that an unusually large slope of the time

varying price impact function is a necessary ingredient for the explanation of extreme stock price changes.

In summary, we find that the virtual price impact calculated from the limit order book is much steeper than the average one. This discrepancy can be explained by strong anticorrelations between returns and limit order flow, indicating that rising prices induce an additional flow of limit sell orders reducing the price change. Since the explanatory power of the average price impact function for large events is weak, we analyze the influence of time varying liquidity. Using the slope of the actual price impact function as a liquidity measure we are able to quantitatively explain the deviations of actual returns from the predictions of the average price impact function.

## References


1. J. Hasbrouck, J. Finance **46**, 179-207 (1991).
2. J. Hausman, A. Lo, and C. MacKinlay, J. Finan. Econ. **31**, 319-379 (1992).
3. A. Kempf and O. Korn, J. Finan. Mark. **2**, 29-48 (1999).
4. V. Plerou, P. Gopikrishnan, X. Gabaix, and H.E. Stanley, Physical Review E **66**, 027104[1]-027104[4] (2002).
5. B. Rosenow, Int. J. Mod. Phys. C **13**, 419-425 (2002).
6. M.D. Evans and R.K. Lyons, J. Political Economy **110**, 170-180 (2002).
7. F. Lillo, J.D. Farmer, and R.N. Mantegna, Nature **421**, 129 (2003).
8. X. Gabaix, P. Gopikrishnan, V. Plerou, and H.E. Stanley, Nature **423**, 267-270 (2003).
9. M. Potters, J.-P. Bouchaud, Physica A **324**, 133-140 (2003).
10. C. Hopman, MIT working paper, Dec. 2002.
11. J.-P. Bouchaud, Y. Gefen, M. Potters, and M. Wyart, eprint cond-mat/0307332 (2003).
12. J.Y. Campbell, A.W. Lo, and A.C. MacKinlay, The Econometrics of Financial Markets, Princeton University Press (New Jersey, 1997).
13. T. Lux, Appl. Financial Economics **6**, 463-475 (1996);
    M. Loretan and P.C.B. Phillips, J. Empirical Finance **1**, 211 (1994).
14. P. Gopikrishnan, M. Meyer, L.A.N. Amaral, and H.E. Stanley, Eur. Phys. J. B **3**, 139 (1998).
15. V. Plerou, P. Gopikrishnan, L. A. N. Amaral, M. Meyer, and H.E. Stanley, Physical Review E **60**, 6519-6529 (1999).
16. J.D.Farmer, L.Gillemot, F.Lillo, S.Mike, A.Sen, eprint cond-mat/0312703, 2003
17. A.S. Kyle, Econometrica **53**, 1315-1335 (1985)
18. L.R. Glosten, Journal of Finance **49**, 1127-1161 (1994)
19. A. Madhavan, M. Richardson, and M. Roomans, Review of Financial Studies **10**, 1035-1064 (1997)
20. T. Chordia, R. Roll, and A. Subrahmanyam, J. Finance **56 (2)**, 501-530 (2001).
21. P. Sandas, Review of Financial Studies **14**, 705-734 (2001)
22. M.T. Coppejans, I.H. Domowitz, A. Madhavan, (December 21, 2001). AFA 2002 Atlanta Meetings
23. H. Beltran, A. Durré, and P. Giot, NBB working paper No. 49 - May 2004.
24. We analyzed the following companies (ticker symbols): AMAT, BRCD, BRCM, CSCO, INTC, KLAC, MSFT, ORCL, QLGC, SEBL.
25. P. Weber and B. Rosenow, eprint cond-mat/0311457 (2003).
26. P. Weber and B. Rosenow, eprint cond-mat/0401132 (2004).

# Prediction oriented variant of financial log-periodicity and speculating about the stock market development until 2010

Stan Drożdż[1,2], Frank Grümmer[3], Franz Ruf[4] and Josef Speth[3]

[1] Institute of Nuclear Physics, Polish Academy of Sciences, PL–31-342 Kraków, Poland
[2] Institute of Physics, University of Rzeszów, PL–35-310 Rzeszów, Poland
[3] Institut für Kernphysik, Forschungszentrum Jülich, D-52425 Jülich, Germany
[4] West LB International S.A., 32-34 bd Grande-Duchesse Charlotte, L-2014 Luxembourg

**Summary.** A phenomenon of the financial log-periodicity is discussed and the characteristics that amplify its predictive potential are elaborated. The principal one is self-similarity that obeys across all the time scales. Furthermore the same preferred scaling factor appears to provide the most consistent description of the market dynamics on all these scales both in the bull as well as in the bear market phases and is common to all the major markets. These ingredients set very desirable and useful constraints for understanding the past market behavior as well as in designing forecasting scenarios. One novel speculative example of a more detailed S&P500 development until 2010 is presented.

**Key words.** Financial physics, critical phenomena, log-periodicity

The concept of financial log-periodicity is based on the appealing assumption that the financial dynamics is governed by phenomena analogous to criticality in the statistical physics sense (Sornette et al. 1996, Feigenbaum and Freund 1996). Criticality implies a scale invariance which, for a properly defined function $F(x)$ characterizing the system, means that

$$F(\lambda x) = \gamma F(x). \tag{1}$$

A constant $\gamma$ describes how the properties of the system change when it is rescaled by the factor $\lambda$. The general solution to this equation reads:

$$F(x) = x^{\alpha} P(\ln(x)/\ln(\lambda)), \tag{2}$$

where the first term represents a standard power-law that is characteristic of continuous scale-invariance with the critical exponent $\alpha = \ln(\gamma)/\ln(\lambda)$ and $P$ denotes a periodic function of period one. This general solution can be interpreted in terms of discrete scale invariance. It is due to the second term that the conventional dominating scaling acquires a correction that is periodic in $\ln(x)$ and may account for the zig-zag character of financial dynamics. It demands however that if $x = |T - T_c|$, where $T$ denotes the ordinary time labeling the original price time series, represents a distance to the critical point $T_c$, the resulting spacing between the corresponding consecutive repeatable structures at $x_n$ seen in the linear scale follow a geometric contraction according to the relation $(x_{n+1} - x_n)/(x_{n+2} - x_{n+1}) = \lambda$. The critical points correspond to the accumulation of such oscillations and, in the context of the financial dynamics, it is this effect that potentially can be used for prediction.

An extremely important related element, for a proper interpretation and handling of the financial patterns as well as for consistency of the theory, is that such log-periodic oscillations manifest their action self-similarly through various time scales (Drożdż et al. 1999). This applies both to the log-periodically accelerating bubble market phase as well as to the log-periodically decelerating anti-bubble phase. Furthermore, more and more evidence is collected that the preferred scaling factor $\lambda \approx 2$ and is common to all the scales and markets (Drożdż et al. 2003). These two elements, self-similarity and universality of the $\lambda$, set very valuable and in fact crucial constraints on possible forms of the analytic representations of the market trends and oscillation patterns, including the future ones as well.

A specific form of the periodic function $P$ in Eq. 2 is as yet not provided by any first principles which opens room for certain, seemingly mathematically unrigorous assignments of patterns. This, on the other hand, allows to correct for frequent market 'imprecisions' when relating its real behavior versus the theory. Very helpful in this respect is the requirement of self-similarity which greatly clarifies the significance of a given pattern and allows to determine on what time scale it operates. Since in the corresponding methodology the oscillation structure carries the most relevant information about the market dynamics, for transparency of this presentation, we use the first term of its Fourier expansion,

$$P(\ln(x)/\ln(\lambda)) = A + B\cos(\frac{\omega}{2\pi}\ln(x) + \phi). \tag{3}$$

This implies that $\omega = 2\pi/\ln(\lambda)$. Already such a simple parametrization allows to properly reflect the contraction of oscillations, especially on the larger time scales. On the smaller time scales just replacing the *cosine* by its modulus often, even quantitatively in addition, describes departures of the market amplitude from its average trend.

One particularly relevant and special, for several reasons, example is shown in Fig. 1. The upper panel (a) illustrates a nearly optimal log-periodic representation of the S&P500 data over the most extended time-period of the

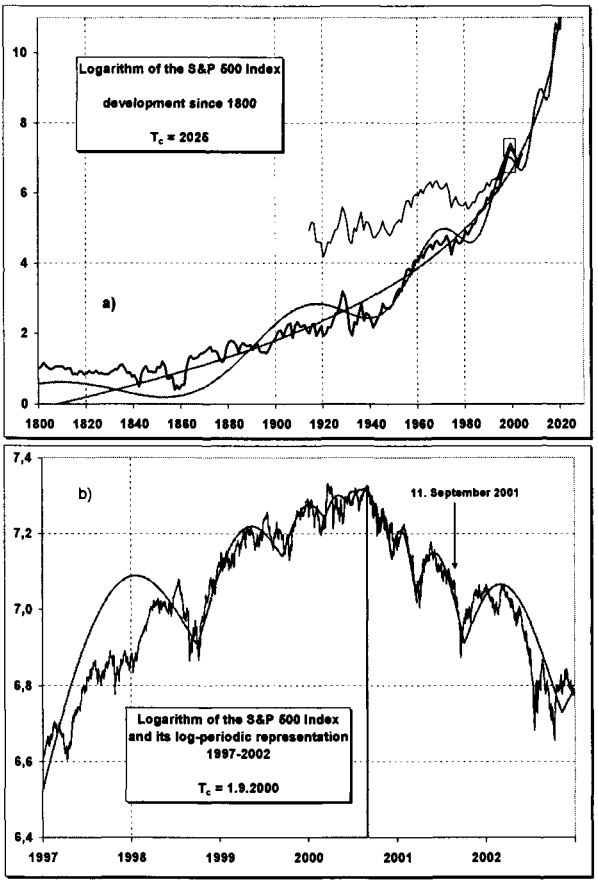


**Fig. 1.** (a) Logarithm of the Standard & Poor's 500 index since 1800 (http://www.globalfindata.com). The thick solid line displays its optimal log-periodic representation with $\lambda = 2$. The thin solid line represents the inflation corrected S&P500 expressed in 2004 US$. It significantly shifts the third minimum to the early 1980s and improves agreement with the theoretical representation. (b) Logarithm of the S&P500 from 1997 till the end of 2002, which corresponds to the magnification of the small rectangle in (a). The solid lines illustrate the log-periodic accelerating and decelerating representations with $\lambda = 2$, modulus of the cosine used in Eq. (3), and a common $T_c = 1.9.2000$.

recorded stock market activity as dated since 1800. As already pointed out (Drożdż et al. 2003) this development signals in around 2025 a transition of the S&P500 to a globally declining phase as measured in the contemporary terms. The magnification of the small rectangle covering the period 1997-2002 is displayed in the lower panel (b) of the same Fig. 1. It thus illustrates the

nature of the stock market evolution on a much smaller time scale of resolution. An impressive log-periodicity with the same $\lambda = 2$ on both sides of the transition date (September 1, 2000) can be seen.

The next stock market top from the perspective of the largest time scale (Fig. 1a) can be estimated to occur in around the years 2010-2011. In the spirit of the log-periodicity its neighborhood is to be accompanied by the smaller time scale oscillations - similar in character to those in Fig. 1b. Of course, when going far away from those large scale transition points such pure log-periodic structures - representative to the one level lower time scale - must get dissolved. A particularly interesting related question then is what characteristics are to govern the stock market dynamics in the transition period when going from 2000 to 2010. The most natural and straightforward way is to view this process as schematically is indicated in Fig. 2. This whole period is thus covered by the two main components represented by the thin lines and the market dynamics is driven by the superposition of of these two components whose phases, slopes and weights are adjusted such that the overall global market trend up to now is reproduced.

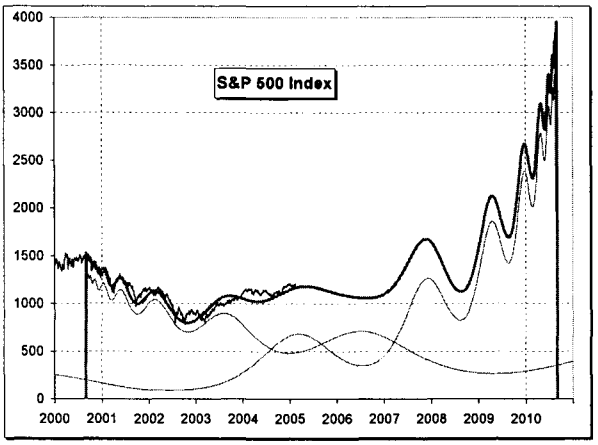


**Fig. 2.** A hypothetical log-periodic scenario, represented by the thick solid line, for the S&P500 development until 2010. This solid line is obtained by summing up the two $\lambda = 2$ components (thin lines): log-periodically decelerating since 1.9.2000 and log-periodically accelerating toward 1.9.2010.

In this scenario, close to the two large-scale transition points (September 2000 and, as provisionally estimated here based on Fig. 1a, September 2010) the market is driven, as needed, essentially by the single log-periodic components, decelerating and accelerating one, correspondingly. More complicated is the situation in the middle of this time interval where the two components contribute comparably. Most interestingly, it indicates that the

period of the stock market stagnation may extend even into the year 2008, before it seriously starts rising. It also demonstrates a possible mechanism that generates modulation structures responsible for the apparent higher order corrections (Johansen and Sornette 1999) to Eq. (3). The changes in the frequency relations observed in the transition period between the bear and the bull market phases originate here from the interference between the two components, both of the simple form as prescribed by Eq. (3) and with the same $\lambda = 2$. Of course, similar effects of interference may occur on the whole hierarchy of different time scales.

There is one more element that from time to time takes place in the financial dynamics and whose identification appears relevant for a proper interpretation of the financial patterns with the same universal value of the preferred scaling factor $\lambda$. This is the phenomenon of a "super-bubble" (Drożdż et al. 2003) which is a local bubble, itself evolving log-periodically, superimposed on top of a long-term bubble. Two such spectacular examples are provided by the Nasdaq in the first quarter of 2000 and by the gold price in the beginning of 1981 (Drożdż et al. 2003).

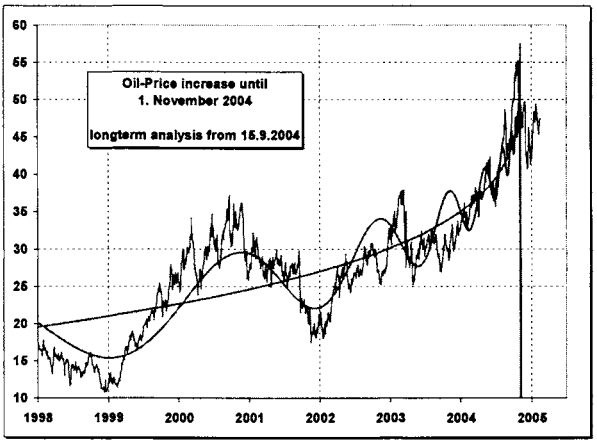


**Fig. 3.** The New York traded oil futures since 1998 and the corresponding log-periodic $\lambda = 2$ representation in terms of Eq. (3).

In connection with this second case it is important to remember that the same value of $\lambda$ as for the stock market turns out appropriate. That such its value may be characteristic to the whole commodities market as well, is shown in Fig. 3 which displays the New York traded oil futures versus the best log-periodic ($\lambda = 2$) representation. In fact, this scenario has been drawn by the authors on September 15, 2004, insisting on using $\lambda = 2$, even though one local minimum (in the beginning of 2004) in the corresponding sequence did

not look very convincing. Designed this way it was indicating a continuation of the increase until the end of October and then a more serious reverse of the trend. Subsequent development of the oil futures provides further arguments in favor of this way of handling the financial log-periodicity.

## References


Drożdż S, Ruf F, Speth J, Wójcik M (1999) Imprints of log-periodic self-similarity in the stock market. Eur. Phys. J. B 10:589-593

Drożdż S, Grümmer F, Ruf F, Speth J (2003) Log-periodic self-similarity: an emerging financial law? Physica A 324:174-182

Feigenbaum JA, Freund PGO (1996) Discrete scale invariance in stock markets before crashes. Int. J. Mod. Phys. B 10:3737-3745

Johansen A, Sornette D (1999) Financial "anti-bubbles": Log-periodicity in gold and Nikkei collapses. Int. J. Mod. Phys. C 10:563-575

Sornette D, Johansen A, Bouchaud J.-P (1996) Stock market crashes, precursors and replicas. J. Physique (France) 6:167-175

# Quantitative Forecasting and Modeling Stock Price Fluctuations

Serge Hayward

Department of Finance
Ecole Supérieure de Commerce de Dijon,
29, rue Sambin, 21000, Dijon, France
shayward@escdijon.com

**Abstract.** Considering the effect of economic agents' preferences on their actions, relationships between conventional summary statistics and forecasts' profit are investigated. Analytical examination demonstrates that investors' utility maximization is determined by their risk attitude. The computational experiment rejects the claims that the accuracy of the forecast does not depend upon which error-criteria are used. Profitability of networks trained with $L_6$ loss function appeared to be statistically significant and stable.

**Keywords:** Artificial Neural Network; Loss Functions; Risk Preferences

## Introduction

The relationship between agents' utility functions and optimal investment decisions (portfolio and saving rules) is a long-standing issue in financial research. This research is motivated by the results of (Chen and Huang 2003), where constant relative risk aversion (CRRA) traders without the best portfolio rules are the best long-term survivors through their saving decisions. In this paper I take a few steps aside. First of all, I examine a mapping of traders' risk attitude into their predictions. Secondly, bearing in mind that stock trading models' time horizons do not typically exceed one-two years, I limit my investigation to short-medium term analysis. Thirdly, considering an environment with agents possessing an 'optimal' stable saving rate (e.g. locked-up saving contracts), allows me to focus on trading decisions, examining the profitability of actions over short and long terms.

The second motivation for this paper comes from (Leitch and Tanner 2001), arguing that traditional summary statistics are not closely related to a forecast's profit. As I consider the effect of agents' risk attitude on their actions' profitability

through loss functions minimization, this relationship is particularly important. If agents' preferences have impact on their wealth, there should be a statistically significant relationship between forecasts' errors and actions' profitability, in order to investigate it with ANN under supervised learning, where the network training is based on a chosen statistical criterion, but when economic performance is sought.

## Methodology

For my experiment, I build ANN forecasts and generate a posterior optimal rule. The rule, using future information to determine the best current trading action, returns a buy/sell signal (B/S) today if prices tomorrow have increased/decreased. A posterior optimal rule signal (PORS) is then modeled with ANN forecasts, generating a trading B/S signal. Combining a trading signal with a strategy warrants a position to be taken. Note that my approach is different from the standard B/S signal generation from a technical trading rule. In the latter, it is only a signal from a technical trading rule that establishes that prices are expected to increase/decrease. In my model, I link a signal's expectations of price change (given by PORS) to a time-series forecast.

To apply my methodology, I develop a dual network structure. The forecasting network feeds into the acting network, from which the information set includes the output of the first network and PORS, as well as the inputs used for forecasting, in order to relate the forecast to the data upon which it was based. It is an effort to relate an action's profitability to forecasting quality, examining this relationship in a computational setting. The model is evolutionary in the sense that it considers a population of networks (individual agents facing identical problems/instances) that generate different solutions, which are assessed and selected on the basis of their fitness. Backpropagation is used in the forecasting net to learn to approximate the unknown conditional expectation function (without the need to make assumptions about a data-generating mechanism and beliefs formation). It is also employed in the acting net to learn the relationship between the statistical characteristics of the forecasts and the economic characteristics of the actions.

A single hidden layer ANN is deemed to be sufficient for my problem, particularly considering the universal approximation property of feedforward nets. Finally, agents discover their optimal settings with a genetic algorithm (GA). GA enhances ANN generalization, and adds additional explanatory power to the analysis. Selecting candidates for the current stage with a probability proportional to their contributions to the objective function at a previous stage, GA reproduces the 'fittest individuals' from a population of possible solutions. As a result, the best suited to performing specific task settings are identified.

## Experimental Design

A loss function, $L$: $\mathbb{R} \rightarrow \mathbb{R}^+$, related to some economic criteria or a statistical measure of accuracy, takes a general form:

$$L(p,\ \alpha,\ \varepsilon) \equiv [\alpha + (1 - 2\alpha)1(\varepsilon < 0)]\varepsilon^p, \tag{1}$$

where $p$ is a coefficient of absolute risk aversion (related to a coefficient of relative risk aversion, ρ through some function h, $p = h(\rho)$); ε is the forecast error; $\alpha \in [0,1]$ is the degree of asymmetry in the forecaster's loss function, and 1 in $1(\varepsilon<0)$ is the indicator function. $L(p, \alpha, \varepsilon)$ is $\mathcal{F}_t$-measurable and also presented as

$$L(p,\ a,\ \theta) \equiv [a + (1 - 2a)1(Y_{t+1} - fc_{t+1}(\theta) < 0)]\left|Y_{t+1} - fc_{t+1}(\theta)\right|^p, \tag{2}$$

where $\alpha$ and $p$ $(\rho)$ are shape parameters of a loss function; vector of unknown parameters, $\theta \in \Theta$. Order of the loss function is determined by $p$. Setting agents attitude towards risk, $p$ to different values allows me to identify the main loss function families. Consider some families and their popular representatives:

1. $L(1, [0,1], \theta)$ – piecewise linear family 'Lin-Lin' or 'Tick' Function.
   - $L(1,\ 1/2,\theta) = |Y_{t+1} - fc_{t+1}|$ – absolute value loss function or mean absolute error (MAE) loss function, $L(\varepsilon_{t+1}) = |\ \varepsilon_{t+1}|$. This loss function determines the error measure, defined as

$$MAE = T^{-1}\sum_{s=1}^{T}\left|\varepsilon_{t+s}\right|. \tag{3}$$

2. $L(2, [0,1], \theta)$ – piecewise quadratic family 'Quad-Quad'.
   - $L(2,\ 1/2,\ \theta) = (Y_{t+1} - fc_{t+1})^2$ – squared loss function or mean squared error (MSE) loss function, $L(\varepsilon_{t+1}) = \varepsilon^2_{t+1}$. Appropriate for this loss function error measure is defined as

$$MSE = T^{-1}\sum_{s=1}^{T}\varepsilon_{t+s}^2. \tag{4}$$

The choice of a loss function is influenced by the object of analysis. In this paper, loss functions that are not directly determined by the value of risk aversion coefficient are limited out. For given values of $p$ and $\alpha$, an agent's optimal one-period forecast is

$$\min_{\theta\in\Theta} E[L(\rho,\ \alpha,\ \theta)] = E[L(Y_{t+1} - fc_{t+1})] = E[L(\varepsilon_{t+1})]. \tag{5}$$

Traders' utility maximization depends on their attitude towards risk (given by a coefficient of risk aversion) and the attitude towards costs of +/- errors (given by a degree of asymmetry in the loss function). Note that a degree of asymmetry is itself a function of a coefficient of risk aversion. Therefore, economic agents' utility maximization is uniquely determined by their attitude towards risk. Training ANN with different loss functions allows me to examine how agents' statistical and economic performances relate to their risk preferences.

## Performance Surface

Loss function determines optimality on the performance surface, given by errors versus weights. As long as gradient descent is used, the output errors injected into the network depend upon a chosen loss function:

$$L = \sum_{i=1}^{I} f(Y_i, \Phi_i), \tag{6}$$

where $Y_i$ is a desired response, $\Phi_i$ is the network's output and $I$ is the number of observations. The function $L$ is minimized when $Y_i = \Phi_i = \psi_{i,j} X_i$, where $X_i$ is the input vector, $\psi_{i,j}$ weights connecting $I$ inputs of the input layer with $J$ neurons of the hidden layer.

The measure of ANN performance is given by the sensitivity of a loss function with respect to the network's output:

$$\partial C / \partial \Phi_i \equiv \varepsilon_i \equiv Y_i - \Phi_i. \tag{7}$$

Recall the $l_p$ norm of a vector $x \in l_p$, defined for the class of measurable functions by $\|x\|_p = (\sum_{i=1}^{\infty} |x_i|^p)^{1/p}$; *for* $1 \le p < \infty$ and consider a loss function of order $p$:

$$L_p = I^{-1} \sum_{i=1}^{I} (Y_i - \Phi_i)^p, \tag{8}$$

where $p$ is a user-defined constant. Since ANN weights' modification depends on the order of a loss function, different values of $p$ produce dissimilar learning and solutions to the optimization problem. By examining a slow step increase in the value of $p$, the behavior of the model with different objective functions is investigated. For comparison I consider $L_\infty$ loss function in the nonlinearly constrained min-max problem.

At $p$ value equal to 1 and 2 common $L_1$ and $L_2$ loss functions are observed. $L_1$, absolute value or MAE loss function takes the form:

$$L_1 = I^{-1} \sum_{i=1}^{I} |Y_i - \Phi_i|. \tag{9}$$

The error function used to report to the supervised learning procedure is the sign of the difference between the network's output and desired response: $\varepsilon_i = -\mathrm{sgn}(Y_i - \Phi_i)$. The cost returned is the accumulation of the absolute differences between the ANN output and the desired response. $L_1$ gives equal weights to large and small errors, weighting the differences proportionally to their magnitude. Learning under $L_1$ loss function de-emphasizes outliers and rare large discrepancies have less influence on results than learning under its main competitor, $L_2$ function. For that reason $L_1$ sometimes viewed as a more robust norm, comparing to $L_2$.

$L_2$, quadratic or MSE loss function takes the form:

$$L_2 = I^{-1} \sum_{i=1}^{I} (Y_i - \Phi_i)^2. \tag{10}$$

The error function is the squared Euclidean distance between the network's output and the target: $\varepsilon_i = -(Y_i - \Phi_i)^2$. The cost returned is the accumulation of the squared errors. Quadratic performance surface is particularly appropriate for linear systems. With $L_2$ loss function the equations to be solved for computing the optimal weights are linear for the weights in linear networks, giving closed form solutions. $L_2$ function is also attractive for giving probabilistic interpretation of the learning output, but might be inappropriate for highly non-Gaussian distributions of the target. Minimizing quadratic loss function corresponds and would be particularly appropriate for agents with a quadratic utility function. Minimizing the error power, $L_2$ weights significantly the large errors. ANN trained with $L_2$ function will assign more weight to extreme outcomes and will focus on reducing large errors in the learning process.

Under MSE and MAE loss functions all errors are considered symmetrically. Since conventional investment behavior implies putting more effort into avoiding large losses, i.e. pursuing an asymmetric target, $L_1$ and $L_2$ loss functions might be less appropriate for agents with these risk preferences. ANN trained under symmetry tends to follow risky solutions.

Generally, for $p > 1$, the cost will always increase at the faster rate than the instantaneous error. Thus, larger errors receive progressively more weight under learning with higher order $L_p$ functions. The upper limit here is given by $L_\infty$ function, where all errors are ignored, except the largest. The $L_\infty$ loss function is an approximation of the $l_\infty$ norm, $\|x\|_\infty = \sup\{|x_1|,\ldots,|x_n|,\ldots\}$. Notice that $l_\infty$ norm is essentially different from $l_p$ norm in the behavior of its tails. $L_\infty$ allows me to minimize the maximum deviation between the target and the net's output:

$$L_\infty = \sum_{i=1}^{I} \left|\tan(Y_i - \Phi_i)\right|. \tag{11}$$

$L_\infty$ locally emphasizes large errors in each output, rather than globally searching the output for the maximum error. The error function is the hyperbolic tangent of the difference between the network's output and the target: $\varepsilon_i = \left|\tan(Y_i - \Phi_i)\right|$. The cost returned is the accumulation of the errors for all output neurons.

On another extreme the performance surface with $p = 0$ is presented. Considering only the sign of the deviations, it is viewed as equivalent to the performance surface optimized solely for directional accuracy (DA). In this research, $L\varpi$ loss (a variant of the $L_2$ function that weight various aspects of time-series data differently) is considered:

$$L\varpi = I^{-\varpi} \sum_{i=1}^{I} \left(Y_i - \Phi_i\right)^2, \tag{12}$$

where $\varpi$ is the weighting factor. Errors are scaled according to the following criteria: DA, recency of observations and magnitude of change.

## Performance Measures

Although ANN is trained to minimize the internal error, testing and optimization of its generalization abilities are arrived at by comparing its performance with the results of a benchmark, an efficient prediction (EP). In forecasting prices, EP is the last known value. For predicting strategies, it is the buy/hold (B/H) strategy. The degree of improvement over efficient prediction (IEP) is calculated as an error from a de-normalized value of the ANN and a desired output, then normalizing the result with the difference between the target and EP value.

I use profitability as a measure of overall success. I examine the following forms of cumulative and individual trade-return measures: non-realized simple aggregate return; profit/loss factor; average, and maximum gain/loss. To assess risk exposure, I adopt common 'primitive' statistics and the Sharpe ratio[1]. To overcome the Fisher effect, I consider trading positions with a one-day delay.

TC is assumed to be paid both when entering and exiting the market, as a percentage of the trade value. TC accounts for broker's fees, taxes, liquidity cost (bid-ask spread), as well as costs of collecting/analysis of information and opportunity costs. According to (Sweeney 1998), TC reasonably range from a minimum of 0.05% for floor traders to somewhat over 0.2% for money managers getting the best prices. Since TC would differ for heterogeneous agents, I report the break-even TC that offsets trading revenue with costs leading to zero profits.

Heterogeneous traders in the experiment use different lengths of past and forward horizons to build their forecasts/strategies. In this paper three memory time horizons, [6; 5; 2½] years are adopted. The simulation is run with a one year testing horizon, as it seems to be reasonable from the actual trading strategies perspective and is supported by similar experiments. Lastly, such forward horizon allows me to investigate trading rules without explicit consideration of saving decisions (made on annual basis). Both long and short trades are allowed in the simulation. Investing total funds for the first trade, subsequent trades (during a year) are made by re-investing all of the money returned from the previous trades. If the account no longer has enough capital to cover TC, trading stops.

## Empirical Application

I consider daily closing prices for the MTMS share index. The time period under investigation is 01/01/97 to 23/01/04. There were altogether 1575 observations in row data sets. ANN with GA optimization was programmed with various topologies. Over one year testing period 19 trading strategies were able to outperform the B/H strategy in economic terms, with an investment of $10,000 and TC of 0.2% of trade value. The average return improvement over B/H strategy

[1] Given by the average return divided by the standard deviation of that return.

was 20%, with the first five outperforming the benchmark by 50% and the last three by 2%. The primary strategy superiority over B/H strategy was 72%. GA model discovery reveals that Multilayer Perceptron (MLP) and Time-Lag Recurrent Network (TLRN); numbers of neurons in the hidden layer in the range [5, 12] and Conjugate Gradients learning algorithm generate the best performance in statistical and economic terms for forecasting and acting nets. For the five best performing strategies, the break-even TC was estimated to be 0.275%; increasing to 0.35% for the first three and nearly 0.5% for the primary strategy. Thus, the break-even TC for at least the primary strategy appears to be high enough to exceed actual TC.

ANN minimizing $L_6$ function performed satisfactory and consistently for all memory horizons. For instance, the annualized return of MLP minimizing $L_6$ function for 1997-2004 data series outperformed $L_2$ counterpart by 12.91% and $L_1$ function by 6.65%; for 1998-2004 return with $L_6$ function minimization was superior to $L_2$ minimization by 1.32% and $L_1$ function by 20.63%. Return of TLRN minimizing $L_6$ function for 2000-2004 series outperformed $L_2$ minimization by 57.17% and $L_1$ function by 27.35%.

If returns of MLP with $L_2$ and $L_1$ functions minimizations were losing to B/H strategy (by 10.85% and 4.59% respectively), the performance of $L_6$ loss minimization has beaten B/H strategy by 2.06% for 7 years series. Returns of TLRN with $L_2$ and $L_1$ functions minimizations were inferior to B/H strategy by 50.67% and 20.87% respectively, where performance of $L_6$ loss minimization was superior to B/H by 6.48% for 3.5 years series. For the same time horizons and ANN topologies, strategies developed with $L_6$ loss minimization were less risky than strategies created with $L_2$ and $L_1$ functions. For instance, SR of strategies with $L_6$ minimization were superior to their competitors in all cases, except one, where risk exposures were equal. Profitability of ANN trained with $L_6$ loss function seems to be stable for multiple independent runs with different random seeds. Table 1, comparing profitability of strategies developed with $L_6$, $L_2$ and $L_1$ loss minimization for three ANN and training periods, demonstrates that strategies with $L_6$ loss minimization generally perform better than those obtained with $L_2$ or $L_1$ functions.

**Table 1.** Profitability of strategies developed with $L_6$, $L_2$ and $L_1$ functions

| Measures/Settings | 1997-2004 MLP | | | 1998-2004 MLP | | | 2000-2004 TLRN | | |
|---|---|---|---|---|---|---|---|---|---|
| Loss Functions | $L_6$ | $L_2$ | $L_1$ | $L_6$ | $L_2$ | $L_1$ | $L_6$ | $L_2$ | $L_1$ |
| Annual Return (%) | 76.75 | 63.84 | 70.10 | 62.09 | 60.77 | 41.46 | 81.17 | 24.02 | 53.82 |
| Sharpe Ratio | 0.16 | 0.12 | 0.15 | 0.12 | 0.12 | 0.10 | 0.14 | 0.06 | 0.12 |

Regarding statistical accuracy of trading strategies, the results were different depending on the ANN topology. MLP with seven (six) years of data, minimizing $L_6$ function, produce results superior to $L_2$ function by 16.66% (0.43%) and to $L_1$ function by 14.76% (10.73%). Accuracy of TLRN with 3.5 years of data, minimizing $L_6$, was inferior to $L_2$ function by 22.51% and $L_1$ function by 22.95%.

Considering price forecasts, accuracy with minimizing $L_6$ function is on average among the best 5%. In fact, a forecast based on $L_6$ loss minimization was the only one that was used in a trading strategy superior to B/H benchmark. Forecasts with $L_2$ minimization slightly underperforms, but is still among the best performing 20%. At the same time $L_1$ function minimization produces top accuracy, as well as being one of the worst performers. If the accuracy of forecast of MSE loss minimization is on average superior to the accuracy of MAE loss minimization, annualized return of trading strategies, based on those forecasts are close to each other. Furthermore, performance surface based only on $L_1$ or $L_2$ loss minimization does not generate profitable strategies.

The results produced with the $L_\infty$ loss minimization are close to the average. At the same time, the detailed examination of the performance surface demonstrates that $L_\infty$ minimization might be appropriate for multi-objective optimization. A natural path for future work is to apply multi-objective GA for this kind of problem. The results of the experiment do not support (Leitch and Tanner 2001) hypotheses that the accuracy of the forecast does not depend upon which error-criteria is used. Unlike $L_2$ and $L_1$ loss minimizations, models with $L_6$ loss functions display strong relationship with the profitability of the forecast.

## Conclusion

The mapping of economic agents' risk preferences into their predictions reveals strong relationships between the value of risk aversion coefficient in loss function minimization and stock trading strategies' economic performances, as well as moderate relationships between a loss function's order and statistical characteristics. Unlike $L_2$ and $L_1$ loss functions minimization, models with $L_6$ error-criterion demonstrate robust relationships with profitability. Traders with CRRA display superior fitness in the short term through their portfolio rules.

ANN and GA have proven to be useful tools in financial data mining, capable of learning key turning points of price movement with the classification of the network output as different types of trading signals. Learning the mapping of forecasts into strategies establishes the predictive density that determines agents' actions and utility of wealth associated.

## References

Sweeney, R. J. (1988) Some Filter Rule Tests: Methods and Results. Journal of Financial and Quantitative Analysis 23: 285-301.

Chen S.-H and Huang Y.-C. (2003) Simulating the Evolution of Portfolio Behavior in a Multiple-Asset Agent-Based Artificial Stock Market. CEF, Washington, USA.

Leitch G. and Tanner E (2001) Economic Forecast Evaluation: Profits Versus the Conventional Error Measure. American Economic Review 81: 580-590.

# Time series of stock price and of two fractal overlap: Anticipating market crashes?

Bikas K. Chakrabarti[1], Arnab Chatterjee[2] and Pratip Bhattacharyya[3]

[1] Theoretical Condensed Matter Physics Division and Centre for Applied Mathematics and Computational Science, Saha Institute of Nuclear Physics, Block-AF, Sector-I Bidhannagar, Kolkata-700064, India.
bikas@cmp.saha.ernet.in
[2] arnab@cmp.saha.ernet.in
[3] pratip@cmp.saha.ernet.in

We find prominent similarities in the features of the time series for the overlap of two Cantor sets when one set moves with uniform relative velocity over the other and time series of stock prices. An anticipation method for some of the crashes have been proposed here, based on these observations.

## 1 Introduction

Capturing dynamical patterns of stock prices are major challenges both epistemologically as well as financially [1]. The statistical properties of their (time) variations or fluctuations [1] are now well studied and characterized (with established fractal properties), but are not very useful for studying and anticipating their dynamics in the market. Noting that a single fractal gives essentially a time averaged picture, a minimal two-fractal overlap time series model was introduced [2, 3, 4].

## 2 The model

We consider first the time series $O(t)$ of the overlap sets of two identical fractals [4, 5], as one slides over the other with uniform velocity. Let us consider two regular cantor sets at finite generation $n$. As one set slides over the other, the overlap set changes. The total overlap $O(t)$ at any instant $t$ changes with time (see Fig. 1(a)). In Fig. 1(b) we show the behavior of the cumulative overlap [4] $Q^o(t) = \int_0^t O(\tilde{t})d\tilde{t}$. This curve, for sets with generation $n = 4$, is approximately a straight line [4] with slope $(16/5)^4$. In general, this curve approaches a strict straight line in the limit $a \to \infty$, asymptotically, where the overlap set comes from the Cantor sets formed of $a - 1$ blocks, taking away

the central block, giving dimension of the Cantor sets equal to $\ln(a-1)/\ln a$. The cumulative curve is then almost a straight line and has then a slope $[(a-1)^2/a]^n$ for sets of generation $n$. If one defines a 'crash' occurring at time $t_i$ when $O(t_i) - O(t_{i+1}) \geq \Delta$ (a preassigned large value) and one redefines the zero of the scale at each $t_i$, then the behavior of the cumulative overlap $Q_i^o(t) = \int_{t_{i-1}}^{t} O(\tilde{t})d\tilde{t}$, $\tilde{t} \leq t_i$, has got the peak value 'quantization' as shown in Fig. 1(c). The reason is obvious. This justifies the simple thumb rule: one can simply count the cumulative $Q_i^o(t)$ of the overlaps since the last 'crash' or 'shock' at $t_{i-1}$ and if the value exceeds the minimum value ($q_o$), one can safely extrapolate linearly and expect growth upto $\alpha q_o$ here and face a 'crash' or overlap greater than $\Delta$ (= 150 in Fig. 1). If nothing happens there, one can again wait upto a time until which the cumulative grows upto $\alpha^2 q_o$ and feel a 'crash' and so on ($\alpha = 5$ in the set considered in Fig. 1).

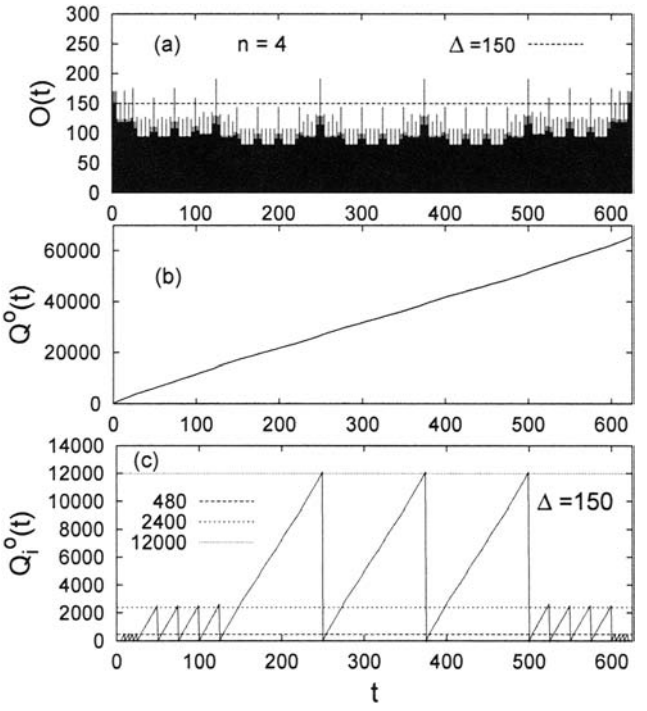


**Fig. 1.** (a) The time series data of overlap size $O(t)$ for a regular Cantor set of dimension ln4/ln5 at generation $n = 4$. (b) Cumulative overlap $Q^o(t)$ and (c) the variation of the cumulative overlap $Q_i^o(t)$ for the same series, where $Q$ is reset to zero after any big event of size greater than $\Delta = 150$.

We now consider some typical stock price time-series data, available in the internet [6]. In Fig. 2(a), we show that the daily stock price $S(t)$ variations for about 10 years (daily closing price of the 'industrial index') from January 1966 to December 1979 (3505 trading days). The cumulative $Q^s(t) = \int_0^t S(t)dt$ has again a straight line variation with time $t$ (Fig. 2(b)). We then define the major shock by identifying those variations when $\delta S(t)$ of the prices in successive days exceeded a preassigned value $\Delta$ (Fig. 2(c)). The variation of $Q_i^s(t) = \int_{t_{i-1}}^{t_i} S(\tilde{t})d\tilde{t}$ where $t_i$ are the times when $\delta S(t_i) \leq -1$ show similar geometric series like peak values (see Fig. 2(d)).

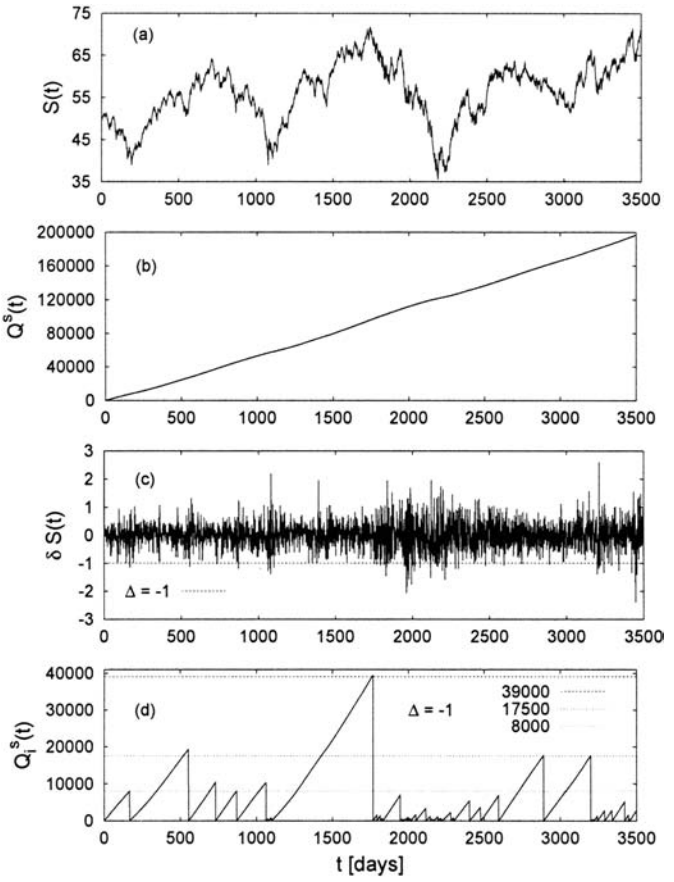


**Fig. 2.** Data from New York Stock Exchange from January 1966 to December 1979: industrial index [6]: (a) Daily closing index $S(t)$ (b) integrated $Q^s(t)$, (c) daily changes $\delta S(t)$ of the index $S(t)$ defined as $\delta S(t) = S(t+1) - S(t)$, and (d) behavior of $Q_i^s(t)$ where $\delta S(t_i) > \Delta$. Here, $\Delta = -1.0$ as shown in (c) by the dotted line.

A simple 'anticipation strategy' for some of the crashes may be as follows: If the cumulative $Q_i^g(t)$ since the last crash has grown beyond $q_0 \simeq 8000$ here, wait until it grows (linearly with time) until about $17,500$ ($\simeq 2.2q_0$) and expect a crash there. If nothing happens, then wait until $Q_i^g(t)$ grows (again linearly with time) to a value of the order of $39,000$ ($\simeq (2.2)^2 q_0$) and expect a crash, and so on.

## 3 Summary

The features of the time series for the overlap of two Cantor sets when one set moves with uniform relative velocity over the other looks somewhat similar to the time series of stock prices. We analyze both and explore the possibilities of anticipating a large (change in Cantor set) overlap or a large change in stock price. An anticipation method for some of the crashes has been proposed here, based on these observations.

## References


1. Sornette D (2003) Why Stock Markets Crash? Princeton Univ. Press, Princeton; Mantegna RN, Stanley HE (1999) Introduction to Econophysics. Cambridge Univ. Press, Cambridge
2. Chakrabarti BK, Stinchcombe RB (1999) Physica A 270:27-34
3. Pradhan S, Chakrabarti BK, Ray P, Dey MK (2003) Phys. Scr. T106:77-81
4. Pradhan S, Chaudhuri P, Chakrabarti BK (2004) in Continuum Models and Discrete Systems, Ed. Bergman DJ, Inan E, Nato Sc. Series, Kluwer Academic Publishers, Dordrecht, pp.245-250; cond-mat/0307735
5. Bhattacharyya P (2005) Physica A 348:199-215
6. NYSE Daily Index Closes from http://www.unifr.ch/econophysics/.

# Short Time Segment Price Forecasts Using Spline Fit Interactions

Ke Xu[1], Jun Chen[3], Jian Yao[1], Zhaoyang Zhao[1], Tao Yu[1], Kamran Dadkhah[2] and Bill C. Giessen[1]

[1]Department of Chemistry and Chemical Biology and Barnett Institute, Boston, MA 02115, USA
[2]Department of Economics, Northeastern University, Boston, MA 02115,USA
[3]Bloomberg LP, 499 Park Ave, New York, NY 10022, USA

**Summary**. Empirically, correlations are seen to exist between market action in specific, short market periods such as the AM, PM and overnight (ON) periods for different days of the week on the one hand and market trends (on various time scales) on the other hand. We use real-time spline fits with tunable smoothness parameters and their signs to obtain signals for these market periods and show that they are stationary (and tradable) for S&P 500 futures.

**Key words.** Intraday periods, Overnight periods, S&P 500 Futures, Price prediction, Spline fits

## Introduction

As part of a futures market analysis research program centering on the identification and optimization of nonrandom futures market features, [1, 2] price movements (local movement (LM) in the following) occurring in suitable, well-defined intra-day periods [such as morning (AM) and afternoon (PM)] and overnight periods (ON) were studied. We have investigated whether LM's follow non-random and possibly tradable patterns, either by themselves or after sorting by suitable criteria.

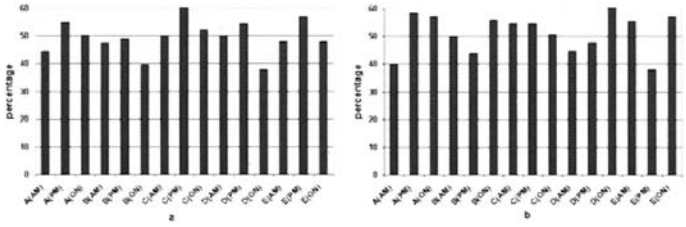

**Fig. 1.** Percentage of up-move price changes for S&P 500 during the 15 LM periods, defined in the text. a) up-move percentages in the training period 01/2001-01/2004; b) up-move percentages in the testing period 01/2004-01/2005.

The five week days (designated A-E) will yield a total of 15 such defined time periods, designed as A(AM), A(PM) etc., as shown on the abscissa of Fig.

1. Since the asymmetry of price changes (up-moves, $\Delta P_u$ or down-moves, $\Delta P_d$) during these periods is the substance of the study, the percentage of up- move price changes ($\Delta P_u$ / ($\Delta P_u$ +$\Delta P_d$)) is obtained and plotted in Fig 1a for the three-year period. Considerable variations are seen in these percentages which would be tradable if they were stationary. However, data for a subsequent test period 01/2004-01/2005 (Fig 1b) shows that this is not the case; thus, a suitable sorting procedure is required to obtain consistency through time.

Based on the insight that both long-term and short-term market movements will influence the LM's and might do so in a stationary way, we present a sorting procedure based on spline fits with selected, optimized smoothness combinations.

## Methodology

Splines: Dual spline fits (using the Matlab toolbox[6]) were made; optimization of the smoothness parameters of the fits is described below. The signs of the two fits at the beginning of each of the 15 LM periods for S&P 500 were recorded during the training period (01/2001-01/2004). It is emphasized that the spline fits used in this stage of the study utilized the total historic database, thus including the "future" at each time point of decision; therefore, the results are valid only to establish the correlation of LM price action with the signs of the spline fit combination, but have only limiting forecasting value.

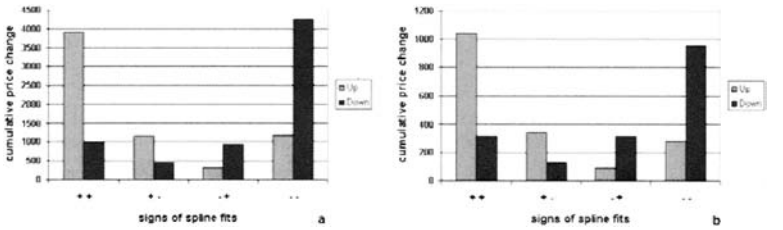


**Fig. 2.** Differentiation of S&P 500 up-moves and down-moves during LM periods after sorting by double spline fit signs. Spline fits are idealized. a) Results during training period 01/2001-01/2004. b) Results during testing period 01/2004-01/2005.

Fig. 2 summarizes the total of the market price changes of all 15 LM's occurring during the learning period, after sorting by these spline fit sign combinations. It is seen that the sorting procedure (with the proviso given above concerning the real-time validity of the spline fits) produces an extremely strong separation of directional movement in the 15 LM's.

Parameter optimization: Fig. 3 shows the process and result of optimizing the spline fit parameters combination used; the optimum for this dataset is seen to occur for fits with smoothness parameters of -9 and -6 (on a log scale). A comment on this result is given in the discussion section.

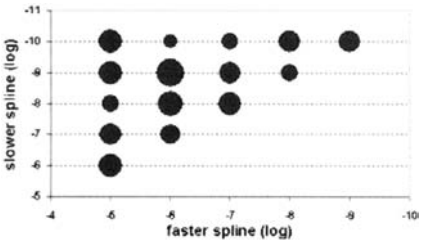


**Fig. 3.** Optimization of smoothness parameter combinations for spline fits used to control LM trade direction. The area of a circle stands for the magnitude of CPL (=P-|L|).

Furthermore the selection threshold can be tuned so as to include more or less strongly discriminating spline combinations for specific LM's, as shown in Fig. 4. Return is measured by the cumulative profit-loss, CPL=P-|L|, and risk avoidance is measured by a stand-in, the figure of merit, FOM= P/ (P+|L|); it is seen that, compared to a relatively unselective threshold (e.g. thr = 0.55), a more selective threshold (e.g. thr = 0.65) would increase the FOM from 0.63 to 0.71 but reduce the CPL from 2,200 to 1,100 S&P units.

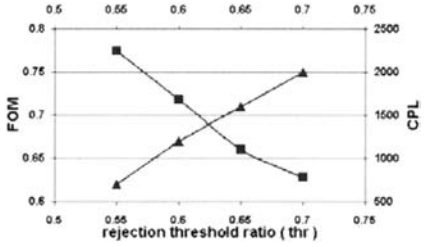


**Fig. 4.** Dependence of net profit (CPL, squares, right scale) and risk avoidance (FOM, triangles, left scale) on the rejection ratio (thr).

## Results

Training period: Table 1a-c summarizes the results obtained for the period 01/2001-01/2004, using it both as a training and a "self"-testing period. It is realized, of course, that this procedure has no probative value concerning stationarity; however, it is used to demonstrate the existence of correlations within the data which is a precondition for a successful stationary test.

Table 1a shows quantitatively the existence of market action differences within the 15 LM periods ("global" result) without the additional benefit of the sorting procedure proposed here; however, as shown below, this result is not stationary.

Table 1b shows the effect of sorting by an idealized spline fit (i.e., a fit using the local future to smoothen the fit). The resulting differentiation of long and

short trades is extremely strong, as expressed by the large CPL and FOM values; however, the idealized spline fits used here can not be obtained in real time.

Table 1c shows the results obtained with real-time (i.e., noisy) spline fits as sorting method. These results are good, but still not realistic in that the 3-year learning and testing periods have been identical.

Table 1: Annualized trading results by CPL and FOM for 15 LM periods during the training period 01/2001-01/2004.

a) Results without further sorting

| | CPL | FOM | % Ideal |
|---|---|---|---|
| Long | 209.8 | 0.55 | 11.5 |
| Short | 272.1 | 0.55 | 10.0 |

b) Results with idealized spline fit sorting

| | CPL | FOM | % Ideal |
|---|---|---|---|
| Long | 1227.9 | 0.77 | 55.1 |
| Short | 1290.2 | 0.77 | 55.9 |

c) Results with real-time spline fit sorting

| | CPL | FOM | % Ideal |
|---|---|---|---|
| Long | 322.1 | 0.61 | 22.9 |
| Short | 356.3 | 0.63 | 25.8 |

Testing period: We now focus on the last and major capstone of our study, the demonstration of stationarity, i.e., the usefulness of the sorting approach presented here, tested by using sorting rules learned in the training period, and applying these rules to a more recent testing period.

Table 2: Results of forecasting price movements for the 15 LM periods during the testing period 01/2004-01/2005, using trading signals derived from the training period, as documented in Table 1.

a) Results without further sorting

| | CPL | FOM | % Ideal |
|---|---|---|---|
| Long | 1.1 | 0.50 | 0.1 |
| Short | -56.6 | 0.35 | -6.4 |

b) Results with idealized spline fit sorting

| | CPL | FOM | % Ideal |
|---|---|---|---|
| Long | 607.6 | 0.71 | 42.7 |
| Short | 503.2 | 0.68 | 36.9 |

c) Results with real-time spline fit sorting

| | CPL | FOM | % Ideal |
|---|---|---|---|
| Long | 164.3 | 0.58 | 17.1 |
| Short | 29.2 | 0.51 | 3.3 |

Table 2a-c is organized analogously to Table 1a-c and compares learned global trading and learned sorted trading for this testing period (01/2004-

01/2005). Global trading (without sorting) is carried out using learning from the previous 3-year training period, i.e., using sorting into the 15 LM periods only (without using spline fits); the results appears to be random, demonstrating non-stationarity of these data. However, spline fit sorted trading, using the parameters and decision algorithms derived from the learning period gives the second set of results, in Table 2b, and trading by realistic spline fits (as described above), provides the third data set, Table 2c.

## Discussion

Bearing in mind that the market had an upward bias of 107 points during the test period (reflected in the much larger "long" revenue) the results (Table1c) for real-time spline fit sorts in the testing period are excellent, yielding a CPL total of 193 S&P points (annualized), again without commission and slippage. The ability to obtain an average FOM of 0.55 by a procedure as automated and reproducible as this one confirms the fact that the spline fits used indeed tap into real market dynamics which are reflected by the price action in the 15 LM's; at the same time the returns confirm that the individual LM's have different characters and behaviors in the market. This aspect is under further study, particularly with respect to possible correlations between successive LM's.

We also observed that sorting the LM data according to market cycle phase combinations produces similar, outstanding results (cycles and their analysis are discussed in a companion paper in this volume[5]). The spline fitting procedure used here in fact simulates these cycles, but was preferred for this presentation because of the transparency of the process and the ready reproducibility of the spline fits.

We thank Cambridge Market Analysis Corporation (CMAC) for financial support.

## References

1. Mantegna, R. N. and Stanley, H. E., An Introduction to Econophycis: Correlation and Complexity in Finance, Cambridge: Cambridge University Press (2000).
2. Murphy, J. J., Technical Analysis of Futures Markets, New York: New York Institute of Finance (1999).
3. Lo, A., Mamaysky, H., and Wang, J., "Foundations of Technical Analysis: Computational Algorithms, Statistical Inference, and Empirical Implementation", *The Journal of Finance,* Vol. LV, No. 4, 1705-1765 (2000).
4. Jun Chen, Ph.D. Thesis, Northeastern University, Boston, MA (2003).
5. Yao, J., Chen, J., and Xu, K., Zhao, Z., Yu, T., Giessen, B., Dadkhah, K., Market Cycle Turning Point Forecasts by an Interactively Learning Algorithm as a Trading Tool for S&P Futures, "Practical Fruits of Econophysics", editor H.Takayasu, Springer, Tokyo (2005).
6. The Mathworks, Inc., Framingham, MA (2004).

# Successful Price Cycle Forecasts for S&P Futures Using TF3, a Pattern Recognition Algorithms Based on the KNN Method

Bill C. Giessen, Zhaoyang Zhao, Tao Yu, Jun Chen[1], Jian Yao and Ke Xu

Department of Chemistry & Chemical Biology and Barnett Institute
Kamran Dadkhah, Department of Economics, Northeastern University, Boston, MA 02115, U.S.A
[1]Now with Risk Management, Bloomberg LP, 499 Park Ave, New York, NY 10022, U.S.A

**Summary.** Basing on the perceived stationary internal structure of market movements on appropriate time scales, a series of interrelated pattern recognition programs was designed to compare specific features of current cycle "legs" with a selected universe of analogous prior market features periods which are then queried to obtain a prediction as to the future of the current cycle leg. Similarities are determined by a K-Nearest-Neighbor (KNN) method. This procedure yields good results in simulated S&P futures trading and demonstrates the hypothesized stationary of market responses to stimuli.

**Key words.** Pattern Recognition by KNN method, Stationarity of market structure, Semiweekly cycle in S&P Futures, Prediction price turning point

## Introduction and Rationale

Technical analysis of futures markets over various time scales, as generally described, postulates that the market has a memory for past events that affect its future. The analyst's task then is to locate which aspects of past market action have relevance in terms of future price action.

In the following, we focus on two specific aspects that we demonstrate in this paper to have predictive qualities if used in conjunction:

- Recent market movements (as explained below);
- Patterns of market response to similar stimuli,

Of these, the former refers to short-term chart patterns such as weekly or semiweekly cycles (In a companion paper[1], the important role of price cycle analysis[2] in our research program on non-random aspects of futures pricing was discussed, relevant cycles[3] were listed and a generic method for forecasting cycle extrema ("tops and valleys") was presented and shown to produce profitable trades). Specifically, the most recent such market cycle is seen as relevant to cyclic market action in the immediate future.

The second, deeper and more fundamental aspect of market predictability is based on the notion that market dynamics represent the collective behavior of multiple decision makers, and can be viewed as a natural phenomenon (analogous to the subjects of the physical sciences), with a statistical internal response structure amenable to analysis and use.

Thus, a current cycle (the "now"-cycle in the parlance of the present paper) can be placed into the context of its historical analogs; from this database, those analogs most "like" the now-cycle in terms of relevant, short-term contexts (discussed in the following) and other aspects of market history can then be identified by pattern recognition methods. In this paper, we choose to use the ½-week cycle (C2), which bisects the fundamental weekly cycle (C5) and which we observe to occur fairly reliably in oscillating markets, being "washed out" only in the most strongly trending markets.

## Methodology

We briefly sketch the market analytical procedure applied and refer to the KNN method of pattern analysis as it is used, e.g., in chemometric practice[4].

As short-term memory-bearing classification parameters of the present market, we use characteristics (price changes and lengths in time) of cycle "leg" market periods immediately preceding the present point in time. For classification, we have designed a family of pattern recognition algorithms designated as TFX. The members of the TFX family of algorithms differ in the specific characteristics chosen (the "markers"), the manner of pattern analysis, and the forecast values sought; as a demonstration, we describe and demonstrate here the use of a specific method, named TF3.

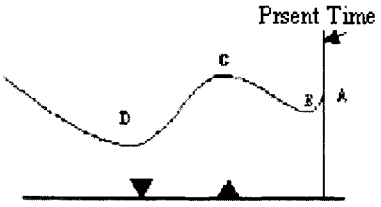


**Fig. 1**.Present time (A) and cycle extrema (B-D) used in TF3 Analysis

**Market Markers Used:** Fig. 1 describes the specific market situation to be analyzed and the markers used in the TF3 analysis. The present point in time, the "now" point, is marked as A; recent market action in a two-day cycle is idealized as an "up-leg" DC from a market bottom D to a top C, and a subsequent "down-leg" CB. It is assumed that both points D and C have been confirmed by subsequent market movements and can be considered to be known at the time $t_A$. It is further assumed that a small upturn BA has taken place, moving the market back up to A from a possible bottom B.

The objective of the analysis to be described is to obtain guidance from historic analogs as to whether BA is merely a fluctuation in the down-leg that began at C (which would then again resume its downward slope beyond B) or whether B was indeed the bottom point of the cycle begun at D, which would mean that the up-leg of a new cycle has begun at B.

**KNN Method Used:** In the TF3 type of analysis, the price changes in the cycle leg DC, the leg CB, and the segment BA are combined to form two dimensionless ratios X and Y, where X = ΔP(AB)/ ΔP(CB) and Y = ΔP(CB)/ ΔP(CD). These ratios are then used as coordinates of an X-Y plot (Fig. 2). This plot contains analogous ratios for analogous cycles from a historic database. As mentioned, we are then seeking guidance from this database for an optimal exit from a short trade which was in progress since point C (or some point before or after C).

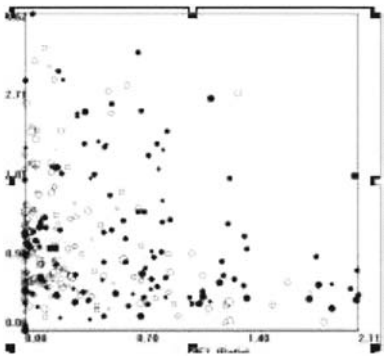

**Fig. 2.** TF3 plot of historic X, Y ratios and current ratio with KNN selector ellipse

The meaning of the points in this plot is as follows: historic cycles which at this point (at B) of their history have already passed their "bottom" are marked in closed circles; those cycles for which this event still lies in the future are marked in open circles. It is seen that open and closed circles are clustered in specific, different regions of the plot, indicating that similar histories predict similar futures, i.e. implying predictivity of the method. The "present-case" point is shown in the plot by a solid rectangle; a surrounding larger circle (shown in Fig. 2, scaled, as an ellipse) is drawn so as to enclose K neighbors (the cohort).

The market histories of these K analogs (here K = 10, see optimization procedure, below) are then retrieved and plotted against time; in this plot (not shown) the times are marked when these analogs either have already reached their last bottom (closed circles in Fig.2) or will reach their next one (open circles). Averaging these historic analogous time periods provides the time signal to terminate the current trade (a "short" in the present instance) and to initiate the reverse trade; the current trade is terminated when the computed time period average passes from a positive value through zero.

The averaged time period (still positive in the case shown) is also indicated by a box in a chart segment (Fig. 3) given here as an example. This chart segment

provides a three-week sample of trades conducted by the rule cited (solid lines=correctly predicted long or short trades, dashed lines = incorrect predictions).

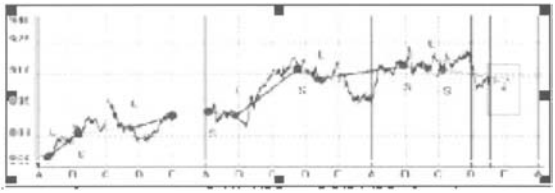

**Fig. 3.** S&P futures charts segment 04/14/03 to 05/01/03 showing program-initiated trades (solid lines, correct longs and shorts; dash lines, incorrect long and shorts) and prediction point (at right)

**Refinement of Cohort Size K:** It is obvious that the value of K, the cohort size, plays a crucial role: too small a value of K will give poor statistics while too large a value will include too many dissimilar points, i. e., past points with inconsistent, non-comparable histories. This is borne out by the results of the refinement study presented here.

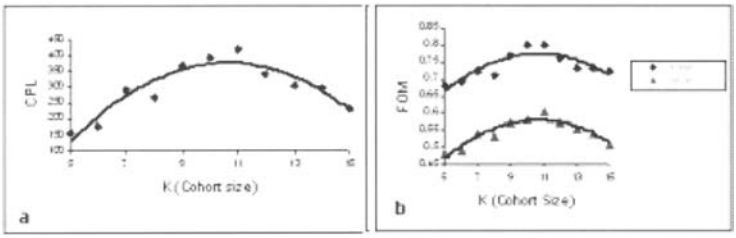


**Fig. 4.** Optimization of CPL (a) and FOM (b) for TF3

Repetition of the total study procedure, with values of K varied from 5 to 15, yields the plots, Fig. 4a (for the cumulative profit/loss, CPL = Profit-|Loss|) and Fig. 4b (for the figure of merit, FOM=Profit/(Profit+|Loss|)) (see caption of Table 1 for these terms) and shows a consistent broad maximum of these optimized quantities at K=11; a value of K=10 was used in this study.

## Results and Discussion

**Results:** Testing as described above was applied in a simulated trading mode (i. e., with a "now"-point moving in simulated time as it would in real time, i.e. with a future unknown to the program).

Table 1(a, b) shows a total return (CPL) of 391.9 S&P points resulting from 183 trades (before commissions and slippage), obtained with high consistency, as measured here by the figure of merit (FOM). Comparison of the CPL to that from

an idealized two-day cycle trading process (using after-the-fact information for this comparison process) shows a profit of 26.5% of the maximum achievable by such trading. In order to establish the consistency of results that can be obtained by the TF3 method, (i.e., stationarity), another, most recent six-months period was chosen for a recheck by the same approach, with results shown in Table 1(c, d).
**Discussion:** The results presented in Tables 1(a, b) and, to a lesser degree, those in Table 1(c, d), are truly remarkable, if it is considered that no other input was used than the algorithm presented and a cycle database resetting program analogous to that described in Ref 1.

**Table 1.** TF3 Trading results 04/03-01/04: a, b; 09/04-02/05: c, d.

| | CPL | FOM | CPL/Ideal Profit |
|---|---|---|---|
| a. Long | 297.3 | 0.80 | 29.03% |
| b. Short | 94.6 | 0.58 | 12.31% |
| c. Long | 93.8 | 0.68 | 19.76% |
| d. Short | 6.3 | 0.51 | 1.65% |

During both test periods, the market strongly and consistently rises by 250 S&P points, suggesting that long trades will fare better during this period, as indeed observed. It is especially satisfying that the program does not lose money (but achieves a small profit) even in the short trade "counter-trend" direction. While the return on the long side is not appreciably better than the result of a correctly executed buy-and-hold strategy, the procedure shown here achieves this result without the inherent speculation and high risk of such a strategy.

In assessing these results, it should also be borne in mind that the TF3 method described is, intrinsically, a trailing indicator and can therefore not deliver the optimal results we believe the full family of TFX signals is capable of capturing.

The results of this study show that the internal market structure is, to a remarkable degree, stationary, and, with tools amenable to further refinement as shown, can be sensed successfully.

We thank Cambridge Market Analysis Corporation (CMAC), Cambridge, MA for sponsorship.

## References

1. Jian Yao, et al. Market Cycle Turning Point Forecasts by an Interactively Learning Algorithm as a Trading Tool for S&P Futures, "Practical Fruits of Econophysics", Editor, H. Takayasu, Springer, Tokyo
2. Murphy J. J., Technical Analysis of Futures Markets, New York: New York Institute of Finance (1999)
3. Jun Chen, Ph.D. Thesis, Northeastern University, Boston, MA (2003)
4. M. Otto, Chemometrics: Statistics and Computer Application in Analytical Chemistry, WILEY-VCH, New York (1999).

# The Hurst's exponent in technical analysis signals

Giulia Rotundo

Department of Business, Technological and Quantitative Studies, University of Tuscia, via del Paradiso 47, 01100 Viterbo, Italy

**Summary.** The fractal nature of financial data has been investigated through literature. The aim of this paper is to use the information given by the detection of the fractal measure of data in order to provide support for trading decisions when dealing with technical analysis signals that can be used to trigger buy/sell orders. Trendlines are considered as a case study.

**Key words.** Fractals, Technical analysis, Financial markets

## Introduction

Market operators often address their buy/sell orders on the basis of decision support systems. Technical analysis methods concern the detection of signals that involve particular patterns of mean reversion of data. To determine the best trading strategy still remains an art, but it can be improved by a deeper knowledge of market phenomena, like the occurrence of brownian motion and of fractional brownian motion that is been widely evidenced through the literature. Whilst the efficient market hypothesis can be validated as a good approximation across markets it concerns an idealized system and residual inefficiences are always present, especially on financial quantities on time scales longer than a month, and not only in high frequency data (Mantegna and Stanley 2000).
This can explain the fact that the estimated degree of long memory of the Dow Jones time series (Ausloos and Ivanova 1999) fall into a range that could comprehend brownian motion as well as persistent and antipertistent behavior.
However there exist cases like Gold and of BGL-USD (Ausloos and Ivanova 1999) that show persistence, whilst the analysis of Italian share FIAT (Menna et al. 2002) exhibits antipersistence over a long period.
It has been shown that speculative bubbles due to endogenous causes are characterized by a super exponential growth with log-periodic corrections to scaling (Johansen and Sornette 2004), thus allowing to perform forecast, in contrast with the brownian motion settings.

During the arise and the deflate of endogenous bubbles it is possible to determine the main growing trend and to detect the causality in the log-periodic part that leads to the reversion to the main trend.
The aim of this paper is to explore the reliability of some technical analysis signals by estimating the probability to get some particular configurations that are used by market operators to trigger the buy/sell signals in the case that data obey a fractional brownian motion measured through the exponent of Hurst $H$. The attention is about the occurrence of the crossing of trendlines over periods that have a time length that can range from a minimum of three weeks to a maximum of several months. Trends of this duration are called intermediate trends and can be useful for future markets. The analyses are performed over closure values of a market index, as assessed by the Dow's theory. The occurrence is examined during the ascent phase of a speculative bubble. The exponent of Hurst can be measured as a global feature of time series and the brownian motion is included in the treatment as a particular case and as a comparison term.

## Theoretical probability bounds for fBM

Let $B_H(t)$ be the fractional brownian motion (fBM) with parameter $H$. For $1/2 < H < 1$, the fBM exhibits long term persistence and memory, whilst antipersistence is characterized by $0 < H < 1/2$. The particular case $H = 1/2$ corresponds to brownian motion. Let $X(t)$ be either a a fBM $B_H(t)$ or a scaled brownian motion $S_H(t) = B(t^{2H})$, and define $A(X,c) = \sup\{X(t) - ct : t \geq 0\}$.
The following results hold (Dębicki et al. 1998):
$P(A(B_H,c) > u) \leq P(A(S_H,c) > u) \quad \forall u \geq 0,\ 1/2 \leq H < 1$
$P(A(B_H,c) > u) \geq P(A(S_H,c) > u) \quad \forall u \geq 0,\ 0 \leq H < 1/2$
The distribution of the suprema of a brownian motion with drift obeys the law
$P(A(B_{1/2},c) > u) = \exp(-2cu) \quad \forall u \geq 0$ (Borodin and Salminen 1996)
An analogous result holds for the scaled brownian motion (Dębicki et al. 1998)
$$P(A(S_H,c) > u) \geq \exp(-2au^{2-2H}) \quad \forall u \geq 0,\ a = \frac{1}{2}\left(c/H\right)^{2H}\left(1/\left(1-H\right)\right)^{2-2H}$$
that allows to provide bounds for the probability that a fractional brownian motion with drift crosses a fixed level.

## Technical analysis signals: trendlines

Technical analysis studies the reaction of financial agents to market conditions than can be detected through the study of charts (Murphy 1986). Several signals were pointed out as good indicators for the triggering of buy/sell orders, the most simple of them being the crossing of a fixed level. Automatic trading running

overnights without control and relying on the simple rule of selling when a lower threshold is crossed sometimes led to big and dangerous drops, and so it is important to analyze the probability of the occurrence of signals.
One of the most easy technical instrument is the trendline. A upward trendline is a straight line that joints successive minima. A downward trendline is a straight line that joints successive maxima. Thus at least two successive minima or maxima are needeed. In order to identify a minimum [maximum] a technical analyst must be sure that a reaction low has been reached, thus he has to wait for a significant increase [decrease] to start. A trendline is more important as more it lasts and its breaking will be more significant. For short time trendline can be considered broken if prices go under or over it for more that 3% over the closure price.

## Numerical results

In this paper the NASDAQ index is examined during the raise of the bubble that started since the beginnings of 1997 and ended in the large crash of April 2000.
The behavior of the logarithm of the index can be approximated by several function. The following approximation

$$y(t) = A + B(t - t_c)^m$$

is considered for the main trend. The values for the parameters $A = 9.36$, $B = -1.60$, $m = 0.26$ and $t_c$ corresponding to April 11$^{th}$, 2000 are obtained by the minimum least squares method (Rotundo 2004). In order to proceed with the long term memory degree estimate it is necessary to deal with a stationary series, thus the logarithm of the NASDAQ has been detrended. Let $\{x(t)\}_t$ be the detrended series. It is worth noting that persistence is not due to a global growth but to the internal order on the values of the series. It is well known that the spectrum of stationary processes with long range memory can be approximated in the neighborhood of the zero frequency as $S(f) \propto f^{-\alpha}, 1 < \alpha < 3, f \to 0^+$ .
The exponent $\alpha$ measures the fractality of the system and it is connected to the Hurst exponent H that describes the degree of dependence among the increments of the analyzed process. The relation $H = (\alpha - 1)/2$ holds. These statistics detect the frequency of trend inversion. On the detrended time series it results that $H = 0.51$ since Jan.1$^{st}$,1997 till Dec. 15$^{th}$, 1998, then $H = 0.46$ till Dec. 8$^{th}$, 1999 and $H = 0.43$ till the crash. This analysis thus reveals correctly the increase in the frequency of the reversion patterns. Intermediate downward trendline were detected over the periods characterized by different long term memory by a least squares method over at least three successive maxima. The analysis for upward trendlines can be carried on analogously. For each trendline $T(t) = ct + d$ the time series $v(t) = x(t) - T(t)$ is a brownian motion with drift. The trendline $T(t)$ is crossed when the supremum of the process $v(t)$ goes over the level $0$. The

probability estimates of the crossings are resumed in Table 1. The time is measured through the discrete units [1,833]. In the region in which $H = 0.51$ the results are close to the brownian case. Thus it is possible to access to the well developed theory (Borodin and Salminen 1996) that estimates the probability of crossings also as a function of the time, hence providing a strong indication for the ending time of the trend. The detaching from the brownian motion evidences as soon as the process switches to $H = 0.46$, and even more in the case $H = 0.43$. $P(A(S_H, c) > u)$ thus provides a lower probability bound for $P(A(B_H, c) > u)$, that is constantly lower than the brownian case, leading to the immediate comparison also about the estimation of crossing times.

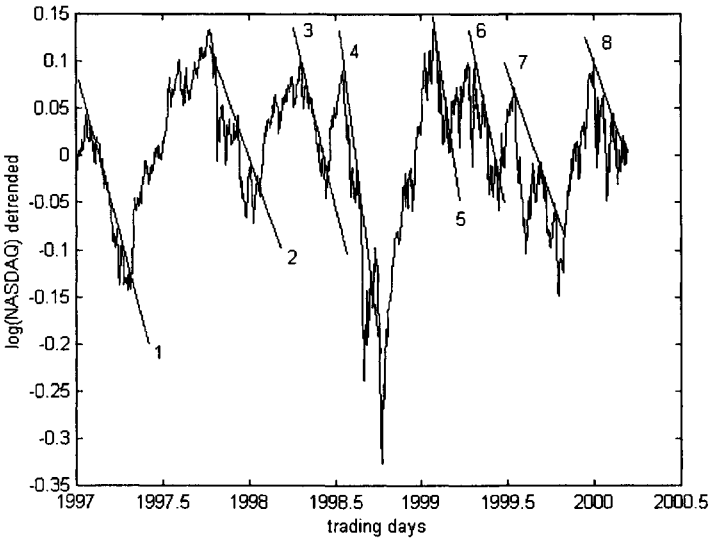


**Fig.1.** The time on the x-axis was rescaled in order to show the years. Lines 1-8 corresponds to the trendlines described in Table 1. Data range from January 1st,1997 to April 11th, 2000.

**Table 1.**Trendlines and probability of crossing.

| N.trendline | $H$ | $c$ | $P(A(B_{1/2}, c) > u)$ | $P(A(S_H, c) > u) \geq$ |
|---|---|---|---|---|
| 1 | .51 | -0.002693 | 0.999318 | 0.999369 |
| 2 | .51 | -0.001991 | 0.997796 | 0.99803 |
| 3 | .51 | -0.003015 | 0.993057 | 0.993836 |
| 4 | .51 | -0.003699 | 0.987651 | 0.989070 |
| 5 | .46 | -0.004860 | 0.994121 | 0.991418 |
| 6 | .46 | -0.002492 | 0.996000 | 0.993699 |
| 7 | .46 | -0.002777 | 0.991671 | 0.986343 |
| 8 | .43 | -0.002067 | 0.993789 | 0.984748 |

## Conclusions

The theory of large financial crashes can lead to the detection of mean reverting patterns among data and to the discover of order through random sequences thus revealing the presence of long term memory. This paper shows how to use the results over the supremum of fractional brownian motion and shifted brownian motion with drift in order to perform a first step towards the probability description for the crossing of trendlines and hence to the measure of the reliability of technical analysis guidelines for pratical decision support. An immediate further development of this research is the analysis of other linear barriers like reference slopes, fan lines, and channels, and of more complex technical analysis pattern, like flags, moving windows averages, head and shoulders, supported by the continuous refinement of probability results over fractional brownian motion.

## References


Ausloos M, Ivanova K (1999) Low q-moment multifractal analysis of Gold price, Dow Jones Industrial Average and BLG-USD exchange rate. Eur. Phys. J. B 8 : 665-669

Borodin A N, Salminen P (1996) Handbook of Brownian Motion - Facts and Formulae. Birkhäuser Verlag Basel

Dębicki K, Michna Z, Rolski T (1998) On the supremum from Gaussian processes over infinite horizon. Probability and Mathematical Statistics 18

Johansen A, Sornette D (2004) Endogenous versus Exogenous Crashes in Financial Markets. Contemporary Issues in International Finance. In press

Lo A W (1991) Long memory in stock market prices. Econometrica 59:1279-1313

Mandelbrot B B, Van Ness J W (1968) Fractional brownian Motions, fractional Noises and Applications. SIAM Review 10:422-437

Mantegna R N, Stanley H E (2000) Introduction to econophysics. Cambridge University Press, Cambridge

Menna M, Rotundo G, Tirozzi B (2002) Distinguishing between chaotic and stochastic systems in financial time series. Int. J. Mod. Phys. C 13:31-39

Murphy J J (1986) Technical analysis of the Futures Markets. Prentice Hall, New York

Rotundo G (2004) Logistic function in large financial crashes. Preprint

Samorodnitsky G, Taqqu, M S (1994), "Stable Non-Gaussian Random Processes", Chapman & Hall, London

# Financial Markets Dynamic Distribution Function, Predictability and Investment Decision-Making (FMDDF)

Gregory Chernizer

Financial Market Universal Dynamics, Inc
6 Marlow Avenue, Manchester, New Jersey 08759, USA

**Summary.** FMDDF system based on the basic scientific ideas from Physics and Economics involved in the procedure for the dynamic probabilistic distribution function of the state (**PDFS**) derivation for any financial market (**FM**). Price moving process defines dynamic FM. Price movement is defined by the volume imbalance V. The necessary condition for the dynamic FM is $V \neq 0$ at the same price, while the sufficient condition is defined by nonzero price volatility $\sigma$. The total probabilistic distribution function of any FM is the sum of the two incompatible terms: the regular probabilistic distribution function (**PDF**) containing the mean value and PDFS. PDFS structured based on the adiabatic integrals of FM motion that include the existing or expected volume imbalance, price volatility and amount of shares or contracts. PDFS is not path dependable (the new trajectories' invariant principle) in the special economic space $E\{\xi\}$. This fact is important in financial engineering, risk control, quantitative FM predictability and investment decision-making.

**Key words.** Volume excess, adiabatic constant, state composite variable, dynamic economic space.

## I.PDFS(Dynamic), Directional and Local Probabilities.

Tthe cumulative volume excess (VE) and volume excess expectation (VEE) V at the certain price with the following corresponding volatility $\sigma$ are the accumulated quantitative measure of FM news and information. **Definition:** FM is (was or will be) dynamic when the price of its financial instrument is (was or will be) moving, otherwise FM is static. Price movement is defined by the volume imbalance V for supply-demand, and the existed market and stop orders (the dynamic orders). The last three sources, governed by the news, are responsible for the price movement and price volatility. **Definition:** the volume excess (VE) for the present and past time or volume excess expectation (VEE) for the future with the common notation V = cumulative volume demand minus cumulative volume supply. It is clear, if $V > 0$ the price will not fall, and if $V < 0$ the price will not rise; FM is static if $V = 0$. The instantaneous dynamic price volatility is equal to zero for the static FM. The necessary condition for a dynamic FM existence is $V \neq 0$ while the sufficient condition is defined by nonzero price volatility $\sigma(V) = \sigma(1-\delta_{V0})$. The supply-demand relationship is the general principle of causation in economic dynamics: V is the source of the dynamic price volatility at the certain price interval due to the non-collinear investors' opinion to the news and information. **Assumption 1 (A1)** The possible VE and VEE local extremes form the set of support and resistant price levels. The state of FM is defined by V, price volatility and total amount of contracts or issued stocks O, where $\sigma$ is dimensionless price volatility measured either in decimals or percentage for the desirable time interval. In the following computation $\sigma$ is measured in decimals. V power is the absolute value of VE or VEE. From the author's data observation during preparing to the report (Chernizer 2000) (Landau and Lifshits 1964), it was found $|V| \sim \sigma^{-1/2}$ or $|V|\sigma^{1/2} \approx$ const when O was constant. It is not the universal constant: every stock has its own "constant" for a certain time interval. It may be compared to the adiabatic process in finance. The observable $V^2\sigma/O$ is the adiabatic constant per share,

$\xi^2 = V^2\sigma/O,$ (1)

$\xi_1=V^+\sqrt{(\sigma/O)}, \quad V^+\in (0; +\infty); \quad \xi_2 = V^-\sqrt{(\sigma/O)}, \quad V^-\in (-\infty; 0),$ (2)

may involve stocks split, and the explicit expressions for the positive and negative V. The new FM state composite variable (SCV) $\xi$ is symmetrical to the volume imbalance, and forms the dynamic economic space $E\{\xi\}$. $\xi_1$, $\xi_2$ may be considered as SCV separately for the price movement direction: V-resistance $\xi^+_1 = \xi_1(V^+,)$ and V-support $\xi^-_2 = \xi_2(V^-)$ states.

The integrals of motion are the certain quantitative expressions in economic space which are either constant during the market motion or provides the conservation for a certain time in the future. Their linear combination in the basic science is the "bricks" to create an implicit expression for the entropy (Landau and Lifshits 1964). Eq. (1) for $\xi^2$ integrates the dynamic features of FM, and may be considered as the adiabatic integral of FM motion. Another integral of the motion is the constant in form LnA describes FM condition at either V = 0 or $\sigma$ = 0, or both of them simultaneously. If V $\equiv$ 0, the supply is equal to demand, and a current price is unchanged. Under this condition FM is predetermined, and its dynamic price volatility $\sigma \equiv 0$. The closed FM is a partial price equilibrium case with V, $\sigma$ are equal to zero. Let us follow to the standard concept in the basic science (Landau and Lifshits 1964) that logarithm of the structured dynamic density of the probabilistic distribution function of the state (PDFS) $\rho_d$ (the state entropy), is the linear combination of the integrals of motion, and may consists in economics of a constant part LnA and adiabatic constant $\xi^2$,

$\mathrm{Ln}\rho_d = \mathrm{Ln}\, A - \xi^2,$ (3)

Constant A>0 and $\xi^2 \geq 0$ with the negative sign in front of it ought to diminish a static FM entropy LnA due to the dynamic FM process when V$\neq$0. FM dynamic equilibrium includes V $\equiv$ 0 and its V two partial derivatives of the first order (with respect to volatility and amount of shares O) equal to zero simultaneously. Therefore, total FM PDFS density $\rho_t$ consists of the sum of the two incompatible probabilistic densities: PDFS $\rho_d$ and the static $\rho$,

$\rho_t = \rho\, \delta_{V0} + (1 - \delta_{V0})\, \rho_d,$ (3a)

Kroneker's operator $\delta_{mn} = 1$ if m = n, and $\delta_{mn} = 0$ if m $\neq$ n. Hence, when FM is dynamic PDFS $\psi$ ought to be normalized $\psi \in [0; 1]$, non-negative and non-decreasing function of SCV.

From (3) dynamic PDFS density may be written as,

$\rho_d = A \exp(-\sigma V^2(P) / O)$ (4)

Constant A may be found from the regular procedure, Eq. (3a) in the case when FM is dynamic (V$\neq$0),

$$A \int_{-\infty}^{\infty} \exp(-\xi^2)\, d\xi = 1 \quad (5)$$

leads to

$A = 1 / \sqrt{\pi},$ (6)

and, therefore,

$\rho_d = (1 / \sqrt{\pi}) \exp(-\xi^2), \quad \xi \neq 0$ (7)

PFDS density $\rho_d$ in (7) makes sense for $\xi$=0 also, when there is no price movements at all (supply is equal to demand and V = 0, or nobody executes the existing V and instantaneous $\sigma$ = 0, or FM closed: V $\equiv$ 0, $\sigma \equiv 0$). $d\psi = \rho_d(\xi)d\xi$ is equal to PDFS differential that the dynamic FM to be found in the interval $\xi$ and $\xi$+d$\xi$. $\psi$ is defined for any $\xi \in (-\infty, \infty)$ on the $\xi\psi$ plane.

Price never falls below zero, which means from the supply-demand relationship that negative VEE ought to be lower than any imaginative number and, furthermore, the efficient support $\sigma$V ought to be lower than any imaginative number. Its definition is "- $\infty$" leads to the following,

$\lim_{P \to 0} \sigma V(P) = -\infty,$ (8)

and hence,

$\lim \rho_d(\xi) \rightarrow 0$
$P \rightarrow 0$

Expression (8) prohibits a negative price. In the static case ($V\sigma = 0$, $\xi \equiv 0$) $\rho$ may be expressed in the dynamic space $E\{\xi\}$ in the form of Dirac's delta function $\rho = \delta(\xi)$, where

$$\int_{-\infty}^{\infty} \delta(\xi)\, d\xi = 1, \qquad (9)$$

Eq. (9) confirms FM existence. The lack $\xi$-continuity describes the reality of the market opportunity to jump from static to non-zero $\xi$ dynamic FM states. $\psi(\xi)$ with the expected V (VEE) for the projective price interval is becoming the expected PDFS for the price interval.

From the Eqs.(7), (10) $\rho_d$ and $\rho$ ($\xi$=0), may be written as follows:

$$\rho_d(\xi) = (1 / \sqrt{\pi}) \exp(-\xi^2), \quad \xi \neq 0; \qquad (10)$$

$$\rho(\xi) = \delta(\xi), \quad \xi = 0. \qquad (11)$$

$E_1\{\xi\}$space defines in the certain $\varepsilon$–vicinity $[-\varepsilon, \varepsilon]$ of $\xi$ due to bid-, offer price uncertainty.

$\rho_d$ derivation based on the integral of FM motion, and, therefore, V is related to the process which prohibits no cost FM arbitrage (no free lunch).

It is a known fact the FM is path-dependent on price historical movements which are the pivotal part of the technical analysis. It is easy to prove that PDFS calculation in the new economic space $E\{\xi\}$ does not sensitive to a trajectory of FM movement, and may be an essential tool to financial engineering, risk estimation and FM predictability. Therefore, path-independent probability calculation may be written in the simple form,

$$\psi(V;\sigma;O|0;0;O) = (\Phi(\xi_2) - \Phi(0))/2 = (1/\sqrt{\pi}) \int_0^{\xi_2} (\exp(-x^2))\, dx =$$

$$(1 / \sqrt{\pi}) \sum_{n=0}^{\infty} (-1)^n \xi_2^{2n+1} / n!(2n+1), \quad \xi << 1. \qquad (12)$$

## II. Dynamic PDFS Application: the Expected Dynamic Trend and Investment Decision-Making.

It is important to find FM stochastic behavior between two local VE or VEE extreme levels for the two given directional accumulative variables: produced by the buyers $V^+ = V > 0$ (sellers $V^- = V < 0$) and possible rising price $P^+$ (declining price $P^-$). The current price in V(P) vicinities may stay, pass through the VEE extreme levels or bounce out them. Let $V_k$ and $V_{k-1}$ mean VEE at local k VEE resistance and k-1 VEE support local extreme VEE levels with their prices $P_{k,1}$, $P_{k-1,2}$ respectively. They are becoming critical in risk control and risk management problems at the considered price interval $[P_{k-1,2}, P_{k,1}]$. The second price subscript index 1 (2) is for resistance (support) level. Bullish $\xi^+$ and bearish $\xi^-$ SCVs mean the following,

$$\xi^+_{k,1} = \xi^+_{k,1}(V^+_k(P_k); \sigma; O); \quad \xi^-_{k-1,2} = \xi^-_{k-1,2}(V^-(P_{k-1}); \sigma; O) \qquad (13)$$

$\xi$-superscript signs in $\xi^+_{k,1}$, $\xi^+_{k-1,2}$ are determined by the current V superscript sign at $V^+ > 0$ or $V^- < 0$ respectively.

$\Psi_k^+$ is the probability to find FM at the resistance $V_k^+$ k level, $\xi^+_{k,1}$ state and its $\varepsilon$-vicinity due to bid-offer price uncertainties for V allocation and, therefore, SCV computation; k numerates V local extreme level which has nothing to do with the second $\xi$-index: 1 for the resistance and 2 for the support. $\psi^+(\xi^+_{k,1})$ is the probability to find FM inside of the $\xi$ interval $(-\infty, \xi^+_{k,1})$ while $\psi^{*+}(\xi^+_{k,1})$ is the probability to find FM outside of the $\xi$ interval $(-\infty, \xi^+_{k,1})$.

$\Psi_{k-1}$ is the probability to find FM at the k-1-th support $V^-_{k-1}$ level and state $\xi^-_{k-1,2}$ ($\xi$ subscript index 2 for any support with $V^-_{k-1} < 0$ always); $\xi^-_{k-1,2}$ is the V-support state with the preceding falling price $P^- > P_{k-1}$, $P^- \in [P_{k-1}; P_k)$ had approached support level $V^-_{k-1}(P_{k-1})$. $\xi^{*-}_{k-1,2}$ is FM state

$\xi^{-}_{k-1,2}$ when the preceding price $P< P_{k-1}$, $P\rightarrow P_{k-1}$ was approaching support $V^{-}_{k-1}$ level by the price rising to the level $V^{-}_{k-1}$. $\xi^{-*}_{k-1,2}$ is complimentary to $\xi^{-}_{k-1,2}$ state in the sense of price direction movement approaching k-1 support level $V^{-}_{k-1}$ and $P_{k-1}$ from the outside of the price interval $[P_{k-1}; P_k)$. Asterisk defines a complimentary notation. The same logic description can be done to the state $\xi^{+}_{k,1}$ and its resistance $V_k^{+}$. If a falling price $P> P_k$ and $P\rightarrow P_k$ moves from the outside of interval $(P_{k-1}; P_k]$, FM state $\xi^{*+}_{k,1}$ is complimentary to $\xi^{+}_{k,1}$. The importance of $\xi$, $\xi^{*}$ is essential to the dynamic FM description if it is bull or bear market in the vicinity of any state $\xi$ and their accumulative quantitative market news $V^{+}$ or $V^{-}$.

$\psi^{+}_{k}(\xi^{+}_{k,1})$ is the probability that expected bull market SCV $\xi^{+}_{k,1}$ on $\xi\psi$ plane does not exceed $\xi_{k,1}-\varepsilon$, $\varepsilon>0$, $\varepsilon \rightarrow 0$ when $\xi_{k,1}{}^{+}\rightarrow \xi_{k,1}$, and $\psi^{*+}(\xi^{*+}_{k,1})$ is the probability for the complimentary to $\xi^{+}_{k,1}$ event with $\xi^{*+}_{k,1}$ SCV. For the given bull and bear markets and their imbalances $V^{+}$, $V^{-}$

$$\psi^{*+}_{k}(\xi^{*+}_{k,1})=1 - \psi_k^{+}(\xi^{+}_{k,1}), \tag{14}$$

$$\psi^{*-}_{k-1}(\xi^{*-}_{k-1,2}) = 1 - \psi^{-}_{k-1}(\xi^{-}_{k-1,2}), \tag{15}$$

The sets of states $\xi^{+*}_{k,1}$, $\xi^{+}_{k,1}$ are incompatible and $\xi^{+*}_{k,1} \cap \xi^{+}_{k,1} = \xi_{k,1}$ at $\varepsilon >0$ price $P_k \pm \varepsilon$ vicinity, $\varepsilon\rightarrow 0$ and $\varepsilon$ less than the price basic point when $P\rightarrow P_k$. From the same consideration $\xi^{-*}_{k-1,2} \cap \xi^{-}_{k-1,2} = \xi_{k-1,2}$.

Therefore, for the given market price directions "+" or "-" the probabilities to find FM at the resistance or support states may be written as

$$\Psi^{+}(\xi_{k,1}) = \psi^{+}(\xi^{+}_{k,1})\,\psi^{*+}(\xi^{*+}_{k,1}),\quad \psi^{*+} = \psi^{+}(\xi_{k,1}{}^{*+}) = 1 - \psi^{+}(\xi^{+}_{k,1}) \tag{16}$$

$$\Psi_{k-1}(\xi_{k-1,2}) = \psi^{-}(\xi^{-}_{k-1,2})\psi^{*-}(\xi^{*-}_{k-1,2}),\quad \psi^{*-} = \psi^{-}(\xi^{*-}_{k-1,2}) = 1 - \psi^{-}(\xi^{-}_{k-1,2}) \tag{17}$$

It is obviously that in the continuous case PDFS $\psi$, (which is not the local (point) probability $\Psi$ !) is defined by PDFS density $\rho_d$ also. Due to that $\psi$ does not depend on FM trajectory in E from $\xi = -\infty$ up to $\xi^{\pm}_{k,m}$ $(V_k;\sigma_1; O_1)$ the probability that FM is in the state $\xi \le \xi_{k,m}{}^{\pm} - \varepsilon$ ($\varepsilon >0$, $\varepsilon\rightarrow 0$ and $\varepsilon$ less than the price basic point) is equal to

$$\psi_k^{\pm}(\xi_{k,m}{}^{\pm}) = \int_{-\infty}^{\xi_{k,m}{}^{\pm}} \rho_d(\xi)\,d\xi = (1/\sqrt{(\pi)}) \int_{-\infty}^{\xi_{k,m}{}^{\pm}} (\exp(-\xi^2))\,d\xi = (1/\sqrt{(\pi)})\,((\sqrt{(\pi)}/2)[1 + (\Phi(\xi_m{}^{\pm}))]$$

$$= [1 + (\Phi(\xi^{\pm}_{k,m}))]/2,\quad m = 1, 2; \tag{18}$$

$$\psi_k^{+} = \psi(\xi_{k,1}{}^{+}),\ \psi_k{}^{-} = \psi(\xi_{k,2}{}^{-}),\ \psi_k{}^{\pm}(-\infty) = 0,\ 0 \le \psi^{\pm}(\xi_{k,m}{}^{\pm}) \le 1;\ \psi_k{}^{\pm}(+\infty) = 1, \tag{19}$$

$\Phi(\xi^{\pm}_{k,m})$ is the probabilistic integral. It is obviously that $\xi^{-}\rightarrow -\infty$ when $V^{-}\rightarrow -\infty$, $\sigma \rightarrow 0$, O is finite number, $\psi_m{}^{\pm}$ means either $\psi^{+}_k$ or $\psi^{-}_k$ depends on either $\xi^{+}_{k,1}{}^{+}$ or $\xi^{-}_{k,2}$ instead of $\xi^{\pm}_{k,m}$ in (18), (19).

Dynamic FM with no additional news leads asymptotically to static FM stability with $V = 0$ and possible minimal PDFS. Therefore the following assumption may be accepted:

**Assumption 2 (A2).** FM price is more stable at state $\xi$ with a lower dynamic probability $\psi$. Assume for the simplicity that in $\varepsilon$ $\xi$-vicinity V and $\sigma$ axes are orthogonal. **Assumption 3 (A3).** Price moves with no additional V-news from the point of higher PDFS $\psi_h$ to the nearest lower $\psi_l$ dynamic probability point in E.

It means that without external additional V perturbation dynamic FM system is characterized by $\psi$ dissipating process and approaching to the static state. The conceivable minimal DFS is $\psi_d(\xi=0) = 0$ and $\psi_{st}(\xi=0) = 1$, describing the lack of dynamic process. Therefore, quantitative most likely price movement criteria and its rate of change is in direction of the vector $\boldsymbol{\eta} = -\text{grad}\psi(\xi)$. Its norm $\eta$ determines the most likely expected FM quantitative measure of PDFS movement from the current state to the fastest $\psi$ falling direction. In this scenario $\eta$ is equal to the rate of $\psi_d$ change to the lower dynamic probability state,

$$\boldsymbol{\eta} = -\text{grad}\psi = -\rho_d(\xi)\,\mathbf{a}\{\eta_1; \eta_2; \eta_3\}, \tag{20}$$

$\mathbf{a}\{\eta_1; \eta_2; \eta_3\}$, $\eta_1 = (\partial\xi/\partial V) = \sqrt{(\sigma/O)}$; $\eta_2 = (\partial\xi/\partial\sigma) = V/2\sqrt{(\sigma O)}$; $\eta_3 = (\partial\xi/\partial O) = -V(\sqrt{(\sigma/O)})/2O$.

It makes $\boldsymbol{\eta}$ the "macro" trend indicating predictor (**TIP**) valid for the interval $(-\infty,\xi)$. This uncertainty does not allow yet to describe FM predictability at the chosen state $\xi^-$ vicinity. When $V\to 0$, volatility $\sigma$ approaches to zero also almost instantaneously (similar to its originating since $V\neq 0$) and, therefore, $\xi\to 0$). The probability that FM is static expressed in Eqs (9), (11). $\psi$ increment may be calculated by the scalar product,

$$d\psi = (\boldsymbol{\eta} \cdot \boldsymbol{\eta}_0\, d\xi) = -\rho_d(\xi)(\sqrt{(\eta_1^2+\eta_2^2+\eta_3 2)})\, d\xi = -\eta d\xi, \qquad \boldsymbol{\eta}_0 = (\boldsymbol{\eta}/\eta) \tag{21}$$

If $\sigma$, O are unchanged in a certain $\xi$ interval, $d\psi$ is equals to the partial differential $d_V\psi$ related to the increment dV,

$$d_V\psi = -\rho_d(\xi)\,(\sqrt{(\sigma/O)})\, dV = -\rho_d(\xi)\,(\sqrt{(\sigma/O)})\,(\partial V/\partial P)\, dP \tag{22}$$

$\partial V/\partial P$ is either known function or ought to be found from independent sources. Current price direction determines by vectors $\boldsymbol{\eta}_0$, $\boldsymbol{\eta}$ and the increment of the news $d\xi$ (21) for PDFS increment $d\psi$. Eq. (22) explains why due to the unexpected V-news at FM price P sometimes does not achieves expected support or resistance levels for the expected price interval.

If V, O are unchanged in a certain $\xi$ interval,

$$d_\sigma\psi = -\rho_d(\xi)\,(V/2\sqrt{(\sigma O)})\, d\sigma = -\rho_d(\xi)\,(V/2\sqrt{(\sigma O)})\,(\partial\sigma/\partial P)\, dP \tag{23}$$

And the last TIP partial differential may be written from Eqs. (24), (25),

$$d_o\psi = \rho_d(\xi)\,(V(\sqrt{(\sigma/O)})/2O)\, dO \tag{24}$$

While TIP $\boldsymbol{\eta}$ plays a "macro" indicator role for FM the interval $(-\infty,\xi)$, there still remains an important problem for local TIP (**LTIP**) in the vicinity of any current or expected state $\xi$. For this purpose $\boldsymbol{\eta}$–technique will be applied to the local PDFS $\Psi_k^+(\xi_{k,1})$, $\Psi_{k-1}^-(\xi_{k-1,2})$ given in Eqs. (16), (17),

$$\boldsymbol{\eta}^+ = -\text{grad}\,\Psi_k^+(\xi^+_{k,1}) = -2\psi^+(\xi^+_{k,1})\,\text{grad}\psi^+(\xi^+_{k,1}) = -[1+(\Phi(\xi^+_{k,1}))]\,(\rho_d(\xi^+_{k,1}))\,\mathbf{a}^+(\xi^+_{k,1}) \tag{25}$$

$$d\Psi_k^+(\xi^+_{k,1}) = -2\psi^+(\xi^+_{k,1})\,(\rho_d(\xi^+_{k,1}))\,(\mathbf{a}^+\cdot\mathbf{a}^+_0)d\xi^+_{k,1} = -[1+(\Phi(\xi^+_{k,1}))]\,(\rho_d(\xi^+_{k,1}))\,a^+ d\xi^+_{k,1}, \tag{26}$$

$$\boldsymbol{\eta}^- = -\text{grad}\Psi_{k-1}(\xi^-_{k-1,2}) = -2\psi^-(\xi^-_{k-1,2})\text{grad}\psi^-(\xi^-_{k-1,2}) = -[1+(\Phi(\xi^-_{k-1,2}))]\,(\rho_d(\xi^-_{k-1,2}))\,\mathbf{a}^-(\xi^-_{k-1,2});$$

$$\mathbf{a}^\pm = (\text{grad}\psi^\pm)/\rho_d(\xi^\pm) \tag{27}$$

$$d\Psi_k^-(\xi^-_{k-1,2}) = -2\psi^-(\xi^-_{k-1,2})(\rho_d(\xi^-_{k-1,2}))\,(\mathbf{a}^-\cdot\mathbf{a}^-_0)d\xi^-_{k-1,2} = -[1+(\Phi(\xi^-_{k-1,2}))]\,*\,(\rho_d(\xi^-_{k-1,2}))\,a^- d\xi^-_{k-1,2} \tag{28}$$

Expression (26), (28) are the quantitative equations for LTIP test when O = const, $\sigma$ = const,

$$d_V\Psi^+_k(\xi^+_{k,1}) = -[1+(\Phi(\xi^+_{k,1}))]\,\rho_d(\xi^+_{k,1})\,(\sqrt{(\sigma/O)})(\partial V^+/\partial P)\, dP \tag{29}$$

$$d_V\,\Psi^-_{k-1}(\xi^-_{k-1,2}) = -[1+(\Phi(\xi^-_{k-1,2}))]\,\rho_d(\xi^-_{k-1,2})\,(\sqrt{(\sigma/O)})\,(\partial V^-/\partial P)\, dP \tag{30}$$

are essential for the market dynamic expectation. As it was discussed above, FM movement tendency to the static state leads to decreasing the dynamic probabilities $(d_V\Psi_k^+(\xi_{k,1})<0$, $d_V\Psi_{k-1}(\xi^-_{k-1,2})<0)$, and, therefore,

price increment sign based on (29), (30) ought to be found from the following $\Psi V$ – test,

$$(\partial V^+(\xi^+_{k,1})/\partial P)\, dP > 0; \qquad (\partial V^-(\xi^-_{k-1,2})/\partial P)\, dP > 0. \tag{31}$$

According to A3, price moves from the higher local probability state to the lower probability state. Its application to V-support and V-resistance levels ($\Psi$-test) may be written as follows. If

$$\Delta\Psi = \Psi^+(\xi^+_1) - \Psi^-(\xi^-_2) > 0, \tag{32}$$

FM is bearish, and if

$$\Delta\Psi = \Psi^+(\xi^+_1) - \Psi^-(\xi^-_2) < 0, \tag{33}$$

FM is bullish.

TIP (21)–(24) for the general trend, LTIP (25)-(29) for the local trend and $\Psi V$–test (31) are practical tools for FM Risk predictability, quantitative trading strategy and probabilities of dynamic FM expected values.

## References


[1] Chernizer G (2000), Volatility forecasting model based upon the least common action principle, Forecasting Financial Markets: Advances for Exchange Rates, Interest Rates and Asset Management, London.

[2] Landau L, Lifshits E (1964), Statistical Physics, Nauka, Moscow, p25.

# Market Cycle Turning Point Forecasts by a Two-Parameter Learning Algorithm as a Trading Tool for S&P Futures

Jian Yao, Jun Chen*, Ke Xu, Zhaoyang Zhao, Tao Yu and Bill C. Giessen,
Department of Chemistry & Chemical Biology and Barnett Institute,
Kamran Dadkhah, Department of Economics, Northeastern University, Boston, MA 02115, U.S.A
* Now with Risk Management, Bloomberg LP, 499 Park Ave., New York, NY10022, U.S.A.

**Summary.** Among the long-term stationary (although complex) behavior characteristics of futures markets is a set of identifiable intermediate-length (2-21.5 days) price cycles. Using a two-parameter extrapolation technique, time and price objectives of these cycles are determined. The valley-to-valley time differences (wavelengths) are more regular than those for top-to-top, with standard deviations of the former about 50% smaller than those of the latter. The substantial profitability in S&P futures trading based on these parameters can be further increased by including additional features.

**Key words.** S&P500 Futures, Optimization of N-φ Prediction Method, Price Cycle Periods, Market Prediction

## Introduction

The occurrence of cyclical price patterns on various time scales [1] is perhaps the most conspicuous manifestation of nonrandom market behavior seen in price charts. Because of their obvious relation to dynamically driven oscillatory phenomena, such patterns are also among the most intriguing potential applications of econophysics [2], as well as chaos theory [3].

Although "average" cycle characteristics (periodicity, amplitude, "leg" ratio in time and price) can be defined and determined, individual cycles show considerable variability of these quantities. In line with a stated purpose of this conference concerning applications to real markets, we deal here with the practical issue of predicting the approximate locations of cycle extrema to allow their use for trading purposes.

As a working model [4], we identify cycles with an average of 5 days (weekly cycle) and 21.5 days (monthly cycle) as well as important "halving" cycles of 2-3 days and 10-11 days; the latter two add up to 5 days and 21.5 days, respectively.

These cycles are referred to by C2, C5, C10 and C20 in the following. We observe that longer cycles share minima and maxima with shorter ones in the manner

**Fig. 1.** Idealized relationship of C2, C5 and C10 market cycles.

schematically shown in Fig.1 ("Concurrency").While there is no "long-range order" (to borrow a term from solid state physics [5] or chemistry) tying the C5 cycle extrema over long range to the periodicity of a specific weekday (or, analogously, the C20 cycle extrema to a specific day of the month), there exists in the data the equivalent of "short-range order", allowing local prediction of tops or valleys from the locations of those for the immediately preceding cycles.

## Methodology

We focus in the following on the C5 (weekly) cycle as a paradigm. To forecast future extrema of a C5 cycle, we use a database of prior weekly extrema (tops "T" and valleys "V") assigned by a variety of methods (discussed below). Fig. 2 illustrates the use of this database for next-T or -V forecasts by a two-parameter process: First one or more (N) prior cycle valleys (V) are used to calculate the location of an idealized average valley(<V>) from these N cycles. A forward count is then made from <V>, adding N/2 cycle lengths to simulate the position of the most recent valley (which may not yet be clearly expressed). Next, a time period $\varphi$ is added to this simulated valley to produce a time count to the next valley (lying in the future). This period $\varphi$ is generally found to be roughly equal to the cycle period. Results are presented in the form of a $\varphi$-N diagram, a plot in which the minimization the time difference between a forecast top or valley and those in the database is given by the lightness of the shading, see Fig. 3. In advanced versions of this approach, the parameter choice is step-wise or continually self-adjusting (learning). For clarity in this demonstration, we present a simplified version, with parameters kept fixed throughout the study period.

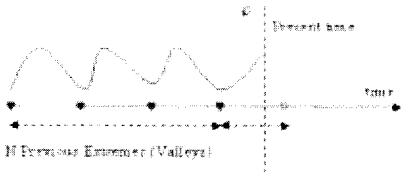

**Fig.2.** Sketch of counting procedure for next-valley prediction by N-$\varphi$ method.

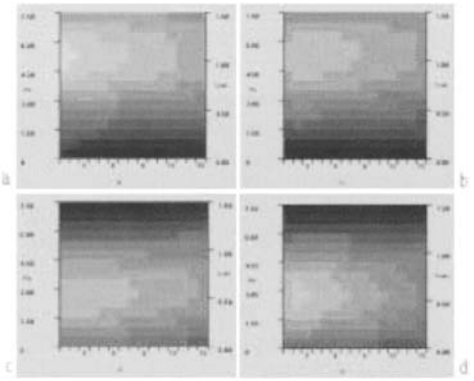

**Fig. 3.** Optimization of N-φ cycle extremum forecasts by minimizing time difference (light shade) between forecast and ideal extremum, a) V-to-V, b) T-to-T, c) V-to-T, d) T-to-V.

## Results

We studied S&P futures over the four-year period 01/2001 to 12/2004. Global application of the cycle extremum forecasting method described above over this period results in the φ-N plots 3a-d which shows the optimization procedure for V-V, T-T, V-T and T-V forecasts, respectively.

The optimal values from these plots (e.g. N=3 periods and φ=5.5 days) are combined and used in forecasting cycle leg end points. (The implied trading command is then to enter long at a valley and reverse short at a top.)

**Table1.** C5 (weekly cycle) trading results for S&P futures

| | Year 2001 | | Year 2002 | | Year 2003 | | Year 2004 | | |
|---|---|---|---|---|---|---|---|---|---|
| | CPL | FOM | CPL | FOM | CPL | FOM | CPL | FOM | Total |
| Long | -24.7 | 0.49 | 18.8 | 0.51 | 62.7 | 0.56 | 193 | 0.67 | 249.8 |
| Short | 123.5 | 0.57 | 285.0 | 0.67 | -132.9 | 0.37 | 101 | 0.63 | 376.6 |
| Total | 98.8 | | 303.8 | | -70.2 | | 294 | | 626.4 |

Carrying out simulated real-time trading with these trading rules yields trading results for this market period summarized in the plots of Fig. 4 (separately presented for long and short trades) and the trading result data in Table 1. To demonstrate stationarity of the approach, trading data for 2004 using the algorithm established from 2001-2003 are included into Table1.

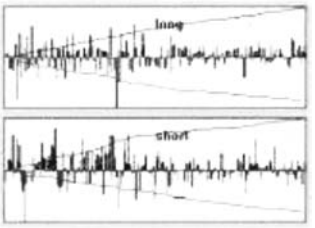


**Fig.4.** Summary of C5 trading for Period 01/2001 too 12/2004.

## Discussion

Trading results: The four-year trading results presented show an annualized net profit (CPL) of over 150 S&P points in about 52 annual C5 market entries/reversals, corresponding to about $7,500 p.a. for an S&P mini contract (i.e., 15% of contract value, without considering leverage, execution cost and slippage), with an average FOM=0.55, indicating acceptable risk.

To put the data in perspective relative to the two overall market directions dominating this 4-year period, one sees the program profiting well on the short side during the declining market (till 03/20/2003, especially during 2002), and earning well on the long side during the rising market of 2004, showing its ability to trade profitably at least on one side independent of overall market direction.

Cycle database and its characteristics: The key to the forecasting process described above is the existence of a usable database for the cycles listed above, and a procedure to extend it into the future, as done here.

To predict futures markets in terms of cycles, a simple strategy used by market practitioners [6] is to visually interpret price charts and to draw in appropriate cyclic chart divisions (coincident with price lows and highs) on specific time scales such that, e.g. 12 monthly (21.5-day) cycles or 52 weekly (5-day) cycles are seen per year.

This manual, inspection-based approach can be systematized by optimizing a suitable combination of price and time premium functions, or by using spline fits of appropriate smoothness parameter, as shown in a companion paper [7], by measuring a "cycle shape quality index" (presently under development), or by considering the superposition of multiple cycles, etc. This work has led to the compilation of a standard database of all pertinent cycles for three major futures markets: S&P, EC and GC.

Drawing on this database, we present in fig 5a-d summaries of the time intervals from V to V, T to T, V to T, and T to V for C5 (S&P). These four histograms show that C5 cycle "wavelengths" and cycle "legs" have broad distributions; however, the V-V wavelength distribution is seen to be much sharper peaked

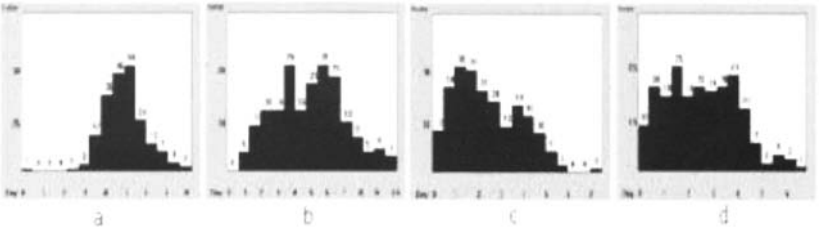

**Fig.5.** C5 cycle leg statistics for 4 year period from 01/2002 to 12/2004, a) V-V time legs, standard deviation $\sigma$ = 1.21days; b) T-T time legs, $\sigma$ = 2.40days; c) V-T time legs, $\sigma$ = 1.64days; d) T-V time legs, $\sigma$ = 1.67days.

around its mean than the T-T distribution, with a standard deviation $\sigma$ for V-V only 50% of that for T-T, with $\sigma$ for the "legs" falling in between. Except for V-V, all distributions appear to be bimodal. (This would be expected for V-T and T-V in combinations of rising and falling markets, and for T-T at changeovers from a rising to a falling market mode and vice versa.)

Outlook and Conclusion: As indicated above, the trading parameter optimization procedure demonstrated in Fig. 2 can be made self-adjusting through time; the results can be further improved by adding a cycle-slope-biasing algorithm. (In fact, the data originally reported at the Third Nikkei conference 11/04 benefited from use of such an algorithm which takes the general market direction into account to bias the up/down leg time ratio; this point should have been noted in the extended abstract.) Positive results were also obtained for the other cycles listed, especially the short-term C2 cycle; multi-cycle superposition is under study for better market performance.

Our results demonstrate the local predictability of cyclic price movements and thus, implicitly, confirm the presence of such cycles in the market data.

We thank Cambridge Market Analysis Corporation (CMAC) for financial support of this work.

## References

1. Murphy, J. J., Technical Analysis of Future Markets, New York: New York Institute of Finance (1999)
2. Mantegna, R.N. and Stanley H.E., An Introduction to Econophysics, Cambridge: Cambridge University Press (2000)
3. Mullin, T., The Nature of Chaos, Oxford: Oxford University Press (1996)
4. Jun Chen, Ph.D. Thesis, Northeastern University, Boston, MA (2003)
5. Kittel, Ch., Introduction to Solid State Physics, 4th edition, New York: Wiley(1971)
6. Bernstein, J., Cyclic Analysis in Futures Trading, New York: Wiley(1988)
7. Xu, K., Chen, J, Yao,J, Zhao,Z., Yu,T, Giessen, B., and Dadkhah, K., Short Time Segment Price Forecasts Using Spline Fit Interactions, "Practical Fruits of Econophysics", editor H.Takayasu, Springer, Tokyo (2005)

# 3. Mathematical Models

# The CTRWs in finance: the mean exit time

Jaume Masoliver, Miquel Montero, and Josep Perelló

Departament de Física Fonamental, Universitat de Barcelona, Diagonal, 647, E-08028 Barcelona, Spain

**Summary.** The continuous time random walk (CTRW) has become a widely-used tool for studying the microstructure of random process appearing in many physical phenomena. We here report the CTRW analysis applied to the market dynamics which has been recently explored by physicists. We focuss on the mean exit problem.

**Key words:** Continuous Time Random Walk, high-frequency data, waiting time, mean exit time

## 1 The random walks: Finance and Physics

The continuous time random walk (CTRW) was first introduced by Montroll and Weiss in 1965. As its name suggests, the CTRW generalizes simple random walk (RW) models. Although the term "random walk" was coined by Pearson in 1905, the formalism had been formulated in the XVIIth century in the context of gambling games such as the probability of ruin after betting $n$ times in a coin tossing game (Weiss 1994). Financial markets have also been studied from the RW point of view. In fact, this formalism was the first tentative model known in finance having been suggested by Bachelier in 1900 to describe stock market dynamics (Cootner 1964). The price evolution is modelled assuming that prices change one unit at each time step with a probability $p$ of going up and $1-p$ of going down. Bachelier showed that the so-called binomial process, after a large number of time steps, tends to the Gaussian distribution.

Several decades passed before there was further progress in the application of RW methodology to analyze different aspects of financial dynamics. In the book edited by Cootner in 1964, there is a chapter devoted to the reexamination of the random walk hypothesis. It is shown there that RW models should be applied to the price return, instead of the price itself as Bachelier asserted. Within these works we mention the articles by Fama and Mandelbrot which study an alternative to the Bachelier Gaussian RW, proposing instead the Pareto distribution. Later on, Cox and Ross (1976) took the Bachelier RW to

provide a discrete time analog to the well-known Black-Scholes option price. They showed that the Bachelier binomial model also gives an option price for the Poisson jump process. Other contributions of the RW approach extend the binomial model adding a third event, a crash, and observe the implications of it to the options (Wilmott 1999). To our knowledge, there are not other models exploiting the possibilities that RW analysis can offer in the study of many phenomena in markets.

The RW formalism mentioned is based on the assumption that step changes are made at equal time intervals but this is a first approximation for many physical phenomena and markets. The CTRW relaxes this restriction since it assumes that time interval between transactions are not constant but random. Ticks have now, and in contrast with the RW, two sources of randomness: one coming from the amplitude and another one from the waiting times between ticks. The deepest structure corresponds to the transaction-to-transaction operations and the CTRW appears to be an appropriate framework to describe the market microstructure (O'Hara 1995). Despite this promising fact, the CTRW is hardly known among financial analysts. In contrast, physicists have studied some applications of the CTRWs to finance with interesting results. The first study was done under the perspective of the Lévy distribution which can be obtained from the Lévy walks (Shlesinger et al. 1995). After this contribution and from 2000, other physicists have proposed CTRW models in a more general approach and deeper exploring their possibilities (Scalas et al. 2000, Mainardi et al. 2002, Raberto et al. 2002 Sabatelli et al. 2002, Kutner and Switala 2003, Masoliver et al. 2003, Masoliver et al. in press, Masoliver et al. 2004).

## 2 An overview of the CTRW formalism

Let $S(t)$ be a financial price and let $t_0$ be an initial time. The log-price or return is defined by $Z(t) = \ln S(t)/S(t_0)$. If $\langle Z(t)\rangle$ is the return mean value, we define the zero-mean return by

$$X(t) = Z(t) - \langle Z(t)\rangle. \tag{1}$$

Suppose that $X(t)$ is described by a CTRW. In this representation any trajectory consists of a series of step functions as shown in Fig. 1. Therefore, $X(t)$ changes at random times starting at $t_0, t_1, t_2, \cdots, t_n, \cdots$ and we assume that sojourns or waiting times, $\tau_n = t_n - t_{n-1}$ $(n = 1, 2, \cdots, n)$, are independent and identically distributed (i.i.d.) random variables described by a given probability density function (pdf) defined by $\psi(t)dt = \text{Prob}\{t < \tau_n \leq t + dt\}$. At the conclusion of a given sojourn the return $X(t)$ suffers a random jump described by the random variable $\Delta X_n = X(t_n) - X(t_{n-1})$ whose pdf is defined by $h(x)dx = \text{Prob}\{x < \Delta X_n \leq x + dx\}$. The jumps are also assumed to be i.i.d. random variables, and the only correlations to be considered are

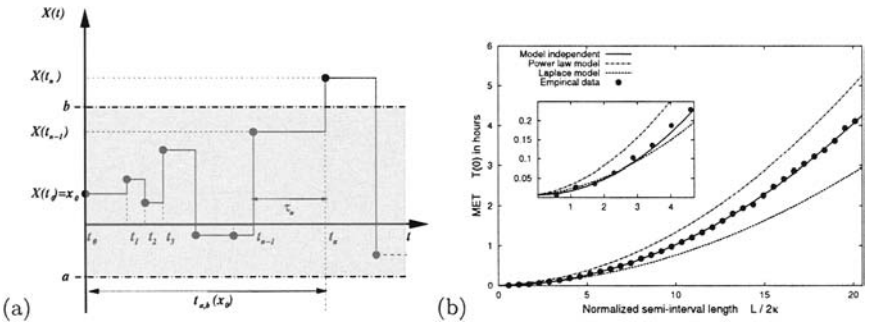


**Fig. 1.** (a) A particular trajectory of the zero-mean return process along with a particular value of the random variable $t_{a,b}(x_0)$. (b) The empirical MET from high frequency data of the U.S. dollar/Deutsche mark futures market with several models specified in Tab. 1.

those between $\Delta X_n$ and $\tau_n$. We must then guess from data (Masoliver et al. in press) the functional form of the joint pdf of waiting times and jumps:

$$\rho(x,t)dxdt = \text{Prob}\{x < \Delta X_n \leq x + dx; t < \tau_n \leq t + dt\}.$$

We will further assume that $\rho(x,t)$ is an even function of $x$ so that there is no net drift in the evolution of $X(t)$. The main objective of the CTRW is obtaining the so-called propagator, that is, the probability density function of the zero-mean return $X(t)$:

$$p(x,t)dx = \text{Prob}\{x < X(t) \leq x + dx\}. \tag{2}$$

Masoliver et al. (2003, in press) have obtained a general expression for the joint Fourier-Laplace transform of the propagator. In terms of the Laplace transform of the waiting time distribution, $\hat{\psi}(s)$, and the Fourier-Laplace transform of the joint distribution, $\hat{\rho}(\omega, s)$. This expression reads

$$\hat{p}(\omega, s) = \frac{[1 - \hat{\psi}(s)]/s}{1 - \hat{\rho}(\omega, s)}. \tag{3}$$

Equation (3) constitutes the most general solution to the problem. There are nonetheless some general results that are independent of the $\rho(x,t)$ chosen:

(a) If the mean waiting time is finite and the jump pdf $h(x)$ has a finite second moment, $\mu_2 = \langle \Delta X^2 \rangle < \infty$, the asymptotic distribution of returns for long times approaches to the Gaussian density: $\tilde{p}(\omega, t) \simeq e^{-\mu_2 \omega^2 t/2\langle\tau\rangle}$ for $t \gg \langle\tau\rangle$.

(b) If $h(x)$ is a long-tailed density, *i. e.*, $h(x) \sim |x|^{-1-\alpha}$ as $|x| \to \infty$. Then $\tilde{h}(\omega) \simeq 1 - k|\omega|^\alpha$ as $\omega \to 0$ for $0 < \alpha < 2$. Moreover, if we assume that for $\omega$ small $\langle \tau e^{i\omega \Delta X} \rangle \simeq \langle\tau\rangle$, then the asymptotic return pdf approaches to the Lévy distribution: $\tilde{p}(\omega, t) \simeq \exp(-k|\omega|^\alpha t/\langle\tau\rangle)$ for $t \gg \langle\tau\rangle$.

**Table 1.** Summary of the models shown in Fig. 1. All cases use $\langle\tau\rangle = 23.65$ s and we add the value of the parameters involved in Eq. (6). The Laplace pdf takes the empirical standard deviation and the rest of parameters are derived automatically. The power-law (Masoliver et al. 2003) fits the empirical tails of $h(x)$ bringing us the corresponding values for $\kappa, H(0)$, and $H(0^+)$. The last row gives the curve with empirical values $\kappa$ and $H(0)$ but chooses $H(0^+)$ to give the best fit.

| | $h(x)$ | $\kappa \times 10^{-4}$ | $H(0)$ | $H'(0^+)$ |
|---|---|---|---|---|
| Laplace | $\gamma \exp(-\gamma\|x\|)/2,\ \gamma^2 = 2/\kappa^2$ | 1.70 | $1/\sqrt{2}$ | -1 |
| Power-law | $\frac{\beta-1}{2\eta(1+\|x\|/\eta)^\beta},\ \eta^2 = \frac{\kappa^2(\beta-2)(\beta-3)}{2}$ | 1.25 | 1.07 | -2.81 |
| Fit | not a model | 1.70 | $4.45 \times 10^{-3}$ | 1.54 |

(c) At intermediate times, $t \approx \langle\tau\rangle$, the behavior of $p(x,t)$ for large values of $|x|$, is the same as that of the jump distribution: $p(x,t) \sim h(x)\ t/\langle\tau\rangle$.

## 3 The mean exit time

We can now ask: at which time interval $X(t)$ leaves a given interval $[a,b]$ for the first time? We call this quantity the exit time out of the interval $[a,b]$ and denote it by $t_{a,b}(x_0)$. Obviously $t_{a,b}(x_0)$ is a random variable since it depends on the particular trajectory of $X(t)$ chosen (see Fig. 1). Our main objective here is to obtain, based on the CTRW formalism, the mean exit time (MET) $T_{a,b}(x_0) = \langle t_{a,b}(x_0)\rangle$. The standard approach to MET problems requires the knowledge of the survival probability of the process in the interval $[a,b]$. Although the interest in knowing the survival probability is beyond any doubt, its attainment turns out to be quite involved. Masoliver et al. (2004) have presented a direct and much simpler derivation

$$T(x_0) = \langle\tau\rangle + \int_a^b h(x - x_0)T(x)dx, \tag{4}$$

where $\langle\tau\rangle$ is the mean waiting time between jumps. From a mathematical point of view Eq. (4) is a Fredholm integral equation of second kind. Depending on the kernel $h(x)$ there are some analytical approaches which allow to get an exact solution. An important point should be emphasized: the fact that the MET does not depend on the possible coupling between waiting times and jumps as shown in Eq. (4). In what follows we will assume that $h(x)$ satisfies the scaling condition $h(x) = H(x/\kappa)/\kappa$, where $\kappa > 0$ is the standard deviation of $h(x)$. Suppose now that the length interval $L$ is small, that is: $L/2\kappa < 1$. An approximate solution to Eq. (4) thus reads

$$T(x_0) \approx \langle\tau\rangle\Big[1 + H(0)\,(L/\kappa) + [H'(0^+)/4 + H(0)^2]\,(L/\kappa)^2 + H'(0^+)(2x_0 - a - b)^2/4\kappa^2\Big]. \tag{5}$$

In the symmetrical case with $x_0 = 0$ we have

$$T(0) \approx \langle \tau \rangle \left[ 1 + H(0)\,(L/\kappa) + \left[ H'(0^+)/4 + H(0)^2 \right] (L/\kappa)^2 \right] \qquad (6)$$

In this way, the MET has for sufficiently small intervals a quadratic growth behavior. In fact, the approximate expression given by Eq. (5) becomes the exact solution for the Laplace jump pdf. In Fig. 1, we compare the empirical MET from the U.S. dollar/Deutsche mark data with several models (Masoliver et al. 2003). We also plot the Laplace model and the power-law model with the parameters obtained from data statistics of $h(x)$ (see Tab. 1). We observe important discrepancies with the empirical MET so that we add a third curve with Eq. (6) taking the optimal value for $H'(0^+)$. Finally, the quadratic growth is still observed even outside the $L/2\kappa < 1$ regime.

This work has been supported in part by Dirección General de Investigación under contract No. BFM2003-04574 and by Generalitat de Catalunya under contract No. 2001 SGR-00061.

## References

Cootner PH (Ed) The random character of stock market prices. MIT Press, Cambridge, 1964

Cox J, Ross S (1976) The valuation of options for alternative stochastic processes. J Fin Econ 3:145-166

Kutner R, Świtała F (2003) Stochastic simulations of time series within Weierstrass-Mandelbrot walks. Quant Fin 3:201-211

Mainardi F, Roberto M, Gorenflo R, Scalas E (2000) Fractional calculus and continuous-time finance II. Physica A 287:468-481

Masoliver J, Montero M, Weiss GH (2003) Continuous-time random-walk model for financial distributions. Phys Rev E 67:021112

Masoliver J, Montero M, Perelló J, Weiss GH, The continuos time random walk formalism in financial markets, J Econ Behav Org (in press)

Masoliver J, Montero M, Perelló J, Extreme times in financial markets. cond-mat/0406556

Montroll EW, Weiss GH (1965) Random walks on lattices, II. J Math Phys 6:167–181

O'Hara M (1995) Market Microstructure Theory. Blackwell, Cambridge

Raberto M, Scalas E, Mainardi F (2002) Waiting-times and returns in high-frequency financial data: an empirical study. Physica A 314:749-755

Sabatelli L, Keating S, Dudley J, Richmond P (2002) Waiting time distributions in financial markets. Eur Phys J B 27:273-275

Scalas E, Gorenflo R, Mainardi F (2000) Fractional calculus and continuous-time finance. Physica A 284:376–384

Shlesinger M, Zaslavski G, Frish U (Eds) (1995) Levy Flights and Related Topics in Physics. Springer, Berlin

Weiss GH (1994) Aspects and Applications of the Random Walk. North-Holland, Amsterdam

Wilmott P (1999) Derivatives. John Wiley & Sons, Chichester

# Discretized Continuous-Time Hierarchical Walks and Flights as possible bases of the non-linear long-term autocorrelations observed in high-frequency financial time-series

Marzena Kozłowska, Ryszard Kutner, Filip Świtała

Department of Physics, Warsaw University, Hoża 69, Pl-00681 Warsaw, Poland

**Summary.** By using regular time-steps we define discrete-time random walks and flights on subordinate (directed) Continuous-Time Hierarchical (or Weierstrass) Walks and Flights, respectively. The obtained results can be considered as a kind of warning that indicates some persistent non-linear long-term autocorrelations (artifacts) accompanying the recording of empirical high-frequency financial time-series by regular time-steps, indeed.

**Key words.** Non-linear long-term autocorrelations, High-frequency financial time-series, Continuous-Time Hierarchical (or Weierstrass) Walks and Flights

## Motivation

We consider the possible reason of non-linear, long-term autocorrelations present in empirical and our synthetic high-frequency (HF) financial time series. The autocorrelations present in empirical time series, which were assumed by physicists as a stylized fact, were studied by them since more than one decade (Paul and Baschnagel 1999, Mantegna and Stanley 2000, Bouchaud and Potter 2001, Ilinski 2001). In distinction the synthetic time-series were obtained by us from the recently developed one-dimensional Continuous-Time Hierarchical Walks (CTHW) (Kutner 2002, Kutner and Świtała 2003) and analogous Hierarchical Flights (CTHF), (Kutner 1999). It seems that the power-law autocorrelations discovered by discretization of the time-series obtained within the CTHW and analogous log-normal ones found for the CTHF, have a persistent character, i.e. they seem to be unavoidable artifacts for the HF time series.

## The model

In this section we consider the above mentioned two types of the hierarchical (Weierstrass) models which cover two types of representations of empirical high-frequency financial time-series and hence two types of the corresponding non-linear autocorrelations (power-law and log-normal in the same time-windows).

## Hierarchical CTRW model and the main result

The present, generalized version of the CTRW model is the combined one defined by the non-separable hierarchical (or Weierstrass) walk which can be occasionally (randomly) intermitted by momentary localizations (WWRIL); the localizations themselves are also described by the Weierstrass (or hierarchical) process. It should be noted that the steps of the walk as well as the momentary localizations are uncorrelated. This approach makes it possible to study by (hierarchical) stochastic (Monte Carlo) simulations the whole spatial-temporal region, while analytically it is possible to study only the initial, pre-asymptotic and asymptotic ones but not the very important intermediate region.

The basic continuous-time series obtained from this stochastic simulation is shown in Fig.1 by a sequence of vectors $\mathbf{A}_1$, $\mathbf{A}_2$, $\mathbf{A}_3$, $\mathbf{A}_4$, $\mathbf{A}_5$,..., connecting the turning points of a single realization of a subordinate random walk trajectory (expanding in positive X-direction as we study only the absolute values of the stock price variations $|\Delta X|$). This simulation is supported by the waiting-time distribution which is the main quantity of our two-state (walking-localization) model. The states of the model are again characterized by their own waiting-time distributions (which give indeed the main distribution in the form of a weighted sum). Each single-state waiting-time distribution is a hierarchical, geometrically weighted superposition of partial waiting-time distributions, describing the regular spatial-temporal processes (connected with single hierarchy generations) which are already easy to simulate.

The synthetic (derivative), discrete time-series was obtained by discretization of the original (basic) continuous-time series at a fixed time horizon $\Delta t$ (shown in Fig.1 by the sequence of characteristic vectors $\mathbf{Q}_1$, $\mathbf{Q}_2$, $\mathbf{Q}_3$, $\mathbf{Q}_4$, $\mathbf{Q}_5$,...,).

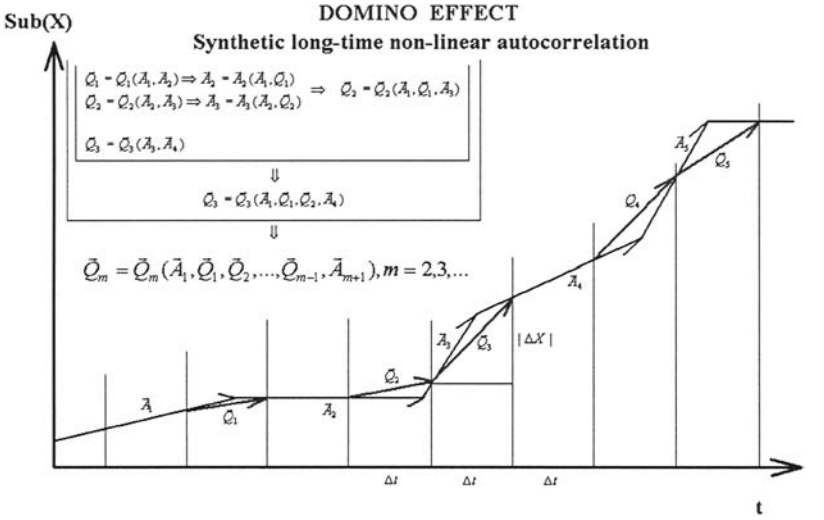


**Fig.1.** Plot of a single realization of a basic synthetic, subordinate (directed) continuous-time trajectory (defined by the sequence of vectors $\mathbf{A}_1$, $\mathbf{A}_2$, $\mathbf{A}_3$, $\mathbf{A}_4$, $\mathbf{A}_5$,...,) and synthetic,

discretized one (defined by a sequence of adequately chosen, characteristic vectors $\mathbf{Q}_1$, $\mathbf{Q}_2$, $\mathbf{Q}_3$, $\mathbf{Q}_4$, $\mathbf{Q}_5$,..., ). The vertical axis denoted as Sub(X) (i.e. subordinate X) is defined as:

$$Sub(X(n\Delta t)) = \sum_{j=0}^{n} |\Delta X(j\Delta t)|$$

As it is seen, the turning points of the basic continuous-time series are, in general, incommensurate with the analogous points supplied by the discrete time series. The autocorrelation function K(t) (defined in the caption to Fig.2) has been studied versus time just for this discrete time-series.

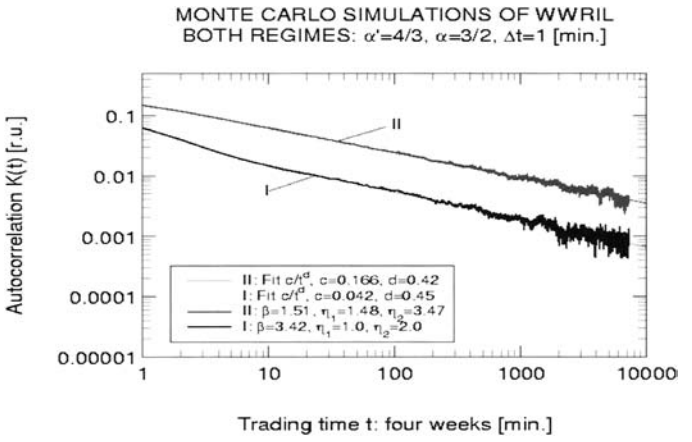


**Fig.2.** Autocorrelation of the centered absolute variations of the stock price (or the walker centered absolute variations of the single step displacement $\Delta X(t) = X(t) - \langle|X(t)|\rangle$, where time $t = n\Delta t$, $n=0,1,2,...$, and $\Delta X(t) = X(t+\Delta t)-X(t))$, defined as usual by the quantity $K(t) = \langle|\Delta X(0)\cdot\Delta X(t)|\rangle - \langle|\Delta X(0)|\rangle\cdot\langle|\Delta X(t)|\rangle$ for the synthetic high-frequency time-series. This quantity was obtained by our time-discretization procedure within the Weierstrass walks randomly intermitted by localizations (WWRIL) for: (I) Gaussian, and (II) non-Gaussian regions of the stock price. The slopes of both curves (defined by exponent $d$ for almost three decades) differ but slightly (viz. for case I: $d=0.42$, and for case II: $d=0.45$). The dynamic exponents, $\eta_1$ and $\eta_2$, define the evolutions of the second and fourth moments of the stock prices (displacements) X(t) (and they depend on the partial dynamic exponents $\alpha'$, $\alpha$, $\beta$ ). The temporal partial dynamic exponents $\alpha'$ and $\alpha$ describe the localization and time-dependence of the walking state, respectively. The spatial exponent $\beta$ defines space penetration within the walking state.

As it is shown in Fig.2, the autocorrelation K(t) exhibits a power-law relaxation over more than three decades both for the Gaussian and non-Gaussian processes.

## Further results and concluding remarks

Hitherto, we studied the representation of financial tick data by the continuous-

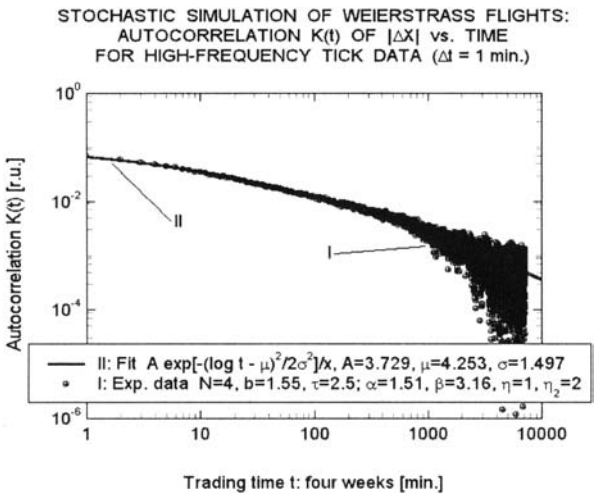


time Weierstrass walk trajectory while in this section we consider the same set of data points represented by the continuous-time Weierstrass flight trajectory. In the latter case, the displacement of the walker or the price variation is shown by the vertical vector (instantaneous jumps) and not by the tagent one (the walk having a

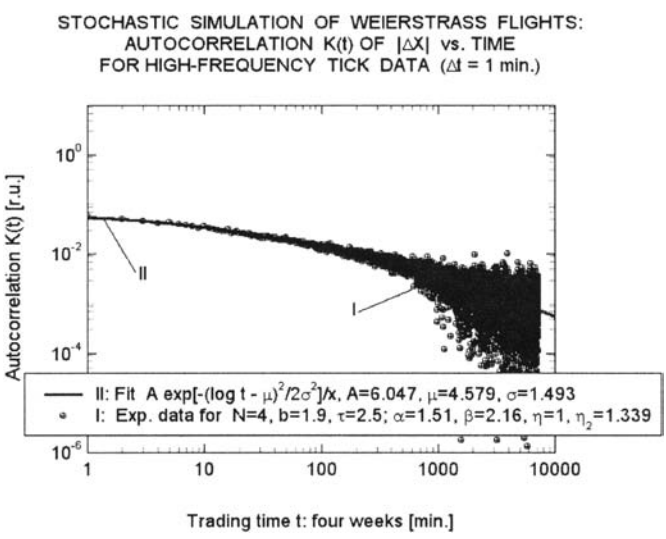


finite velocity such as, for example, that shown by vectors $\mathbf{A_j}$, j=1,2,..., in Fig.1).

Fig.3. The log-normal dependence of the autocorrelation function K(t) (defined in caption to Fig.1) vs. time within a four weeks time-window for the Gaussian (upper figure) and non-Gauusian (lower figure) regions of the price variations.

As it is seen in Fig.3, the autocrrelation function K(t) exhibits log-normal correlations after high-frequency time discretization (at time-horizon $\Delta t = 1$ min.). It should be noted that these correlations can be mistaken locally for a power-law (Montroll 1984, Sornette 2000). Again the log-normal autucorrelations have a long-term, persistent character.

The above considerations have shown that the obtained autocorrelations come from the 'domino effect' occurring within the discrete time-series (as shown, for example, in Fig.1). This domino effect occurs as each pair of displacements (obtained after the discretization) shown by vectors $\mathbf{Q}_j$ and $\mathbf{Q}_{j+1}$, j=1,2, ... , have common 'bonds' given by the corresponding basic vectors $\mathbf{A}_{j+1}$, j=1,2, ... . We suppose that this effect is indeed responsible for the analogous long-term autocorrelations commonly occurring in the empirical financial high-frequency time-series.

## References


Bouchaud J-P and Potter M (2001) Theory of Financial Risks. From Statistical Physics to Risk Management. Cambridg Univ. Presss, Cambridge

Ilinski KI (2001) Physics of finance. Gauge modeling in non-equilibrium pricing. J. Wiley & Sons Ltd., New York

Kutner R (1999) Coherent Spatio-Temporal Coupling in Fractional Wanderings. Renewed Approach to Continuous-Time Lévy Flights. In: Kutner R, Pękalski A, Sznajd-Weron K (Eds) Anomalous Diffusion. From Basics to Applications. Lecture Notes in Physics Vol. 519. Springer, Berlin, Heidelberg, New York, pp.1-14.

Kutner R (2002) Extreme events as foundation of Lévy walks with varying velocity. Chem. Phys. 284; 481-505

Kutner R and Świtała F (2003) Study of the non-linear autocorrelations within the Gaussian regime. Eur. Phys. J. B **33;** 495-503

Kutner R and Świtała F (2003) Stochastic simulations of time series within Weierstrass-Mandelbrot walks. Qunat. Finance **3;** 201-211

Mantegna RN and Stanley HE (2000) An Introduction to Econophysics. Correlations and Complexity in Finance. Cambridge Univ. Presss, Cambridge

Paul W, Baschnagel J (1999) Stochastic Processes. From Physics to Finance. Springer, Berlin, Heidelberg, New York

Lebowitz JL and Montroll EW (1984) In: Nonequilibrium Phenomena II. From Stochastics to Hydrodynamics. Studies in Statistical Mechanics Vol. XI. North-Holland, Amsterdam, Oxford, New York, Tokyo

Sornette D (2000) Critical Phenomena in natural Sciences. Chaos, Fractals, Selforganization and Disorder: Concepts and Tools.

# Evidence for Superdiffusion and "Momentum" in Stock Price Changes

Morrel H. Cohen[1], and Prasana Venkatesh[2]

[1]Department of Physics and Astronomy, Rutgers University, Piscataway. NJ 08854-8019, USA. E-Mail: mhcohen@prodigy.net

[2]Derivatives Research, Lehman Brothers Japan, 6-10-1 Roppongi Hills, Tokyo 106-6131, Japan. E-mail: Prasana.Venkatesh@Lehman.com

**Summary.** It is now well established that the probability distribution of relative price changes of stock market aggregates has two prominent features. First, in its central region, the distribution closely resembles a Levy stable distribution with exponent $\alpha \cong 1.4$. Secondly, it has power-law tails with exponent $\nu \leq 4$. Both these results follow from relatively low resolution analyses of the data. In this paper we present the results of a high-resolution analysis of a database consisting of 132,000 values of the S&P 500 index taken at 10 minute intervals. We find a third prominent feature, a delta function at the origin the amplitude of which shows power-law decay over time with an exponent $c \cong 2/3$. We show that Continuous-Time Random-Walk (CTRW) theory can account for all three features, but predicts subdiffusion with a growth of the variance of the ln(price) as the $c$*th* power of time. We find instead superdiffusion with an exponent $c \cong 9/8$ instead of $2/3$. We conclude that CTRW theory must be extended to incorporate the effects of "Price Momentum".

**Key words.** Levy Stable, Continuous Time Random Walks, Stock Price Statistics

## I. Introduction.

The interpretation of financial time series as random walks of price over time has a deep history well reviewed by Mantegna and Stanley [1]. Mantegna, Stanley, and collaborators, via careful statistical analysis of large data sets, have argued that the relative changes of stock prices over a fixed time interval follow a Levy-stable distribution in the central region with inverse power law tails [1]. The index $\alpha$ of the Levy region is approximately 1.4 [2] and the exponent $\nu$ of the decay of the tails is typically somewhat less than 4 [3, 4]. Sokolov, Chechkin, and Klafter (SCK) have shown [5] that a suitable generalization of the diffusion equation containing a fractional "space" derivative has as its solution a distribution which is Levy-like in the central region and crosses over to power-law decay in the tails, with the remarkable feature that $\alpha + \nu = 5$, not inconsistent with the data.

For any such generalized Smoluchowski equation there is an underlying fractional random walk [6].

The problem of finding a random-walk description of financial time series encompassing all empirically established facts thus appeared close to solution. Accordingly, we decided to test the quality of the fit of the SCK theory to the empirical yield distributions computed from 132, 000 values of the S&P 500 stock price index at 10 minute intervals in the period 1984 through 1996 [7]. We found a good fit to the tails, but a poorer fit in the central region. More precisely, we fitted integrals of the distribution over approximately 130 intervals chosen to contain approximately 100 data points each.

We chose to fit intervals because we knew from prior unpublished work [8, 9] that the central region of the distribution contains a zero-yield delta function surrounded by gaps. In Section II, we confirm that feature in the S&P 500 data via a high-resolution analysis. In Section III, we argue that it would be difficult to account for those features via fractional diffusion equations or stochastic differential equations but that all known features can be accounted for by Continuous Time Random Walk (CTRW) theory [10-12]. In Section IV, we show that because of the slow decay of the delta function reported in Section II, it follows rigorously that the ln(Price) undergoes subdiffusion. Nevertheless, we find that the S&P 500 data show superdiffusion, in direct contradiction to the CTRW theory as we have formulated it. We conclude in Section V, that a conceptual change is required in the way random walk theory is used to interpret financial time series.

## II The Delta Function.

In our notation $x(t)$ the natural logarithm of the price of the S&P 500 index at time $t$, is the basic random variable, assumed to undergo a CTRW. $X(t, \tau) = x(t + \tau) - x(t)$ is the excursion in $x$ over the interval $\tau$. $Y(t,\tau) = X(t,\tau)/\tau$ is the yield over the interval $\tau$. $n(X,t)$ is the probability density of excursions $X$ over the interval $t$. $n(X,0) = \delta(X)$ is the initial condition on $n(X,t)$. We have chosen to compile the statistics of the yield $Y$ after subtracting its mean. Note that for small price change or small interval $\tau$, $X(t,\tau)$ is just the widely studied [1] relative price change.

In the Figure we plot a yield-frequency histogram for a 10 minute interval at low resolution. A prominent feature stands out. It is the spike in the box centered at zero yield. Every entry in that box corresponds to zero yield and no change in $X$, so the spike is direct evidence of a delta function in $n(X,t)$ centered at $X = 0$ similarly for $n(Y,t)$.

The probability distribution $n(X,t)$ thus has the form $n(X,t) = A(t)\delta(X) + m(X,t)$ where $A(t)$ is the amplitude of the delta function and $m(X,t)$ is the non-singular portion of the distribution. Because

$n(X,0)=\delta(X)$, $A(0)=1$ and $m(X,0)=0$. We find a slow decay of $A(t)$ with time which is well fitted by the form $A(t)=(1+t/\tau)^{-b}$ with $b=0.6665\pm0.0021 (b\cong 2/3)$ and $\tau=0.769\pm0.003$ seconds. All our data are in the asymptotic domain.; $m(X,t)$ contains the smooth power law tails with $v=3.65\pm0.21$.

## III. Continuous Time Random Walks.

It is quite extraordinary that after a century of quantitative analysis of financial time series, the existence of the delta function has not previously been reported. Generalized diffusion equations can be found which give the delta function [14], but getting its time decay right would be difficult. On the other hand, CTRW theory provides a natural basis for constructing models which contain the delta function, the Levy-like central region, and the power law tails within a unified formalism. In a CTRW, a walker jumps from one point to another after a waiting time $t$. The waiting time is random with a distribution $f(t)$. It is straightforward to prove that a delta function exists in $n(X,t)$ and that $f(t)=-dA(t)/dt$. Our empirical form, Equation (2), and measured values of $b$ and $\tau$ thus fix $f(t)$. The CTRW theory can thus yield all features of $n(X,t)$ known at this point.

## IV. The Diffusion of the Natural Logarithm of the Price.

It is tempting to stop at this point and say that with CTRW theory yielding the known features of $n(X,t)$, it is time to try to understand how and why the behavior of agents in the marketplace manifests itself as a CTRW in the natural logarithm of the price. It would be safer to do so, however, after confirmation of an actual prediction of the CTRW theory. One property simple to extract both from CTRW theory and the data is the time-dependence of the variance $V(X,t)$ of $X(t)$. The form for $\phi(t)$ yields $V(X,t)\approx t^{-b}$ for the asymptotic dependence of $V(X,t)$ on $t$. Thus the natural logarithm of the price undergoes subdiffusion.; *i.e.*, its variance changes with time with a power less than unity since $b\approx 2/3$. We have measured the variance of the yield $Y$, $V(Y,t)$, for which CTRW requires that it be asymptotically proportional to $t^{b-2}=t^{-4/3}$ with decay exponent greater than unity. We do indeed get a good fit of $V(Y,t)$ to the power law $at^{-c}$ with $a=1.039\times10^{-6}\pm1.083\times10^{-7}$ but $c=0.877\pm0.082$ is *less than unity*. This implies an exponent for $V(X,t)$ of $2-c=1.123\cong 9/8$, which is greater than

unity. Thus the ln(Price) undergoes *superdiffusion* in direct contradiction to the subdiffusion predicted by CTRW given the decay of the delta function found in the data.

## V. Conclusion.

Despite its inability to capture the superdiffusion of the ln(Price), the CTRW theory gets so many other features of $n(X,t)$ correctly – the decaying delta function, the quasi-cusp-like behavior evident at low resolution, the power-law tails – that it must be close to a fully satisfactory theory. An example of a simple stochastic model which shows superdiffusion has been given by Zumofen and Klafter [15]. Its import for financial time series is that it contains what is termed momentum in financial analysis, albeit in a highly oversimplified form. We conclude that our finding of superdiffusion can be reconciled with CTRW theory without loss of its attractive features through introduction of correlation of successive jumps or in the underlying dynamic yields. This would require a generalization of the conceptual and formal structure of CTRW theory.

### References


1. R. N. Mantegna and H. Eugene Stanley (2000), An Introduction to Econophysics; Correlations and Complexity in Finance, Cambridge University Press, Cambridge
2. R. N. Mantegna and H. E. Stanley (1995), Scaling Behavior in the Dynamics of an Economic Index, Nature, 376, 46 – 49.
3. P. Gopikrishnan, M. Meyer, L. A. N. Amaral, and H. E. Stanley (1998), Inverse Cubic Law for the Distribution of Stock Price Variations, Eur. Phys. J. B, 3, 139-140.
4. X. Gabaix, P. Gopikrishnan, V. Plerou, and H. Eugene Stanley (2003), A theory of power-law distributions in financial market fluctuations, Nature, 423, 267 – 270.
5. I. M. Sokolov, A. V. Chechkin, and J. Klafter (2004), Fractional Diffusion Equation for a Power-Law-Truncated Levy Process, Physica A, 336, 245-251.
6. R. Metzler and J. Klafter (2000), The Random Walk's Guide to Anomalous Diffusion; a Fractional Dynamics Approach, Physics Reports, 339, 77 – 140.
7. We are deeply grateful to Dr, P. Gopikrishnan and Professor H. Eugene Stanley for so generously providing us with the data.
8. Morrel H. Cohen and V. D. Natoli (2002), unpublished.
9. Morrel H. Cohen and Prasana K. Venkatesh (2002), presented at the Second Nikkei Symposium on "Applications of Econophysics" Tokyo, Nov 12 – 14, 2002; unpublished.
10. E. W. Montroll and M. F. Shlesinger (1984), On the Wonderful World of Random Walks, in Non-equilibrium Phenomena II; from Stochastics to Hydrodynamics, eds. J. L. Lebowitz and E. W. Montroll, North Holland, Amsterdam pp 1 – 121.
11. H. Scher and M. Lax (1973), Stochastic Transport in a Disordered Solid. I Theory, Physical Review B, 7, 4491-4502.
12. J. Klafter and R. Silbey (1980), Coherence and Incoherence, Exciton Motion in the Framework of the Continuous Time Random Walk, Physics Letters A, 76, 143-146.
13. M. F. M. Osbourne (1959), Brownian Motion in the Stock Market, Operations Research, 145-173

14. Morrel H. Cohen, Unpublished.
15. G. Zumofen and J. Klafter (1995), Laminar localized-phase coexistence in dynamical systems, Physical Review E 51, 1818 – 1821. We are grateful to Professor Klafter for bringing this paper to our attention.

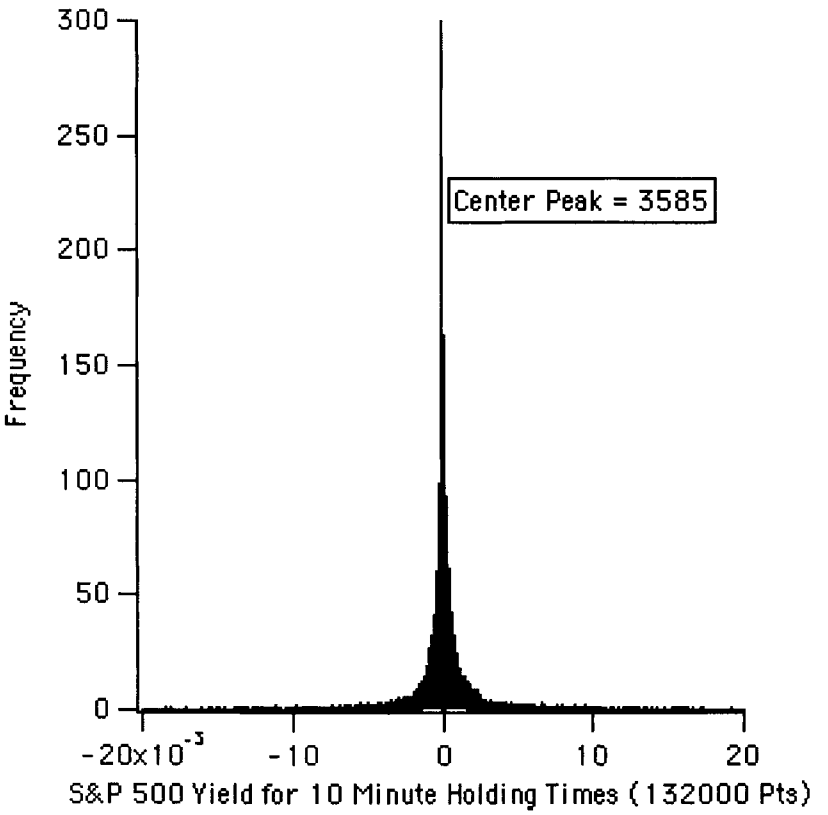

# Beyond the Third Dimension: Searching for the Price Equation

Antonella Sabatini[1]

[1]Finbest Spa, CEO, Engineering, Project and Portfolio Manager. Via San Domenico, 70, Florence, 50133, Italy - *as@alum.mit.edu*

The purpose of this study is to examine the deterministic structure of financial time series of prices in presence of chaos and a low-dimensional attractor. The methodology used consists of transforming the observed system, typically exhibiting higher dimensional characteristics, into its *corresponding best two dimensional system*, via attractor or phase space reconstruction method, with subsequent intersection of the reconstructed attractor with the best two-dimensional (2D) hyperplane. The 2D system resulting from this slicing operation can be used for financial market analysis applications, by means of the determination of the *price equation.*

**Key words.** Non-Linear Dynamics, Attractor Reconstruction, Embedding Dimension, Dimension Reduction, Price Equation

## Phase Space and Attractor Reconstruction

A phase or state space is a space in which each point describes the state of a dynamical system as a function of the non-constant parameters of the system. Implicit in the notion is that a particular state in phase space specifies the system completely; it is all we need to know about the system to have complete knowledge of the immediate future.

It has been demonstrated (Packard et al. 1980) that the characteristics of the phase space can be derived by a plot, named *return map* or *phase space reconstruction*, obtained from the time series, which is the observed output of the dynamical system. The basic idea of phase space reconstruction is that evolution of any state component of a system depends on other interacting components within the same system, so the information of these related components is hidden under the evolution of the single component. In order to reconstruct an *equivalent* high dimensional space that the system embeds in, we need only to investigate the one component we are able to observe and measure, by utilizing some time-delay data of observed time series as new coordinates for the phase space.

The observations are a projection of the multivariate state space of the system onto the one-dimensional axis of the phase space. The purpose of time-delay

embedding is to unfold the projection back to a multivariate state space that is representative of the original system. Suppose that the time series to be investigated is represented by scalar x(t), sampled at rate h, giving rise to the observations $x_1,x_2,..x_N$. We need to reconstruct the state space by the well know technique of attractor reconstruction by time delays, as follows:

The delay state vector, for every state i, is defined as

$$\mathbf{x}_i=(x_i,x_{i-\tau},x_{i-2\tau},\ldots x_{i-(m-1)\tau})'$$

Where m is the embedding dimension, $\tau$ is the time lag. The notation V' represents the transpose of the vector V.

The choice of the parameter m is crucial for the efficacy of the model representing the system under investigation. One algorithm commonly used to determine m is the *method of false neighbors*. The proper choice of time delay $\tau$ is also essential in reconstructing procedures, (Fraser and Liebert). Several methods are known and used frequently. Empirical studies discussed the determination of $\tau$, which should be defined by the relation $m=g/\tau$, where g is the average length of non-periodic cycles in the series. One method of determining $\tau$ is by using the *average mutual information function* or the autocorrelation method.

### Poincarè Sections

Assume a state space of a system in 3D is x,y,z. Then, a set of points sampled at constant z constitute a *Poincarè section* - in other words - a subset of state space that slices the attractor non tangential to the trajectories. A Poincarè section has the property of reducing the phase space dimension by one. The Poincarè section is defined not by a fixed time interval, but by successive times when an orbit crosses a fixed surface in phase space ("surface" here means a manifold of dimension one less than the phase space dimension, m). The placement of the Poincaré surface is of high relevance for the usefulness of the result. An optimal surface maximizes the number of intersections, i.e. it minimizes the time intervals between them. Another aspect for the choice of the surface of section is that one should try to maximize the variance of the data inside the section.

## The Method

Poincarè sections would be perfect and would work quite well if the embedding dimension of the system under investigation were three dimensional. Most financial time series are high-dimensional processes and a Poincarè section has the property of reducing the phase space dimension only by one. Since the purpose of this study is to reduce the dimension of the original system from a high number of dimensions (on the order of 10 dimensions) to two dimensions by reconstructing a system carrying equivalent information, or with the minimal information loss,

another approach needs to be used. The concept of Poicarè sections is utilized in its essence, but the idea is extended further: let's assume that the system object of this investigation has been estimated of embedding dimention, m. Let's further assume that the delay factor has been estimated to be $\tau$; This paper presents the following algorithm to transform the original time series with N states or observations, inherently embedded in a m-dimensional (12- dimensional) space, into its corrisponding best two-dimensional system. The algorithm is as follows:

1. Reconstruct the attractor by the well known procedure of attractor reconstruction by time delay, obtaining the delay vector, for all states (observations), i, of the system: $\mathbf{x}_i=(x_i,x_{i-\tau},x_{i-2\tau},\ldots x_{i-(m-1)\tau})'$.
2. Define $\mathbf{x}_{i,s}=(x_i,x_{i-\tau},x_{i-2\tau},\ldots x_{i-(s-1)\tau},c_{const},\ x_{i-(s+1)\tau},\ldots x_{i-(m-1)\tau})'$, where $1 < s \leq m-1$ and c is the value of the ith observation for the $x_{i-(s)\tau}$ component, kept constant (or defined in a small range), $\forall$ i; repeat $\forall$ s.
3. $\forall$ i and $\forall$ s, compute $\chi_i \cap \chi_{i,s} \cap \chi_{i,s} \ldots \cap \chi_{i,s}$ for m-2 components, This operation is equivalent to the intersection between the vector of $x_i$ and the hyperplane H (vector defined by all its components equal to a constant, c [realization of state i], except for two components).
4. Find $x_{s_{\max}} = \max\left(\chi_i \cap \chi_{i,s} \cap \chi_{i,s} \ldots \cap \chi_{i,s}\right)$, where max() returns the intersection result vector with the maximum number of points,

$\chi_{s_{\max}}$ will yield the best two-dimensional reconstruction of the original m-dimensional system. The resulting system, being now embedded in two dimensions, is not an exact homoeomorphism of the original system, as the technique of Poincarè section would have achieved. On the other hand, this method provides the practitioner in the financial markets analysis and trading industry, with a two dimensional system much easier to deal and to work with: that is, the system formed by the number of points left after the intersection operation of the original vector $\mathbf{x}_i$ with the hyperplane H.

The transformed two dimensional system is then best fitted to obtain an equation which relates the current information as a function of its corresponding $\tau$-lagging value.

The computational complexity of the algorithm for the determination of the corresponding two-dimensional system is $O(N^2)$. Improvements can be made in the attempt to achieve a computational complexity of O(NLogN). Considering that N is relatively small, for practitioners in the financial markets, the algorithm should not require very intense computational efforts.

## Empirical Studies

Three different time series are depicted below (Fig. 1). By a qualitative assessment, it is obvious that the financial market time series is not two-

dimensional. Its higher dimensional dynamics projected onto a 2D plane exhibits non-ordered behavior (Fig. 1).

A 3D attractor reconstruction of the Eur/Usd time series (Fig. 2.a) also exhibits a non-ordered pattern. It is the result of a multidimensional attractor being projected onto a 3D surface. However, for illustrative purposes only, the dimension reduction procedure is depicted in the 3D case, starting from a 3D reconstructed attractor: various slices (two dimensional planes) are selected from the 3D attractor (Fig. 2.b-d). It is necessary to select the slice containing the maximum number of point.

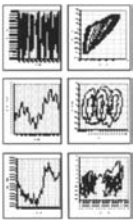

**Fig. 1**. Non-linear systems: (from top to bottom): Logistic Equation, Standard Time Series, portion of Eur/Usd Time Series. Time domain plot (left); Phase space plot (right).

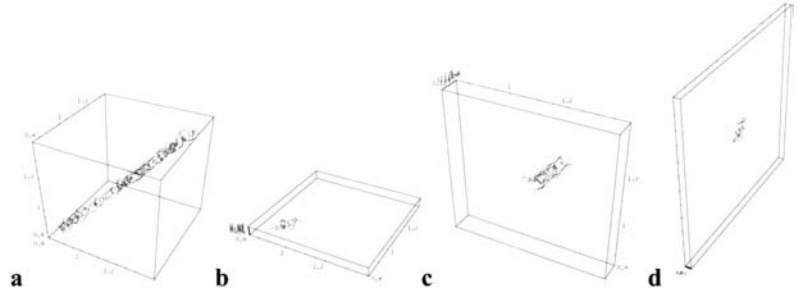


**Fig. 2**. Eur/Usd - Example of a 2D slice of a 3D Attractor Reconstruction **a.** 3D Attractor Reconstruction; **b-d** different slices.

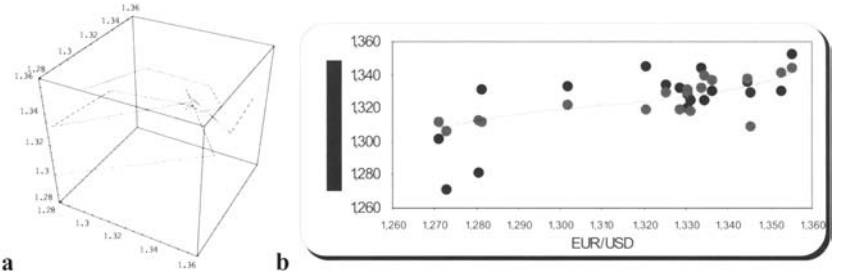


**Fig. 3**. Eur/Usd (Weekly data from 10.02.1995 to 31.12.2004) - Example of a 2D slice of a 8D Attractor Reconstruction; **a**. best 2D corresponding system; **b.** *price equation.*

By using the technique of attractor reconstruction with time delay the best 2D corresponding system for the Eur/Usd series is calculated. Next, a best-fitting procedure is implemented to determine the best curve approximating the best 2D reconstructed system. Such curve, expressed in closed form, represents the desired *price equation.*

## Practical Conclusions

An instance of the price equation for the Eur/Usd is:

$$y=1.3251 + 0.0021 \sin(t) + 0.0032 \cos(t) - 0.0025 \sin(2t) + 0.0161 \cos(2t)$$

To illustrate: for y = 1,3093 its corresponding Eur/Usd value is 1,345 (mid December 2004). Recall that the y curve, deriving from Eur/Usd(t-$\tau$), is lagging by $\tau$ units of time. This indicates a growing trend in the near term (next two o three weeks). By virtue of self-similarity and fractal properties, longer-term determinism can be achieved by changing scale and zooming out to a lower frequency chart (i.e. monthly chart). An important issue to be further investigated is whether the magnitude of loss of information derived from the application of the procedure of attractor reconstruction with dimension reduction to the observed time series can be acceptable for the financial markets money management industry.

### Acknowledgments

The author wishes to thank Prof. D. Ruelle for his insightful observations on Poincarè sections and embedding dimension, Prof. H. E. Stanley for his invaluable expertise and comments on various econophysics issues. Prof. Giulia Rotundo for her interesting remarks and suggestions on this work.

## References

Abarbanel, H.D.I., *Analysis of observed chaotic data.* N.Y. Springer-Verlag, 1996

Grassberger, P, *Generalized Dimensions of Strange Attractors*, Phys.Lett.97A, 227 (1983).

Grassberger, P, Procaccia, I., *Characterization of Strange Attractors.* Physical Review Letters, (1983), 50, 346-369.

Grassberger, P., Procaccia, I., *Measuring the Strangeness of Strange Attractors.* Physica D, 9, (1983), 189-208.

Hamilton, J. G., *Time Series Analysis,* Princeton University Press, 1994.

Hayashi, K., *The Applications of Econophysics*, Proceedings of the Second Nikkei Econophysics Symposium, H. Takayasu Ed., Tokyo, 2002, Springer 2004, *Chaotic Structure in Intraday Data of JGB Futures Price*, Pag. 140-145

Hurst, H.E.., *Long Term Storage Capacity of Reservoirs*, Trans. Am. Soc. Civil Engineers, 116, 770-799

Kennel MB, Brown R, Abarbanel HDI (1992), *Determining Embedding Dimension for Phase Space Reconstruction using a Geometrical Construction.* Phys Rev A 45: 3403±3411

Lezos G. et. Al., *Predicting the Future with the Appropriate Embedding Dimension and Time Lag*, 1999 IEEE, 2509

Mandelbrot, B., *The Variation of Certain Speculative Prices*, in P. Cootner, ed., *The Random Character of Stock Prices. Cambridge*, MIT Press, 1964

Markowitz, H. M., *Portfolio Selection*, Blackwell Publishers Inc. 2002

Mantegna R.N., Stanley H.E., An *Introduction to Econophysics; Correlations and Complexity in Finance*, Cambridge University Press, Cambridge, UK

Packard, N., Ruelle, D. and Takens, F. - 1981.

Peters, E. E., *Chaos and Order in the Capital Markets*, Wiley Finance Edition, Second Edition, 1996

Poincaré H., *The Foundations of Science*, University Press of America, New York, 1982.

Ruelle D., *Chaotic Evolution and Strange Attractors*, Cambridge University Press, Cambridge, 1989.

Software: Microsoft Office 2000 Excel; Wolfram Research Mathematica ver. 5.0

Sprott J.C., *Chaos and Time-Series Analysis*. Oxford University Press, 2003, Oxford, UK, & New York, US. 2003.

Strogatz, S.H., *Non Linear Dynamics and Chaos*, Westview Press, December 2000.

Takens F., *Detecting Strange Attractors in Turbulence*. Dynamical Systems and Turbulence, ed. Rand, D. A. & Young, L.-S., New York: Springer-Verlag. Lecture Notes in Math. 898. pp. 366-81 (1981).

# An agent-based model of financial returns in a limit order market

Koichi Hamada[1], Kouji Sasaki[2] and Toshiaki Watanabe[3]

[1]Department of Economics, Yale University, 28 Hillhouse Avenue, New Heaven, CT 06511, USA
[2]Institute for Monetary and Economic Studies, Bank of Japan, 2-1-1 Nihonbashi Hongokucho Chuo-Ku, Tokyo, 103-8660, Japan
[3]Faculty of Economics, Tokyo Metropolitan University, Minami-Osawa 1-1, Hachioji-Shi, Tokyo, 192-0397, Japan

**Summary.** A set of finance literature shows that asset return processes are characterized by a GARCH class conditional volatility and fat-tail distributed disturbances, such as mixture of normal distributions and $t$-distribution (Watanabe 2000; Watanabe and Asai 2004). This paper finds that this type of complicated process arises by aggregating returns of a risky asset traded in a limit order market. The conditional volatility of generated return series can be modeled as a GARCH class since the volatility gradually diminishes as the price assimilates the new information about the future asset return. The reason why the error term of estimated model is fat-tail distributed is that the return of transaction prices is distributed as a mixture of normals; one of the two distributions represents the drift of the price process, and the other represents the liquidity effect.

**Key words.** Agent model, Liquidity, Limit order market

## The model

We consider a security market where traders exchange a risky asset. The number of trading days and the number of traders' arrivals on a particular trading day are denoted by $T$ and $J$, respectively. On a trading day $t$, new information about the log return innovation arrives at the market. The stochastic innovation is given by the following binomial form.

$$\log(v_t) - \log(p_{t-1}) = \begin{cases} +\sigma, & \text{with probability } \phi \\ -\sigma, & \text{with probability } 1-\phi \end{cases} \tag{1}$$

where $v_t$ is the end-of-the-day "true" asset value implied by the information, and $p_{t-1}$ is the closing price of the previous trading day, $t-1$. The parameters $\sigma(>0)$ and $\phi$ denote the log return innovation and the probability that the price innovation is upward, respectively. We assume that $\sigma$ and $\phi$ are constant for all the trading days. Traders know the distribution of the log return process as in equation (1), but do not know the realization of the innovation, either $+\sigma$ or $-\sigma$, until the trading session of the day finishes. We assume that the timing that the trading session finishes is stochastically determined. The session finishes when $J$-th trader arrives at the market if the following condition is first satisfied.

$$\tilde{u} > 1 - \left(\frac{1}{10}\right)^{\frac{F}{1}} \tag{2}$$

where $\tilde{u}$ is a random draw from the uniform distribution $U(0,1)$. The draw is performed at every trader's arrival. $F$ is a positive constant. Under this specification the number of traders arriving at the market in a trading day is expected to be high with a high value of $F$. When the trading session finishes the latest transaction price becomes the closing price of the day. We let $p_{t,J}$ denote the closing price at day $t$. On the next day $t+1$, the information is overwritten on the remaining information, $\log(v_t) - \log(p_{t,J})$. This specification describes the situation that traders cannot trade after the closure even though the information about the return innovation is not completely assimilated into the price. Before the next day's trading session starts new information arrives and is overwritten on the previous day's remaining information.

We consider that this asset is traded in a limit order market, where there is no intermediary to quote the bid-ask prices and to execute orders, and thus traders need to exchange the asset voluntarily. On a day the asset return innovation is positive (with probability $\phi$) a trader arriving at $j$-th is a buyer with probability $\frac{1}{2}(1+\pi)$ and a seller with probability $\frac{1}{2}(1-\pi)$. On a day the asset return innovation is negative (with probability $1-\phi$) a trader arriving at $j$-th is a buyer with probability $\frac{1}{2}(1-\pi)$ and a seller with probability $\frac{1}{2}(1+\pi)$. Each trader submits an order with specified trade conditions, i.e. price and quantity. The orders are collected and prioritized by a centerized market system. The buy (sell) order with a higher (lower) order price submitted earlier in the trading session obtains priority of execution. The prioritized orders are recorded in a limit order book and immediately published. An order is executed if the order price of incoming buy (sell) order is not lower (higher) than the lowest (highest) order price in the limit order book on the sell (buy) side. When the trading session of a particular day finishes the book is cleared and the next day's session starts with an empty book. A main characteristic of this market mechanism is that a pile of already submitted orders play a role of liquidity suppliers for incoming traders, and incoming traders become either liquidity suppliers if their orders are not immediately executed, or liquidity demanders if the orders are executed immediately.

In such a market traders are likely to determine their order strategies conditional on the state of the order book. We assume in this paper that they determine the order price and quantity conditional on their posterior beliefs about the return innovation. The posterior is formed conditional on a summary statistic of the state of the book, $n$. The value of $n$ describes the number of waiting buy orders exceeding that of waiting sell orders. If $n > 0$ the number of already submitted buy orders is greater than that of already submitted sell orders by $n$, and if $n < 0$ the number of already submitted buy orders is less than that of already submitted sell orders by $|n|$. Then a buyer (a seller), arriving at the market when the state of the book is $n$, submits the order with following price $p_t^b(n)$ and quantity $q_t^b(n)$ ($p_t^s(n)$ and $q_t^s(n)$).

$$p_t^b(n) = p_{t-1,J} \exp\left(-\sigma \frac{\left(\frac{1-\pi}{1+\pi}\right)^n - \gamma}{\left(\frac{1-\pi}{1+\pi}\right)^n + \gamma}\right), \qquad q_t^b(n) = \frac{1}{1 + |p_t^b(n) - p_{t-1,J}|} \tag{3}$$

$$p_t^s(n) = p_{t-1,J} \exp\left(+\sigma \frac{\left(\frac{1-\pi}{1+\pi}\right)^{-n} - \gamma}{\left(\frac{1-\pi}{1+\pi}\right)^{-n} + \gamma}\right), \qquad q_t^s(n) = \frac{1}{1 + |p_t^s(n) - p_{t-1,J}|} \tag{4}$$

We note that the order prices of buyers and sellers increase as $n$ increases, and decrease as $n$ decreases. This is rationalized by the fact that on the day of positive return, the likelihood of buyers' arrival is $\frac{1}{2}(1+\pi)$ and the likelihood of sellers' arrival is $\frac{1}{2}(1-\pi)$. The symmetric argument holds on the day of the negative return.

Trade takes place if $p_t^b(n)$ is not less than the lowest order price in the order book proposed by sellers, denoted by $\underline{P}^{ask}$, or $p_t^s(n)$ is not greater than the highest order price in the book proposed by buyers, denoted by $\overline{P}^{bid}$. That is, if $p_t^b(n) \geq \underline{P}^{ask}$ or $p_t^s(n) \leq \overline{P}^{bid}$. If these conditions do not hold the submitted orders are not executed and recorded in the book.

If $p_t^b(n) \geq \underline{P}^{ask}$ the transaction price and quantity are determined as follows.

$$(p^*, q^*) = (p_t^b(n), q_t^b(n)) \qquad \text{if } p_t^b(n) = \underline{P}^{ask} \tag{5.1}$$

$$(p^*, q^*) = \left(\underline{P}^{ask}, \frac{1}{1+|\underline{P}^{ask}|}\right) \qquad \text{if } p_t^b(n) > \underline{P}^{ask} \tag{5.2}$$

Similarly if $p_t^s(n) \leq \overline{P}^{bid}$ the transaction price and quantity are determined as follows.

$$(p^*, q^*) = (p_t^s(n), q_t^s(n)) \qquad \text{if } p_t^s(n) = \overline{P}^{bid} \tag{6.1}$$

$$(p^*, q^*) = \left(\overline{P}^{bid}, \frac{1}{1+|\overline{P}^{bid}|}\right) \qquad \text{if } p_t^s(n) < \overline{P}^{bid} \tag{6.2}$$

In practice we often observe transactions with a large quantity cleaning up all the waiting orders at the best quotes, $\underline{P}^{ask}$ and $\overline{P}^{bid}$. To capture this phenomena, we assume that when the transaction occurs a trader submits a large order cleaning up all the waiting orders at the best quote with probability $q^{large}$, and an ordinary order quantity specified by equation (5.2) or (6.2) with probability $1-q^{large}$. Under this simple framework of the trading system and traders' behavior, we show that the simulated transaction price processes exhibit several important characteristics of asset return processes observed in practice.

## Simulation results

This section simulates the model presented in the previous section and examines the characteristics of simulated asset returns. To implement the simulation we set the parameter values as follows; the initial value $v_0 = 100$, the probability of return innovation being positive $\phi = 0.55$, the return innovation $\sigma = 2.5$, the trading days $T = 250$, the survival rate parameter $F = 5$, and the parameters for order price and quantity $\pi = 0.03$, $\gamma = 0.975$, $q^{large} = 0.3$. We let $\tau$ denote the event time when the transaction occurs. Then the transaction-based log return is written as follows.

$$R_\tau = \log(p_\tau) - \log(p_{\tau-1}) \tag{7}$$

To examine the effects of aggregation we compare the distributional characteristics of log return series without aggregation to those aggregating every two, five and ten transactions. We let $R1$, $R2$, $R5$ and $R10$ denote the log return series without aggregation, aggregating every two, five and ten transactions, respectively. The following table shows the descriptive statistics of these series.

**Table 1.** The descriptive statistics of simulated return series

| | price | R1 | R2 | R5 | R10 |
|---|---|---|---|---|---|
| No. of observation | 45,789 | 45,789 | 22,894 | 9,158 | 4,579 |
| mean | 126.65 | 0.00001 | 0.00001 | 0.00003 | 0.00007 |
| standard deviation | 12.20 | 0.00144 | 0.00174 | 0.00227 | 0.00295 |
| skewness | -0.18 | -1.78300 | -1.33550 | -1.05930 | -0.69787 |
| kurtosis | 2.25 | 72.49700 | 44.46500 | 18.24700 | 9.24270 |

The table shows that the log return series exhibit strong negative skewness and strong leptokurtosis. Interestingly the skewness and kurtosis become less significant as the log return is aggregated more. This observation can be explained as the liquidity effect. When there is a large number of waiting orders at the best quote, for instance at the best ask $\underline{P}^{ask}$, several buy orders may successively arrive at the market. Then they would successively hit the waiting orders at $\underline{P}^{ask}$ until all the waiting sell orders at that price are executed. Consequently it is possible to have many successive zero transaction-based returns. The frequency mass at zero return becomes less significant as the returns are aggregated more since zero returns are sumed up with non-zero returns.

The theoretical and empirical literature suggest that the time series with these distributional characteristics can be modeled as a GARCH class with fat-tailed disturbances. Thus we examine whether the generated return series is well fit to the following GARCH class, AR(1)-GARCH(1, 1) with disturbances drawn from a mixture of normal distributions (Bollerslev, Engle and Nelson 1994).

$$R_s = \rho_0 + \rho_1 R_{s-1} + e_s \tag{8}$$

where $s$ denotes $s$-th return of each series. The distribution of disturbances $\{e_s\}$ is a mixture of two normal distributions with mean zero and the conditional variance $h_s$. The conditional variance $h_s$ is characterized as follows.

$$h_s = \omega + \alpha e_{s-1}^2 + \beta h_{s-1} \qquad \text{where} \qquad h_s = \eta\xi\sigma_s^2 + (1-\eta)\sigma_s^2 \tag{9}$$

The mixture of normal distributions for the disturbances is

$$f(e_s) = \frac{\eta}{\sqrt{2\pi\xi\sigma_s^2}} \exp\left(-\frac{1}{2}\frac{e_s^2}{\xi\sigma_s^2}\right) + \frac{1-\eta}{\sqrt{2\pi\sigma_s^2}} \exp\left(-\frac{1}{2}\frac{e_s^2}{\sigma_s^2}\right) \tag{10}$$

This specification suggests that the residual series is distributed as $N(0, \xi\sigma_s^2)$ with probability $\eta$ and $N(0, \sigma_s^2)$ with probability $1-\eta$. Table 2 shows the estimates of the model. All the estimates in the table are significant at 1% level. The results suggest that the process of $h_s$ is highly persistent. We can confirm this by observing that the persistence parameter $\alpha+\beta$ is close to unity for all return series. Our agent model, where traders trading a risky asset in a limit order market, generates the return series with GARCH with fat-tail distributed disturbances, which captures several important characteristics of the wide range of return series observed in practice.

**Table 2.** The estimates of AR(1)-GARCH(1, 1)-mixture of normals

| | R1 | R2 | R5 | R10 |
|---|---|---|---|---|
| log likelihood | -262,438.15 | -122,005.92 | -44,499.47 | -20,622.15 |
| omega | 0 | 0 | 0 | 0 |
| alpha | 0.11406 | 0.15981 | 0.1974 | 0.22278 |
| beta | 0.88224 | 0.83921 | 0.79921 | 0.70408 |
| alpha+beta | 0.9963 | 0.99902 | 0.99661 | 0.92686 |
| rho(0) | 0.00014 | 0.00013 | 0.00015 | 0.0002 |
| rho(1) | -0.02129 | -0.04787 | -0.05429 | -0.05121 |
| eta | 0.80198 | 0.80246 | 0.76302 | 0.5398 |
| xi | 0.05558 | 0.1053 | 0.15306 | 0.17486 |

## Conclusion

This paper shows that the log return series of a risky asset traded in a limit order market can be modeled as AR(1)-GARCH(1, 1) with fat-tail distributed disturbances. The conditional volatility of simulated return series can be modeled as the GARCH class since the volatility gradually decreases as the price assimilates the information about the future asset return. The reason the disturbances of the model is fat-tail distributed is that there are two factors driving the return series; one of the two distributions represents the drift of the price process, and the other represents the liquidity effect. These explanations are well fit to what we observe in practice.

## References

Bollerslev T, Engle R F and Nelson B (1994) ARCH models, in Engle R F and McFadden D eds., The handbook of econometrics, 4, North-Holland: Amsterdam, 2959-3038

Watanabe T (2000) Excess kurtosis of conditional distribution for daily stock returns: The case of Japan, Applied Economics Letters, 7, 353-355

Watanabe T, and Asai M (2004) Stochastic volatility models with heavy-tailed distributions: A Bayesian analysis, COE Discussion Paper Series No.1, Faculty of economics, Tokyo Metropolitan University

(Views expressed in this paper are those of the authors and do not necessarily reflect those of the Bank of Japan or Institute for Monetary and Economic Studies. This work is partly supported by the Grant-in-Aid for the 21st Century COE program "Microstructure and Mechanism Design in Financial Markets" from the Ministry of Education, Culture, Sports, Science and Technology of Japan.)

# Stock price process and the long-range percolation

Koji Kuroda[1] and Joshin Murai[2]

[1] Graduate school of Integrated basic sciences, Nihon University, Tokyo, Japan
kuroda@math.chs.nihon-u.ac.jp
[2] Graduate school of Humanities and Social Sciences, Okayama University, Okayama, Japan murai@e.okayama-u.ac.jp

**Summary.** Using a Gibbs distribution developed in the theory of statistical physics and a long-range percolation theory, we present a new model of a stock price process for explaining the fat tail in the distribution of stock returns.

We consider two types of traders, Group A and Group B: Group A traders analyze the past data on the stock market to determine their present trading positions. The way to determine their trading positions is not deterministic but obeys a Gibbs distribution with interactions between the past data and the present trading positions. On the other hand, Group B traders follow the advice reached through the long-range percolation system from the investment adviser. As the resulting stock price process, we derive a Lévy process.

## 1 Group A traders

Group A consists of $N$ traders. The random variable $\omega_u(i)$ stands for the types of trading positions of a Group A trader $i = 1, \ldots, N$ at time $u = 1, \ldots, n$. We denote by $\omega_u(i) = +1, -1$ and 0 for a buy position, a sell position and neutral position, respectively. Let $\omega_u^+$ or $\omega_u^-$ be the number of traders in Group A who make a buying or selling order at time $u$, respectively. We define the *number of market participants* of Group A by $|\omega_u| = \omega_u^+ + \omega_u^-$, and the *surplus orders* for Group A traders by $< \omega_u >= \omega_u^+ - \omega_u^-$.

We shall define a configuration $\hat{\omega}$ of Group B traders and a random interval $I_n^{\hat{\omega}}(k) \subset \{1, \ldots, n\}$ in the next section.

We define *Hamiltonian* of trading strategies of Group A traders at time $u \in I_n^{\hat{\omega}}(k)$ by

$$H^{u,\hat{\omega}}(\omega) = \beta_1 |\omega_u|^2 + \beta_2 \Phi(\omega_u | \omega_{u-a}^k, \ldots, \omega_{u-1}^k) - \beta_3 f_1(|\omega^k|_{u,a}, k/n^q)|\omega_u| - \frac{\beta_4}{\sqrt{n}} f_2(< \omega^k >_{u,a}, k/n^q) < \omega_u >, \quad (1)$$

where $\beta_1$, $\beta_2$, $\beta_3$, $\beta_4$ are positive constants, $a$ is a positive integer, $\omega_u^k = \omega_u$ if $u \in I(k)$, and $\omega_u^k(i) = 0$ otherwise, $f_1(x,t)$, $f_2(x,t)$ are real valued functions continuous in $t$, and $|\omega^k| = \sum_{\ell=1}^a |\omega_{u-\ell}^k|$, $< \omega^k >= \sum_{\ell=1}^a < \omega_{u-\ell}^k >$. The first term in (1) controls the activities of Group A. The second term expresses the trading strategies of traders who analyse the past data $\{\omega_{u-\ell}; 1 \leq \ell \leq a-1, u-\ell \in I_n^{\hat{\omega}}(k)\}$. The third term plays a role to generate a volatility of the stock price process. If $f_1(\cdot,\cdot) > 0$ then the activity is increasing and a large volatility is obtained, otherwise the activity is decreasing and a small volatility is obtained. The forth term derives a drift (or trend) of the stock price process. If $f_2(\cdot,\cdot) > 0$ then the stock price process is in an up trend, otherwise is a down trend. A *Gibbs measure* is defined by

$$\mathbf{P}^{\hat{\omega}}(\omega) = \frac{1}{Z_n^{\hat{\omega}}} \exp\left[-\sum_{u=1}^{n} H^{u,\hat{\omega}}(\omega)\right], \tag{2}$$

where $Z_n^{\hat{\omega}}$ is a normalization constant.

## 2 Group B traders and long-range percolation model

Group B traders are located in $\mathbb{Z}$ and *an investment adviser* is in its origin $0 \in \mathbb{Z}$. The random variable $\bar{\omega}_u$ stands for the type of news the investment adviser receives at time $u = 1, \ldots, n$. We denote by $\bar{\omega}_u = +1$, $-1$ or $0$, if a good, a bad or no news is received, respectively.
Let $\mathbb{B} = \{\{x,y\}\,;\, x, y \in \mathbb{Z}\}$ be the set of all pairs of Group B traders. We denote by $\tilde{\omega}_u(x,y) = +1$ or $0$, if the channel between $x$ and $y$ is open or closed, respectively. We denote a configuration of Group B traders by $\hat{\omega}_u = (\bar{\omega}_u, \tilde{\omega}_u)$.

We say a pair $\{x,y\} \in \mathbb{B}$ of traders belongs to the same *open component* at time $u$ if there is a sequence of traders $x = x_0, x_1, \ldots, x_k = y \in \mathbb{Z}$ such that $\tilde{\omega}_u(\{x_{\ell-1}, x_\ell\}) = +1$ for all $\ell = 1, \ldots, k$. The event that a pair $\{x,y\} \in \mathbb{B}$ of traders belongs to the same open component is denoted by $x \leftrightarrow y$.

At each time $u = 1, \ldots, n$, if the news is good (bad), the investment adviser sends an advice to buy (sell) the stocks to the traders belonging to the same open component with him. The set of all traders who receive the advice is $C_\infty = C_\infty(0) = \{x \in \mathbb{Z}\,;\, 0 \leftrightarrow x\}$. We also denote by $C_\infty(x)$ the open component including $x \in \mathbb{Z}$.

Let $N_n$ be a positive integer increasing in $n$ and let $B_{N_n} = [-N_n, N_n] \cap \mathbb{Z}$. We assume that only traders in $B_{N_n}$ can participate in the trading, we call them *the selected traders*. A set of the selected traders who receive the advice is $C_{N_n} = \{x \in B_{N_n}\,;\, 0 \leftrightarrow x\}$. Also, we assume that each Group B trader can trade $1/|B_{N_n}|$ unit of stocks at each time. As all traders in $C_{N_n}$ behave in the same way according to the type $\bar{\omega}_u$ of news, *the modified surplus orders for Group B traders* is given by $< \hat{\omega}_u >= \bar{\omega}_u |C_{N_n}|/|B_{N_n}|$.

Let $\delta$ be a constant with $\frac{3}{8} < \delta < \frac{1}{2}$. Let $T_0(\hat{\omega}) = 0$ and $U_0(\hat{\omega}) = 0$. We define stopping times by $T_k(\hat{\omega}) = \min\{u \geq 1\,;\, \sum_{\ell=1}^u < \hat{\omega}_{U_{k-1}+\ell} >\geq n^\delta\}$,

$U_k(\hat{\omega}) = U_{k-1}(\hat{\omega}) + T_k(\hat{\omega})$ for $k \geq 1$. Let $q = 1/2 - \delta$ $(< \delta)$. We decompose the set of discrete times $\{1, \ldots, n\}$ into random intervals $I_n^{\hat{\omega}}(1), \ldots, I_n^{\hat{\omega}}(n^q + 1)$:

$$I_n^{\hat{\omega}}(k) = \begin{cases} \{U_{k-1}(\hat{\omega}) + 1, \ldots, U_k(\hat{\omega})\}, & \text{for } k = 1, \ldots, n^q, \\ \{U_{n^q}(\hat{\omega}) + 1, \ldots, n\}, & \text{for } k = n^q + 1. \end{cases}$$

We assume that the advice from the investment adviser spreads over Group B via the long-range percolation model. It is known that the long-range percolation model exhibits the first order phase transition. We state some known results on this model as follows.

**Theorem 1.** ([1], [3], [5]) *For any $\beta > 1$, the following statements holds.*

(1) *There exists a critical value $p_c(\beta) \in (0, 1)$ such that*

$$P_p(|C_\infty| = \infty) \begin{cases} = 0, & (p < p_c(\beta)), \\ \geq \beta^{-1/2}, & (p \geq p_c(\beta)). \end{cases}$$

(2) *For any $p \geq p_c(\beta)$, there is a unique infinite cluster almost surely.*

(3) *For any $p < p_c(\beta)$, there is a constant $c_0(p, \beta) < \infty$ such that $\tau(x, y) \leq c_0(p, \beta)|x - y|^{-2}$ for any $x, y \in \mathbb{Z}^2$, where $\tau(x, y) = P_p(x \leftrightarrow y)$ is a connectivity function.*

We fix $\beta > 1$. Let $0 < p_0 < p_c(\beta)$. We define the *nearest neighbor percolation probability* $\{p_k\,;\, k = 1, \ldots, n^q + 1\}$ by $p_k = p_0 + k\{p_c(\beta) - \varepsilon(n) - p_0\}/n^q$ for $1 \leq k \leq n^q$ and $p_{n^q+1} = p_c(\beta)$, where $\varepsilon(n) > 0$ is decreasing in $n$ and converges to 0 as $n \to \infty$.

For $u \in I_n^{\hat{\omega}}(k)$, A probability distribution of $\tilde{\omega}_u$ is given as the long-range percolation model, that is

$$\hat{\mathbf{P}}(\tilde{\omega}_u(\{x, y\}) = +1 | \hat{\omega}_1, \ldots, \hat{\omega}_{u-1}) = \begin{cases} p_k, & (|x - y| = 1), \\ \beta|x - y|^{-2}, & (|x - y| \geq 2), \end{cases}$$

and $\hat{\mathbf{P}}(\tilde{\omega}_u(\{x, y\}) = 0 | \hat{\omega}_1, \ldots, \hat{\omega}_{u-1}) = 1 - \hat{\mathbf{P}}(\tilde{\omega}_u(\{x, y\}) = +1 | \hat{\omega}_1, \ldots, \hat{\omega}_{u-1})$.

We assume that $\{\bar{\omega}_u, \tilde{\omega}_u(x, y)\,;\, (x, y) \in \mathbb{B}\}$ are independent for each $u$.

## 3 Statement of results

A coupled probability measure $\mathbf{P}$ for both groups is defined by

$$\mathbf{P}(\omega, \hat{\omega}) = \mathbf{P}^{\hat{\omega}}(\omega)\hat{\mathbf{P}}(\hat{\omega}).$$

When the total amount of modified surplus orders $< \omega_u > + < \hat{\omega}_u >$ is positive, it is expected that there is a strong driving activity on the part of buyer and the stock price is going to move in upper direction. On the other hand, market is going to fall when $< \omega_u > + < \hat{\omega}_u >$ is negative. We define the stock price change at time $u$ by

$$\frac{S_u}{S_{u-1}} = e^{c_0(<\omega_u>+<\hat{\omega}_u>)}, \tag{3}$$

where $c_0 > 0$ is a constant called the *market depth*. (Note that we think $S_u$ is the *closing price* other than opening price.) This recurrence formula implies

$$S_u = S_0 \exp\{c_0 \sum_{l=1}^{u}(<\omega_l> + <\hat{\omega}_l>)\}, \tag{4}$$

where $S_0$ is the initial stock price at time 0.

We consider the processes

$$W_u = \sum_{l=1}^{u} <\omega_l>, \qquad \hat{W}_u = \sum_{l=1}^{u} <\hat{\omega}_l> .$$

Then by (4), the stock price process is described as $S_u = S_0 e^{c_0(W_u+\hat{W}_u)}$.

Let $k(n,t) \in \{1, \ldots, n^q+1\}$ be a unique number with $[nt] \in I_n^{\hat{\omega}}(k(n,t))$. Let $\frac{1}{4} < \lambda < \frac{1}{2}$. A scaled process $\{W_t^{(n)}\}_{t\in[0,1]}$ of $\{W_u\}_{u=1}^n$ is given by $W_0^{(n)} = 0$ and

$$W_t^{(n)} = \begin{cases} \frac{1}{\sqrt{n}} W_{U_{k(n,t)}}, & \text{if } k(n,t) \le n^q, \\ \frac{1}{\sqrt{n}} W_{U_{n^q}+n^{1-\lambda}}, & \text{if } k(n,t) = n^q + 1, \end{cases} \qquad \text{for } t \in (0,1],$$

A scaled process $\{\hat{W}_t^{(n)}\}_{t\in[0,1]}$ of $\{\hat{W}_u\}_{u=1}^n$ is also given in a similar way.

We define a process by

$$X_t^{(n)} = W_t^{(n)} + \hat{W}_t^{(n)}.$$

Let $\tau \in (0,1)$ be a fixed time and $f_3(t) > 0$ be a continuous function on $[0,1]$ such that

$$\int_0^1 \frac{1}{f_3(x)} \mathrm{d}x = \tau.$$

A continuous function $s(t), t \in [0,\tau]$ is defined implicitly by

$$\int_0^{s(t)} \frac{1}{f_3(x)} \mathrm{d}x = t. \tag{5}$$

Since $f_3(t)$ is a positive function, $s(t)$ is well-defined.

**Theorem 2.** *For $\frac{3}{8} < \delta < \frac{1}{2}$, $\frac{1}{4} < \lambda < \frac{1}{2}$ and $q = \frac{1}{2} - \delta$, the process $X_t^{(n)}$ converges in finite dimensional distribution to the process*

$$X_t = \int_0^t (\mu_A(v) + \mu_B(v))\mathrm{d}v + \int_0^t \sigma_A(v)\mathrm{d}B_v + h1_{\{t=\tau\}}, \quad \textit{for all } t \in [0,\tau], \tag{6}$$

*where $B_t$ is a standard Brownian motion and $h$ is a jump length. Trend terms and the volatility term of the limit price process are described in terms of the polymer functionals in the theory of cluster expansion as follows.*

$$\mu_A(t) = \beta_4 \sum_{i(A)=0} < A > f_2(A, s(t))\phi_0(A)e^{\beta_3 f_1(A,s(t))}\frac{\alpha^T(A)}{A!}f_3(s(t)), \quad (7)$$

$$\mu_B(t) = f_3(s(t)), \quad (8)$$

$$\sigma_A^2(t) = \sum_{i(A)=0} < A >^2 \phi_0(A)e^{\beta_3 f_1(A,s(t))}\frac{\alpha^T(A)}{A!}f_3(s(t)). \quad (9)$$

Let $\{\tau_i\,;\, i = 1, 2, \ldots\}$ be i.i.d. sequence of exponential holding times with mean $1/c$, and we write $\tau_0 = 0$. When $\tau_i \leq 1$, the stock price is continuous on each random interval $(\tau_{i-1}, \tau_i)$, and it jumps at each random time $\tau_i$, and jumps are i.i.d. with distribution $\rho$.The stock price process on $(\tau_{i-1}, \tau_i]$ behaves just like on $(0, \tau_1]$. Then by using the same argument in the proof of Theorem 2 repeatedly, we will obtain the following.

**Theorem 3.** *For $\frac{3}{8} < \delta < \frac{1}{2}$, $\frac{1}{4} < \lambda < \frac{1}{2}$ and $q = \frac{1}{2} - \delta$, The scaled process $X_t^{(n)}$ converges in finite dimensional distribution to the process*

$$X_t = \int_0^t (\mu_A(v) + \mu_B(v))\mathrm{d}v + \int_0^t \sigma_A(v)\mathrm{d}B_v + Y_t, \quad \textit{for all } t \in [0, 1],$$

*where the jump term $Y_t$ is a compound Poisson process, that is*

$$Y_t = \int_{[0,t]} \int_{(-\infty,\infty)\setminus\{0\}} xN_p(\mathrm{d}s\mathrm{d}x),$$

*where $N_p(\mathrm{d}s\mathrm{d}x)$ is a Poisson random measure. The Lévy measure of $Y_t$ is $\mu(\mathrm{d}x) = c\rho(\mathrm{d}x)$ with $c > 0$ and $\rho((-\infty, \infty)) = 1$.*

## References


1. AIZENMAN, M. AND NEWMAN, C.M. (1986). Discontinuity of the Percolation Density in One Dimensional $1/|x - y|^2$ Percolation Models. *Commun. Math. Phys.* **107,** 611–647.
2. CONT, R. AND BOUCHAUD, J.P. (2000). Herd behavior and aggregate fluctuations in financial markets. *Macroeconomic Dynamics.* **4 (2),** 170–196.
3. GANDOLFI, A., KEANE, M.S. AND NEWMAN, C.M. (1992). Uniqueness of the infinite component in a random graph with applications to percolation and spin glasses. *Probab. Theory Related Fields* **92,** 511–527.
4. MANTEGNA, R.N. AND STANLEY, H.E. (2000). An introduction to Econophysics: Correlatons and Complexity in Finance. *Cambridge University Press.*
5. NEWMAN, C.M. AND SCHULMAN, L.S. (1986). One Dimensional $1/|j - i|^s$ Percolation Models: The Existence of a transition for $s \leq 2$. *Commun. Math. Phys.* **104,** 547–571. *Sūrikaisekikenkyūsho Kōkyūroku.* **1264,** 203–218.

# What information is hidden in chaotic time series?

Serge F. Timashev[1], Grigory V. Vstovsky[2], Anna B. Solovieva[2]

[1]Karpov Institute of Physical Chemistry, 10 Vorontsovo pole Street, Moscow, 103064, Russia
[2]Semenov Institute of Chemical Physics, Russian Academy of Science, 4 Kosygina, Moscow, 119991, Russia

**Summary.** Foundations of Flicker-Noise Spectroscopy (FNS) which is a new phenomenological approach to extract information hidden in chaotic signals are presented. The information is formed by sequences of distinguished types of signal irregularities – spikes, jumps, and discontinuities of derivatives of different orders – at all space-time hierarchical levels of systems. The ability to distinguish irregularities means that parameters or patterns characterizing the totality of properties of the irregularities are distinguishably extracted from the power spectra $S(f)$ ($f$ – frequency) and difference moments $\Phi^{(p)}(\tau)$ ($\tau$ – temporal delay) of the $p^{th}$ order. It is shown that FNS method can be used to solve the problems of two types: to show of the parameters characterizing dynamics and peculiarities of structural organization of open complex systems; to reveal the precursors of the sharpest changes in the states of open dissipative systems of various nature on the base of a priori information about their dynamics. Applications of the FNS for getting information hidden in economical data (daily market prices for the Nasdaq- and Nikkei-Index time series) are presented.

**Key words.** Time series, flicker-noise spectroscopy, information, irregularities of dynamic variables, power spectrum, difference moment, non-stationary process, daily market prices

The image of "complexity" is introduced to underline the complex essence of information hidden in chaotic signals (temporal, spatial, energetic), which are produced by non-linear complex dissipative systems. Chaotic time series obtained under studying dynamics of economic phenomena (market price fluctuations, cash flow data, etc.), among other chaotic signals, contain much information. What type of information is hidden in chaotic signal? In what way this initial information could be extracted from the chaotic series of measured dynamic variables to be a base for phenomenological study of economic phenomena? Is it possible to propose an algorithm for taking out as much hidden information as one needs for solving problems under consideration? In this paper we demonstrate that the practical problems related to revealing the informative essence of various chaotic signals could be resolved by introducing a new image of information hidden in chaotic signals. This image is presented in Flicker-Noise Spectroscopy (FNS)

(Timashev 1999), (Timashev 2000a, b), (Timashev 2002), (Timashev and Vstovsky 2003), (Descherevsky et al. 2003), (Parkhutik et al. 2003).

According to this phenomenological approach, the main information hidden in chaotic signals is formed by sequences of distinguished types of irregularities – the spikes, jumps, and discontinuities of derivatives of different orders at all space-time hierarchical levels of the systems under consideration. FNS approach classifies the irregularities of different types by the generalized functions with zero carrier (compact support in $\{0\}$) expressed as a sum over $\delta$-functions and their derivatives for actual singularities, and functions containing various types of discontinuities for potential singularities (the Heaviside $\theta$-functions and functions with discontinuities of the first-, second-, and higher-order derivatives). In this case it is possible to introduce different types of information ("colours"), and the ability to distinguish irregularities means that parameters or patterns characterizing the totality of properties of the irregularities are distinguishably extracted from the power spectra $S(f)$ ($f$ – frequency):

$$S(f) = \left| \int_{-T/2}^{T/2} \langle V(t)V(t+t_1) \rangle \cdot \exp(2\pi i f t_1) dt_1 \right|, \quad \langle (...) \rangle = \frac{1}{T} \int_{-T/2}^{T/2} (...) dt \tag{1}$$

where angle brackets are for averaging over the $T$ interval (we refuse the ergodic hypothesis), and transient difference moments $\Phi^{(p)}(\tau)$ ($\tau$ – temporal delay) of the $p^{\text{th}}$ order $\Phi^{(p)}(\tau)$ ($p$ = 1, 2, 3, ...) and dimensionless "transient semi-invariants" or "quasi-qumulants" for $p \geq 3$:

$$\Phi^{(p)}(\tau) = \left\langle \left[ V(t) - V(t+\tau) \right]^p \right\rangle, \mu^{(p)}(\tau) = \frac{\Phi^{(p)}(\tau)}{\left[ \Phi^{(2)}(\tau) \right]^{p/2}}, \tag{2}$$

It is easy to see that $\Phi^{(p)}(\tau)$ is formed exclusively by jumps of the dynamic variable at different space-time hierarchical levels of the system, and $S(f)$ is formed by both the spikes and jumps. The characteristic information extracted from the $S(f)$ and $\Phi^{(2)}(\tau)$ dependences represents the correlation time, the parameters characterizing the loss of "memory" for this correlation time, or "passport patterns" characterizing the sequences of spikes, jumps and discontinuities of derivatives of different orders (in the latter case time series for "quasi-derivatives" must be calculated). It means that in the FNS frame the power spectra and difference moments of the 2nd order carry out different informations, which are complement for each other unlike the standard point of view which could be adequate only for smooth signals. According to FNS, the term "stationary" means that the every set of informative parameters is the same for each space-time level of hierarchical organization of the system under study in the considered range of time scales.

For solving practical problems on the base of FNS we developed (Timashev and Vstovsky 2003) a new "relaxation procedure" to split the studied signal $V(t)$ to low-frequency $V_R(t)$ and high-frequency component $V_F(t)$ components: $V(t) = V_R(t) + V_F(t)$. We can calculate $S(f)$ and $\Phi^{(p)}(\tau)$ for each of the functions $V_J(t)$ ($J = R, F$ or $G$), where the subscripts $R$, $F$ and $G$ refer to $V_R(t)$, $V_F(t)$ and $V(t)$, respectively. In these cases the corresponding subscripts for $S_J(f)$ and $\Phi_J^{(p)}(\tau)$ are used.

The investigations carried out by now show that FNS method with getting information by analyzing the $S_J(f)$ and $\Phi_J{}^{(2)}(\tau)$ dependences can be used to solve the problems of two types.

**1. Determination of the parameters or patterns characterizing dynamics of complex systems.** As an example of using the FNS for finding passport patterns of chaotic series we present in Fig.1 the results of the corresponding processing of the daily (open, close, high and low) market prices for the Nasdaq- and Nikkei-Index time series. Fig. 1 demonstrates the high degree of diversity of every presented pattern other than the $S_G(f)$ dependences which are considered usually.

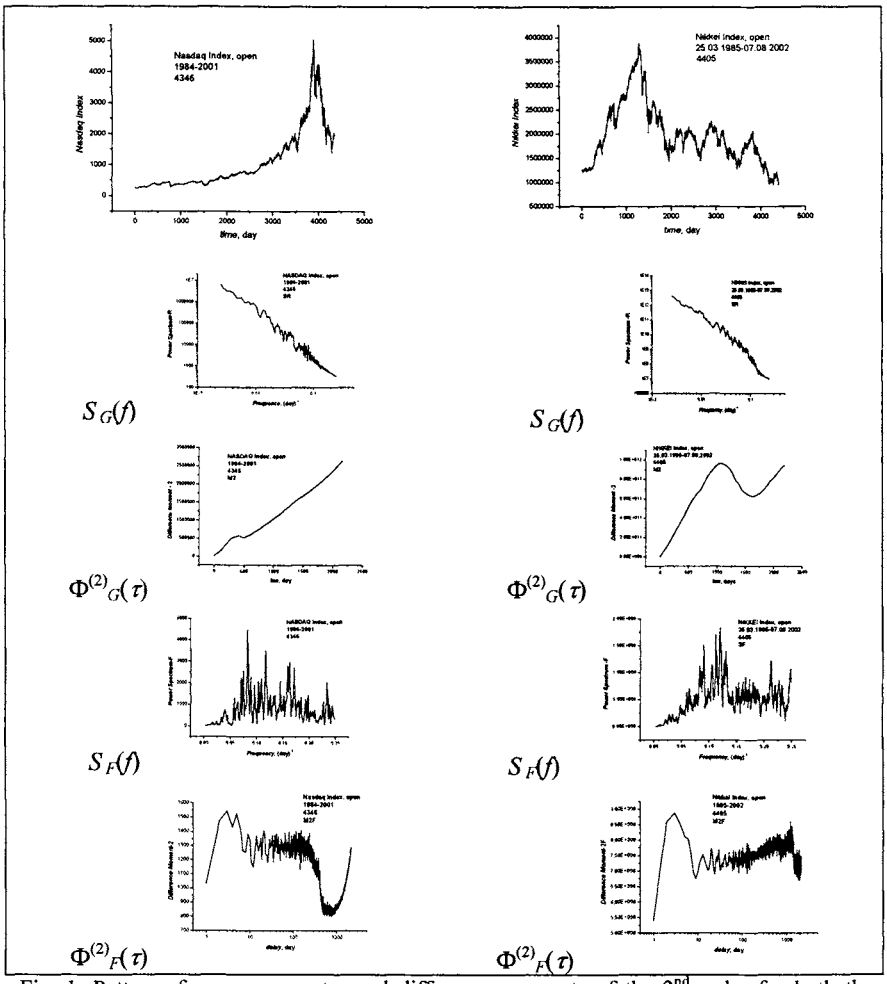


Fig. 1. Patterns for power spectra and difference moments of the 2nd order for both the regular and high frequency parts of Nasdaq(open) and Nikkei(open)-Index (on the right hand) time series.

**2. Revelation of the precursors of sharpest changes in the states of open dissipative systems.** We introduce a new factor, which characterizes the non-stationary character of analyzed signals. It could be considered as precursor signaling about forthcoming catastrophic reorganization in the system under study. To obtain such precursors we analyze the time variation of power spectrum $S_J(f)$ or difference moments $\Phi_J^{(2)}(\tau)$ that are calculated within the averaging interval $[k\Delta T, t_k = k\Delta T+T]$ of duration $T$, where $k = 0, 1, 2, 3, \ldots$, shifting discretely over the series of entire observation period $T_{tot}$ by steps $\Delta T$. The time intervals $T$ and $\Delta T$ should be physically chosen. So, if there are some "minor" processes with the characteristic times $\tau_i$ gently influencing the main non-stationary process in the system, a condition $\tau_i << T$ must be fulfilled. It means, contrary to stationary case, that non-stationary evolution of complex system is characterized by a set of characteristic times $T_{sn}$, and the prediction problem becomes, in a general case, multi-parametric. We relate the "precursor" to the sharpest changes in the variations of $S_J(f)$ and $\Phi_J^{(p)}(\tau)$ when the upper boundary of the averaging interval $t_k$ becomes closer to the time of a catastrophic event $t_c$. The simplest "precursors" are defined on the base of the difference moments $\Phi_J^{(2)}(\tau)$. Taking delay $\tau$ in the range $[0, \alpha T]$ with $\alpha \leq 0.5$, we introduce the dimensionless factors:

$$C_J(t_{k+1}) = 2 \cdot \frac{Q_{k+1}^J - Q_k^J}{Q_{k+1}^J + Q_k^J} \Big/ \frac{\Delta T}{T}; \quad Q_k^J = \int_0^{\alpha T} \left[\Phi_J^{(2)}(\tau)\right]_k d\tau. \tag{3}$$

Here $t_{k+1} = (k+1)\Delta T+T$, ($k = 0, 1, 2, \ldots$) and subscripts of square brackets show that $\Phi_J^{(2)}(\tau)$ dependence was calculated for time interval $[k\Delta T, k\Delta T + T]$. The peak values of these factors characterize a "measure of non-stationarity" of the signals when the sharp variations of $\Phi_J^{(p)}(\tau)$, during the shifting the averaging interval $T$, are due to large changes of signal on "forward" and "back" boundaries of interval $T$ as the "forward" boundary approaches to the time $t_c$ of the expected event. This problem is resolved by analysis of temporal behavior of corresponding criteria for varied $T$: it is evident that when $T$ increases by value $\Delta T_1$ the effects of non-stationarity due to signal behavior at "back" boundary must appear with the same

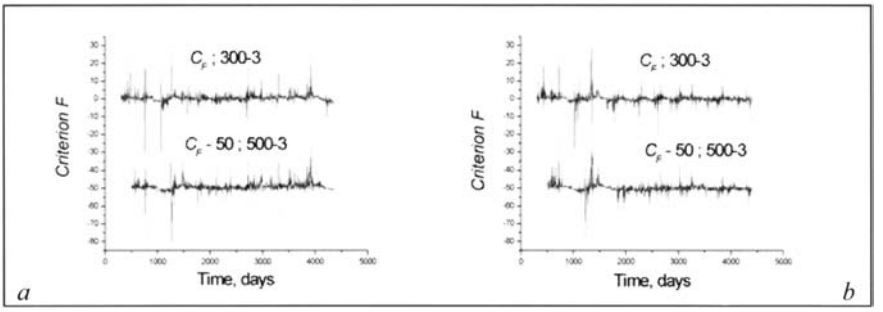


Fig. 2. Non-stationarity factors $C_F(t_{k+1})$ calculated for Nasdaq(open) (*a*) and Nikkei(open) (*b*) Indexes in Fig.1 for $\Delta T = 3$ days and averaging "windows" $T$=300 and $T$=500 days. ($C_F$ and $C_F$-50, respectively)

delay time $\Delta T_1$, whereas the effects due to signal behavior at "forward" boundary must not sharply depend on averaging interval value. Evidently, $C_J(t_{k+1}) = 0$ for the stationary processes for $T \to \infty$. As an example we found the factors of non-stationarity for the daily Nasdaq(open)- and Nikkei(open)-Index time series, Fig.2. Note, that every $C(t_{k+1})$ large peak on the "forward" boundary appearing at real time during computer processing of the time series under study can be considered as a signal of serious "changes" in the time series origin which could become a precursor of more catastrophic changes (Descherevsky et al. 2003), (Parkhutik et al. 2003). In any case, the peak appearance means that it is necessary to be more attentive to the analysis of additional information concerning the studied system and to deal with analysis of the time series with higher sampling frequency. In the case of the market price fluctuations it is necessary to get additional information which can be obtained from analysis of more detailed (sampled by hours or minutes) measured financial time series.

Eventually, FNS is a new informative methodology. The "distinguishability" of the irregularities means that the parameters or patterns characterizing the totality of properties of the irregularities are distinguishably extracted from the power spectra and difference moments of different order. In FNS formalism, in contrary to the theory of deterministic chaos, a multi-parametric representation of the information image indicating the information loss rate is introduced.

The work was supported by the ISTC Grant #2280.

## References

Timashev S F (1999) Complexity and Evolutionary Law for Natural Systems. In: Annals of the New York Academy of Science, Tempos in Science and Nature: Structures, Relations, and Complexity. 879: 129-143

Timashev S F (2000a) A New Dialogue with Nature. In: Broomhead D.S, Luchinskaya E.A., P.V.E. McClintock, T. Mulin (Eds) Stochastic and Chaotic Dynamics in the Lakes – STOCHAOS. Melville, New York: AIP Conference Proceedings, pp. 238-243

Timashev S F (2000b) Self-Similarity in Nature. Ibid, pp. 562-566

Timashev S F (2002) On the microscopic origin of the Second Law. In: Quantum Limit to the Second Law. Ed. D.P. Sheehan. AIP Conference Proceedings, pp. 367-372

Timashev S F, Vstovsky G V (2003) Flicker-Noise Spectroscopy in analysis of chaotic time series of dynamic variables and the problem of "signal-noise" relation. Russian J. Electrochemistry 39: 156-169

Descherevsky A V, Lukk A A, Sidorin A Ya, Vstovsky G V, Timashev S F (2003) Flicker-noise spectroscopy in earthquake prediction research. Natural Hazard and Earth System Sciences 3 N 3/4: 159-164.

Parkhutik V, Rayon E, Ferrer C, Timashev S, Vstovsky G (2003) Forecasting of electrical breakdown in porous silicon using flicker-noise spectroscopy. Physica Status Solidi (a) 197: 471-475.

# Analysis of Evolution of Stock Prices in Terms of Oscillation Theory

Satoshi Nozawa[1] and Toshitake Kohmura[2]

[1]Josai Junior College, 1-1 Keyakidai, Sakado, Saitama 350-0295, Japan
[2]Josai University, 1-1 Keyakidai, Sakado, Saitama 350-0295, Japan

**Summary.** Taking advantage of the oscillatory evolution of stock prices, we analyze the evolution of stock prices in terms of the oscillation theory. We apply the formalisms to Nikkei225 data and compare with the predictions of the random walk theory.

## 1. Introduction

We study the time evolution of stock prices, for example, the Nikkei225 in terms of physics tools. It appears that stock prices vary randomly without any causal laws. It seems that a stock price in this month varies independently of the price in last month. Nevertheless, we introduce a theory for oscillations in order to analyze the time evolution of the stock prices (Kohmura and Nozawa 2003a, 200b, Nozawa and Kohmura 2004). The theory of oscillations is a very common approach in physics, which has an advantage to be solved analytically and to predict future development.

The present paper is organized as follows. In section 2 we present an analytic formulation for the time evolution of the stock price indices in terms of the theory for oscillations. In section 3 we apply the formalisms to Nikkei225 data and compare with the predictions of the random walk theory.

## 2. Analysis in Terms of Oscillation Theory

Let us assume that stock prices fluctuate according to the theory for oscillations. Namely a stock price index $x(t)$ at a time $t$ oscillates

around a mean value $b$. Then $x(t)$ is determined by the following differential equation.,

$$\frac{d^2}{dt^2}x(t) = -\omega^2\{x(t) - b\}, \tag{1}$$

where $\omega$ is the angular frequency, which represents the speed of oscillations. The solution is given as follows,

$$x(t) = a\cos(\omega t + \theta) + b, \tag{2}$$

where $a$ and $\theta$ are parameters. In the present case, we treat $\omega$ and $b$ as parameters as well. Let $\Delta t$ be a constant time interval. Then the variations of $x$ between two successive time points are defined as follows,

$$y(t + \frac{1}{2}\Delta t) = \Delta x(t + \frac{1}{2}\Delta t) = x(t + \Delta t) - x(t). \tag{3}$$

Similarly, the second order of difference of the variation $y(t)$ of the stock price $x(t)$ varying in the oscillation motion in equation (2) yields the difference equation of motion,

$$\Delta^2 y(t) = -4\sin^2\left(\frac{\omega\Delta t}{2}\right)y(t), \tag{4}$$

where the second order of difference of $y(t)$ is defined to be

$$\begin{aligned}\Delta^2 y(t) &= \Delta y(t + \frac{1}{2}\Delta t) - \Delta y(t - \frac{1}{2}\Delta t) \\ &= y(t + \Delta t) - 2y(t) + y(t - \Delta t).\end{aligned} \tag{5}$$

From the actual values of the stock price $x(t)$ for the given corporation recorded at four consecutive points in time in the stock market, we obtain the variation $y(t)$ and its second order difference in equation (5) and evaluate the following ratio R. If the stock price $x(t)$ features the oscillation motion in equation (2), then the ratio is given by

$$R \equiv \frac{\Delta^2 y(t)}{y(t)} = -4\sin^2\left(\frac{\omega\Delta t}{2}\right). \tag{6}$$

This relation shows that for the stock price $x(t)$ varying in an oscillation

motion, the ratio is bound as

$$-4 < R < 0. \tag{7}$$

From the analysis of the actual stock prices belonging to Tokyo Stock Market, we have found that about 60 percent of the stock prices satisfy the above condition for oscillation motion. This will be discussed in more detail in the next section. But there are some other cases when the stock prices $x(t)$ yield the ratio

$$R > 0, \tag{8}$$

which indicates that the stock prices $x(t)$ vary exponentially. There are also other cases when the stock prices $x(t)$ yield the ratio

$$R < -4, \tag{9}$$

which indicates that the stock prices $x(t)$ vary in a zigzag motion.

The ratio $R$ is a very useful index to classify the current trend of the evolution of the stock prices. From the values of the ratio, we can figure out the current evolution state of the stock prices and predict the medium length period (a few month) trend of the evolution.

## 3. Application to Nikkei225 data

In this section we analyze stock price data in terms of the theory for oscillations derived in section 2. In the present paper, in particular, we study general trends of stock prices. Therefore, we use Nikkei225 data instead of individual issues. In order to reduce statistical uncertainties as much as possible, we try to include large number of data available for us.

In Figure 1 we have plotted a histogram of Nikkei225 data as a function of $R$. The data are Nikkei225 stock price indices at the end of months. The total number of data is 400 (months) for the last 33 years in the period of 1970-2003. Each bar in Figure 1 denotes the number of frequency for the interval $\Delta R = 0.1$. The solid curve is the prediction of the random walk theory, which is normalized to the total number of frequencies. As far as the gross structure of the frequency distribution is concerned, both of the shape and the peak position of the frequency distribution of the practical data seem to be consistent with the random walk theory prediction. However, number

of data points (400 points) is not sufficient enough to exclude statistical errors.

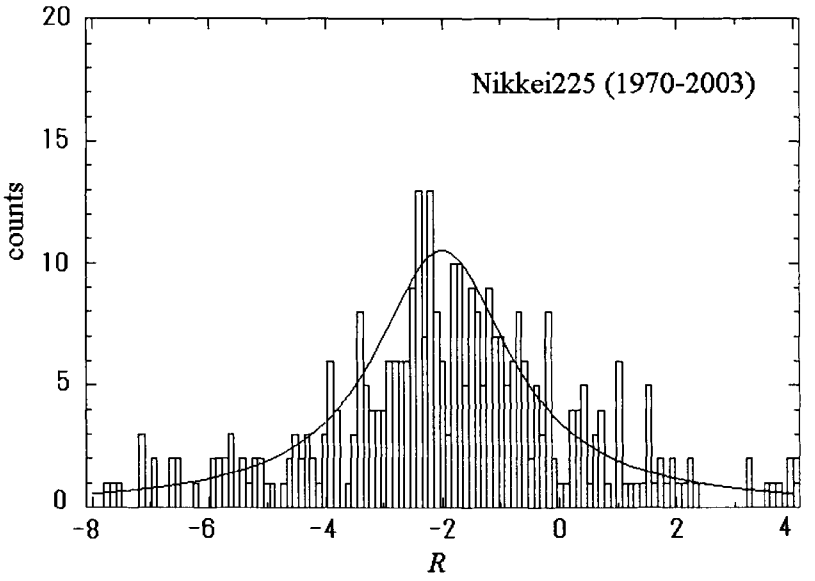


**Fig. 1** Frequency distribution of Nikkei225 data for the last 33 years as a function of R. Total number of data is 400 (months) for the period of 1970-2003. The curve is a result of the random walk theory, which is normalized to the total number of data.

In Table 1 we have calculated the frequencies (in percent) of the same Nikkei225 data for the period of 1970-2003 for each fluctuation mode. The first, second and third lines stand for oscillation fluctuations, zigzag fluctuations and divergent fluctuations, respectively. The third column shows the prediction by the standard random walk theory. Again, the gross structure of the frequency distribution of Nikkei225 seems to be described by the random walk theory reasonably well. However, there exists a significant deviation in specific fluctuation modes. Again higher statistics is necessary to draw a definite conclusion.

In summary we have introduced a formulation for the evolution of the stock prices indices in terms of a theory for oscillations. We have shown that the ratio of $R$ is an essential quantity in analyzing the stock price

indices. We have compared the data with a standard random walk theory result.

**Table 1** Frequency distribution of Nikkei225 data for the last 33 years in various fluctuation modes. Total number of data is 400 (months) for the period of 1970-2003.

| Fluctuations | Nikkei225 Data | Random Walks |
|---|---|---|
| Oscillations $(-4 < R < 0)$ | 0.595 | 0.608 |
| Zigzag $(R > 0)$ | 0.215 | 0.196 |
| Divergent $(R < -4)$ | 0.190 | 0.196 |
| Total | 1.000 | 1.000 |

## References


Kohmura T and Nozawa S (2003a)

Analytical Study on the Evolution of Economical Indices, Josai University Bulletin the Department of Ecomomics, 21: 1--14

Kohmura T and Nozawa S (2003b)

Analytical Study on the Evolution of Economical Indices II, Annual Reports of Josai Graduate School of Economics, 19: 23--37

Nozawa S and Kohmura T (2004)

A Study of the evolution of Stock Price Indices in Terms of Oscillation Theory, The Josai Journal of Business Administration, 1: 45--54

# Simple stochastic modeling for fat tails in financial markets

Hans-Georg Matuttis

Department of Mechanical Engineering and Intelligent Systems, The University of Electro-Communications, Tokyo 182-8585, Japan hg@mce.uec.ac.jp

## 1 Introduction

Stochastic theories for the description of financial markets, e.g. via the Langevin equation, are usually based on terms with uncorrelated noise. The purpose of this paper is to investigate how correlations in the market can introduce "fat tails" in Random Walk (RW)-like models as well as a narrow center in the distribution as found in the S&P500[1]. Using the discrete version for the RW

$$x_i = \mu + x_{i-1} + \xi_i \tag{1}$$

as a starting point, where $\mu$ is the "trend" and $\xi_i$ is Gaussian/ normally distributed uncorrelated noise, we focus on de-trended random walks with $\mu = 0$. Correlated noise for our purpose can easily be produced by "mixing" successive random numbers from the Gaussian random number sequence in a weighted average, e.g.

$$\tilde{\xi}_i = \sum_{j=i-M}^{j} (1-\epsilon)\xi_j + \epsilon\xi_{j-1}. \tag{2}$$

For different $\epsilon$, we get different distributions all narrower than the standard normal distribution, which nevertheless still can all be fitted to a Gaussian with standard deviation $\sigma < 1$. Therefore the narrow center in the S&P500-Data of Mantegna et al.[1] may be explained by short-term/local correlations in the "noise" of the random walk, which corresponds to the correlated information/noise the players receive in the financial world. In the remaining part, Gaussian white noise with reduced variance is used instead of explicitly correlated noise to model the center of the distribution, which nevertheless cannot account for the fat tails, because it does narrow, not widen, the distributions. From here on, we use "correlated noise" $\tilde{\xi}_i = a\xi_i$, from a Gaussian distribution $\xi_i$ with the standard deviation $\sigma = a < 1$, so eqn. (1) becomes

$$x_i = x_{i-1} + a\xi_i. \tag{3}$$

## 2 Technical analysis, correlation and fat tails

A possible reason for much wider market swings than local correlation in market data is the synchronous reaction of many market players to signals from technical/chart analysis: Erratic chart data are averaged or fitted (in a very loose sense of the word), and the market players adapt their expectations and strategies accordingly, which is reflected in the price evolution. As the basis for our "technical analysis", we will use "moving averages", which are computationally easier accessible than chart formations like "double tops", "shoulder-head-shoulder-configurations" or "resistance-lines", on which market analysts often don't agree among themselves.

### 2.1 The Model: RW with Moving Averages

We set up our model equation for the technical analysis random walk (TARW)

$$x_i = x_{i-1} + a\xi_i + b\eta_i, \tag{4}$$

with Gaussian distributed mini-trends $\eta_i$, which react to the crossing of the averages in "bullish" or "bearish" manner as follows: The standard-normal-distributed "mini-trends" $\eta_i$ with prefactor $b$ don't change as long as the chart $x_i$ does not cross the moving average $\langle x_i \rangle_N = \frac{1}{N} \sum_{j=i-N}^{i} x_j$ from the previous $N$ market transactions:

$$\eta_i = \eta_{i-1} \text{ if } \eta_{i-1} > 0 \text{ and } x_i > \langle x_i \rangle_N \tag{5}$$

$$\eta_i = \eta_{i-1} \text{ if } \eta_{i-1} < 0 \text{ and } x_i < \langle x_i \rangle_N \tag{6}$$

Whenever the chart $x_i$ crosses the moving average $\langle x_i \rangle_N$, a new "mini-trend" $\eta_i$ with sign opposite the previous one is selected:

$$\text{new } \eta_i < 0 \text{ if } \eta_{i-1} > 0 \text{ and } x_i < \langle x_i \rangle_N \tag{7}$$

$$\text{new } \eta_i > 0 \text{ if } \eta_{i-1} < 0 \text{ and } x_i > \langle x_i \rangle_N. \tag{8}$$

The result for the distribution[1] of such a TARW is shown in Fig. 1(a) with fit parameters $a = 0.4$, $b = 4$. The inclusion of technical-analysis-like decision-making leads to fat tails and also a curvature change similar to the one seen in the empirical S&P500-data. Nevertheless, the fat tails in Fig. 1(a) branch

[1] This and all the following distributions have been plotted with the maximum probability normalized to one to allow the simple comparison with the empirical data, with 300000 time steps, 8000 equilibration steps before the first measurement, and moving averages of length $N = 5000$. Distributions did not change significantly if the moving averages were computed for $N = 5000$, $N = 50000$, or $N = 500$. Our "technical analysis" is "time-scale-free" in the sense that the sum of Gaussian random numbers produces a Gaussian again. The structure of the time-series itself varied considerably with the length of the moving averages.

out at too high probabilities compared to the data from Mantegna[1]. The TARW-mechanism can be interpreted as the superposition of two Gaussian distributions, one narrow, one wide, where the wider distribution is selected due to the relative motion of chart and moving average very rarely. Though we can conclude that the "technical analysis" (i.e. a quantifiable herd-like behavior produced by the herd itself) is a very efficient way to obtain "fat tails" when introduced in random walk models, the TARW-mechanism is not the final answer: The simulated curve deviates significantly from the empirical data, the "onset" of the fat tails is much too high.

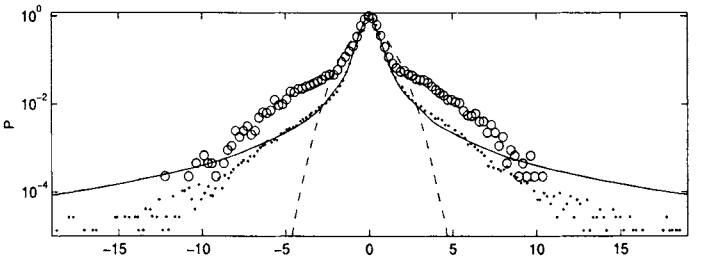


(a) After eqn. (4)-(8) with $a = 0.4$, and $b = 3$,

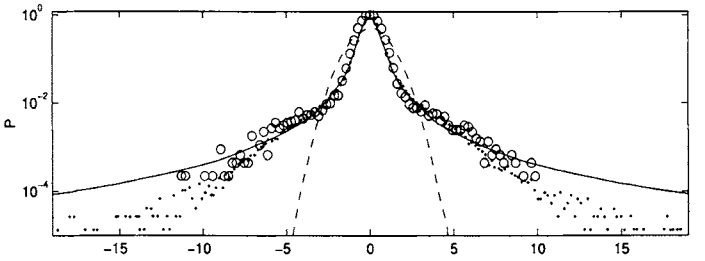


(b) After eqn. (9) -(8) with $a = 0.4$, $b = 1.4$ and $D = 25$.

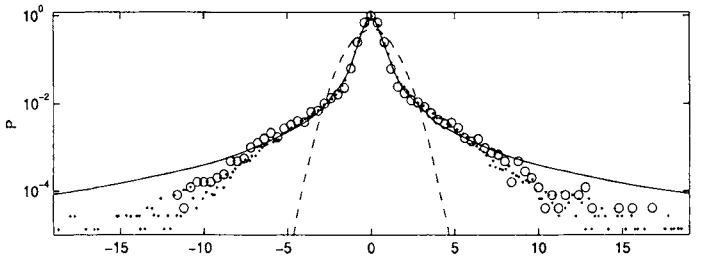


(c) After eqn. (9)-(8), (10)-(15), $a = 0.32$, $b = 1$ and $D = 15$.

**Fig. 1.** Comparison for TARW (a), DTARW (b) and DTARWB (c) (moving averages of length $N = 5000$, circles) with the empirical data for the S&P500 (full dots), the fitted Levy-distribution (solid line) and Gaussian (broken line) after Ref. [1]

## 2.2 Introducing Delay

In our TARW-Model, each transaction relates to the previous one as reference level. In reality, in the trader-based New York Stock exchange, transactions for the S&P500 do not take place instantaneously, but there is a certain time lag between the transaction decision, the completion of the transaction and the actual display of the new price. Data for the duration of this delay are hard to come by, Wall Street seems to be quite reluctant to talk it. To mimic the time lag, we introduce the delay time $D$ so that between display-timestep $j$ and the next display-timestep $j+D$ all players base their transaction decision on the data at the display-timestep $j$, so

$$x_{j+i} = x_j + a\xi_{j+i-1} + b\eta_{j+i-1}, \quad D \geq i \geq 1, \tag{9}$$

all other terms are defined as in the TARW-model. For this "delayed technical analysis random walk model"[2] (DTARW), the delay parameter of $D$ means that the average number of transactions between a transaction and the reference price is $D/2$. The "best fit" for the empirical S&P500-data obtained with the parameters $a = 0.4$, $b = 1.4$ and delay $D = 25$ is shown in Fig. 9. For the DTARW, the variance $b$ for the "mini-trend" has decreased to 1.4, from 4 for the TARW, which is an improvement for the sake of plausible simulation parameters. Nevertheless, the simulation data are higher than the empirical distribution for the probability interval between $10^{-2}$ and $10^{-4.5}$. Another setback of the model is that we had to introduce an additional simulation parameter, the delay $D$ (again the distribution did not change with the length of the moving average), so the DTARW needs three fit parameters, which should account for any curve symmetric to the y-axis with two different curvatures, not very satisfying from the point of data modeling.

## 2.3 Bollinger Bands

Our models up to here[2] allowed only a change from "down" to "up" in the mini-trends, and vice versa. A convenient way to implement a steepening or flattening of a trend in the same direction is via Bollinger Bands, so that

$$\eta_i > \eta_{i-1} \text{ if } \eta_{i-1} > 0 \text{ and } x_i > \langle x_i \rangle_N + 2\mathrm{STD}(x_i) \tag{10}$$

$$\eta_i = \eta_{i-1} \text{ if } \eta_{i-1} > 0 \text{ and } \langle x_i \rangle_N + 2\mathrm{STD}(x_i) > x_i > \langle x_i \rangle_N \tag{11}$$

$$\text{new } \eta_i < 0 \text{ if } \eta_{i-1} > 0 \text{ and } x_i < \langle x_i \rangle_N \tag{12}$$

$$\eta_i < \eta_{i-1} \text{ if } \eta_{i-1} < 0 \text{ and } x_i < \langle x_i \rangle_N - 2\mathrm{STD}(x_i) \tag{13}$$

$$\eta_i = \eta_{i-1} \text{ if } \eta_{i-1} < 0 \text{ and } \langle x_i \rangle_N - 2\mathrm{STD}(x_i) < x_i < \langle x_i \rangle_N \tag{14}$$

$$\text{new } \eta_i > 0 \text{ if } \eta_{i-1} < 0 \text{ and } x_i > \langle x_i \rangle_N, \tag{15}$$

[2] This model is not a delay differential equation in the conventional sense where each $x_i$ would be computed from the previous $x_{i-D}$.

where the "mini-trends" $\eta_i$ are chosen with absolute value larger than the previous one, but the same sign, if the market breaks out beyond the Bollinger bands (twice the standard deviation above and below the moving average[3]). The result for this "Delayed technical analysis random walk with Bollinger Bands" (DTARWB) can be seen in Fig. 1(c) for $a = 0.32$, $b = 1$ and delay interval $D = 15$. The tails have been significantly straightened in comparison to the DTARW-case. Not only are the simulated data very close to the empirical data, the scattering in the tails and the convex part are quantitatively well reproduced. The delay-parameter $D$ to model the empirical S&P500-data has been reduced to 15 in the DTARWB from 25 for the DTARW, so between a transaction decision and the display of the price on average 7 to 8 transactions have occurred. More important: The previous fit-parameter $b$ has been reduced to unity, which means that though the returns $x_i - x_{i-1}$ are not Gaussian distributed, the mini-trends $\eta_i$ are. Therefore, our DTARWB needs only two free fit-parameters, the local correlation $a$ and the delay $D$, so it seems to contain some "true" information about the market.

## 3 Summary and Conclusions

We have shown that the return distributions observed in the S&P500 can be obtained for a random-walk which reacts to moving averages in the technical analysis sense. Characteristic ingredients are mini-trends in accordance with moving averages, which lead to fat tails, delay in trading, which shifts the tails lower in the distributions and a reaction to break-outs of the market (in our case, Bollinger bands) which straighten out the curvature of the tails. Though the chart values of the S&P500 are not Gaussian distributed, it is the mini-trends which follow a random walk/ Gaussian distribution with unit variance. This leaves considerable doubts about the actual "efficiency" of the market. It will be interesting to analyze other market data whether the local correlation $a$ is universal, the mini-trends $\eta_i$ are always standard-normal-distributed and whether the delay $D$ is shorter in markets with electronic trading.

## References


1. R. N. Mantegna, H. E. Stanley, Scaling Behavior in the Dynamics of an Economic Index, Nature 376, p. 46-49 (1995).
2. H.-G. Matuttis, Simple stochastic modeling for financial markets, Meeting Abstracts of the Physical Society of Japan, Vol. 59, Issue 1, part 2, p. 346, March 2004.


[3] Changes in the definition of the Bollinger bands from a prefactor two to three gave only moderate changes in the distributions. A publication with a more detailed discussion of the scattering is in preparation.

# Agent Based Simulation Design Principles – Applications to Stock Market

Lev Muchnik[1], Yoram Louzoun[2], Sorin Solomon[3,4]

[1] Department of Physics, Bar Ilan University, Ramat-Gan, Israel
[2] Department of Mathematics, Bar Ilan University, Ramat-Gan, Israel
[3] Racah Institute of Physics, The Hebrew University, Jerusalem 91904, Israel.
[4] Complex Multi-Agent Systems Division, ISI Torino

**Summary.**
We present a novel agent based simulation platform designed for general-purpose modeling in social sciences. Beyond providing convenient environment for modeling, debugging, simulation and analysis, the platform automatically enforces many of the properties inherent to the reality (such as causality and precise timing of events). A unique formalism grants agents with an unprecedented flexibility of actions simultaneously isolating researchers from most of the overhead of the virtual environment maintenance.

**Key words.** Agent-Based Simulation; Experimental Markets; Artificial Financial Markets; Market Microstructure.

## Introduction

The classic analysis of financial phenomena is usually based on simple (often linear) *macroscopic* models, which preferably can be solved analytically. Such models can reproduce basic market macroscopic features. This type of models fails to reproduce emergent features of markets that cannot be directly deduced from the microscopic interaction producing them.

Emergent phenomena, were studied over the last couple of decades in a wide range of systems. A general approach is to model the system in question as a set of *microscopic elements* and define *microscopic interactions* between them so that the desired *macroscopic phenomenon* emerges. Being frequently and successfully exploited in physics, this method is now being applied in social sciences as well. In the specific context of the stock market, a variety of simplified *microscopic* models have been introduced over the last decade, (Bak et al. 1997, Stauffer 2000, Levy et al. 1994, Mantegna R., Stanley 1999, Maslov 2000, Solomon 2000 and many others). Most of these models focus on specific aspects of the problem: basic features of the agent's behavior or of the stock exchange procedures. They show that even a small set of simple assumptions can explain the set of "stylized" experimental facts characterizing generically the market (Mantegna, Stanley 1999, Cont 2001, Lux, Heitger, Takayasu): power (Pareto–Zipf) laws, fat tails (and/or

Levy-stable distributions), (multi-) fractal dynamics (Hurst exponents), long range correlations (clustered volatility), criticality (scaling exponents).

Similar models explaining stylized facts exist in practically all domains of social sciences ranging from social influence and opinion dynamics (Weidlich, Haag, 1983) to wealth distribution (Levy et. al 2000). It is obvious that in order to go beyond these generic "stylized" facts, one has to consider more realistic features (Solomon, 1999). In the context of the stock market, we would need to consider: detailed stock market procedures, individual trader behavior, communication lags, external events (news arrival, economic fundamentals, etc.) (Levy et al. 1994, Moss et al. 1999).

We developed a platform that simulates an arbitrary number of agents interacting with an arbitrary range of behaviors. A demand for such a tool has been present for quite some time already and several attempts were made to satisfy it (Jacobs et al. 2004, Minar et al. 1996, LeBaron 2002,2004). However, to the best of our knowledge, none of them possessed all the properties required to satisfy the growing community of researchers who could use it. We hereby introduce the basic concepts for the general simulation platform we have developed, named *NatLab* for ***N***atural ***A***synchronous-***T***ime Event-***L***ead ***A***gent-***B***ased Platform. *NatLab* is a realistic continuous time causal asynchronous event driven simulator. It is highly efficient - the cost of each event is proportional to the log of the number of candidate events. In *NatLab* the communication between agents is through a novel efficient messaging mechanism. In the next section first, the design principles of the simulation will be detailed, then a concrete application will be used to exemplify its potential.

## *NatLab* Design Principles and Implementation Details.

*NatLab* deals with any arbitrary system of interacting agents unless they experience continuous interactions. As long as the microscopic inter-agent interactions can be presented as sequence of momentary "collisions", the entire system can be simulated precisely. Each agent can engage any other agent, group of agents or the entire population. The spatial structure in *NatLab* is implemented using a fixed (or evolving) network of nodes and links, effectively introducing neighbors. The basic design principles of *NatLab* are as follow:

- Timing
    - Asynchronous update - Active agents are allowed to initiate actions as opposed to the conventional passive agents that are delayed until polled.
    - Event-Driven - The simulation engine schedules future events and processes them one by one, skipping the time in-between
    - Continues time - Unlike in conventional discrete time simulations, times of the events are precise as they are not confined to any discrete time.
- Causality - Being event-driven and executing all events at the precise time of their occurrence, the simulation does not accumulate inaccuracies as it evolves.

Moreover, the platform ensures the correct ordering of events, continuously maintaining the cause-effect principle. This allows each and every agent to respond and adjust by re-scheduling his future actions. The schedule of upcoming events is constructed on the fly, while the first event is executed.

- Realistic action cycle - Agents may exploit the asynchronous nature of the platform implementing a realistic multi-stage action cycle. Being isolated between events and exogenous to the agent messages, each agent can evolve in parallel until it either spontaneously decides to initiate some action or responds to an interaction coming from outside (either directly induced by an other agent or indirectly in response to an objective state change following some event execution). Since events are scheduled and executed when their time arrives, realistic delays in agents evolution and action time lags are naturally ensured.
- Messages - Agents interact by exchanging arbitrary delayed messages. The simulation platform engine guarantees delivery of the messages when the simulation time is promoted to the appropriate time. The same message can be delivered to a group or even all agents, which may either ignore it or respond by scheduling some future action (simulating natural delayed response).
- Efficacy -*NatLab* is optimally efficient. *NatLab* deals uniquely with events execution, wasting no resources on looping over the pool of agents, and very few resources on scheduling future events. The execution time scales as O(N*log(M)), where N is the total number of events, and M is the number of events currently in the queue. *NatLab* CPU cost does not depend on the total number of agents in the system.
- Multilevel - *NatLab* is suited to simulate not only relatively small isolated systems (such as the stock exchange), but can deal with systems of arbitrary complexity at several scales (time scales and organizational complexity). One could in principle model the entire economy– starting from individuals acting as employees through firms, banks, the stock exchanges, etc. All the interactions between them can be made as precise as required.

We will not provide all algorithmic details and the software implementation, as these are mainly technical and do not contribute to understanding the function of *NatLab*. There are, however some particulars which are essential in order to understand the general function of the simulation.

**General structure:** The platform is divided into three independently developed modules with a strictly defined interface and communication protocols between them. This structure allows the optimization of *NatLab*, and its implementation on very different platforms. Moreover, it allows the user to ignore the internal structure when designing agents. The basic elements are:

- *The Autonomous engine*. The highly optimized core of the platform, whose task is to automatically manipulate user-defined agents by delivering their messages.
- *Simulation User Interface* (Figure 1). This module provides the user with a convenient user interface, and is independent on of the simulation core.
- *Agents*. To reduce requirements from developers, we do not require inter-platform compatibility from each agent. However, each agent should be based

either on the template supplied with the platform, or strictly support the interface, specified by us.

**Agents:** *NatLab* implements a modular concept which requires each agent to be implemented and compiled as a separate binary module. These modules are automatically recognized and imported by the simulation platform as it loads or when at the configuration stage of a specific simulation run. All agents should be based upon the single basic agent class and provide the functionality required by *NatLab*. Moreover, they should all provide a common binary interface to allow the platform to operate them. The functionality includes mainly the agent ability to filter and respond to messages they receive, and to send new messages.

**Messages:** Messages are used for communication between agents. All messages must provide the minimal information required for their transfer and delivery: A) Issuing agent ID, B) Issue time, C) Destination agent ID, D) Delivery time, E) Message type (ENUM) and may include arbitrary additional information.

## Application

Let us demonstrate the simulation platform by schematically presenting a simple stock exchange model where the spontaneous herding behavior of a tiny fraction of the traders populating it causes formation of a bubble and a crash, followed by a long recovery period. This simulation shows the huge effect of the uncoordinated action of a very small portion of traders. We do not intend to replicate or explain any of the real market properties, but to merely present an example of the platform use.

The model framework consists of a single stock traded by means of a

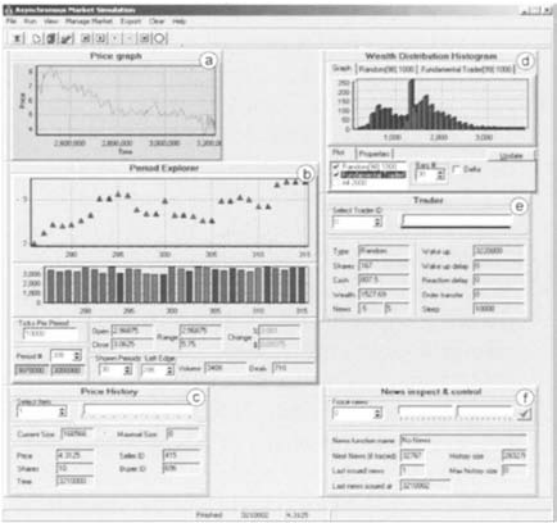


Fig. 1 GUI of NatLab. The graphical user interface of the Platform is designed to provide a comprehensive insight into the dynamical processes of any specific model at both macroscopic and microscopi levels. The windows providing textual or graphical representation of model parameters at the run time are also implemented as agents, each updating it's own content on demand. Similartly to model-specific agents, each window can be designed to update periodically or to respond to specific events. They can also allow the user to interfer into the simulation by providing the interface for setting parameters and issuing system-wide or specific messeges. In this particular example: (a)Shows the price evolution. (b)Daily price and volume. (c)Exposes details of every transaction. (d)Comparative distribution of traders' wealth for each type. (e)Provides acccess to detailed information about each agent. (f) Allows the user to inspect and issue news.

classical orders book similar to the one employed today by most stock exchanges[1]. The market is mainly populated (98% in our runs) by one type of agents. These agents act randomly by occasionally submitting relatively small (~2% of their wealth) limit orders. The limit orders' prices are drawn from the neighborhood of the current market price. Each order has 50% probability to be a buy or a sell order. If these agents would be the only agents acting in the market, the stock value distribution would be approximately a narrow Gaussian around the value determined by the amount of money and the stock number. One could argue that the inclusion of a few uncoordinated agents should not significantly affect the market dynamics. We actually show that a small minority, trying (naively) to identify the market's behavior and to follow it can drastically change the market dynamics.

Let us, thus, assume a second small population (2% in our case, but it can be even smaller). Unlike the random traders, each of the agents belonging to the second type continuously tries to identify and exploit price trends. Those *occasional* traders represent people that do not invest in stocks unless they identify (to the best of their knowledge) a clear opportunity. In our case, we have selected a persistent positive price trend as an indicator for occasional traders to enter the market. They start with no shares at all and keep inspecting the prices until they recognize a trend. From this moment on, the agent gradually buys stocks until either its entire capital is invested or the price starts to drop. When the opposite trend is detected, the agent starts selling by submitting market orders. Note again that these minority traders (2%) are not synchronized.

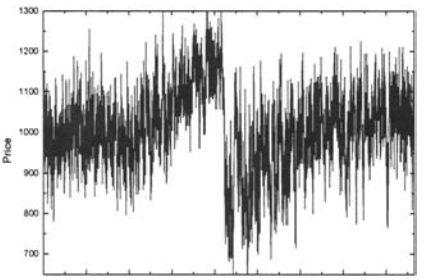

Fig. 2 The price evolution shows region of regular trade followed by gradual price raise due to massive acquisition by ocasional agents, crash and slow recovery.

In our runs executed for a population of 10,000 random traders and 200 occasional traders (Fig. 2) we observe the emergence of a herding behavior which causes a gradual increase of the price, followed by sudden crash. Each agent acts independently from the others, having personal criteria for its behavior. Occasional traders start with no stocks and watch the market sporadically identifying random fluctuation as appearing trends. In response to such an initially (erroneous) trigger the demand increases. This demand in turn actually raises the price, increasing the chance for other agents to identify it as a (real) emerging trend. Eventually, all occasional traders will interpret the raising price as an opportunity and will start competing with the rest for the available stocks (obviously raising the price even more). The process will continue until most of the occasional agents are exhausted and have no more cash to invest. At this point,

[1] www.nyse.com

the price stops rising. The traders interpret this by realization that no additional profits can be made in this situation and start realizing them as fast as they can. This, naturally enough, causes the price to crash. As soon as the majority of occasional traders manage to get rid of their stocks, the price stabilizes and even climbs gradually. The reason for the positive trend in this case is the interaction between the random agents. By definition, they do not distinguish between any of the two assets (the money and the stocks) and operate caring only for the volume of transactions. Therefore, they will tend to sell more shares at low prices, effectively causing the price to rise. This effect stabilizes the price near the price determined by the total amount of money and stocks random agents have. Note that none of the agents involved has to know what those numbers are.

## References


P. Bak, M. Paczuski and M. Shubik, Price Variations in a Stock Market with Many Agents, Physica A, Dec 1997. cond-mat/9609144.

Cont R., Empirical properties of asset returns: stylized facts and statistical issues, Quantitative Finance, Volume 1, (2001) 223-236

Jacobs B. I., Levy K. N., Markowitz H.. Financial market simulations. Journal of Portfolio Management, 30th Anniversary, 2004.

LeBaron B. Building the santa fe artificial stock market. Physica A, 2002. Working Paper, Brandeis University.

LeBaron B. Agent-based computational finance. 2004. Priliminary draft.

Levy M., Levy H., Solomon S.. Microscopic Simulation of Financial Markets: From Investor Behavior to Market Phenomena. Academic Press, 2000. ISBN 0124458904

Lux T., Heitger F., Takayasu H., Micro-Simulations of Financial Markets and the Stylized Facts. The Empirical Science of Financial Fluctuations: Econophysics Approach on the Horizon. Berlin: Springer, in press.

Mantegna R. & Stanley H.E. An Introduction to Econophysics, Cambridge University Press, 1999. ISBN: 0521620082

Maslov S., Simple model of a limit order-driven market, PHYSICA A, 278, April 14, 2000, pp 571-578,cond-mat/9910502

Minar N., Burkhart R., Langton C., Askenazi M.. The Swarm Simulation System: A Toolkit for Building Multi-agent Simulations, 1996

de Oliveira S. M., de Oliveira P.M.C., Stauffer D., Evolution, Money, War, and Computers - Non-Traditional Applications of Computational Statistical Physics, Teubner, Stuttgart-Leipzig (1999), ISBN 3-519-00279-5

Solomon S. Towards behaviorly realistic simulations of the stock market. Computer Physics Communications 121 (1999) 161. http://xxx.lanl.gov/abs/adap-org/9901003

Solomon S., Generalized Lotka Volterra (GLV) Models of Stock Markets , Applications of Simulation to Social Sciences, Hermes Science Publications 2000, p 301

Stauffer S., Econophysics - a new area for computational statistical physics, International Journal of Modern Physics C, Vol. 11, No. 6 (2000) pp 1081-1087

Weidlich W., Haag G., Concepts and models of quantitative sociology. Springer, Berlin, 1983



*Acknowledgement*: This research was partially supported by the Israeli Science Foundation

# Heterogeneous agents model for stock market dynamics: role of market leaders and fundamental prices

Janusz A. Hołyst and Arkadiusz Potrzebowski

Faculty of Physics and Center of Excellence for Complex Systems Research
Warsaw University of Technology
Koszykowa 75, PL–00-662 Warsaw, Poland
jholyst@if.pw.edu.pl

**Summary.** We have developed a microscopic model of interacting agents where agents buy or sell shares depending on the information they get from neighbours and a relation of a temporary price to a fundamental price. Depending on the magnitude of the noise present in the system (magnitude of market temperature) prices oscillate between the bull and the bear phases or around a mean fundamental value. The oscillation period can be calculated from a mean field theory. A very influencial investor (market leader) does not get larger profits than a typical one. A crucial role for profits is played by a coupling constant to a fundamental price.

*pacs 89.65.Gh, 75.10.Hk*
*keywords: multi-agents models, stock market*

We use the social impact theory [1, 2] to describe behaviour of a group of $N$ investors described by constant in time strengths $s_i > 0$ and the state variables $\sigma_i(t) = \pm 1$ that define their investment attitude as follows: $\sigma_i(t) = 1$ if the trader wants to buy a share and $\sigma_i(t) = -1$ if the trader wants to sell a share at time $t$. For simplicity we assume that every investor can buy/sell at every moment not more than one share. Orders are reduced to ensure a constant number of all shares available at the market. Each investor $j$ influences the opinion of other investor $i$ with a magnitude proportional to the strength $s_j$ of the investor $j$ and their market immediacy $m_{ij} > 0$ where the constant $m_{ij}$ does not need to be equal to $m_{ji}$.

Investor attitudes $\sigma_i(t)$ may change simultaneously (synchronous dynamics) in discrete time steps according to the Glauber–like rule : $\sigma_i(t+1) = +1$ with the probability $\alpha$ and $\sigma_i(t+1) = -1$ with the probability $1 - \alpha$ where $\alpha = 1/[1 + \exp(-2I_i/T)]$. Here $I_i$ corresponds to the local information field acting at the investor $i$ and it has been assumed as

$$I_i = \sum_{j=1}^{N} s_j m_{ij} \sigma_j(t) - \gamma_i \ln[p(t)/p_i^f] \tag{1}$$

where $p(t)$ is a temporary price, $p_i^f$ is a value of a fundamental price chosen by the investor $i$ while $\gamma_i > 0$ is a constant characterizing sensitivity of the attitude of investor $i$ to price changes. The parameter $T$ may be interpreted as a "market temperature" describing a degree of randomness in the behaviour of individuals, but also their average volatility.

Price $p(t)$ changes as $\Delta p(t-1) = \beta p(t-1) \sum_{j=1}^{N} \sigma_j(t-1)$ where $\beta > 0$ is a constant.

The model belongs to the similar class of Ising-like models that were studied among others in [3, 4] but instead of coupling the attitude of interacting traders to the global attitude $\sigma_i(t)|\sum_{j=1}^{N} \sigma_j(t-1)|$ as in [4] we have introduced the coupling to the temporary price $p(t)$. We assume also that one can not distinguish between fundamental and interacting traders and all traders are influenced by trader–trader interactions and by ratio between the temporary price and the individually chosen fundamental price.

Using the mean field approximation after some algebra one can write average attitude of investors as

$$\langle \sigma(t+1) \rangle = \tanh[(Nsm/T)\langle \sigma(t) \rangle - (N\gamma\beta/T) \sum_{\tau=1}^{t-1} \langle \sigma(\tau) \rangle] \tag{2}$$

where $s$, $m$, $\gamma$ are corresponding mean values. As one can see due to the coupling of investment attitudes to the local price there is a memory term in the above equation. This term induces either oscillations of the mean attitude (investor mood) $\langle \sigma(t) \rangle$ around the zero value for $Nsm/T < 1$ (the paramgentic phase of weak interactions) or *between* two values that follow from the standard mean field solution for $Nsm/T > 1$ (the ferromagnetic phase of strong interactions). The second kind of dynamics corresponds to switching bwetween the bull ($\langle \sigma(t) \rangle > 0$) and bear ($\langle \sigma(t) \rangle < 0$) market. A typical dynamics for weak and strong interactions regime is presented at Fig. (1).

It easy to show that in the case when the discrete time equation for price changes can be approximated by a differential equation then the switching time between two ferromagnetic phases is inversely proportional to the coupling constant $\gamma$ what in fact has been observed in our numerical experiments.

We have studied the influence of the leader on the market dynamics. The leader has been characterized by a large market strength $s_L$. In the presence of such a leader the evolution of prices has been shifted towards lower or towards higher values depending on a characteristic value of a fundamental price $p_L^f$ assumed by the market leader. In fact the presence of such a leader resembles the effect of the external field $h$ that breaks the symmetry in the considered system. It is remarkable that in average the leader doee not have larger profits than less influential players (see Fig. 2).

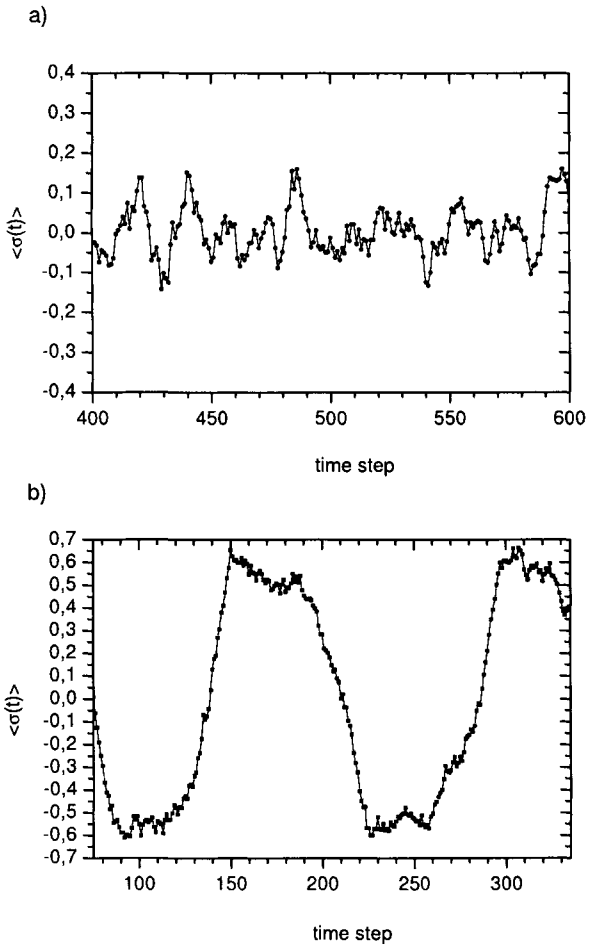


**Fig. 1.** Solutions: oscilations of the mean investor mood in a paramagnetic phase or between two ferromagnetic phases

Various test have been performed to find optimal values for an individual to get the largest profit. Our simulations have shown that the best strategies correspond to larger values of the coupling constants $\gamma_i$ that characterize the role of fundamental aspects in the trader strategy (see Fig. 3 and Fig. 4)

It interesting that values of assumed fundamental prices $p_i^f$ play only a minor role and investors with different $p_i^f$ get in average the same profits if they coupling constants $\gamma_i$ are the same.

In conclusions we show that in a simple model of heterogenous investors an influential market player does not have large benefits. Such benefits can be

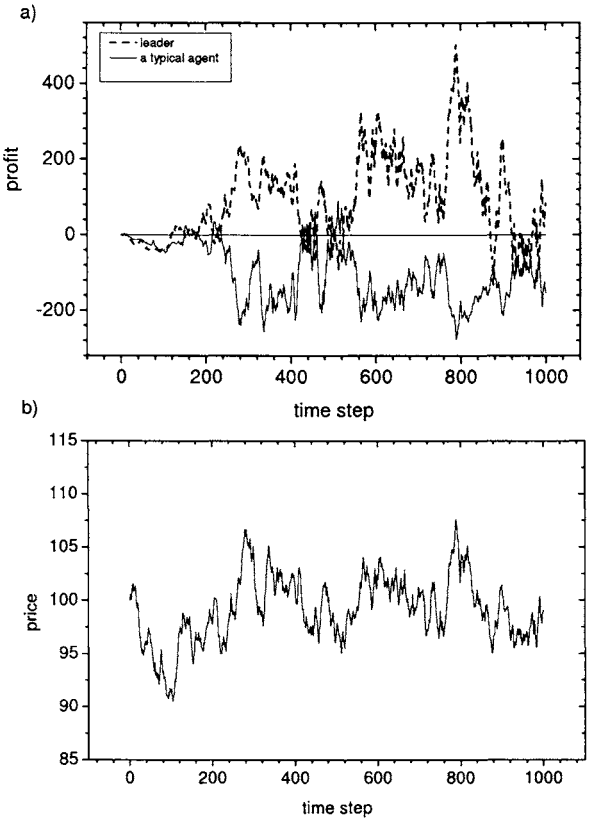


**Fig. 2.** Strong leader does not get larger profits !

a result of a strong coupling between an investor strategy and a fundamental price.

## References


1. K. Kacperski and J. A. Hołyst, Physica A **269**, 511 (1999), Physica A **287**, 631 (2000). and
2. A. Krawiecki and J. A. Hołyst, Physica A **317**, 597 (2003),
3. T. Kaizoji, Physica A **287**, 493 (2000).
4. T. Kaizoji, S. Bornholdt and Y. Fujiwara, Physica A **316**, 441 (2002).

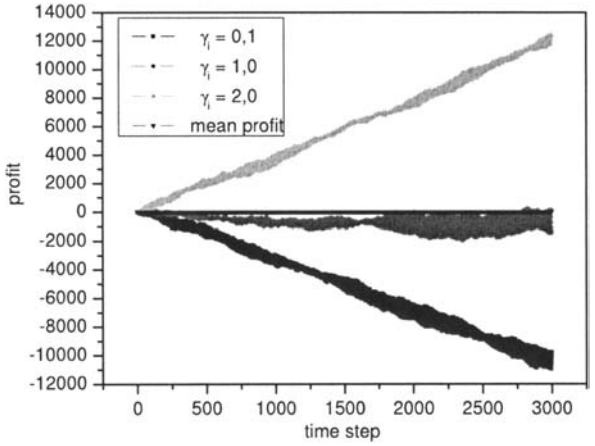


**Fig. 3.** Changes of cumulative profits for agents with different fundamental weights $\gamma_i$

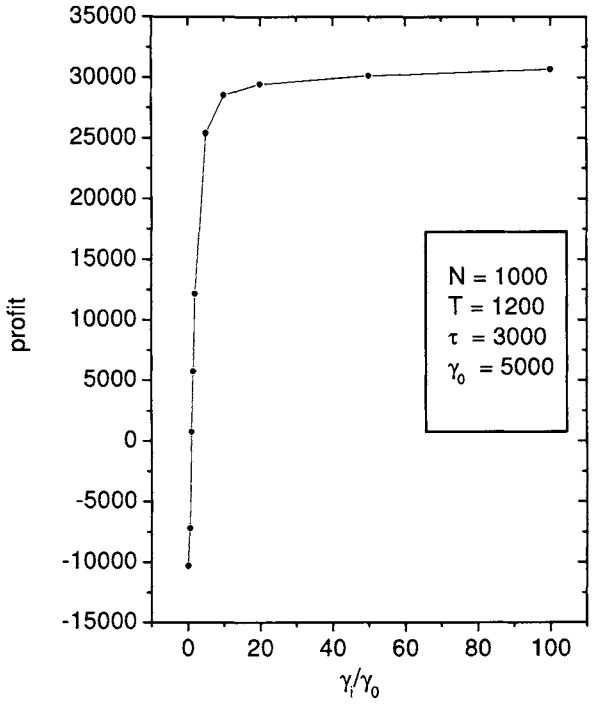


**Fig. 4.** Average cummulative profits for agents with different fundamental weights $\gamma_i$ calculated after $\tau$ time steps

# Dynamics of Interacting Strategies

Masanao Aoki[1] and Hiroyuki Moriya[2]

[1] Department of Economics, University of California, Los Angeles
aoki@econ.ucla.edux
[2] Oxford Financial Education
moriya@quasars22.co.jp

**Abstract.** This paper presents the model of the dynamics process of switching the strategies adopted by a large number of agents according to their views of what they deem as the most advantageous strategy in relation to the behavior of other agents and/or exogenous environments. The process of switching the strategies is modeled by the master equation by suitably specifying the transition rates of continuous time Markov chains. The computer simulation explains the effects of demand-supply imbalance created by short-medium term traders in the dollar-yen foreign exchange market.

## 1 Introduction

We examine nonlinear dynamics generated by a large number of heterogeneous agents when they switch, enter or exit their strategies. They change, enter or exit their strategies over time, because they can not foresee the consequences of their choices exactly at the moment of their choice. Consequences of their choices are distributed stochastically, and over time new information may become available as to desirability of some choices over the others.

Consequently, clusters of agents of the same choices may develop and disappear over time. Aoki (1996,2002) has discussed problems for the case where each agent has binary choices. As in these cases, we use the master equation, that is, the backward Chapman-Kolmogorov equation, to discuss the dynamics of agent behavior.

In the late 1980s and until the mid 1990s, Hogg and Huberman (1991), Youssefmir and Huberman (1995) or Adjali, Gell and Lunn (1994), and their collaborators have published a number of papers in which agents have many choices over resources and strategies. While these authors use error functions to express distributions of the consequences of choices. We use Ingber's approximation to the error function and introduce Gibbs distributions into transition rates of continuous time Markov chains.

Here, the computer simulations focus on the states that agents implement two strategies in dollar-yen foreign exchange market.

## 2 The model

Suppose that there are a fixed number $K$ strategies. The total number of agents is fixed at $\mathbf{N}$. At any time $n_i$ is the number of agents with strategy $i$, where $\sum_i n_i = \mathbf{N}$. The master equation describe how the probability $Pr(\mathbf{n}, t)$ evolves over time, where $\mathbf{n}$ is the vector whose $i$-th component is $n_i$. We say agent is of type $i$ when it uses strategy $i$.

The probability $Pr(\mathbf{n}, t + \Delta)$ increases over $Pr(\mathbf{n}, t)$ by the net inflow of probability flux, that is, the difference between the inflow and outflow, where inflow arise from some agent of type $j$ deciding to drop strategy $j$ and adopting strategy $i$, $j \neq i$, and outflow is due to one agent of type $i$ deciding to switch to a different strategy.

Since we model those processes as birth-and-death type Markov process, at most one such strategy switch takes place over a small time interval $\Delta$.

The master equation is derived from

$$Pr(\mathbf{n}, t + \Delta) = Pr(\mathbf{n}, t) - \sum_{\mathbf{n}' \neq \mathbf{n}} Pr(\mathbf{n}, t)\omega(\mathbf{n}, \mathbf{n}') + \sum_{\mathbf{n}' \neq \mathbf{n}} Pr(\mathbf{n}', t)\omega(\mathbf{n}', \mathbf{n})$$

Assuming that $\lambda$ is the rate of strategy examination over time, denoting the number of agents of type $j$ before revision by $n'_j$, and let $\eta_{j,i}$ the probability that strategy $i$ is regarded by agent $j$ to be the most desirable, we write the transition probability over time interval $\Delta$ as

$$\omega(\mathbf{n}', \mathbf{n}) = n'_j \eta_{j,i}(\mathbf{n}')\Delta$$

Aoki(2002) has shown that on the derivation that $\eta$ has a Gibbs distribution $e^{\beta g_{j,i}}/Z$, where $Z$ is a partition function, where $\beta$ is a parameter which embody the uncertainty associated with this switch of strategy, and $g_{j,i}$ is the expected difference in the discounted present value of adopting strategy $j$ over strategy $i$. Here we use Ingber's approximation to error functions for approximating transition rates in the way described by Aoki (1996,page 133;1998;2002,chap 6). Hence the master equation is rewritten as

$$Pr(\mathbf{n}, t + \Delta) - Pr(\mathbf{n}, t) = \lambda\Delta(O - I),$$

where $O - I$ stands for inflow - outflow, where

$$I = \sum_i \sum_{j \neq i} n'_j \eta_i Pr(\mathbf{n}', t),$$

and

$$O = \sum_i \sum_{j \neq i} n_j \eta_j Pr(\mathbf{n}, t),$$

up to $o(\Delta)$.

Dividing both sides by $\Delta$ and letting it go to zero we arrive at

$$\frac{\partial Pr(\mathbf{n}, t)}{\partial t} = \lambda(O - I)$$

## 3 Interacting or No interacting patterns

**Calculating $\eta_{i,j}$ for interacting patterns:** Let $V_i$ be the random discounted present value of using strategy $i, i = 1, \ldots, n$ for some specified length of time. Define $\eta_{i,j}$ to be the probability that agents who have been using strategy $i$ want to switch from strategy $i$ to $j$,

$$\eta_{i,j}(x) = Pr(V_j \geq \max_{i \neq j}\{V_i\}|x)$$

Under certain sets of assumptions, it is known that this expression is given by a Gibbs distribution, Aoki(2002,Sec.6.3). We can use a program called MULNOR, introduced by Shervich(1984,1985), to calculate such probabilities with agents interactions.

**Calculating equilibrium probability for no interacting patterns** The master equation with the entry and exit without any switching the strategies provides the equilibrium probabilities of the strategy i based on Poisson distribution.

$$P_i(\theta = \nu) = e^{-\theta} \frac{\theta^\nu}{\nu!}$$

where $\theta = \alpha/(\mu k)$ ; $\alpha$:the entry rate; $\mu k$:the exit rate: $k$:the number of traders.

## 4 Simulation

The simulation is made for identifying how the behavior of trading groups with a short-medium term horizon affects price movements in the foreign exchange market. We focus on two types of traders in the market: trend followers and contrarians. Type 1 is a trend follower who buys(or sells) currency when the currency is appreciating(or depreciating). They are sub-divided into type 1a and type 1b. Type 1a is a upward trend follower who gets profits when the market has upward trend. As a large number of trading strategies are available for upward trend viewers, we use option strategies to replicate their behavior. The trading with buying calls represents type 1a strategy. Type 1b is a downward trend follower who makes money when the market has downward trend. Buying puts represents type 1b strategy. The trend followers switch

the sub-strategy from 1a to 1b or vice versa, depending on their profits and losses. These interactions are described as birth-death process. Type 1a and type 1b have the master equation with transition rates that are functions of the profits and losses.

Type 2 is a contrarian who buy(or sell) the currency when it is depreciating(or appreciating), because they believe that the market will stay in the range. Selling calls and puts represents type 2 strategy.

We assume that the trend followers and the contrarians do not change their types in a short-medium term horizon. However, they enter and exit the strategy over time depending on profits and losses of the strategy. Each of type 1 and type 2 has the master equation with the entry and exit without any interacting patterns.

The simulations are made as follows:

1. Trend followers : Type 1a(type 1b) buys one unit of at the money call(put) with one(or three) month(s) maturity every day. They hold the positions until the maturity. Simplifying the problems, one(or three) month(s) consists of 20(or 60) working days. Therefore, the portfolios of options held by each sub-group include 20(or 60) different options. A set of daily historical data is used for the evaluations: spot price, implied volatilities, and domestic and foreign interest rates. In case of type 1a with one month maturity, the portfolio is evaluated daily as

$$V_{1a}(t) = \sum_{t_p=0}^{20-1} (w_{t-t_p} \times c_{t-t_p,t} - r_{t-t_p})$$

where $c_{t-t_p,t}$ is the value of the call option at time $t$ starting at time $t-t_p$ as the at the money option with maturity of one month, and is evaluated by using the Black-Scholes type currency option model(M.b.Garman and S.W.Kohlhagen,1983). $w_{t-t_p}$ is the weight of the option and equal to the inverse of $c_{t-t_p,t-t_p}$. $r_{t-t_p}$ is the funding cost for the option starting at time $t-t_p$. Based on the standard deviations and means of $V_{1a}(t)$, we estimate the rates, $\eta_{1a,1b}(t)$ by using Mulnor program,

$$\eta_{1a,1b}(x(t)) = Pr(V_{1a} \geq V_{1b}|x(t)) = \int_{-\infty}^{\infty}\int_{a}^{\infty} f(x_{1a}, x_{1b})dx_{1a}dx_{1b}.$$

The probabilities of type 1a at time $t+\Delta$ based on a set of empirical data are obtained from

$$Pr(n_{1a}, t+\Delta) = Pr(n_{1a}, 0) + \sum_{t=0} Pr(n_{1a}, t)\omega(n_{1a}, n_{1b}, t)$$

$0 \leq Pr(n_i, t) \leq 1$ for any t, where $\omega(n_{1a}, n_{1b}, t) = l \times \eta_{1a,1b}(x(t))$. $l$ is constant over time and determined as maximizing the profit of the trend followers.

Consequently, we get the daily values of the portfolio held by the trend followers.

$$V(t) = Pr(n_{1a}, t + \Delta) \times V_{1a}(t) + (1 - Pr(n_{1a}, t + \Delta)) \times V_{1b}(t)$$

2. Contrarians : Contrarians sell one unit of at the money call and put with one(or three) month(s) maturity every day and keep these positions until the maturity. The value of the portfolio is calculated by the same way as above.

3. Entry to and Exit from the strategy : Finally, we calculate the standard deviation of the portfolio value of both the trend followers and the contrarians, and estimate the equilibrium probabilities of each strategy $P_{i,t}, i = 1, 2$ with the entry and exit at time t based on Pisson distribution.

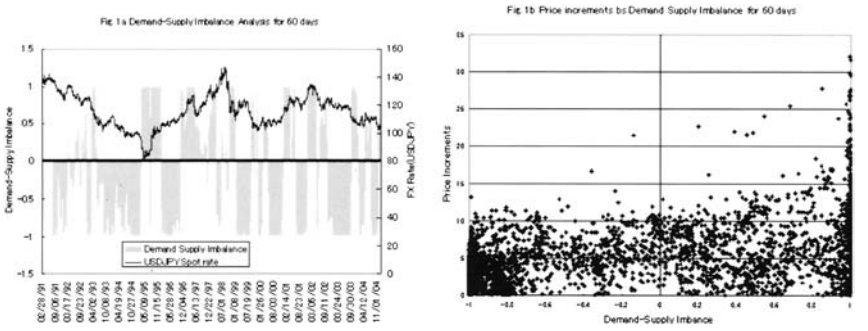


**Fig. 1.** Three months simulation (1a) provides the relationship between demand/supply imbalance and dollar-yen price movements. (1b) provides the relationship between price increments and demand/supply imbalance.

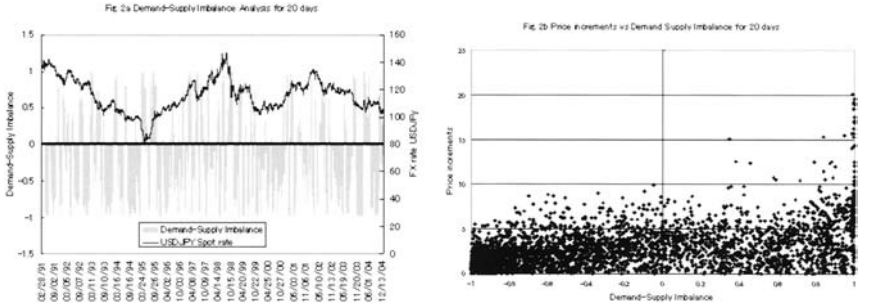


**Fig. 2.** One month simulation (2a) provides the relationship between demand/supply imbalance and dollar-yen price movements. (2b) provides the relationship between price increments and demand/supply imbalance.

The decisions of entry to and exit from each group are made independently, therefore, there are the imbalance between demand and supply of the currency(options). This imbalance is balanced by market-makers and day traders in the market, however, we currently focus on the imbalance created by the short-medium term traders. In general, we can understand when trend followers dominate the market, they will provide the positive feedback of the price movements that may emerge the trend in the market. On the other hand, when contrarians dominate the market, the market may stay in the range due to the negative feedback of the price movements. The imbalance at time t is obtained by $P_{1,t} - P_{2,t}$ . Fig 1 and 2 show us the simulation results that explain the demand-supply imbalance affects the price movements in dollar-yen market, visually and intuitively.

## 5 Conclusion

We examine nonlinear dynamics generated by trend followers and contrarians with a short-medium term view in the dollar-yen market. Based on the analysis of computer simulation, we currently conclude that behavior of heterogeneous agents may be one of the reasons for generating trending or trendless market.

## References


1. Adijali, I,M.Gell, and T. Lunn (1994), "fluctuations in a decentralized agent-resource system," Phy. Rev. E 49 3833-3842
2. Aoki,M.(1996) New Approaches to Macroeconomic Modeling: Evolutionary stochastic dynamics, multiple equilibria, and externalities as field effects, Cambridge University Press, New York.
3. Aoki,M.(1998) "A simple model of asymmetrical business cycles: Interactive dynamics of large number of agents with discrete choices," Macroeconomic Dynamics,2,427-442.
4. Aoki,M.(2002) Modeling Aggregate Behavior and Fluctuations in Economics, Cambridge University Press, New York.
5. Garman,Mark B. and Kohohagen, Steven W., "Foreign Currency Option Values", Journal of International Money and Finance,Vol.2,No.3,Dec.1983,231-237
6. Hogg, T., and B. A. Huberman (1991) "Controlling chaos in distributed systems," IEEE Trans. Systems, Man, and Cybernetics, 21, 1325-1331.
7. Ingber, L. (1982), "Statistical mechanics of neocortical interactions," Physica A, 5, 83-107.
8. Schervish, M. (1984), "Multivariate normal probabilities with error bound," Appl. Stat., 33, 81-87.
9. Schervish, M. (1985), "Correction to Algorithm AS 195: Multivariate normal probabilities with error bound", Appl. Stat., 34, 103-104.
10. Youssefmir, M., and B. A. Huberman (1995), "Clustered Volatility in Multiagent Dynamics", arX:adap-org/9502006.

# Emergence of two-phase behavior in markets through interaction and learning in agents with bounded rationality

Sitabhra Sinha[1] and S. Raghavendra[2]

[1] The Institute of Mathematical Sciences, CIT Campus, Taramani, Chennai 600113, India.
sitabhra@imsc.res.in
[2] Madras School of Economics, Anna University Campus, Chennai 600 025, India.

Phenomena which involves collective choice of many agents who are interacting with each other and choosing one of several alternatives, based on the limited information available to them, frequently show switching between two distinct phases characterized by a bimodal and an unimodal distribution respectively. Examples include financial markets, movie popularity and electoral behavior. Here we present a model for this biphasic behavior and argue that it arises from interactions in a local neighborhood and adaptation & learning based on information about the effectiveness of past choices.

## 1 Introduction

The behavior of markets and other social agglomerations are made up of the individual decisions of agents, choosing among a number of possibilities open to them at a given time. Let us consider the example of binary choice, where the agent can make one of two possible decisions, e.g., to buy or to sell. If each agent makes a choice completely at random, the outcome will be an unimodal distribution, a Gaussian to be precise, of the collective choice (i.e., the sum total of all the individual decisions), at whose mean value the distribution will have its peak. In our example this implies that, on the average, there are equal numbers of buyers and sellers.

However, empirical data in financial markets [1, 2], movie popularity [3] and electoral behavior [4] indicate that there is another phase, corresponding to the agents predominantly choosing one option over the other. This is reflected in a bimodal distribution of the collective choice (Fig. 1).

To account for this we argue that, in a society, agents make choices based on their personal beliefs as well as opinions of their neighbors about the possible outcomes of a choice. These beliefs are not fixed but evolve over time according to changing circumstances, based on previous choices (adaptation)

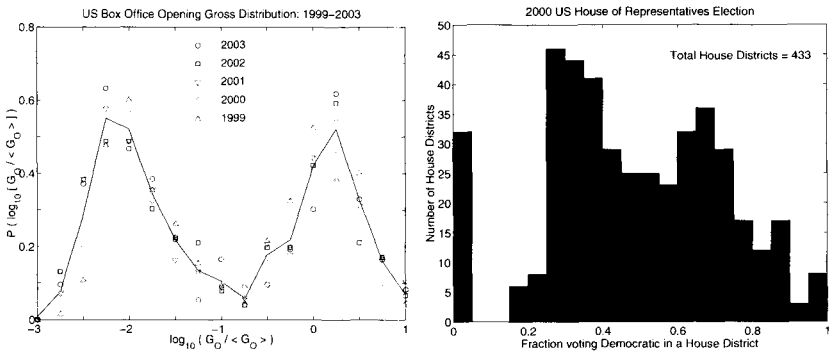


**Fig. 1.** Examples of empirical bimodal distributions. (Left) The distribution of opening week gross earning, $G_O$ (scaled by the average value for a particular year, $< G_O >$) for movies released in the USA during the period 1999-2003. The different symbols correspond to individual years, while the curve represents the average over the entire period. (Right) Frequency histogram of vote share for the Democratic Party candidate in each House district at the 2000 US Federal House of Representatives election.

and how they accorded with those of the majority (learning). We propose a model of collective choice dynamics where each agent has two variables associated with it, one corresponding to its choice and the other corresponding to its belief regarding the possible outcome of the choice.

The bounded rationality of the agents in our model is due to the limited information available to the agent at a given point of time. However, subject to this constraint, the agent behaves deterministically. One of the striking observations obtained from the model is that although each agent may behave rationally and change their beliefs (and hence their choices) periodically, the collective choice may get polarized and remain so for extremely long times (e.g., the entire duration of the simulation).

## 2 The Model

Our model is defined as follows. Consider a population of $N$ agents, each of whom can be in one of two choice states $S = \pm 1$ (e.g., to buy or to sell, to vote Party A or Party B, etc.). In addition, each agent has a personal preference or belief, $\theta$, that is chosen from a uniform random distribution initially. At each time step, every agent considers the average choice of its neighbors at the previous instant, and if this exceeds its belief, makes the same choice; otherwise, it makes the opposite choice. Then, for the $i$-th agent, the choice dynamics is described by:

$$S_i^{t+1} = \text{sign}(\Sigma_{j \in \mathcal{N}} J_{ij} S_j^t - \theta_i^t), \tag{1}$$

where $\mathcal{N}$ is the set of neighbors of agent $i$ ($i = 1, \ldots, N$), and sign $(z) = +1$, if $z > 0$, and $= -1$, otherwise. The coupling coefficient among agents, $J_{ij}$, is

assumed to be a constant (= 1) for simplicity and normalized by $z$ (= $|\mathcal{N}|$), the number of neighbors. In a lattice, $\mathcal{N}$ is the set of spatial nearest neighbors and $z$ is the coordination number.

The individual belief $\theta$ in turn evolves, being incremented or decreased at each time step, according to the agent's choice:

$$\begin{aligned} \theta_i^{t+1} &= \theta_i^t + \mu S_i^{t+1} + \lambda S_i^t, \text{ if } S_i^t M^t < 0, \\ &= \theta_i^t + \mu S_i^{t+1}, \text{otherwise,} \end{aligned} \tag{2}$$

where $M^t = (1/N)\Sigma_j S_j^t$ is the collective choice of the entire community at time $t$. The adaptation parameter $\mu$ is a measure of how frequently an agent switches from one decision to another. Belief also changes according to whether the previous choice agreed with the majority decision. In case of disagreement, the belief is increased/decreased by a quantity $\lambda$ that measures the relative importance of global feedback (e.g., through information obtained from the media). The desirability of a particular choice is assumed to be related to the fraction of agents in the community choosing it; hence, at any given time, every agent is trying to coordinate its choice with that of the majority.

## 3 Results

Although some analytical results can be obtained under mean field theory, here we present only numerical simulation results for the case where the agents are placed on a two-dimensional regular lattice (see Ref. [5] for details). Note that, in absence of either adaptation or global feedback ($\mu = \lambda = 0$) the model reduces to the well-studied random field Ising model.

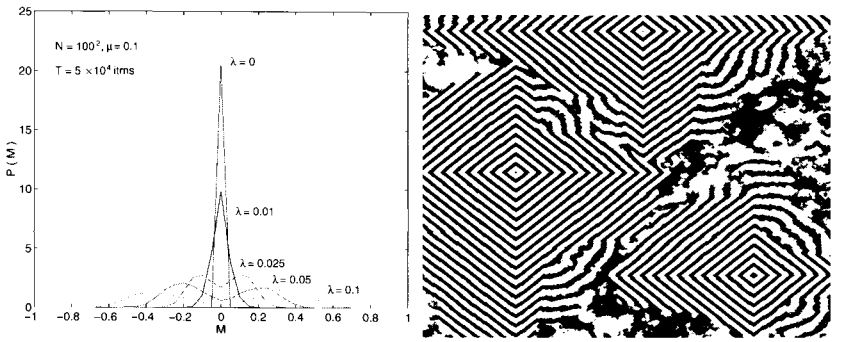


**Fig. 2.** (Left) Probability distribution of the collective choice $M$ at different values of the global feedback parameter $\lambda$. A phase transition from a bimodal to an unimodal distribution occurs as $\lambda \to 0$. The simulation results shown are for $100 \times 100$ agents interacting in a 2-D lattice for 50,000 iterations. The adaptation rate is $\mu = 0.1$. Compare with Fig. 1a in Ref. [1]. (Right) Spatial pattern in the choice behavior for $1000 \times 1000$ agents interacting in a square lattice after $10^5$ iterations with $\mu = 0.1$ and $\lambda = 0.05$.

In the presence of adaptation but absence of learning ($\mu > 0, \lambda = 0$), starting from an initial random distribution of choices and personal preferences, we observe only very small clusters of similar choice behavior and the average choice $M$ fluctuates around 0. In other words, at any given time equal number of agents have opposite choice preferences (on an average). Introduction of learning in the model ($\lambda > 0$) gives rise to significant clustering as well as a non-zero value for the collective choice $M$. We observe a phase transition of the probability distribution of $M$ from an unimodal to a bimodal form as a result of the competition between the adaptation and global feedback effects (Fig. 2 (left)).

The collective choice switches periodically between a positive value and a negative value, having an average residence time which diverges with $\lambda$ and with $N$. For instance, when $\lambda$ is very high relative to $\mu$, $M$ gets locked into one of two states (depending on the initial condition), corresponding to the majority preferring either one or the other choice. This is reminiscent of lock-in in certain economic systems subject to positive feedback [6]. The existence of long-range correlations in the choice of agents in the bimodal phase often results in striking spatial patterns such as vortices and spiral waves [Fig. 2 (right)] after long times. These patterns often show the existence of multiple domains, with the behavior of agents belonging to a particular domain being highly correlated and slaved to the choice behavior of an "opinion leader".

We have also introduced partial irrationality in the model by making the choice dynamics stochastic. Each agent may choose the same as or opposite to that of its neighbors if their overall decision exceeds its personal belief, according to a certain probability function with a parameter $\beta$ that is a measure of the degree of reliability that an agent assigns to the information it receives. For $\beta \to 0$, the agent ignores all information and essentially chooses randomly; in this case, expectedly, the distribution becomes unimodal. Under mean-field theory, one sees that the bimodal distribution occurs even for $\lambda = 0$ as $\beta \to \infty$; however, as $\beta$ is gradually decreased a phase transition to the unimodal distribution is observed.

## 4 Discussion and Summary

Our model seems to provide an explanation for the observed bimodality in a large number of social or economic phenomena, e.g., in the initial reception of movies, as shown in the distribution of the opening gross of movies released in theaters across the USA during the period 1997-2003 [3]. Bimodality in this context implies that movies either achieve significant success or are dismal box-office failures initially. We have considered the opening, rather than the total, gross for our analysis because the former characterizes the uncertainty faced by the moviegoer (agent) whether to see a newly released movie, when there is very little information available about its quality. Based on the model presented here, we conclude that, in such a situation the moviegoers' choice depends not only on their neighbors' choice about this movie, but also on how well previous action based on such neighborhood information agreed with

media reports and reviews of movies indicating the overall or community choice. Hence, the case of $\lambda > 0$, indicating the reliance of an individual agent on the aggregate information, imposes correlation among agent choice across the community which leads to bimodality in the opening gross distribution.

Our model also provides justification for the two-phase behavior observed in the financial markets wherein volume imbalance clearly shows a bimodal distribution beyond a critical threshold of local noise intensity [1]. In contrast to many current models, we have not assumed a priori existence of contrarian and trend-follower strategies among the agents [7]. Rather such behavior emerges naturally from the micro-dynamics of agents' choice behavior.

Similar behavior possibly underlies biphasic behavior in election results. The distribution of votes in a two-party election will show an unimodal pattern for elections where local issues are more important than the role of the mass media (hence $\lambda = 0$) and a bimodal distribution for elections where voters are more reliant on media coverage for individual-level voting cues ($\lambda > 0$).

One can also tailor marketing strategies to different segments of the population depending on the role that global feedback plays in their decisions. Products, whose consumers have $\lambda = 0$, can be better disseminated through distributing free samples in neighborhoods; while for $\lambda > 0$, a mass media campaign blitz will be more effective.

In summary, we have presented here a model of the emergence of collective choice through interactions between agents who are influenced by their personal preferences which change over time through processes akin to adaptation and learning. We find that introducing these effects produce a two-phase behavior, marked by an unimodal distribution and a bimodal distribution of the collective choice, respectively. Our model explains very well the observed two-phase behavior in markets, not only in the restricted context of financial markets, but also, in a wider context, movie income and election results.

## References


1. Plerou V, Gopikrishnan P, Stanley HE (2003) Two-phase behavior of financial markets, Nature 421: 130
2. Zheng B, Qiu T, Ren F (2004) Two-phase phenomena, minority games and herding models, Phys. Rev. E 69: 046115
3. Sinha S, Raghavendra S (2004) Hollywood blockbusters and long-tailed distributions: An empirical study of the popularity of movies, Eur. Phys. J. B 42: 293–296
4. Mayhew D (1974) Congressional elections: The case of the vanishing marginals, Polity 6: 295–317
5. Sinha S, Raghavendra S (2004) Phase transition and pattern formation in a model of collective choice dynamics, SFI Working Paper 04-09-028
6. Arthur W B (1989) Competing technologies, increasing returns and lock-in by historical events, Economic Journal 99: 106–131
7. Lux T (1995) Herd behaviour, bubbles and crashes, Economic Journal 105: 881–896

# Explanation of binarized tick data using investor sentiment and genetic learning

Takashi Yamada and Kazuhiro Ueda

Department of General Systems Studies, Graduate School of Arts and Sciences, University of Tokyo, 3-8-1 Komaba, Meguro-ku, Tokyo 153-8902, Japan.
tyamada@blake.c.u-tokyo.ac.jp ueda@gregorio.c.u-tokyo.ac.jp

**Summary.** This paper attempts to clarify some time series properties of binarized tick data by investor sentiment and genetic algorithm. For this purpose, first we explore the conditions for genetic algorithm to describe investor sentiment. Then we calculate auto-correlations and conditional probabilities using binarized sample paths generated by estimated models of investor sentiment. The most fitted parameter set of genetic algorithm have the following implications: First, a herd behavior is likely to emerge. Second, traders try to perceive brand-new information even if it is not completely correct.

**Key words:** investor sentiment, genetic learning, binarized time series

## 1 Introduction

The recent development of econophysics has enabled us to capture another time series properties of high frequency data. The main contributions of this aspect are to reveal some differences of time scales and to clarify some predictabilities of markets (e.g. [6, 10]). While spin lattice models or Ising models have successfully described some emergent phenomena (e.g. [3, 4]), but it is not clear what drives such features of high frequency data, since those models have not taken into account behaviors of market participants so much.

On the other hand, behavioral economics and agent-based computational economics (ACE) allow us to offer descriptive models about behaviors of investors or to replicate market dynamics. Among ACE models, genetic algorithm has been often used as a method of agents' learnings [1, 5, 11]. Besides, some studies have stated that there needs some models which incorporate behavioral economics into ACE models [9, 13].

We investigated whether genetic algorithm learning (hereafter GAL) with investor sentiment (A model of investor sentiment: hereafter MIS) [2] was able to reproduce actual tick data. For this purpose, we determined the conditions from the viewpoints of agents towards market which were obtained when some

series of typical asset-returns were given. Then we explored more plausible conditions by comparing time series properties between actual data and the generated sample paths using the estimated variables of MIS.

## 2 Description of MIS by GAL

The constitutions of MIS are twofold; First, a market is either in a stable state or in an unstable one. If the market is in a stable state, the probability $\pi_H$ that the price movement will be the same as the previous one is over 0.5. On the other hand, if the market is in an unstable condition, the probability $\pi_L$ is under 0.5. And the parameter $\lambda_1$ ($\lambda_2$) is the probability of transition from unstable (stable) state to stable (unstable) one. Second, the price movement in the economy is $+1$ or $-1$. Therefore $q_t$, the probability that the market is unstable, becomes to be higher in case that the asset return is different from the previous one, or to be lower otherwise[1].

In order to determine conditions requisite for GAL to describe MIS, we fed two kinds of price movements ($-+---++$ and $+-$) to agents with five binary bits (one of them was to judge a market condition, and others were to make a prediction).

The simulation was ran by altering parameters of genetic algorithm, i.e. crossover (0.6 or 0.8), mutation (0.01 or 0.05), learning frequency (LF) (every period or every 19-period), time horizon (last 1 or 19-period, or all periods), and fitness calculation[2]. We obtained the following conditions: First, the agents needed to know the market condition for their learnings. Second, the information used when the agents selected their parents must be up-to-date[3].

## 3 Relations between estimated MIS and binarized time series

To describe some features of binarized data, first we generated 100 sample paths, each consisted of 10000 periods, using estimated and other variables of MIS, and learning frequency used in the previous section. Price movements and the renewal of $q_t$ were determined by random number and those five variables in MIS respectively, i.e. (1) in case that the previous change was $+1$ and (2) otherwise:

[1] For more details, see [2].

[2] There are three types: (fa) An agent receives $+1$ if she predicts the asset return precisely. (fb) She receives $+1$ if she predicts the asset return and, at the same time, judges the market condition properly. (fc) She receives $+1$ if she judges only the market condition properly. While she receives $+3$ if her expectation is also right about the price movement.

[3] For more details, see [14].

**Table 1.** Auto-correlations of binarized data

| | $\lambda_1$ | $\lambda_2$ | $\pi_L$ | $\pi_H$ | Lag 1 | Lag 2 |
|---|---|---|---|---|---|---|
| GAL 1*1 | $5.09 \times 10^{-3}$ | $12.63 \times 10^{-3}$ | 0.406 | 0.509 | −0.129 | 0.025 |
| GAL 2*2 | $7.96 \times 10^{-3}$ | $10.06 \times 10^{-3}$ | 0.440 | 0.532 | −0.040 | 0.008 |
| GAL 3*3 | $6.50 \times 10^{-3}$ | $16.68 \times 10^{-3}$ | 0.403 | 0.501 | −0.135 | 0.021 |
| GAL 4*4 | $4.72 \times 10^{-3}$ | $5.53 \times 10^{-3}$ | 0.398 | 0.540 | −0.073 | 0.009 |
| Barberis [2] | $1.00 \times 10^{-1}$ | $3.00 \times 10^{-1}$ | 0.333 | 0.750 | −0.120 | 0.151 |
| Nikkei225 daily [7] | $1.00 \times 10^{-3}$ | $8.00 \times 10^{-3}$ | 0.310 | 0.690 | −0.174 | 0.047 |
| USD/JPY tick [12] | | | | | −0.350 | 0.050 |

*1: crossover: 0.8, mutation: 0.01, LF: every period, fitness: (fc)
*2: crossover: 0.6, mutation: 0.01, LF: every period, fitness: (fc)
*3: crossover: 0.8, mutation: 0.01, LF: every 19-period, fitness: (fc)
*4: crossover: 0.8, mutation: 0.05, LF: every 19-period, fitness: (fc)

$$\begin{cases} +1, & \text{if } rnd() < q_t\pi_L + (1-q_t)\pi_H \\ -1, & \text{otherwise} \end{cases} \tag{1}$$

$$\begin{cases} +1, & \text{if } rnd() < q_t(1-\pi_L) + (1-q_t)(1-\pi_H) \\ -1, & \text{otherwise} \end{cases} \tag{2}$$

where $rnd() \in (0,\ 1)$ is uniform random number. Then auto-correlations [12] and conditional probabilities [8] were calculated after eliciting the last 9000 periods from each of the generated sample paths.

First, we confirmed that each parameter of genetic algorithm, especially fitness calculation, influenced the first-order auto-correlation. If a parameter set was the one estimated by the fitness calculation (fb), the auto-correlation was nearly zero. On the other hand, the auto-correlation was around $-0.100$ in case that the fitness calculation was (fc) (Table 1). These results imply that traders try to perceive brand-new but not perfectly correct information.

Second, we found that the predictabilities hinged mostly on the learning frequencies and on the fitness calculations. Especially we can say the following implications with respect to the former parameter of genetic algorithm; The $q_t$ remained high in case that the learning interval was every 19-period (Fig. 1a). This means that since the over half investors considered the market to be unstable, a trend-following prediction could not be seen. On the other hand, the $q_t$ dropped to be under 0.5 in case of fast learning (Fig. 1b). Besides, speculators switched their recognition before a predictability situation emerged. As a consequence, a trend-following prediction dominated the market.

Finally, we show some results of other variables for comparison; The one is from [2] and the other is from [7] (Table 1 and Fig. 1c). From the most fitted parameter set, namely GAL 1, and the experimental ones, we draw some inferences as follows: First, a herd behavior is likely to emerge due to a high probability of crossover and a low probability of mutation. Second, speculators try to get brand-new information as soon as possible even if it is

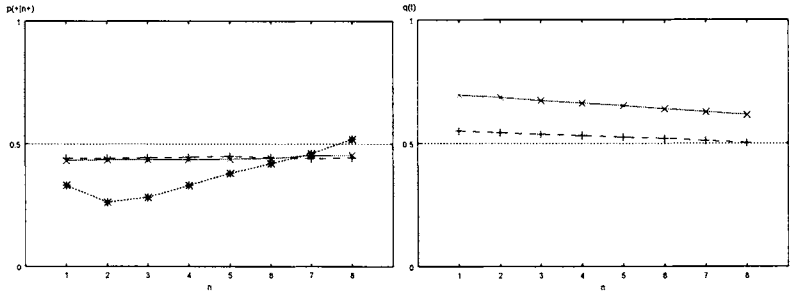

Solid line: GAL 3, Dashed line: GAL 4, Dotted line: USD/JPY tick data
a. Slow learning

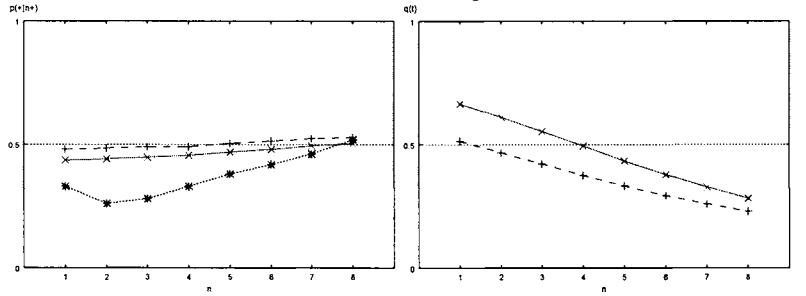

Solid line: GAL 1, Dashed line: GAL 2, Dotted line: USD/JPY
b. Fast learning

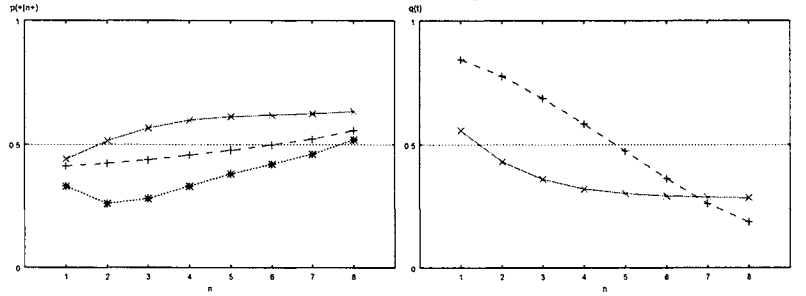

Solid line: Barberis et al., Dashed line: Nikkei225, Dotted line: USD/JPY
c. Practical application

**Fig. 1.** Differences of conditional probabilities (left panel) and $q_t$s (right panel)

not completely correct. Probably lower $\pi_L$ and higher $\pi_H$ will describe actual tick data more precisely.

## 4 Conclusion

This paper attempts to explain what drives time series properties of binarized tick data by investor sentiment and genetic algorithm. Our results imply that a herd behavior is likely to emerge and that speculators perceive brand-new information as soon as possible even if the information is not completely correct. For further research, we need to extend our model by altering parameters of genetic algorithm or by adding fundamentalists in order to distinguish between actual data and our results, or conduct other time series analyses.

## References


1. Arifovic J, Gençay R (2000) Statistical properties of genetic learning in a model of exchange rate. Journal of Economic Dynamics and Control 24:981–1005
2. Barberis N, Shleifer A, Vishny R (1998) A model of investor sentiment. Journal of Financial Economics 49:307–343
3. Chowdhury D, Stauffer D (1999) A generalized spin model of financial markets. European Physical Journal B 8:477–482
4. Cont R, Bouchaud J-P (2000) Herd behavior and aggregate fluctuations in financial markets. Macroeconomic Dynamics 4:170–196
5. LeBaron B (2000) Agent-based computational finance: suggested readings and early research. Journal of Economic Dynamics and Control 24:679–702
6. Liu Y, Gopikrishnan P, Cizeau P, Meyer M, Peng C-K, Stanley H E (1999) The statistical properties of the volatility of price fluctuations. Physical Reviews E 59:1390–1423
7. Miwa K, Ueda K (2005) The influence of investor's behavioral biases on the usefulness of the dual moving average crossovers. New Generation Computing 23:67–75
8. Mizuno T, Kurihara S, Takayasu M, Takayasu H (2003) Analysis of high-resolution foreign exchange data of USD-JPY for 13 years. Physica A 324:296–302
9. Nakamura S, Izumi K, Ueda K (2001) Jinkou-shijou to jikken-shijou no deai: mogi-trading jikken ni yoru atarashii agent-model no teishou (in Japanese). Operations Research 46:549–554
10. Ohira T, Sazuka N, Marumo K, Shimizu T, Takayasu M, Takayasu H (2003) Predictability of currency market exchange. Physica A 308:1–4
11. Riechmann T (2001) Genetic algorithm learning and evolutionary games. Journal of Economic Dynamics and Control 25:1019–1037
12. Sazuka N, Ohira T, Marumo K, Shimizu T, Takayasu M, Takayasu H (2003) A dynamical structure of high frequency currency exchange market. Physica A 324:366–371
13. Ueda K, Uchida Y, Izumi K, Ito Y (2004) How do expert dealers make profits and reduce the risk of loss in a foreign exchange market? Proceedings of 26th annual conference of the Cognitive Science Society, Chicago, USA, 1357–1362
14. Yamada T, Ueda K (2005) Can genetic algorithm learning represent investor sentiment? IEICE Transactions on Information and Systems, to appear

# A Game-theoretic Stochastic Agents Model for Enterprise Risk Management

Yuichi Ikeda, Shigeru Kawamoto, Osamu Kubo, Yasuhiro Kobayashi, and Chihiro Fukui
Hitachi Research Laboratory, Hitachi Ltd., Omika 7-1-1, Hitachi, Ibaraki 319-1292, Japan

**Summary.** A model of business scenario simulation is developed by applying game theory to the stochastic agents described by the Langevin equations for enterprise risk management (ERM). Business scenarios of computer-related industries are simulated using the developed model, and are compared with real market data. Economic capital was calculated based on the business scenario, as the most basic requisite of ERM.

**Key words.** Langevin equation, game theory, agent model, enterprise risk management

## 1. Introduction

Business scenario simulation is a crucial task for the decision-making of enterprise risk management (ERM) [1], in order to cope with an uncertain business environment, a business scenario simulation model, i.e. the game-theoretic stochastic agent [2, 3], was developed by applying game theory to the stochastic agents [4, 5] described by the Langevin equations in order to analyze uncertain business environments. In this paper, the business scenarios of computer-related industries, which consist of three industrial sectors, i.e. the large scale integrated circuit (LSI) sector, the personal computer (PC) sector, and the liquid crystal display (LCD) sector, were simulated using the game-theoretic stochastic agent model, and the results were compared with real market data. The importance of the herding behavior of firms was demonstrated to reproduce the formation and collapse of the bubble in the computer-related industry market in Japan during the late 90s. The economic capital of each sector was calculated, based on the business scenario, as the most basic requisite of ERM.

## 2. Game-theoretic Stochastic Agent Model

The revenue $R_i(t)$ $(i=1,\cdots,N)$ for the $i^{\text{th}}$ agent is described by the Langevin equation,

$$\frac{dR_i}{dt} = \sum_k D_i w_{ik} \delta(t-t_k) - \gamma_i R_i - \frac{\partial U}{\partial R_i} + \sigma_i \xi_i(t) + \eta(t) R_{c(i)}, \qquad (1)$$

where $\gamma_i$, $U$, $\sigma_i$, and $\xi_i$ are a friction coefficient, an interaction energy, volatility, and the Gaussian white noise, respectively. Rational decision-making of

the i[th] agent is made by the first term of the RHS of Eq. (1). $D_i w_{ik} = \pm D_i$ ( $k = 1, \cdots, K$ ) is the planned revenue of the i[th] agent. $w_{ik} = w_{ik}(PV_i)$ is a transition probability at a decision-making point in time $k$, and depends on the payoff $PV_i$ of the i[th] agent, which is the summed discounted cash flow over $l = t/\Delta t$ ,

$$PV_i = (1-T)\sum_l \{R_i(l\Delta t) - C_i(l\Delta t)\}/(1+r)^l , \qquad (2)$$

where $T$ is a tax rate. The cost $C_i$ is assumed to be linear and quadratic, proportional to the revenue, $C_i(t) = \alpha R_i(t) + \beta R_i(t)^2$ . The second term of the cost corresponds to the fact that larger firms are less efficient. A transition probability $w_{ik}$ , which corresponds to the Nash equilibrium, is evaluated using backward induction. The third term of the RHS of Eq. (1) represents an interaction acting on the i[th] agent, $\partial U/\partial R_i = \sum_{j \neq i}^{N} F_{ij}\left(R_i - R_j - \overline{R_i - R_j}\right)$, where $\overline{R_i - R_j}$ is the average difference of revenue between the i[th] agent and the j[th] agent. The last term of the RHS of Eq. (1) represents the irrational herding behavior. $\eta(t)$ and $c(i)$ are the time-varying strength of the herding behavior and the competitor of the i[th] agent, respectively. The time-varying strength of the herding behavior $\eta(t)$ is assumed to be externally given in this model.

## 3. Simulation

The market data for the LSI, PC, and LCD sectors among the computer-related industries in Japan were divided into three periods, i.e. (I) the normal period, (II) the bubble period, (III) the post-bubble period. The model parameters were calibrated in order to reproduce the market data of the computer-related industries during Period I as a Nash equilibrium [3]. Scenarios of revenues for Periods II and III were generated for the six-agents system, i.e. the LSI1 agent, the LSI2 agent, the PC1 agent, the PC2 agent, the LCD1 agent, and the LCD2 agent, using a Monte Carlo simulation according to Eq. (1). The time-varying strength of the herding behavior $\eta(t)$ was given as follows, $\eta(t) = +0.1$ for Period II and $\eta(t) = -0.1$ for Period III. The generated mean scenarios of revenues for Periods II and III are shown in Fig. 1 (a). Fig. 1 (a) shows that the bubble formation during Period II and the bubble collapse during Period III were reproduced fairly well for all sectors. It is, however, noted that the calculated revenue for the LCD sector was larger than the market data during Period III. The importance of the herding behavior of firms was demonstrated to reproduce the formation and collapse of the bubble in the computer-related industry market in Japan during the late 90s.

The revenue distributions of the PC sector at 2Q-01 are shown in Fig. 1 (b). One is for the Gaussian random number, and the other is for the power random number. The same standard deviation was used for both random numbers. The revenue distribution with the power random number has a fat tail.

The payoff distributions $PV_{PC}$, calculated using Eq. (2) for the Gaussian and the power random number, are shown in Fig. 1 (c) and (d), respectively. The economic capital, which is equal to the capital exposed to risk according to the Earning-at-Risk technique, was calculated as the most basic requisite of ERM. The calculated economic capitals were $6.05\times10^{9}$ JPY and $6.05\times10^{9}$ JPY for Fig. 1 (c) and (d), respectively.

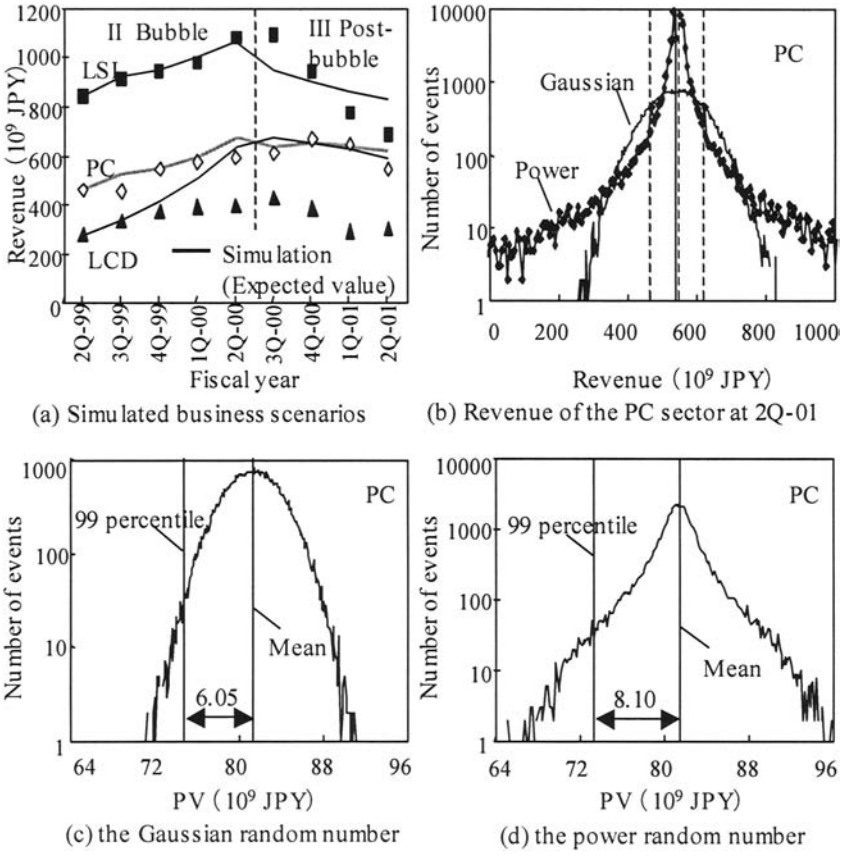


Fig. 1 Revenues for Periods II and III for the six-agents system with herding behavior are shown in Fig. 1 (a). The symbols are real market data. The revenue distribution of the PC sector at 2Q-01 is shown in Fig. 1 (b). The revenue distribution with the power random number has a fat tail. The payoffs with the Gaussian and the power random number are shown in Fig. 1 (c) and (d), respectively. The calculated economic capitals as the requisite of ERM were $6.05\times10^{9}$ JPY and $6.05\times10^{9}$ JPY for Fig. 1 (c) and (d), respectively.

## 4. Conclusions

Business scenario simulation is a crucial task for the decision-making of ERM, in order to cope with the uncertain business environment. A model of business scenario simulation was developed by applying game theory to the stochastic agents described by the Langevin equations for ERM. Business scenarios of computer-related industries were simulated using the developed model, and were compared with real market data. The importance of the herding behavior of firms was demonstrated to reproduce the formation and collapse of the bubble in the computer-related industry market in Japan during the late 1990s. The economic capital, which is equal to the capital exposed to risk according to the Earning-at-Risk technique, was calculated as the most basic requisite of ERM, and used for the obtained payoff distribution. An appropriate implementation of the model will be valuable to analyze the uncertain business environment and to provide feasible decision-making for ERM.

## References


1. The committee of sponsoring organizations of the Treadway commission, Enterprise Risk Management - Integrated Framework, the American Institute of Certified Public Accountants, 2004
2. Y. Ikeda et al., Forecast of Business Performance using an Agent-based Model and Its Application to a Decision Tree Monte Carlo Business Valuation, Physica A 344 (2004) 87-94
3. Y. Ikeda et al., Firm Dynamics Simulation using Game-theoretic Stochastic Agents, Workshop on Economics and Heterogeneous Interacting Agents, 2004, in press.
4. P. Richmond et al., Peer pressure and Generalized Lotoka Volterra models, Physica A 344 (2004) 344-348
5. W. Souma et al., Wealth Distribution in Scale-Free Networks, Meeting the Challenge of Social Problems via Agent-Based Simulation, T. Terano et al. (Eds.), Springer-Verlag Tokyo, 2003

# 4. Correlation and Risk Management

# Blackouts, risk, and fat-tailed distributions

Rafał Weron[1] and Ingve Simonsen[2]

[1] Hugo Steinhaus Center for Stochastic Methods,
Wrocław University of Technology, 50-370 Wrocław, Poland
[2] Department of Physics, NTNU, NO-7491 Trondheim, Norway

**Summary.** We analyze a 19-year time series of North American electric power transmission system blackouts. Contrary to previously reported results we find a fatter than exponential decay in the distribution of inter-occurrence times and evidence of seasonal dependence in the number of events. Our findings question the use of self-organized criticality, and in particular the sandpile model, as a paradigm of blackout dynamics in power transmission systems. Hopefully, though, they will provide guidelines to more accurate models for evaluation of blackout risk.

Electric power transmission networks are complex systems.[1] Due to economic factors, they are commonly run near their operational limits. Major cascading disturbances or blackouts of these transmission systems have serious consequences. Although, each blackout can be attributed to a particular cause: natural peril, equipment malfunction or human behavior, an exclusive focus on the causes of these events can overlook the global dynamics of a complex system. Instead, it might be interesting to study blackouts from a top-down perspective. Following Carreras *et al.* (2004) we analyze a time series of blackouts to explore the nature of these complex systems. However, despite the fact that we are using the same database we obtain different results. Consequently, we challenge their arguments that lead to modeling blackouts as a self-organized criticality (SOC) phenomenon (Bak *et al.*, 1987).

The reliability events — like the August 1996 blackout in Northwestern America that disconnected 30,390 MW of power to 7.5 million customers or the even more spectacular August 2003 blackout in Northeastern America that disconnected 61,800 MW of power to 50 million people — demonstrate that the necessary operating practices, regulatory policies, and technological tools for dealing with the changes are not yet in place to assure an acceptable level of reliability. In a restructured environment, prices are a matter of private choice, yet the reliability of the delivery system affects everyone.

[1] For a brief review of approaches to complex systems and cascading failure in power system blackouts see Dobson *et al.* (2004).

Naturally, the operation of the electric system is more difficult to coordinate in a competitive environment, where a much larger number of parties are participating. For example, in North America about one-half of all domestic generation is now sold over ever-increasing distances on the wholesale market before it is delivered to customers (Albert *et al.*, 2004). Consequently the power grid is witnessing power flows in unprecedented magnitudes and directions. Unfortunately, it seems that the development of reliability management reforms and operating procedures has lagged behind economic reforms in the power industry. In addition, responsibility for reliability management has been disaggregated to multiple institutions (Carrier *et al.*, 2000). All this results in an increase of the risk of blackouts, not only in North America, but also world-wide.

The Disturbance Analysis Working Group (DAWG) database[2] summarizes disturbances that have occurred in the electric systems in North America. The database is based on major electric utility system disturbances reported to the U.S. Department of Energy (DOE) and the North American Electrical Reliability Council (NERC). The data arise from government incident reporting requirements criteria detailed in DOE form EIA-417.

Carreras *et al.* (2004) analyzed the first 15 years of data (1984-1998) from the DAWG database. As currently four more years of data are available[3] we study two datasets: D98 covering the period 1984-1998 and D02 covering the full data set 1984-2002. The first one is used for comparison with the previous findings, while the second lets us extend the analysis and draw more up-to-date conclusions. The data are of diverse magnitude and of varying causes (including natural perils, human error, equipment malfunction, and sabotage). It is not clear how complete these data are, but it seems to be the best-documented source for blackouts in the North American power transmission system. Besides the date and the region of occurrence, two measures of the event's severity are given: the amount of power lost (in MW) and the number of customers affected.

There are 435 documented blackouts in the first 15 years (dataset D98), which gives on average 29 blackouts per year. A few events have missing data in one or both of the severity fields. For the analysis of blackout sizes we have used only those 427 occurrences which have complete data in both columns.[4] The average inter-occurrence time is 12.6 days, but the blackouts are distributed over the 15 years in a non-uniform manner with a maximum waiting time of 252 days between event origins. Furthermore, the mean and the maximum restoration times are 14 hours and 14 days, respectively, indicating

[2] Publicly available from http://www.nerc.com/~dawg/database.html.

[3] The delay in data distribution is due to the complexity of the problem. It can take months after a large blackout to dig through the records, establish the events occurring and reproduce a causal sequence of events.

[4] However, for the waiting time distribution analysis we have used all occurrences. A preprocessed, spreadsheet-ready ASCII format datafile is available from http://www.im.pwr.wroc.pl/~rweron/exchlink.html.

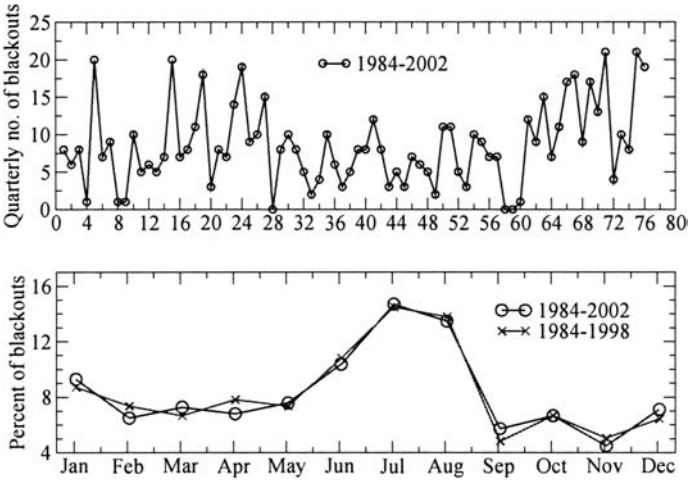


**Fig. 1.** The quarterly number of blackout events from 1984 till 2002 (top) and annual distribution of monthly events (bottom) for the North-American power grid.

that the inter-occurrence times are more or less equivalent to the quiet times (the lapses of time between the end of a blackout and the beginning of the next one).

In the full dataset (D02) there are 646 documented blackouts, yielding on average 34 blackouts per year. However, only 578 occurrences have complete severity data, since – especially in 1999 and 2000 – there are many missing values. The average period of time between blackouts is now only 10.7 days, indicating a recent increasing trend in the number of blackouts, while the mean and the maximum restoration times are slightly higher: 16 hours and 15 days, respectively.

Although the scarcity of data limits sound statistical inference, looking at the top panel of Fig. 1 we can intuitively divide the dataset into three parts: an initial period of relatively volatile activity (1984-1990; quarters 1-28), followed by a fairly calm period (1991-1998; quarters 29-60), and, most recently, a period of increasing activity (1999-2002; quarters 61-76). Whether this is a consequence of deregulation, different incident reporting procedures or simply randomness remains an open question. However, the seasonal behavior of the outages is indisputable. Roughly 30% of all blackouts take place in July and August, see the bottom panel of Fig. 1, regardless of the dataset analyzed. Our observations contradict earlier reports, where the authors detected no evidence of systematic changes in the number of blackouts or (quasi-)periodic behavior (Carreras *et al.*, 2004).

A closer inspection of the waiting times between blackouts reveals a non-trivial nature. The distribution does not have an exponential tail, as reported

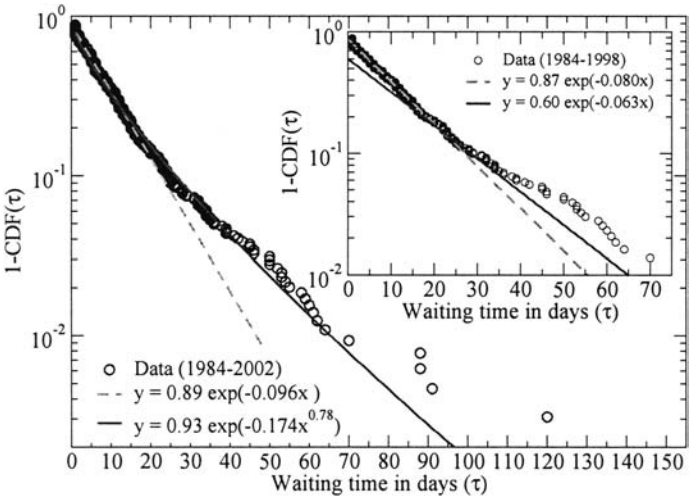


**Fig. 2.** The complementary cumulative distribution function $(1 - \mathrm{CDF}(\tau))$ of the waiting times $\tau$ (measured in days) between two consecutive blackout origins for the North-American power transmission system using the D02 (main panel) and D98 data sets (inset). The dashed lines represent exponential fits to the distributions. The solid lines correspond to a stretch exponential fit (main panel) and the exponential fit obtained by Carreras *et al.* (2004) using the same data set (inset).

e.g. by Chen *et al.* (2001), but rather a fatter one.[5] As can be seen in Fig. 2 the deviation is significant for both D98 and D02. These findings question the SOC-type approach to modeling blackout dynamics (Carreras *et al.*, 2004) since SOC-type dynamics should exhibit exponential decay in the waiting time distribution (Boffetta *et al.*, 1999, Carreras *et al.*, 2004).

It is apparent that large blackouts, as the mentioned earlier August 1996 and August 2003 events, are rarer than small blackouts. But how much rarer are they? Analysis of the D98 and D02 datasets shows that the complementary cumulative probability distribution of the blackout sizes does not decrease exponentially with the size of the outage, but rather has a power-law tail of exponent $\alpha = 1$, see Fig.3. Hence, if we evaluate the risk of a blackout as the product of its frequency and cost (commonly regarded to be proportional to unserved energy, see e.g. Billinton and Allan (1996)), then the total risk associated with the large blackouts is – due to the power-law type distribution of blackout sizes – much greater than the risk of small outages. This is strong motivation for investigating the global dynamics of series of blackouts that can lead to power-law tails. The investigated models, though, should take into account all or at least most of the characteristics revealed in this study.

[5] Waiting time distribution of high-frequency financial data show similar fatter-than exponential distributions (Scalas *et al.*, 2005).

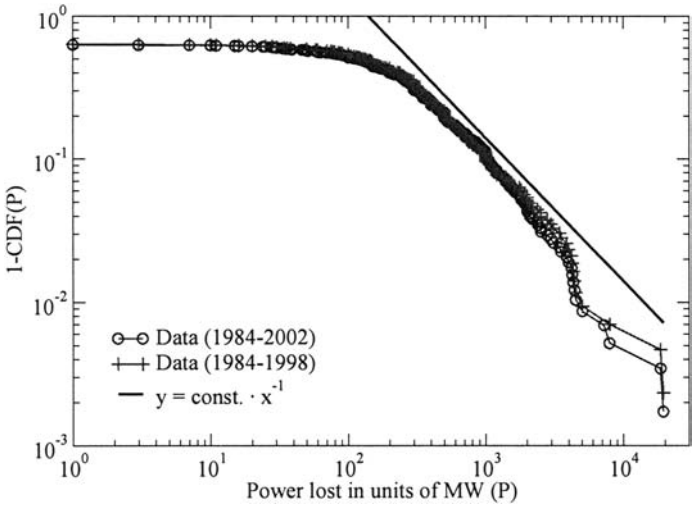


**Fig. 3.** The complimentary cumulative distribution (1 – CDF(P)) of power lost (P) due to blackouts for the North-American electric power transmission system.

## References


Albert, R., Albert, I., Nakarado, G.L. (2004) Structural vulnerability of the North American power grid. Phys. Rev. E 69, 025103(R).

Bak, P., Tang, C., Wiesenfeld, K. (1987) Self-organized criticality: an explanation of 1/f noise. Phys. Rev. Lett. 59, 381-384.

Billinton, R., Allan, R.N. (1996) Reliability evaluation of power systems, 2nd ed. Plenum Press, New York.

Boffetta, G., Carbone, V., Guliani, P., Veltri, P., Vulpiani, A. (1999) Power laws in solar flares: Self-organized criticality or turbulence? Phys. Rev. Lett. 83, 4662-4665.

Carreras, B.A., Newman, D.E., Dobson, I., Poole, A.B. (2004) Evidence for self-organized criticality in a time series of electric power system blackouts. IEEE Trans. Circuits and Systems 51(9), 1733-1740.

Carrier, P., *et al.* (2000) Findings from the summer of 1999. Interim Report of the U.S. Department of Energy's Power Outage Study Team.

Chen, J., Thorp, J.S., Parashar, M. (2001) Analysis of electric power system disturbance data. In: Proc. 34th Hawaii Int. Conf. on System Sciences, Maui.

Dobson, I., Carreras, B.A., Lynch, V., Newman, D.E. (2004) Complex systems analysis of series of blackouts: Cascading failure, criticality, and self-organization. Proc. Bulk Power System Dynamics & Control - VI, Cortina d'Ampezzo.

Scalas, E., Gorenflo, R., Luckock, H., Mainardi, F., Mantelli, M., Raberto, M. (2005) Anomalous waiting times in high-frequency financial data. Quantitative Finance, *in print.* See also: arXiv:cond-mat/0310305.

# Portfolio Selection in a Noisy Environment Using Absolute Deviation as a Risk Measure

Imre Kondor[1,2], Szilárd Pafka[1,3], Richárd Karádi[4] and Gábor Nagy[3]

[1]Department of Physics of Complex Systems, Eötvös University, Pázmány P. sétány 1/a, H–1117 Budapest, Hungary
[2]Collegium Budapest–Institute for Advanced Study, Szentháromság u. 2., H–1014 Budapest, Hungary
[3]Risk Management Department, CIB Bank, Medve u. 4–14., H–1027 Budapest, Hungary
[4]Finance and Accounting Department, Procter&Gamble Central Europe South, Váci út 35., H–1134 Budapest, Hungary

**Summary.** Portfolio selection has a central role in finance theory and practical applications. The classical approach uses the standard deviation as risk measure, but a couple of alternatives also exist in the literature. Due to its computational advantages, portfolio optimization based on absolute deviation looks particularly interesting and it is widely used in practice. For the practical implementation of any variant, however, one needs to estimate the parameters from finite return series, which inevitably introduces measurement noise that, in turn, affects portfolio selection. Although much research has been devoted to investigating the noise in the classical model, hardly any attention has been paid to the problem in the case of absolute deviation. In this paper, we study the effect of estimation noise in the case of absolute-deviation-based portfolio optimization. We show that the key parameter determining the effect of noise is the ratio of the length of time series to portfolio size and that, other things being equal, the effect of noise is higher than in the classical, variance-based model. This finding points to the importance of checking whether theoretically „better" portfolio selection models can indeed outperform the classical one in practice.

**Key words:** portfolio optimization, absolute deviation, estimation error

## Introduction

Starting with the seminal work of Markowitz (1952, 1959) the problem of portfolio selection has gained a central role in finance, both in theory and practical applications (see e.g. Elton and Gruber (1995) and the numerous references therein). Mean–variance portfolio selection along with the subsequently developed Capital Asset Pricing Model (CAPM) form the pillars of

modern investment theory and have led to important investment and risk management applications such as, for example, capital allocation or risk adjusted performance measurement.

However, it has been clear from the very outset that the practical implementation of the theory is less than straightforward. First, the input parameters in the optimization problem (expected returns and the covariance matrix) have to be determined from empirical data. Estimating „expected" returns is notoriously hard, but one is left with the task of estimating covariances even in those cases, where one attempts to minimize risk without any reference to expected returns (e.g. in several hedging problems or benchmark tracking). Covariance matrices of returns are usually estimated from financial time series. Since one has to estimate $O(N^2)$ covariance matrix elements ($N$ denotes the number of assets) from $NT$ datapoints ($T$ denotes the length of the time series), it is clear that, unless $T \gg N$ (which is usually not the case in practical applications), these estimates will contain considerable noise, which can in turn adversely affect the determination of the optimal portfolio. This was recognized very early in the literature and several procedures, for example factor models (see e.g. Elton and Gruber 1995) or Bayesian shrinkage estimators (e.g. Frost and Savarino 1986), have been introduced in order to reduce the estimation error. By decreasing the effective dimensionality of the problem, most of these techniques can achieve a significant reduction of noise.

Second, since mean–variance portfolio selection requires the minimization of a quadratic form (in the asset portfolio weights) subject to different constraints, it usually leads to a quadratic programming problem that needs to be solved numerically[1]. Although (thanks to spectacular advances in computing technology) this does not constitute an impassable barrier anymore, for large portfolios the practical implementation of the mean–variance portfolio selection framework can still require considerable resources and sometimes non-standard optimization techniques. It is, therefore, important to consider alternatives to the classical mean–variance optimization, preferably such that the idea of mean–risk optimization be preserved (with some other measure of risk, instead of the standard deviation).

One such portfolio optimization framework, based on absolute deviation as a risk measure, has been advanced by Konno and Yamazaki (1991). Here, the risk of a portfolio (of weights $w_i$) of $N$ assets with returns described by random variables $r_i$ of means $\mu_i$ is given by

$$\mathrm{E}\Big(\Big|\sum_i w_i(r_i - \mu_i)\Big|\Big), \tag{1}$$

where $\mathrm{E}(\cdot)$ denotes expected value and $i = 1, 2, \ldots, N$. In practice, one has to minimize (subject to different constraints) an *estimator* for this, based on a sample of finite time series:

[1] Except in the simple case when the only constraints are the budget constraint and the one on the expected returns, when the problem can be solved analytically.

$$\frac{1}{T}\sum_t \left|\sum_i w_i(r_{it}-\mu_i)\right| \tag{2}$$

where $r_{it}$ denotes the return on asset $i$ at time $t$ ($t = 1,2,\ldots,T$) and $\mu_i = \frac{1}{T}\sum_t r_{it}$. The main advantage of the above mean–absolute deviation portfolio optimization model is computational: as long as the accompanying constraints remain linear, the problem can be solved by linear programming, which requires significantly less computational effort than the classical, mean–variance optimization.

Due to its computational ease, mean–absolute deviation portfolio selection has gained important ground also in practice. For example, Algorithmics, a leader in risk management solutions, has built its portfolio optimization tool on absolute deviation as risk measure[2] (Dembo and Rosen 2000, Algorithmics 2002). Besides the usual mean–risk optimization, the software can be used to minimize risk without constraints on expected returns, providing solutions, for example, for benchmark tracking, portfolio compression or different hedging or pricing problems.

However, little attention has been paid to the estimation error in the mean–absolute deviation framework. Even if we only consider a situation where expected returns are irrelevant, there might be considerable noise stemming from the finiteness of the time series in Eq. (2). It is therefore important to know the magnitude of the effect of this noise on the selected portfolio.

Since very early, much research has focused on the estimation noise and the performance of different noise reduction techniques in the case of mean–variance optimization (e.g. Elton and Gruber 1973, Eun and Resnick 1984, Chan, Karceski and Lakonishok 1999). In contrast with the empirical approach in the literature, in an earlier paper (Pafka and Kondor 2002) we proposed a model/simulation–based approach. Making use of an appropriate metric for the effect of noise, we applied this framework to systematically investigate the effect of noise in the problem of variance-based risk minimization. We showed that the effect of noise depends essentially on the ratio $T/N$ of the length of the time series to the size of the portfolio (Pafka and Kondor 2003), and that, indeed, dimension reduction techniques can be very efficient in reducing this estimation noise (Pafka and Kondor 2004). However, (except Simaan 1997) we are not aware of a similar study of the effect of noise in mean–absolute deviation portfolio optimization.

In this paper we extend our earlier methodology to investigate the effect of noise in the risk minimization problem based on absolute deviation. Very much like in Simaan (1997), we find that noise can cause a significant error in the optimal portfolio and, for the same set of parameters, this error is higher than in the case of variance-based risk optimization. In addition, we identify the key factor determining the impact of noise in the mean–absolute deviation

[2] More precisely, the user can choose from different forms of absolute deviation (e.g. considering all or only the negative returns, respectively) or a form of „maximal loss" (which also leads to a linear programming problem).

framework and show that (for a wide choice of the random process generating the time series) the effect of noise depends essentially only on the ratio $T/N$ again, similarly to the case of variance minimization.

## Results and Discussion

For our present study we adapt the simplified portfolio optimization framework advanced by Pafka and Kondor (2003): the portfolio risk (estimator) $\frac{1}{T}\sum_t |\sum_i w_i r_{it}|$ is minimized under the budget constraint $\sum_i w_i = 1$, where $r_{it}$ represents (normally distributed) surrogate return series generated using various covariance structures. The „optimal" portfolio in the presence of noise is determined by solving the above minimization problem (which reduces to linear programming), while the „true" optimal portfolio is determined by solving the minimization of $\mathrm{E}\big(|\sum_i w_i r_i|\big)$ under the same budget constraint, which, for normally distributed returns, is equivalent to solving the corresponding variance minimization problem (Konno and Yamazaki (1991)). Using the same metric as in Pafka and Kondor (2002), we quantify the effect of noise by $q_0$, the ratio of the risk (in this case the absolute deviation) of the optimal portfolio in the presence of noise and the risk of the true optimal portfolio[3].

For different values of portfolio size $N$ and time series length $T$, and for different covariance structures $\sigma_{ij}^{(0)}$ (Pafka and Kondor 2004), we determined the effect of noise ($q_0$) using Monte Carlo simulations. The results are summarized in Fig. 1. It can be seen from the figure that for large sizes, the effect of noise depends essentially only on the ratio $T/N$ (for a large choice of the covariance structure of returns). Pafka and Kondor (2003) found a similar dependence in the classical variance-based case[4], also shown in the figure. Therefore the key factor determining the effect of noise in the absolute deviation based portfolio optimization is $T/N$, similarly to the classical variance-based case. Moreover, (in both cases) as $T$ approaches $N$ from above, $q_0$ diverges, anticipating the fact that for $T < N$ the optimization problem becomes degenerate (and meaningless from a practical point of view).

The other remarkable feature of the results presented in Fig. 1 is that for the same choice of input parameters the level of noise in absolute–deviation–based optimization is higher than in the classical case with standard deviation. An interesting (although not rigorous) explanation for this can be obtained

[3] We emphasize that by risk (of a portfolio of weights $w_i$) we mean $\mathrm{E}\big(|\sum_i w_i r_i|\big)$, which in the case of normally distributed returns is proportional to the standard deviation of $\sum_i w_i r_i$, i.e. to $\big(\sum_{ij} w_i \sigma_{ij}^{(0)} w_j\big)^{1/2}$, where $\sigma_{ij}^{(0)}$ is the covariance matrix used for generating the return series.

[4] In addition to simulation results, tools from random matrix theory allow one to derive a closed, analytical formula for $q_0$ in the $N \to \infty$ limit: $q_0 = 1/\sqrt{1 - N/T}$ (Pafka and Kondor 2003), which fits the simulation results already for $N \sim 50$.

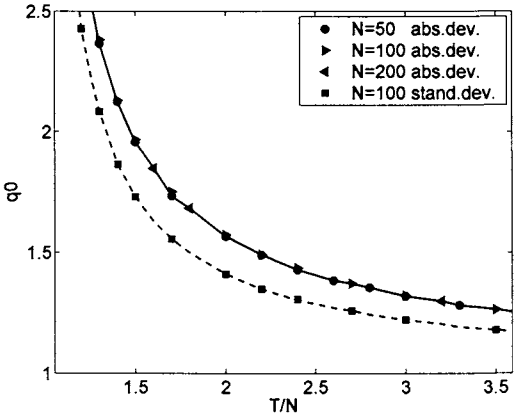


**Fig. 1.** $q_0$ as a function of $T/N$ for different $N$, $T$ and different covariance structures (solid line). For comparison, we also display the corresponding results for variance minimization (dashed line).

by considering the iso-risk level surfaces (in the space of portfolio weights) of standard and absolute deviation, respectively. If returns are, for example, independent, normally distributed, the „true" iso-risk surfaces of both standard and absolute deviation are ellipsoids. However, when risk must be estimated from finite return series, the iso-risk surfaces become „deformed" and, in general, a higher level of noise will cause more significant deformation. The deformation (relative to the ideal case) can be significant in both cases. However, while the iso–risk surfaces of standard deviation remain ellipses, those for absolute deviation become polygons (that go over into ellipses for infinitely long time series). Similarly, in higher dimensions we will have risk ellipsoids and risk polyhedra. The solution to the risk minimization problems is at the points where these level surfaces first touch the hyperplane of the budget constraint; in the case of absolute deviation this happens at one of the corners of the risk polyhedron. It is clear that the slightest change (due to noise) in the orientation of the risk polyhedron will cause the solution to jump to another corner, while a small reorientation of the ellipsoid corresponding to the variance will cause a smooth shift in the solution. This explains the enhanced sensitivity of the absolute deviation framework to noise. We can see then that „linearizing" the problem by using the absolute deviation for a risk measure comes not only with the computational advantage of linear programming, but also with the inevitable increase in instability and estimation noise.

## Conclusion

Due to its computational advantages, portfolio optimization based on absolute deviation as risk measure (instead of the standard deviation of the classical approach) has recently become wide–spread in practice. Although much research has focused on the effect of estimation noise in the classical (standard–deviation–based) problem, little attention has been paid to the case of absolute deviation. In this paper we have analyzed the effect of estimation noise in absolute–deviation–based portfolio optimization. We found that the level of noise can be significant and it is, in general, higher than in the case of standard–deviation–based optimization. This points to a possible trade off between computational advantage and noise level, which should be carefully analyzed whenever one chooses a risk measure for practical application.

## References


Algorithmics (2002) Scenario, risk/reward and risk/risk optimization. Technical report Algorithmics Inc.

Chan L, Karceski J, Lakonishok J (1999) On portfolio optimization: Forecasting covariances and choosing the risk model. Reviews of Financial Studies 12:937–974

Dembo R, Rosen D (2000) The practice of portfolio replication. Algo Research Quarterly 3(2):11–22

Elton E, Gruber M (1973) Estimating the dependence structure of share prices - Implications for portfolio selection. Journal of Finance 28:1203–1232

Elton E, Gruber M (1995) Modern portfolio theory and investment analysis. J Wiley and Sons

Eun C, Resnick B (1984) Estimating the correlation structure of international share prices. Journal of Finance 39:1311–1324

Frost P, Savarino J (1986) An empirical bayes approach to efficient portfolio selection. Journal of Financial and Quantitative Analysis 21:293–305

Konno H, Yamazaki H (1991) Mean-absolute deviation portfolio optimization model and its applications to Tokyo stock market. Management Science 37:519–531

Markowitz H (1952) Portfolio selection. Journal of Finance 7:77–91

Markowitz H (1959) Portfolio selection: Efficient diversification of investments. J Wiley and Sons

Pafka S, Kondor I (2002) Noisy covariance matrices and portfolio optimisation. European Physical Journal B 27:277–280

Pafka S, Kondor I (2003) Noisy covariance matrices and portfolio optimisation II. Physica A 319:487–494

Pafka S, Kondor I (2004) Estimated correlation matrices and portfolio optimization. Physica A 343:623–634

Simaan Y (1997) Estimation risk in portfolio selection: The mean variance model versus the mean absolute deviation model. Management Science 43:1437–1446

# Application of PCA and Random Matrix Theory to Passive Fund Management

Yoshi Fujiwara[1], Wataru Souma[1], Hideki Murasato[1], and Hiwon Yoon[2]

[1] ATR Network Informatics Laboratories, Kyoto 619-0288, Japan
yfujiwar@atr.jp, souma@atr.jp, h-mura@atr.jp
[2] CMD Research, Ltd., Nihonbashi 1-chome Bldg. 15F, Tokyo 103-0027, Japan
yoon@cmdr.co.jp

**Summary.** We use principal component analysis (PCA) for extracting principal components having larger-power in cross correlation from risky assets (Elton and Gruber 1973), and random matrix theory (RMT) for removing noise in the correlation and for choosing statistically significant components (Laloux et al 1999, Plerou et al 1999) in order to estimate expected correlation in portfolio optimization problem. In addition to correlation between every pairs of asset returns, the standard mean-variance model of optimal asset allocation requires estimation of expected return and risk for each assets. Asset allocation is, in practice, quite sensitive to how to estimate the expected return. We applied estimation based on "beta" (following the idea of Black and Litterman 1992) to portfolio optimization for 658 stocks in Tokyo Stock Exchange (TSE). By using daily returns in TSE and verifying that TSE has qualitatively similar principal components as NYSE (Plerou et al 1999), we show (i) that the error in estimation of correlation matrix via RMT is more stable and smaller than either historical, single-index model or constant-correlation model, (ii) that the realized risk-return in TSE based on our method outperforms that of index-fund with respect to Sharpe ratio, and (iii) that the optimization gives a practically reasonable asset allocation.

**Key words.** random matrix theory, cross correlation, portfolio optimization

In the standard of mean-variance paradigm (Elton et al 2003), portfolio optimization problem is to allocate a fraction $w_i$ of total asset to each risky asset $i$ by minimizing the variance $\sum_{ij} \rho_{ij}\sigma_i\sigma_j w_i w_j$ under the constraints (a) total return $\bar{r}_p = \bar{r}_i w_i$, (b) normalization $\sum_i w_i = 1$, and (c) some constraints such that $w_i > 0$ forbidding short-selling. Here $r_i$ is return of asset $i$, $\bar{r}_i$ is its expected value, $\sigma_i^2$ is expected variance of asset $i$, and $\rho_{ij}$ is correlation coefficient matrix (normalized such that $\rho_{ii} = 1$).

The optimization problem involves estimation of expected return $\bar{r}_i$, expected risk $\sigma_i$ and correlation of every pairs of assets $\rho_{ij}$. For practical appli-

cation of portfolio optimization, one has to overcome several problems. First, since the number of risky assets involved is typically hundreds or thousands, it is a formidable task for a practitioner to estimate every elements of correlation matrix. Although the cross correlation matrix has components of correlated movement of returns (Elton and Gruber 1973), one often assumes some simplification in the correlation matrix (Elton et al 1978). Several years ago, Laloux et al 1999 and Plerou et al 1999 independently applied random matrix theory to estimate a noise level appearing in the eigen-value spectrum of correlation matrix (see also Bouchaud and Potters 2000, Plerou et al 2002, Rosenow et al 2002). There have been some recent works (Ma et al 2004, Sharifi et al 2004, Utsugi et al 2004) for example. We have verified that TSE has qualitatively similar principal components as what had been found in other markets (see principal components in Fig. 4).

Second, when solving the optimization problem without constraint such as (c) above, one often gets large short positions in many assets. When one rules out short positions by constraint (c) and uses historical values for estimation of return $\bar{r}_i$, they frequently obtain "corner" solutions with zero weights in many assets, and at the same time, unreasonably large weights in a small number. This would invalidate the diversified portfolio itself (see Fig. 1). We employ the idea in solving these problems developed by Black and Litterman 1992, and use "beta" estimation of return $\bar{r}_i$, while we use historical values for estimation of risk $\sigma_i$ in solving the optimization. For estimation of correlation $\rho_{ij}$, we use RMT-denoised historical correlation as done in Plerou et al 2002.

We show that this approach of denoising by RMT and "beta" estimation of return can be used for passive fund management, in which a portfolio needs to track market index. The result outperforms return and decreasing risk by diversification into a smaller number of assets, rather than by investment into all the assets. Specifically, by using TSE daily returns for 658 stocks, we show (i) that the error in estimation of correlation matrix via RMT is more stable and smaller than that for historical values, single-index model and constant correlation model (Fig. 2), (ii) that the realized risk-return in TSE based on our method outperforms that of index-fund (Fig. 3), and (iii) that the optimization gives a practically reasonable (not "non-sense" as what one gets by using historical returns) asset allocation (Fig. 1).

We developed a prototype of software which does the PCA and RMT analysis, then denoising, calculates efficient frontier, and tests out-of-sample data. Visualization of principal components with firm sectors, and correlation structure by classic methods including multi-dimensional scaling and clustering-dendrogram analysis can be done in the software (Fig. 4 lower-panel).

**acknowledgement** This research was selected as one of the 2003 Exploratory Software Projects by IPA (Information-technology Promotion Agency). We would like to thank the project manager, Nobukuni Kino, for encouragement. This research was supported in part by the National Institute of Information and Communications Technology.

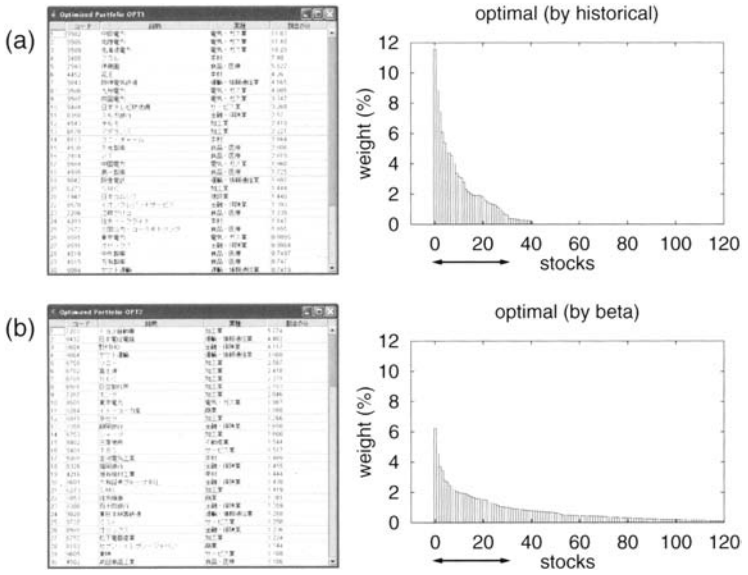


**Fig. 1.** (a) Optimal portfolio for 658 stocks in TSE, obtained by using historical values for expected return $\bar{r}_i$. The right plot is its weights $w_i$, and the left list is the names of stocks with the highest 30 weights. The list mainly includes electric-power, local railway companies etc. of little practical interest. (b) The same plot and list obtained by using historical beta $\beta_i$ for expected return $\bar{r}_i = \beta_i r_m$ where $r_m$ is historical market-index return. The list includes majors such as Toyota, NTT, Sony, Fujitsu, NEC, Hitachi, Honda, Sharp, Matsushita, Takeda etc. Both for (a) and (b), historical value of $\sigma_i$ and RMT-denoised correlation matrix $\rho_{ij}$ are used with past period being 750 days.

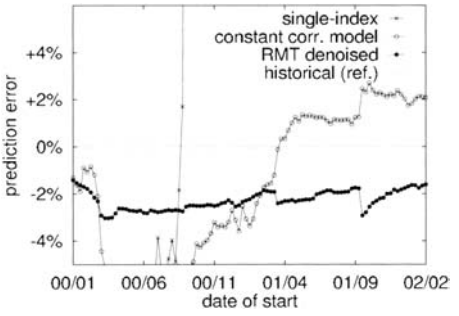


**Fig. 2.** Prediction error in correlation coefficient $\rho_{ij}$. One year for correlation calculation. The prediction error is defined as follows: take the quantity $|\rho_{ij}(\text{realized}) - \rho_{ij}(\text{predicted})|$ averaged over all pairs $(i, j)$, and calculate fractional error compared with that for simple-minded historical-value prediction. The x-axis is beginning date of one-year (starting from Jan 2000 to Feb 2002). Single-index and historical correlation model (Elton et al 1978) are compared with RMT-denoised result.

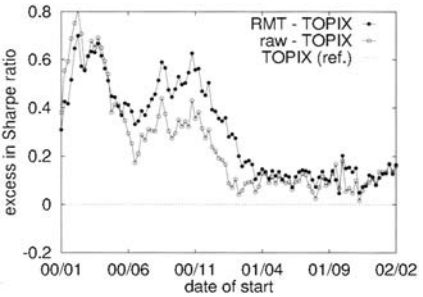


**Fig. 3.** The portfolio optimization in Fig. 1 (b) is used to measure the performance of portfolio for 1-year "buy-and-hold" passive fund management. The performance is measured by Sharpe ratio in the 1-year period. Horizontal dotted-line corresponds to the Sharpe ratio of TOPIX, with respect to which the result of raw correlation (open circles) and that of RMT-denoised correlation (filled circles) are compared. RMT outperforms others almost all the period from Jan 2000 to Feb 2002.

## References


1. Black F, Litterman R (1992) Global portfolio optimization. Financial Analysts Journal Sep-Oct:28–43
2. Bouchaud JP, Potters M (2000) Theory of Financial Risk. Cambridge University, Cambridge
3. Elton EJ, Gruber MJ, Brown SJ, Goetzmann WN (2003) Modern Portfolio Theory and Investment Analysis, sixth ed. John Wiley & Sons, New York
4. Elton EJ, Gruber MJ (1973) Estimating the dependence structure of share prices — implications for portfolio selection. J Finance 28:1203–1232
5. Elton EJ, Gruber MJ, Urich TJ (1978) "Are betas best?". J Finance 33:1375–1384
6. Laloux L, Cizeau P, Bouchaud JP, Potters M (1999) Noise dressing of financial correlation matrices. Phys Rev Lett 83:1467–1470
7. Ma WJ, Hu CK, Amritkar RE (2004) Stochastic dynamical model for stock-stock correlation. Phys Rev E 70:026101
8. Plerou V, Gopikrishnan P, Rosenow B, Amaral LAN, Guhr T, Stanley HE Universal and nonuniversal properties of cross correlations in financial time series. Phys Rev Lett 83:1471–1474
9. Plerou V, Gopikrishnan P, Rosenow B, Amaral LAN, Guhr T, Stanley HE (2002) Random matrix approach to cross correlations in financial data. Phys Rev E 65:066126
10. Rosenow B, Plerou V, Gopikrishnan P, Stanley HE (2002) Portfolio optimization and the random magnet problem. Eur Phys Lett 59:500–506
11. Sharifi S, Crane M, Shamaie A, Ruskin H (2004) Random matrix theory for portfolio optimization: a stability approach. Physica A 335:629–643
12. Utsugi A, Ino K, Oshikawa M (2004) Random matrix theory analysis of cross correlations in financial markets. Phys Rev E 70:026110

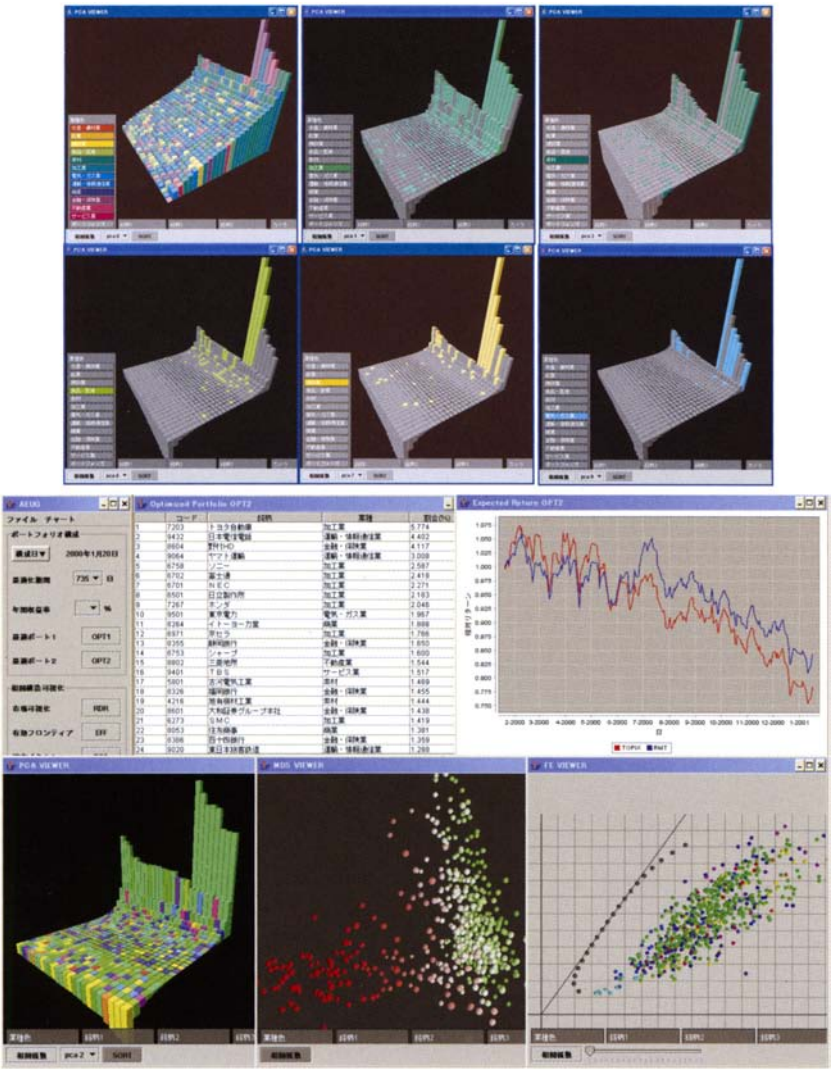

**Fig. 4.** *Upper panel:* Principal component with large eigen-values. Each column represent the contribution of each stock to the component. The color of column represents business-sector which the stock belongs to. Top left corresponds to the largest eigen-value. The others corresponds industrial processing, material industries, pharmaceutical/bio-technologies, construction, and electricity/power. *Lower panel:* A prototype of software for analysis of PCA and RMT, denoising, calculation of efficient frontier (bottom right), weights in the optimal portfolio with Sharpe ratio maximum (top middle), tests out-of-sample data (top right), visualize principal components (bottom left) as well as multi-dimensional scaling (bottom middle).

# Testing Methods to Reduce Noise in Financial Correlation Matrices

Per-Johan Andersson, Andreas Öberg and Thomas Guhr

Matematisk Fysik, LTH, Lunds Universitet, Sweden thomas.guhr@matfys.lth.se

Noise dressing of financial correlation matrices leads to spectral properties which have much in common with those of purely random matrices. Efficient noise reduction methods are needed. We study two such methods which have been proposed recently. The first method, the *filtering*, is based on a principal component analysis. The second method, the *power mapping*, is a shrinkage approach. Due to the definition of the correlation matrix itself, the optimal shrinkage parameter is uniquely determined. Hence, *filtering* and *power mapping* are conceptually different methods. We apply the two methods to Swedish and US market data.

## 1 Introduction

The noise dressing of financial correlation matrices was revealed and clearly demonstrated for empirical data in Refs. [1, 2]. The spectral properties of financial correlation matrices are compatible with those of purely random matrices. A major reason for the presence of noise is the finiteness of the time series used to calculate the correlation matrix elements. Obviously, this issue is important for any kind of risk management involving correlations, particularly for portfolio optimization. Various authors addressed this problem and suggested methods to reduce the noise. Here we focus on two methods: the *filtering*, put forward in Refs. [3, 4], and the *power mapping*, developed in Ref. [5]. Reference to other approaches is given in the paper [5]. These proceedings contain further contributions dealing with noise dressing and noise reduction. More references can also be found there.

The filtering method relies on the observation that the spectral density, i.e. the probability density function of finding an eigenvalue at a certain position, consists of, first, a generic *bulk part* which is well described by the analytically known spectral density for random matrices and, second, a part reflecting the *industrial branches* [3, 4]. Thus, only the information in the latter is directly usable, while the information in the former is buried under

noise. To remove the noise one proceeds as follows. The financial correlation matrix for $K$ companies or, more generally, risk factors, is diagonalized, yielding the eigenvalues $\lambda_k$, $k = 1, \ldots, K$. A fit to the random matrix spectral density gives a cut–off eigenvalue $\lambda_c$ such that the eigenvalues below $\lambda_c$ represent the bulk. The whole set of eigenvalues $(\lambda_1, \ldots, \lambda_c, \lambda_{c+1}, \ldots, \lambda_K)$ is then replaced by the filtered set $(0, \ldots, 0, \lambda_{c+1}, \ldots, \lambda_K)$ where the remaining larger eigenvalues can be associated with industrial branches. These eigenvalues are reexpressed in the original basis which gives the filtered correlation matrix, comprising the desired information.

The filtering has been proven to be very successful. Nevertheless, it is always good to have an alternative method. If the dimension $K$ of the correlation matrix is relatively small, the random matrix properties are not developed so well making the cut–off $\lambda_c$ ambiguous. Moreover, if some branches are small, the corresponding eigenvalues are small and can even be smaller than the cut–off such that the filtering would remove relevant information. The power mapping proposed in Ref. [5] is such an alternative method. It does not use any random matrix input and it is thus parameter free.

## 2 Power Mapping

The elements $C_{kl}$ of the correlation matrix $C$ are scalar products of the properly normalized time series for companies $k$ and $l$. Hence, each element contains the information about the length of the time series. We mention in passing the close formal connection to *chirality* encountered when studying the spectra of the Dirac operator, see Refs. [4, 5]. Remarkably, this can be used to map the correlation matrix $C$ via the power mapping

$$C_{kl} \quad \longrightarrow \quad \mathrm{sign}\,(C_{kl})\,|C_{kl}|^q \;=\; C_{kl}^{(q)} \tag{1}$$

onto another correlation matrix $C^{(q)}$ in which the noise–dressed information is partly recovered [5]. The optimal power $q \approx 1.5$ is automatically determined by the very definition and normalization of the correlation matrix. The effect is illustrated in Fig. 1 for the bulk part of the spectral density. These correlation matrices were generated from a one–factor–model. Two peaks emerge due to the power mapping, the left one stems from the true correlations, while the right one is produced by remainders of the noise. This clearly shows that even the information in the bulk can partly be reconstructed. The power mapping can be viewed as an "artificial prolongation" of the time series. A heuristic explanation: Some elements $C_{kl}$ comprise a *true* part $u$, say, and a *noisy* part $v$ which scales with $1/\sqrt{T}$ where $T$ is the length of the time series. Purely noisy elements lack the true part. The power mapping yields

$$\begin{aligned} \left(u + \frac{v}{\sqrt{T}}\right)^q &= u^q + q\frac{u^{q-1}v}{\sqrt{T}} + \mathcal{O}\left(\frac{1}{T}\right) \\ \left(\frac{v}{\sqrt{T}}\right)^q &= \frac{v^q}{T^{q/2}}\,. \end{aligned} \tag{2}$$

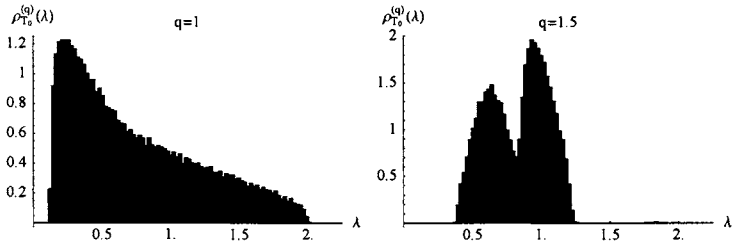


**Fig. 1.** Bulk part of the spectral density for synthetic correlation matrices, before (left) and after (right) the power mapping. Taken from Ref. [5]

Thus, the elements which only contain noise are stronger suppressed than those with a true part, if $q > 1$. The larger eigenvalues associated with the industrial branches are little affected. The power mapped correlation matrices $C^{(q)}$ are used as they stand instead of the original ones for risk management.

## 3 Application to Market Data

### 3.1 Observables and Data

We apply both noise reduction methods to portfolio optimization, using the standard Markowitz theory. We calculate the correlation matrices for our empirical data by sampling over a certain (longer) period, reduce the noise and then evaluate the portfolio over a certain (shorter) period with the noise reduced correlation matrices. As historical data are employed, we can compare, at the end of the evaluation period, risk and return involving the correlation matrices without noise reduction (simply referred to as *sample*) with risk and return after noise reduction has been applied. To obtain some statistical significance, the lengths of sample and evaluation period is chosen in such a way that the latter can be moved through the available data, allowing for several repetitions. We have two data sets: (i) daily Swedish stock returns [6] for 197 companies from July 12th, 1999, to July 18th, 2003, sampling period one year, evaluation period one week, and (ii) monthly US portfolio returns [7] for 48 branches from January 1973 to December 2002, sampling period five years, evaluation period one year.

### 3.2 Results

We set the expected return to 0.3% per week and work out the daily risk and the monthly return as functions of time. In a first study, we impose no constraints in the optimization procedure, the results are shown in Fig. 2. The yearly actual risk which amounts to 20.7% without noise reduction is considerably lowered by the noise reduction, we find 11.3% for power mapping

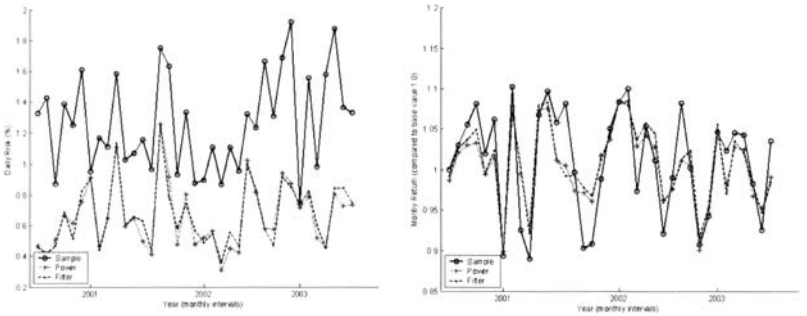

**Fig. 2.** Daily risk (left) and and monthly return (right) for the Swedish market data, no constraints imposed: no noise reduction, i.e. plain sample (circles), power mapping (crosses) and filtering (dashes).

and 11.4% for filtering. Although statements about the return are, in general, less meaningful in such a study, we believe that they are still of interest as relative information, when comparing the results for the two noise reduction methods. The yearly actual return is 11.1% without noise reduction and is given by 5.0% and 10.5% for power mapping and filtering, respectively. Thus both methods reduce the risk very efficiently, but the filtering seems to do better for the return. In a second study, we impose the constraint that no short selling is allowed. The outcome which is quite different is displayed in Fig. 3. The yearly actual risk of 10.1% without noise reduction is only

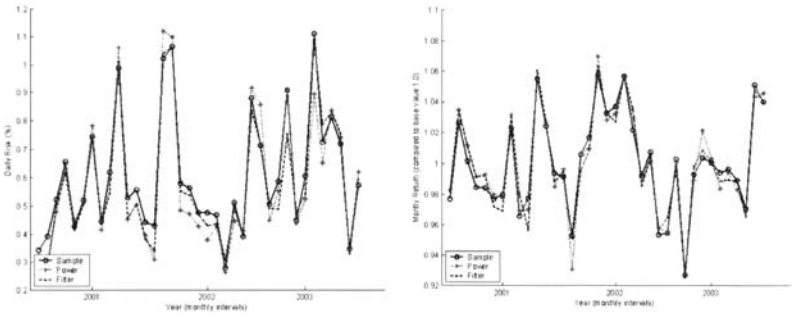

**Fig. 3.** Daily risk (left) and and monthly return (right) for the Swedish market data, no short selling allowed: no noise reduction, i.e. plain sample (circles), power mapping (crosses) and filtering (dashes).

very slightly lowered to 9.9% for both noise reduction methods. The yearly actual return is 0.5% without noise reduction and is improved to 1.1% for power mapping and 0.7% for filtering. In spite of the caveat applying to the

evaluation of returns in this context, we find it interesting that the power mapping in this case seems to perform better than the filtering.

The striking difference between the studies without and with constraints becomes understandable when looking at the fractions of wealth invested in the individual companies, which are the result of the optimization procedure. Without constraints, the fractions scatter almost symmetrically around zero implying that there are many negative fractions. Thus, short selling is very important to achieve the optimal portfolio. When short selling is forbidden, all weights must be positive. Apparently, the power mapping handle this situation well by yielding diversification with less fluctuations than filtering.

The results for the US portfolio returns are qualitatively the same. This is remarkable, because the correlation structure changes over the period of almost thirty years — which was our main motivation to study these data. It is also surprising that the filtering works well: as the dimension $K = 48$ is so small, basically only one eigenvalue survives the filtering, representing the entire market.

## 4 Conclusions

As the two noise reduction methods are conceptually different, they also produce different results. Our preliminary studies cannot serve as a basis to make schematic suggestions as to which method ought to be preferred in which situation. This will always be difficult. But further and systematic studies extending the ones presented here might yield some guidelines.

## References


1. Laloux L, Cizeau P, Bouchaud JP, Potters M (1999), Noise Dressing of Financial Correlation Matrices, Phys. Rev. Lett. 83:1467–1470
2. Plerou V, Gopikrishnan P, Rosenow B, Amaral LAN, Stanley HE (1999), Universal and Nonuniversal Properties of Cross-Correlations in Financial Time Series, Phys. Rev. Lett. 83:1471–1474
3. Gopikrishnan P, Rosenow B, Plerou V, Stanley HE (2001), Quantifying and Interpreting Collective Behavior in Financial Markets, Phys. Rev. E64:035106(R)
4. Plerou V, Gopikrishnan P, Rosenow B, Amaral LAN, Guhr T, Stanley HE (2002), A Random Matrix Approach to Cross-Correlations in Financial Data, Phys. Rev. E65:066126
5. Guhr T, Kälber B (2003), A New Method to Estimate the Noise in Financial Correlation Matrices, J. Phys. A36:3009–3032
6. `www.stockholmsborsen.se` (2003), web download
7. Fama E, French K (2003), web download

# Application of noise level estimation for portfolio optimization

Krzysztof Urbanowicz[1] and Janusz A. Hołyst[2]

[1] Max Planck Institute for the Physics of Complex Systems, Nöthnitzer Str. 38, D–01187 Dresden, Germany
urbanow@pks.mpg.de;http://www.chaosandnoise.org
[2] Faculty of Physics and Center of Excellence for Complex Systems Research Warsaw University of Technology
Koszykowa 75, PL–00-662 Warsaw, Poland
jholyst@if.pw.edu.pl

**Summary.** Time changes of noise level at Warsaw Stock Market are analyzed using a recently developed method basing on properties of the coarse grained entropy. The condition of the minimal noise level is used to build an efficient portfolio. Our noise level approach seems to be a much better tool for risk estimations than standard volatility parameters. Implementation of a corresponding threshold investment strategy gives positive returns for historical data.

*pacs 05.45.Tp,89.65.Gh*
*keywords: Noise level estimation, stock market data, time series, portfolio diversification*

## 1 Introduction

Although it is a common believe that the stock market behaviour is driven by stochastic processes [1, 2, 3] it is difficult to separate stochastic and deterministic components of market dynamics. In fact the deterministic fraction follows usually from nonlinear effects and can possess a non-periodic or even chaotic characteristics [4, 5]. The aim of this paper is to study the level of stochasticity in time series coming from stock market. We will show that our noise level analysis can be useful for portfolio optimization.

We employ here a method of noise-level estimation that has been described in details in [6]. The method is quite universal and it is valid even for high noise levels. The method makes use of a functional dependence of coarse-grained correlation entropy $K_2(\varepsilon)$ [7] on the threshold parameter $\varepsilon$. Since the function $K_2(\varepsilon)$ depends in a characteristic way on the noise standard deviation $\sigma$ thus $\sigma$ can be found from a shape of $K_2(\varepsilon)$. The validity of our method has

been verified by applying it for the noise level estimation in several chaotic models [7] and for the Chua electronic circuit contaminated by noise. The method distinguishes a noise appearing due to the presence of a stochastic process from a non-periodic *deterministic* behaviour (including the deterministic chaos). Analytic calculations justifying our method have been developed for the gaussian noise added to the observed deterministic variable. It has been also checked by numerical experiments that the method works properly for a uniform noise distribution and at least for some models with a dynamical noise corresponding to the Langevine equation [6]. The method has been already successfully applied for noise level calculations of engine process [8] and has given similar results to an approach basing on neighboring distances in Takens space [9].

## 2 Choosing low noise portfolio

In the present paper we define the noise level as the ratio of standard deviation of estimated noise $\sigma$ to the standard deviation of data $\sigma_{data}$

$$NTS = \frac{\sigma}{\sigma_{data}} \tag{1}$$

In the first step we construct a portfolio from $M$ stocks with the minimal value of the stochastic variable [10]. We assume that one can do this by maximization of the following quantity:

$$\mathcal{B} = \sum_{i=1}^{M} \sum_{j=1}^{M} p_i p_j \frac{\sigma_{i,D}}{\sigma_i} \frac{\sigma_{j,D}}{\sigma_j} \rho_{i,j} = max \tag{2}$$

where $\sigma_{i,D}$ is the standard deviation of deterministic part of the stock $i$, $\sigma_i$ is the standard deviation of the noise for this stock and $\rho_{i,j}$ is the correlation coefficient between deterministic parts of stocks $i$ and $j$. The maximal value of $\mathcal{B}$ can be received with the help of the steepest descent method by changing variables $p_i$ and keeping the normalization constraint $\sum_{i=1}^{M} p_i = 1$.

In some cases for practical reasons it is more efficient not to minimize the noise level in the portfolio but to maximize it. This is because the method for noise level estimation can fail and it can occasionally give wrong values of $NTS$. When we minimize the noise level it can happen that one stock with an artificially very low noise level dominates the whole portfolio and the risk increases without any additional profit.

## 3 Investment method

In our investment method we make use of additional information, available due to the knowledge of the noise level, to increase profits from selected portfolios. The simplest approach is to introduce a threshold for a noise level. We

divide all portfolios into two classes: profitable and nonprofitable taking into account high or low values of the noise level and a positive or a negative past trend. The partition into high/low noise classes is based on the threshold parameter $NTS_{th}$ that should be optimized. Additionally we label portfolio by calculations of an average return for the last $N_{win}$ data. We use the following algorithm: if the past trend from $N_{win}$ data of the portfolio is positive $m_p > 0$ and the noise level of the portfolio is small ($NTS_p < NTS_{th}$) we consider the portfolio as a profitable. We have a profitable portfolio also when it is more stochastic ($NTS_p > NTS_{th}$) but its trend is negative $m_p < 0$. In the remaining two cases we consider the portfolio as a nonprofitable. In such a way we create the basic strategy giving $\{p_i\}$, which involves the information on the noise level and the past trend in the portfolio selection. This basic strategy should then be adjusted using a *risk parameter* $\mathbf{r}$ that is introduced below. The process of the final portfolio selection is based on the comparison of the optimized portfolio to the simplest portfolio consisting of equal contributions from all stocks ($p_i = 1/M$, $i = 1, ..., M$). We set up a composition of the final portfolio $\{\tilde{p}_i\}$ with a use of certain risk parameter $\mathbf{r}$ on the preliminary optimized portfolio $\{p_i\}$ as follows:

$$\tilde{p}_i = \frac{1}{M} + \mathbf{r}\left(p_i - \frac{1}{M}\right) \tag{3}$$

One should mention that for a negative value of the parameter $\mathbf{r}$ we have the opposite investing to the composition $p_i$.

At Fig. 1 the level of success of our investment method as a function of the parameter $NTS_{th}$ is shown. Here the percent of success corresponds to a fraction of positive returns from our strategy. We have used a negative risk parameter $\mathbf{r} = -10$ to get a positive profit for small values of $NTS_{th}$: $NTS_{th} < 0.85$ in the above simulations. A similar dependence on the parameter $N_{win}$ is shown at Fig. 2. The percent of the success in both cases is above 50% and for some regions of selected parameters the strategy brings positive returns after commissions deduction.

It is clear that to use our approach we have to find optimal threshold parameters $NTS_{th}$ and $N_{win}$. Our optimization method is quite straightforward and it resembles a genetic algorithm. During the optimization process we change the selection probability for actual values of optimized parameters i.e. we increase the probability if the profit from portfolio is positive and we decrease in the opposite case. The optimization process is terminated when we reach a satisfactory mean value of a yearly profit from past data (here it is 30%). In such a way we optimize simultaneously two parameters $N_{win}$ and $NTS_{th}$.

We begin our algorithm by generating randomly chosen stocks in the initial portfolio. Then we randomly select a starting moment for our virtual investment. The next step is to optimize the parameters $N_{win}$ and $NTS_{th}$ using available data from the period prior to the selected starting point. Finally we invest in the portfolio described by the risk value $\mathbf{r} = -3$ (see Eq. 3). The

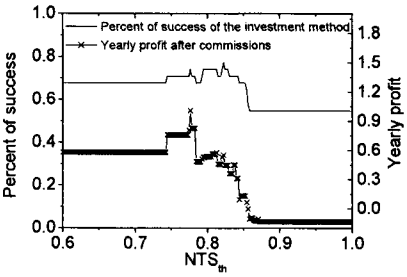


**Fig. 1.** Plot of the investment success as a function of parameter $NTS_{th}$ in the period of January - July 2003 at the Warsaw Stock Exchange ($N_{win}$ = 2500). Portfolio consists of 18 stocks from WSE.

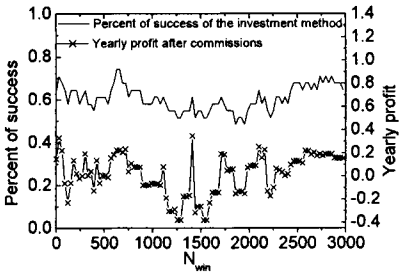


**Fig. 2.** Plot of the investment success as a function of parameter $N_{win}$ in the period of January - July 2003 at Warsaw Stock Exchange ($NTS_{th}$ = 0.85). Portfolio consists of 18 stocks from WSE.

procedure was repeated 10000 times and at the end we calculated an average profit i.e. the efficiency of the method. At Fig. 3 we show a distribution of returns for our portfolio at Warsaw Stock Exchange. We have calculated recommendations for windows $17 - 41$ days long on the period July 2002 - December 2003 (see Fig. 4). The annual return received in such a way after commissions substracting is around 56% (the commission level has been set to 0.25%). To omit artificially large price changes that can be caused by such effects as stock splitting, extreme returns larger than 12 standard deviation of data have been rejected.

## 4 Conclusions

In conclusion we have analyzed noise level for data from Warsaw Stock Exchange. We show that our noise level estimations can be useful for portfolio optimization. The resulting investment strategy brings larger profits than a simple average from the same stocks.

## References

1. Voit J (2001) The Statistical Mechanics of Financial Markets. Springer-Verlag, Berlin Heidelberg New York Barcelona Hong Kong London Milan Paris Singapore Tokyo
2. Bouchaud JP, Potters M (2000) Theory of financial risks - from statistical physics to risk management. Cambridge University Press, Cambridge
3. Mantegna RN, Stanley HE (2000) An Introduction to Econophysics. Correlations and Complexity in Finance. Cambridge University Press, Cambridge

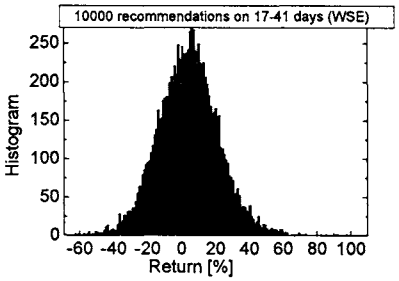


**Fig. 3.** Histogram of returns received by our strategy. The mean return equals to 4.33% while the histogram dispersion is about 17%.

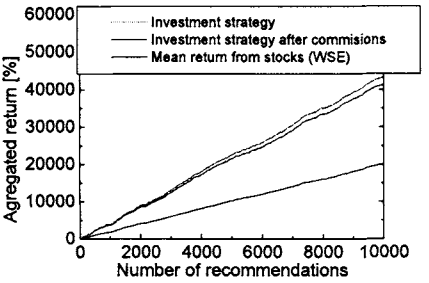


**Fig. 4.** The aggregated return for our investment strategy applied for the Warsaw Stock Exchange. The return corresponds to the mean annual return 56% while the mean annual return of Warsaw Stock Index was about 28% at the same time period.


4. Peters EE (1997) Chaos and Order in the Capital Markets. A new view of cycle, Price, and Market Volatility. John Wiley & Sons, New York.
5. Hołyst JA et al. (2001) Observations of deterministic chaos in financial time series by recurrence plots, can one control chaotic economy? European Physical Journal B 20:531-535
6. Urbanowicz K, Hołyst JA (2003) Noise-level estimation of time series using coarse-grained entropy. Phys. Rev. E 67:046218; http://www.chaosandnoise.org
7. Kantz H, Schreiber T (1997) Nonlinear Time Series Analysis. Cambridge University Press, Cambridge
8. Kaminski T et al. (2004) Combustion process in a spark ignition engine: Dynamics and noise level estimation. Chaos 14(2):461-466; Litak G et al. (2005) Estimation of a Noise Level Using Coarse-Grained Entropy of Experimental Time Series of Internal Pressure in a Combustion Engine. Chaos Solitons & fractals 23(5):1695-1701
9. Urbanowicz K, Hołyst JA (2004) Noise estimation by the use of neighboring distance in Takens space and its application to the stock market data. Proceedings of the Conference Complexity in science and society, International Journal of Bifurcation and Chaos, arXiv:cond-mat/0412098; http://www.chaosandnoise.org
10. Urbanowicz K and Hołyst JA (2004) Investment strategy due to the minimization of the noise level in a portfolio. Physica A 344:284-288

# Method of Analyzing Weather Derivatives Based on Long-range Weather Forecasts

Masashi Egi[1], Shun Takahashi[2], Takeshi Ieshima[2], and Kaoru Hijikata[3]

[1]Hitachi, Ltd., Central Research Laboratory, 1-280, Higashi-koigakubo, Kokubunji-shi, Tokyo 185-8601, Japan
[2]Hitachi, Ltd., Business Solution Systems Division, Hitachi Systemplaza, Shin-kawasaki, 890 Kashimada, Saiwai, Kawasaki, Kanagawa, 212-8567, Japan
[3]Hitachi, Ltd., Finance Department II, Financial Business Planning Group, 6, Kanda-Surugadai 4-chome, Chiyoda-ku, Tokyo 101-8010, Japan

**Summary.** We examined the effectiveness of long-range weather forecasts applied to analyze weather derivatives. We carried out 651 back tests for different historical periods and confirmed that the accuracy of evaluating the risk of weather derivatives could be drastically improved by using long-range weather forecasts.

**Key words.** weather derivative, weather forecast, Monte Carlo simulation

## Introduction

Weather derivatives are financial instruments for companies to hedge against the risk of weather-related losses. The investor who sells a weather derivative accepts the risk by charging the buyer a premium. For example "The company pays $5M to the investors as a premium beforehand. If there are days cooler than 20°C next July in Tokyo, the investor must pay $1M per day to the company as compensation." If nothing happens, then the investor makes a profit. However, if the weather turns bad, the company claims the money.

The premium, i.e. the price of a weather derivative, is determined based on a predicted distribution of compensation, which can be obtained by Monte Carlo simulation generating virtual weather scenarios based on stochastic weather time-series models. So far, various stochastic models have been proposed to describe various characteristics of weather transitions (Briggs and Wilks 1996, Caw and Wei 1999, Dischel 1999, Jewson and Caballero 2002, Richardson 1981, Torró et al. 2001, Wilks 2002).

The accuracy of the distribution depends on the values of the model parameters, which have been simply determined to fit into historical data. However it is obvious that these values do not have specific information about weather in future. To

improve the accuracy, we need to feed information about future weather into the model parameters.

Long-range weather forecasts (LWF hereafter) are one type of such future weather information provided by the Meteorological Agency. LWFs are periodically broadcast for monthly average temperatures and monthly precipitation amounts, and consist of three probabilities $(p_b, p_n, p_a)$ pertaining to the three classes "below-normal", "near-normal", and "above-normal", respectively. The normal range is defined in such a way that historical data for the last 30 years is equally divided among the three classes.

However, reflecting LWFs that have a temporally aggregated nature in stochastic weather time-series models presents a significant challenge. In the next section, we explain, a method to solve this difficulty.

## Parameter Estimation Methods Reflecting Long-Range Weather Forecasts

We briefly review a model-independent method proposed by Briggs and Wilks (1996) to reflect LWF in stochastic weather time-series models, and refer to this method as a biased sampling method. Schematic diagrams of traditional and biased sampling methods are shown in Figure 1. The original population consists of 30 samples for the last 30 years of data. According to the definition of the normal range, each of the three classes has 10 samples. In a traditional method, the model parameter values are estimated to fit well into the original population.

The biased sampling method is as follows. First, we construct a biased population sampling from each of the three classes of the original population on the weights $(p_b, p_n, p_a)$ according to LWF. In figure 1, we show an example when the forecast is $(p_b, p_n, p_a) = (20\%, 30\%, 50\%)$. In this case the biased population can be constructed by sampling 20, 30, and 50 items of data from each of the three classes. Then, the model parameter values are estimated to fit well into the biased population. In this way, we can reflect LWF in stochastic weather time-series models, which is obviously independent of the model details.

Briggs and Wilks (1996) proposed the biased sampling method for use in the hydrometeorology field rather than in financial engineering, so an application for weather derivatives was not discussed. Zeng (2000) independently proposed the biased sampling method to analyze weather derivatives. However, the effectiveness has never been examined. In the next section, we comprehensively verify the effectiveness of the method applied to analyze weather derivatives.

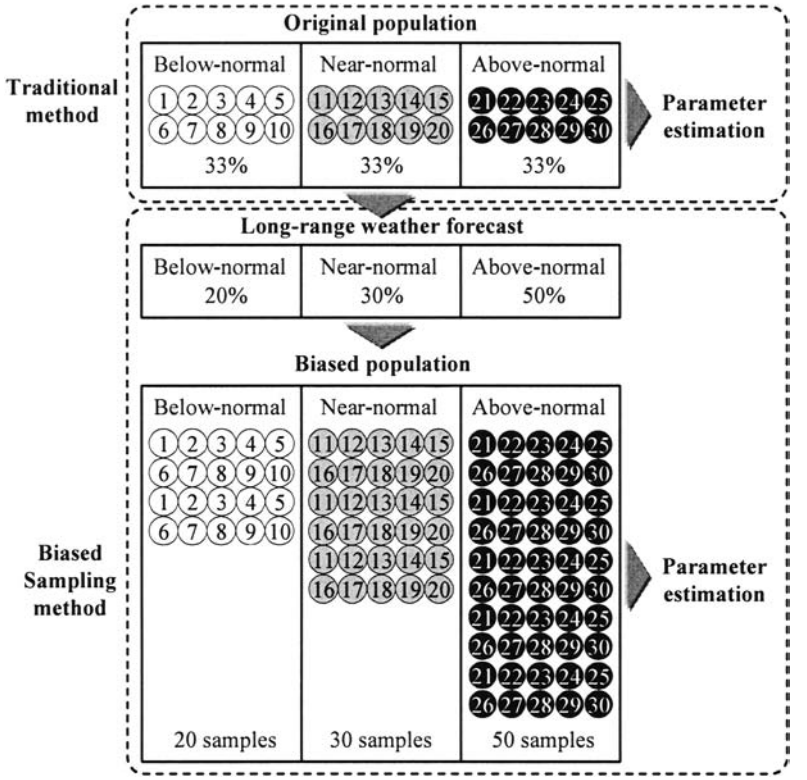


**Fig. 1.** Schematic diagrams of traditional and biased sampling methods. Each circle represents a sample of historical data over the last 30 years, and the number in the circle represents the order among the 30 samples.

## Verification of Effectiveness

We carried out $M = 651$ back tests for different historical periods shifting a time-window, using actual past data observed in Japan, and compared the accuracy of the compensation distribution of traditional and biased sampling methods. We assumed the following weather derivatives against heavy rain "In the forthcoming 31 days, if there are days in which the daily precipitation exceeds 1 mm, then the investor will pay \$10K per a day."

Here we notice that the accuracy of the biased sampling method depends on the accuracy of the LWF itself. To focus our attention on the accuracy of the biased sampling method, we used the artificial LWF constructed to have an ideal accu-

racy in which the observed occurrence rates in each class exactly equal the forecasted values $(p_b, p_n, p_a)$.

Employing the model developed by Richardson (1981) for daily precipitation, we generated 10000 virtual weather scenarios to construct the predicted compensation distribution function for each period. We evaluated the following two performance indicators to quantify the accuracy of the predicted compensation distribution function $f_t(x)$ and $f_b(x)$ predicted by each method, where $x$ denotes compensation value and the indices represent traditional and biased sampling methods, respectively.

One performance indicator is the absolute error between the expectation value of the predicted compensation distribution and the realized compensation, namely

$$\varepsilon_t = \frac{1}{M}\sum_{i=1}^{M}\left|E_t[x_i] - x_i'\right|,\ \varepsilon_b = \frac{1}{M}\sum_{i=1}^{M}\left|E_b[x_i] - x_i'\right| \tag{1}$$

where index $i$ represents the period number, $x'$ represents the realized compensation, and $E_t[]$, $E_b[]$ represent expectation values of $x$ by each method.

The second performance indicator is the goodness of fit in terms of the $\chi^2$ value in order to evaluate the adequacy of risk estimation. The percentile of a realized compensation in the predicted compensation distribution is given by

$$q = \int_0^{x'} f(x)dx \tag{2}$$

If the predicted compensation distribution is ideal, the percentiles are uniformly distributed in a range [0,1]. We evaluated the deviation from the ideal uniformity by the $\chi^2$ value. Dividing the range [0,1] into $N$ equal intervals, we counted the number of periods appearing in each interval denoted by $n(i)\,; i = 1, \cdots, N$ where $\sum_{i=1}^{N} n(i) = M$. Then the goodness of fit is given by

$$\chi_t^2 = \frac{1}{N}\sum_{k=1}^{N}\frac{\left(n_t(k) - m\right)^2}{m},\ \chi_b^2 = \frac{1}{N}\sum_{k=1}^{N}\frac{\left(n_b(k) - m\right)^2}{m} \tag{3}$$

where $m = M / N$ and assumed $N = 10$.

We obtained the results listed in table 1, which shows that both indicators are improved, and the goodness of fit is drastically improved.

**Table 1.** Results of our examinations of performance indicators.

| Performance Indicator | Traditional method | Biased sampling method | Improveness |
|---|---|---|---|
| Absolute erorr | \$25.6K | \$24.6K | 4% |
| Goodness of fit | 28.1 | 13.9 | 51% |

## Conclusion

We examined the effectiveness of LWF applied to analyze weather derivatives. We carried out 651 back tests for different historical periods and confirmed that it was possible to drastically improve the accuracy of evaluating the risk of weather derivatives by using LWFs. Therefore, LWF may have a great deal of potential to improve the quality of weather risk managements.

## References


Briggs W.M., and Wilks D.S., "Modifying Parameters of a Daily Stochastic Weather Generator Using Long-Range Forecasts", Conference on probability and statistics in the atmospheric sciences, Vol. 13, 243-246 (1996)

Caw M., and Wei J., "Pricing Weather Derivatives: An Equilibrium Approach", Department of Economics, Queen's University, Kingston, Ontario, Working Paper (1999)

Dischel B., "The D1 Stochastic Temperature Model for Valuing Weather Futures and Options", Applied Derivatives Trading (1999)

Jewson S., and Caballero R., "Multivariate Long-Memory Modeling of Daily Surface Air Temperatures and the Valuation of Weather Derivative Portfolios", http://ssrn.com/abstract=405800 (2002)

Richardson C. W., "Stochastic simulation of daily precipitation, temperature and solar radiation", Vol. 17, 1820190, Water Resources Research (1981)

Torró H., Meneu V., Valor E., "Single Factor Stochastic Models With Seasonality Applied to Underlying Weather Derivative Variables", working paper in European Financial Management Association (2001)

Wilks D.S., "Realizations of daily weather in forecast seasonal climate", Vol. 3, Part 2, 195-207, Journal of Hydrometeorology (2002)

Zeng L., "Pricing Weather Derivatives", The Journal of Finance, Vol.1, No.3, 72-78 (2000)

# Investment horizons : A time-dependent measure of asset performance

Ingve Simonsen[1], Anders Johansen[2], and Mogens H. Jensen[3]

[1] Department of Physics, NTNU, NO-7491 Trondheim, Norway
[2] Teglgårdsvej 119, DK-3050 Humlebæk, Denmark
[3] Niels Bohr Institute, Blegdamsvej 17, DK-2100 Copenhagen Ø, Denmark

**Summary.** We review a resent *time-dependent* performance measure for economical time series — the (optimal) investment horizon approach. For stock indices, the approach shows a pronounced gain-loss asymmetry that is *not* observed for the individual stocks that comprise the index. This difference may hint towards an synchronize of the draw downs of the stocks.

As an investor or practitioner working in the financial industry, you are continuously faced with the challenge of how to chose and manage a portefolio under varying market conditions; as the market change, you have to decide whether to adjust your positions in order to make the portfolio, as you see it, more optimal. The way such important decisions are made, with dramatic economic consequences if done badly, is rather complex; most market players have their very own methods for this purpose, and they are only rarely disclosed to the public. The clients risk aversion, which is based on individual psychology, plays a major role in the task of choosing a portfolio and hence quantifiable and rational measure must be used in for example stress testing of the portfolio.

As the financial industry became fully computerized, the distribution of returns approach became popular for measuring asset performance from historic data records. Today, this method is considered one of the classic approaches for gauging the performance of an asset [1, 2]. The method relies on the distribution of returns (to be defined below) corresponding to a *fixed* time window (or horizon as we will refer to it below). In order to look into the performance over a different time horizon, the return distribution has to be regenerated for the new window size. Actually, one of the most successful strategies for actively investing when the risk aversion is not low, is to, *a priori*, decide for a return level and then liquidate the position when this level has been reached.

It is not at all clear that the natural scenario for an investor is to consider fixed time windows. There has therefore lately been a lot of interest in time dependent measures, *i.e.* measures where the time period over which the asset is hold, is non-constant, and allowed to depend on the specific market condi-

tions which in general is not known in detail. A change in time horizon used by an investor may be due to for instance a changes in the market itself, or new investment strategies being implemented by the investor.

In this work, we will review a recent development in such time-dependent measures — the *investment horizon approach*. This approach is motivated by progress in turbulence [3], and it represents an adaption of a more general concept, known as *inverse statistics*, to economics. The investment horizon approach was first introduced into economics by the present authors [4], and later considered in a series of publications [5, 6, 7, 8]. The method has recently been applied to different types of financial data with success; stock index data [4, 5, 6], like the Dow Jones Industrial Average (DJIA), NASDAQ, Standard and Poor 500 (SP500), individual stocks [8], and high frequency foreign exchange (FX) data [6]. A similar approach, however without a fixed return level, has been studied in Refs. [9, 10] with the prime focus on losses.

Let $S(t)$ denote the asset price, and $s(t) = \ln S(t)$ the corresponding logarithmic price. Here time $(t)$ can be measured in different ways [2], but the various choices may result in different properties for the inverse statistics [6]. The logarithmic return at time $t$, calculated over a time interval $\Delta t$, is defined as [1, 2] $r_{\Delta t}(t) = s(t + \Delta t) - s(t)$.

We consider a situation where an investor is aiming for a given return level denoted by $\rho$. This level may be both positive (gains) or negative (losses). If the investment is made at time $t$, then the investment horizon is defined as the time $\tau_\rho(t) = \Delta t$ so that the inequality $r_{\Delta t}(t) \geq \rho$ $(r_{\Delta t}(t) \leq \rho)$ for $\rho \geq 0$ $(\rho < 0)$ is satisfied for the *first* time. In mathematical terms, this can be expressed as

$$\tau_\rho(t) = \begin{cases} \inf\{\Delta t \mid r_{\Delta t}(t) \geq \rho\}, & \rho \geq 0, \\ \inf\{\Delta t \mid r_{\Delta t}(t) \leq \rho\}, & \rho < 0. \end{cases} \tag{1}$$

The investment horizon distribution, $p(\tau_\rho)$, is then the distribution of investment horizons $\tau_\rho$ estimated from the data (cf. Fig. 1a). This distribution will go through a maximum, as should be apparent from the discussion to follow. This maximum — the *optimal investment horizon* — will be denoted $\tau_\rho^*$. It quantifies the most likely time period (obtained from historic data) needed to reach the investment outcome characterized by $\rho$.

For later use, we stress that if the price process $S(t)$ is a geometrical Brownian motion — the classic assumption made in theoretical finance — then the solution to the investment horizon (first passage time) problem is known analytically [11]. It can be shown that the investment horizon distribution is given by the Gamma-distribution: $p(t) = |a| \exp(-a^2/2t)/(\sqrt{2\pi}t^{3/2})$, where $a \propto \rho$. Hence, in the limit of large (waiting) times, one recovers the well-known first return probability $p(t) \sim t^{-3/2}$.

Figures 1 show empirical investment horizon distributions, $p(\tau_\rho)$ with $\rho = \pm 0.05$. for an index (Fig. 1a) and an individual stock (Fig. 1b). Drift-terms that were "smooth" up till a time scale of roughly 4 years, were removed from the logarithmic prices prior to the analysis (consult Ref. [4] for details).

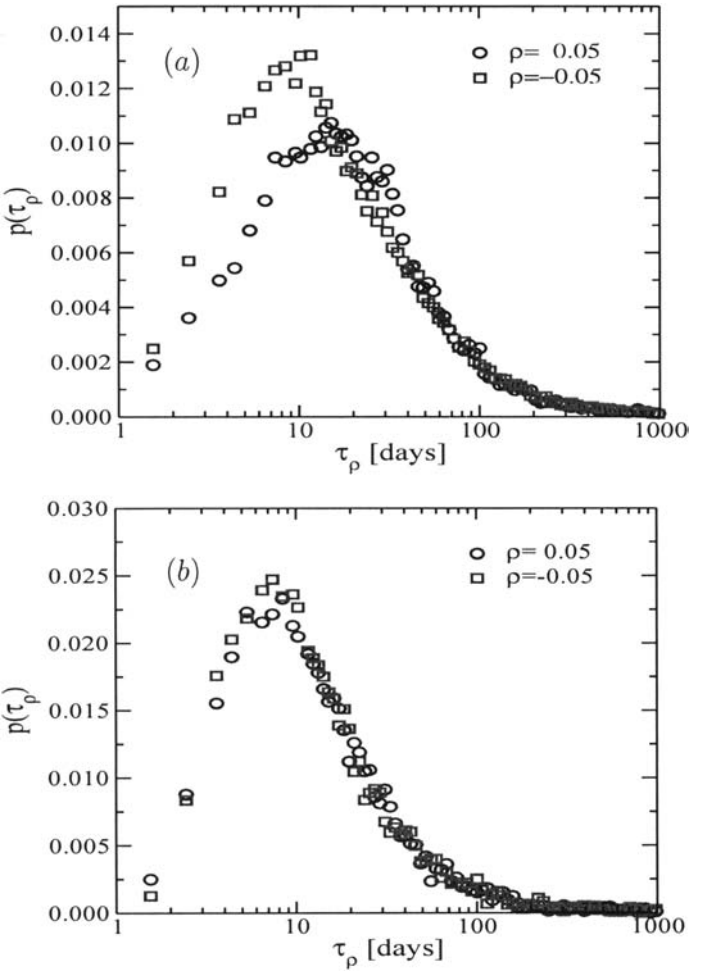


**Fig. 1.** (a) The investment horizon distributions of the DJIA closing prices from 1896 till present, at a return levels $|\rho| = 0.05$. (b) The same as Fig.1(a), but now for the single stock of IBM for the period from the beginning of 1962 till June 2000. IBM has been part of DJIA since June 29, 1979.

This pre-processing of the data was done in order to enable a more consistent comparison of the results corresponding to positive and negative levels of returns due to differences in economic fundamentals such as inflation, interest rates, *etc.* The data set used to produce the results of Fig. 1a was the daily close of the Dow Jones Industrial Average taken over its whole history up till present. From this same figure, two well-pronounced, but not coinciding, optimal investment horizons can be observed from the empirical distributions

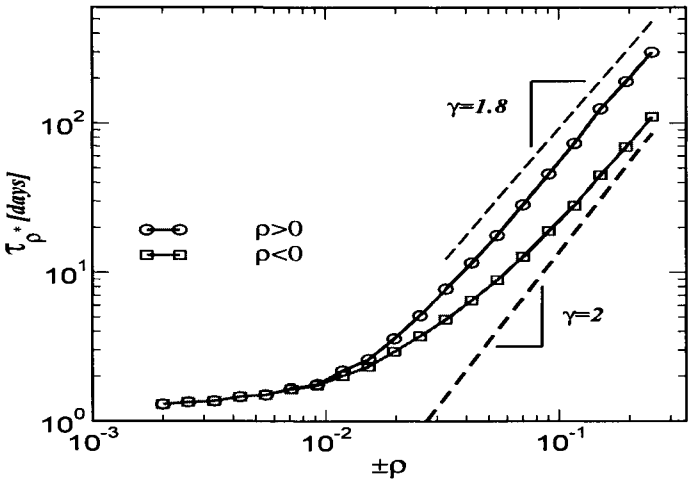


**Fig. 2.** The optimal investment horizon $\tau_\rho^*$ for positive (open circles) and negative (open squares) levels of return $\pm\rho$. In the case $\rho < 0$ one has used $-\rho$ on the abscissa for reasons of comparison.

$p(\tau_\rho)$. With $|\rho| = 0.05$ they are both of the order of $\tau_\rho^* \sim 10$ days. In general, the values of $\tau_\rho^*$ will depend on the return level $\rho$, and we presents results for the DJIA in Fig. 2 for positive and negative return levels. Recall that if the price process is consistent with a geometrical Brownian motion, one has $\tau_\rho^* \sim \rho^\gamma$ with $\gamma = 2$ for *all* values of $\rho$ (lower dashed line in Fig. 2). The empirical results are observed not to be consistent with such a behavior. For rather small levels of returns — a fraction of a percent — the dependence on return level is quite weak. When $|\rho|$ is increased, however, the dependence becomes more pronounced and it gradually becomes more and more like, but still different from, the geometrical Brownian result. As a whole, the dependence of $\tau_\rho^*$ (on $\rho$) over the range of return levels considered in Fig. 2, resembles more a double logarithmic behavior than a power law. However, for the range of $\rho$-values considered and the fact that the statistics become poorer for increasing levels of return, we are unable from the empirical data alone to uncover the actual functional dependence of $\tau_\rho^*$ on the return level.

One of the most striking features of Fig. 2 is the apparent fact that the optimal investment horizon for positive and negative return levels are *not* the same. This asymmetry starts to develop when the return level $|\rho|$ is not too small (cf. Fig. 2). Such a *gain-loss asymmetry* is actually a rather general feature of the investment horizon of stock indices [6]. On the other hand, for individual stocks that together comprise the index, this phenomenon is less pronounced [8] and an asymmetry can often hardly be seen at all. In Fig. 1b this is exemplified by the investment horizons of IBM for $\rho = \pm 0.05$, a company that is part of the DJIA index. Similar results hold for most other stocks

being part of the DJIA [8]. The attentive reader could ask: How is it possible that an asymmetry is present in the index, but not in the individual stocks that *together* make out the index? At the time of writing, there is no consensus on what is causing this behavior. It has been speculated that it might be caused by cooperative effects taking place among the stocks and causing them to partly synchronize their draw-downs (conditional serial correlation). If that was to be the case, the index — that is some average of the individual stocks — will experience an increased probability of shorter investments horizons $\tau_{-|\rho|}$ compared to the similar results found for the same positive level of return. Other speculations go in the direction of this phenomenon being related to the so-called leverage effect [12]. These questions are being addressed by ongoing research efforts, and it is hoped that they will be satisfactory answered in the immediate future.

Before ending this contribution, we would like to add a few comments regarding possible practical implications (as we see it) of the investment horizon approach [13]. Two applications will be mentioned here, both taken from portfolio management. The first application is related to the problem of consistent allocation of VAR-like (quantile) and stop-loss limits. For such problems, the correlation structure over different time horizons is important. Our approach naturally use non-fixed time windows, and it is therefore hoped that it might contribute some new insight onto these issues. The second application is concerned with the calculation of risk measures for portfolios. When the market is moving against you, you are forced to liquidate. In this process, "liquidation horizons" that are used across assets of a portfolio, are normally not the same. By taking advantage of the negative return levels, investment horizon distributions $p\left(\tau_{-|\rho|}\right)$ for the different assets of the portfolio, may be used to design an *optimal liquidation* procedure depending on the nature of the position, *e.g.*, long or short. The exploration of possible applications of the concept of inverse statistics in economics is at its infancy. We hope that the future will demonstrate this approach to be fruitful also from a practical standpoint.

A new measure of asset performance that represents an alternative to the classic distribution of returns approach has been described. Unlike the classic method, the new technique is *time-dependent*. This opens the possibility of studying and measure asset performance over a non-constant time scale, an idea that lately has attracted a great deal of attention.

**Acknowledgements**
The first author wishes to thank Drs. Ted Theodosopoulos and Marc Potters for fruitful discussions and valuable comments and suggestions. IS also acknowledges the financial support kindly provided by Nihon Keizai Shimbun Inc.

## References


1. J.-P. Bouchaud and M. Potters. *Theory of financial risks : from statistical physics to risk management.* Cambridge University Press Cambridge 2000.
2. R. N. Mantegna and H. E. Stanley. *An Introduction to Econophysics: Correlations and Complexity in Finance.* Cambridge University Press Cambridge 2000.
3. M.H. Jensen. *Multiscaling and Structure Functions in Turbulence: An Alternative Approach.* Phys. Rev. Lett. **83**, 76 (1999).
4. Ingve Simonsen, Mogens H. Jensen and Anders Johansen. *Optimal Investment Horizons.* Eur. Phys. J. B **27**, 583 (2002).
5. M.H. Jensen, A. Johansen and I. Simonsen. *Inverse Fractal Statistics in Turbulence and Finance.* Int. J. Mod. Phys. B **17**, 4003 (2003).
6. M.H. Jensen, A. Johansen and I. Simonsen. *Inverse Statistics in Economics : The gain-loss asymmetry.* Physica A **324**, 338 (2003).
7. M.H. Jensen, A. Johansen, F. Petroni and I. Simonsen. *Inverse Statistics in the Foreign Exchange Market.* Physica A **340**, 678 (2004).
8. A. Johansen, I. Simonse and M.H. Jensen. *Unpublished work.* 2004.
9. A. Johansen and D. Sornette. *Stock market crashes are outliers.* Eur. Phys. J. B **1**, 141 (1998).
10. A. Johansen and D. Sornette. *Large stock market price drawdowns are outliers.* J. of Risk **4** (2), 69 (2001/2002).
11. D. Kannan. *Introduction to Stochastic Processes.* North Holland New York 1979.
12. J.-P. Bouchaud, A. Matacz and M. Potters. *Leverage Effect in Financial Markets: The Retarded Volatility Model.* Phys. Rev. Lett. **87**, 228701 (2001).
13. Ted Theodosopoulos. *Private communication.* 2004.

# Clustering financial time series

Nicolas Basalto[1] and Francesco De Carlo[2]

[1] Institute for Advanced Studies at University of Pavia, via Bassi 6, I-27100 Pavia, Italy nicolas.basalto@unipv.it
[2] Department of Physics, University of Bari, via Amendola 173, I-70126 Bari, Italy francesco.decarlo@ba.infn.it

**Summary.** We analyze the shares aggregated into the Dow Jones Industrial Average (DJIA) index in order to recognize groups of stocks sharing synchronous time evolutions. To this purpose, a pairwise version of the Chaotic Map Clustering algorithm is applied: a map is associated to each share and the correlation coefficients of the daily price series provide the coupling strengths among maps. A natural partition of the data arises by simulating a chaotic map dynamics. The detection of clusters of similar stocks can be exploited in portfolio optimization.

**Key words:** Clustering algorithms, Chaotic maps, Portfolio optimization

## 1 Introduction

In recent years, the analysis of several social systems (economics, finance, urban planning, etc.) has dramatically aroused the attention of many quantitative scientists. Because of their features, the analysis of financial markets is especially challenging. We focus here on a specific level of their complexity: the cross-correlation among temporal series of stock prices. Clustering is the natural approach to a problem like this one. In particular, non-parametric methods are the optimal strategy when no prior knowledge on the clusters to find is available: these methods make few assumptions about the structure of the data, rather they employ local criteria for reconstructing the clusters and are particularly suited when a hierarchical structure, rather than a fixed partition, of the data should be obtained. Here we implement a non-parametric version of a clustering technique, named Chaotic Map Clustering (CMC) (Basalto et al. 2005) (Angelini et al. 2000), which relies on the synchronization properties of a chaotic map system (Manrubia et al. 1999) in order to obtain a hierarchy of classes. The matter in hand is the analysis of the financial time series of the 30 stocks belonging to the DJIA (Dow Jones Industrial Average) index. We aim to find, by means of mathematically rigorous methods, economically significant partitions to be further exploited into portfolio optimization.

## 2 Preliminary notions

In general, clustering consists in partitioning a set of $N$ elements into $K$ clusters on the basis of a suitable *similarity* criterion (Fukunaga 1990). A number of criteria can be used to define this intuitive concept leading, in general, to different resulting partitions, each one deeply influenced by the strategy adopted by the observer in reason of his own ideas and preconceptions on the problem. Furthermore, the clustering techniques differ from each other depending on a number of features of the algorithm used to implement them. The CMC algorithm we apply can be classified as: *non-parametric*, which is a neutral approach whenever no prior knowledge is available; *hierarchical*, as it yields nested partitions; *pairwise*, as the data are indirectly represented by a similarity matrix which provides pairwise comparisons among elements.

## 3 Physical model

In this section we give a brief review of the chaotic map algorithm. In a $D$-dimensional feature space, the data-points are viewed as sites of a lattice, each one hosting a map $x_i \in [-1, 1]$, $i = 1, \ldots, N$. Short-range interactions between neighboring maps are introduced as exponential decreasing function of the site distances. In the stationary regime, clusters of synchronized maps appear, corresponding to high density regions in the original data space. The mutual information between maps is used as both a similarity index for building the clusters, and a scale parameter for reconstructing the hierarchical tree (Angelini et al. 2000). As the data at hand are the similarity matrices of the financial times series, rather than feature vectors, a pairwise version of this algorithm would be more suitable. The CMC algorithm shares the same philosophy of the Super Paramagnetic Clustering (SPC) algorithm (Blatt et al. 1996) where the physical system used to partition the data is an inhomogeneous ferromagnetic model: Potts spin $s_i$ are assigned, instead of map variables, to each data-point and short-range interactions between neighboring sites are introduced. The spin-spin correlation function replaces the mutual information as similarity index for clustering the data. In the super-paramagnetic regime, domains of aligned spins appear, corresponding to the classes present in the data. Kertesz et al. generalized the SPC to the case of anti-ferromagnetic couplings by introducing the following spin-spin strength as a function of the correlation coefficients $c_{ij}$ (Kertesz et al. 2000):

$$J_{ij} = \mathrm{sgn}(c_{ij})\Big(1 - \exp\Big\{ - \frac{n-1}{n}\Big[\frac{c_{ij}}{a}\Big]^n\Big\}\Big) \,, \tag{1}$$

where $n$ is an even positive integer tuning the shape of the interaction function (whose value should be chosen so that a stable non-trivial partition can be obtained inside the hierarchical solution), and $a$ is the average of the largest correlation coefficients for each sequence (Kertesz et al. 2000):

$$a = \frac{1}{N} \sum_{i=1}^{N} \max_{j}(c_{ij}) \ . \tag{2}$$

We shall try to follow a similar strategy in our CMC approach. We are naturally led to adopt the couplings (1) for $c_{ij} \geq 0$, while setting $J_{ij} = 0$ for $c_{ij} < 0$. In this way, we build up a partially coupled map lattice with exponential increasing interactions between positively correlated data-points. The evolution of the maps is driven by a chaotic dynamics:

$$x_i(\tau + 1) = \frac{1}{C_i} \sum_{j \neq i} J_{ij} f\left(x_j(\tau)\right) \ , \tag{3}$$

where $f(x) = 1 - 2x^2$ is the logistic map, $C_i = \sum_{j \neq i} J_{ij}$ is a normalization factor, and $\tau$ denotes the evolution time of the chaotic map system (not to be confused with the real time $t$ of the financial series). A detailed description of the above mentioned dynamics for clustering purposes is described elsewhere (Angelini et al. 2000); roughly speaking, after a certain equilibration time, the dynamics (3) yields a stable partition of the maps $x_i$ into synchronized clusters. In order to evaluate the synchronicity in the evolution of the maps and to explore the entire resulting hierarchical structure we adopt the Shannon mutual information $I$ (Basalto et al. 2005).

## 4 Application to financial data

We applied the CMC algorithm to cluster the $N = 30$ shares composing the DJIA index collecting their daily closure price during the period 1998-2002. The analysis has been performed either over each single year and over the whole period. We look at the temporal series of the logarithmic differences

$$Y_i(t) \equiv \ln P_i(t) - \ln P_i(t-1), \tag{4}$$

where $P_i(t)$ is the closure price of the $i$-th share at day $t$. The natural measure to quantify the degree of similarity between two time series, namely the synchronicity in their time evolution, is the correlation coefficient:

$$c_{ij} = \frac{\langle Y_i Y_j \rangle - \langle Y_i \rangle \langle Y_j \rangle}{\sqrt{(\langle Y_i^2 \rangle - \langle Y_i \rangle^2)(\langle Y_j^2 \rangle - \langle Y_j \rangle^2)}} \ . \tag{5}$$

In our framework, each stock is represented by a map. Once we have set the coupling strength between each pair of them (1), they evolve according to the dynamics (3) in order to reach a stable partition. Exploring the whole mutual information range of values, the complete hierarchy of clustering is obtained. In Fig. 1, we display, by means of a dendrogram, the resulting partition of stocks over the whole time period. Each firm is labeled by mean of its ticker. Tickers and their corresponding companies are shown in Table1.

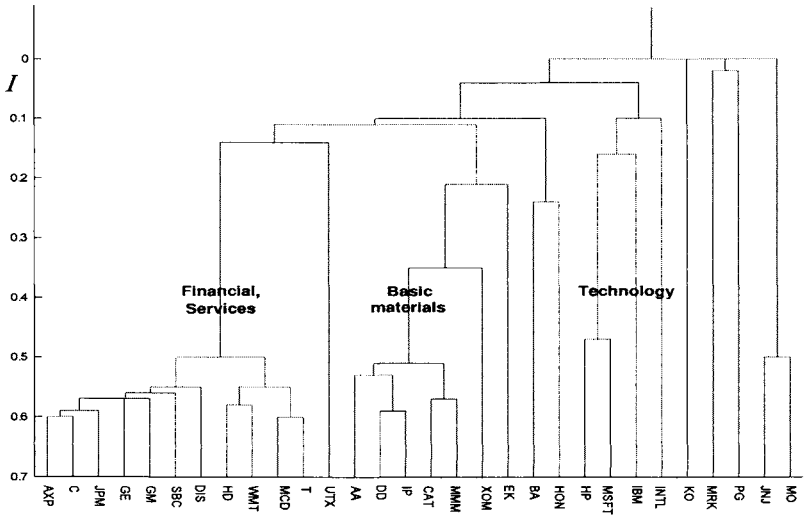


**Fig. 1.** Dendrogram obtained from the whole 5-year time period 1998-2002, with $n = 18$. The main branches have been marked by the industrial areas of the companies they are made of

Analyzing the outcomes, it is worth stressing the presence of some economically meaningful cores of companies which remain strongly linked together over periods longer than one year: financial companies (AXP, C, JPM, 98-02), services (DIS, MCD, T, WMT, 98-99, 01), consumers non-cyclical (KO, MO, PG, 98-99), basic materials (AA, DD, IP, 00-02), capital goods (BA, CAT, HON, 99-01), technology (HPQ, IBM, MSFT, 01-02), healthcare (JNJ, MRK, 98-99), conglomerates (MMM, UTX, 00-02). Let us stress that these resulting partitions come out from a purely mathematical algorithm, using no economical information but the price of stocks. In this sense, the partitions are provided by the market itself and should have an immediate pertinence in a matter of great interest for financial institutions: the portfolio optimization. According to the portfolio theory, in order to minimize the risk involved in a financial investment, one should diversify among different assets by choosing those stocks whose price time evolutions are as different as possible. In our opinion, a proper selection of stocks can be performed by means of the chaotic map clustering approach.

## 5 Conclusions

In the present work, a pairwise version of the chaotic map algorithm has been applied to the analysis of the stocks aggregated into the DJIA index. The correlation coefficients between financial time series have been used as similarity

**Table 1.** Companies belonging to the Dow Jones Industrial Average: tickers and their extended names

| Ticker | Name | Ticker | Name |
|---|---|---|---|
| AA | Alcoa Inc. | IP | Intl Paper |
| AXP | American Express Co | JNJ | Johnson & Johnson |
| BA | Boeing | JPM | JP Morgan Chase |
| C | Citigroup | KO | Coca Cola Inc. |
| CAT | Caterpillar | MCD | McDonalds Corp. |
| DD | DuPont | MMM | Minnesota Mining |
| DIS | Walt Disney | MO | Philip Morris |
| EK | Eastman Kodak | MRK | Merck & Co. |
| GE | General Electrics | MSFT | Microsoft |
| GM | General Motors | PG | Procter & Gamble |
| HD | Home Depot | SBC | SBC Communications |
| HON | Honeywell Intl | T | AT&T |
| HPQ | Hewlett-Packard | UTX | United Technology |
| IBM | Intl Business Machine | WMT | Wal-Mart Stores |
| INTC | Intel Co | XOM | Exxon Mobil |

measures to cluster the temporal patterns. Once the coupling interactions between maps are taken to be functions of these coefficients, the dynamics of such a system leads to the formation of clusters of companies that can often be identified as different industrial branches. The resulting analysis can be exploited into a suitable portfolio selection and optimization procedure.

## References


1. Angelini L, De Carlo F, Marangi C, Pellicoro M,Stramaglia S (2000) Clustering data by inhomogeneous chaotic map lattices. Phys Rev Lett 85:554.
2. Basalto N, Bellotti R, De Carlo F, Facchi P, Pascazio S (2005) Clustering stock market companies via chaotic map synchronization. Physica A 345:196-206
3. Blatt M, Domany E, Wiseman S (1996) Super-paramagnetic clustering of data. Phys Rev Lett 76: 3251-3254
4. Fukunaga K (1990) Introduction to Statistical Pattern Recognition. Academic Press, San Diego
5. Kertesz J, Kullmann L, Mantegna RN (2000) Identification of Clusters of Companies in Stock Indices via Potts Super-Paramagnetic Transitions. Physica A 287:412-419
6. Manrubia SC, Mikhailov AS (1999) Mutual synchronization and clustering in randomly coupled chaotic dynamical networks. Phys Rev E 60:1579-1589

# Risk portofolio management under Zipf analysis based strategies

M. Ausloos and Ph. Bronlet

SUPRATECS, B5, Sart Tilman Campus, B-4000 Liège, Euroland
marcel.ausloos@ulg.ac.be; philippe.bronlet@ulg.ac.be

**Summary.** A so called Zipf analysis portofolio management technique is introduced in order to comprehend the risk and returns. Two portofoios are built each from a well known financial index. The portofolio management is based on two approaches: one called the "equally weighted portofolio", the other the "confidence parametrized portofolio". A discussion of the (yearly) expected return, variance, Sharpe ratio and $\beta$ follows. Optimization levels of high returns or low risks are found.

## 1 Introduction

Risk must be expected for any reasonable investment. A portofolio should be constructed such as to minimize the investment risk in presence of somewhat unknown fluctuation distributions of the various asset prices [1,2] in view of obtaining the highest possible returns. The risk considered hereby is measured through the variances of returns, i.e. the $\beta$. Our previous approaches were based on the "time dependent" Hurst exponent [3]. In contrast, the Zipf method which we previously developed as an investment strategy (on usual financial indices) [4,5] can be adapted to portofolio management. This is shown here through portofolios based on the $DJIA30$ and the $NASDAQ100$. Two strategies are examined through different weights to the shares in the portofolio at buying or selling time. This is shown to have some interesting features. A key parameter is the *coefficient of confidence*. Yearly expected levels of returns are discussed through the Sharpe ratio and the risk through the $\beta$.

## 2 Data

Recall that a time series signal can be interpreted as a series of words of $m$ letters made of characters taken from an alphabet having $k$ letters. Here below $k = 2$: $u$ and $d$, while the words have a systematic (constant) size ranging between 1 and 10 letters.

Prior to some strategy definition and implementation, let us introduce a few notations. Let the probability of finding a word of size $m$ ending with a $u$ in the $i$ (asset) series be given by $P_{m,i}(u) \equiv P_i([c_{t-m+2}, c_{t-m+1}, \cdots, c_{t+1}, c_t; u])$ and correspondingly by $P_{m,i}(d)$ when a $d$ is the last letter of a word of size $m$. The character $c_t$ is that seen at the end of day $t$.

In the following, we have downloaded the daily closing price data available from the web: (i) for the $DJIA30$, 3909 data points for the 30 available shares, i.e. for about 16 years[1]; (ii) for the $NASDAQ100$, 3599 data points[2] for the 39 shares which have been maintained in the index, i.e. for about 14.5 years. The first 2500 days are taken as the preliminary *historical* data necessary for calculating/setting the above probabilities at time $t = 0$. From these we have invented a strategy for the following 1408 and 1098 possible investment days, respectively, i.e. for ca. the latest 6 and 4.5 years respectively. The relevant probabilities are recalculated at the end of each day in order to implement a *buy* or *sell* action on the following day. The daily strategy consists in buying a share in any index if $P_{m,i}(u) \geq P_{m,i}(d)$, and in selling it if $P_{m,i}(u) \leq P_{m,i}(d)$.

However the weight of a given stock in the portofolio of $n$ assets can be different according to the preferred strategy. In the equally weighted portofolio (EWP), each stock $i$ has the same weight, i.e. we give $w_{i\in B} = 2/n_u$ and $w_{i\in S} = -1/n_d$, where $n_u$ ($n_d$) is the number of shares in $B$ ($S$) respectively such that $\Sigma[w_{i\in B} + w_{i\in S}] = 1$, with $n_u + n_d = n$ of course. This portofolio management strategy is called $ZEWP$.

In the other strategy, called $ZCPP$, for the confidence parametrized portofolio (CPP), the weight of a share depends on a confidence parameter $K_{m,i} \equiv P_{m,i}(u)$ - $P_{m,i}(d)$. The shares $i$ to be bought on a day belong to the set $B$ when $K_{m,i} > 0$, and those to be sold belong to the set $S$ when $K_{m,i} < 0$. The respective weights are then taken to be $w_B = \frac{2K_{m,i\in B}}{\Sigma K_{m,i\in B}}$, and $w_S = \frac{-K_{m,i\in S}}{\Sigma K_{m,i\in S}}$.

## 3 Results

The yearly return, variance, Sharpe ratio, and $\beta$ are given in Table 1 and Table 2 for the so called $DJIA30$ and so called $NASDAQ39$ shares respectively as a function of the word length $m$. The last line gives the corresponding results for the $DJIA30$ and the $NASDAQ100$ respectively. We have calculated the average (over 5 or 4 years for the $DJIA30$ and $NASDAQ39$ respectively) yearly returns, i.e. $E(r_P)$ for the portofolio $P$. The yearly variances $\sigma_P$ result from the 5 or 4 years root mean square deviations from the mean. The Sharpe ratio $SR$ is given by $SR = E(r_P)\ /\ \sigma_P$ and is considered to measure the portofolio performance. The $\beta$ is given by $cov(r_P, r_M)/\sigma_M^2$ where the $P$ covariance $cov(r_P, r_M)$ is measured with respect to the relevant financial

[1]From Jan. 01, 1989 till Oct. 04, 2004

[2]From June 27, 1990 till Oct. 04, 2004

index, so called market ($M$), return. Of course, $\sigma_M^2$ measures the relevant *market* variance. The $\beta$ is considered to measure the portofolio risk. For lack of space the data in the tables are not graphically displayed.

It is remarkable that the $E(r_P)$ is rather low for the $ZEWP$, and so is the $\sigma_P$, but the $E(r_P)$ can be very large, but so is the $\sigma_P$ in the $ZCPP$ case for both portofolios based on the $DJIA30$. The same observation can be made for the $NASDAQ39$. In the former case, the highest $E(r_P)$ is larger than 100% (on average) and occurs for $m$ =4, but it is the highest for $m$=3 in the latter case. Yet the risk is large in such cases. The dependences of the Sharpe ratio and $\beta$ are not smooth functions of $m$, even indicating some systematic dip near $m = 6$, in 3 cases; a peak occurs otherwise.

The expected yearly returns $E(r_P)$ *vs.* $\sigma$ are shown for both portofolios and for both strategies in Figs.1-2, together with the equilibrium line, given by $E(r_M)(\sigma/\sigma_M)$, where it is understood that $\sigma$ is the appropriate value for the investigated case. Except for rare isolated points below the equilibrium line, data points fall above it. They are even very much above in the $ZCPP$'s. cases.

| | ZEWP | | | | ZCPP | | | |
|---|---|---|---|---|---|---|---|---|
| $m$ | $E(r_P)$ | $\sigma_P$ | SR | $\beta$ | $E(r_P)$ | $\sigma_P$ | SR | $\beta$ |
| 1 | 20.00 | 16.98 | 1.18 | 0.97 | 20.16 | 17.95 | 1.12 | 1.02 |
| 2 | 18.10 | 16.21 | 1.12 | 0.92 | 20.36 | 17.66 | 1.15 | 1.00 |
| 3 | 22.00 | 14.05 | 1.57 | 0.79 | 65.24 | 39.52 | 1.65 | 0.08 |
| 4 | 24.93 | 11.90 | 2.09 | 0.57 | 104.85 | 47.02 | 2.23 | -1.11 |
| 5 | 22.60 | 9.16 | 2.47 | 0.38 | 95.96 | 56.54 | 1.70 | -1.58 |
| 6 | 18.37 | 11.68 | 1.57 | 0.47 | 67.97 | 40.55 | 1.68 | 0.09 |
| 7 | 17.33 | 8.93 | 1.94 | -0.06 | 65.27 | 30.18 | 2.16 | -0.50 |
| 8 | 9.84 | 7.73 | 1.27 | 0.11 | 53.83 | 37.52 | 1.43 | 0.32 |
| 9 | 11.23 | 4.91 | 2.29 | -0.01 | 44.23 | 38.12 | 1.16 | 0.58 |
| 10 | 6.46 | 7.11 | 0.91 | 0.15 | 37.40 | 61.05 | 0.61 | 1.92 |
| | $E(r_M)$ | $\sigma_M$ | SR | $\beta$ | | | | |
| DJIA30 | 17.09 | 17.47 | 0.98 | 1 | | | | |

**Table 1.** Statistical results for a portofolio based on the 30 shares in the $DJIA30$ index for two strategies, i.e. $ZEWP$ and $ZCPP$ based on different word sizes $m$ for the time interval mentioned in the text. The last line gives the corresponding results for the $DJIA30$. All quantities are given in %

## 4 Conclusion

We have translated the time series of the closing price of stocks from two financial indices into letters taken from a two character alphabet, searched for

| | ZEWP | | | | ZCPP | | | |
|---|---|---|---|---|---|---|---|---|
| $m$ | $E(r_P)$ | $\sigma_P$ | SR | $\beta$ | $E(r_P)$ | $\sigma_P$ | SR | $\beta$ |
| 1 | 12.68 | 22.01 | 0.58 | 0.89 | 5.41 | 26.30 | 0.21 | 0.55 |
| 2 | 11.43 | 19.99 | 0.57 | 0.81 | 2.25 | 28.12 | 0.08 | 0.63 |
| 3 | 20.25 | 16.92 | 1.20 | 0.24 | 149.27 | 192.91 | 0.77 | -1.87 |
| 4 | 27.08 | 15.74 | 1.72 | -0.04 | 131.69 | 149.75 | 0.88 | -1.70 |
| 5 | 27.84 | 11.49 | 2.42 | -0.18 | 106.63 | 103.30 | 1.03 | -1.08 |
| 6 | 24.89 | 8.77 | 2.84 | -0.05 | 90.11 | 68.89 | 1.31 | -0.26 |
| 7 | 15.99 | 9.19 | 1.74 | -0.10 | 67.28 | 32.58 | 2.07 | 0.37 |
| 8 | 13.93 | 12.39 | 1.13 | -0.25 | 68.34 | 44.33 | 1.54 | 0.06 |
| 9 | 17.52 | 11.13 | 1.57 | -0.32 | 99.20 | 38.84 | 2.55 | 0.21 |
| 10 | 14.77 | 10.81 | 1.37 | -0.32 | 71.42 | 32.09 | 2.23 | 0.30 |
| | $E(r_M)$ | $\sigma_M$ | SR | $\beta$ | | | | |
| NASDAQ100 | 7.36 | 24.11 | 0.31 | 1 | | | | |

**Table 2.** Statistical results for a portofolio based on 39 shares from the $NASDAQ100$ index for two strategies, i.e. $ZEWP$ and $ZCPP$ based on different word sizes $m$ for the time interval mentioned in the text. The last line gives the corresponding results for the $NASDAQ100$. All quantities are given in %

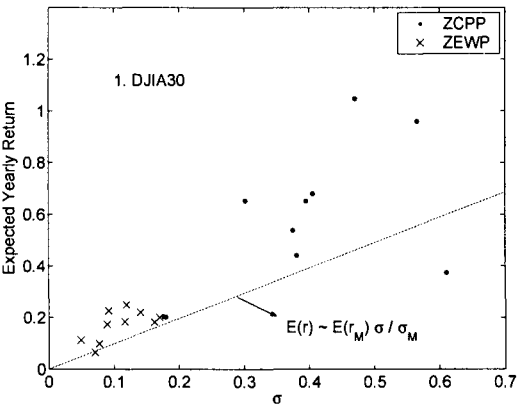


**Fig. 1.** Expected yearly return as a function of the corresponding variance for two investment strategies involving the shares in the $DJIA30$. The time of investigations concerns the latest 5 yrs

words of $m$ letters, and investigated the occurrence of such words. We have invented two portofolios and maintained them for a few years, buying or selling shares according to different strategies. We have calculated the corresponding yearly expected return, variance, Sharpe ratio and $\beta$. The best returns and weakest risks have been determined depending on the word length. Even though some risks can be large, returns are sometimes very high.

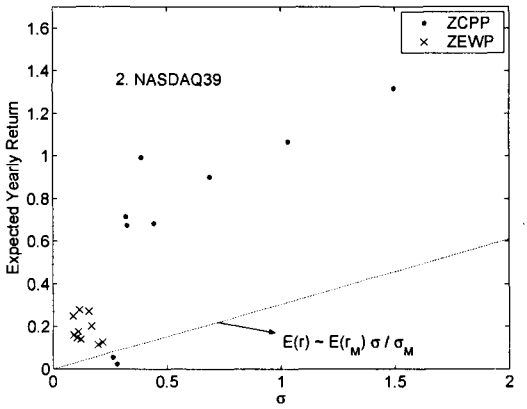


**Fig. 2.** Expected yearly return as a function of the corresponding variance for two investment strategies involving 39 shares taken from the $NASDAQ100$. The time of investigations concerns the latest 4 yrs


### Acknowledgments

MA thanks the organizers of the 3rd Nikkei symposium for financial support received in order to present the above results.


## References


[1] H.M. Markowitz, Portofolio Selection, J. Finance 8 (1952) 77 - 91.

[2] M. H. Cohen and V.D. Natoli, Risk and utility in portfolio optimization, Physica A 324 (2003) 81 - 88.

[3] M. Ausloos, N. Vandewalle and K. Ivanova, Time is Money, in *Noise, Oscillators and Algebraic Randomness*, M. Planat, Ed. (Springer, Berlin, 2000) pp. 156-171.

[4] M. Ausloos and Ph. Bronlet, Strategy for Investments from Zipf Law(s), Physica A 324 (2003) 30 - 37.

[5] Ph. Bronlet and M. Ausloos, Generalized (m,k)-Zipf law for fractional Brownian motion-like time series with or without effect of an additional linear trend, Int. J. Mod. Phys. C. 14 (2003) 351 - 365.

# Macro-players in stock markets

**Bertrand M. Roehner** [1]

**Institute for Theoretical and High Energy Physics, University Paris 7**

[1] Postal address: LPTHE, University Paris 7, 2 place Jussieu, 75005 Paris, France.
E-mail: ROEHNER@LPTHE.JUSSIEU.FR

**Abstract** It is usually assumed that stock prices reflect a balance between large numbers of small individual sellers and buyers. However, over the past fifty years mutual funds and other institutional shareholders have assumed an ever increasing part of stock transactions: their assets, as a percentage of GDP, have been multiplied by more than one hundred. The paper presents evidence which shows that reactions to major shocks are often dominated by a small number of institutional players. Most often the market gets a wrong perception and inadequate understanding of such events because the relevant information (e.g. the fact that one mutual fund has sold several million shares) only becomes available weeks or months after the event, through reports to the Securities and Exchange Commission (SEC). Our observations suggest that there is a radical difference between small ($< 0.5\%$) day-to-day price variations which may be due to the interplay of many agents and large ($> 5\%$) price changes which, on the contrary, may be caused by massive sales (or purchases) by a few players. This suggests that the mechanisms which account for large returns are markedly different from those ruling small returns.

## 1 Introduction

Very broadly speaking, there are two ways to represent stock markets and also two different methodologies to choose between them (Fig. 1). In the micro-player representation, the number of players is large enough to be treated by using statistical methods. In this case, each individual player has only a negligible impact on daily price changes. On the contrary, in the macro-player representation, the number of players is small and each one has a substantial impact not only on daily price changes but even on weekly or monthly price changes. In the second case a game theoretic approach would be more sensible than a statistical approach. The main objective of this paper is to find out which of these descriptions corresponds to the actual situation in 2004. A first hint is provided by the sheer weight of macro-players. In 1900, the share of financial institutions in total corporate stock outstanding was 6.7%, in 1974 it was 33%, in 2002 it was of the order of 50% (Kotz 1978, Statistical Abstract of the United States 2003, p. 755).

The purpose of this paper is to show that many (though not all) important phenomena that occur nowadays in stock markets are due to macroplayers. Our analysis

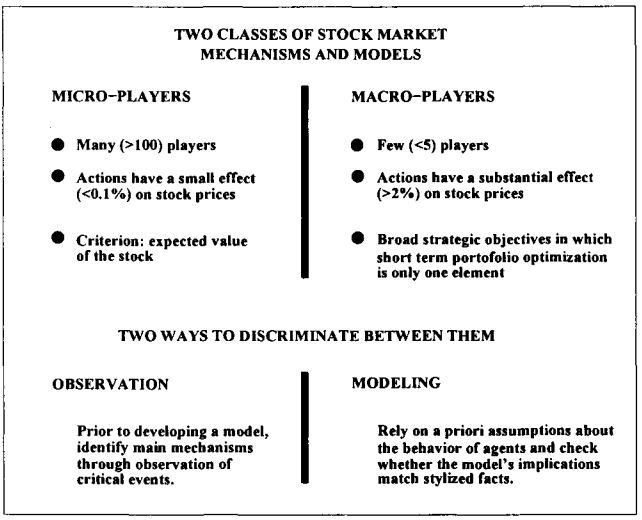


**Fig.1** In this paper we want to discriminate between the micro- and macro-player representations by observing the reactions of stocks to major shocks. Trying to unravel market mechanisms prior to any attempt at constructing specifi c mathematical models can be labeled as ex-ante analysis, as opposed to ex-post analysis which in econometrics is the standard approach.

starts from the insight provided by some pertinent case-studies. First we consider two typical examples, then we discuss their broader relevance. This provides an overall framework for model building, a step that we leave to a subsequent paper. To begin with, I consider the case of Kmart, the American retail store company.

## 2 Kmart: background information

As several of the episodes to be considered below concern Kmart, it is in order to give some background information for this company. It was founded in 1899 by Sebastian Kresge and was called the Kresge company until 1977 when its name was changed to Kmart. As shown by Fig. 2a it has been a highly successful discount retailer for many decades, but fell into trouble in the 1980s[1]. Eventually it had to ask for Chapter 11 bankruptcy protection in January 2002. The losing battle that Kmart fought against Wal-Mart can be summarized by the following figures.

[1] Symbolizing this trend was the fact that back in 1988, in the Oscar-winning fi lm "Rain-man", the character played by Dustin Hoffman repeatedly refers to Kmart by saying "Kmart sucks" meaning that the stores were shabby and displayed low quality items.

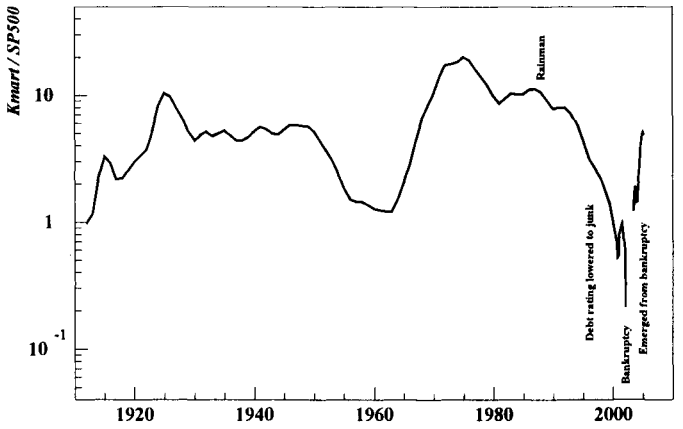


**Fig.2a Ratio of Kmart stock price to the Standard and Poor's 500 index (1910-1999)** In the 1950s In the late 1980s after becoming confronted to Wal-Mart's competition Kmart entered a downward spiral that lasted over 20 years and eventually lead to its bankruptcy in January 2002. After the company emerged from bankruptcy in May 2003, its shareprice increased more than 5 times within 18 months. The reference to the fi lm "Rainman" is explained in the text. *Source: Common stock (1992), Kmart Fact Book (1999).*

| | Kmart | Wal-Mart |
|---|---|---|
| Revenue 1990 [billion dollars] | 32 | 32 |
| Revenue 1994 [billion dollars] | 36 | 83 |

In 1993, Kmart had to close 5% of its stores and in 1994 it experienced a loss of one billion dollars. These poor performances led to increased indebtedness and in 1996, the rating of its debt was lowered below investment grade. For a company of the size of Kmart to be rated at junk level is something which is not common. In subsequent years, Kmart continued to lose market shares to Wal-Mart. The fall of its.share price shown in Fig. 2a is consistent with this loss of momentum. However, the evolution of Kmart's stock price (Fig. 2b and c) raises at least two questions:

- Why did it increase by almost 100% between September 2000 and August 2001?
- Why did it abruptly drop in January 2002 leading the company into bankruptcy?

In the expected value framework one would wish to know which innovations in Kmart's growth perspectives justified these changes. In fact, there were none. Both the increase and the sharp fall were due to causes which had very little to do with Kmart's growth perspectives. The 100% rise resulted from the strategic move of a single investor, Ronald Burkle, a billionaire and head of an investment firm. The bankruptcy resulted from the withdrawal of Fidelity, a major shareholder.

## 3 Burkle's deal with Kmart

Between October 2000 and October 2001, Burkle bought 7.2% of Kmart's outstanding shares (Fig. 2b) representing about $ 300 million. We know this because an in-

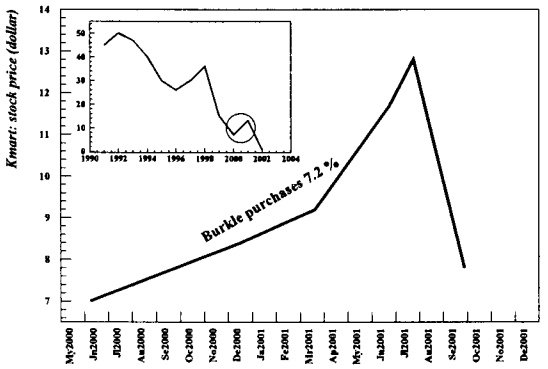


**Fig.2b Kmart share price (July 2000 - December 2001).** The insert shows how the price increase that took place between June 2000 and August 2001 (as delimited by the circle) fi ts into the broader picture; this increase was mainly due to the fact that a consortium led by billionaire Ronald Burkle purchased 7.2% of Kmart's outstanding shares. Once Burkle's share purchases stopped the price resumed its downward trend. *Source: CNN Money (January 22, 2002).*

vestor who wishes to buy more than 5% of the shares has to notify the Securities and Exchange Commission in advance which he did on October 13, 2000. In the present case we are fortunate to know his global strategy, something which is rarely the case. The purchase of Kmart shares was in fact part of a broader deal. Before 2001, Kmart had two grocery suppliers: Supervalue (for $ 2.3 billions) and Fleming (for $ 1.3 billion). In February 2001, that is to say 5 months after Burkle began his massive purchases, it became known that Kmart had chosen Fleming as exclusive supplier for the next 10 years, a deal whose value was estimated at $45 billions. As it happens, Burkle had a stake of almost 10% in Fleming. This makes the deal fairly clear. Burkle invests about $ 300 million in Kmart shares and in return he gets an exclusivity contract that is worth at least 10 times more (CNN, February 7, 2001)

Naturally, Kmart denied that there was any link between the two transactions. However, one should keep in mind that in 1999 Kmart tried to initiate a buyback program of its own shares for a total amount of $ 1 billion; assuming a price range from $ 5 to $ 10 per share, this represented between 20% and 40% of its outstanding shares. Unable to complete this program by itself because of its indebtedness, Kmart certainly relied on the deal with Burkle for implementing its objective, albeit on a smaller scale than planned initially.

To sum up, the 100% price increase in Fig.2b had much to do with Burkle and Fleming, but very little with Kmart itself. We now turn to the events which occurred in the weeks before Kmart's bankruptcy.

## 4 The withdrawal of Fidelity from Kmart

In a CNN financial report of February 15, 2002 one reads:

> Jim Lowell, editor of the newsletter "Fidelity Investor" said Fidelity recently slashed its holding in Kmart. Kmart had represented almost 10% of assets at Fidelity parent company Fidelity Management and Research Corporation (FMR) until recently, before the company slashed its position to 1.3%.

We posit that Fidelity's move (which was certainly imitated by other institutional holders even though we don't have explicit statements) accounts for much of Kmart's stock price collapse in January 2002 (Fig. 2c). Because holdings are reported only every three months we do not know when exactly the sales occurred. As a result the term "recently" used in the above excerpt is fairly elastic: it refers to a date comprised between November 15, 2001 and January 22, 2002.

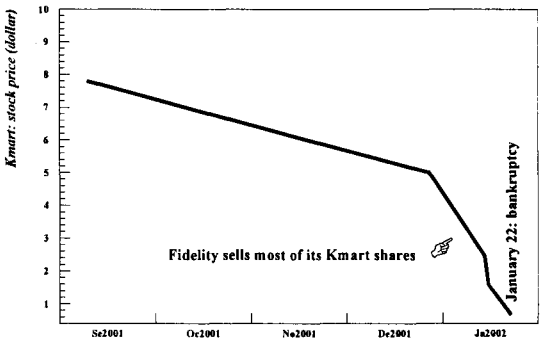


**Fig.2c Kmart share price in January 2002.** When Fidelity began to sell its shares, it became obvious that Kmart no longer had the support of its major institutional shareholders. *Source: New York Times (January 2002).*

FMR is the world's largest investment fund with assets estimated in 2003 at about 1 trillion dollars ($\sim$ 10% of US GDP in 2001). The company has several subsidiaries such as Fidelity Magellan, Fidelity Growth Company, Fidelity Leveraged Company which manage its funds. Unfortunately, in contrast to the previous case, we do not know precisely the reason of Fidelity's move. Of course, if Kmart had been unable to avoid bankruptcy that would have been a sufficient motive for share holders usually

lose 100% of their assets in a bankruptcy. However, my reading is that Kmart was not driven into bankruptcy by its debt but rather by the withdrawal of its major share holders. That feeling relies on the fact that Kmart's assets in terms of real estate (land and stores) was estimated at $ 15 billions in a report published by the Deutsche Bank in July 2004[2]; no doubt that, in early 2002 prior to the bankruptcy, the value of this asset was substantially larger. As Kmart's debt never exceeded $ 4 billions, it was not in an Enron-like situation with debt being larger than real worth of assets.

Naturally, if major investors withdraw their support, if the company's debt is downgraded by rating agencies (which indeed happened on January 17, 2002), then it cannot get new short-term loans and bankruptcy becomes unavoidable.

Let us summarize what we learned from the K-Mart case-study.

1) Until 1999-2000 there was a connection between Kmart's share price and its achievements as a discount retailer.

2) After October 2000, there is a one-year episode marked by a strong price rise due to a deal with a supplier which bears no relationship whatsoever with Kmart's performances.

3) The bankruptcy occurred when one of the major share holders withdrew its support. Although it is difficult to distinguish with certainty between cause and consequence, the question must be examined in the light of what happened subsequently, namely the fact that the corporation fell under the control of Lampert's hedge fund.

4) The 700% price increase between May 2003 and September 2004, that is to say after K-Mart had emerged from bankruptcy, was completely at variance with the evolution of Kmart's growth fundamentals.

Similar mechanisms are at work in many other cases. This is illustrated by the following example.

## 5 Converium

Converium (NYSE: CHR) is a Swiss reinsurer which ranks among the top 10 reinsurers and employs approximatively 850 people in 23 countries around the world. Why did I select Converium among many other possible cases? My attention was attracted to it because it experienced a sharp price fall in July 2004. Subsequently I discovered that one of our colleagues, econophysicist Michel Dacorogna, is a senior member of its Risk Modeling team; naturally, this further increased my interest in the company. The graph (Fig. 3) of its share price is particularly striking because it has been very stable during two years before dropping sharply by 50% on July 21, 2004. After this date it continued to fall albeit more slowly. As of September 23, 2004 its share price was as low as $ 7.80 which means that it had been divided by

[2] In late July 2004 Kmart actually sold 78 of its 2000 stores for about $ 1 billion.

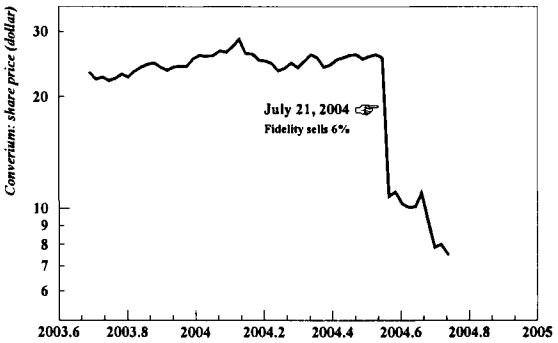


**Fig.3 Converium share price (September 2003 - September 2004.** Converium, a Swiss reinsurer began to be listed on the New York Stock Exchange in January 2002. From that date to mid-July 2004 its price remained within a fairly narrow margin of 25 ± 5 dollars. Then, on July 21, it suddenly dropped 50% after the company's announcement that it will have to increase its reserves. *Source: http://finance.yahoo.com.*

more than 4 with respect to the price level of January 2004. The comments offered by analysts in the wake of the fall of July 21 were not very convincing. They attributed the fall to a net loss amounting to 22% of its capitalization and to the fact that it had to strengthen its reserves by a similar amount. Although fairly serious, such a problem did not imperil the existence of the company especially because the loss was limited to its activity in the United States[3]. A more tangible explanation came two weeks later, on August 3 2004, in the form of the following statement made by the company:

> Converium Holding hereby informs that Fidelity International (based in Hamilton, Bermuda) has reduced its holding in Converium from 9.87% to 3.81%.

As is common in such announcements, it did not say when exactly Fidelity had sold its shares.

To what extent is it possible to generalize the results of these case-studies? One can give the following answers.

- The Kmart episode was not an isolated example. As a matter of fact, the strategy Lampert used at Kmart had been used previously in others of its acquisitions such as Autonation (NYSE:AN), America's largest retailer of new and used vehicles, Autozone (NYSE: AZO), Deluxe (NYSE: DLX) and finally Sears, Roebuck and Co (NYSE: S).
- The fact that an investment fund reduces its stake in a company to a considerable extent in a short time interval is relatively common. Table 2 gives a number

[3] As one of the main activities of Converium was the reassurance of airspace industries, it is possible that the loss was a consequence of 9/11.

of illustrations for FMR. Usually the growth fundamentals of a company do not change sharply in a few months which means that such massive sales (or purchases) pursued broader strategic objectives.

**Table 1 Effect on share prices of a change in holdings by Fidelity Management and Research (FMR)**

| | Date | Company | Ticker symbol | Initial stake [%] | Subsequent stake [%] | Price variation [%] |
|---|---|---|---|---|---|---|
| 1 | 2002 Dec. | Teradyne | NYSE:TER | 15 | 8.24 | −61 |
| 2 | 2003 Dec. | Delta Airlines | NYSE:DAL | 7.3 | 0.5 | −72 |
| 3 | 2003 Oct. | Forrester Research | NASDAQ:NM | 9.4 | 2.8 | −30 |
| 4 | 2004 Feb. | Boeing | NYSE:BA | 2.2 | 3.6 | 17 |

Notes: FMR is the world's largest investment fund with about one trillion dollar under management (which represents 10% of the US GDP in 2001). The price variation refers to the quarter during which the sales or purchases were made (we do not know the exact dates of the transactions). Earlier FMR moves include the reduction of its stake in (i) United Airlines from 6% to 2% (June 1994), (ii) Apple Computer from 11% to 2.5% (August 1995), (iii) Technology stocks (end of 1995), (iv) US Airways from 11.3% to 5.8% (May 1996), (v) Digital Equipment Corporation from 13.7% to 7% (June 1996), (vi) Chrysler Corporation from 12.2% to 7.8% (June 1996) Besides FMR there are several other mutual funds giants (e.g. Vanguard Group, Capital Research and Management, State Street) whose moves have substantial impacts on stock prices.
Sources: Boston Business Journal (Dec. 10 2002, Oct. 10 2003); Atlanta Business Chronicle (Dec. 19 2003); The News Tribune of Tacoma, Washington (Feb. 18 2004), New York Times (June 11 1994, January 12 1996, Aug. 15 1996); Wall Street Journal (Oct. 12 1995); USA Today (May 9 1996); Boston Herald (July 11 1996).

## 6 Conclusion

The main message of this paper is the observation that many of the major shocks to which companies are confronted are due to the moves of a small number of investment funds. In the case of Kmart we have seen that single investors played a central role in each of the three successive episodes which sealed the fate of the corporation between 2000 and 2004: first it was Burkle, then FMR and finally Lampert.

The key role played by major investment funds can be further illustrated by comparing the major holders of three airline companies, namely American Airlines, Delta Airlines, and US Airways. Two observations can be made.

1) Several institutional holders have a stake in both American and Delta. Examination of other airlines (e.g. Continental, NorthWest, Southwest) shows that these players also hold substantial stakes in those other airlines.

2) There is a fundamental difference between the major holders of American and Delta on the one hand and those of US Airways on the other. In the latter we do not find any major investment funds with a substantial (say over 1%) stake. Most of the shares are in the hands of the Alabama Retirement Fund which, through its links with Social Security, is probably partly funded by federal money. This striking difference is certainly to be attributed to the fact that US Airways went through bankruptcy in August 2002. As seen previously, stocks are likely to lose all their worth in a bankruptcy process. For major holders the main problem therefore is to be able to sell before the price has collapsed. Naturally, such tactics are double edged because the withdrawal of a major holder may drive down the market price to a point which makes bankruptcy ineluctable.

Fig. 4 shows that, since 1945, mutual funds experienced an exponential growth which was shortly interrupted only by the bear market of 1968-1978. As for any

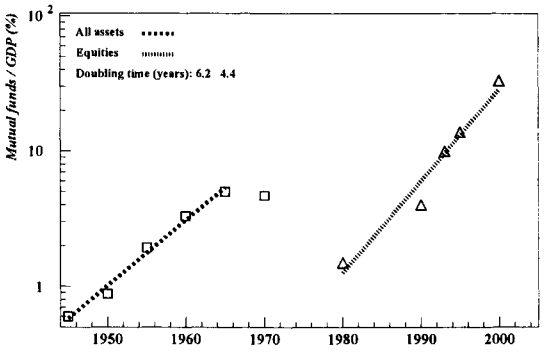


**Fig.4 Growth of American mutual funds compared to the growth of the US gross domestic product (1945-2000).** Between 1947 and 2000 the assets of mutual funds as a proportion of GDP have been multiplied by a factor of the order of 100. We had to rely on two different series because the pre-1970 data available in the Historical Statistics of the United States refer to total assets (i.e. stocks plus bonds), whereas the Statistical Abstract more specifi cally gives equity assets. Both trajectories are exponential. Naturally, mutual funds represent only one class (albeit the most important) of institutional share holders besides insurance companies, banks, state retirement funds, hedge funds, etc. *Source: Historical Statistics of the US (1975), Statistical Abstract of the US (various years).*

exponential growth, the beginnings were inconspicuous. It is only in recent years that mutual funds were able to get a firm grip on American stock markets. If this evolution continues the conception based on micro-players will become less and less relevant.

In a previous paper (Roehner 2005) it was shown that, through buyback programs, corporations can influence the price level of their own stock. In this paper we tried to scrutinize the economic rationale of the moves of major players. Such an approach is complimentary to the comprehensive macrodynamic analysis of market structure carried out by other researchers such as for instance Elroy Dimson et al. (2002), Rosario Mantegna et al. (2000) or Didier Sornette (2003). Finally, there is an important question which we did not consider and which should be addressed in a subsequent study. What is the kind of interaction between macro-players. Is it a competitive or cooperative linkage, or perhaps both depending on circumstances?

**Acknowledgements** I am most grateful to Stanislaw Drozdz, Olivier Gérard, Cornelia Küffner, Joseph MacCauley and Michel Dacorogna for their helpful comments.

## References

Common stock price histories 1910-1987. Logarithmic supplement (1988) WIT Financial Publishers. Morristown (New Jersey).

Dimson (E.), Marsh (P.), Staunton (M.) 2002: Triumph of the optimists: 101 years of global investment returns. Princeton University Press, Princeton.

Kotz (D.M.) 1978: Bank control of large corporations in the United States. University of California Press. Berkeley.

Mantegna (R.N.), Stanley (H.E.) 2000: An introduction to econophysics: correlations and complexity in finance. Cambridge University Press, Cambridge.

Roehner (B.M.) 2005: Stock markets are not what we think they are: the key roles of cross-ownership and corporate treasury stock. Physica A 347, 613-626.

Sornette (D.) 2003: Why stock markets crash: critical events in complex financial systems. Princeton University Press, Princeton.

# Conservative Estimation of Default Rate Correlations

Bernd Rosenow[1] and Rafael Weißbach[2]

[1] Institut für Theoretische Physik, Universität zu Köln, D-50937 Köln, Germany
[2] Institut für Wirtschafts- und Sozialstatistik, Universität Dortmund, D-44221 Dortmund, Germany

**Summary.** The risk of a credit portfolio depends crucially on correlations between the probability of default (PD) in different economic sectors. We present statistical evidence that a (one-) factorial model is sufficient to describe PD correlations, and suggest a method of parameter estimation which avoids in a controlled way the underestimation of correlation risk.

## 1 Introduction

A reliable forecast of losses is mandatory for the credit business of a bank. Modeling losses stochastically enables the focus on high quantiles denoted as Credit Value-at-Risk (CreditVaR). The difference between the CreditVaR and the expected loss needs to be covered by the economic capital of a bank. Diversification of credit risk is possible by distributing debt across different business sectors. However, correlations between sector PDs determine to which degree diversification is successful.

In CreditRisk+, concentration risk in industry sectors is modeled as a multiplicative random effect on the PD per counterpart in a given sector. Correlations between PD fluctuations in different sectors can be integrated into CreditRisk+ with the method of Bürgisser et al. [1]. For the calculation of the CreditVaR it is important whether input parameters like the correlation coefficients between sector PDs are known or must be estimated. In the latter case, this estimation leads to an additional variability of the target estimate, i.e. the portfolio loss. In this way, uncertainty in the estimation of PD correlations translates itself into uncertainty of the economic capital.

The estimation of cross-correlations is difficult if the length $T$ of the available time series is comparable to the number $K$ of industry sectors. In such a situation, the number of estimated correlations coefficients is of the same order as the number of input parameters, and estimation errors are large. The

use of a factor model with a reduced dimensionality of the parameter space is a way out of this dilemma. By using a test for the equivalence of the empirical correlation matrix to the unit matrix, we show that the PD correlations for $K = 20$ industry sectors are captured by a one-factor model. However, even the parameter estimation for a parsimonious model is subject to large statistical fluctuations. We suggest a method which allows to find an upper limit for these parameters, and briefly discuss the influence of different conservative estimates on the CreditVaR of a realistic portfolio.

## 2 Description of data set

As the economic activity and the probability of default in a given industry sector is not directly observable, we approximate it by the probability of insolvency $PD_{kt}$ of sector $k$ in year $t$

$$\hat{PD}_{kt} = \frac{\sum_{A \in \text{sector k in year t}} I_{\{A \text{ fails}\}}}{\sum_{A \in \text{sector k in year t}}} \quad . \tag{1}$$

With the help of insolvency rates, the default probability for a given company $A$ can be factorized into an individual expected PD $p_A$ and the sector specific relative PD movement $X_k$ with expectation $\langle X_k \rangle = 1$ according to $P(A \text{ fails}) = \mathrm{p_A X_k}$ with $\mathrm{X_{kt}} = \hat{\mathrm{PD}}_{\mathrm{kt}}/(\frac{1}{\mathrm{T}} \sum_{\mathrm{t}} \hat{\mathrm{PD}}_{\mathrm{kt}})$. For this study, we use sector specific default histories as supplied by the federal statistical office of Germany. We analyze default rates for $T = 7$ years for a segmentation of the economy into $K = 20$ sectors and assume stationarity of these default rates in the following. We estimate the sample correlation matrix as $C_{ij}^{\text{emp}} = \frac{1}{T-1} \sum_{t=1}^{T} (X_{it} - 1)(X_{jt} - 1)/\sigma_{X_i}\sigma_{X_j}$ with $\sigma_{X_i}$ denoting the standard deviation of $X_i$.

## 3 Test for independent sectors

We first ask whether the sample correlation matrix of the PD time series is compatible with the hypothesis of zero correlations. Ideas for testing this hypothesis for covariance matrices date back to the seventies [3], and were recently generalized to situations where the number of time series is larger than the sample size [4]. Here, we use an adaption of the tests [3, 4] to test for the equivalence of correlation matrix to the unit matrix. The test statistics

$$R = \frac{1}{K} \mathrm{tr}\left[\mathsf{C}^2\right] - 1 \ , \tag{2}$$

for a correlation matrix $\mathsf{C}$ is both $K$– and $T$–consistent with the $T$–limiting distribution $(T-1)KR/2 \xrightarrow{D} \chi^2_{K(K-1)/2}$ [5]. The prefactor $T - 1$ rather than $T$ is chosen to improve the finite $T$ properties of the test. For our example with

$T = 7$ and $K = 20$, we find $R = 5.805$, whereas the critical value for $\alpha = 0.05$ is $R_{\text{crit}} = 3.719$. Hence, the independence of sector PDs must not be assumed and a model describing sector correlations is needed.

## 4 Description of one–factor model

We diagonalize the empirical cross correlation matrix $\mathsf{C}^{\text{emp}}$ and rank order its eigenvalues $\lambda_{i,\text{emp}} < \lambda_{i+1,\text{emp}}$. As we are interested in modeling correlations rather than covariances, we normalize the $X_{it}$ such that they have the same, namely the average variance $\sigma_X^2 = (1/K)\sum_{i=1}^{K} \sigma_{X_i}^2$ and subtract the mean

$$\tilde{X}_{it} = (X_{it} - 1)\frac{\sigma_X}{\sigma_{X_i}} \quad . \tag{3}$$

We use the components of the eigenvector $\mathbf{u}_{\text{emp}}^{(K)}$ corresponding to the largest eigenvalue $\lambda_{K,\text{emp}} = 10.38$ to define a factor time series

$$Y_t = \sum_{i=1}^{K} u_{i,\text{emp}}^{(K)} \tilde{X}_{it} \quad . \tag{4}$$

In the context of stock returns, a time series defined according to the prescription of Eq. (4) was found to agree well with a value weighted stock index [6]. We expect that the factor time series Eq. (4) describes economy wide changes of relative PD.

We model the correlations between relative PD movements by a one–factor model

$$\tilde{X}_{it} = b_i Y_t + \epsilon_{it} \quad . \tag{5}$$

The coefficients $\{b_i\}$ are found by performing a linear regression. To see whether a one–factor model fully describes the correlations between the $\{\tilde{X}_{it}\}$, we apply the test Eq. (2) to the correlation matrix of the residuals $\{\epsilon_{it}\}$. Taking into account that the regression reduces the effective length of the residual time series from $T$ to $T - 1$, we find $R = 4.409$ slightly below the threshold $R_{\text{crit}} = 4.463$. As the assumption of uncorrelated residuals is not rejected, no further factors are needed for the description of correlations.

The point estimator can now be calculated under the assumption that the residua $\{\epsilon_{i,t}\}$ are iid random variables. Defining the factor variance $\sigma_Y^2 = \frac{1}{T-1}\sum_{t=1}^{T} Y_t^2$, one finds the point estimator for the cross correlation matrix as

$$C_{ij}^{\text{point}} = \delta_{ij} + (1 - \delta_{ij}) b_i b_j \sigma_Y^2 / \sigma_X^2 \quad . \tag{6}$$

The largest eigenvalue of $\mathsf{C}^{\text{point}}$ is found to be $\lambda_{K,\text{point}} = 10.66$ in good agreement with the original largest eigenvalue. In addition, the corresponding eigenvector $\mathbf{u}_{\text{point}}^{(K)}$ is found to be very close to the original eigenvector (Fig. 1a).

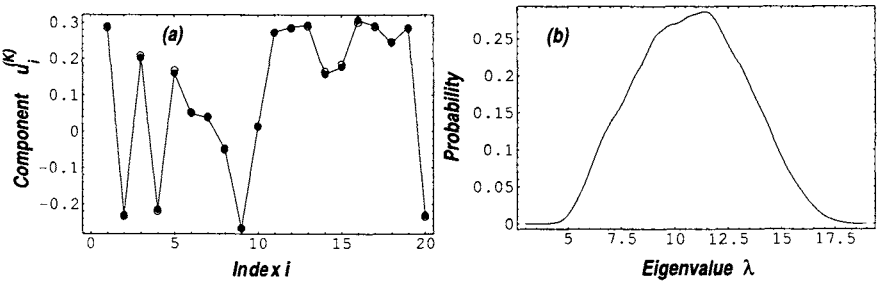


**Fig. 1.** (a) The components of the eigenvector $\mathbf{u}_{\text{emp}}^{(K)}$ of the empirical correlation matrix (connected full symbols) are almost identical to the components of the eigenvector $\mathbf{u}_{\text{point}}^{(K)}$ of the point estimator $\mathsf{C}^{\text{point}}$ (open symbols). (b) Distribution of the largest eigenvalue from simulations of a one–factor toy model with $\lambda_{K,\text{model}} = 10.38$ and $u_{i,\text{model}}^{(K)} \equiv 0.22$.

## 5 Fluctuations in empirical correlation matrices

By using the test statistic $R = \frac{1}{K}\text{tr}\left[\mathsf{C}^2\right] - 1$, we found that a one-factor model is both necessary and sufficient to reproduce the correlation structure of the empirical relative PDs. However, even for a one–factor model, the "true" correlation matrix $\mathsf{C}^{\text{model}}$ resulting from infinitely long model time series differs significantly from matrices $\mathsf{C}^{\text{sim}}$ numerically calculated from finite time series of length $T = 7$. We use Monte Carlo simulations to quantify the fluctuations of the ensemble of matrices $\mathsf{C}^{\text{sim}}$. Details of the simulations are described in [2]. We find that the largest eigenvalue of $\lambda_{K,\text{sim}}$ fluctuates strongly around the true $\lambda_{K,\text{model}}$ with a standard deviation $\sigma_\lambda = 2.42$ (Fig. 1b). Similarly, the components of the corresponding eigenvector $\mathbf{u}(K)_{\text{sim}}$ fluctuate around the value $\mathbf{u}(K)_{\text{model}}$ with a standard deviation $\sigma_u = 0.083$ (Fig. 2a).

## 6 Conservative Estimates

Using the empirical correlation matrix $\mathsf{C}^{\text{emp}}$, the bank risks that the correlations are "accidently" low. The most conservative approach would be to assume all correlations to be one, i.e. $u_i^{(K)} = \frac{1}{\sqrt{K}}\ \forall\ i$ and $\lambda_K = K$. As a controlled mediation we introduce "cases" of add-ons of $x = 1, 2, 3$ standard deviations to the fluctuating quantities such that the predicted risk for a portfolio is increased [2]. This means correcting the eigenvalue by $x$ standard deviations $\sigma_\lambda$ towards larger values and the eigenvector components by $x$ standard deviations $\sigma_u$ towards the value $u_i^{(K)} \equiv 1/\sqrt{K}$ indicating the same correlation strength for all sectors (see Fig.2).

To judge the economic implications of the various correlation estimates, we study the differences in the CreditVaR resulting from them for a realistic

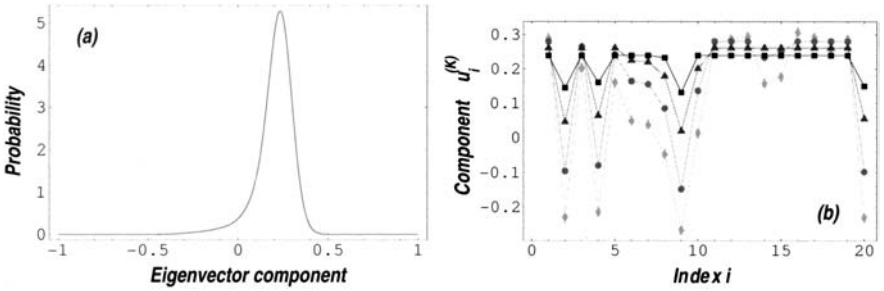


**Fig. 2.** (a) Distribution of the components of the eigenvector with the largest eigenvalue from simulations of a one–factor toy model with $\lambda_{K,\mathrm{model}} = 10.38$ and $u_{i,\mathrm{model}}^{(K)} = 0.22$. (b) Comparison between the empirical eigenvector $\mathbf{u}_{\mathrm{emp}}^{(K)}$ (diamonds) and the conservative estimates $\mathbf{u}_{1\sigma}^{(K)}$ (circles), $\mathbf{u}_{2\sigma}^{(K)}$ (triangles), and $\mathbf{u}_{3\sigma}^{(K)}$ (squares).

– although fictitious – portfolio of an international bank [2]. Using the CreditVaR without including any correlations as a reference point, we find that the CreditVaR increases by 26.5 % for $\mathrm{C}^{\mathrm{emp}}$, by 24.5 % for $\mathrm{C}^{\mathrm{point}}$, by 37.8 % for $\mathrm{C}_{1\sigma}^{\mathrm{model}}$, by 52.5 % for $\mathrm{C}_{2\sigma}^{\mathrm{model}}$, and by 61.5 % for $\mathrm{C}_{3\sigma}^{\mathrm{model}}$. In comparison, the assumption of full correlations between all business sectors leads to an increase of CreditVaR by 74.1 %. We find that the use of the two–$\sigma$ estimate guarantees a sufficient forecast reliability on the one hand and allows for some guidance for economical decision on the other hand.

## References


1. Bürgisser, P., A. Kurth , A. Wagner, and M. Wolf, *Integrating Correlations*, Risk, 07/1999.
2. B. Rosenow, R. Weißbach, and F. Altrock, eprint cond-mat/0401329 (2004).
3. John, C.,*Some optimal multivariate tests*, Biometrika **58**, 123-127 (1971).
4. Ledoit, O. and M. Wolf, *Some hypothesis tests for the covariance matrix when the dimension is large compared to the sample size*, Annals of Statistics **30**, 1081-1102 (2002).
5. B. Rosenow, to be published. For correlation matrices, the test statistics $R$ is equivalent to the statistics $W$ studied in [4]. $R$ has a limiting distribution $\chi^2_{K(K-1)}$ as compared to the limiting distribution $\chi^2_{K(K+1)}$ for $W$ as the diagonal elements of a correlation matrix are fixed and do not fluctuate.
6. P. Gopikrishnan, B. Rosenow, V. Plerou, and H.E. Stanley, *Quantifying and interpreting collective behavior in financial markets*, Phys. Rev. E **64**, 035106(R) (2001).

# Are Firm Growth Rates Random? Evidence from Japanese Small Firms

Yukiko Saito[1] and Tsutomu Watanabe[2]

[1] Fujitsu Research Insitute, 1-16-1 Kaigan, Minato-ku, Tokyo 105-0022, Japan saito@fri.fujitsu.com
[2] Institute of Economic Research, Hitotsubashi University, Kunitachi, Tokyo 186-8603, Japan tsutomu.w@srv.cc.hit-u.ac.jp

**Summary.** Anecdotal evidences suggest that a small number of firms continue to win until they finally acquire a big presence and monopolistic power in a market. To see whether such "winner-take-all" story is true or not, we look at the persistence of growth rates for Japanese small firms. Using a unique dataset covering half a million firms in each year of 1995-2003, we find the following. First, scale variables, such as total asset and sales, exhibit a divergence property: firms that have experienced positive growth in the preceding years are more likely to achieve positive growth again. Second, other variables that are more or less related to firm profitability exhibit a convergence property: firms with positive growth in the past are less likely to achieve positive growth again. These two evidences indicate that firm growth rates are not random but history dependent.

**Key words:** Firm growth; Gibrat's Law; history dependence; winner-take-all; persistence of growth

## 1 Introduction

It is often said that a small number of firms continue to win until they finally acquire a big presence and strong monopolistic power in a market. For example, "winner-take-all" is said to be an important phenomena observed in IT (information technology) related industries, in which technology-driven network externalities enable a small number of firms to acquire a dominant presence in markets. Also, at least partially due to developments in financial technology, more and more firms are now engaged in mergers and acquisitions, thereby contributing to the emergence of highly concentrated markets. Given this tendency, should we expect that each market will be monopolized in the near future? This is an important question to be addressed, partly be-

cause highly concentrated market structure might lead to less competition, and consequently to the deterioration of economic welfare.

Previous studies on firm growth give us some hint to think about this issue. Famous Gibrat's Law tells us that firm size evolves according to a random walk, so that there is no reason to believe that big firms grow faster than smaller ones. If this is true, what we currently observe in markets is just an illusion or, at best, a very short-life phenomena. More importantly, many of recent empirical studies, which tend to report results against Gibrat's Law, typically find that big firms grow *more slowly* than small ones, with an implication that firm size tend to converge over time to a common long-run level (See Sutton (1997) for an extensive survey). This is clearly against the winner-take-all story.

The purpose of this paper is to investigate whether firm growth rates are random or not. More specifically, we try to detect persistence in firm growth rates. The rest of this paper is organized as follows. Sections 2 and 3 explain our empirical strategy and data. Section 4 presents empirical results.

## 2 Empirical Strategy

The common model used to explain firms' growth rate is

$$\triangle x_{it} = \beta x_{it-1} + \epsilon_{it}, \tag{1}$$

where $x_{it}$ is the logarithm of the size of firm $i$ in period $t$, $\triangle x_{it}$ is the growth rate, which is defined by $\triangle x_{it} \equiv x_{it} - x_{it-1}$, $\beta$ is a parameter, and $\epsilon_{it}$ is a disturbance. This equation can be rewritten as

$$\triangle x_{it} = \epsilon_{it} + \beta\epsilon_{it-1} + \cdots + \beta(1+\beta)^{t-2}\epsilon_{i1} + \beta(1+\beta)^{t-1}x_{i0}. \tag{2}$$

It is straightforward to see that $x_{it}$ follows a random walk if (1) $\beta = 0$ and (2) $\mathrm{Cov}(\epsilon_{it}, \epsilon_{it-k}) = 0$. Put differently, we have

$$\Pr(\triangle x_{it} \mid \triangle x_{it-1}, \triangle x_{it-2}, \triangle x_{it-3}, \cdots) = \Pr(\triangle x_{it}) \tag{3}$$

if these two conditions are satisfied. In words, firm $i$'s growth rate in period $t$ does not depend on its past performance. However, if either of the two conditions is violated, equation (3) does not hold any more, and firm $i$'s growth rate in period $t$ depends on its past performance. This is what we call history dependence.

More specifically, we are interested in whether

$$\Pr(\triangle x_{it} \geq 0 \mid \triangle x_{it-1} \geq 0, \triangle x_{it-2} \geq 0, \cdots) = \Pr(\triangle x_{it} \geq 0) \tag{4}$$

$$\Pr(\triangle x_{it} < 0 \mid \triangle x_{it-1} < 0, \triangle x_{it-2} < 0, \cdots) = \Pr(\triangle x_{it} < 0) \tag{5}$$

hold or not. For example, if the conditional probability in equation (4) is smaller than the unconditional one, it implies "mean-reversion" or "convergence": those firms with positive growth in the past are more likely to turn to

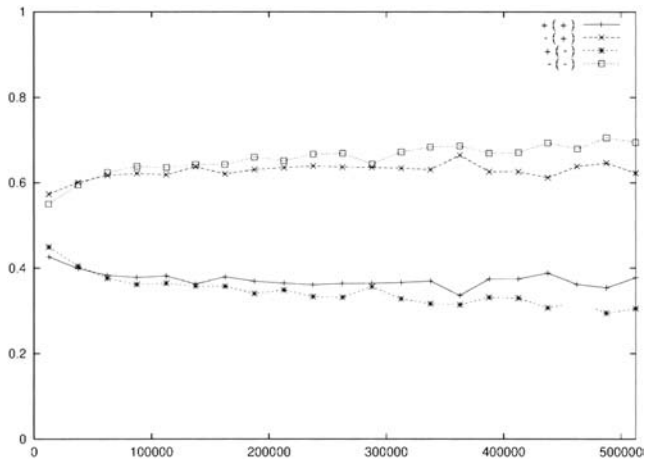


**Fig. 1.** Growth Rates of Total Assets in Two Consecutive Years

negative growth in period $t$. On the other hand, if the conditional probability is greater than the unconditional one in equation (4), it implies "trend movements" or "divergence": those firms with positive growth in the past are more likely to achieve positive growth again in period $t$, which is consistent with the winner-take-all story. In what follows, we will compare the conditional and unconditional probabilities to see whether or not the data supports such a story.

## 3 Data

The data we use are from the Credit Risk Database (CRD) collected by the CRD Association. The sample is well suited for our purposes; it consists of more than half a million incorporated enterprises of small size (i.e., about twenty employees per firm) in each year and covers the nine years of 1995-2003. Basic B/S and P/L information, which is reported by firms to their banks each year, is available for those small firms.

## 4 Empirical Results

### 4.1 Growth rates in two consecutive years

Fig. 1 looks at the relationship between the growth rates of total assets in 2001 ($\triangle x_{i01}$) and those in 2002 ($\triangle x_{i02}$). We classify firms into 21 categories depending on the amount of total assets, which is measured by the horizontal axis,

and calculate four conditional probabilities for each category: $\Pr(\triangle x_{i02} \geq 0 \mid \triangle x_{i01} \geq 0)$, represented by the line with "+"; $\Pr(\triangle x_{i02} \geq 0 \mid \triangle x_{i01} < 0)$, represented by the line with "$*$"; $\Pr(\triangle x_{i02} < 0 \mid \triangle x_{i01} \geq 0)$, represented by the line with "$\times$"; $\Pr(\triangle x_{i02} < 0 \mid \triangle x_{i01} < 0)$, represented by the line with "$\square$". The vertical axix measures probabilities.

It is seen that the line with "+" is almost always above the line with "$*$", implying that those firms with positive growth in 2001 are more likely to achieve positive growth again in 2002.[3] On the other hand, the line with "$\square$" is almost always above the line with "$\times$", implying that those firms with negative growth in 2001 are more likely to have negative growth again in 2002.

The divergence property observed in Fig. 1 is consistent with the "winner-take-all" story, but clearly not consistent with the results reported by the previous studies, which typically estimate $\beta$ in equation (1) under the assumption that $\mathrm{Cov}(\epsilon_{it}, \epsilon_{it-k}) = 0$, and find that $\beta$ is slightly smaller than zero. To compare our finding with those of the previous studies, observe that, under the assumption of $\mathrm{Cov}(\epsilon_{it}, \epsilon_{it-k}) = 0$, equation (1) implies

$$\mathrm{Cov}(\triangle x_{it}, \triangle x_{it-k}) = \frac{\beta(1+\beta)^{k-1}}{2+\beta}\sigma_\epsilon^2, \tag{6}$$

where $\sigma_\epsilon$ is the standard deviation of $\epsilon_{it}$. It is straightforward to see that $\mathrm{Cov}(\triangle x_{it}, \triangle x_{it-k})$ cannot be positive as long as $\beta \in (-1, 0]$. In this sense, our finding is against those of the previous studies. Our finding implies that the typical assumption adopted in the previous studies, $\mathrm{Cov}(\epsilon_{it}, \epsilon_{it-k}) = 0$, might not be appropriate, or their estimates of $\beta$ might be biased.[4]

### 4.2 Growth rates in five consecutive years

Table 1 extends the analysis to more than two years. The upper part of the table presents the unconditional and conditional probabilities for those firms with positive growth in 2000; namely, the second column shows the unconditional probability ($\Pr(\triangle x_{i00} \geq 0)$) and the third column shows the conditional probability $\Pr(\triangle x_{i00} \geq 0 \mid \triangle x_{i99} \geq 0)$, and the fourth column shows the conditional probability $\Pr(\triangle x_{i00} \geq 0 \mid \triangle x_{i99} \geq 0, \triangle x_{i98} \geq 0)$, and so on. The lower part of the table presents similar probabilities for those firms with negative growth in 1999.

Table 1 shows several important features. First, the conditional probability $\Pr(\triangle x_{i00} \geq 0 \mid \triangle x_{i99} \geq 0)$ is slightly lower than the corresponding unconditional probability, and similarly, the conditional probability $\Pr(\triangle x_{i00} < 0 \mid$

[3] If one looks at the two lines more closely, one finds that they overlap with each other for those firms with smaller total assets.

[4] Chesher (1979) is a notable exception in which $\beta$ is estimated allowing for the possibility of serial correlation of the disturbance term. Using 183 UK firms in 1960-1969, he finds that the disturbance term is positively autocorrelated ($E(\epsilon_{it}, \epsilon_{it-k}) > 0$), while the estimate of $\beta$ is close to zero.

**Table 1.** Multi-year history dependence: Total asset

| | $\Pr(+)$ | $\Pr(+ \mid +)$ | $\Pr(+ \mid ++)$ | $\Pr(+ \mid +++)$ | $\Pr(+ \mid ++++)$ |
|---|---|---|---|---|---|
| | 0.41878 | 0.41665 | 0.44522 | 0.47158 | 0.50012 |
| Error bar | | 0.00284 | 0.00441 | 0.00646 | 0.00869 |
| | $\Pr(-)$ | $\Pr(- \mid -)$ | $\Pr(- \mid --)$ | $\Pr(- \mid ---)$ | $\Pr(- \mid ----)$ |
| | 0.58122 | 0.57942 | 0.60377 | 0.64643 | 0.69962 |
| Error bar | | 0.00261 | 0.00341 | 0.00497 | 0.00742 |

$\triangle x_{i99} < 0$) is slightly higher than the corresponding unconditional probability. These results imply a convergence property, but the differences between the conditional and unconditional probabilities are not substantial, and in fact not statistically significant.[5]

Second, the conditional probability $\Pr(\triangle x_{i00} \geq 0 \mid \triangle x_{i99} \geq 0, \triangle x_{i98} \geq 0)$ is higher than the corresponding unconditional probability, implying that those firms with positive growth in two consecutive years are more likely to achieve positive growth again in the third year. Similarly, we see that those firms with negative growth in two consecutive years are more likely to experience negative growth again in the third year.

Third, the conditional probability of positive growth is higher for those firms experiencing positive growth for a longer period: namely, firms with three consecutive positive growth are more likely to achieve positive growth again than those with two consecutive positive growth, and similarly, firms with four consecutive positive growth are more likely to experience positive growth than those with three consecutive growth. The second and third findings strongly suggest that the data is consistent with the winner-take-all story.

### 4.3 Growth rates in terms of various measures

Tables 2 and 3 repeat the same exercise as we did in Table 1, but now we use two different variables: firm sales and firm profits. Table 2 shows that firm sales exhibit a divergence property that is similar to what we observed for total assets: positive (negative) growth is more likely to occur for those firms with positive (negative) growth in the preceding years. On the other hand, Table

[5] Error bars in table 1 are calculated as follows. Denote the total number of occurrences of the event $\triangle x_{it-1} \geq 0$ by $n_1$. If the event $\triangle x_{it} \geq 0$ occurs totally independently of past events (in particular, independently of the event $\triangle x_{it-1} \geq 0$), the number of occurrences of $\triangle x_{it} \geq 0$ obeys a binomial distribution whose mean and variance are given by $n_1 \Pr(\triangle x_{it} \geq 0)$ and $n_1 \Pr(\triangle x_{it} \geq 0)(1 - \Pr(\triangle x_{it} \geq 0))$, where $\Pr(\cdot)$ represents an unconditional sample mean. Then the error bar for $\Pr(+ \mid +)$ is defined by $[\Pr(\triangle x_{it} \geq 0)(1 - \Pr(\triangle x_{it} \geq 0))/n_1]^{1/2}$. Similarly, the error bar for $\Pr(+ \mid ++)$ is given by $[\Pr(\triangle x_{it} \geq 0 \mid \triangle x_{it-1} \geq 0)(1 - \Pr(\triangle x_{it} \mid \triangle x_{it-1} \geq 0))/n_2]^{1/2}$, where $n_2$ represents the number of occurrences of the event $\triangle x_{it-1} \geq 0$ and $\triangle x_{it-2} \geq 0$. Other error bars are calculated in a similar way.

**Table 2.** Multi-year history dependence: Firm sales

| | $\Pr(+)$ | $\Pr(+ \mid +)$ | $\Pr(+ \mid ++)$ | $\Pr(+ \mid +++)$ | $\Pr(+ \mid ++++)$ |
|---|---|---|---|---|---|
| | 0.44894 | 0.44097 | 0.48341 | 0.53885 | 0.58402 |
| Error bar | | 0.00329 | 0.00546 | 0.00770 | 0.01061 |
| | $\Pr(-)$ | $\Pr(- \mid -)$ | $\Pr(- \mid --)$ | $\Pr(- \mid ---)$ | $\Pr(- \mid ----)$ |
| | 0.55106 | 0.54683 | 0.55443 | 0.60868 | 0.67304 |
| Error bar | | 0.00240 | 0.00290 | 0.00436 | 0.00672 |

**Table 3.** Multi-year history dependence: Firm profits

| | $\Pr(+)$ | $\Pr(+ \mid +)$ | $\Pr(+ \mid ++)$ | $\Pr(+ \mid +++)$ | $\Pr(+ \mid ++++)$ |
|---|---|---|---|---|---|
| | 0.53415 | 0.42148 | 0.36042 | 0.34043 | 0.35099 |
| Error bar | | 0.00280 | 0.00389 | 0.00601 | 0.01012 |
| | $\Pr(-)$ | $\Pr(- \mid -)$ | $\Pr(- \mid --)$ | $\Pr(- \mid ---)$ | $\Pr(- \mid ----)$ |
| | 0.46585 | 0.36140 | 0.31090 | 0.28990 | 0.29349 |
| Error bar | | 0.00270 | 0.00303 | 0.00425 | 0.00663 |

3 shows that firm profits exhibit a convergence property: positive (negative) growth is less likely to occur for those firms with positive (negative) growth in the preceding years. Such a convergence property is observed for other variables, such as ROA (return on assets), probability of defaults, interest payments, that are more or less related to firm profitability (Not reported here). These two contrasting evidences seem to suggest that it is possible for firms to grow in terms of scale variables (such as total asset or firm sales) if they want to so, but larger scale operation does not necessarily guarantee higher profitability.

## Acknowledgement

We would like to thank Hideki Takayasu and Mitsuru Iwamura for helpful comments and suggestions.

## References

1. Chesher, A. 1979. "Testing the law of proportionate effect." Journal of Industrial Economics 27: 403-411.
2. Sutton, J. 1997. "Gibrat's legacy." Journal of Economic Literature 35: 40-59.

# Trading Volume and Information Dynamics of Financial Markets

S.G. Redsun, R.D. Jones, R.E. Frye, and K.D. Myers

CommodiCast, 552 Agua Fria, Santa Fe, NM 87501, USA

**Summary.** We describe a new financial diagnostic method, related to the entropy generated when a limit trader satisfies market demand by filling orders, thereby playing the role of a Maxwell Demon. By comparing the real cumulative trading volume to some measure of historically "normal" demand, one may determine whether the market shows excess order or disorder, and accordingly adjust one's trading strategy.

**Key words.** Entropy, Maxwell Demon, Trading volume

## Introduction

Information-theoretical analysis of financial markets has historically focused on prices. The Efficient Market Hypothesis states that all information about a stock or a market is contained in its price. Since every trader has access to the current stock price, no trader has an advantage in predicting future prices.

In our model, we consider the information contained not in prices but in volume, the number of shares traded or offered for trade. While trading volume and price are not independent (they are related through liquidity or price impact), volume is more directly related than price to supply and demand for orders, and can be expressed in familiar probability measures from information theory. In particular, we make an econophysical analogy between financial markets and the Maxwell Demon.

## Analogy with the Maxwell Demon

In the Maxwell Demon thought experiment, an intelligent "demon" observes particles moving in a box with two chambers separated by a trapdoor. The Demon collects fast particles in one chamber and slow particles in the other by opening or closing the trapdoor as each particle approaches. While the order created by the Demon seems to violate the Second Law of Thermodynamics, in fact the stream of

information collected by the Demon in determining whether to open or close the trapdoor more than offsets this.

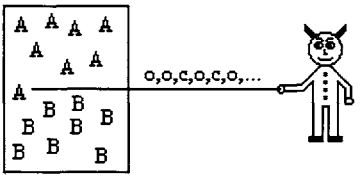


**Fig. 1.** The Maxwell Demon in thermodynamics. The Demon sorts molecules of gases A and B, generating a stream of information. There are four molecule states: (A, top), (A, bottom), (B, top), (B, bottom), and two sorting operations: (open, close).

In our idealized model of a financial market, market orders play the role of particles, and a limit trader plays the role of the Demon. By placing limit orders at meaningful prices that add liquidity to the market, the limit trader effectively sorts market orders into filled and unfilled states, analogous to the chambers of the box. The limit trader creates order in the market while generating excess entropy in the universe.

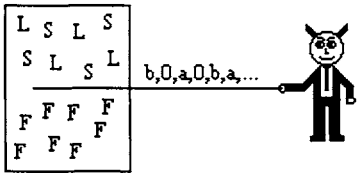


**Fig. 2.** The Maxwell Demon in financial trading. Limit traders sort market orders by placing bids and asks. There are three order states (long, short, filled) and three sorting operations (bid, ask, do nothing).

## Idealized Stock Market Model

Consider an idealized stock market in which:

1. Supply and demand vary in time according to the quantity of unfilled short and long market orders present.
2. A single limit trader fills all market orders. The market is efficient, so the limit trader knows the proper stock price (to within the bid-ask spread).

In our model, at the beginning of a trading day there are N unfilled market orders (N/2 short, N/2 long) waiting to be filled. At any subsequent time, the limit

trader observes a market order and places either a bid or ask to fill it (if unfilled), or no order (if already filled). By the end of the day, all N market orders are filled.

We have shown elsewhere (Jones et al. 2004) that the market's entropy change over the trading day is -N. The market becomes more ordered by 1 bit per market order filled, as expected. The corresponding increase in entropy of the limit trader is $(1 + \eta^*)N$, where

$$\eta^* = \pi^2 / (6 \ln 2) \approx 2.37 \text{ bits/order.} \quad (1)$$

This excess entropy generation (information collection) is identical to the minimum increase in entropy for sorting initially anti-sorted particles in the Maxwell Demon problem (Jones et al. 2003). This result is surprising, as the two systems (particles v. market) are physically unrelated and have a different number of states and sorting operations.

## Practical Implementation

The essence of this diagnostic method is tracking the cumulative trading volume v. time, and comparing it to a standard reference. As a simple example, when the trading volume exceeds that predicted for constant demand, the market is relatively ordered, otherwise it is relatively disordered.

In real trading, we do not expect orders to arrive at a constant rate. Markets are most active at the open and close of trading. There are flurries of trading in response to financial news. Traders may place an excess of long or short orders during runs. Hence a more realistic diagnostic should compare the cumulative trading volume to a "normal" day or intraday interval.

We have developed trading strategies that use various pattern recognition techniques to detect meaningful volume dynamics, but the details are beyond the scope of this article. In summary, trading volume reveals useful information about the order or disorder of financial markets, providing a valuable complement to conventional predictive models based on price history.

## References

Jones RD, Redsun SG, Frye RE (2003) Entropy of Sorting and Control I: The Maxwell Demon, Complexica Report 030729a

Jones RD, Redsun SG, Frye RE, Myers KD (2004) Minimal Information Required to Fill Orders in a Financial Market, Complexica Report 040111

# Random Matrix Theory Applied to Portfolio Optimization in Japanese Stock Market

Masashi Egi[1], Takashi Matsushita[2], Seiji Futatsugi[2], and Keizaburo Murakami[3]

[1]Hitachi, Ltd., Central Research Laboratory, 1-280, Higashi-koigakubo, Kokubunji-shi, Tokyo 185-8601, Japan
[2]Hitachi, Ltd., Business Solution Systems Division, Hitachi Systemplaza, Shin-kawasaki, 890 Kashimada, Saiwai, Kawasaki, Kanagawa, 212-8567, Japan
[3]QUICK Corp., 2-2-20 Toyo, Koto-ku, Tokyo 135-8386, Japan

**Summary.** We examined the effectiveness of random matrix theory applied to portfolio optimization using Japanese stock market data. We carried out 48 back tests for different historical periods and confirmed that it was possible to drastically improve the accuracy of portfolio risk evaluation using random matrix theory.

**Key words.** random matrix theory, portfolio optimization, cross-correlation

## Introduction

Portfolio optimization is one of the most important and fundamental problem in finance. According to Markowitz theory, a portfolio is optimized by minimizing the predicted risk using the cross-correlation matrix of stock returns (Markowitz 1959). Conventionally, the matrix has been directly calculated from historical data. However, recent studies of random matrix theory (RMT hereafter) have revealed that such a cross-correlation matrix is heavily contaminated with noise (Bouchaud et al. 2000, Laloux et al. 1999a, Plerou et al. 2001, Plerou et al. 2002, Utsugi et al. 2003), which causes a substantial margin of error in risk prediction (Bouchaud et al. 2000, Laloux et al. 1999b, Plerou et al. 2002, Rosenow et al. 2002). Noise reduction methods applying RMT have also been proposed and the effectiveness in portfolio optimization has been shown in some examinations of the European and US stock markets (Bouchaud et al. 2000, Laloux et al. 1999b, Plerou et al. 2002, Rosenow et al. 2002, Pafka et al. 2004). In this paper, we comprehensively verified the effectiveness of RMT applied to portfolio optimization in the Japanese stock market.

## Portfolio Optimization Theory

A portfolio is defined by the fraction of money to be invested into each stock $x_i$ where $i$ runs over $N$ different stocks. The predicted return $R(\boldsymbol{x})$ and risk $S(\boldsymbol{x})$ of the portfolio in the investment interval $T$ are given by

$$R(\boldsymbol{x},\boldsymbol{m}) = \frac{T}{\Delta t}\sum_{i=1}^{N} x_i m_i \tag{1}$$

$$S(\boldsymbol{x},\sigma,\boldsymbol{C}) = \left\{\frac{T}{\Delta t}\sum_{i=1}^{N}\sum_{j=1}^{N} x_i x_j \sigma_i \sigma_j C_{ij}\right\}^{\frac{1}{2}} \tag{2}$$

where $\boldsymbol{m}$, $\sigma$ and $\boldsymbol{C}$ are parameters which describe the average, standard deviation, and cross-correlation of the relative price change of stocks at every time interval $\Delta t$, respectively (Markowitz 1959, Rosenow et al. 2002). These parameter values are predicted for the investment interval.

The portfolio optimization problem is to solve on $\boldsymbol{x}$, which minimizes $S(\boldsymbol{x},\sigma,\boldsymbol{C})$ under the constraints $R(\boldsymbol{x},\boldsymbol{m}) = r$ and $\sum_{i=1}^{N} x_i = 1$. With the aid of Lagrange's undetermined multiplier method, we can easily obtain the optimal portfolio $\boldsymbol{x} = \tilde{\boldsymbol{x}}(r,\boldsymbol{m},\sigma,\boldsymbol{C})$ and the predicted minimum risk $S\left(\tilde{\boldsymbol{x}}(r,\boldsymbol{m},\sigma,\boldsymbol{C}),\sigma,\boldsymbol{C}\right)$.

The realized return and risk of the optimal portfolio in the actual investment interval can be written as $R\left(\tilde{\boldsymbol{x}}(r,\boldsymbol{m},\sigma,\boldsymbol{C}),\boldsymbol{m}'\right)$ and $S\left(\tilde{\boldsymbol{x}}(r,\boldsymbol{m},\sigma,\boldsymbol{C}),\sigma',\boldsymbol{C}'\right)$, where $\boldsymbol{m}'$, $\sigma'$ and $\boldsymbol{C}'$ are the realized values in the actual investment interval. Then, each gap between predicted and realized values for return and risk are understood as prediction errors.

In order to accurately predict the return and risk of a portfolio, we need the accurate values of $\boldsymbol{m}$, $\sigma$ and $\boldsymbol{C}$ beforehand. Of these, $\boldsymbol{C}$ has been directly calculated usign the following familiar formula

$$C_{ij} = \frac{\left\langle G_i(t)G_j(t)\right\rangle_t - \left\langle G_i(t)\right\rangle_t \left\langle G_j(t)\right\rangle_t}{\sqrt{\left\langle G_i(t)^2\right\rangle_t - \left\langle G_i(t)\right\rangle_t^2}\sqrt{\left\langle G_j(t)^2\right\rangle_t - \left\langle G_j(t)\right\rangle_t^2}} \tag{3}$$

where $G_i(t)$ is past time-series data for relative price change of stock $i$ in every time interval $\Delta t$ and $\langle\ \rangle_t$ indicates a temporal average. However, there has been a problem that even if $\boldsymbol{m} = \boldsymbol{m}'$ and $\sigma = \sigma'$, $\boldsymbol{C}$ calculated by eq.(3) causes a large gap between the predicted and realized risk. Recently, the RMT has revealed that $\boldsymbol{C}$ calculated by eq.(3) is heavily contaminated with noise, causing the problem described below.

## Random Matrix Theory

We start from a null hypothesis that all stock price changes are purely independent of each other and consider a cross-correlation matrix calculated by eq.(3) using the time-series data of length $L$. According to RMT, in the limit $N, L \to \infty$ with

$Q = L/N \geq 1$ is fixed, the density function of eigen values $\lambda$ of the matrix can be explicitly written as follows (Bouchaud et al. 2000, Laloux et al. 1999b, Plerou et al. 2002, Rosenow et al. 2002)

$$\rho(\lambda) = \frac{Q}{2\pi} \frac{\sqrt{(\lambda - \lambda_-)(\lambda_+ - \lambda)}}{\lambda} \tag{4}$$

$$\lambda_\pm = 1 + \frac{1}{Q} \pm 2\sqrt{\frac{1}{Q}} \tag{5}$$

There is a critical upper bound $\lambda_+$ on $\lambda$. Therefore the range $\lambda < \lambda_+$ can be understood as a noise-level region, and $\lambda_+ < \lambda$ can be understood as a signal-level region.

We plotted two eigen value distributions in figure 1. One is the observed distribution of a cross-correlation matrix calculated by eq.(3) using actual past data from the Japanese stock market, and the other is the RMT distribution given by eq.(4). We can see from the figure 1 that the overwhelming majority of the observed eigenvalues are found in the noise-level region. We can therefore understand that this noise is the root cause of risk prediction error.

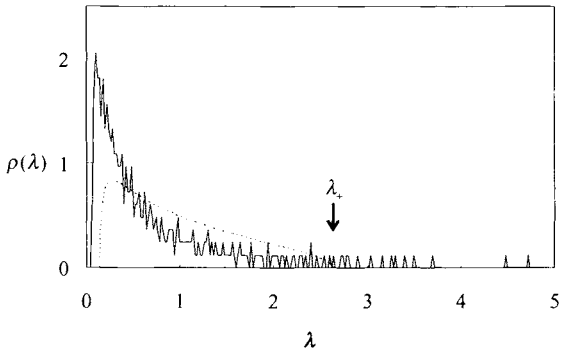


**Fig. 1.** Eigenvalue distributions of cross-correlation matrices. The dashed line is distribution given by eq.(4). The solid line is distribution of observed cross-correlation matrix using real stock price data from Tokyo Stock Exchange from July 16, 2001 to January 15, 2002. Assuming $\Delta t = 30$ minutes corresponding to $L = 1079$, we selected $N = 414$ stocks with high liquidity whose data deficient rates were less than 1%.

Noise reduction methods applying RMT have previously been proposed (Bouchaud et al. 2000, Laloux et al. 1999b, Plerou et al. 2002, Rosenow et al. 2002, Pafka et al. 2004), and the simplest one is as follows (Rosenow et al. 2002). First, we perform eigenvalue decomposition of $\boldsymbol{C}$, that is, $\boldsymbol{C} = \boldsymbol{P}\Lambda\boldsymbol{P}^t$, $\Lambda = \mathrm{diag}(\lambda_1, \cdots, \lambda_N)$ where $\lambda_1 < \cdots < \lambda_N$. Second, we eliminate noise-level eigenvalues from $\Lambda$ and define $\tilde{\Lambda} = \mathrm{diag}(0, \cdots, 0, \lambda_k, \cdots, \lambda_N)$, where $\lambda_{k-1} < \lambda_+ < \lambda_k$. Finally, we obtain the noise-reduced cross-correlation matrix $\tilde{\boldsymbol{C}}$ constructed by $\tilde{\boldsymbol{C}} = \boldsymbol{P}\tilde{\Lambda}\boldsymbol{P}^t$ setting the diagonal elements to one. The effectiveness of this noise-reduction method in portfolio optimization is explained in the next section.

## Verification of Effectiveness

We carried out 48 back tests for different historical periods shifting a time-window, using actual past data of the Japanese stock market, and compared the accuracy of risk prediction methods using matrices before and after noise reduction. We set the time-window to 12 months, and considered the first and second 6 months as virtual past and future. Using the virtual past data, we obtained optimal portfolios and their predicted risks using each method. Then, using the virtual future data, we evaluated the realized risks for each optimal portfolio. To quantify the accuracy of each method, we defined error ratios at $r = 1$ as

$$\varepsilon_{\text{before}} = \frac{S\left(\tilde{x}(1,\boldsymbol{m},\sigma,\boldsymbol{C}),\sigma,\boldsymbol{C}'\right) - S\left(\tilde{x}(1,\boldsymbol{m},\sigma,\boldsymbol{C}),\sigma,\boldsymbol{C}\right)}{S\left(\tilde{x}(1,\boldsymbol{m},\sigma,\boldsymbol{C}),\sigma,\boldsymbol{C}\right)} \tag{6}$$

$$\varepsilon_{\text{after}} = \frac{S\left(\tilde{x}(1,\boldsymbol{m},\sigma,\tilde{\boldsymbol{C}}),\sigma,\boldsymbol{C}'\right) - S\left(\tilde{x}(1,\boldsymbol{m},\sigma,\tilde{\boldsymbol{C}}),\sigma,\boldsymbol{C}\right)}{S\left(\tilde{x}(1,\boldsymbol{m},\sigma,\tilde{\boldsymbol{C}}),\sigma,\boldsymbol{C}\right)} \tag{7}$$

The results we obtained are plotted in figure 2. The average error ratios before and after noise reduction are 1.51 and 0.69, respectively. We confirmed that the optimization method using matrices after noise reduction always reduces the error ratio to about 80% compared to the method using matrices before noise reduction.

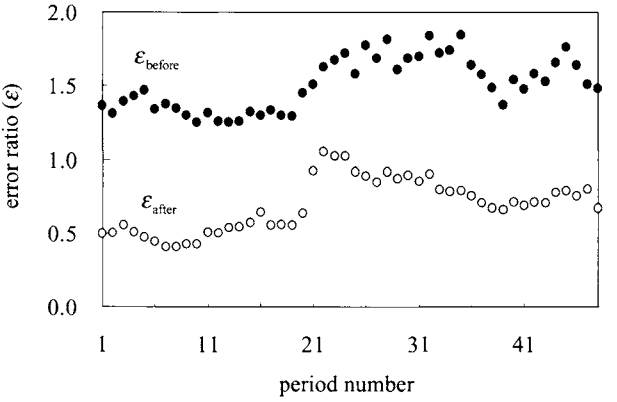


**Fig. 2.** Error ratios before and after noise reduction. The solid and open circles represent error ratios before and after noise reduction for each period. We carried out examinations shifting the time-window by one week using real market data from July 16 2001 to July 11 2003. We set $\Delta t = 30$ minutes corresponding to $L \sim 1000$ by average and selected $N = 414$ stocks with high liquidity whose data deficient rates were less than 1%.

## Conclusion

We examined the effectiveness of RMT applied to portfolio optimization using Japanese stock market data. We carried out 48 back tests for different historical periods and confirmed that it was possible to dramatically improve the accuracy of portfolio risk evaluation using RMT. Therefore, RMT may have a great deal of potential to improve risk management and portfolio optimization for various kinds of financial assets.

## References


Bouchaud J.P. and Potters M., Theory of Financial Risks, Cambridge University Press, Cambridge (2000)

Laloux L., Cizeau P., Bouchaud J.P. and Potters M., Phys. Rev. Lett., 83, No7, 1467-1470 (1999a)

Laloux L., Cizeau P., Bouchaud J.P. and Potters M., Risk 12, No.3, 69, (1999b)

Markowitz H., Portfolio Selection, J. Wiley and Sons, New York (1959)

Pafka S., Potters M., Kondor I., preprint cond-mat/0402573 (2004)

Plerou V., Gopikrishnan P, Rosenow B, Amaral L.A.N., Stanley H.E., Physica A, 299, No.1-2, 175-180 (2001)

Plerou V., Gopikrishnan P, Rosenow B, Amaral L.A.N., Guhr T., Stanley H.E., Phys. Rev. E65, 066126 (2002)

Rosenow B., Plerou V., Gopikrishnan P. and Stanley H.E., Europhys. Lett., 59, 500-506 (2002)

Utsugi A., Kazusumi I., Oshikawa M., preprint cond-mat/0312643 (2003)

# Growth and Fluctuations for Small-Business Firms

Yoshi Fujiwara[1], Hideaki Aoyama[2], and Wataru Souma[1]

[1] ATR Network Informatics Laboratories, Kyoto 619-0288, Japan
yfujiwar@atr.jp, souma@atr.jp
[2] Graduate School of Science, Kyoto University, Kyoto 606-8501, Japan
aoyama@phys.h.kyoto-u.ac.jp

**Summary.** Small-business firms have qualitatively different characteristics of firm-size growth from those for large firms. Credit Risk Database (CRD) is the largest database of japanese small and midsize companies, which covers nearly 1 million small-business firms, more than 60% of all companies in Japan. By employing stock (total assets and debts) and flow (sales) quantities in the CRD, we show that Gibrat's law breaks down for the small and midsize companies corresponding to non-power-law region, while the law asymptotically holds in the larger-size region, for all the variables examined. In fact, standard deviation $\sigma$ of logarithmic growth rate $r = \log R = \log(x_2/x_1)$ (where $x_1$ and $x_2$ are the variable for two successive years) scales as firm size becomes larger ($\sigma \propto x_1^{-\beta}$), but asymptotically approaches non-scaling regime ($\sigma \sim$ const). We also show that there is scaling relation of growth rates for different time-scales with which one observes firm-size. Standard deviation $\sigma$ of growth rate $r = \log R = \log(x_{t+\Delta t}/x_t)$ from time $t$ and $t + \Delta t$ scales as $\sigma \propto (\Delta t)^{-\gamma}$.

**Key words.** company growth, Pareto-Zipf distribution, Gibrat law, scaling relation

## Introduction

Financing small-business firms is one of the biggest financial problems in Japan. The problem concerns about how a financial institution should finance small and midsize companies with an appropriate interest rate for a duration of period. Although this is a fundamental issue for any financial sector, japanese institutions have been lacking an applicable database for quantitative study.

Credit Risk Database (CRD) is a database of about one million japanese small-business firms. This is the largest database for small and midsize companies, which covers more than 60% in the year 2001, for example. Small-business firms have qualitatively different characteristics of firm-size growth from those for large firms. It was found, for example, that Gibrat's law (growth rate is independent of starting size) does not hold, i.e. smaller firms have larger vari-

ation in their growth (Stanley et al. 1996, Amaral et al. 1997, Amaral et al. 1998, Mizuno et al. 2002, Aoyama et al. 2004).

As a first step to state the financing problem in a quantitative way for small-business firms, we examine the growth process of such firms by employing the CRD and by examining stock and flow variables in financial statements. In this paper, due to the limit of space, we focus on the empirical facts about growth rates as overall cross-sectional data for all business-sectors and geographical regions.

## Small and midsize companies

According to survey by statistics bureau of a japanese ministry, the number of japanese companies is approximately 1.6 million in the year 2001. Data in the CRD is sampled annually by credit guarantee association, government-affiliated institutions and private-sector financial institutions all over Japan since the year 1997. It mainly covers small and midsize companies, the definition of which can be stated as follows, basically in accordance with the japanese Small and Medium Enterprise Basic Law; either the capital (when established) or the number of employees is less than a threshold. The threshold depends on the business-sector to which the company belongs. For wholesales, the threshold of capital is 0.1 billion yen, and that of employees number is 100. For retails, 50 million and 50. For services, 50 million and 100. And for manufacturing and other sectors, 0.3 billion and 300. The data coverage is more than 60 % of such companies in the year 2001. The database includes financial statements, non-financial facts (establishment etc.) and default facts. We used only those firms that satisfy the threshold conditions for analysis.

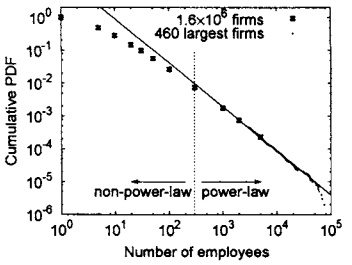


**Fig. 1.** Cumulative probability distribution of japanese firm-size in the year 2001. The squares correspond to a tabulated data by sample survey (Establishment and Enterprise Census 2001 by Ministry of Internal Affairs and Communications). The dots show an exhaustive list of largest 460 firms (database by Diamond, Inc.). The line is simply a guide for eyes with $\mu = 1.34$ in the power-law $P_>(x) \propto x^{-\mu}$.

Firm size distribution with respect to the number of employees is depicted in Fig. 1. One can observe that there exists a transition from non-power-law regime to power-law regime (cf. Stanley et al. 1995, Hart and Oulton 1997,

Takayasu and Okuyama 1998, Axtell 2001). The transition occurs at around several hundreds in terms of the number of employees. The CRD, therefore, covers the non-power-law regime and the transition region[3]. While company growth in the power-law regime has been extensively studied (see Steindl 1965, Stanley et al. 1996, Amaral et al. 1997, Amaral et al. 1998, and more recent works, Mizuno et al. 2002, Aoyama et al. 2003, Fujiwara et al. 2004), little has been known for the growth and fluctuations for small-business firms.

## Growth and fluctuations

Let $x$ be a quantity that measures firm size (such as total-assets and sales), and $x_1$ and $x_2$ be the quantities measured at two successive years. The joint probability $P(x_1, x_2)$ is shown in Fig. 2. It can be observed that detailed-balance condition holds approximately in the sense that $P(x_1, x_2) = P(x_2, x_1)$. This means that the empirical probability for a firm to change its size from a value to another is statistically the same as that for its reverse process in the ensemble.

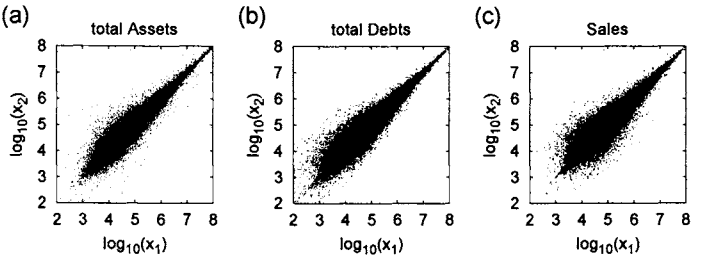


**Fig. 2.** Scatter plots corresponding to joint probabilities $P(x_1, x_2)$ for total-assets (a), total-debts (b) and sales (c). The values of $x_1$ and $x_2$ are in units of $10^3$ yen.

Our concern is the annual change of individual firm-size, namely its growth. Growth rate is defined as $R = x_2/x_1$. It is customary to use the logarithm of $R$, $r \equiv \log_{10} R$. We examine the probability density for the growth rate $P(r|x_1)$ on the condition that the size $x_1$ in an initial year is fixed. If $P(r|x_1)$ does not depend on $x_1$, it is said that Gibrat's law holds (see Sutton 1997). For large firms in the power-law regime, we showed in Fujiwara et al. 2004 (see also Aoyama et al. 2003 for firm-income) that Gibrat's law holds and that Gibrat's law implies the existence of power-law in the firm-size distribution under the detailed-balance condition. However, for small and midsize ones, Gibrat's law was shown to break down for total-assets (Aoyama et al. 2004).

[3] In what follows, we shall examine stock quantities of total assets and total debts, and flow quantity of sales. We verified the existence of strong correlation between each of these quantities and the number of employees. Especially, the range of each such quantity corresponds to the range of the number of employees approximately coinciding to the non-power-law regime and the transition region.

Fig. 3 (a)–(c) shows the breakdown of Gibrat's law by depicting the probability density function $P(r|x_1)$ for logarithmic growth rate $r$. The probability density has explicit dependence on $x_1$ showing the breakdown of Gibrat's law. In order to quantify the dependence, we examine how the standard deviation of $r$ in the ensemble defined in each bin of $x_1$ scales as $x_1$ becomes larger. Let the standard deviation of $r$ be denoted by $\sigma$. Fig. 3 (d)–(f) shows that $\sigma$ scales as a function of $x_1$ ($\sigma \propto x_1^{-\beta}$), but asymptotically approaches non-scaling regime ($\sigma \sim$ const). The breakdown of Gibrat's law in the non-power-law regime and its holding in the power-law regime are consistent with what we showed in our work (Fujiwara et al. 2004).

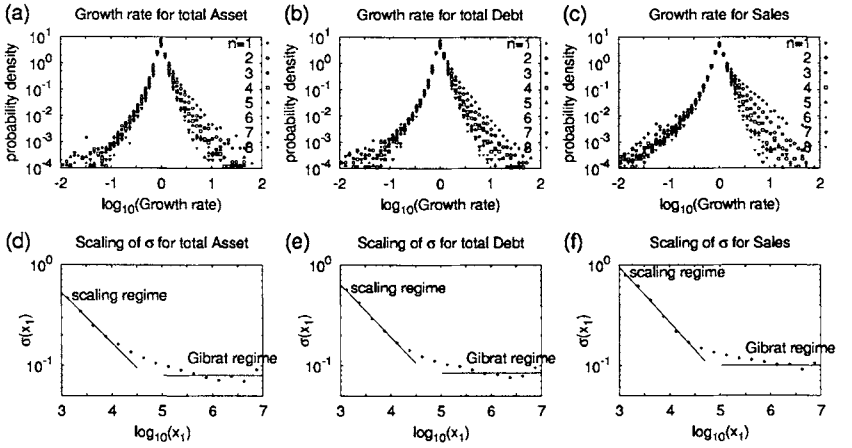


**Fig. 3.** *Upper panels:* Probability density function $P(r|x_1)$ for $r = \log_{10}(R)$. For conditioning $x_1$, we use different bins of initial firm-size with equal interval in logarithmic scale as $x_1 \in [10^{4+0.25(n-1)}, 10^{4+0.25n}]$ $(n = 1, \cdots, 8)$ for total-assets (a), total-debts (b) and sales (c). *Lower panels:* Standard deviation $\sigma$ of $r$ as a function of initial year's firm-size $x_1$ for total assets (d), total debts (e) and sales (f).

We also examine the growth rate for different time-scales $\Delta t$, namely $r = \log R = \log(x_{t+\Delta t}/x_t)$, for $\Delta t$ changed from 1 to 6 years. Fig. 4 shows $\sigma$ as a function of $\Delta t$. It is obvious that there is a scaling relation $\sigma \propto (\Delta t)^{-\gamma}$. This finding is thought to be quite important when one considers temporal change of financial state of stock (balance-sheet) and flow (profit-and-loss), as it is relevant to growth and default process of small and midsize companies (see also Fujiwara 2004 for bankruptcy of large firms).

**acknowledgement** The authors would like to thank the CRD Association (CRD: Credit Risk Database) in Japan for providing datasets and information. This research was supported in part by the National Institute of Information and Communications Technology.

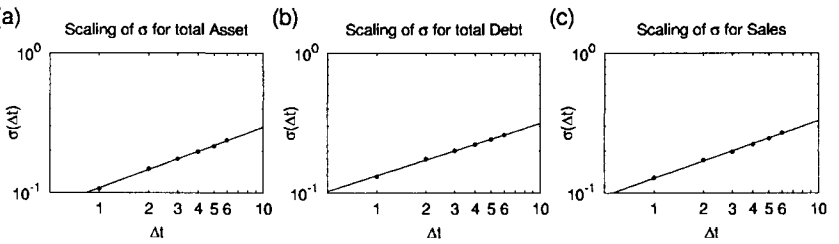


**Fig. 4.** Standard deviation $\sigma$ of $r = \log_{10} R$. The growth rate $R = x_{t+\Delta t}/x_t$ is for different time-scales $\Delta t$ which ranges from 1 year to 6 years. Scaling relation in the form $\sigma \propto (\Delta t)^{-\gamma}$ is evident for total-assets (a), total-debts (b) and sales (c). The values of $\gamma$ are respectively (a) 0.44, (b) 0.38 and (c) 0.41.

## References


1. Amaral LAN, Buldyrev SV, Havlin S, Leschhorn H, Maass P, Salinger MA, Stanley HE, Stanley MHR (1997) J Phys (France) I 7:621–633
2. Amaral LAN, Buldyrev SV, Havlin S, Salinger MA, Stanley HE (1998) Power law scaling for a system of interacting units with complex internal structure. Phys Rev Lett 80:1385–1388
3. Aoyama H, Souma W, Fujiwara Y (2003) Growth and fluctuations of personal and company's income. Physica A 324:352–358
4. Aoyama H, Fujiwara Y, Souma W (2004), talk presented at Japan Physical Society meeting at Kyushu University, March 27 2004
5. Axtell RL (2001) Zipf distribution of U.S. Firm Sizes. Science 293:1818–1820
6. Fujiwara Y, Di Guilmi C, Aoyama H, Gallegati M, Souma W (2004) Do Pareto-Zipf and Gibrat laws hold true? An analysis with European firms. Physica A 335:197–216
7. Fujiwara Y (2004) Zipf Law in Firms Bankruptcy. Physica A 337:219–230
8. Hart PE, Oulton N (1997) Zipf and the size distribution of firms. Applied Economics Letters 4:205–206
9. Mizuno M, Katori M, Takayasu H, Takayasu M (2002) In: Takayasu H (ed) Empirical Science of Financial Fluctuations: The Advent of Econophysics. Springer-Verlag, Tokyo
10. Stanley MHR, Buldyrev SV, Havlin S, Mantegna RN, Salinger MA, Stanley HE (1995) Zipf plots and the size distribution of firms. Economics Letters 49:453–457
11. Stanley MHR, Amaral LAN, Buldyrev SV, Havlin S, Leschhorn H, Maass P, Salinger MA, Stanley HE (1996) Scaling behaviour in the growth of companies. Nature 379:804–806
12. Steindl J (1965) Random processes and the growth of firms: A study of the Pareto law. Griffin, London
13. Sutton J (1997) Gibrat's legacy. J Economic Literature 35:40–59
14. Takayasu H, Okuyama K (1998) Country dependence on company size distributions and a numerical model based on competition and cooperation. Fractals 6:67–79

# 5. Networks and Wealth Distributions

# The skeleton of the Shareholders Networks

Guido Caldarelli[1], Stefano Battiston[2], and Diego Garlaschelli[3]

[1] INFM-CNR Istituto dei Sistemi Complessi via dei Taurini 19 00185 Roma, ITALY Guido.Caldarelli@roma1.infn.it.
[2] Lab. de Physique Statistique, Ecole Normale Supérieure, 24 rue Lhomond, 75005, Paris FRANCE battiston@ens.fr.
[3] Dip. di Fisica, Univ. di Siena, Via Roma 56, 53100 Siena ITALY garlaschelli@cscfw.pendola.unisi.it.

## 1 The Markets

We have collected the data of the Shareholding Network (SN) as it appeared in 2002 in two US stock market (NYSE and NASDAQ, [1]) and in one European stock market (MIB, [2]). We have performed a systematic study of the topological properties of such networks using a complex networks approach [3], with particular attention at edges weights [4].

In a previous paper [5] we have addressed the issue of whether it is possible to classify stock markets based on the scale free nature of the connectivity properties. Here we want to investigate the inner organization of such networks. While some network properties are common to different markets, others are dramatically different and may be used to classify financial systems. In our previous work [5] we have found that the in-degree distribution follows a power law, but exponents are different for MIB and US stock markets. The in-degree corresponds to the number of stocks in agents' portfolio and we will refer to it as ***portfolio diversification*** or ***portfolio size*** in the rest of the paper. The power law distribution implies that there is no characteristic value for the portfolio diversification and that the network is self similar. Many social and biological networks have been recently found to display this property, the World Trade Web [6] and food webs [7] among others [8], suggesting common underlying mechanisms leading to self-organization.

The set of companies quoted on a stock market, together with their respective top-holders form the Shareholding Network (SN). Vertices of the graph represent either companies or shareholders (either another company or a mutual fund or an individual, hereafter we denote this as an economic "agent"). A link is drawn from the company to the shareholder, forming a weighted oriented graph. Each link is weighted by the fraction of shares held. Restricting only to vertices that are quoted on the same market, we obtained a subnetwork, the Stock Shareholding Network (SSN).

Whenever considering the whole investment relationships we will instead refer to the "extended net". We found in our previous work [5] that the portfolio diversification $k_{in}$ is correlated to the invested volume $v$ in such a way that:

$$k_{in} \propto v^{\beta} \tag{1}$$

This empirical correlation allowed us to relate, with a simple model of network formation, the distribution of $k$ to the distribution of $v$. The probability density of the portfolio diversification is a power law $P(k) \propto k^{-\gamma}$, where the values of the exponent $\gamma$ are given by $\gamma_{nys} = 2.37$, $\gamma_{nas} = 2.22$, $\gamma_{mib} = 2.97$.

The tail of the distribution of the invested volume (see [5]) displays too a power-law behavior $\theta(v) \propto v^{-\alpha}$, with $\alpha_{nys} = 1.95, \alpha_{nas} = 2.09, \alpha_{mib} = 2.24$.

Since $v$ represents the invested wealth, the observed power-law tails generalize to a market investment context the well-known Pareto tails describing the right part of the wealth distribution of different economies.

It is also important to notice that if we re-define the weights as $\tilde{w}_{ij} = w_{ij}c_j$ then the invested volume is analogous to the notion of strength $s_i$ for weighted graphs, recently introduced in [4]

$$v_i = \sum_j w_{ij}c_j = \sum_j \tilde{w}_{ij} = s_i \tag{2}$$

Differently from social networks which are characterized by high clustering, shareholding networks have very small clustering coefficient, especially the US markets ($CC_{MILA} = 1.8 \cdot 10^{-3}$, $CC_{NYSE} = 2.7 \cdot 10^{-5}$, $CC_{NASD} = 2.3 \cdot 10^{-6}$ ).

An argument to explain this feature is the following. Recall that we are dealing with large, long term investments. If a portfolio contains two companies A and B, and B owns shares of A, then if A has financial difficulties this could propagate to B. Hence in general holders might prefer to avoid having connected stocks in their portfolios.

It is important to understand whether the network can be decomposed in *subnetworks* of comparable size (in this case the market would be separated in sub-markets) or whether there exist a *giant connected component* including most of the nodes. We find 65 connected components of at least 2 nodes in MIB, while 14 in NYSE and 41 in NASDAQ. The largest connected component takes 73% of the whole network in MIB, while the 99.7% in NYSE and the 99.2% in NASDAQ.

## 2 Effective Control Indices

We now want to take into account the relative importance of a shareholder of a stock with respect to the other shareholders of that same stock. It is clear that the concentration of the ownerships plays a crucial role in financial strategy. We thus compute two indexes that capture the fact that a 10%

shareholder holds much more control if the other shareholders hold 1% each, than if they hold 10% each. This information is not contained in the amount of share alone, nor in the distribution of shares $w_{ij}$ over all nodes. We define the following quantities.

$$SI_i = \frac{(\sum_{j \in holders} w_{ij})^2}{\sum_{j \in holders} w_{ij}^2} \tag{3}$$

$SI_i$ gives the effective number of holders of the company $i$. SI is close to 1 when there is a dominating holder. SI is equal to N when there are N equally important holders.

For each holder $j$ and each stock $i$ we also compute:

$$\frac{w_{ij}^2}{(\sum_{k \in holders} w_{ik}^2)} \tag{4}$$

This quantity ranges in $[0, 1]$ and reflects to what extent the company $i$ is controlled by the holder $j$. Then we sum up the above quantity for each of the stocks in the portfolio of the agent $i$.

$$HI_j = \frac{\sum_{i \in stocks.owned.by.j} w_{ij}^2}{(\sum_{k \in holders.of.stock.i} w_{ik}^2)} \tag{5}$$

$HI_j$ gives the effective number of stocks controlled by the holder $j$.

We note that HI and SI are quantities analogous to the connectivity in-degree $k_{in}$ and out-degree $k_{out}$ for a weighted network, because they measure the effective number of in-going and out-going links.

We report the distributions of SI and HI in **Figure 1**. While in the US markets the typical value of SI is around 6, in MIB the typical value is 1. These results shows that in MIB the concentration of power among holders is distributed in a very different way from US markets. In MIB companies are typically controlled by a single holder. In the US markets the large majority of companies is controlled by 6 holders.

As for HI, the distribution has a power law behavior similarly to the $k_{in}$ distribution [5]. Note the difference of range across the markets: holders control up to the equivalent of 3 companies in the Italian market and up to the equivalent of 200 companies in the US markets.

Imagine now to rebuild the network keeping only the effective holders of a company as measured by SI. The fact that in MIB companies are typically controlled by one holder, means that stocks have mostly one outgoing link. Which implies that the network has a *tree-like structure* or a forest-like structure in case there are several disconnected trees. The fact that HI ranges up only to 3 means that most holders have one or two in-going links. Putting together the two pieces of information we can expect the network of the prominent relationships to be a tree (or a forest) with branching factor mostly 1 or

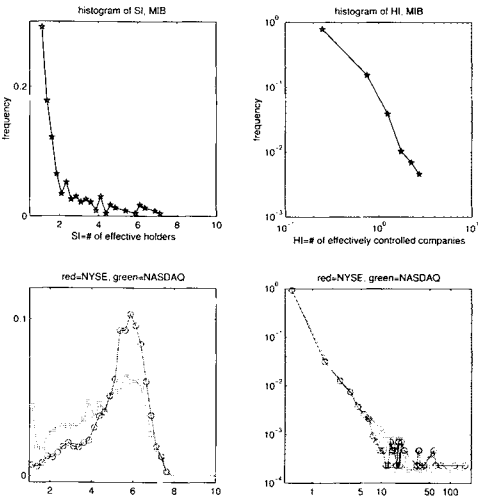


**Fig. 1.** Distributions of HI and SI computed on the extended networks.
SI measures the effective number of holders for a stock. HI measures the number of stocks effectively controlled by a holder.

2. To know whether the network is a single tree or a forest, we need to count the connected components (see next section).

In the US markets, the distribution of HI shows that there are some very powerful holders who control dozens and even hundreds of stocks. But a stock typically has 6 prominent out-going links. Hence for sure we cannot build a tree out of the original network. Moreover we still do not know whether these powerful holders control separate sets of stocks or if instead they control together overlapping sets of stocks.

## 3 Conclusions

We have studied the topology of the Shareholding Networks of three different stock markets with a complex network approach. The portfolio diversification was known from our previous work to have a power law distribution in all those markets. This result can be explained with a 'Fitness model' as done in [5]. Here we have provided a further characterization of the network structure. We have introduced a novel method for extracting the backbone of the network by means of two quantities HI and SI, analogous to in-degree and out-degree for weighted graph. These quantities capture the notion of number of companies controlled by a holder and number of holders controlling a company. The quantities HI and SI allow on one hand to characterize statistically the ownership concentration of stocks and the power of holders at a local level.

On the other hand they allow to identify the investors that control most of the market. It turns out that they are 1% of all the investors in the US markets and 12% in the MIB. Finally the number of effective holders SI allow us to extract the subnetwork of the prominent shareholding relationships. We can thus unveil the essential structure of the market core, obtaining very different pictures for our cases of study: the MIB splits into several separated groups of interest, while the US markets is characterized by very large holders sharing their control on overlapping subsets of stocks.

## 4 Acknowledgments

This work is supported by FET-IST department of the European Community, Grant IST-2001-33555 COSIN.

## References

1. single companies informations are available at *http://finance.lycos.com.*
2. (2002) Banca Nazionale del Lavoro, La meridiana dell'investitore 2002, Class Editori, Milano.
3. (2002) Albert R. and Barabasi A.-L. , Rev. Mod. Phys. 74, 47.
4. (2004) Barrat A. and Barthélémy M. and Pastor-Satorras R. and Vespignani A., The architecture of complex weighted networks Proceedings of the National Academy of Sciences USA 101 3747-3752
5. (2005) Garlaschelli D. and Battiston S. and Castri M. and Servedio V.D.P. and Caldarelli G., The scale free nature of market investment network, Physica A 350, 491-499.
6. (2003) Serrano M.A. and Boguñá M. , Topology of the World Trade Web,ArXiv:cond-mat/0301015
7. (2003) Garlaschelli D. and G.Caldarelli and L.Pietronero, Universality in Food Webs, Nature 423 165-168.
8. (2003) Dorogovtsev S.N. and Mendes J.F.F., Evolution of Networks: From Biological Nets to the Internet and WWW, Oxford University Press, Oxford.

# Financial Market - A Network Perspective

Jukka-Pekka Onnela[1], Jari Saramäki[1], Kimmo Kaski[1], and János Kertész[2]

[1] Laboratory Computational Engineering, Helsinki University of Technology, P.O.Box 9203, FIN-02015 HUT. jonnela@lce.hut.fi
[2] Department of Theoretical Physics, Budapest University of Technology and Economics, Budafoki út 8, H-1111 Budapest, Hungary.

We construct a weighted financial network for a subset of NYSE traded stocks, in which the nodes correspond to stocks and edges to interactions between them. We identify clusters of stocks in the network, based on the Forbes business sector classification, and study their intensity and coherence. Our approach indicates to what extent the business sector classifications are visible in market prices, enabling us to gauge the extent of group-behaviour exhibited by stocks belonging to a given business sector.

## 1 Introduction

Complex networks provide a very general framework, based on the concepts of statistical physics, for studying systems with large numbers of interacting agents [1]. The nodes of the network represent the agents and a link connecting two nodes indicates an interaction between them. In the complex networks framework, interactions have typically been considered to be binary in nature, meaning that either two nodes interact (are connected) or they do not (are not connected). Imposing a binary interaction requires setting a threshold value for interaction strength, such that interactions falling below it are discarded. Although this approach is a suitable first approximation, thresholding can lead to a loss of information. Consequently, a natural step forward is to assign weights on the links to reflect the strengths of interactions.

In a financial market the performance of a company is compactly characterised by a single number, the stock price, which results from a large number of interactions between different market participants. Although the exact nature of these interactions is not known, they are certainly reflected in the equal-time return correlations. In this paper we study a financial network in which the nodes correspond to stocks and links to return correlation based interactions between them. Mantegna [2] was the first to construct such networks and the idea was followed and extended by others [3, 4, 5, 6, 7].

## 2 Methods

### 2.1 Constructing the Network

We start by considering a price time series for a set of $N$ stocks and denote the daily closing price of stock $i$ at time $\tau$ (an actual date) by $P_i(\tau)$. Since investors work in terms of relative as opposed to absolute returns, logarithmic returns are commonly used in studies, and thus we denote the daily logarithmic return of stock $i$ by $r_i(\tau) = \ln P_i(\tau) - \ln P_i(\tau - 1)$. We extract a time window of width $T$, measured in days and in this paper set to $T = 1000$ (equal to four years, assuming 250 trading days a year), and obtain a return vector $\boldsymbol{r}_i^t$ for stock $i$, where the superscript $t$ enumerates the time window under consideration. Then equal time correlation coefficients between assets $i$ and $j$ can be written as

$$\rho_{ij}^t = \frac{\langle \boldsymbol{r}_i^t \boldsymbol{r}_j^t \rangle - \langle \boldsymbol{r}_i^t \rangle \langle \boldsymbol{r}_j^t \rangle}{\sqrt{[\langle \boldsymbol{r}_i^{t\,2} \rangle - \langle \boldsymbol{r}_i^t \rangle^2][\langle \boldsymbol{r}_j^{t\,2} \rangle - \langle \boldsymbol{r}_j^t \rangle^2]}}, \tag{1}$$

where $\langle ... \rangle$ indicates a time average over the consecutive trading days included in the return vectors. These correlation coefficients between $N$ assets form a symmetric $N \times N$ correlation matrix $\mathbf{C}^t$ with elements $\rho_{ij}^t$. The different time windows are displaced by $\delta T$, where we have used a step size of one week, i.e. $\delta T = 5$ days.

Next we define interaction strengths, or link weights, based on the correlation coefficients. One of the simplest alternatives is to use the absolute values of the correlation coefficients, in which case the interaction strength reflects the strength of linear coupling between the logarithmic returns of stocks $i$ and $j$ in time window $t$. If we use $w_{ij}^t$ to denote the weight on the link connecting node $i$ and node $j$, with this choice we have $w_{ij}^t = |\rho_{ij}^t|$, or in matrix form $\mathbf{W}^t = |\mathbf{C}^t|$. Because the correlation coefficients $\rho_{ij}^t$ vary between $-1$ and 1, the interaction strengths $w_{ij}^t$ are naturally limited to the $[0, 1]$ interval. In the correlation matrix $\mathbf{C}^t$ we have estimated the correlations between all the assets. Thus, the resulting network will be fully connected consisting of $N$ nodes and $N(N-1)/2$ links, corresponding to the elements in the upper (or lower) triangular part of the the weight matrix.[3]

### 2.2 Characterising Network Clusters

Let us now consider any cluster or subgraph $g$ in the above defined network. To characterise how compact or tight the subgraph is, we use the concept of subgraph *intensity* $I(g)$ introduced in [8]. Put differently, subgraph intensity allows us to characterise the interaction patterns within clusters. If we use $v_g$

[3] It is possible, using some heuristic, to insert only a fraction of all the links in the network, but this would result in an additional parameter to be determined.

to denote the set of nodes and $\ell_g$ the set of links in the subgraph with weights $w_{ij}$, we can express subgraph intensity as the *geometric mean* of its weights:

$$I(g) = \left( \prod_{(ij) \in \ell_g} w_{ij} \right)^{1/|\ell_g|} . \tag{2}$$

Due to the nature of the geometric mean, the subgraph intensity $I(g)$ may be low because one of the weights is very low, or it may result from all of the weights being low. In order to distinguish between these two extremes, we use the concept of subgraph *coherence* $Q(g)$ [8]. It assumes values from the interval $[0, 1]$ and is close to unity only if the subgraph weights do not differ much, i.e. are internally coherent. Subgraph coherence is defined as the ratio of the geometric to the arithmetic mean of the weights as

$$Q(g) = I|\ell_g| / \sum_{(ij) \in \ell_g} w_{ij}. \tag{3}$$

In order to compare intensity and coherence values, we need to establish a reference. A very natural reference system is obtained by considering the entire market. In other words, we take all of the $N$ nodes and $N(N-1)/2$ links making up the network $G$, and then using the above definitions compute $I(G)$ and $Q(G)$. We can also use *relative cluster intensity* for cluster $g$, given by $I(g)/I(G)$, and *relative cluster coherence*, given by $Q(g)/Q(G)$, if instead of absolute values we wish to examine the cluster intensity or coherence relative to the reference system.

## 3 Results

In this section we consider a subset of 116 NYSE-traded stocks from the S&P 500 index from 1.1.1982 to 31.12.2000. We deal with the closing price, resulting in a total of 4787 price quotes for each stock. To divide the stocks into clusters, we obtained the Forbes business sector labels for each stock [9]. The stocks in our dataset fall into 12 business sectors, such as Energy and Utilities. Given these labels for each stock, we use the concepts of subgraph intensity and coherence to gauge how how similarly stocks belonging to a given business behave as a function of time.

Let us consider a cluster $g$, constructed such that all of its nodes $v_g$ belong to the same business sector, and let $n$ denote the number of nodes in this cluster. Then we add all the $n(n-1)/2$ links corresponding to the interaction strengths between any pair of nodes within $g$. In one extreme, if all the link weights are equal to unity, every node participating in $g$ interacts maximally with its $n-1$ neighbours. In the other extreme, if one or more of the weights are zero, the subgraph intensity for the *fully connected subgraph* $g_n$ tends to zero because the original topological structure no longer exists.

In Figure 1, we show the relative cluster intensity as a function of time for selected business sector clusters. Values above unity indicate that the intensity of the cluster is higher than that of the market. This implies that in most cases stocks belonging to a given business sector are tied together in the sense that intra-cluster interaction strengths are considerably stronger than those of the market on the whole. It is also worth noting the high value for the absolute cluster intensity for the market roughly between 1986 and 1990. This elevated value is due to the 1987 stock market crash (Black Monday), which caused the market to behave in a unified manner[4]. The crash also compresses the relative cluster intensities, which means that the cluster-specific behaviour is temporarily suppressed by the crash, and after the market recovers the clusters regain their characteristic behaviour.

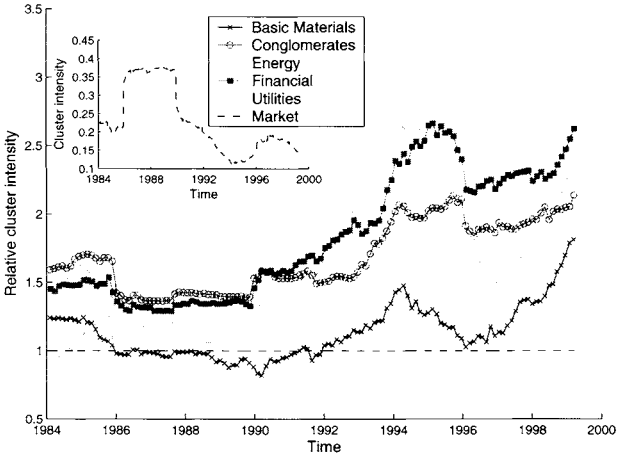


**Fig. 1.** Relative (to the market) cluster intensity as a function of time for select clusters. Inset: The (absolute) cluster intensity for the market used for normalisation.

Business sector clusters are also more coherent than the market, as shown in Figure 2, except for Basic Materials. One explanation is obtained from the industry classifications, which is a finer classification scheme, of stocks comprising the BM cluster. These include Metal Mining, Paper, Gold & Silver and Forestry & Wood Products. Therefore, it is clear that the Basic Materials business sector is extremely diverse. Also, the price of some of these items is determined, at least partially, outside the stock market. Consequently, it is not so surprising that the cluster intensity remains low, at times even falling below the market reference. Similarly, the low coherence values indicate that there are stocks in this cluster with very high correlations (those belonging

[4] The length of this elevated period is related to the window width parameter.

to the same industry, such as gold mining), but also very low (companies belonging to different industries). In conclusion, our results indicate that, in most cases, stocks belonging to the same business sector have higher intensity and more coherent intra-cluster than inter-cluster interactions.

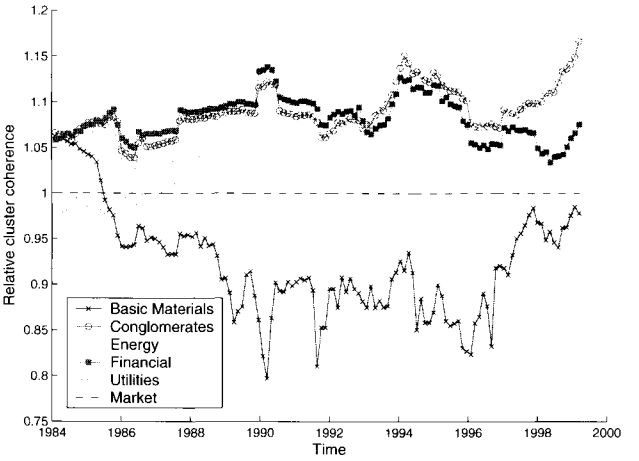


**Fig. 2.** Relative (to the market) cluster coherence as a function of time.

## References


1. Albert R, Barabasi A-L (2002) Statistical mechanics of complex networks. Reviews of Modern Physics 74, 47-97
2. Mantegna R N (1999) Hierarchical structure in financial markets. European Physical Journal B 11, 193-197
3. Vandewalle N, Brisbois F, Tordoir X (2001) Non-random topology of stock markets. Quantitative Finance 1, 372-374
4. Marsili M (2002) Dissecting financial markets: Sectors and states. Quantitative Finance 2, 297-302
5. Caldarelli G, Battiston S, Garlaschelli D, Catanzaro M (2004) In: Ben-Naim E, Frauenfelder H, Toroczkai Z (eds) Complex Networks. Springer
6. Onnela J-P, Chakraborti A, Kaski K, Kertesz J, Kanto A (2003) Dynamics of market correlations: Taxonomy and portfolio analysis. Physical Review E 68, 056110
7. Onnela J-P, Chakraborti A, Kaski K, Kertesz J, Kanto A (2003) Asset trees and asset graphs in financial markets. Physica Scripta T106, 48-54
8. Onnela J-P, Saramäki J, Kertész J, Kaski K Intensity and coherence of motifs in weighted complex networks. cond-mat/0408629
9. The website of Forbes at www.forbes.com

# Change of ownership networks in Japan

Wataru Souma[1], Yoshi Fujiwara[2], and Hideaki Aoyama[3]

[1] ATR Network Informatics Laboratories, Kyoto 619-0288, Japan. souma@atr.jp
[2] ATR Network Informatics Laboratories, Kyoto 619-0288, Japan. yfujiwar@atr.jp
[3] Department of Physics, Graduate School of Science, Kyoto University, Yoshida, Kyoto 606-8501, Japan. aoyama@phys.h.kyoto-u.ac.jp

**Summary.** As complex networks in economics, we consider Japanese shareholding networks as they existed in 1985, 1990, 1995, 2000, 2002, and 2003. In this study, we use as data lists of shareholders for companies listed on the stock market or on the over-the-counter market. The lengths of the shareholder lists vary with the companies, and we use lists for the top 20 shareholders. We represent these shareholding networks as a directed graph by drawing arrows from shareholders to stock corporations. Consequently, the distribution of incoming edges has an upper bound, while that of outgoing edges has no bound. This representation shows that for all years the distributions of outgoing degrees can be well explained by the power law function with an exponential tail. The exponent depends on the year and the country, while the power law shape is maintained universally. We show that the exponent strongly correlates with the long-term shareholding rate and the cross-shareholding rate.

**Keywords.** Shareholding network, Power law, Long-term shareholding, Cross-shareholding

## 1 Introduction

Recently, many studies have revealed the true structure of real-world networks [1, 3]. This development also holds true in the field of econophysics. Such studies have investigated business networks [9], shareholding networks [10, 11, 12, 5], world trade networks [6, 7], and corporate board networks [2, 4].

By common practice, if we intend to discuss networks, we must define their nodes and edges. Edges represent the relationships between nodes. The subject of this study is the ownership network. Accordingly, we consider companies as nodes and the shareholding relationships between them as edges.

**Table 1.** Change in the size of shareholding network $N$, the total number of edges $K$, and the exponent $\gamma$ of the outgoing degree distribution $p(k_{\text{out}}) \propto k_{\text{out}}^{-\gamma}$

| Year | 1985 | 1990 | 1995 | 2000 | 2002 | 2003 |
|---|---|---|---|---|---|---|
| $N$ | 2,078 | 2,466 | 3,006 | 3,527 | 3,727 | 3,770 |
| $K$ | 23,916 | 29,054 | 33,860 | 32,586 | 30,000 | 26,407 |
| $\gamma$ | 1.68 | 1.67 | 1.72 | 1.77 | 1.82 | 1.86 |

In this article, we consider Japanese shareholding networks as they existed in 1985, 1990, 1995, 2000, 2002, and 2003 (see Ref. [5] for shareholding networks in MIB, NYSE, and NASDAQ). We use data published by Toyo Keizai Inc. This data source provides lists of shareholders for companies listed on the stock market or on the over-the-counter market. The lengths of the shareholder lists vary with the companies. The data before 2000 contain information on the top 20 shareholders for each company. On the other hand, the data for 2002 and 2003 contain information on the top 30 shareholders for each company. Therefore to uniformly analyze the data we consider the top 20 shareholders for each company.

Types of shareholders include listed companies, non-listed financial institutions (commercial banks, trust banks, and insurance companies), officers, and other individuals. In this article, we don't consider officers and other individuals, so the shareholding networks are constructed only from companies. The number of nodes, $N$, and the total number of edges, $K$, vary with the years, and these are summarized in Table. 1.

This paper is organized as follows. In Sec. 2 we consider the degree distribution for outgoing edges and show that the outgoing degree distribution follows a power law function with an exponential cutoff. In addition, we show that the exponent depends on the year and the country, while the power law shape is maintained universally. We also discuss correlations between the exponent and the long-term shareholding rate and the cross-shareholding rate. From this examination, we show that the exponent strongly correlates with these quantities. The last section is devoted to a summary and discussion.

## 2 Change of outgoing degree distribution

If we draw arrows from shareholders to stock corporations, we can represent a shareholding network as a directed graph. If we count the number of incoming edges and that of outgoing edges for each node, we can obtain the degree distribution for incoming degree, $k_{\text{in}}$, and that for outgoing degree, $k_{\text{out}}$. However, as explained in Sec. 1, the lengths of the shareholder lists vary with the companies, and thus we consider only the top 20 shareholders for consistency. Therefore, the incoming degree has an upper bound, $k_{\text{in}} \leq 20$, while the outgoing degree has no bound.

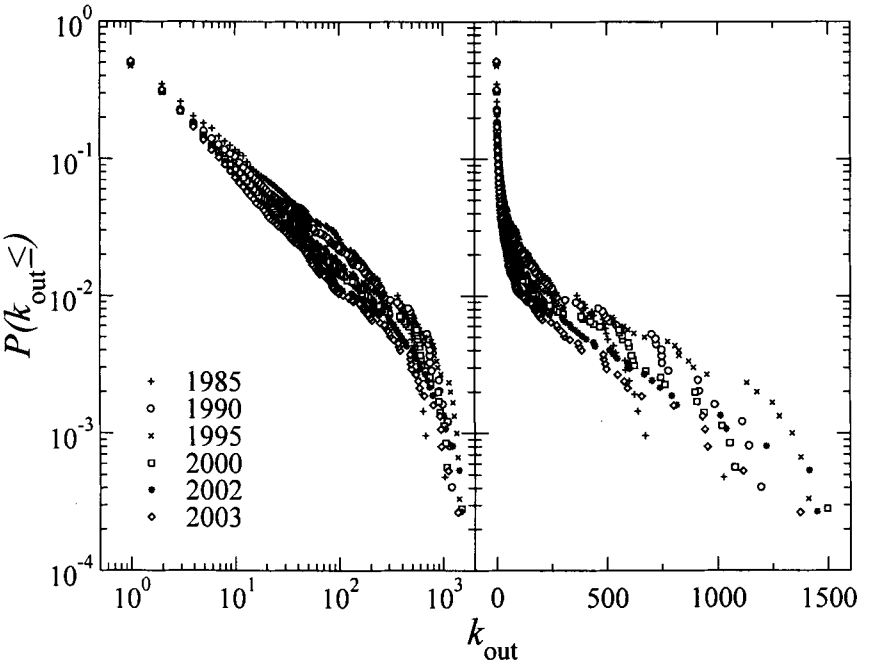


**Fig. 1.** Log-log plot (left) and semi-log plot (right) of the cumulative probability distribution, $P(k_{\rm out} \leq)$, of the outgoing degree $k_{\rm out}$.

The log-log plot of $k_{\rm out}$ is shown in the left panel of Fig. 1. In this figure, the horizontal axis corresponds to $k_{\rm out}$, and the vertical axis corresponds to the cumulative probability distribution $P(k_{\rm out} \leq)$ that is defined by the probability distribution function $p(k_{\rm out})$,

$$P(k_{\rm out} \leq) = \int_{k_{\rm out}}^{\infty} dk'_{\rm out}\, p(k'_{\rm out}),$$

in the continuous case. We can see that the distribution follows the power law function, $p(k_{\rm out}) \propto k_{\rm out}^{-\gamma}$, except for the tail part. The exponent $\gamma$ depends on the year, as summarized in Table. 1. It has also been reported that the degree distributions of shareholding networks for companies listed on the Italian stock market (Milano Italia Borsa; MIB), the New York Stock Exchange (NYSE), and the National Association of Security Dealers Automated Quotations (NASDAQ) each follow the power law distribution [5]. The exponents are $\gamma_{\rm MIB} = 1.97$ in 2002, $\gamma_{\rm NYSE} = 1.37$ in 2000, and $\gamma_{\rm NASDAQ} = 1.22$ in 2000. These are not so different from the Japanese case.

The semi-log plot is shown in the right panel of Fig. 1, and the meaning of the axes is the same as in the left panel. We can see that the tail part of the distribution follows approximately the exponential function. The exponen-

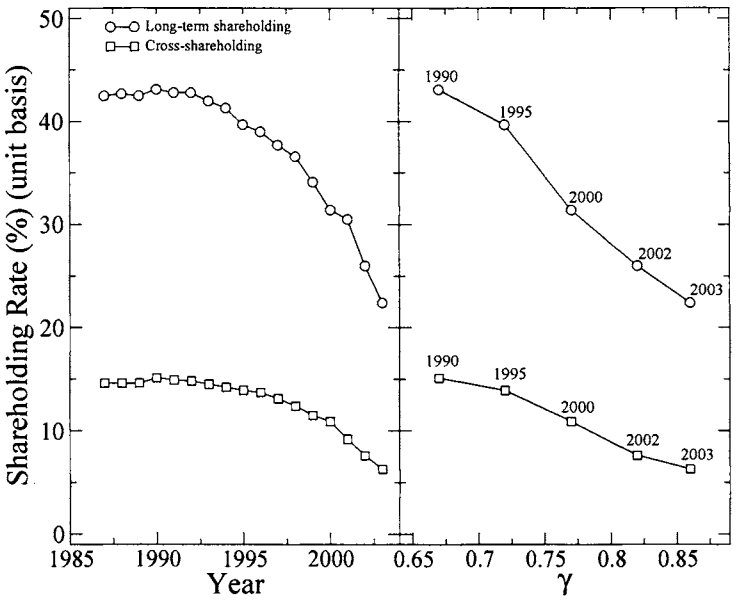


**Fig. 2.** Change in the long-term shareholding rate and that in the cross-shareholding rate (left), and the correlations between these rates and the exponent $\gamma$ (right).

tial part of the distribution is mainly constructed from financial institutions. On the other hand, almost all of the power law part of the distribution is constructed from non-financial institutions. The above results suggest that different mechanisms work in each range of the distribution, and some of the reasons for the emergence of this distribution are discussed in Ref. [12].

It is reasonable to assume that the change in the exponent $\gamma$ can be attributed to the change in the pattern of shareholding. In Japan, since 1987, a long-term shareholding rate and a cross-shareholding rate have been reported by Nippon Life Insurance (NLI) Research Institute [8].

The changes in these rates are shown in the left panel of Fig. 2. In this figure, the horizontal axis corresponds to the year, and the vertical axis corresponds to the shareholding rate calculated on the basis of number of shares. The open circles corresponds to long-term shareholding, and the open squares corresponds to cross-shareholding. We can see that both the long-term shareholding rate and the cross-shareholding rate decrease after 1990.

Correlations of the exponent with the long-term shareholding rate and with the cross-shareholding rate are shown in the right panel of Fig. 2. In this figure, the horizontal axis corresponds to the exponent $\gamma$, and the vertical axis, the open circle, and the open square are the same as in the left panel. We can see that the exponent has strong and negative correlations with both the long-term shareholding rate and the cross-shareholding rate.

## 3 Summary

In this article, we considered Japanese shareholding networks as they existed in 1985, 1990, 1995, 2000, 2002, and 2003. These networks were represented as a directed graph by drawing arrows from shareholders to stock corporations. For these directed shareholding networks, it was shown that the outgoing degree distribution for each year can be well explained by the power law distribution, except for the tail part. The exponent depends on the year and the country, while the power law shape is maintained universally. We also showed that the exponent has strong and negative correlation with both the long-term shareholding rate and the cross-shareholding rate. This means that the dissolution of long-term shareholding and cross-shareholding causes the exponent to increase.

## References


1. Barabási AL (2002) Linked: The New Science of Networks. Perseus Press, Cambridge, MA
2. Battiston S, Bonabeau E, Weisbuch G (2003) Decision making dynamics in corporate boards. Physica A 322: 567–582
3. Dorogovtsev SN, Mendes JFF (2003) Evolution of Networks: From Biological Nets to the Internet and WWW. Oxford University Press, Oxford
4. Davis G, Yoo M, Baker WE (2003) The small world of the American corporate elite, 1982–2001. Strategic Organization 3: 301–326
5. Garlaschelli D, et al. (2003) The scale-free topology of market investments. to be published in Physica A. arXiv:cond-mat/0310503
6. Li X, Jin YY, Chen G (2003) Complexity and synchronization of the World trade Web. Physica A 328: 287–296
7. Li X, Jin YY, Chen G (2004) On the topology of the world exchange arrangements web. Physica A 343: 573–582
8. NLI Research Institute Financial Research Group (2004) The fiscal 2003 survey of cross-shareholding. http://www.nli-research.co.jp/index.html
9. Souma W, Fujiwara Y, Aoyama H (2003) Complex networks and economics. Physica A 324: 396–401
10. Souma W, Fujiwara Y, Aoyama H (2004) Random matrix approach to shareholding networks. Physica A 344: 73–76
11. Souma W, Fujiwara Y, Aoyama H (2005) Heterogeneous economic networks. In: Namatame A, et al. (eds) the proceedings of the 9th Workshop on Economics and Heterogeneous Interacting Agents. Springer-Verlag, Tokyo, to be published. arXiv:physics/0502005
12. Souma W, Fujiwara Y, Aoyama H (2005) Shareholding networks in Japan In: Mendes JFF, et al. (eds) the proceedings of the International Conference "Science of Complex Networks: from Biology to the Internet and WWW". Springer-Verlag, Berlin, to be published. arXiv:physics/0503177

# G7 country Gross Domestic Product (GDP) time correlations. A graph network analysis

J. Miśkiewicz[1] and M. Ausloos[2]

[1] Institute of Theoretical Physics, University of Wrocław, pl. M. Borna 9, 50-204 Wrocław, Poland jamis@ift.uni.wroc.pl
[2] SUPRATECS, B5, University of Liège, B-4000 Liège, Euroland marcel.ausloos@ulg.ac.be

## 1 Introduction

The G7 countries (France, USA, United Kingdom, Germany, Japan, Italy, Canada) are the most developed countries in the world, but such statement leaves unanswered the question on which of those is the most important one and of course what kind of dependencies exists between them. Of course this subject has been considered along various lines of analysis (Frankel 2000), which usually require a detailed knowledge of the analysed objects and therefore are difficult to pursue. Our own question is to investigate the dependence and leadership problem on a very limited number of data. Within this paper correlations between G7 countries, are investigated on the basis of their Gross Domestic Product (GDP). GDP is one of the most important parameters describing state of an economy and is extensively studied (Lee et al. 1998, Ormerod 2004).

The annual GDP records[3], considered as a discrete time series are used over the last 53 years (since 1950 till 2003) in order to evaluate GDP increments and distances between those countries. Different distance functions are used and the results compared. Distance matrices are calculated in the case of discrete Hilbert spaces $L_q$ $(q = 1, 2)$, Eq. (1), a statistical correlation distance, Eq. (2), and a difference between increment distributions, Eq. (4). The distance functions were chosen here below taking into account considerations on basic properties of the data. The distance matrices are then analysed using graph methods in the form of a unidirectional or bidirectional chain (UMLP and BMLP respectively) (Ausloos and Miskiewicz 2005) as well as through the locally minimal spanning distance tree (LMST).

## 2 Distance and graph analysis

In the case of discrete time series the metrics can be defined in the Hilbert space $L_q$ $(q = 1, 2)$ in a standard way (Maurin 1991)

[3] http://www.ggdc.net/index-dseries.html#top

$$d_q(A,B) = (\sum_{i=1}^{n} |a_i - b_i|^q)^{\frac{1}{q}}, \tag{1}$$

where $A, B$ are time series: $A = (a_1, a_2, \ldots, a_n)$, $B = (b_1, b_2, \ldots, b_n)$. The statistical correlation distance is used in the form:

$$d(A,B)_{(t,T)} = \sqrt{\frac{1}{2}(1 - corr_{(t,T)}(A,B))}, \tag{2}$$

where $t$ and $T$ are the final point and the size of the time window over which an average is taken respectively; the correlation function is defined as:

$$corr_{(t,T)}(A,B) = \frac{< AB >_{(t,T)} - < A >_{(t,T)} < B >_{(t,T)}}{\sqrt{(< A2 >_{(t,T)} - < A >^2_{(t,T)})(< B2 >_{(t,T)} - < B >^2_{(t,T)})}}. \tag{3}$$

The brackets $< \ldots >$ denote a mean value over the time window $T$ at time $t$.

Additionally the distribution $p(r)$ function of GDP yearly increments $(r)$ is evaluated and the correlations between countries are investigated using $\mathcal{L}_q$ $(q = 1)$ metrics (Maurin 1991)

$$d_{\mathcal{L}_q}(A,B) = [\int_{-\infty}^{+\infty} |p_A(r) - p_B(r)|^q dr]^{\frac{1}{q}}. \tag{4}$$

Since the statistical parameters describing GDP increments are very close to the normal distribution (Ausloos and Miskiewicz 2005) it is assumed that this distribution well describes the GDP increments distribution.

There are different advantages to each of those distance functions. The discrete Hilbert space $L_q$ distance Eq. (1) can be applied to any data and does not require any special properties of the data so this method seems to be very useful for comparing various sets of data. The second method Eq. (2), a statistical distance, is specially sensitive to linear correlations. The third method Eq. (4) is the most sophisticated one since it requires a knowledge of the data distribution function, but then points out to similarities between data statistical properties. The main disadvantage of the last method is that it is sensitive to the size of the data set, since it is based on the whole distribution function.

The distance matrices are built in a varying size time window moving along the time axis. The distance matrices are analysed by network methods - in the form of LMST and correlation chains (CC). The topological properties of such trees and graphs, generated as a visualisation of the correlation between GDP in G7 countries allow us to gain some practical information about the weakest points of the networks and some possible roots for crashes, recessions or booms as will be investigated in details in a following paper.

Our present analysis focuses on the globalization process of G7 country economies, which is understood as an increasing resemblance between development patterns. The question is investigated by means of the total graph

weight which is defined as a sum of distances between the countries for a given graph type (for LMST) and the mean distance for CC. LMST is a modification of the Minimum Spanning Tree algorithm (Cormen et al. 2001). It is built under the constraints that the initial pair of nodes on the tree are the countries with the strongest correlation between their GDP. CC are investigated in two forms: unidirectional and bidirectional minimum length chains (called UMLP and BMLP respectively) (Ausloos and Miskiewicz 2005). UMLP and BMLP algorithms are simplifications for LMST, where the closest neighbouring countries are attached at the end of a chain. In the case of the unidirectional chain the initial node is an arbitrary chosen country. Therefore in the case of UMLP the chain is expanded in one direction only, whereas in the bidirectional case countries might be attached at one of both ends depending on the distance value.

Moreover a percolation threshold is defined as the distance value at which all countries are connected to the network. The percolation threshold has been investigated for the different distance measures. This technique allows us to observe structures in GDP relationships between countries.

## 3 Results

The analysis is discussed here for a 15 years time window, which allows to observe the globalization process and statistically compare results obtained by different methods. The graph and percolation analysis were performed in the case of $L_1$, $L_2$, $\mathcal{L}_1$ and statistical distances. Figs 1,2 show the results of graph analysis and Fig 3 the time evolution of the percolation threshold for different distance measures. Despite differences in values between results obtained by LMST and CC methods (the graph weight takes its maximal value up to 12 in the case of $\mathcal{L}_1$ in LMST, whereas in CC the maximal value of the mean distance is not larger than 1.2) the time evolutions of the measured parameters show that the distances between countries are monotonically decreasing in time whatever the method of analysis. However for the LMST and percolation threshold in $\mathcal{L}_1$ metrics the evolution is not monotonous. Yet, since the distances between countries are usually decreasing with time this can be interpreted as a proof of a globalization process. A similar conclusion may be obtained by analysing the percolation threshold of G7 countries (Fig 3). However the results depend on the applied distance measures, which are sensitive to different properties of the analysed time series. In the case of $L_1$ and $L_2$ distances the results do not significantly depend on the visualisation method. But in the $\mathcal{L}_1$ and statistical distances the results are not unique specially in the case of the percolation threshold Fig (3).

[3]In Figs 1,2 and 3, $\mathcal{L}_1$ and statistical distances are denoted as Gauss and Mantegna respectively.

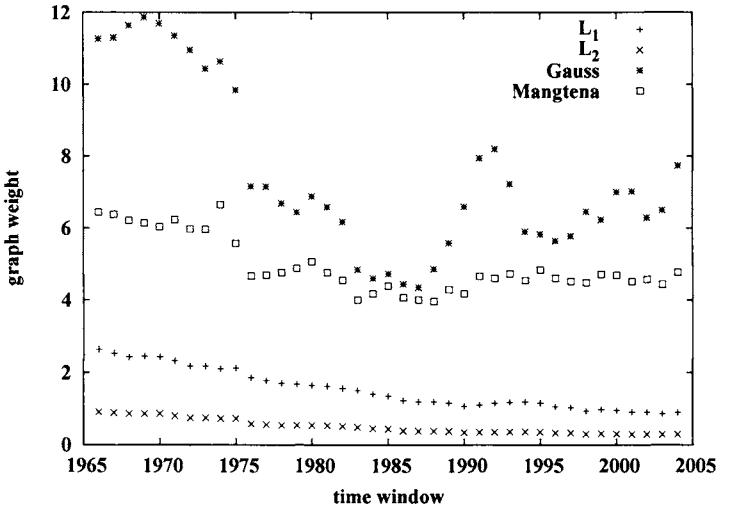


**Fig. 1.** The time evolution of the graph weight for different distance measures. The time window size is equal to 15 yrs.

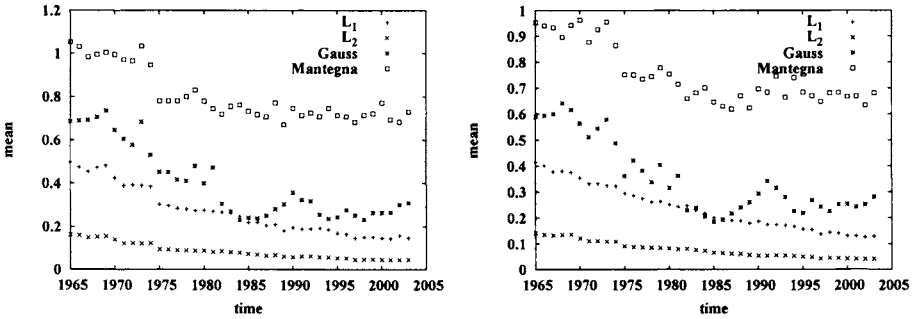


**Fig. 2.** The time evolution of the total length of uni- and bidirectional chains for different measures. The time window size is equal to 15 yrs.

## 4 Conclusions

The correlation between G7 countries has been analysed using different distance functions and various graph methods. Despite the fact that most of the methods allow to observe a globalization like process it is obvious that their sensitivity to observe correlations are different. It seems that the percolation threshold methods is the most sensitive one, since even for $L_1$ and $L_2$ distance functions it reveals different stages of globalization. One can observe that the correlations achieve their highest value in 1990, at well known significant political changes in Europe. Later on, the correlations remain on a

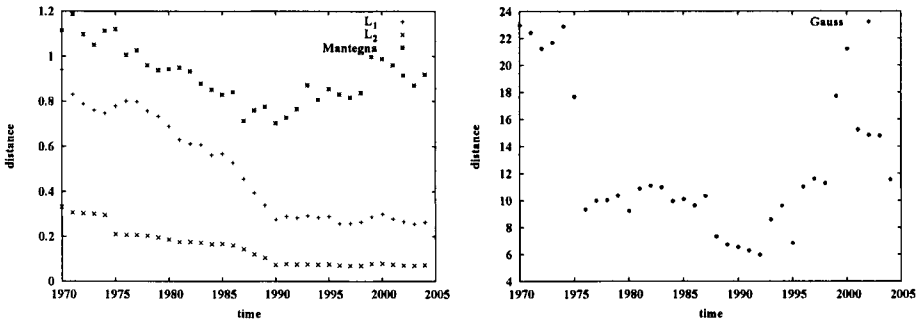


**Fig. 3.** The time evolution of percolation threshold for different measures. The time window size is equal to 15 yrs.

relatively stable level. Analysing the applied distance functions it has been observed that the noise level is the highest in the case of the $\mathcal{L}_1$ distance since this method is the most sensitive to the length of the data (required for calculating the distribution parameters). However the $\mathcal{L}_1$ method seems to be the most appropriate, because it compares the distribution functions taking into considerations all properties of the process.

**Acknowledgement**

This work is partially financially supported by FNRS convention FRFC 2.4590.01. J. M. would like also to thank SUPRATECS for the welcome and hospitality and the organizers of the 3rd Nikkei symposium for financial support received in order to present the above results.

## References

Ausloos, M. and Miskiewicz, J. (2005) An attempt to observe economy globalization: the cross correlation distance clustering of the top 19 GDP countries. *submitted for publication.*

Cormen, T. H., Leiserson, C. E., Rivest, R. L., and Stein, C. (2001) *Introduction to Algorithms, Second Edition.* The MIT Press.

Frankel, J. (2000) in Nye J. S. and Donahue, J., editors, *Governance in a Globalizing World,* pages 45–71. Brookings Inst. Press, Washington.

Lee, Y., Amaral, L. A. N., Canning, D., Meyer, M., and Stanley, H. E. (1998) Universal features in the growth dynamics of complex organizations. *Phys. Rev. Lett.*, 81:3275–3278.

Maurin, K. (1991) *Analiza.* PWN, Warszawa.

Ormerod, P. (2004) Information cascades and the distribution of economic recessions in capitalist economies. *Physica A*, 341:556–568.

# Dependence of Distribution and Velocity of Money on Required Reserve Ratio

Ning Xi, Ning Ding, and Yougui Wang*

Department of Systems Science, School of Management, Beijing Normal University, Beijing, 100875, People's Republic of China ygwang@bnu.edu.cn

**Summary.** The impacts of money creation on the statistical mechanics of money circulation were investigated by focusing on the dependence of monetary wealth distribution and the velocity of money on the required reserve ratio in this paper. In reality, money creation is important to economic system. The process of money creation can be represented by the multiplier model of money in traditional economics. From this model, it can be known that the required reserve ratio set by the central bank is one of the main determinants of the monetary aggregate and under some assumptions the monetary aggregate can be expressed as the product of the monetary base and the required reserve ratio in steady state. Taking the role that the required reserve ratio plays in the monetary system into account, we developed a random transfer model by introducing a fractional reserve banking system and carried out some simulations to observe how the monetary aggregate evolves over time, how monetary wealth is distributed among agents, as well as how fast money is transferred in the transferring process. Monetary wealth is found to follow asymmetric Laplace distribution, and the fact that latency time of money follows exponential distribution indicates that the transferring process is Poisson type. The theoretical formulas of monetary wealth distribution and the velocity of money in terms of the required reserve ratio are given respectively which are in a good agreement with the simulation results.

**Key words:** Money creation, Reserve ratio, Statistical distribution, Velocity of money, Random transfer

## 1 Introduction

Models of environments where money is transferred among traders, have recently undergone rapid development and contribute prominently to econophysics on wealth distribution [1, 2, 3]. This kind of models can be applied to investigate not only monetary wealth distribution but also the velocity of money [4, 5]. However, most of the works in this line studied the case without money creation. In reality, money plays an important role in economy and

most of money in circulation is created by loaning behavior of banks. Cognising the significance of money creation, Robert Fischer and Dieter Braun analyzed the process of creation and annihilation of money from a mechanical perspective by proposing analogies between assets and the positive momentum of particles and between liabilities and the negative momentum, and applied this approach into the study on statistical mechanics of money [6]. To be closer to reality, the required reserve ratio, one of the main determinants of the monetary aggregate, should be considered. In this work, we further examine the impacts of the required reserve ratio on two outcomes of money transfer: monetary wealth distribution and the velocity of money.

## 2 Money Creation and Simplified Multiplier Model

Modern banking system is a fractional reserve banking system, which absorbs savers' deposits and loans to borrowers. As purchasing, the public can pay in currency or in deposits. In this sense, currency held by the public and deposits in bank can both play the role of exchange medium. Thus, in economics, the monetary aggregate is measured by the sum of currency held by the public and deposits in bank. When the public saves a part of their currency into commercial banks, this part of currency turns into deposits and the monetary aggregate does not change. Once commercial banks loan to borrowers, usually in deposit form, deposits in bank increase and currency held by the public keeps constant. So loaning behavior of commercial banks increases the monetary aggregate and achieves money creation.

Economists have developed a model to represent this process. It is called the multiplier model of money [7]. Here we introduce its simplified version. In economy, commercial banks are required to keep a percentage of their deposits in currency form as required reserves, which is determined by central bank and named as the required reserve ratio. The simplified multiplier model requires that all the currency is saved in commercial banks and commercial banks only hold reserves as much as required reserves. Thus commercial banks try to grant loans till all the currency is held as required reserves, then the monetary aggregate can be expressed as

$$M = \frac{M_0}{r}, \tag{1}$$

where $M$ denotes the monetary aggregate, $M_0$ the monetary base and $r$ the required reserve ratio.

Although all factors involved in money creation except the required reserve ratio are ignored in the simplified multiplier model, it conveys us the essence of money creation in reality. This suggests that the role of money creation can be investigated by focusing on the impacts of the required reserve ratio on relevant issues. Thus we simply introduced a bank into the random transfer model to examine how the required reserve ratio affects monetary wealth distribution and the velocity of money.

## 3 Model and Simulation

We made an extension of the model in Ref. [6] by introducing a fractional reserve banking system. The economy consists of $N$ traders and a bank. At the beginning, a constant monetary base $M_0$ is equally allocated to these traders and all the monetary base is saved in the bank. In the transferring process of money, each of the traders chooses his partner randomly in each round, and yield $N$ trade pairs. Then one is chosen as "payer" randomly and the other as "receiver" in each trade pair. If the payer has deposits in the bank, he pays one unit of money to the receiver in deposit form. If the payer has no deposit and the bank has excess reserves, the payer borrows one unit of money from the bank and pays it to the receiver. But if the bank has no excess reserve, the trade is cancelled. After receiving one unit of money, if the receiver has loans, he repays his loans. Otherwise the receiver holds this unit of money in deposit form.

Since the initial settings of the amount of money and the number of traders have no impacts on the final results, we performed several simulations with $M_0 = 2.5 \times 10^5$ and $N = 2.5 \times 10^4$, while altering the required reserve ratio. It is found that given a required reserve ratio the monetary aggregate increases approximately linearly for a period, and after that it approaches and remains at a steady value, as shown in the left panel of Figure 1. We recorded the steady values of the monetary aggregate for different required reserve ratios and found the relation between them in a good agreement with that drawn from the simplified multiplier model. We also collected the values of time when the monetary aggregate begins to be steady for different required reserve ratios. Since the maximal value among them is $1.2 \times 10^5$ or so, after $8 \times 10^5$ rounds we collected the data of deposit volume, loan volume and latency time which is defined as the time interval between the sampling moment and the moment when money takes part in trade after the sampling moment for

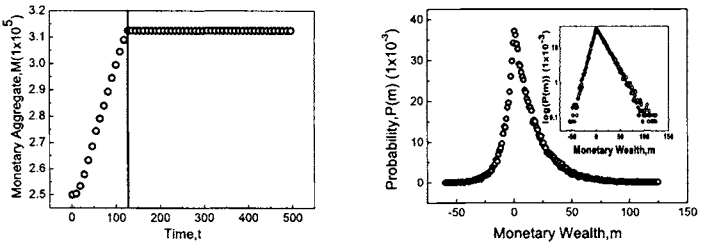


**Fig. 1.** Time evolution of the monetary aggregate for the required reserve ratio $r = 0.8$ (left). The vertical line denotes the moment at which the monetary aggregate reaches the steady value. The stationary distribution of monetary wealth for the required reserve ratio $r = 0.8$ (right). It can be seen that the distribution follows asymmetric Laplace distribution from the inset.

the first time. We are fully convinced that the whole economic system has reached a stationary state by that moment. Please note that each transfer of the deposits can be regarded as that of currency chosen randomly from reserves in the bank equivalently as collecting the data of latency time.

Defining monetary wealth as the difference between deposit volume and loan volume of a trader, we found that monetary wealth follows asymmetric Laplace distribution, as shown in the right panel of Figure 1. Using the method of the most probable distribution [8], we can obtain the formula of stationary distribution of monetary wealth in terms of the required reserve ratio as follows,

$$\begin{aligned} p_+(m) &= \frac{N_0}{N} e^{-\frac{m}{\overline{m}_+}} \quad \text{for } m \geq 0; \\ p_-(m) &= \frac{N_0}{N} e^{\frac{m}{\overline{m}_-}} \quad \text{for } m < 0, \end{aligned} \tag{2}$$

where $N_0$ denotes the number of the traders with no monetary wealth, $\overline{m}_+$ is equal to the average amount of positive monetary wealth and $\overline{m}_-$ is equal to the average amount of negative monetary wealth. The expressions of $\overline{m}_+$ and $\overline{m}_-$ can be written as

$$\overline{m}_+ = \frac{1 + \sqrt{1-r}}{r} \frac{M_0}{N} \tag{3}$$

and

$$\overline{m}_- = \frac{1 - r + \sqrt{1-r}}{r} \frac{M_0}{N}. \tag{4}$$

Theoretical results are in good agreement with simulation results, as shown in the left panel of Figure 2.

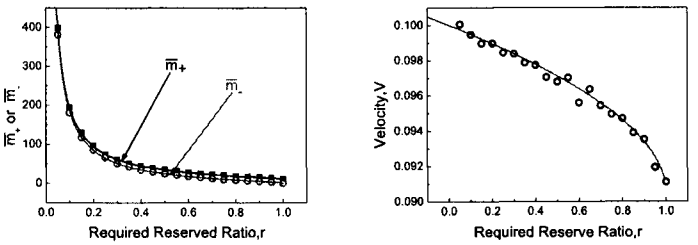


**Fig. 2.** $\overline{m}_+$ (left, upper), $\overline{m}_-$ (left, lower) and the velocity of money (right) versus the required reserve ratio obtained from simulation results (dots) and the corresponding analytical formulas (continuous curves) respectively.

From simulation results, it is also seen that latency time follows an exponential law, which indicates that the transferring process of currency is a Poisson type. In this case, the velocity of money can be calculated by latency

time [4]. From the detailed balance condition which holds in steady state, we can obtain the expression of the velocity of money in terms of the required reserve ratio as follows,

$$V = \frac{N}{M_0} e^{-\frac{1}{m_+}}. \tag{5}$$

Theoretical results are in good agreement with simulation results, as shown in the right panel of Figure 2.

## 4 Conclusion

In this paper, in order to look into how money creation affects the statistical mechanics of money circulation, we develop a random transfer model of money by introducing a fractional reserve banking system. In this model, the monetary aggregate is determined by the monetary base and the required reserve ratio. Simulation results show that the steady monetary wealth distribution follows asymmetric Laplace type and latency time of money obeys exponential distribution regardless of the required reserve ratio. The distribution function of monetary wealth in terms of the required reserve ratio are presented. Likewise, the expression of the velocity of money is also presented. These theoretical calculations are in quantitative agreement with the corresponding simulation results. We believe that this study is helpful for understanding the process of money creation and its impacts in reality.

## References


1. Drăgulescu A, Yakovenko VM (2000) Statistical mechanics of money. The European Physical Journal B 17:723–729
2. Chakraborti A, Chakrabarti BK (2000) Statistical mechanics of money: how saving propensity affects its distribution. The European Physical Journal B 17:167–170
3. Chatterjee A, Chakrabarti BK, Manna SS (2004) Pareto law in a kinetic model of market with random saving propensity. Physica A 335:155–163
4. Wang Y, Ding N, Zhang L (2003) The circulation of money and holding time distribution. Physica A 324:665–677
5. Ding N, Xi N, Wang Y (2003) Effects of saving and spending patterns on holding time distribution. The European Physical Journal B 36:149–153
6. Fischer R, Braun D (2003) Transfer potentials shape and equilibrate monetary systems. Physica A 321:605–618
7. Garfinkel MR, Thornton DL (1991) The multiplier approach to the money supply process: a precautionary note. Federal Reserve Bank of St. Louis Review 73:47–64
8. Gaskell DR (2003) Introduction to the Thermodynamics of Materials. Taylor & Francis, New York

# Prospects for Money Transfer Models

Yougui Wang*, Ning Ding, and Ning Xi

Department of Systems Science, School of Management, Beijing Normal University, Beijing, 100875, People's Republic of China ygwang@bnu.edu.cn

**Summary.** Recently, in order to explore the mechanism behind wealth or income distribution, several models have been proposed by applying principles of statistical mechanics. These models share some characteristics, such as consisting of a group of individual agents, a pile of money and a specific trading rule. Whatever the trading rule is, the most noteworthy fact is that money is always transferred from one agent to another in the transferring process. So we call them money transfer models. Besides explaining income and wealth distributions, money transfer models can also be applied to other disciplines. In this paper we summarize these areas as statistical distribution, economic mobility, transfer rate and money creation. First, money distribution (or income distribution) can be exhibited by recording the money stock (flow). Second, the economic mobility can be shown by tracing the change in wealth or income over time for each agent. Third, the transfer rate of money and its determinants can be analyzed by tracing the transferring process of each one unit of money. Finally, money creation process can also be investigated by permitting agents go into debts. Some future extensions to these models are anticipated to be structural improvement and generalized mathematical analysis.

**Key words:** Transfer model, Distribution, Mobility, Transfer rate, Money creation

## 1 Introduction

Money does matter to an economy. To understand the role that money plays in the performance of economic system, many theoretical studies have been performed in traditional economics. Recently, a small branch of "econophysicists" shifted their attentions to this issue. Several models have been developed by applying principles of statistical mechanics to the questions of income and wealth distribution [1, 2, 3, 4, 5]. These models share some characteristics, such as consisting of a group of individual agents, a pile of money and a specific trading rule. The most noteworthy fact is that money is always transferred from one agent to another in the transferring process. So this kind of models could be referred as money transfer models. The prime theme of constructing such models is to explore the mechanism behind wealth or income

distribution. In fact, they can be applied more widely in some other economic issues. In this paper, we prospect for some applications of these transfer models and anticipate that considerable achievements can be made on the basis of them. We also argue that further improvements should be accomplished to make these models much more realistic.

The purpose of this paper is to identify what issues could be analyzed on the basis of money transfer models. This kind of models is very easy to grasp, for only two elements are involved: money and agents. Money is possessed or held by agents, and may be transferred among them via trading. Based on these models, recent efforts were mainly devoted to the formation of monetary wealth distribution, the circulation of money [6, 7] and creation of money [8]. We would like to summarize and expand the scope of their applications in the following four routes.

## 2 Applications

### 2.1 Distribution

Money transfer models are originally used to demonstrate steady distributions of money. This can be achieved by recording the quantity of money stock possessed by each agent in the simulations. In the basic model proposed by A. Drăgulescu and V.M. Yakovenko, the money distribution follows a Boltzmann-Gibbs law [1]. B.K. Chakrabarti et al. introduced the saving behavior into the model [2, 3], and found the money distribution obeys a Gamma law when all the agents are set with the same saving factor, but a power law as the saving factor is set randomly. N. Ding et al. introduced the preferential dispensing behavior into the trading process and also obtained a stationary power-law distribution [4]. From these results we can see that the shape of distribution is determined by the trading rule.

Besides these theoretical studies, econophysicists also performed the empirical studies on the distribution in the economy, following the earlier Pareto's work. The analysis showed that in many countries the income distribution typically presents with a power-law tail, and majority of the income distribution can be described by an exponential distribution [9, 10, 11]. It is worthy noting that account of these empirical studies is taken of income distribution. Income corresponds to money flow which is different from money amount. However, all the distributions presented in previous simulations do not refer to the money flow. Actually, in the money transferring process, we can also record the level of money flow received by each agent during a given period. The statistics of them yields the flow type distribution. Thus, embodying the money flow generation mechanism, the transfer models can also provide a convenient tool for investigating the mechanism behind the income distribution in reality.

## 2.2 Mobility

During the simulations of money transfer models, the amount of money held by agents varies over time. This phenomenon is called mobility in economics. In the view of economists, mobility is an indispensable supplement to distribution because the former can cure the anonymity assumption of the latter [12]. And the analysis of mobility is greatly helpful to comprehend the dynamic mechanism behind the distribution. In addition, like distribution, economic mobility should be an essential criterion when evaluating a relevant theoretical model.

In the transferring process, the economy will reach its steady state and the distribution will keep unchanged. After that, the amount of money still fluctuates over time for each agent, meanwhile the rank of each agent shifts from one position to another. To show the mobility phenomenon with clarity, we can record agents' rank instead of the amount of money. The time series of rank for any agent's can be obtained by sorting all of agents according to their money in the end of each round. We performed some simulations and the primary results show all of agents are equal in the economies of models in Ref. [1] and [2]. They have the same probability to be the rich or the poor. It can be found that the frequency of the rank fluctuation decreases as the saving rate increases. By contrast, the economy in Ref. [3] is stratified where agents are not equal any longer for their saving rates are set diversely. Based on these results, it can be concluded that different models exhibit different mobility characters.

## 2.3 Transfer Rate

In reality, money does not remain motionless. Instead, it is transferred from hand to hand consecutively. This phenomenon is called the circulation of money in economics. The term usually used to describe the circulation is the velocity of money, which can be computed by the ratio of total transaction volume to the money stock. In fact, it refers to the transfer rate of money that measures how fast the money moves between agents. This rate can be observed by recording the time intervals for each unit of money to be held. This kind of time interval is called "holding time" or "latency time" of money. It can be found that there is not only a distribution of money among agents, but also a steady distribution of holding time as the economy reaches its equilibrium state. The holding time distribution also shifts its shape depending on the trading rule. For instance, in the simulation of the model with uniform saving factor the stationary distribution of holding time obeys exponential law, while in the model with diverse saving factor the distribution changes to a power type [7].

The transfer rate of money has an inverse relation with the average holding time of money. When the circulation process is in the nature of Poisson one,

the probability distribution of the latency time of money takes the following form [6]

$$P(t) = \frac{1}{T} e^{-\frac{t}{T}}, \tag{1}$$

where $1/T$ corresponds to the intensity of Poisson process, and $T$ signifies the average holding time of money. In this case, the velocity of money can be written as

$$V = \frac{1}{T}. \tag{2}$$

Since the average holding time is governed by the money holders (agents in the models), the above equation suggests that the velocity is determined by the behavior patterns of economic agents. Employing the well-known life-cycle model in economics, Wang et al. demonstrated that the velocity of money can be obtained from the individual's optimal choice [13]. Thus the study on the transferring process provides a new insight into the velocity of money circulation.

### 2.4 Money Creation

With the help of money transfer models, we can still discuss the impact of money creation on the statistical mechanics of money circulation. In reality, most part of the monetary aggregate that circulates in the modern economy is created by debts through banking system. Thus money creation has important influence on the characteristics of monetary economic system.

Recently, some investigations have been carried out in this line mainly from two perspectives. One is from physics perspective. Adrian Drăgulescu and Victor Yakovenko demonstrated the equilibrium probability distribution of money follows the Boltzmann-Gibbs law, allowing agents to go into debt and putting a limit on the maximal debt of an agent [1]. Robert Fischer and Dieter Braun analyzed the process of creation and annihilation of money using a mechanical method and examined how money creation affects statistical mechanics of money [8]. The other is from economics perspective. It is known that the essence of money creation can be represented by the required reserve ratio from the multiplier model of money in economics. Thus we can examine the dependence of monetary wealth distribution and the velocity of money on the required reserve ratio based on a transfer model of money and computer simulations. We extended a money transfer model by introducing a banking system, where money creation is achieved by bank loans and the monetary aggregate is determined by the monetary base and the required reserve ratio. The simulation results show that monetary wealth follows asymmetric Laplace distribution, and the velocity decreases as the required reserve ratio increases. For more details you can see Ref. [14].

## 3 Discussion and Conclusion

The money transfer models were constructed originally for explaining the real income or wealth distribution. They also can be applied to other economic issues, such as economic mobility, transfer rate and money creation. These applications will bring this kind of models to be rival to the prevailing models in monetary economics. Of course, the current version of these models is far from perfectness. In order to fulfill the goal, some further improvements and modifications are required. One is to make the agents in the model closer to rational economic ones. Another one is to analyze the model in a generalized mathematical way, which would help us to understand the model deeply and completely and show the right way to structural modification.

## References


1. Drăgulescu A, Yakovenko VM (2000) Statistical mechanics of money. The European Physical Journal B 17:723–729
2. Chakraborti A, Chakrabarti BK (2000) Statistical mechanics of money: how saving propensity affects its distribution. The European Physical Journal B 17:167–170
3. Chatterjee A, Chakrabarti BK, Manna SS (2004) Pareto law in a kinetic model of market with random saving propensity. Physica A 335:155–163
4. Ding N, Wang Y, Xu J, Xi N (2004) Power-law distributions in circulating money: effect of preferential behavior. International Journal of Modern Physics B 18:2725–2729
5. Hayes B (2002) Follow the money. American Scientist 90:400–405
6. Wang Y, Ding N, Zhang L (2003) The circulation of money and holding time distribution. Physica A 324:665–677
7. Ding N, Xi N, Wang Y (2003) Effects of saving and spending patterns on holding time distribution. The European Physical Journal B 36:149–153
8. Fischer R, Braun D (2003) Transfer potentials shape and equilibrate monetary systems. Physica A 321:605–618
9. Drăgulescu A, Yakovenko VM (2001) Evidence for the exponential distribution of income in the USA. The European Physical Journal B 20:585–589
10. Silva AC, Yakovenko VM (2005) Temporal evolution of the thermal and superthermal income classes in the USA during 1983–2001. Europhysics Letters 69:304–310
11. Souma W (2001) Universal structure of the personal income distribution. Fractals 9:463–470
12. Schiller BR (1977) Relative earnings mobility in the United States. The American Economic Review 67:926-941
13. Wang Y, Qiu H (2005) The velocity of money in a life-cycle model. Physica A in press
14. Xi N, Ding N, Wang Y (2005) Dependence of distribution and velocity of money on required reserve ratio. In: Takayasu H (eds) this contributed works. Springer, Tokyo

# Inequalities of Wealth Distribution in a Society with Social Classes

J. R. Iglesias[1,2], S. Risau-Gusman[1] and M. F. Laguna[3]

1. Instituto de Física, Univ. Fed. do Rio Grande do Sul, Porto Alegre, Brazil
2. Programa de Pós-Graduação em Economia, Univ. Fed. do Rio Grande do Sul, Porto Alegre, Brazil
3. The Abdus Salam International Center for Theoretical Physics, Strada Costiera 11, (34014) Trieste, Italy

**Summary.** We study a simple model of capital exchange among economic agents in which the effect of a correlation between wealth and connectivity is considered within two different hypotheses: a) agents interact within their own social or economic class and b) agent's connectivity is related to its success in exchange transactions. The wealth distribution in the first case may generate a two-class society with a clear gap in the middle and highly unequal power law distributions with a great number of strongly impoverished agents and a few very rich ones. In the second case the wealth distribution is modified by the dynamics of the lattice, getting closer to a power law for some values of the parameters of the model. As expected, the lattice itself is different from the random initial one.

**Keywords:** Econophysics, Wealth Distribution, Pareto's Law, Dynamic Network

Wealth and income distribution in developed societies follow a kind of modified Pareto's law: a power law behavior is generally observed in the high income classes (with an exponent that changes from country to country [1]) while for intermediate and low income groups the distribution follows a different law that could be Gibbs or log-normal [2-5]. Different models of capital exchange among economic agents have been proposed trying to obtain the power law distribution for the wealthiest strata [6-14]. Most of these models consider two important factors: the existence of risk aversion and an asymmetric probability that, in the exchange, the poorer agent will be somehow privileged. Nevertheless, almost all of them consider exchanges on a fixed lattice or with no lattice at all, which corresponds to just pick two agents, either at random [12], or following an extremal dynamics [13,14]. In almost all cases a Gibbs-exponential distribution is obtained, and the results are in good agreement with the income distribution of welfare states such as Sweden [15]. Other models have been proposed, in which agents save a fraction of their capital, and put at risk only a fraction of their resources [6,8,9,12]. In the language of economics this saved part of the assets is a measure of the agent risk aversion and its effect on the wealth distribution has been also studied for different dynamics. A power law is obtained in some limits, but the Gibbs-exponential distribution is the most frequent result [12].

In all those models there are no correlations between the wealth of the agents and the probability of interaction between them: the choice of the interacting partner is determined either by a minimum dynamics [13,14] or completely at random. This seems to be at odds with the idea that people have a tendency to interact mainly with other members of their own social and economic class. For example: Inaoka et al. [16] analyzes the exchanges between Japanese banks, concluding that the bigger ones have more interactions between them and with the others than the small banks. The resulting network of interactions is very different for big banks (almost fully connected) than for small ones (a star-like network).
In this paper we include correlations between the agent's connectivity and its wealth. The first case considered corresponds to a society in which agents interact only if they belong to a similar wealth class: we impose the difference of wealth between two agents to be within a given threshold to allow them to have an exchange. In the second case a correlation between the success of an agent in their economic exchanges and its degree of connectivity is considered: agents are initially placed on a random lattice, with a given average connectivity. When the transfer of wealth between agents takes place, every time an agent increases its wealth it also increases the number of neighbors linked to it.

**a) Model with wealth classes**

This is a variation of the model we presented in a previous work [12]: We consider a set of economic agents characterized by an initial wealth uniformly distributed between 0 and $w_{max}$ and by a risk aversion factor $\beta_i$, being $0 \leq \beta_i \leq 1$, so that $1-\beta_i$ is the percentage of wealth that the $i$-agent is willing to risk. Each transaction will take place between two agents chosen at random and we prescribe that no agent can win more than the amount he puts at stake, so that the value exchanged is the minimum value of the available resources of both agents, i.e. $dw = min\,[(1-\beta_i)w_i; (1-\beta_k)w_k]$, being $\beta_i$ the risk-aversion and $w_i$ the wealth of the $i$-agent. Finally, we introduce a probability $p \geq 0.5$ of favoring the poorer of the two partners [9]. Increasing the probability of favoring the poorer agent is a way to simulate the action of the state or of some type of regulatory policy that tries to redistribute the resources [14,15]. Here we take this probability given by a formula proposed in previous works [9,12]: if the two agents participating in the exchange are $i$ and $k$, the probability of favoring the poorer one is given by:

$$p = 0.5 + f \times \frac{|w_i - w_k|}{w_i + w_k} \qquad (1)$$

In ref. [12] the two agents were chosen with no restrictions. Here they can only interact if they belong to the same wealth class, i. e., if the difference between their wealth's is such that $|w_i - w_k| < u$, where $u$ is a *threshold* parameter. The idea behind this hypothesis is that the exchanges are more frequent or probable between agents belonging to the same economic strata [16]. We present numerical results for a system of $N=10,000$ agents and performing a number of transactions big enough to guarantee that the distribution is stationary ($10^4$ to $10^5$ steps per agent).

Fig.1 shows the results for two values of the parameter $f$ of Eq. (1): $f=0.1$ (low probability of favoring he poorer agent) and $f=0.5$ (the highest probability of favoring the poorer agent) and several values of the threshold $u$. We start the simulation with a uniform wealth distribution in the range [0,500].
For very low values of $u$ the wealth distribution presents a sharp peak for very low income, meaning that a substantial fraction of the population owns almost zero income, while for higher values of $w$ the distribution is almost flat: the small value of $u$ prevents wealth redistribution. For intermediate values of the threshold ($u$ =25 and 50) an interesting effect occurs: the formation of two "social classes", one with very small wealth, $w \approx 0.1$, and a richer one with a maximum near $w = 100$.

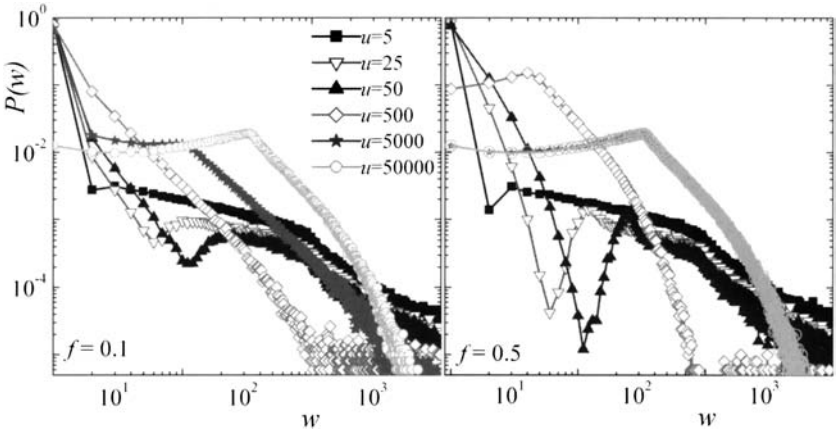


Fig. 1: Wealth distribution for case (a) with two values of the probability of favoring the poorer agent: $f=0.1$ (left panel) and $f=0.5$ (right panel) and several values of the threshold $u$. The results are averaged over 100 runs.

Finally, for bigger values of $u$ the wealth distribution looks more familiar: In the case of $f=0.1$ a maximum is observed for low values of the wealth ($w \approx 100$) and a power law for the wealthiest sector of the population (see $u=5000$). For $f=0.5$ the maximum is more pronounced, the society is "fairer", and the number of very rich people decreases faster with a kind of exponential behavior. We have also calculated the Gini coefficients, finding that they increase as a function of $u$. It means that the presence of "wider" classes lessens inequalities. Correlations between wealth and risk-aversion will be discussed in a forthcoming article.

**b) Model with correlation between wealth and connectivity**

We consider a system where the agents are connected at random, but the links are not static and change as a function of the success in the individual exchanges. Each agent is characterized by an initial wealth $w_i$, and by a risk aversion factor $\beta_i$. The simulation parameters are the same as in the previous case. We investigate

several values for the average number of links per agent, $\nu$, going from *5* to *80* links per agent, for $N=5000$ agents. The initial distribution of links is a Gaussian. In order to update the lattice at each exchange, we divide the total wealth of the system by the total number of links, attributing a "monetary" value to each link. The winner in a transaction wins the amount of wealth defined in the previous subsection, but also wins the equivalent number of links, rounded by elimination of any fractional number. At each time step one chooses at random one agent and, also at random, one of the ``neighbors" connected with him by a link. This implies that more connected agents interact more frequently. We have studied three cases: the static lattice, in order to have a reference for comparison, the case (i) where after the transaction the winner takes links from the loser (up to a limit of leaving the loser connected by at least one link), and the case (ii) where the winner gets links taken at random from the population. Notice that in all three cases the total number of links remains constant throughout the evolution. This dynamics modifies the lattice: in all cases the resulting link distribution deviates significantly from the initial one, with a few agents having a number of links much higher than the average, whereas most of the population has very few links. This effect is most dramatic in the case $f=0.1$, and for big values of $\nu$.

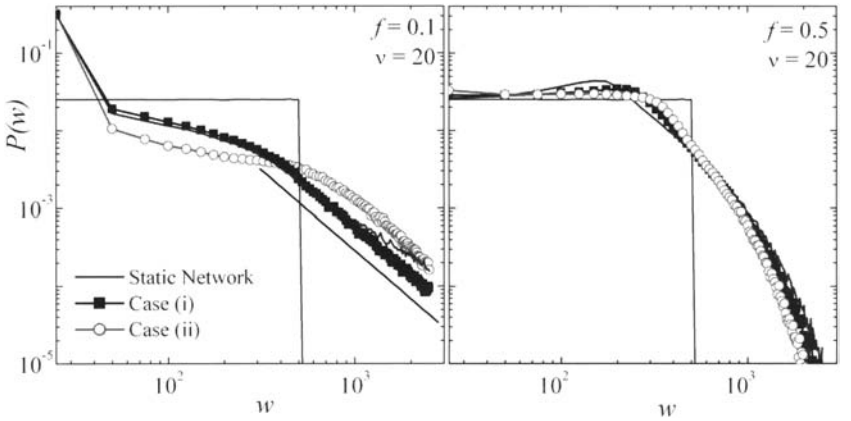


Fig. 2: Asymptotic wealth distribution for f=0.1 (left panel) and f=0.5 (right panel) and ν=20. The results are averaged over 100 runs. The lines correspond to the fit by a power law, and are only guides to the eye. The exponent of the power law is –2.06

Concerning the asymptotic wealth distribution, in Fig. 2 we present results for $\nu=20$, with $f=0.1$ and $f=0.5$. For $f=0.1$ a very high peak for low values of income appears: about *60* per cent of the agents own about *1/10* of the average wealth. On the other hand, a few very rich individuals own most of the wealth: each one owns about five times the average wealth. The differences between the three cases concern mainly the number of people in the middle class, loosely defined as the wealth interval between $w_{max}/10$ and $w_{max}$, and the number of people in the upper class ($w > w_{max}$). One striking feature observed for $f=0.1$ is that in the high class the asymptotic distribution for case (ii) follows a power law, whose exponent is $\approx$

*-2.06* (corresponding to a Pareto exponent *-1.06*). Also, it is rather surprising that the distribution for case (i) and the static one are almost identical for $f=0.1$, even though the underlying lattices are very different. The three cases look similar for high values of $f$. When $f=0.5$, the redistribution of links does not seem to play an important role in the redistribution of wealth. In this case, the wealth distribution looks similar to that of developed countries like Japan or England [3,4]: a maximum in the distribution is observed for a "middle class" and for high income a power law may be drawn in a relatively narrow strip of wealth. The income of that middle class is almost the same as the average initial wealth, while the number of very rich people is smaller by a factor of *2* compared with the case $f=0.1$. In all cases, we have found a linear relationship between the connectivity of each agent and its wealth. Thus, interactions take place mostly between rich agents. A full description of this model is going to be published elsewhere [17].

## Conclusions

We have presented two models where the exchange of wealth is either related to the respective wealth of the agents or to the success in individual exchanges. In spite of the simplicity of the models, the results reproduce some features of observed real wealth distributions. If the probability of favoring the poorer partner in individual transactions is small the distributions exhibits clear peaks for very low income (less than one hundredth of the average initial value). Those peaks contain a significant fraction of the total population, while the number of very rich agents is small but they concentrate most of the total wealth of the society. In a fairer society ($f \approx 0.5$) the distribution looks more like that of developed societies, with a maximum in the middle class and a smaller number of very rich agents. But there is a deviation of the power law to an exponential law, suggesting that this value of $f$ is too high to a detailed description of real societies.

## References:


[1] V. Pareto, Cours d'Economie Politique, Vol. 2, F. Pichou, Lausanne (1897).
[2] J.P. Bouchaud and M. Mézard, Phys. A **282**(2000), 536.
[3 ]W. Souma, Fractals **9** (2001), 463.
[4] A. Dragulescu, V.M. Yakovenko, Eur.Phys.J. B **20** (2001) 585; Phys.A **299** (2001) 213.
[5] F. Clementi and M. Gallegati, cond-mat/0408067 (2004)
[6] A.Chatterjee, B.K. Chakrabarti and S.S. Manna, Physica A **335** (2004), 155.
[7] T. Di Matteo, T. Aste, S. T. Hyde, cond-mat/0310544 (2003).
[8] A. Chakraborti and B.K. Charkrabarti, Eur. Phys. J. B **17** (2000), 167.
[9] N. Scafetta, S. Picozzi and B.J. West, cond-mat/0209373v1 and cond-mat/0306579v2 .
[10] S. Ispolatov, P.L. Krapivsky and S. Redner, Eur. Phys. J. B **2** (1998), 267.
[11] S. Solomon and P. Richmond, Eur. Phys. J. B **27** (2002), 257.
[12] J. R. Iglesias, S. Gonçalves, G. Abramson and J.L. Vega, Phys. A **342** (2004), 186.
[13] S. Pianegonda, J. R. Iglesias, G. Abramson and J.L. Vega, Phys. A **322** (2003), 667.
[14] J. R. Iglesias *et al.*, Phys. A **327** (2003), 12.

[15] S. Pianegonda and J.R. Iglesias, Physica A **342** (2004), 193.
[16] H. Inaoka, H. Takayasu, T. Shimizu, T. Ninomiya and K. Taniguchi., Phys. A **339** (2004), 621.
[17] S. Risau Gusman and J.R. Iglesias, submitted to Physica A.

# Analyzing money distributions in 'ideal gas' models of markets

Arnab Chatterjee[1], Bikas K. Chakrabarti[1] and Robin B. Stinchcombe[2]

[1] Theoretical Condensed Matter Physics Division and Centre for Applied Mathematics and Computational Science, Saha Institute of Nuclear Physics, Block-AF, Sector-I Bidhannagar, Kolkata-700064, India.
arnab@cmp.saha.ernet.in, bikas@cmp.saha.ernet.in

[2] Rudolf Peierls Centre for Theoretical Physics, Oxford University, 1 Keble Road, Oxford, OX1 3NP, UK. stinch@thphys.ox.ac.uk

We analyze an ideal gas like models of a trading market. We propose a new fit for the money distribution in the fixed or uniform saving market. For the market with quenched random saving factors for its agents we show that the steady state income ($m$) distribution $P(m)$ in the model has a power law tail with Pareto index $\nu$ exactly equal to unity, confirming the earlier numerical studies on this model. We analyze the distribution of mutual money difference and also develop a master equation for the time development of $P(m)$. Precise solutions are then obtained in some special cases.

## 1 Introduction

The distribution of wealth among individuals in an economy has been an important area of research in economics, for more than a hundred years. Pareto [1] first quantified the high-end of the income distribution in a society and found it to follow a power-law $P(m) \sim m^{-(1+\nu)}$, where $P$ gives the normalized number of people with income $m$, and the exponent $\nu$, called the Pareto index, was found to have a value between 1 and 3.

Considerable investigations with real data during the last ten years revealed that the tail of the income distribution indeed follows the above mentioned behavior and the value of the Pareto index $\nu$ is generally seen to vary between 1 and 2.5 [2, 3, 4, 5]. It is also known that typically less than 10% of the population in any country possesses about 40% of the total wealth of that country and they follow the above law. The rest of the low income population, in fact the majority (90% or more), follow a different distribution which is debated to be either Gibbs [3, 6] or log-normal [4].

Much work has been done recently on models of markets, where economic (trading) activity is analogous to some scattering process [6, 7, 8, 9, 10, 11,

12]. We put our attention to models where introducing a saving factor for the agents, a wealth distribution similar to that in the real economy can be obtained [7, 8]. Savings do play an important role in determining the nature of the wealth distribution in an economy and this has already been observed in some recent investigations [13]. Two variants of the model have been of recent interest; namely, where the agents have the same fixed saving factor [7], and where the agents have a quenched random distribution of saving factors [8]. While the former has been understood to a certain extent (see e.g, [14, 15]), and argued to resemble a gamma distribution [15], attempts to analyze the latter model are still incomplete (see however, [16]). Further numerical studies [17] of time correlations in the model seem to indicate even more intriguing features of the model. In this article, we intend to study both the market models with savings, analyzing the money difference in the models.

## 2 The model

The market consists of $N$ (fixed) agents, each having money $m_i(t)$ at time $t$ ($i = 1, 2, \ldots, N$). The total money $M$ ($= \sum_i^N m_i(t)$) in the market is also fixed. Each agent $i$ has a saving factor $\lambda_i$ ($0 \leq \lambda_i < 1$) such that in any trading (considered as a scattering) the agent saves a fraction $\lambda_i$ of its money $m_i(t)$ at that time and offers the rest $(1 - \lambda_i)m_i(t)$ for random trading. We assume each trading to be a two-body (scattering) process. The evolution of money in such a trading can be written as:

$$m_i(t+1) = \lambda_i m_i(t) + \epsilon_{ij}\left[(1-\lambda_i)m_i(t) + (1-\lambda_j)m_j(t)\right], \qquad (1)$$

$$m_j(t+1) = \lambda_j m_j(t) + (1-\epsilon_{ij})\left[(1-\lambda_i)m_i(t) + (1-\lambda_j)m_j(t)\right] \qquad (2)$$

where each $m_i \geq 0$ and $\epsilon_{ij}$ is a random fraction ($0 \leq \epsilon \leq 1$). In the fixed savings market $\lambda_i = \lambda_j$ for all $i$ and $j$, while in the distributed savings market $\lambda_i \neq \lambda_j$ with $0 \leq \lambda_i, \lambda_j < 1$.

## 3 Numerical observations

In addition to what have already been reported in Ref. [8, 9, 10] for the model, we observe that, for the market with fixed or uniform saving factor $\lambda$, a fit to Gamma distribution [15],

$$P(m) \sim m^{\eta} \exp(-m/T), \quad \eta = \frac{3\lambda}{1-\lambda} \qquad (3)$$

is found to be better than a log-normal distribution. However, our observation regarding the distribution $D(\Delta)$ of difference $\Delta \equiv |\Delta m|$ of money between any two agents in the market (see Fig. 1a) suggests a different form:

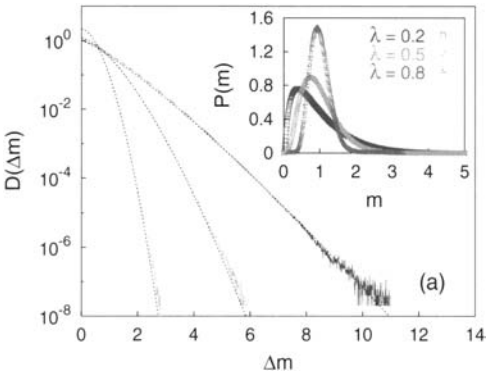


**Fig. 1.** $D(\Delta)$ in the fixed or uniform savings market, for $\lambda = 0.2, 0.5, 0.8$ (right to left) and their fitting curves: $D(\Delta) \sim \exp(-\Delta^{1+\lambda}/T')$; the corresponding $P(m)$ the inset.

$$P(m) \sim m^{\delta} \exp(-m^{\kappa}/T'); \quad \kappa = 1 + \lambda. \tag{4}$$

In fact, we have checked, the steady state (numerical) results for $P(m)$ asymptotically fits even better to (3), rather than to (4).

With heterogeneous saving propensity of the agents with fractions $\lambda$ distributed (quenched) widely ($0 \leq \lambda < 1$), where the market settles to a critical Pareto distribution $P(m) \sim m^{-(1+\nu)}$ with $\nu \simeq 1$ [8], the money difference behaves as $D(\Delta m) \sim (\Delta m)^{-(1+\gamma)}$ with $\gamma \simeq 1$. In fact, this behavior is invariant even if we set $\epsilon_{ij} = 1/2$ [18]. This can be justified by the earlier numerical observation [7, 8] for fixed $\lambda$ market ($\lambda_i = \lambda$ for all $i$) that in the steady state, criticality occurs as $\lambda \to 1$ where of course the dynamics becomes extremely slow. In other words, after the steady state is realized, the third term containing $\epsilon = 1/2$ becomes unimportant for the critical behavior. We therefore concentrate on this case in this paper.

## 4 Analysis of money difference

In the process as considered above, the total money $(m_i + m_j)$ of the pair of agents $i$ and $j$ remains constant, while the difference $\Delta m_{ij}$ evolves for $\epsilon = 1/2$ as

$$(\Delta m_{ij})_{t+1} = \alpha_{ij}(\Delta m_{ij})_t + \beta_{ij}(m_i + m_j)_t, \tag{5}$$

where $\alpha_{ij} = \frac{1}{2}(\lambda_i + \lambda_j)$ and $\beta_{ij} = \frac{1}{2}(\lambda_i - \lambda_j)$. As such, $0 \leq \alpha < 1$ and $-\frac{1}{2} < \beta < \frac{1}{2}$. The steady state probability distribution $D(\Delta)$ can be written as (cf. [18]):

$$D(\Delta) = \int d\Delta'\, D(\Delta')\, \langle \delta(\Delta - (\alpha+\beta)\Delta') + \delta(\Delta - (\alpha-\beta)\Delta') \rangle$$
$$= 2\langle \left(\frac{1}{\lambda}\right)\, D\left(\frac{\Delta}{\lambda}\right) \rangle, \qquad (6)$$

where we have used the symmetry of the $\beta$ distribution and the relation $\alpha_{ij} + \beta_{ij} = \lambda_i$, and have suppressed labels $i, j$. Here $\langle \ldots \rangle$ denote average over $\lambda$ distribution in the market. Taking now a uniform random distribution of the saving factor $\lambda$, $\rho(\lambda) = 1$ for $0 \leq \lambda < 1$, and assuming $D(\Delta) \sim \Delta^{-(1+\gamma)}$ for large $\Delta$, we get

$$1 = 2 \int d\lambda\, \lambda^{\gamma} = 2(1+\gamma)^{-1}, \qquad (7)$$

giving $\gamma = 1$. No other value fits the above equation. This also indicates that the money distribution $P(m)$ in the market also follows a similar power law variation, $P(m) \sim m^{-(1+\nu)}$ and $\nu = \gamma$.

## 5 Master equation approach

We also develop a Boltzmann-like master equation for the time development of $P(m,t)$, the probability distribution of money in the market [18]. We again consider the case $\epsilon_{ij} = \frac{1}{2}$ in (1) and (2) and rewrite them as

$$\begin{pmatrix} m_i \\ m_j \end{pmatrix}_{t+1} = \mathcal{A} \begin{pmatrix} m_i \\ m_j \end{pmatrix}_t \text{ where } \mathcal{A} = \begin{pmatrix} \mu_i^+ & \mu_j^- \\ \mu_i^- & \mu_j^+ \end{pmatrix}; \quad \mu^{\pm} = \frac{1}{2}(1 \pm \lambda). \qquad (8)$$

Collecting the contributions from terms scattering in and subtracting those scattering out, we can write the master equation for $P(m,t)$ as

$$\frac{\partial P(m,t)}{\partial t} + P(m,t) = \langle \int dm_i \int dm_j\, P(m_i,t) P(m_j,t)\, \delta(\mu_i^+ m_i + \mu_j^- m_j - m) \rangle, \qquad (9)$$

which in the steady state gives

$$P(m) = \langle \int dm_i \int dm_j\, P(m_i) P(m_j)\, \delta(\mu_i^+ m_i + \mu_j^- m_j - m) \rangle. \qquad (10)$$

Assuming, $P(m) \sim m^{-(1+\nu)}$ for $m \to \infty$, we get [18]

$$1 = \langle (\mu^+)^{\nu} + (\mu^-)^{\nu} \rangle \equiv \int \int d\mu^+ d\mu^- p(\mu^+) q(\mu^-) \left[ (\mu^+)^{\nu} + (\mu^-)^{\nu} \right]. \qquad (11)$$

Considering now the dominant terms ($\propto x^{-r}$ for $r > 0$, or $\propto \ln(1/x)$ for $r = 0$) in the $x \to 0$ limit of the integral $\int_0^{\infty} m^{(\nu+r)} P(m) \exp(-mx) dm$, we get from eqn. (11), after integrations, $1 = 2/(\nu+1)$, giving finally $\nu = 1$.

## 6 Summary

We consider the ideal-gas-like trading markets where each agent is identified with a gas molecule and each trading as an elastic or money-conserving (two-body) collision [7, 8, 9, 10]. Unlike in a gas, we introduce a saving factor $\lambda$ for each agents. Our model, without savings ($\lambda = 0$), obviously yield a Gibbs law for the steady-state money distribution. Our numerical results for uniform saving factor suggests the equilibrium distribution $P(m)$ to be somewhat different from the Gamma distribution reported earlier [15].

For widely distributed (quenched) saving factor $\lambda$, numerical studies showed [8, 9, 10] that the steady state income distribution $P(m)$ in the market has a power-law tail $P(m) \sim m^{-(1+\nu)}$ for large income limit, where $\nu \simeq 1.0$, and this observation has been confirmed in several later numerical studies as well [16, 17]. It has been noted from these numerical simulation studies that the large income group people usually have larger saving factors [8]. This, in fact, compares well with observations in real markets [13, 19]. The time correlations induced by the random saving factor also has an interesting power-law behavior [17]. A master equation for $P(m,t)$, as in (9), for the original case (eqns. (1) and (2)) was first formulated for fixed $\lambda$ ($\lambda_i$ same for all $i$), in [14] and solved numerically. Later, a generalized master equation for the same, where $\lambda$ is distributed, was formulated and solved in [16] and [18]. We show here that our analytic study (see [18] for details) clearly support the power-law for $P(m)$ with the exponent value $\nu = 1$ universally, as observed numerically earlier [8, 9, 10].

## 7 Acknowledgments

BKC is grateful to the INSA-Royal Society Exchange Programme for financial support to visit the Rudolf Peierls Centre for Theoretical Physics, Oxford University, UK and RBS acknowledges EPSRC support under the grants GR/R83712/01 and GR/M04426 for this work and wishes to thank the Saha Institute of Nuclear Physics for hospitality during a related visit to Kolkata, India.

## References

1. Pareto V (1897) Cours d'economie Politique. F. Rouge, Lausanne
2. Moss de Oliveira S, de Oliveira PMC, Stauffer D (1999) Evolution, Money, War and Computers. B. G. Tuebner, Stuttgart, Leipzig
3. Levy M, Solomon S (1997) Physica A 242:90-94; Drăgulescu AA, Yakovenko VM (2001) Physica A 299:213; Aoyama H, Souma W, Fujiwara Y (2003) Physica A 324:352
4. Di Matteo T, Aste T, Hyde ST (2003) cond-mat/0310544; Clementi F, Gallegati M (2004) cond-mat/0408067

5. Sinha S (2005) cond-mat/0502166
6. Chakrabarti BK, Marjit S (1995) Ind. J. Phys. B 69:681; Ispolatov S, Krapivsky PL, Redner S (1998) Eur. Phys. J. B 2:267; Drăgulescu AA, Yakovenko VM (2000) Eur. Phys. J. B 17:723
7. Chakraborti A, Chakrabarti BK (2000) Eur. Phys. J. B 17:167
8. Chatterjee A, Chakrabarti BK, Manna SS (2004) Physica A 335:155
9. Chatterjee A, Chakrabarti BK; Manna SS (2003) Phys. Scr. T 106:36
10. Chakrabarti BK, Chatterjee A (2004) in Application of Econophysics, Proc. 2nd Nikkei Econophys. Symp., ed. Takayasu H, Springer, Tokyo, pp. 280-285
11. Hayes B (2002) Am. Scientist (Sept-Oct) 90:400; Sinha S (2003) Phys. Scr. T 106:59; Ferrero JC (2004) Physica A 341:575; Iglesias JR, Gonçalves S, Abramson G, Vega JL (2004) Physica A 342:186; Scafetta N, Picozzi S, West BJ (2004) Physica D 193:338
12. Slanina F (2004) Phys. Rev. E 69:046102
13. Willis G, Mimkes J (2004) cond-mat/0406694
14. Das A, Yarlagadda S (2003) Phys. Scr. T 106:39
15. Patriarca M, Chakraborti A, Kaski K (2004) Phys. Rev. E 70:016104
16. Repetowicz P, Hutzler S, Richmond P (2004) cond-mat/0407770
17. Ding N, Xi N, Wang Y (2003) Eur. Phys. J. B 36:149
18. Chatterjee A, Chakrabarti BK, Stinchcombe RB (2005) cond-mat/0501413
19. Dynan KE, Skinner J, Zeldes SP (2004) J. Pol. Econ. 112:397.

# Unstable periodic orbits and chaotic transitions among growth patterns of an economy

Ken-ichi Ishiyama and Yoshitaka Saiki

Department of Mathematical Sciences, Graduate School of Mathematical Sciences, The University of Tokyo, 3-8-1 Komaba, Meguro-ku, Tokyo 153-8914, Japan
(e-mail: ishiyama@ms.u-tokyo.ac.jp; saiki@ms.u-tokyo.ac.jp)

**Summary.** We analyze a chaotic growth cycle model which represents essential aspects of macroeconomic phenomena. Unstable periodic solutions detected from a chaotic attractor of the model are categorized into some hierarchical classes, and relationships between each class of them and characteristics of the attractor are discussed. This approach may be useful to clarify economic laws hidden behind complicated phenomena.

## 1 Introduction

There is a close relation between a business cycle model and periodic solutions even if it shows chaotic dynamics. This suggests that taking periodic solutions from the chaotic dynamics leads to clarifying laws hidden behind complicated economic dynamics.

There have been some studies to understand complicated chaotic phenomena by detecting unstable periodic solutions. For example, an unstable periodic solution of Navier-Stokes equation found by Kawahara and Kida (2001) exhibits a regeneration cycle of wall turbulence and makes it possible for us to recognize a coherent structure obviously. We examine chaotic dynamics shown by a generalized Goodwin model through finding unstable periodic orbits embedded in the chaotic attractor.

The next section gives a Keynes-Goodwin model[1] and shows a chaotic attractor generated by the model. In section 3 we study unstable periodic orbits numerically found in the attractor, and attempt to understand characteristics of the model through classified orbits. The final section concludes our results.

[1] Wolfstetter (1982) first generalized the original model (Goodwin (1967)) to a model with dissipative structure by introducing a government taking a Keynesian fiscal policy.

## 2 The model and its attractor

A two-country model with capital mobility is extended from a model representing the domestic growth cycle of a country by interactions among three variables. The two-country growth cycle model is described by the following six-dimensional system (Ishiyama and Saiki (2005b)):

$$\frac{du_i}{dt} = 0.5(\frac{0.1}{1-v_i} - 0.48 + \pi_i^e - \alpha)u_i, \tag{1}$$

$$\frac{dv_i}{dt} = (0.1(h_i + 0.7\mu_i(v^* - v_i) - 0.7(1-\delta)(1-u_i)) - (\alpha+\beta))v_i, \tag{2}$$

$$\frac{d\pi_i^e}{dt} = 0.4(\frac{0.1}{1-v_i} - 0.48 - \pi_i^e - \alpha), \tag{3}$$

where investment function $h_i = 1.5(1-u_i)^5 + 3.5(u_j - u_i)^3$; $i, j = 1, 2$ $(i \neq j)$. Variables $u_i$, $v_i$ and $\pi_i^e$ denote the $i$-th country's labor share rate, employment ratio and expected inflation respectively. Parameters $\alpha$, $\beta$ and $\delta$ are the rate of technical progress, the population growth rate, and the income tax rate respectively. These parameters are common in both countries, while parameters of fiscal policy $\mu_i$ are different. The relation $\mu_2 > \mu_1 (> 0)$ means the government of country 2 takes more positive fiscal policy. Symbol $v^*$ means the equilibrium employment ratio determined by $1/u_i \cdot du_i/dt = 0$ and $d\pi_i^e/dt = 0$. The function $h_i$ contains a term of mutual actions between countries. For an economically meaningful parameter setting the trajectory starting from almost every point reaches the chaotic attractor shown in Fig. 1.

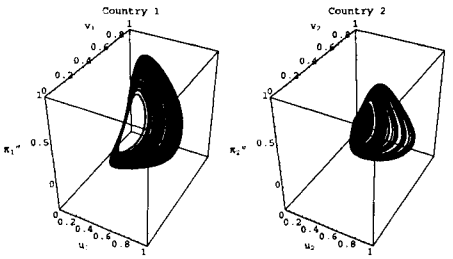


**Fig. 1.** A chaotic attractor depicted by the model

Parameters are fixed as $\alpha = 0.02$, $\beta = 0.01$, $\delta = 2/7$, $\mu_1 = 1.25$, $\mu_2 = 6$ hereafter. The first Lyapunov exponent of the attractor is 0.099.

## 3 Unstable periodic orbits in the attractor

Ishiyama and Saiki (2005a,b) have already pointed out the importance of unstable periodic orbits (UPOs) to recognize characteristics of business cycles

to some extent. In this section we consider classes of periodic solutions focusing on the labor share rate in country 1 ($u_1$). Relationships between each class of the solutions and the chaotic solution will be discussed further. It is essential in this context that periodic orbits are to be embedded.[2]

### 3.1 Unstable periodic solutions with simple dynamics

The simplest periodic solution (Fig. 2) is a representative of business cycles observed in the chaotic attractor. Intervals between the nearest local maxima of $u_1$ of the cycles approximately equal the period of this solution.[3] Here we

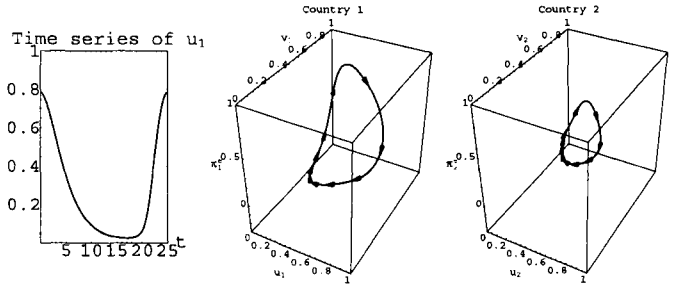


**Fig. 2.** Time series and phase diagram of the simplest periodic solution ($UPO_1$)

Period of this orbit is about 25.22. Arrows on the periodic orbit indicate traveling directions. They also show how an economy typically goes in the chaotic solution.

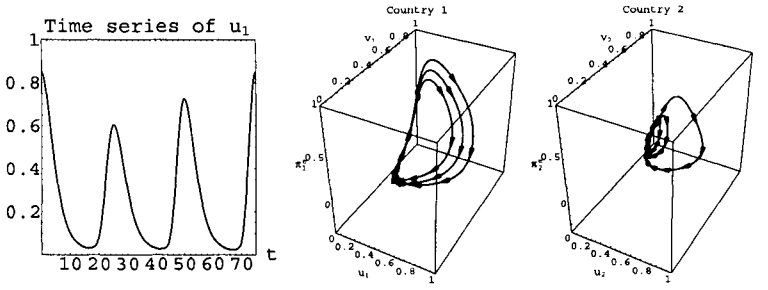


**Fig. 3.** Time series and phase diagram of an example of $\mathrm{UPO_n}$ ($UPO_3$)

This unstable periodic orbit can be seen as a series of three expanding tides.

[2] See Ishiyama and Saiki (2005b).

[3] Some statistical similarities between the simplest solution and the chaotic solution are referred to in Ishiyama and Saiki (2005b).

consider a class $\mathrm{UPO_n}$ including the simplest solution. It consists of $UPO_k$, where $UPO_k$ is a set of periodic solutions with $k$ times of monotonic expansions of $u_1$ (See Fig. 3.). Only $UPO_1$, $UPO_2$, $\cdots$, $UPO_7$ are found as the members of $\mathrm{UPO_n}$ for our parameter setting.

### 3.2 Unstable periodic solutions with complicated dynamics

We have found more than 500 unstable periodic orbits with transitions among patterns. Each pattern is a series of expanding oscillations like $UPO_n$, and called regime $n$ in Ishiyama and Saiki (2005a,b). We name the transition from $UPO_m$ type pattern (regime $m$) to $UPO_n$ type pattern (regime $n$) transition $m \rightarrow n$. $\mathrm{UPO_{m,n}}$ is a class of periodic solutions which contains transition $m \rightarrow n$ and transition $n \rightarrow m$, while $\mathrm{UPO_{l,m,n}}$ is a class of periodic solutions consisting of transitions $l \rightarrow m$, $m \rightarrow n$ and $n \rightarrow l$. Fig. 4 gives examples of these classes.

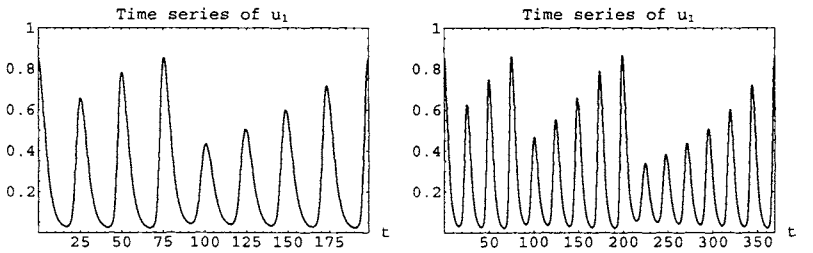


**Fig. 4.** Time series of examples of $\mathrm{UPO_{m,n}}$ ($UPO_{3,5}$) and $\mathrm{UPO_{l,m,n}}$ ($UPO_{3,5,7}$)

Each orbit of these classes is considered as a cyclical series of growth patterns of $u_1$.

### 3.3 Hierarchical structure of solutions

Let us consider correspondences between chaos-transitions and transitions in unstable periodic orbits with respect to the classes mentioned above. Chaos-transitions are transitions observed in the chaotic behavior. Fig. 5 suggests that the more complicated periodic solutions with many patterns we find, the more sorts of chaos-transitions can be covered with their transitions. In fact it is confirmed that transition $4 \rightarrow 2$ is covered with the transitions in $UPO_{2,3,3,4}$ for example. No transitions other than chaos-transitions are covered with the transitions of any periodic orbits in the attractor. Thus there is duality between chaos-transitions and transitions represented by detectable periodic orbits in the attractor.

Transition in the chaotic attractor

| From \ To | 1 | 2 | 3 | 4 | 5 | 6 | 7 | 8 | 9 |
|---|---|---|---|---|---|---|---|---|---|
| 1 | 34 | 197 | 33 | 0 | 0 | 0 | 0 | 0 | 0 |
| 2 | 125 | 517 | 223 | 0 | 0 | 0 | 0 | 0 | 0 |
| 3 | 29 | 51 | 197 | 179 | 92 | 40 | 0 | 0 | 0 |
| 4 | 26 | 42 | 44 | 37 | 33 | 37 | 74 | 0 | 0 |
| 5 | 24 | 29 | 27 | 23 | 21 | 22 | 36 | 8 | 0 |
| 6 | 9 | 13 | 18 | 21 | 27 | 22 | 20 | 6 | 0 |
| 7 | 14 | 15 | 41 | 21 | 15 | 16 | 23 | 7 | 0 |
| 8 | 0 | 0 | 5 | 13 | 3 | 0 | 0 | 0 | 0 |
| 9 | 0 | 0 | 0 | 0 | 0 | 0 | 0 | 0 | 0 |

**Fig. 5.** Distribution of chaos-transitions and transitions represented by $UPO_{m,n}$ and $UPO_{l,m,n}$ (Value in each cell is the frequency of a chaos-transition divided by 100.)

The $c$-th cell in the $r$-th row with positive number denotes chaos-transition $r \to c$. The cells bounded by dashed lines and thick lines mean chaos-transitions corresponding to $UPO_{m,n}$ and $UPO_{l,m,n}$ respectively. Note that the existence of $UPO_k$ implies transition $k \to k$ is observable in the chaotic economic growth.

## 4 Conclusions

We focus on three classes of unstable periodic solutions embedded in the chaotic attractor of a growth cycle model. We study correspondences between these classes and the general chaotic behavior. Typical patterns and properties of economic growth of the model can be represented by the simplest class. The other classes contain recursive transitions among two or three typical patterns corresponding to transitions observed in the chaotic growth. We have successfully related the presence of such a transition of chaotic economic dynamics generated by the two-country Keynes-Goodwin model to the existence of unstable periodic solutions embedded in the attractor. Generally infinite number of unstable periodic orbits are embedded in a chaotic attractor. This implies usefulness of unstable periodic orbits to study business cycle models.

## References


1. Goodwin RM (1967) A growth cycle. In: Feinstein CH (ed) Socialism, capitalism, and economic growth. Cambridge University Press, Cambridge
2. Ishiyama K, Saiki Y (2005a) Unstable periodic orbits embedded in a chaotic economic dynamics model. Applied Economics Letters, in press
3. Ishiyama K, Saiki Y (2005b) Unstable periodic orbits and chaotic economic growth. Chaos, Solitons & Fractals, in press
4. Kawahara G, Kida S (2001) Periodic motion embedded in plane Couette turbulence: regeneration cycle and burst. Journal of Fluid Mechanics 449:291–300
5. Wolfstetter E (1982) Fiscal policy and the classical growth cycle. Journal of Economics 42:375–393

# Power-law behaviors in high income distribution

Sasuke Miyazima[1] and Keizo Yamamoto[2]

[1]Department of Natural Science, Chubu University, 1200 Matsumoto, Kasugai, Aichi, 487-8501, Japan
[2]Faculty of Engineering, Setsunan University, 17-8 Ikeda-Nakamachi, Neyagawa, Osaka, 572-8508, Japan

**Summary.** We discussed a model in this paper which shows the power-law behavior in a ranking problem of income. The Monte Carlo simulation of our model shows a satisfactory fit with the data for Japanese and US CEOs. We have investigated the origin of the power-law behavior which is proven by some fractal structure formed in our model system.

**Key words.** High-income ranking, Power-law distribution, Fractals, High-income model

## 1. Introduction

A log-normal distribution for a wide range of income and Pareto distribution (Power-law distribution) for high-income people have been investigated since 1897: (Pareto 1987); (Champernowne 1953); (Shlesinger and Montroll 1983); (Aoyama et al. 2000); (Yamamoto and Miyazima 2001). The simple explanation of the log-normal distribution has been made by the product of independent events and the central limit theorem. The power law distribution has not been explained simply by introducing some adjusting parameters: (Champernowne 1953); (Lydal 1959); (Mandelbrot 1960); (Montroll and Shleginger 1983); (Takayasu and Okuyama 1998); (Kawamura and Hatano 2002).

The main source of income of each person is proportional to sales amounts of companies. The series of those processes perform an endlessly complicated and hierarchical nest structure of trades, where a person gets the incomes from another person who loses the resource money. Therefore, we can find an intricate nest of structures, and consequently these should form some fractality.

In this paper we will suggest a model for the distribution of income. Our present model is so simple that we can obtain an analytical solution and power-law distribution assuming existence of stationary solution. But we don't expect that our model can be robust enough to explain all properties of economics. We are very interested in understanding why the economic system shows the fractality, which we consider, one of important reasons why the data in real economical activity and our model show the power law in high income.

## 2. Random Competitive Model Showing the Power Law

We proposed a model which reproduces a power law behavior of the highest income amounts against ranking of income without any adjusting parameter: (Yamamoto et al. 2002, 2003). Our high income data in Japan are derived from tax amounts of high tax payers which we can obtain annually from the tax office publications. The tax rate is constant for these high-tax payers who are the top 100,000 wage-earners in Japan. Therefore, the income is proportional to the tax amount for those people. For our model system we assume two following conservation conditions:

C1. Our system consists of $N$ homogeneous members at the initial stage. The number of persons $N$ is fixed.

C2. Our system reserves $2N$ units as resource money. Each member keeps one unit as a minimum amount.

We tried to simulate several cases of $N$=100, $N$=1,000, $N$=10,000 and $N$=100,000 and generally averaged the ranked incomes over 100 trials of simulation.

We introduce the following simple competition rule to our system:

M1. Two members who are picked up randomly from the whole group scramble for their total money by doing an economic activity. One of the two members collects all the money of the two members, and the other loses all of his and her resource money. In order to maintain the number of active members with resource money, we add one unit of money to the loser.

M2. In order to keep the whole resource money in our system we reduce one unit from a member who has resource money more than or equal to two units and is also selected randomly.

Hereafter, a step of process which consists of both M1 and M2 is referred to one Monte Carlo step(1M.C.). If this simulation is carried out more than $N^2$ Monte Carlo steps, we obtain a stationary distribution from any arbitrary initial condition. This model is so simple that we can take into account more factors of complicated situations for our simulation with ease. A good fit with the combined data of CEOs in the USA and Japan was obtained previously even in the present model. We show the comparison of the real data (1998) and the simulation result ($N$=10,000) in Fig.1. Now, in this simulation a minimum unit of resource money is converted in a hundred million yen in real data. Both slopes of these data are about –0.7, which shows a good fit with the power law slope.

## 3. Intricate Nests of Structures

We investigate the origin of the power law which has been proven here by the fact that the fractality is formed in our model system. Evidence of the fractality is shown to be a nest of structures. It has been investigated how intricate nests of structures are formed in our system. It is our attractive point how many members have joined to the competition until a certain member in the system gets the present wealth. We trace backward the flow of the money from the top of the tree.

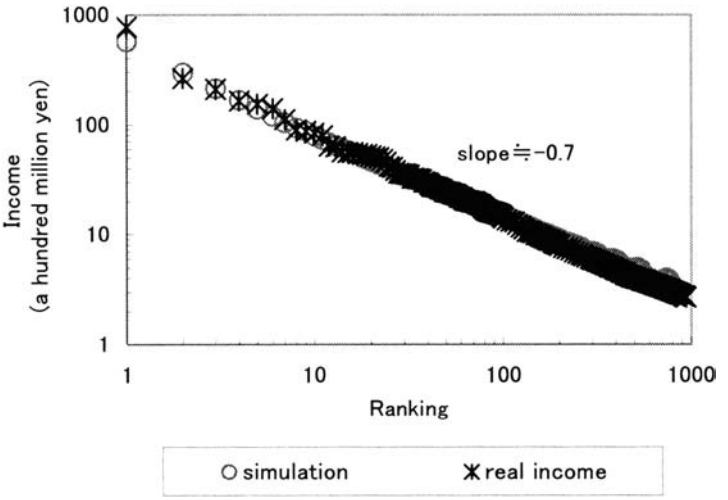


**Fig. 1.** The comparison of the real data (1998) and the simulation result($N$=10,000)

An example of the intricate nests of structures is shown in Fig.2 for $N$=1,000. The number on the left-hand side in Fig.2 indicates the M.C. step, and time goes to upward. The first figure in the box is the wealth amount at the M.C. step and the second figure is the member's identification number. The shaded box indicates that the member lost his whole resource money in the previous competition. The beginning of the tree (top in Fig.2) is defined by a member who lost his whole resource money in a competition. The ends of the tree (bottom in Fig.2) are defined by a pair of members whose resource money is one (for example, the two members #725 and #947 at the M.C. step of 939051, #827 and #978 at M.C. step of 939086 and #625 and #469 at M.C. of 939162 in Fig.2). This tree is so large that only parts of the top and bottom are shown, omitting M.C. Step of 939162 to 997091.

Thus we can find various sizes of trees where many members are joined into the competition. The dot-dash-line in the vertical direction in Fig.2 shows that one unit or occasionally more units are reduced from the winner in the intervals of these Monte Carlo steps (the step M2 in the second section). Therefore, the wealth on the top of the tree becomes less than the size of tree.

Naturally, the size of a tree is equal to the number of competitions in the tree or the number of shaded boxes in the tree. Therefore, if one unit or occasionally more units were not reduced from the winner in the intervals of these Monte Carlo steps, like dot-dash-lines in Fig.2, the wealth on the top of the tree could become the same amount of the tree size under the enough resource money in the system. The fractality in the size of trees (the number of members joined) and the number of trees has been investigated.

We show the size of trees against the ranking ($N$=1,000) and the wealth on the top of the tree against the ranking is shown in Fig.3 in the log-log diagram. The

slope of power-law of the tree size in Fig. 3 is –1.94, and the coefficient of determination-R2 is 0.999 by least squares method, which means that the size of tree

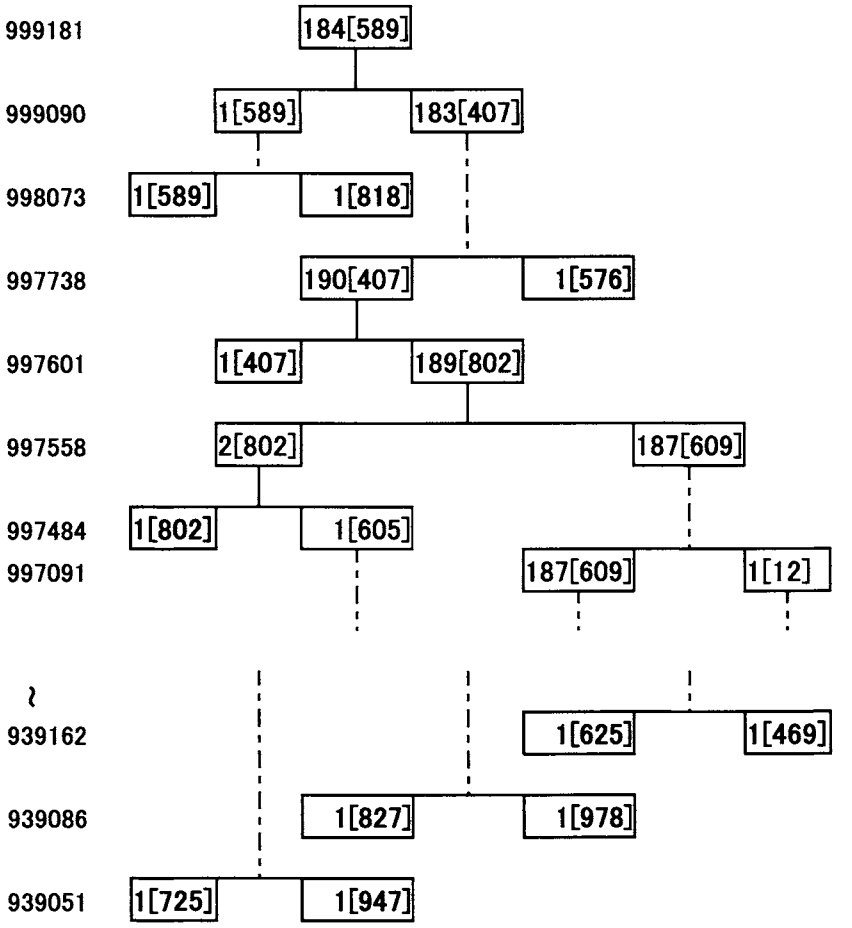


**Fig. 2.** An example of the intricate nests of structures $N$=1.000

is expressed by the power-law of the ranking. Similarly, the slope of power-law of the wealth is –0.721. These results show good fits with the power-law in Fig. 1. Therefore, we consider that the fractality of our model is clearly illustrated by the fractality of the tree size distribution.

## References

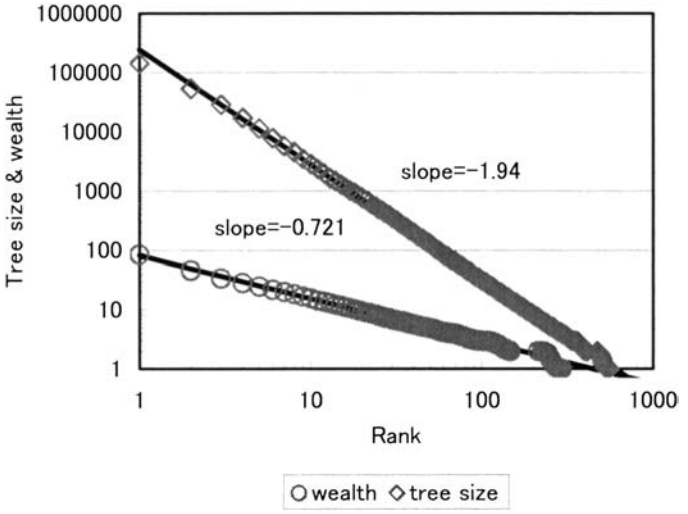


**Fig. 3** The size of the tree and the wealth on the top of the tree against the ranking ($N$=1,000). The lozenge, the circle and the straight line are obtained from the present simulation and curve fitting, respectively

Aoyama H, Souma W, Nagahara Y, Okazaki M P, Takayasu H, Takayasu M (2000) Pareto's law for income of individuals and debt of bankrupt companies. Fractals **8:**293-300

Champernowne GD (1953) A model of income distribution. Economic Journal 63:318-351

Kawamura K, Hatano N (2002) Universality of Zipf's law. Journal of the Physical Society of Japan **71:** 1211-1213

Lydall H F (1959) The distribution of employment incomes. Econometrica 27:110-115

Mandelbrot BB (1960) The Pareto-Levy law and the distribution of income. International Economic Review 1:79-106

Montroll EW, Shlesinger MF (1983) Maximum entropy formalism, fractals, scaling phenomena, and 1/f noise: A tale of tails. J Stat Phys 32:209-230

Pareto V (1897) Le Cours d'Economie Politique. Macmillan, London

Shlesinger MF, Montroll EW (1983) Fractal stochastic process: clusters and intermittancies. Lecture Note in Math 1035:138-152

Takayasu H, Okuyama K (1998) Country dependence on company size distributions and a numerical model based on competition and cooperation. Fractals 6:67-79

Yamamoto K, Miyazima S (2001) Power-law Distribution of High Income Taxes in Japan (in Japanese). Sociological Theory and Methods 16:133-138

Yamamoto K, Miyazima S, Koshal KR, Yamada Y (2002) A model for distribution of high-tax payers. Physica A 314:743-748

Yamamoto K, Miyazima S, Koshal KR, Koshal M, Yamada Y (2003) A Model for Distribution of High-Tax Payers. Japan J Indust Appl Math 20:147-154

# The power-law exponent and the competition rule of the high income model

Keizo Yamamoto[1], Sasuke Miyazima[2], Hiroshi Yamamoto[3], Toshiya Ohtsuki[3] and Akihiro Fujihara[3]

[1]Faculty of Engineering, Setsunan University, 17-8 Ikeda-Nakamachi, Neyagawa, Osaka 572-8508, Japan
[2]Department of Natural Science, Chubu University, 1200 Matsumoto, Kasugai, Aichi 487-8501, Japan
[3]Graduate School of Integrated Science, Yokohama City University, 22-2 Kana-zawaku-seto, Yokohama, Kanagawa 236-0027, Japan

**Summary.** We propose a model for power-law problem in high-income against ranking. This model is so simple that we can examine the effect of some differences in competition rules where we obtain different power-law exponents as well as exact analysis by the master equation.

**Key words.** High-income model, Power-law exponent, High-income ranking, Fractal, Master equation

## 1. Introduction

Economic activities have a very intricate structure consisting of many factors such as production of natural resources, disasters, labor power supply, relation between goverments, and so on to be considered. The economic system can be viewed as a prototype of complex system. These gains which are obtained by the competition among companies are distributed to employees. These processes perform endlessly complicated nests of trades that people get incomes from unspecific random objects and give incomes other people more and more. Therefore here are intricate nests of structures and these should exist some fractality.

Power-law distributions for high-income have been investigated since 1897 (Pareto 1897); (Chanpernowune 1953); (Lydall 1959); (Shlesinger and Montroll 1983); (Takayasu and Okuyama 1998); (Aoyama et al. 2000) ; (Yamamoto et al. 2001, 2002) and (Kawamura and Hatano 2002). Power-law distributions are found in many other examples of social and economical events as well as in high-income ranking problems, such as word counting (Zipf 1932), family name distribution (Miyazima at al. 2000), firm size (Stanley 1996), fluctuation in finance (Mandelbrot 1997), passengers at stations (Fujita and Miyazima 2003) and so on. Here we show some earlier power-law exponents of high-income data in Table 1.

In high-income ranking problem, our main interests are why the high-income distribution shows power-law and what kinds of factors determine the power-law exponent. In addition, it is also interesting what the power-law exponent means in the real economical phenomena. In this paper we suggest a model which indicates some different power-law exponents depending on competition rules.

**Table 1.** Some earlier data of the power-law exponent ($X$: Income. $P(t>X)$: The probability with income more than $X$. $R$: The rank means the number of persons who earn more than $X$. Equation $R \sim P(t>X) \sim X^{-\alpha}$)

| Year | Name | $\alpha$ | Income Data |
|---|---|---|---|
| 1897 | Pareto | 1.5 | Some Euro cities |
| 1953 | Champernone | 1.7 | U.K. 1951/1952 |
| 1959 | Lydall | 1.5 | U.K. 1954/1955 |
| 1983 | Montroll. et al. | 1.63 | USA 1935/1936 |
| 1998 | Takayasu. et al. | 0.5 | Model |
| 2000 | Aoyama. et al. | 2.05 | Japan 1998 |
| 2002 | Yamamoto. et al. | 1.39 | Model |
| 2002 | Yamamoto. et al. | 1.32 | Japan & USA 1998 |
| 2002 | Kawamura. et al. | 1.0 | Model |

When we change the competition rule in our model, different power-law exponents are obtained. If we can investigate and analyze the relation between the competition rule and the power-law exponent sufficiently, it will become clear that we can estimate the competition rule. Our presented model is simple enough to get exact solution by analytical method.

## 2. Model and simulation

Our common procedures are as follows.

Step1. Our system consists of $N$ homogeneous members. The number of members $N$ is fixed.

Step2. One of two members who are chosen randomly from the members gets their total money after the following competition rule.

Step3. $S$ units of money are kept constant as total resource during the process. Each member keeps one unit of money as a minimum amount. The total resource money $S$ is fixed except for the following Type 2.

We introduce our system to the competition rule of the following three different types.

**Type 1**: One of the two members collects all the money of the two members, and the other loses all of his or her resource money. In order to maintain the number of active members with resource money, we add one unit of money to the loser. In order to keep the whole resource money in our system we reduce one unit from a randomly selected member who has the resource money more than or equal to two units. Here, the total amount of the resource money $S$ is fixed $2N$.

**Type 2**: One of the two members acquires all the money of the two members, and the other loses all of his or her resource money. In order to maintain the number of active members with resource money, we add one unit of money to the loser. Therefore, the total resource money increases by one unit per competition. We relax the above common condition Step3 and the system is simulated under the condition $N^2 < S < (N+1)^2$ for the member $N$ and the total resource money $S$.

**Type 3**: When amounts of the resource money for the two members are different, a winner acquires less amount of two resource moneys and the other loses the amount of money. A winner who has smaller money doesn't get the all of the money of a loser. The remaining part of the rule is almost the same as Type 1. Here, the total resource money $S$ is fixed $7N$.

We show simulation results of three different types against ranking in Fig. 1. The power-law exponent of incomes against ranking of Type 1,Type 2 and Type 3

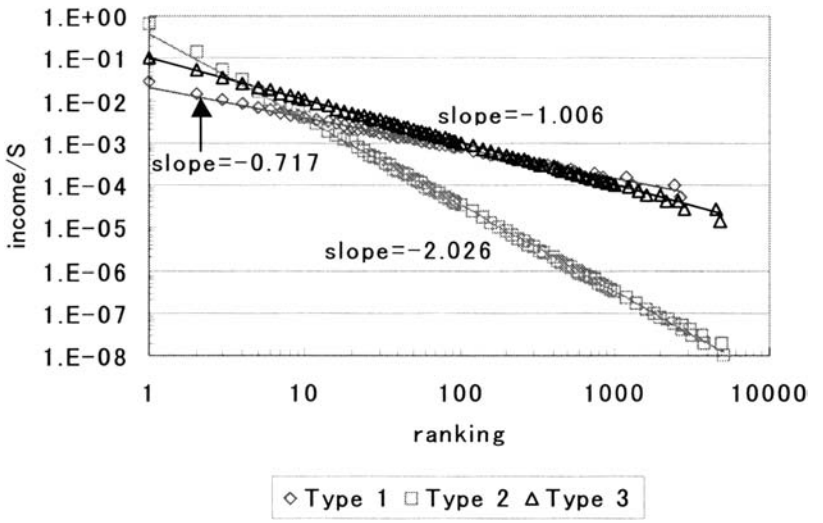


**Fig. 1.** Three log-log plots of income against ranking, $N$ =10,000.

are –0.717, –2.026 and –1.006, respectively.

Simulation results of the frequency $F(X)$ against the income $X$ are shown in Fig.2 for three different types. The power-law exponent of the frequency $F(X)$ against the income $X$ of Type 1,Type 2 and Type 3 are –2.45, –1.55 and –1.98, respectively. Now we compare above exponents with $\alpha$ in Table 1. When we

change the exponents of the frequency $F(X)$ in Fig. 2 to the exponents of the cumulative quantity, the exponents of Type 1, Type 2 and Type 3 become –1.45, –0.55 and –0.98, respectively. The exponent of Type 1 corresponds to the indices of $\alpha$ of Pareto's, Champernowne's, Lydall's, Montroll's and Yamamoto's data. The Type 2 corresponds to the index of $\alpha$ of Takayasu's data. The Type 3 corresponds to the index of $\alpha$ of Kawamura's data.

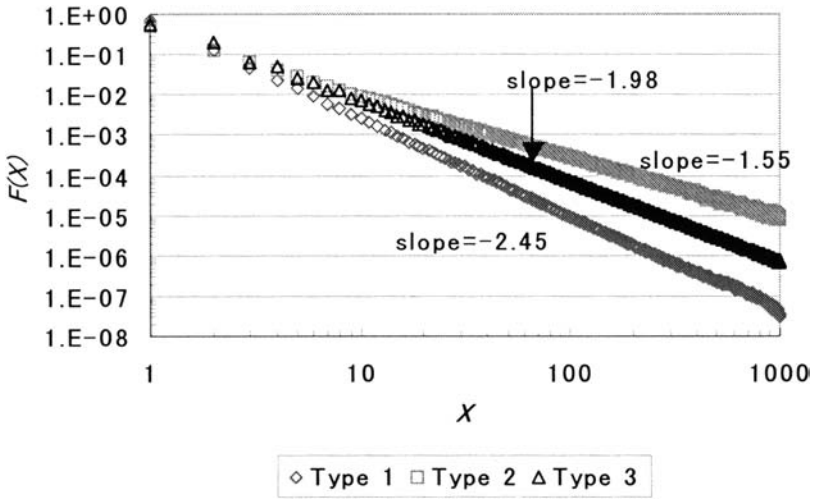


**Fig. 2.** Tree log-log plots of the frequency $F(X)$ against the income $X$, $N$ =10,000.

We also obtain the asymptotic solution of our model. Our model is simple enough to be solved by the generating function of the master equation. When income $X$ is sufficiently larger than order 1, the asymptotic probability $P(X)$ behaves as a power-law. As for the Type 1 model, the power-law exponent of the asymptotic probability $P(X)$ becomes –5/2 and as for the Type 2 model, the power-law exponent of the asymptotic probability $P(X)$ becomes –3/2, respectively. These results show a good agreement with the slopes in Fig.2.

## References


Aoyama H, Souma W, Nagahara Y, Okazaki M P, Takayasu H, Takayasu M (2000) Pareto's law for income of individuals and debt of bankrupt companies. Fractals **8**:293-300

Champernowne GD (1953) A model of income distribution. Economic Journal 63:318-351

Kawamura K, Hatano N (2002) Universality of Zipf's law. Journal of the Physical Society of Japan **71**: 1211-1213

Lydall H F (1959) The distribution of employment incomes. Econometrica 27:110-115

Mandelbrot BB (1997) Fractals and Scaling in Finance in France, Springer, Berlin

Miyazima S. Lee Y. Nagamine T. Miyajima H (2000) Power-law distribution of family names in Japanese societies. Physica A 278:282-288
Fujita H. Miyazima S Master Thesis of H. Fujita. Department of Engineering Physics. Chubu University. March 2003
Pareto V (1897) Le Cours d'Economie Politique. Macmillan. London
Shlesinger MF. Montroll EW (1983) Fractal stochastic process: clusters and intermittancies. Lecture Note in Math 1035:138-152
Stanley M H R. Amaral L A N. Buldyrev S V. Havlin S. Leschhron H. Maass P. Salinger M A and Stanley H E (1996) Scaling behavior in the growth of companies. Nature. 379:804-806.
Takayasu H. Okuyama K (1998) Country dependence on company size distributions and a numerical model based on competition and cooperation. Fractals 6:67-79
Yamamoto K. Miyazima S (2001) Power-law Distribution of High Income Taxes in Japan (in Japanese). Sociological Theory and Methods 16:133-138
Yamamoto K. Miyazima S. Koshal KR. Yamada Y (2002) A model for distribution of high-tax payers. Physica A 314:743-748
Zipf G K (1932) Selected studies of the principle of relative frequency in language. Harvard University Pree. Cambridge. MA

# 6. New Ideas

# Personal versus economic freedom

Katarzyna Sznajd-Weron[1] and Józef Sznajd[2]

[1] Institute of Theoretical Physics,
University of Wrocław, Poland
[2] Institute for Low Temperature and Structural Research, Polish Academy of Sciences, Wrocław, Poland

**Summary.** In this paper we present a model which allows to discriminate between two kinds of behavior connected with areas which we will call personal and economic. It seems that an attitude with regard to the personal area spreads in a different way than that with regard to the economic area. We assume that each agent tries to influence its neighbors, but in the personal area the information flows inward from the neighborhood (like in most opinion dynamic models), whereas in the economic area the information flows outward from the agent or group of agents to the neighborhood (like in the Sznajd model).

## 1 Introduction

Much of economic and financial theory is based on the notion that individuals act rationally and consider all available information in the decision-making process. However, researchers have uncovered a surprisingly large amount of evidence that this is frequently not the case [1]. Human decision-making deviates in one way or another from the standard assumptions of the rationalistic paradigm in economics. Psychologists consider an interactive process where several factors may influence a decision in a non-trivial way. In the seventies Daniel Kahneman and Amos Tversky began to benchmark their cognitive models of decision making under risk and uncertainty against economic models of rational behavior. In 2002 they were rewarded by the Nobel Prize in Economic Sciences.

Starting with the works of Kahneman and Tversky a field known as "behavioral finance" has evolved. It attempts to better understand and explain how emotions and cognitive errors influence investors and the decision-making process. Many researchers believe that the study of social sciences can shed considerable light on the efficiency of financial markets as well as explain many stock market anomalies, market bubbles, and crashes.

One of the most powerful phenomena that influence human decision is the so-called *Social Validation* - the fundamental way that we decide what to do

in a situation is to look at what others are doing [2]. An isolated person does not convince others; a group of people sharing the same opinion influences the neighbors much more easily. Motivated by this phenomenon we introduced a novel concept of spin dynamics, known presently as the Sznajd model (SM) [3]. The crucial difference of our model compared to voter or Ising-type models is that information flows outward. In our model each site of a one-dimensional lattice carries an Ising spin. Two neighboring parallel spins, i.e. two neighboring people sharing the same opinion, convince their neighbors of this opinion. SM has been successfully applied in marketing, finance and politics (for reviews see [4, 5, 6]).

However, it is known that social validation is not equally powerful in all parts of life. Here we present a new approach, which allows to discriminate between two kinds of behavior, connected with areas which we will call personal and economic.

## 2 Motivation - politics

One of the sociological (or political) problems that attracts much attention is the building of consensus in a society whose members represent several different attitudes. In particular Stauffer [7] has asked the following question: 'What happens when there are several parties on the political stage, say two extremist and two centrist?'. Such a situation pertained in the United Kingdom in the early 1980s, when the Liberals and the Social Democratic Party held the middle ground between the left-wing Labour Party and the right-wing Conservative Party. The two middle parties soon realized that there was not enough room for both of them, and merged in the late 1980s [8]. In the model proposed by Stauffer each lattice site is initially either empty, with probability 1/2, or has one of four possible opinions 1, 2, 3 or 4 (like in the Potts model), with probability 1/8 each. Then, at each time step every occupied site tries to move to an empty neighbor. Afterwards, randomly selected pairs of nearest neighbors, who share the same opinion, convince all those neighbors of the pair's opinion, which differ by at most one unit. Stauffer found that parties 2 or 3 always win: they have more power of persuasion. But in most cases, one party other than the winner retained a small minority. This minority was always an extremist position, either 1 or 4.

Recently we have proposed another approach to describe a political stage with four parties [9]. Our approach is based on the so-called Political Compass, which works by separating ideology into two major areas: economic and personal [10]. It allows us to discriminate between two kinds of behavior, connected with areas which we call personal and economic. It seems that an attitude with regard to the personal area can change in a different way than that with regard to the economic area. We assume that each agent tries to influence its neighbors, but in the personal area the information flows inward

from the neighborhood (like in Glauber dynamics), whereas in the economic area the information flows outward to the neighborhood (like in SM).

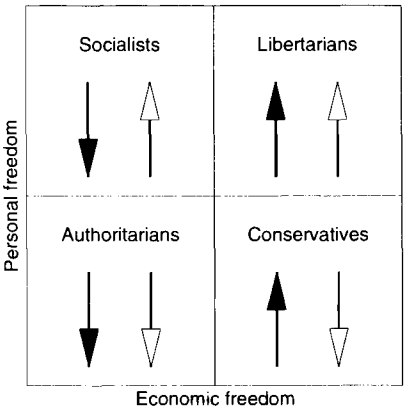


**Fig. 1.** Political Compass and the representation of 4 types of political attitude in our model. Black arrows represent attitude to economic and white - to personal freedom.

## 3 The Model

Each person is characterized by two traits $(\sigma_i, S_i)$, where $\sigma_i$ describes the attitude to personal freedom and $S_i$ describes the attitude to economic freedom. Both traits are represented by Ising spins (like in the Ashkin-Teller model [11]). This representation is simply a discretization of the diagram presented in Fig.1:

1. Socialists: $(\sigma_i = 1, S_i = -1)$
2. Libertarians: $(\sigma_i = 1, S_i = 1)$
3. Authoritarians: $(\sigma_i = -1, S_i = -1)$
4. Conservatives: $(\sigma_i = +1, S_i = 1)$

Since social validation seems to be really powerful in economic parts of life, the attitude to economic freedom $(S_i)$ is driven by the SM dynamics. On the other hand, it seems that the social validation phenomenon is less pronounced in private aspects of life, such as e.g. religion. The personal area attitudes are mostly influenced by the family or friends. For this reason we have decided to model the evolution of $\sigma_i$ using zero-temperature Glauber dynamics. It is obvious that some agents who share opinions in one area (e.g. economic) can be at variance in the other (personal). It is also natural to assume that a disagreement in one area can destroy or at least weaken the

convincing force of these agents also in the other area. To take into account the mutual influence of both aspects (personal and economic) of social life we introduce a tolerance factor $p$.

Results for a two dimensional system can be found in [9]. Here we describe he algorithm and results of computer simulations on the chain. In each Monte Carlo step we repeat $N$ (number of agents in the system) times the following:

1. Change the attitude to economic freedom:
   a) Choose at random a pair of neighboring spins (persons) $S_i$ and $S_{i+1}$.
   b) If $\sigma_i * \sigma_{i+1} = 1$ then the spins $S_{i-1}$ and $S_{i+2}$ follow SM dynamics, i.e. $S_{i-1} = S_{i+2} = S_i$ if $S_i * S_{i+1} = 1$.
   c) If $\sigma_i * \sigma_{i+1} = -1$ then the spins $S_{i-1}$ and $S_{i+2}$ follow SM dynamics with probability $p$.
2. Change the attitude to personal freedom:
   a) Choose at random a spin $\sigma_i$.
   b) If $S_{i-1} * S_{i+1} = 1$ then the spin $\sigma_i$ follows the zero-temperature Glauber dynamics, i.e. $\sigma_i = \sigma_{i-1}$ if $\sigma_{i-1} * \sigma_{i+1} = 1$, in the opposite case ($\sigma_{i-1} * \sigma_{i+1} = -1$) the spin $\sigma_i$ is flipped with probability $\frac{1}{2}$.
   c) If $S_{i-1} * S_{i+1} = -1$ then the spin $\sigma_i$ follows the zero-temperature Glauber dynamics with probability $p$.

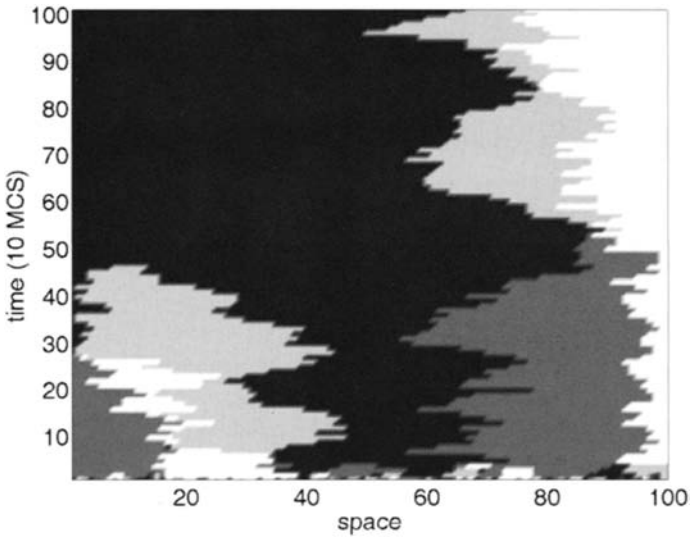


**Fig. 2.** Time evolution from random initial conditions of the chain. Four colors describe four attitudes. Some attitudes can become extinct or appear during the evolution.

We have found that independently of the initial attitudes distribution and independently of the tolerance factor $p$, consensus is always reached as a final steady state in one dimension, in contrast to the results for two dimensions [9]. However, consensus in the economic area is reached much faster than in the personal area. Interestingly, some options can disappear from the system and appear again (see Fig.2) during time evolution. If we start, for example, with only two options, say Socialists and Libertarians, randomly distributed we can end with Conservatives or any other one of four possible steady states.

In case the initial conditions consist of two opposite attitudes (disagreement in both areas, e.g. Authoritarians and Libertarians) separated by a border line the evolution always takes place in two steps. In the first step consensus in the economic area is reached. Then for a long time two attitudes that differ only in the personal area (e.g. Libertarians and Socialists) compete eventually leading the system to a consensus in both areas. It should be noted that in this case the behavior of a one dimensional system differs from the behavior in two dimensions, where a "phase transition" was observed as a function of the tolerance factor [9]. Below a certain value of $p$ consensus is not reached. Moreover, in two dimensions the relaxation time is $p$-dependent, in contrast to the one dimensional case.

The main conclusion of our paper is the observation (based on computer simulations) that it is quite easy to convince others in the economic area, and almost impossible in the personal area.

## References


1. D. Kahneman and A. Tversky, eds. (2000). Choices, values and frames. Cambridge University Press, Cambridge.
2. R. Cialdini *Influence Science and Practice (4th Edition)* Allyn & Bacon, 2000
3. K. Sznajd-Weron and J. Sznajd, Int. J. Mod. Phys. C **11**, 1157 (2000).
4. D. Stauffer, Comput. Phys. Commun. **146**, 93 (2002)
5. B. Schechter, New Scientist **175**, 42 (2002)
6. S. Fortunato and D. Stauffer, in: Extreme Events in Nature and Society, edited by S. Albeverio, V. Jentsch and H. Kantz. Springer, Berlin - Heidelberg (2005)
7. D. Stauffer, Advances in Complex Systems, **5** 97 (2002)
8. P. Ball, Nature News Service (27 February 2002)
9. K. Sznajd-Weron and J. Sznajd, Physica A **351**, 593 (2005)
10. D.F. Nolan, 'Classifying and Analysing Politico-Economic Systems', in Advocates for Self-goverment(1995), Nolan Chart Reader, Advocates for Self-Government Inc., Atlanta, GA, pp. 3-9.
11. J. Ashkin and E. Teller, Phys. Rev. **64**, 178 (1943).

# Complexity in an Interacting System of Production

Yuji Aruka[1] and Jürgen Mimkes[2]

[1] Faculty of Commerce Chuo University aruka@tamacc.chuo-u.ac.jp
[2] Department of Physics, Paderborn University
mimkes@zitmail.uni-paderborn.de

## 1 Introduction: Entropy in the Disaggregated Production Function

Mimkes [3] gave a concise formulation of *entropy* of production by the use of disaggregated neoclassical production function:

$N$ different elements(factors of production) : $K$, capital, $L$, labor, and so forth.
$M$ different classes (production processes) : $W_1, W_2, \cdots, W_m$.
Disaggregated production function $W_i = F_i(K, L)$ for each process $i = 1, \cdots, m$.
*Entropy* $S$ then is defined by the use of the probability $P$ of the distribution of the $N$ elements in $M$ classes of categories: $S = N \ln N - N_i \ln N$

In this article, we replace this idea of *entropy* of production with a more concrete idea of *complexity* in economic point of view. In particular, we use the idea of *hierarchical inclusion*. This can be illustrated in Table 1. The idea is associated with an idea of *truncation* of production system. Truncation here implies *microscopic reversibility* in a sense that any activity or its subset after truncation could be feasibly changeable under the economic feasibility condition.

**Table 1.** The Idea of Hierarchical Inclusion

| | Production **simple** | | Subset **complex** | *hierarchical* |
|---|---|---|---|---|
| **Technology** | $s$ | $\preceq$ | $\boxed{c}$ | $\searrow$ $s \cup c$ |
| **Real wage** | $< \omega^s >$ | $>$ | $< \omega^c >$ | **average** |
| **Probability** | $Pr(\omega^{higher} \mid s) > Pr(\omega^{lower} \mid s) <$ | | $Pr(\omega^{higher} \mid c)$ $Pr(\omega^{lower} \mid c)$ | $\nearrow$ |

## 2 Complexity and Interaction in Production

### 2.1 Producers' Set: The Winery Example

A simpler process could be regarded as a process with a younger vintage $t$. According to the Austrian theory, the process series of different vintages $\alpha_t$ in production can build into a newly more complex process to produce a final produce of higher quality $\alpha_n$, e.g., the winery to make the vintages variety of bottle of wine:

$$\{\{\{\{\alpha_1\}^1\alpha_2\}^2\alpha_3\}^3\cdots\alpha_n\}^n$$

This suggests the idea of *vertically integrated* process of production since this may be decomposed as follows: The elder process $\{\{\alpha_1\}^1,\alpha_2\}^2$ contains a set of intermediate produces of simpler independent processes $\{\alpha_1\}^1\{\alpha_1\alpha_2\}^2$ and so forth. Here thus are two sources of production for each intermediate good e.g., $\alpha_2$, i.e., one source from a simpler separate process as such $\{\alpha_1\}^1$, the other as a by-product from a more complex process $\{\alpha_1\alpha_2\}^2$.

### 2.2 The Essential Feature of Productive Arrangements

The key notions in economics could just become active when *the price-cost criteria* or *profitability* are applied to them. A simpler or more complex process could then not stand alone irrespective of a lower or higher welfare or real wage. As shown later, we encounter some dilemma from the following table:

**Table 2.** Complexity and Profitability

| | Complexity | |
|---|---|---|
| Average welfare | **simple** | **complex** |
| **lower** | $\{\alpha_1\}^1$ | $\{\alpha_1\alpha_2\}^2$ |
| **higher** | $*$ | $\{\alpha_1\}^1\cup\{\alpha_1\alpha_2\}^2$ |

### 2.3 A Roundabout as well as Hierarchical Inclusion

We must now be careful to distinguish the two cases of more complex system: (a)The element $(1,2)$ of the above matrix, and (b)the element $(2,2)$ of the matrix. Production in both cases includes *roundabout production.* In our *wine* example, by *roundaboutness*, $\alpha_2$ must be embodied a higher added value, as indicating a possibility of higher net income. We however have only $\alpha_2$ as a final produce in the system (a). $\alpha_1$ just serves as an intermediate one as an input. In our terms, we call the system (b), i.e., $\{\alpha_1\}^1\cup\{\alpha_1\alpha_2\}^2$ the *hierarchical* system of production, because there are contained a simpler way as well as a higher way of production, and then providing two different commodities as the final produces. A *hierarchical inclusion* may have a better *quasi-average* welfare system in terms of a convex combination of both subsystems.

### 2.4 Complexity in the Activity Analysis: Extension

We shall formulate an extensive form of complexity in production as above mentioned in terms of the Activity Analysis of *von Neumann* growth model type. This model may be of a typical model of *CAS*: Complex Adaptive System. See Holland [2]. This can depict an aspect of *interaction of heterogeneous processes* of production.

In the Analysis, by means of the idea of *truncations* of the production system into many productive subsystems,[3] we could again seize the point of *hierarchical* sets even in our more extensive case than the previous case.

## 3 Average Welfare of the Hierarchical Inclusion

### 3.1 A Numerical Example of Production and Truncations

We then introduce a new commodity $\beta^t$, e.g., *chemical* at time $t$ in our production system, by the use of which a new wine could be made. We for simplicity set $\beta^t = \beta$ for any $t$. Such an addition to Table 2 will complete a usual input-output matrices $A, B$. Here $a_i^j$ indicates the input of good $j$(super-suffix) required per unit of process activity $q_i$. $b_i^j$ indicates the output of good $j$ per unit process activity $q_i$.

So far we furthermore have neglected the input of primary factor of production like *labor* input. Now we introduce labor $l_i$ as indispensable factor for each process of production $i$. Our numerical values will be as follows:

**Table 3.** A Numerical Example of von Neumann Growth Model

| process $i$ | labor | input $A$ $a_i = (a_i^1, a_i^2)$ | | output $B$ $b_i = (b_i^1, b_i^2)$ | |
|---|---|---|---|---|---|
| **process 1** | 1 | 5.333 | 16 | 12.333 | 36 |
| **process 2** | 1 | 6 | 1.5 | 16 | 13.25 |
| **process 3** | 1 | 0.1 | 0.8 | 7.9 | 11.5 |

Finally we close our model to introduce the final demand vector:

$$d = (d^1, d^2) = (5, 6.5)$$

In our numerical example, the system as a whole will thus produce two final goods by choosing any single process or an two processes from the given system $\{A, B, l\}$.

[3] Schefold B [5]

### 3.2 Cost Minimization Systems: CMS

According to the idea of von Neumann [4], we formulate the dual system of price $p$ and quantity $q$ system underlying the above example. Here $p$ is a column vector, $q$ a row vector.

**The price system** for $i = 1, 2, 3$:

$$(1 + r)a_i p + wl_i \geq b_i p \tag{1}$$

Here $w$ is the rate of wage; $r$ is the rate of interest.

**The quantity system** for $j = 1, 2$:

$$(1 + g)qa^j + d_j \leq qb^j \tag{2}$$

Here $d$ is the final demand; $g$ is the rate of growth. Under these inequalities conditions, we will choose **the Cost Minimizing System: CMS**:[4]

$$\text{Minimize } ql \text{ s.t. } [B - (1 + r)A]p \leq wl \tag{3}$$

**Income Maximization**, as the dual problem,:

$$\text{Maximize } dp \text{ s.t. } q[B - (1 + r)A]p \geq dp \tag{4}$$

The von Neumann *equilibrium* could be achieved if the rules of *profitability* and *free goods* were applied;[5]. In this framework, in particular, the rule of free goods may contribute to income maximization by way of much use of the free good. This may be an intuitive reason why we could often *empirically* find an optimal solution of the form of *single process operation*, even if there were any multiple processes available to us.

**Lemma 1.** [6] *Welfare of a multiple process operation system could thus be higher by including a single process operation into its own system.*

### 3.3 The Number of Subsystem in a Given Production Set

We call the subsystems of solutions finding a minimal price subsystem *truncations*. In our example, we have 9 ways of truncations *in toto*:

$$\{1, 2\}, \{1, 3\}, \{2, 3\}, 1^1, 1^2, 2^1, 2^2, 3^1, 3^2$$

Here we denote a subsystem of process $h \cap i$ by $\{h, i\}$; We also denote the single process operation of process $i$ to produce good $j$ only by $i^j$.

[4] $B = [(b_i^j)]$, the output matrix; $A = [(a_i^j)]$, the input matrix

[5] The rule of profitability means that the process operation is halted if the strict inequality is held in (3)The rule of free good means that the price of the goods is set zero (a free good) if the strict inequality is held in (4)(overproduction).

[6] Aruka [1]

2 commodity production by 3 processes : ${}_3C_2 +_3 C_1 \times 2 = 9$ ways of truncation.

3 commodity production by 3 processes : ${}_3C_3 + 3({}_3C_2 \times_2 C_2) +_3 C_1 \times 3 = 16$ ways of truncation.

**Lemma 2.** *The larger both the numbers of process and commodity are, the larger the number of truncation will be. Also it will similarly as for the number of hierarchical inclusion of subsystems.*

### 3.4 Wage Curves of CMS subsystems

We employ the notion of *real wage* to judge the level of *welfare* of a subsystem of production. Given the final demand $d = (d^1, d^2)$, The real wage $\omega$ is defined as:

$$\omega = \frac{\text{the wage payment}}{\text{the standard of living}} = \frac{\sum_i^3 wq_i l_i}{\sum_{j=1}^2 d^j p_j} \tag{5}$$

By substituting the solution of a CMS $p(r)$,[7] thus we have the wage curve of the form:[8]

$$\omega(r) = \frac{1}{dp(r)}$$

The *wage curve* can measure the level of *welfare* in the society. Similarly, it follows the *consumption curve* from the dual maximization problem:

$$c(g) = \frac{1}{q(g)l}$$

### 3.5 The Characterization of CMS' Solutions

We can solve a CMS for any nonnegative plane $(r, g)$. The economically meaningful range for the solutions are limited to the range $g \leq r$. The golden age growth $r = g$ is merely a very special case. Economy will be located in the lower triangle of the $r-g$ plane, i.e., the non-golden age growth area. As shown in Lemma 1, we may often observe that a single process operation could often be found a solution among the CMS truncations, in other words, a most profitable one for producers. In users' view of welfare, however, it must not be.[9] We could use the idea of hierarchical inclusion to enlarge our subsystems into a more comprehensive system. We could then obtain a larger welfare in average.

[7] We use the normalization rule $ql = 1$.

[8] The curve usually is of hyperbolic on the plane $(r, \omega)$.

[9] In addition, a higher rate of profitability may be accompanied by a higher *risk* in the financial economy.

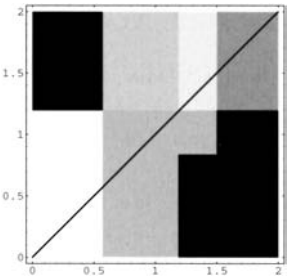


**Fig. 1.** The horizontal axe: rate of interest $r$; The vertical axe: rate of growth $g$

### 3.6 The Real Wage $\omega$ and Complexity

We see that there may coexist some multiple truncations at a given rate of interest under the economic feasibility condition $g \leq r$, as shown as the *black colored areas* in Figure 1. Thus a certain *hierarchical inclusions* of subsystems could be *formed*. In our example Table 3, we find a multiplicity of truncations $\{\{2,3\} \cup 2^2\}$ at $r = 1.2$ for a feasible $g \geq 1.2$. In view of Lemma 1-2, hence, we will have the statement on *complexity of production*:

**Theorem 1.** *The probability of multiple truncations compatible to a given rate of interest $r$ must be augmented if the number of truncations increases in the range of $g \leq r$. Average welfare could then be risen by a hierarchical inclusion of a single process operation of higher profitability, i.e., by an increase of complexity.*

## References

1. Aruka Y (1996) Dictatorship, price hike like bubble and employment adjustment on the non-goldenpath of the von Neumann growth model with joint -production. In Proceedings of econometric society Australasian meeting, 1:475-504, University of Western Australia, Perth.
2. Holland JH(1992) Adaptation in natural and artificial systems. MIT Press, Cambridge Massachusetts
3. Mimkes J et.al. (2004) Dynamics of heterogeneous agents in socio-economic systems. University of Paderborn, Paderborn
4. von Neumann J (1937) Über ein Ökonomisches Gleichungssystem und eine Verallgemeinung des Brouwerschen Fixpunktsatzes, Ergebnisse eines Mathematischen Kolloquiums 8: 73-83(translated as "A model of general economic equilibirum", Review of Economic Studies 13:1945-1946)
5. Schefold B (1997) Mr. Sraffa on joint production and other essays. Unwin Hyman, London

# Four Ingredients for New Approaches to Macroeconomic Modeling

Masanao Aoki
Department of Economics, University of California, Los Angeles
aoki@econ.ucla.edu; fax 1-310-825-9528

Abstract

This paper outlines some of the concepts and tools which, although not in the mainstream macroeconomics literature, have been effective either in providing new results, or insights to known results. [1]

Briefly put, the new approaches borrow concepts and tools from population genetics, condensed matter physics, and recently developped stochastic combinatorial analysis in statistics. Continuous-time Markov chains are constructed for clusters of heterogeneous types of interacting economic agents. We can then draw macroeconomic policy implications by examining solutions of master (Chapman-Kolomogorv) equations, Fokker-Planck equations or Langevin equations, as the needs call for them.

This paper attempts to introduce the reader to some of these new notions, and procedures to gain new insights and results.[2]

This paper reports on some of these by loosely organizing them into four sections.

## Introduction

In mid 1990's, new approaches to macroeconomic modeling have been proposed in Aoki (1996), and elaborated further in Aoki (2002).

His modeling approaches have been suggested by examples in population genetics, condensed matter physics, and in stochastic combinatorial analysis, and differ substantially from the mainstream macroeconomics in model constructions. Some of the similarities in models in condensed matter physics and biology have already been noted in Higgs (1995), Mekjian and Chase (1997), and in Derida and Flyvbjerg (1987). We extend similar approaches to modeling macroeconomics. For example, the notion of the relative sizes of basins of attractions in random map models in physics, the Herfindahl index as an economic idea of shares of markets, Aoki (2002, p.142, 173-174),

[1] For details of the methods and some examples see Aoki (1996, 2002), and their corrected versions Aoki (1998, 2004),and recentWehia conference proceedings.

[2] Some of the reported results have been obtained in cooperation with a few of like-minded economists, statisticians, and physicists. In particular the author gratefully acknowleges several important insights he obtained as the results of many discussions with H. Yoshikawa, and D. Costantini.

and Ewens distributions in population genetics are remarkably similar or identical.

Models we use are dynamic, that is, model states change over time. The model dynamics are described by the continuous time Markov chains. Instead of differential (difference) equations for the states, we use differential (difference) equations for the *probability* of state variables. They are the Chapman-Kolomogorov equations. We call them master equations following the physics usage.

We loosely classify our approaches and results into four groups or categories depending on what new "ingredients" or viewpoints are used in modeling or in describing the models. First, the notion of equilibria is extended to stationary or equilibrium stochastic distributions. Equilibria are stationary distributions. See Yoshikawa (2003) for elaboration.

Second, we do not use representative agents in our models. Instead, several types of agents are considered. Sets of agents are partitioned into subsets, called clusters. Clusters are composed of agents of the same characteristics, called type for short. In considering these partitions, combinatorial considerations naturally come into play in counting the number of different configurations that these partitions can assume. The notion of entropy and various distributions on the set of clusters of agents in different configurations also become necessary. Less well-known distributions such as Ewens, Poisson-Dirichlet, residual allocation models, and Lévy distributions are some of the examples.

These clusters are not treated symmetrically. Some are closer together than others. We introduce a notion of distance of clusters that is transitive. Correlations will not do since they are not transitive, as is well known from the literature on numerical taxonomy. We use the notion of ultrametrics.

The clusters are organized as leaves of trees and dynamics on trees are examined as in the physics literature by assuming that stochastic transition rates between clusters are functions of the ultrametric distances between clusters. Dynamics of states organized into trees are used to examine the effects of idiosyncratic shocks to one of the clusters spreading throughout the trees. We have shown that sluggish spread of the idiosyncratic shocks throughout the trees are one of the causes for slow responses of macroeconomic signals to these shocks. The tree structures help explain sluggish macroeconomic indices, and policy ineffectiveness under uncertainty which is touched on next.

Third, uncertainty also contributes to sluggish responses of macroeconomy. Uncertainty of the forecasts of the effects of current actions has been shown to make policy actions less effective. Uncertainty, moreover, has implications not fully explored in the existing mainstream macroeconomics, as has been demonstrated in Aoki and Yoshikawa (2005a,b,c), and in Aoki, Yoshikawa, and Shimizu (2005).

Fourth, dynamics of clusters lead us naturally to examine fat-tailed distributions, also known as power-laws, and (scale-invariant truncated) Lévy distributions. These distributions are well-known in finance but not in macroeconomics.

We have examined labor market dynamics as a vehicle of illustration of

some of the points touched on here. Unlike the traditional approach, our model of labor market dynamics dispenses with the traditional matching functions. We derive Okun's law and Beveridge curves in economies which respond to aggregate demands.

In this connection we mention new Schumperterian perspective on long-run behavior as another example. We model interaction between innovation and imitation processes as birth-death with immigration models and examine long-run behavior of this model, by solving a model of two-sector economy composed of innovative and immitative sectors. Explicit stationary solutions of the first and second moments are obtained for the sizes of the two sectors, using cumulant generating functions for dynamically interacting two sectors. Distributions of relative sizes of technically efficient and inefficient sectors are quite similar to those we obtain in our labor market model. See Aoki, Nakano, and Yoshida (2004), and Aoki and Yoshikawa (2005 b) for detail.

## Stochastic Equilbria

Bellman was the first to identify probability distributions as the proper notion of state in stochastic dynamics, hence equilibria aare stationary probability distributions, Bellman (1961), and Bellman and Dreyfus (1962). There usually are several basins of attractions. Models are not confined to some basins of attractions. They eventually wander out of the basins they currently occupy. The idea of equilibrium selections in macroeconomics loses its meaning in stochastic context.

## Sluggish Macroeconomic Behavior

Our approach in explaining sluggishness in macroeconomy is different from the well-known Taylor's explanation of staggered labor contract, Taylor (1980). His model and virtually all multi-sector models treat sectors symmetrically with equal distance between any two sectors. There is no notion of adjustment speeds as functions of some similarity measures among clusters.

Dynamics of trees have two aspects to it. There are multiplier lags or impluse or step responses. These are lags in responses at the output of dynamics when a *known* input, such as an impulse or a step input is applied to the input. There is another kind of lags related to the delay in exogenous disturbances to one of the leaves of a tree spreading throughout the tree as the input signals to other leaves or nodes on higher levels of trees. These are multiplier and information transmission lags. For further detail see Aoki and Yoshikawa (2005).

## Uncertainty Trap

To explain this notion simply, suppose that a large number, $N$ of agents face a binary choice optimization problem. There is externality because the current number ,$n$ of the agents with one choice may influence how the rest

of the agents choose, and consequently the dynamics of how the size of the fraction evolve. The number of ways $n$ agents out of $N$ form one cluster turns out to be important. Here the entropy of this patterns matter as has been shown in Aoki (1996, pp. 137-147).

The same formulation can be used to conclude that in situations with a large degree of uncertainty policy effectiveness is greatly reduced. See Aoki and Yoshikawa (2005a) for detail.

## New Features of Multi-Sector Economy

In Aoki (2002, Sec. 8.6) a new multi-sector economy has been examined where sectors have different productivity coefficients to illustrate effectiveness of demand manangement. Despite the simplicity of the model, its output (GDP) has been shown to respond to demand management policies. Later in Aoki and Yoshikawa (2005) the model has been extended to examine Okun's law and the Beveridge curves, all without the traditional matching functions. They exhibit an unexpected effects of demand share switching when the model is not in equilibrium. Expanding demand shares of less productive sectors lead to the increase in size of the less productive sectors. When more demands are directed to more productive sectors, the sizes of the less productive sectors shrink faster than the sizes of the more productive sectors grow. This leads to decrease in GDP, contrary to our intuition. A similar phenomenon has also been observed in a more elaborate model in Schumperterian spirit, Aoki, Nakano, and Yoshida 92004).

## Concluding Remarks

One area that requires further attention is the construction of macroeconomic model with asset markets. There are many proposals using representative agents, and some with heterogeneous agents where agents solve very complicated intertemporal optimization problems under ad hoc sets of assumptions.

Asset market behavior has been extensively modeled by the econophysicists, a group of physicists who turn their training to discover power-laws and scale invariant properties with almost no work being done in macroeconomics.

We try to match their efforts in modeling financial phenomena by focusing on the real phenomena such as consumption streams and GPD.

There are other results not included in this list. See the forthcoming book by Aoki and Yoshikawa (2005).

## References

Aoki, M.(1996) *New Approaches to Macroeconomic Modeling:Evolutionary stochastic dynamics, multiple equilibria, and externalities as field effects* , Cambridge University Press, New York.

——.(1998) "A simple model of asymmetrical business cycles: Interactive dynamics of large number of agents with discrete choices," *Macroeconomic Dyncmics*, **2**, 427–442

——. (2002) *Modeling Aggregate Behavior and Fluctuations in Economics* Cambridge University Press, New York.

Aoki, M., and H. Yoshikawa, (2003), "Uncertainty,policy ineffectiveness, and long stagnation of the macroeconomy," Working Paper No.316, Stern School of Business, New York University, forthcoming in *Japan and World Economy*, 2005.

—,and ——. (2003),"A new model of labor market dynamics: ultrametrics, Okun's law, and transient dynamics", Forthcoming in Proceeding of Wehia03 Conference, Springer-Verlag, Heidelberg,

—, and —.(2005a), "Why macroeconomic price indicies are sluggish in large economy ?" forthcoming in the Proceeding of 2004 Wehia conference", Springer-Verlag.

Aoki, M., and H. Yoshikawa (2005b) *Stochastic approach to macroeconomics and financial markets*, under preparation for Japan-US. Center UFJ monograph series on international financial markets

—,—, and T. Shimizu. (2003) "The long stagnation and monetary policy in Japan: A theoretical explanation" in *Monetary Pokicy and Labor Markets* W. Semmler (ed), Routeledge, London, forthcoming.

Aoki. M., T.Nakano, G. Yoshida (2004) An example of Schumperterian dynamics:effects of innovation and imitation in the long run of two sector dynamic models". Working paper, Institute of Research and Developments, Chuo Univ. Tokyo,

Bellman, R. E.(1961) *Adaptive Control Processes: A Guided Tour*, Princeton Univ. Press, N.J.

—, and S. E. Dreyfus (1962) *Applied Dynamic Programming* Princeton Univ. Press. N.J.

Derrida, B., and H. Flyvbjerg. (1987) "The random map model: A disordered model with deterministic dynamics", *J. Phy. (Paris)* **48**,971–878.

Higgs, P. G. (1995)"Frequency distributions in population genetics parallel those in statistical physics", *Phy. Rev. E.* **51** 95–99.

Mekjian, A.Z., and K. C. Chase (1997). "Disordered systems, power laws and random processes," *Phys. Lett. A* **229** 340–346.

Yoshikawa, H. (2003), "The role of demand in macroeconomics" 2003 Presidential address, the Japanese Economic Association. *The Japanese Econ. Rev.* **54**, 1–27

# Competition phase space: theory and practice

Dmitri B. Berg[1,2], Valerian V. Popkov[1,2]

[1]International A.Bogdanov Institute, Mira str. 44, PO BOX 212, Ekaterinburg, 620078, Russia
[2]Urals State Technical University, Mira str. 19, Ekaterinburg, 620002, Russia

**Summary.** Competition phase space approach is proposed. Theoretical background is presented. Practical applications of the proposed approach to competition media monitoring are discussed.

**Key words.** Competition, Phase diagram, Multi-agent simulation model, Bank system.

## Introduction

Competition is considered to be a motive power of evolution in economical systems and it lies in the focus of both empirical and theoretical studies. A correct and well-timed monitoring of the competition media is one of the main problems for headquarters and top managers. A lot of competition analysis techniques are known nowadays: SWOT, 7S, Porter model, GAP and so on.

In the present paper we propose the competition phase space approach that is based on main results of our studies of competition in physics, ecology and economy carried out for the last five years, including: i) quantitative technique for identification of agents' competitive strategic behavior (Popkov and Berg 2001); ii) general numerical model of the competition life cycle (Berg and Popkov 2003); iii) software for empirical data analysis (Popkov et al. 2001). All these tools have been applied to monitoring of banks' competition (Popkov et al. 2002). Current paper is the first one summarizing our theoretical and practical studies in the field of phase space approach to competition analysis.

## Phase space of the competition behavior (theory)

Competition between economic agents for limited amount of resources takes place in any economical system. The most universal resource is payable demand of customers. Agents do their best in order to maximize income money flow. So agent's competitive behavior (behavior strategy) means the agent's response to the

changing external conditions (according to Mintzberg et al. 1998). Usually the economic agents' behavior strategies are described in a qualitative verbal form: companies are compared to different kinds of animals (foxes, lions etc.) because similarity in competition between animals and firms helps to understand behavior of economic agents. Main (primary or basic) well-known strategies (according to the different classifications) are the following:

1. "Skimming the cream off" (profit maximizes) / swallows / explerents / ruderals.
2. "Leading in costs" / lions, elephants / violents / competitors.
3. "Market niche players" (differentiation) / foxes / patients / stress-tolerants.

Traditional qualitative techniques ascribe the certain agent's behavior to one of these classes. Real economic agent is usually combining the features of different classes that makes qualitative classification useless.

Phase diagram is used to discover the quantitative (in %) superposition of the three basic competitive strategies of agents' behavior, that makes 100%. So the phase diagram is a three-component one (two of the components are independent) and a triangle. Components are the basic strategies. Detailed identification of competitive behavior strategies was described in our recent study (Popkov and Berg 2001).

Phase space inside the 2D triangle is the space of competition behavior, fig. 1. As with description of dynamic systems in physics, independent coordinates are «agent's assets $A$ – assets normalized growth rate $A'$» where $A'=1/A \bullet dA/dt$. So the agent's position inside this triangle is determined by two dynamic empirical parameters $(A, A')$.

This diagram was tested by a computer model of the competition life cycle (CLC). This numerical model, describing the competition self-development in a closed system, is defined on a two-dimensional lattice using "cell automata" technique. Agents' competition for a limited amount of resource takes place under their growth. Growth/dissimilation of each agent is the result of in- and out-coming resource flows (income and costs). For the detailed description of the model see paper by Berg and Popkov (2003).

Trajectories of the competition life cycle were calculated and set at the above mentioned phase diagram together with the empirical data. Stages of the competition life cycle at the calculated trajectory correspond to the well known empirical observations of the market development, described, for example, by M. Porter, P. Kotler and others.

As it was shown earlier the proposed phase diagrams make it possible to: i) identify the type of the agents' strategic behavior and calculate the share (superposition) of each basic strategy it comprises; ii) compare the competitive behavior of all the agents both in qualitative and quantitative way; iii) find the position of one individual agent among others (concerning behavior features); iv) analyze the time dependence of the evolution of each agent's behavior strategy as well as the whole market evolution.

## Competition monitoring (practice)

The idea of the competition media monitoring is based on the fact that the same agents are competing with each other on different product markets (micro level of competition) at one and the same time. Results of the competition are income and costs flows of agents, summarized in total assets ($A$) and profit growth (aggregated, macro level of competition). The banking sector of the Russian economy has been selected for the demonstration of the competition monitoring due to the following features: i) high level of competition; ii) better data base (as compared to the other economy branches); iii) high speed of evolutionary changes within a short time period.

At the micro level of competition sales of four banking products/services (deposits of firms and citizens and credits to firms and citizens), that form more than 80% of the bank's profit, are taken into consideration. At the macro level the banks' assets dynamics is analyzed. So parameter $A$ corresponds to assets of bank at macro level and sales of certain product at micro level

Banks' competition media monitoring in Ekaterinburg was performed during the period 2000-2003 (14 banks, database of banks' balances: over 150 parameters per each bank, quarterly). Some brief results are described below.

Comparison of banks' competitive behavior was carried out and is shown at the Table and fig. 1a,b. The Table demonstrates the quantitative identification of competitive strategies for 4 banks (the other 10 are not shown) at 3 of 4 markets ("Deposits of firms" column is not shown). For example: real behavior of the bank № 3 at the citizens' deposits market is 50% competitive ($C$), 40% - ruderal ($R$) and only 10% - stress-tolerant ($S$), see also fig. 1a.Percentages ($\pm$1%) of $S$, $R$ and $C$ strategies are calculated by means of triangle phase diagrams. Fig. 1 shows only 2 of them.

**Table.** Comparison of banks' competitive behavior (in %).

| Bank № | Credits to firms | | | Deposits of citizens, fig.1a | | | Credits to citizens | | | <Average> behavior* (4 markets) | | | Aggregated behavior,** fig. 1b | | |
|---|---|---|---|---|---|---|---|---|---|---|---|---|---|---|---|
| | *S* | *R* | *C* | *S* | *R* | *C* | *S* | *R* | *C* | *S* | *R* | *C* | *S* | *R* | *C* |
| 3 | 17 | 28 | 55 | 10 | 40 | 50 | 34 | 23 | 43 | 32 | 30 | 38 | 5 | 38 | 57 |
| 4 | 20 | 46 | 34 | 36 | 40 | 24 | 90 | 0 | 10 | 55 | 27 | 18 | 8 | 52 | 40 |
| 10 | 74 | 20 | 6 | 87 | 10 | 3 | 87 | 11 | 2 | 81 | 16 | 3 | 78 | 16 | 6 |
| 14 | 75 | 22 | 3 | 90 | 10 | 0 | 90 | 10 | 0 | 82 | 17 | 1 | 72 | 26 | 2 |

*S, R, C* are the basic competitive strategies: *S* – stress-tolepant, *R* – ruderal, *C* – competitive behavior (see classification above).

*"<Average> behavior" means, that the percentage of *S*, *R* and *C* types in bank's behavior at each of 4 investigated markets is averaged.

**"Aggregated behavior" means, that the behavior is calculated according to bank's assets that are summarizing the bank's activity in financial sphere, including the markets investigated.

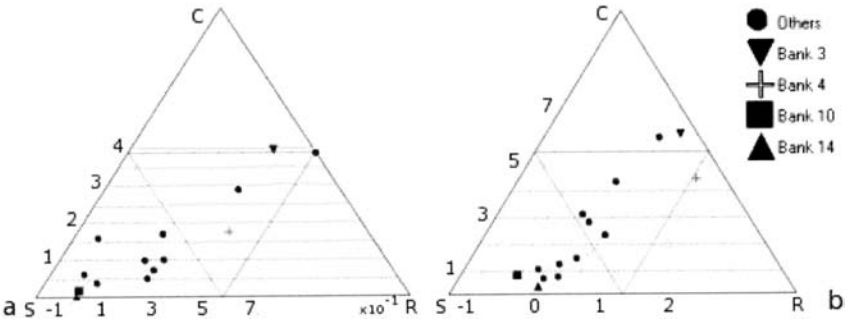


**Fig.1ab.** Phase diagrams of banks' competitive behavior for the last quarter of 2004. The position of each bank inside the triangle reflects it's competitive behavior as compared to the other banks. This position is recalculated in percents according to the three basic strategy types (*S, R, C*) and shown at the Table. **a** Citizens' deposits market (micro level of competition). Horizontal axis – growth rate of deposits volume (quarterly) without normalization, left axis – total volume of deposits. **b** Aggregated behavior calculated by assets (macro level of competition). Horizontal axis – growth rate of assets volume (quarterly) without normalization, left axis – total volume of assets. All units – in billions of Russian rubles.

Fig. 1 shows the competition phase space in micro level (fig. 1a corresponds to "Deposits of citizens" column of the Table) and macro level (fig. 1b corresponds to "Aggregated behavior" column).

Comparative analysis of banks' competitive behavior, summarized in the Table and fig. 1, shows, that the phase space technique discovers new important information about agents' behavior. Main results of the competition monitoring are the following:

1. One and the same bank demonstrates different competitive behavior at the different markets. For example, behavior of the bank № 3 at the market of credits to firms is characterized as competitive in the part of 55%, while at the market of credits to citizens – only in the part of 43%. At the same time the average behavior is competitive only in part of 38% and aggregated one – in the part of 57%.
2. The aggregated behavior (macro level) is not a simple average of behavior at each product market (micro level). Comparison of two last columns of the Table makes it clear (especially for bank № 4). The main reason lies in the fact that the bank can redistribute it's profits and assets among the different markets (that would result in shift of sales growth rate), while the total assets amount remains the same.

Besides, the phase diagram of the total sales (that is not shown) easily indicates the most attractive market of bank products (or a group of markets) in respect of profits and sales growth, which is important in directing further managers' efforts.

## Conclusion: other useful applications

Phase space inside the proposed triangle diagram, used for competition monitoring, can be applied to other dynamic systems analysis in management practice:

1. Industry monitoring with the help of phase space technique helps banking top managers to find the most attractive branches for investments and determines an empirical rule of banking management, based on the life cycles of it's clients monitoring.
2. Business-cycles analysis in macro and microeconomics activities (including successful and unsuccessful projects).
3. Monitoring of all ongoing projects of the company helps to observe and compare their efficiency (portfolio project management).

Also the phase space proposed has certain advantages in cognitive data presentation in comparison with ordinary tables and time-dependency curves (see, for example, the Table column "Aggregated behavior" and the diagram at fig. 1b).

### Acknowledgments

The research has been carried out under the partial financial support of Russian Humanitarian Scientific Foundation, grant No 04-02-00076a.

## References

Berg D, Popkov V (2003) General numerical model of the competition life cycle: from physics to economy. Physica A 324:167-173

Mintzberg H, Ahlstrand B, Lampel J (1998) Strategy safari. Prentice Hall, London N.-Y Toronto, pp 10-25

Popkov V, Berg D (2001) Empirical identification of competitive strategies: russian bank system. In: Takayasu H (Ed) Empirical science of financial fluctuations: the advent of econophysics. Springer, Tokyo, pp 331-340

Popkov V, Berg D, Kuznetsov R (2002) Evolutionary dimension of strategic bank management. Uralskii Rabotchii, Ekaterinburg, pp 210-280 (in Russian)

Popkov V, Berg D, Kapralov M, Kuznetsov R, Shipitsyn E (2001) Competition strategies' recognitioner. Rus. patent office reg. № 2001610971 for software.

# Analysis of Retail Spatial Market System by the Constructive Simulation Method

Hirorhide Nagatsuka[1], Katsuya Nakagawa[2]
[1] DMR, Ltd., 2-3-1105,Kugenumahigasi, Fujisawa, Kanagawa 251-0026 Japan
[2] UNITEC, Inc.1-3-905,Nissincho,Kawasakiku,Kawasaki,Kanagawa.210-0024,Japan

In the spatial interaction theories of geography, the regional system is given as OD matrix from the beginning, the attractiveness of each store is given exogenously, and parameters are estimated using survey trip data Tij. These theories don't account for the idea that the macro regional system would be generated self-organizationally from micro interactions of elements. D. L. Huff (1962) studied individual shopping behavior and made a probability model for the choice of stores. In Huff's model the attractiveness of each store is also given exogenously and the resistance parameter is estimated from inquiry survey data. His theory also doesn't account for the idea of a self-organizing retail spatial market system. In this paper we will take up habitual shopping in all types of shopping behavior. We'll take the consumer's store choice model as the micro non-linear interaction of elements setting the attractiveness as endogenous variables, and also parameters as endogenous ones. Using the constructive simulation method we'll show that in specific regional areas, under what kind of conditions of the model, and how, a macro regional market system will be generated self-organizationally. The characteristic of a regional space concerning the consumer's store choice behavior will be expressed by the combination of two parameters [ $\lambda$ ,Sg] introduced into the model. Each store's attractiveness will be estimated to give an account of the real sales.

## Assumptions and Model

### Types of business taken into consideration

We'll take up the GMS (general merchandising store) and SM (supermarket) as the retail type that corresponds to habitual shopping. We'll divide the SM into two types, SM1 and SM2. SM1=selling area 500~1999 ㎡, monthly sales over one hundred million yen. When sales are unknown we'll take selling area over 1000 ㎡. SM2=2000~5999 ㎡.GMS=over 6000 ㎡. SM1 type stores merchandize perishable foods, processed foods, domestic non-durable goods, and utensils. SM2 type stores merchandize the same goods as SM1, and other categories. Here, GMS is an original Japanese type of business. The GMS merchandize the same categories as SM2 but also merchandize clothes, home fashion and recreational goods.

### Input data and the subject of the model

The input data is firstly so called mesh census data base (in 2000) that is published with

digital media by the government, secondly family income and expenditure survey data (in 2000) by the government, finally supermarket data base (in 2000, including selling area, gross sales, latitude and longitude data) by the Shogyokai Inc. The subject of consumption is households with 2 or more members. We will divide the analyzing regional area into many small spaces in the simulation, and consider the shopping behavior of the group of the small space instead of individuals. Next we assume that the mean probability and mean consumption of monthly shopping behavior correspond to the small group, and follows the model. We label the small group as a collective consumer just like an individual.

**The choice model and the share of consumption Sg at g retail type**

We assume that the probability of choosing a store is in proportion to the store's attractiveness and inversely proportional to the power function on the Euclid distance from residence point i to the j store like $R_{ij}^{\lambda}$. We assume that resistance parameter $\lambda$ corresponds to the average of all traffic modes and is indigenous to each regional area. The normalization of the probabilities is carried out through the 3 retail types at each i-point. There is the problem of I.I.A.( Independence from Irrelevant Alternatives) in this case. Then the total consumption of the analyzed area at the all stores is not changed in spite of the existence of any stores being outside of the model. To express and solve this problem we introduce a new parameter Sg that means the share of consumption at g retail type in our model. If we write C for household's monthly expenditure of goods (it was 116,535 yen in 2000 except some goods which GMS or SM didn't merchandise) we can find out Sg, with it C*Sg becomes to mean the household's average monthly expenditure at g retail type. Sg is also indigenous to each regional area.

**Store's attractiveness and the coefficient of attractiveness**

According to habitual shopping behavior, at first a store is chosen, then goods are chosen. This means each store possesses the whole attractiveness. Also we consider that the attractiveness is a realized utility (satisfaction) in the consumers' habitual experience. Therefore attractiveness per $m^2$ would be around the sales per $m^2$. So we introduce j store's attractiveness per $m^2$ Aj (we call this the coefficient of attractiveness). Next we write Aj*Mj as the j store's whole attractiveness. Mj means selling area, and these are constants in the simulation. Aj is an endogenous variable that is estimated as a solution of the simulation. On the other hand we relativize each store's sales per $m^2$ by dividing with the GMS's average sales per $m^2$ of the Kanto plain (it was 55,600 yen in 2000). We call this as relative sales per $m^2$ and write it Kj. We put this Kj as the initial value of Aj in the simulation. GMS's average $K_{gms}$=1.0, SM2's average $K_{SM2}$=1.23, SM1's average$K_{SM1}$=2.21. If we can't discover a store's sales on the data base we estimate it's theoretical sales using this average of each retail type. With these initial values if we find out Sg with the Sg the simulation converges very rapidly, then finally Aj would be around each Kj. Then Sg would take the meaning of real share of consumption at g retail type. Because we can say that from the equation (2) if all the variables

take their real meanings, except Sg, then Sg must take it's real meaning. (The simulation could converge at any Sg but the corresponding Aj could not be interpreted.)

**The size of store choice set**

The size of store's choice set is the number of stores chosen mostly close to the consumer's residence on their monthly shopping at each retail type. If we put many stores for the set in the simulation, the possibility of assigning the probabilities to unnatural stores from the viewpoint of the collective consumer would arise. We simulated changing the number and found that the case of 4 stores on SM2 and SM1, 8 stores on GMS were very natural and realistic in our 3 specific regional areas.

## System equation and the method of simulation

We write the mean probability that consumers of i-point choose j-store in their monthly total shopping trips as follows:

$$\mathrm{P\,ij} = (AjMj / R^{\lambda}ij) \Big/ \Big( \sum_{SM1:l=1}^{n1} A_l M_l / R^{\lambda}_{il} + \sum_{SM2:m=1}^{n2} A_m M_m / R^{\lambda}_{im} + \sum_{GMS:n=1}^{n3} A_n M_n / R^{\lambda}_{in} \Big) ; \quad \text{from definition} \quad \sum_{l=1}^{n1} \mathrm{Pil} + \sum_{m=1}^{n2} \mathrm{Pim} + \sum_{n=1}^{n3} \mathrm{Pin} = 1$$

At all points in the regional area. n1, n2, n3 = number of chosen stores at each retail type. We write the theoretical sales per month of j store Ujt. Then we can write as follows:

$$\mathrm{Ujt} = \sum_i \mathrm{P\,ij}^*\mathrm{C}^*\mathrm{Sg}^*\mathrm{Ni}^*\Delta\mathrm{i} = \sum_i \alpha_i{}^*\mathrm{Aj}^*\mathrm{Mj}^*\mathrm{Ni}^*\Delta\mathrm{i}^*\mathrm{C}^*\mathrm{Sg} \quad \cdots\cdots (1)$$

$\alpha_i$=constant, $\Delta$i=the small area around i-point, Ni= household density around i-point.

If we want Aj with which j-store's theoretical sales Ujt equal to real sales Ujr under given $\lambda$ and Sg, we would write this as follows:

Ujt= Ujr j=1~m (at each store in the analyzed area) ・・・・・・・・・(2)

These are kinds of non-linear large simultaneous equations concerning Aj, and the number of formulae is m. To solve these equations we developed large simulation software. The method of simulation is as follows. At first we set the number of contour lines of probability and the value of probability from 100% to 1%. On the points of the subdivided mesh line the software estimates the value of probability and gets all the contour lines of each store. Next, the software calculates the inter-area of each contour line and multiplies the inter-area with Ni and C*Sg and the value of probability so as to get the theoretical sales of j store. Next it compares this Ujt to real sales Ujr. If the relative error is over the specified % it calculates modifying Aj little by little, and finishes when each relative error of all stores is reached under a specified %.

There are infinite solutions concerning Aj in the above simultaneous equations. The reason is that if we multiply this variable by any constant, the value of the probability is not changed. So we must select a really meaningful solution. Therefore, as already mentioned, we must set Sg so that Aj will converge around it's initial value, that is relative sales per $m^2$.

## Conclusion

We have run this simulation in 3 areas, i.e. the Shonan area, the Yamato area, the Sagamihara area in Kanagawa which are similar suburban areas of Tokyo (see Fig.1), and we found the following conclusion. (The boundary of the first-degree trade area is defined as 30% line of the probability, second-degree trade area as 15%, third-degree trade area as 7%, fourth-degree trade area as 1%, as follows.)

1.Table 1 shows the corresponding value of Sg and the value of C*Sg in each area which can be found when we change the value of $\lambda$ from 1.8 to 3.0. Each value of C*Sg means the necessary condition for convergence. We can show that only one or a small range of the set of C*Sg is real and true. The stability of the system becomes higher when $\lambda$ is lower, i.e. the simulation converges rapidly. But in each area when $\lambda$=1.8~2.0 the average expenditure at SM1 or SM2 is larger than the expenditure at GMS. This is converse to reality. In other words under conditions of high mobility like $\lambda$=1.8~2.0, many consumers concentrate on GMS, therefore SM1 or SM2 would be not able to exist due to lower demand. Conversely when $\lambda$ =2.8~3.0 the stability of the system becomes lower, i.e. Aj of some stores of GMS would become larger further away from Kj to converge. The power function causes that the first-degree trade area becomes larger, and the second-degree trade area doesn't change. However the third and fourth degree trade areas become smaller in all stores of these analyzed areas compared with the case of $\lambda$=2.4. As a result, because of such low mobility, SM1 needs less demand to operate. Conversely GMS needs an unrealistically larger demand if the real sales were to be realized in the simulation. According to the statistics by the government (the 1999 National Survey of Family Income and Expenditure) we can neglect the case of $\lambda$=2.2 because of lower expenditure at GMS. Thus we can estimate that the real value of $\lambda$ may be 2.4~2.6, but from the stability of the system we could say $\lambda \fallingdotseq$2.4. Table 2 shows the estimated values of Aj and Kj of GMS in the Shonan area when $\lambda$=2.4 as an example.

2.The Shonan area is covered all over with the contour lines of all GMSs. Fig.2 shows the first-degree trade area of all stores of the 3 retail types. Thus under the trade area of the GMSs the smaller SMs also have similarly broad first-degree trade areas when $\lambda$=2.4. From the shape of power function the boundary of the second-degree trade area is close to the boundary of the first-degree trade area at each store. 60% of stores in the Shonan area take a share of sales over 60% in the first- plus second-degree trade area. So the trade area could be seen as a monopolistic area, and because of this each store can avoid a strongly competitive situation.


Fig.1

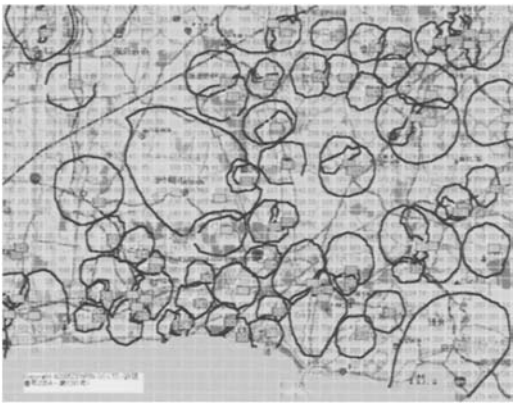

Fig. 2

**Table 1.** λ & share of expenditure Sg & average expenditure per month C*Sg estimated from simulation

| Shonan area | Sg | | | C*Sg | | |
|---|---|---|---|---|---|---|
| λ | gms | sm2 | sm1 | gms | sm2 | sm1 |
| 1.8 | 0.41 | 0.43 | 0.47 | 47779 | 50110 | 54771 |
| 2 | 0.43 | 0.41 | 0.43 | 50110 | 47779 | 50110 |
| 2.2 | 0.46 | 0.4 | 0.4 | 53606 | 46614 | 46614 |
| 2.4 | 0.48 | 0.4 | 0.37 | 55937 | 46614 | 43118 |
| 2.6 | 0.5 | 0.4 | 0.35 | 58268 | 46614 | 40787 |
| 2.8 | 0.52 | 0.39 | 0.34 | 60598 | 45449 | 39622 |
| 3 | 0.54 | 0.39 | 0.33 | 62929 | 45449 | 38457 |
| Yamato area | Sg | | | C*Sg | | |
| λ | gms | sm2 | sm1 | gms | sm2 | sm1 |
| 1.8 | 0.41 | 0.47 | 0.47 | 47779 | 54771 | 54771 |
| 2 | 0.43 | 0.46 | 0.43 | 50110 | 53606 | 50110 |
| 2.2 | 0.46 | 0.44 | 0.41 | 53606 | 51275 | 47779 |
| 2.4 | 0.48 | 0.43 | 0.39 | 55937 | 50110 | 45449 |
| 2.6 | 0.5 | 0.42 | 0.37 | 58268 | 48945 | 43118 |
| 2.8 | 0.53 | 0.42 | 0.36 | 61764 | 48945 | 41953 |
| 3 | 0.54 | 0.41 | 0.35 | 62929 | 47779 | 40787 |
| Sagamihara area | Sg | | | C*Sg | | |
| λ | gms | sm2 | sm1 | gms | sm2 | sm1 |
| 1.8 | 0.39 | 0.47 | 0.45 | 45449 | 54771 | 52441 |
| 2 | 0.41 | 0.45 | 0.42 | 47779 | 52441 | 48945 |
| 2.2 | 0.44 | 0.43 | 0.39 | 51275 | 50110 | 45449 |
| 2.4 | 0.47 | 0.43 | 0.36 | 54771 | 50110 | 41953 |
| 2.6 | 0.49 | 0.42 | 0.35 | 57102 | 48945 | 40787 |
| 2.8 | 0.51 | 0.41 | 0.33 | 59433 | 47779 | 38457 |
| 3 | 0.53 | 0.4 | 0.32 | 61764 | 46614 | 37291 |

**Table 2.** Aj & Kj of GMS in the Shonan

| store | Aj | Kj |
|---|---|---|
| 160 | 0.84 | 0.97 |
| 165 | 1.05 | 0.98 |
| 166 | 1 | 1.08 |
| 167 | 1.47 | 1.47 |
| 168 | 0.98 | 0.86 |
| 169 | 1.21 | 1.21 |
| 170 | 1.35 | 1.81 |
| 194 | 1.27 | 1.27 |
| 195 | 1.27 | 1.27 |
| 196 | 0.85 | 0.69 |
| 197 | 1 | new entry |
| 198 | 1.75 | 1.43 |
| 200 | 1.25 | 1.02 |
| 219 | 0.84 | 1.04 |
| 221 | 1.8 | 1.37 |
| 222 | 1.45 | 1.18 |
| 223 | 0.74 | 0.96 |
| 224 | 1.21 | 1.06 |
| 225 | 0.67 | 0.92 |
| 226 | 1.05 | 0.86 |
| 228 | 0.65 | 0.75 |
| 229 | 0.58 | 0.78 |
| 230 | 1.07 | 1.07 |

# Quantum-Monadology Approach to Economic Systems

Teruaki Nakagomi

Kochi University, Kochi 780-852 Japan, nakagomi@is.kochi-u.ac.jp

**Summary.** In order to describe non-classical nature of economic phenomena, the use of quantum monadology, a quantum world model reinforced with Leibnizian monadology, is proposed, which provides not only the way of thinking but also a mathematical system that enables us to simulate personal and social human behaviors and to describe integrative or anomalous processes of economic systems.

**Key words:** Quantum monadology, Whole-individual reflection

## Quantum brain produces economic phenomena

Economic phenomena are produced by human activities. Human activities are created by the brain, which is "material" and ultimately governed by quantum mechanics. The traditional average image of the brain might be a complex neural network system. Recently, however, another scientific trend appears which asserts that the ultimate origin of the decision making and the consciousness is in quantum mechanics associated with the "brain matter" and that the neural system serves as an enhancer and a supporter to the quantum brain system. Symbolically, it is called "quantum brain dynamics (QBD)." You will find comprehensive discussions on this trend from science and philosophy in the monograph edited by Globus et al. (2004). In order to make a linkage between QBD and the traditional approach, the author proposed *quantum monadology*, which provide a mechanism of integrating quantum individuals to make a unified whole (Nakagomi 1992, 1995, 2004a, 2004b). In this line of thinking, it is expected that economic systems should be described by quantum models rather than classical models, since econo-systems are the result of monadistic integration of elemental quantum systems.

A main objection to such an approach will be that quantum structure on the microscopic level is averaged out on the macroscopic level and the classical population dynamics is sufficient and effective, as is true in chemical reactions. Indeed, typical theories of econo-dynamics are base on the statistical

mechanics of chemical reaction models. In this objection, econo-systems are considered to be macroscopic, but what is the material scale that characterizes the macroscopicness of an econo-system? Different from chemical reaction systems, an econo-system is not uniform not only in real space but also in abstract econo-space, and cannot be considered as a simple macroscopic system that is subject to statistical mechanics.

## Monadistic examples

We can see some examples of monadistic structures in our daily experience.

*Computer games.* In a computer game through networks, each player battles in a battlefield that his computer produces. The battlefields of different players are correspondent to each other by the communication through networks, and players feel themselves to be playing in a common battlefield, which does not exist anywhere.

*Traffic of cars.* Consider many cars running on a road. The distances between cars vary smaller or larger as they are running, but normally they do not collide with each other except for rare accidents. Observing such phenomena, physicists may consider that there is a repulsive force between cars and they may succeed in explaining average motions of cars. However, the force assumption would not describe the motion of individual cars. We find a similar situation in quantum physics. The motion of a car is determined by the mind of the driver. Decisions of the driver depend on the memory of the past and the prediction of the future and are not affected by those of the other drivers. Also in quantum mechanics, the behavior of a particle is affected by the wave function belonging to the particle and not by the wave functions of the other particles. Each driver has his image of the motion of his car and surrounding ones, which, normally, is correspondent to those of other drivers, and the cars run smoothly. However, if the correspondence is broken, then it may cause accidents. Not physical law of motion of cars but correspondent images of drivers produce the harmonized external world, the smooth motion of the whole cars.

*The market.* The motion of the market is determined by the action of market players, who choose their action by the image of the motion of the market that they have in their mind. If you want to control the market, you must consider to control the image of the market players. It is important to know the laws of motion of the image, some of which we know and use by experience, though we do not have a systematic theory of them.

## Whole-individual reflection

The author considers that the essential feature of economic phenomena consists in the whole-individual reflection in the sense that the internal images

of the whole in respective individuals determine the whole and inversely the whole reflects into individual's internal worlds, in other word, the preestablished harmony in the Leibnizian philosophy, monadology.

The whole-individual reflection provides a integration scheme of individuals, which is different from that in statistical mechanics, the latter averages out varieties of individuals, and makes spatially uniform structures.

From the point of view of quantum monadology, the first origin of the whole-individual reflection scheme is in the ultimate basic physical level of quantum mechanics and relativity, and the scheme is iterated simulatively to make a hierarchy of monadistic structures each of which has its own semantic system. In this way, the quantum field structure on the basic physical level is inherited into the systems of human activities, in particular, in political and economic systems.

## Quantum logic

In the hierarchy of monadistic structures, the quantum nature of the basic physical level would be inherited into the human-level monadology. In this inheritance, though incomplete, quantum structure remains in the logic used in the decision making system of individuals or monads. The logic with quantum nature is represented mathematically as an *orthomodular lattice*, which includes both standard quantum logic (generated on a Hilbert space) and classical (or Boolean) logic.

An orthomodular lattice, sometimes symbolically called "quantum logic", is a logic system of AND, OR, NOT that satisfies the "orthomodular law" and is not required to be subject to the distributive law, different from Boolean logic.

Decision making systems based on non-classical types of logic are discussed in Nakagomi(1995). A salient characteristic of quantum logic is that the order of two decisions may affect its consequence. Quantum logic is adopted in the axioms of quantum monadology.

## Mathematical scheme of NL world

A monadistic system is specified by a mathematical scheme called NL world $W$, which consists of three sets and five mappings and is subject to the two rules given below.

$$W = (V, F, L, \eta, \rho, \omega, \lambda, \beta). \tag{1}$$

Each item is as follows: $V$ is a finite set of *monad-images* with a special element $v_{\mathrm{self}}$, *self-image*. $F$ is a set of *internal states*. $L$ is a $\sigma$-complete orthomodular lattice (or quantum logic) of *contents of consciousness*. $\eta$ is a mapping $\psi \in F \mapsto \eta(\psi) \geq 0$, *appetite*. $\rho$ is a mapping $\psi \in F \mapsto \rho(\cdot|\psi)$ (a probability measure

on $L$), *preferability.* $\omega$ is a mapping $\psi \in F \mapsto \omega(\psi)$ (an orthogonal system of elements of $L$), *list of choice.* $\lambda$ is a mapping $(r, \psi) \in \mathfrak{S}(V) \times F \mapsto \lambda(r, \psi)$ (an automorphism on $L$), *interpreter*, where $\mathfrak{S}(V)$ is the symmetric group of $V$ (the group of all one-to-one and onto mappings from $V$ to $V$). $\beta$ is a mapping $(\ell, \psi) \in L \times F \mapsto \beta(\ell)\psi \in F$, *state-change operator.* The orthogonal system $\omega(\psi)$ is assumed to be complete with respect to the measure $\rho(\cdot|\psi)$, i.e., $\sum_{\ell \in \omega(\psi)} \rho(\ell \mid \psi) = 1$.

## Rule 1 (Monads and correspondences)

With the NL world $W$, a set $M_W$ of *monads* is associated, whose number of elements is the same as that of $V$. For any pair of monads $m$ and $m'$, there exists a image-image correspondence $r_{mm'} : V \to V$ (one-to-one and onto) with condition that

$$r_{mm'}(v_{\text{self}}) \neq v_{\text{self}} \ (m \neq m') \quad \text{and} \quad r_{mm'} r_{m'm''} = r_{mm''}. \tag{2}$$

Each monad $m$ then has an entity-image correspondence $c_m : M_W \to V$ defined by

$$c_m(m') = r_{mm'}(v_{\text{self}}), \tag{3}$$

which is uniquely derived from the condition $r_{mm'} c_{m'} = c_m$ and $c_m(m) = v_{\text{self}}$.

## Rule 2 (Current states and renewal cycle)

Each monad $m$ has a variable $\Psi_m$, *current state*, that takes values in $F$, and follows the renewal cycle of three steps given below:

Step 1. Each monad $m$ is urged one time to make a decision, and *one* monad, say $m_1$, is hit with probability proportional to the appetite $\eta(\Psi_{m_1})$.

Step 2. The hit monad $m_1$ chooses an item $\ell$ from $\omega(\Psi_{m_1})$ with probability proportional to the preferability $\rho(\ell \mid \Psi_{m_1})$.

Step 3. Each monad $m \in M_W$ interprets the choice $\ell$ by the monad $m_1$ as $\ell_m = \lambda(r_{mm_1}, \Psi_m)\ell$, and renews its current state $\Psi_m$ by the substitution formula

$$\Psi_m := \beta(\ell_m)\Psi_m. \tag{4}$$

## Symmetry and substructures

The NL world has the basic correspondence given by Rule 1. It is extended to a higher-level correspondence among internal worlds of individual monads in a situation in which 1) the symmetric group $\mathfrak{S}(V)$ has a representation $R$ on the transformations over $F$, that is, for each $r \in \mathfrak{S}(V)$, $R(r)$ defines a

mapping from $F$ to $F$ such that $R(rr') = R(r)R(r')$ and $R(I) = I$, and 2) the definition of the NL world $W$ has "symmetry" under the transformation $R(r)$ for any $r \in \mathfrak{S}(V)$.

On this symmetry assumption, it is derived that if the following relation holds for any pair of monads $m$ and $m'$ at some time

$$\Psi_m = R(r_{mm'})\Psi_{m'}, \tag{5}$$

then, at any time after that time, this relation holds for any pair of monads $m$ and $m'$.

Relation (5) means that all the monads share a common world image. Different from the original Leibnizian world model, the correspondence (or harmony) between monads is not all pre-established, but partly post-established in the NL world scheme. This mechanism makes it possible to produce higher-level monadistic structures. There are various possibilities as the representation $R$ by restricting to subsets of monads (if necessary), and we have various monadistic substructures superposed on each other.

The explanation of quantum monadology remains quite insufficient in this paper due to the limitation of pages. Among omitted subjects, there is the concept of *null monads*, which plays an important role in generating higher-level monadistic structures.

The author expects that the NL world scheme is implemented adaptable to econo-systems, and is used to simulate their dynamics and to answer various economic problems from fundamental to practical.

## References


1. Globus GG, Pribram KH, Vitiello G (2004) (eds) Brain and Being - At the boundary between science, philosophy, language and arts. John Benjamins, Amsterdam Philadelphia
2. Nakagomi T (1992) Quantum Monadology: A Word Model to Interpret Quantum Mechanics and Relativity. Open Sys. & Information Dyn. 1: 355-378
3. Nakagomi T (1995) Feeling decision systems and quantum mechanics. Cybernet. Syst. 26: 601-19
4. Nakagomi T (2003a) Mathematical formulation of Leibnizian world: a theory of individual-whole or interior-exterior reflective systems. BioSystems 69: 15-26
5. Nakagomi T (2003b) Quantum monadology: a consistent world model for consciousness and physics. BioSystems 69: 27-38

# Visualization of microstructures of economic flows and adaptive control

Yoshitake Yamazaki[1-4], Zhong-can Ou-Yang[1], Herbert Gleiter[2], Kunquan Lu[3], Dianhong Shen[3] and Xing Zhu[4]
[1]Institute of Theoretical Physics (CAS), P.O.Box2735, Beijing 100080, China
[2]Institut fuer Nanotechnologie (FZK), D-76021 Karlsruhe, Germany
[3]Institute of Physics (CAS), P.O.Box 603, Beijing 100080, China
[4]School of Physics, Peking University, Beijing 100871, China

**Summary.** Economic flows are modeled based on the microscopic particle pictures, and studied by renormalized stochastic dynamics and simulations. From the universal behavior obtained, every catastrophic behavior of the flows may be understood, as well as which sub-system is concerned and how to avoid it by suitable control measures.

Key words. economic flows, economic catastrophe, microstructures and control

## Introduction

Aims of this paper are to improve our understanding of the economic flows on the basis of a particle model. Assuming typically important types of microeconomic structures, we discuss how to derive various catastrophic points and their behavior by understanding how to control them. We compare these results with those of the actual economic flow behavior. In section 2, general model systems are specified and methods and results are summarized. And also the relationship between the results and the evolution of option pricing is summarized in section 2. Finally, in section 3 concluding remarks are given. For further details we refer to three references.

## General model systems, methods and results

**Model systems**. Money is proposed to possess certain characteristics {like mass, charge, and spin (internal degrees of freedom)} while it flows via commercial societies, termed "groups". The money with inherent characteristics averaged over a certain group is regarded as a "particle" with a certain *group-dependent character*. Every particle flows according to the balance of influences of the pairwise interactions between particles, on the external-field interactions, on local external fields and a certain environment as a whole. The groups consist of various

*financial groups, industrial sectors/nations*. The external fields are related to certain *economic policies/reviews* acting on the particles. The environment may be parametrized by a "*temperature*".

For the simulations, particles at a position $\mathbf{r}_i$ in space possess the following characters {spin $\mathbf{s}_i$, kinetic energy $K_i$}. Pairwise interactions result in magnetic and/or elastic interactions described as $\{J_{ij}, A_{ij}=J_{ij}[\kappa \mathbf{s}_i \bullet \mathbf{s}_j+(1-\kappa)], B_{ij}=J_{ij}[\kappa\delta_{sisj}+(1-\kappa)]\}$, where a Lennard-Jones potential $J_{ij}=J(r)=4\varepsilon[(\sigma/r)^{12}-(\sigma/r)^6]$ (giving a minimum potential $-\varepsilon$, and zero potential at the distances $\sigma$, $\infty$). The parameters $0<\kappa<1$ are adopted. External (magnetic, pressure) fields $\mathbf{h}_i$, $\mathbf{P}_i$ represent *micropolicy/review*, and temperature T *macropolicy*. The state of money is assumed to vary by *individual* and *group* states, which are called "magnetic" and "elastic", respectively.

(S1) Elastic type systems: $E= \Sigma_i K_i+\Sigma_{i>j}J_{ij}-\Sigma_i \mathbf{P}_i \bullet \mathbf{v}_i$,

(S2) Magnetoelastic type systems: $E= \Sigma_i K_i+\Sigma_{i>j}A_{ij}-\Sigma_i \mathbf{h}_i \bullet \mathbf{s}_i-\Sigma_i \mathbf{P}_i \bullet \mathbf{v}_i$, (S=1,...,S),

(S3) Fractured elastic type systems: $E=\Sigma_i K_i+\Sigma_{i>j}B_{ij}-\Sigma_i h_{si} m_{si}-\Sigma_i \mathbf{P}_i \bullet \mathbf{v}_i$, (S=0,...,q-1),

where $\mathbf{v}_i$ and $m_{si}$ are a surface vector and a spin-moment at a point *i*, respectively.

(SO) Other theoretical systems with various interacting mechanisms like anisotropic-magnetic/binary-fluid/quantum-fluid/Heisenberg-magnetic type.

In (S1) the money flow is represented by the money configuration in space under the interactions with the external field and temperature. In (S2)-(S3) it is determined by the magnetic and elastic interactions under the influence of the fields {h,P,T}. The difference in these systems results from the different type of the pairwise interactions. The models (S1)-(SO) may become the economic standard models, and the results obtained indicate the measures required for the analysis of microeconomic dynamics.

**Methods and results.** In our model, economic flows consist of groups, "grains" of various sizes and individual of investors in "interfaces" between the "grains". Individual dealers make decisions by their own judgments under the policy of their groups. Each group competes with other groups to get customers. In an assembly of *groups of different sizes*, the smallest group disappears at the lowest T. This process is iterated until the largest group makes transition to another phase, with increasing T. In the solid phase the system possesses long-range order, magnetic order and periodic order in space, whereas in the liquid and gas phases it has only short-range correlations, to form clusters. In the gas phase, particles are assumed to obey Boltzmann's equation. In an *assembly of same sized groups*, all groups are frustrated to compete with each other. Finally, one group loses the competition, and this process is repeated until the largest group makes a transition, with increasing T. This case is related to the glass-like state.

*Monte Carlo simulation and results for (S1), (S2), (S3).* The economic systems are divided into small block-cells so that a block-cell system may be regarded as a local equilibrium state. Monte Carlo simulation is performed, and the averages of economic quantities over each block-cell are taken leading to the following results. Many *mesoscopic phases hierarchically* appear in the "solid-like/liquid-like/gas-like" phase regions, e.g., their curves of order parameter vs temperature are drawn with hierarchical stepwise curves. In the liquid-like/gas-like phases, the stepwise curves change to those with nearly discontinuous jump as a "first-order-like"

phase transition, and "spinodal-like" behavior appears. The order of the transition temperatures corresponds to that of the group sizes in the weak nonlinear regime, whereas an irregular ordering occurs in strong nonlinear regime. For every mesoscopic transition point, critical regions exist that exhibit power-law behaviors and non-critical regions are present displaying non-power-law behaviors. The position, height and half-width of the peaks for every block-cell, e.g. in the curves of specific heat, susceptibility, and autocorrelation are different, depending on the block-cell positions. As competing phenomena of the magnetic and elastic interactions, a higher transition temperature results for stronger average pairwise interactions. At the balancing point of both interactions, both mesoscopic phase transitions simultaneously occur. Competition between groups arises, to get more customers. This competition between same-sized groups continues for longer times with high energies. The reason is that larger groups become more stably ordered. Wherever the size of interfacial regions is larger than the interacting potential range, more stably ordered groups are newly created in the interfacial regions. Simultaneously, the energy of the system rapidly changes and the creation of a new group occurs in a large interfacial region. Afterwards the system becomes more stable. Similarly, this situation happens in the glass-like phase. Due to an economic policy of quench-anneal, changing from a certain hard policy $T_1$ to a soft policy $T_2$ in some period of time $\tau$, and returning to the same hard policy $T_1$, the economic system can find more stable new states. By an appropriate choice of $T_1, T_2, \tau$, the optimal economic situations can be induced. In these simulation systems, the visualization, the estimation and the adaptive control of the economic situations may become possible for every mesoscopic phase.

*Renormalized stochastic dynamics and results.* Every particle in economic flows is affected with random forces inside its own group and with stochastic forces inside the other groups and interfaces. Let us now consider generalized systems of extended-defect N-component type $H(\phi, V, f) = \int dx[(1/2)\Sigma^N_{\alpha=1} \{|\nabla_\perp \varphi_\alpha|^2 + a^2_b|\nabla_\parallel \varphi_\alpha|^2 + r_b\varphi_\alpha^2 + V(x_\perp)\varphi_\alpha^2 + u_{sb}(\Sigma^N_{\alpha=1}\varphi_\alpha^2)^2/4! + u_{cb}\Sigma^N_{\alpha=1}\varphi_\alpha^4/4! - (H+f)\cdot\varphi\}$ . The $\varepsilon_d$-dimensional extended-defects; $\varepsilon_d$ is 0 for point defects, 1 for line defects, 2 for plane defects, and non-integers for fractal defects. The dimensional analysis deduces the dimensions $\varepsilon = 6-d$ for the quartic interactions, and $\varepsilon \hat{} = \varepsilon_d + \varepsilon$ for the defect interaction. The mesoscopic critical behaviors for each grain system were obtained by the renormalizing approaches. For almost all representative systems also, they were studied and summarized in the last reference.

*Different sized groups* of mesoscopic critical temperatures $\{T_{ic}\}$, $T_{1c} < T_{2c} < \ldots T_{ic}$ is the critical temperature of i-th group with average size $L_i = 2R_i$. It appears in the ascending order of group sizes for weak nonlinear regime. This ordering irregularly changes for strong nonlinear regime. Every mesoscopic phase possesses the inherent, characters and mesoscopic critical behaviors. The economic states of every group are estimated and controlled by these properties.

*Same-sized groups.* A reference group surrounded by other groups makes motions inside the accumulated potential. It may overcome the potential barrier and make random walk, after some of the surrounding groups open a path. We define the jumping rate $R(p) = 1/\tau(p)$, characteristic evolution time $\tau(p)$, interacting time $\Theta$

and interacting momentum given by $R(p)\Theta=1$. Use $R(p)=(1/\tau_0)(p/p_0)^{\alpha}$. This state of a "glass-like" phase is described by the nonequilibrium distribution $L_{\mu}(x)=\mu\tau_b^{\mu}/x^{1+\mu}$ with $\mu=d/\alpha$: $\alpha=2$ for nonconserved fields, and 4 for conserved fields, in mean field approximation. By renormalizing approaches, the mesoscopic critical behavior of the effective homogeneous functions and critical exponents $\alpha,\ldots$, are obtained. The economic states can be estimated and controlled by them.

**Evolution of option pricing.** For the above results of each group, we use the conventional methods. Consider the relationship of the fluctuating volatility distribution $P_T(t)$, the option price $O(t)$, and the expected price, based on the microeconomic pictures. The option price is assumed to have larger fluctuations than its stock price. For *Gaussian price fluctuations*, consider evolution of option price. Denote the price and the number by $S(t)$, $N_S(t)$ for stocks, by $O(S,t)$, $N_O(t)$ for options, and by $B(t)$, $N_B(t)$ for short-time bonds. The total wealth is expressed as $W(t)=N_S(t)S(t)+N_O(t)O(S,t)+N_B(t)B(t)$. Consider a smooth exponential growth *without fluctuations*; $dW(t)/dt\approx r_W W(t)$, $dB(t)/dt\approx r_B B(t)$. Conventional relationship between the growth rate $r_W$ and the short-term bond rate $r_B$ is adopted as $r_W\approx r_B$. The self-financing strategy is expressed by $dN_S(t)/dtS(t)+dN_O(t)/dtO(S,t)+dN_B(t)/dtB(t)=0$; $N_S(t)/N_O(t)=-\partial O(S(t),t)/\partial S(t)$. Use the Fokker-Planck equation for the option price $\partial O/\partial t=r_W O-r_{xW}\partial O/\partial x+H\hat{}(i\partial_x)O$, where $r_{xW}=r_W+H\hat{}(i)$ and the probability distribution $P(x_b t_b|x_a t_a)=\exp[-r_W(t_b-t_a)]\int_{-\infty}^{\infty}(dp/2\pi)\exp[ip(x_b-x_a)-\{H\hat{}(p)+ir_{xW}p\}(t_b-t_a)]$ with $H\hat{}(p)=H(p)-H'(0)=(1/2)c_2p^2-(1/3!)ic_3p^3-(1/4!)c_4p^4+(1/5!)ic_5p^5+\ldots$. An option for a certain strike price E of the stock is written as $O(x_b,t_b)=\theta(S_b-E)(S_b-E)=\theta(x_b-x_E)[\exp(x_b)-\exp(x_E)]$ with $\theta$ step function and $x_E=\ln E$. The result deduces the Black-Scholes formula $O(x_a,t_a)=S(t_a)N(y_+)-\exp[-r_W(t_b-t_a)]EN(y_-)$ with $y_{\pm}=[\ln\{S(t_a)/E\}+(r_W\pm\sigma^2/2)(t_b-t_a)]/\{\sigma^2(t_b-t_a)\}^{1/2}$. For the option pricing *with nonGaussian fluctuations* $O(x(t),v(t),t)$, consider the riskfree portfolio $W(t)=N_S(t)S(t)+N_O(t)O(S,t)+N_V(t)V(t)+N_B(t)B(t)$. By accounting up to the second derivatives in the time evolution equation for the option price, using Ito rule and putting $N_V(t)/N_O(t)=-\partial O(S(t),v(t),t)/\partial v(t)$, we can use the smooth growth $dv(t)/dt\approx-\gamma[v(t)-v\hat{}]$. The renormalizing contributions to the corrective price of volatility risk $-\lambda v$ are accounted as $\gamma^*=\gamma+\lambda$, $v\hat{}^*=\gamma v\hat{}/\gamma^*$. We can use the Fokker-Planck equation $\partial O/\partial t=r_W(O-\partial O/\partial x)+(H\hat{}^*+\gamma^*+\epsilon\rho\partial_x+\epsilon^2\partial_v)O$, where $H\hat{}^*=-(1/2)\partial_x v-\gamma^*\partial_v(v-v\hat{}^*)-(1/2)\partial_x^2 v-(1/2)\epsilon^2\partial_v^2 v-\epsilon\rho\partial_x\partial_v v$, and the probability distribution $P_v(x_b v_b t_b|x_a v_a t_a)=\exp[-(r_W+\gamma^*)\Delta t]P\hat{}_v(x_b v_b t_b|x_a v_a t_a)$, with the arguments shifted to $x_b-x_a\rightarrow x_b-x_a-(r_W-\epsilon\rho)$, $v_b-v_a\rightarrow v_b-v_a-\epsilon^2$.

Stock market indices in each group is represented by the logarithmic divergence of the index y for t near $t_c$ as $y=A+B[\ln(1-t/t_c)][1+C\sin\{\omega\ln(1-t/t_c)+\varphi\}]$ for $t<t_c$, where $t_c$ is estimated by the Levenberg-Marquardt and Monte Carlo algorithms $dy/dt=-B/(t_c-t)$. For every group, using the relation of the wealth vs time, the catastrophic point and the option pricing are estimated from Fig.1, upper-right. The fine structure of the curve of the volatility vs time for every group may deduce the relation of temperature vs time illustrated in the lower-left figure because the volatility is related to the inverse susceptibility, relative temperature shift. From this figure and the phase diagram illustrated in the upper-left figure, the contributions to the wealth of every group for each moment may be evaluated. It indicates which group contributes from which phase states at which rate. For

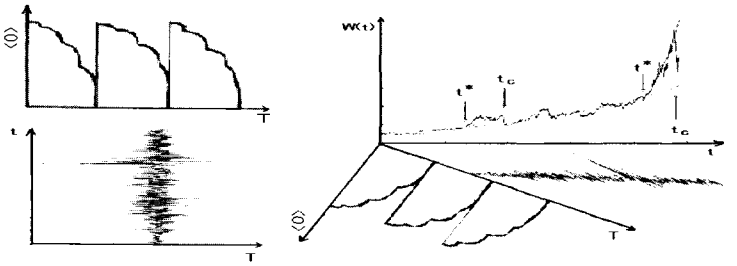


Fig. 1 Evolution of option price.

macrocatastrophic changes a number of groups cooperatively change their states over wide phase states, whereas for every mesocatastrophic change particular groups are concerned with special phase states. By identifying the mesoscopic critical properties of the actual system with those of economic standard models, the characters of every concerned group, the dynamic estimation and the controlling methods are known.

## Concluding remarks

Catastrophic properties of the economic systems were studied based on interacting microeconomic pictures. Every system divided into the "groups" with different characters exhibits the respective characteristic properties in its own catastrophic point. The group-size, catastrophic temperature and the magnitude of pairwise interactions are identified with the economic standard model. They are obtained from the height, position and half-width of the reference peak in the curves like specific heat and susceptibility. The essential features of every group are estimated as the spin components and the type of models like ferromagnetic/simple-fluids/ super-fluids. From these facts, the interacting mechanisms and structures of micro economic flows may be understood. The crucial states are estimated, in which each group works in phases (like solid-like/liquid-like/gas-like/glass-like phases) under certain values of the external fields and the temperature. As a result, they may be controlled by the external fields and the temperature, inherent to the macro and micro policies/reputations/reviews. Before planning or performing certain policies, it may be possible to estimate the consequences and to adjust the original plan, based on the simulations to realize a most acceptable situation for the public.

### References

Yamazaki Y and Gleiter H (2003) Adaptive intelligent control of economical flows by stochastic dynamics, Intell. Aut. Soft Comp.**9**, 129

Yamazaki Y, Gleiter H, Lu K-Q., Ou-Yang Z-C., and Zhu X. (2004) Mesoscopic phase transition of nanostructured materials, Surf. Interface Anal. **36**, 177

Yamazaki Y, Ou-Yang Z-C., Lu K-Q., Gleiter H, Zhu X., Wilde G, Shen D-H., Abe Y, and Watanabe M, Mesoscopic relaxation and elastic properties of two dimensional magnetic nanostructured materials, J.Comp.Theor.Nanosci., in press.